

**SOIL RESPONSE TO ACID DEPOSITION  
AT DIFFERENT REGIONAL SCALES**

**Field and laboratory data,  
critical loads and  
model predictions**

CENTRALE LANDBOUWCATALOGUS



0000 0572 0491

40951

**Promotor:** dr. ir. N. van Breemen  
Hoogleraar in de Bodemvorming en Ecopedologie

**Co-promotor:** dr. ir. A. Breeuwsma  
Hoofd van de afdeling Bodem- en Natuurbescherming  
Dienst Landbouwkundig Onderzoek  
Instituut voor Onderzoek van het Landelijk Gebied (SC-DLO)

NNO8701, 1812

**W. de Vries**

**SOIL RESPONSE TO ACID DEPOSITION AT DIFFERENT REGIONAL SCALES**  
**Field and laboratory data, critical loads and**  
**model predictions**

Proefschrift  
ter verkrijging van de graad van doctor  
in de landbouw- en milieuwetenschappen  
op gezag van de rector magnificus  
dr. C.M. Karssen  
in het openbaar te verdedigen  
op vrijdag 2 september 1994  
des namiddags te vier uur in de Aula  
van de Landbouwniversiteit te Wageningen

Isn 296722

The research presented in this thesis was performed at

DLO Winand Staring Centre for Integrated Land, Soil and Water  
Research (SC-DLO)  
Postbus 125, 6700 AC Wageningen (The Netherlands)

Most investigations were supported by the Dutch Ministry of Housing,  
Physical Planning and Environment (VROM)

The publishers of *Water, Air and Soil Pollution*, *Geoderma*, *Ecological Modelling* and *Journal of Applied Ecology* are acknowledged for their kind permission to include papers in this thesis.

Cover design : M. Jansen  
Text processing : L.C. van Liere


CIP-GEGEVENS KONINKLIJKE BIBLIOTHEEK, DEN HAAG

Vries, W. de

Soil response to acid deposition at different regional scales: Field and laboratory data, critical loads and model predictions / W. de Vries,  
Wageningen: DLO Winand Staring Centre. - III. Thesis Wageningen.  
With ref. - With summary in Dutch.

ISBN 90-327-0255-6

Subject headings: soil acidification / critical loads / acid deposition

 **BIBLIOTHEEK**  
**LANDBOUWUNIVERSITEIT**  
**WAGENINGEN**



UN08201,1812

Stellingen behorend bij het proefschrift van  
W. de Vries

"Soil response to acid deposition at various regional scales:  
Field and laboratory data, critical loads and model predictions"

Wageningen, 2 september 1994

Ontvangen

01 SEP. 1994

UB-CARDF

## STELLINGEN

- 1 De door Krug en Frink (1983) veronderstelde geringe bijdrage van zure depositie aan bodemverzuring biedt wel een nieuw, maar geen juist perspectief.  
*E.C. Krug and C.R. Frink, 1983. Acid rain on acid soils: a new perspective. Science 221: 520-525.*
- 2 Ondanks de hoge stikstofbelasting is zwaveldepositie de belangrijkste oorzaak van de verzuring van kalkloze bosgronden in Nederland.  
*Dit proefschrift.*
- 3 Een afname van zwavel- en stikstofdepositie leidt tot een evenredige afname van de uitspoeling van aluminium in kalkloze bosgronden in Nederland.  
*Dit proefschrift.*
- 4 Zuurneutralisatie in kalkloze zandgronden wordt op lange termijn veelal gedomineerd door aluminiumverwerking uit secundaire anorganische verbindingen, hoewel het vrijkomen van veelal organisch gecomplexiseerd aluminium in de bovengrond een relatief belangrijke rol kan spelen.  
*Dit proefschrift.*
- 5 De invloed van pH op de aluminiumverwerking kan redelijk tot goed worden beschreven op basis van de onderverzadiging van opgelost aluminium ten opzichte van gibbsiet.  
*Dit proefschrift.*
- 6 De door Higashi et al. (1981) berekende maximale metaal/koolstof ratio in organische stof is veel te hoog en leidt tot de onjuiste conclusie dat natriumpyrofosfaat een betrouwbaar extractiemiddel is voor organisch gecomplexiseerd aluminium.  
*T. Higashi, F. de Coninck and F. Gelaude, 1981. Characterization of some spodic horizons of the campine (Belgium) with dithionite-citrate, pyrophosphate and sodiumhydroxide-tetra borate. Geoderma 125: 131-142.*
- 7 De door James en Riha (1986) experimenteel vastgestelde hoge zuurbuffering in ecto-organische horizonten is, in tegenstelling tot wat zij beweren, weinig relevant voor de buffering van bosgronden.  
*B.R. James and S.J. Riha, 1986. pH buffering in forest soil organic horizons: relevance to acid precipitation. Journal of Environmental Quality 13: 229-234.*
- 8 Onzekerheden over kritische depositieniveaus voor stikstof en zwavel voor bossen worden in sterke mate bepaald door de onzekerheid van kritische waarden voor de chemische samenstelling van naalden en bodemvocht.  
*Dit proefschrift.*
- 9 Overschrijding van kritische depositieniveaus voor stikstof is geen typisch Nederlands probleem.  
*Dit proefschrift.*

- 10 Een afname van het depositieniveau van stikstof en zwavel leidt op relatief korte termijn tot een verbetering van de bodemvocht kwaliteit.  
*Dit proefschrift.*
- 11 In duingronden langs de Nederlandse kust met een laag kalkgehalte kan, bij handhaving van het huidige depositieniveau, binnen enkele decennia een pH-daling van 3 tot 4 eenheden optreden.  
*Dit proefschrift.*
- 12 Bij uitvoering van het voorgenomen beleid in het bestrijdingsplan verzuring is uitputting van de snel beschikbare aluminium voorraad in bosgronden pas op zeer lange termijn een reëel gevaar.  
*Dit proefschrift.*
- 13 Het is te verwachten dat voorgenomen reducties in de emissie van  $SO_4$ ,  $NO_x$  en  $NH_3$  in Nederland tot een verbetering, maar in Europa tot een verslechtering van de bodem- en bodemvocht kwaliteit zullen leiden.  
*Dit proefschrift.*
- 14 De stelligheid waarmee Krug (1991) blijft stellen dat zure depositie nauwelijks bijdraagt aan de verzuring van bodem- en oppervlaktewater stelt voor raadsels en lijkt meer het gevolg van een vooringenomen opstelling dan van een wetenschappelijke instelling.  
*E.C. Krug, 1991. Review of acid-deposition-catchment interaction and comments on further research needs. Journal of Hydrology 128: 1-27.*
- 15 De toenemende noodzaak van externe financiering voor wetenschappelijk onderzoek kan ertoe leiden dat onderzoeksinstituten en ingenieursbureau's in de toekomst niet meer van elkaar te onderscheiden zijn.
- 16 De grote vraag naar (kleuren)kaarten voor milieueffecten, in combinatie met de opkomst van geavanceerde ARC-Info systemen, kan zeer gemakkelijk leiden tot producties van een dubieus wetenschappelijk gehalte.
- 17 Uitgaande van de gemiddelde Nederlander is het zeer aannemelijk dat alleen gratis openbaar vervoer tot een afname van het autogebruik zal leiden.
- 18 In de woningbouw zijn stellingen essentiëler dan in de wetenschap.
- 19 De meest belang(stelling)wekkende stellingen werden in 1517 op een slotkapel gespiekerd.
- 20 De enige toekomstverwachting die voor een christen volkomen zekerheid heeft, is die welke beschreven is in Openbaring 22 vers 12.

## ABSTRACT

De Vries, W., 1994. Soil acidification on a regional scale: Critical loads and long-term impacts of acidic deposition. Doctoral thesis, Agricultural University, Wageningen, the Netherlands; 487 pp; 105 figs; 161 tables; 498 refs.

Enhanced soil, ground water and surface water acidification by elevated deposition of S and N compounds is one of the most important large-scale environmental problems today. This thesis deals with the quantification of:

- (i) natural and man-induced sources of acidification in agricultural soils and forest soils in the Netherlands;
- (ii) present impacts of atmospheric S and N deposition on the solution chemistry of acid sandy forest soils in the Netherlands;
- (iii) various buffermechanisms (i.e. mineral weathering, cation exchange and Al dissolution) in acid sandy soils in the Netherlands;
- (iv) average critical deposition levels (loads) for N and acidity (N and S) for forests, heathlands, ground water and surface water in the Netherlands;
- (v) spatial variability in critical loads for N, S and acidity and the degree by which these loads are exceeded at present on forests in the Netherlands and in Europe;
- (vi) long-term impacts of acidic deposition on representative non-agricultural soils;
- (vii) spatial variability in long-term impacts of acidic deposition on forest soils in the Netherlands and in Europe.

Quantification was performed on the basis of interpretation of literature information, combined with field research (i and ii), laboratory research (iii), and model research, (iv, v, vi and vii). In order to derive critical loads, steady-state soil models were developed, i.e. a one-layer model (START) for application on a European scale and a multi-layer model (MACAL) for application on a national scale. Similarly, two dynamic soil models were developed to assess the long-term soil response to acidic deposition, i.e. a one-layer model (SMART) for application in Europe and a multi-layer model (RESAM) for application in the Netherlands.

Results showed that:

- (i) the contribution of acid deposition to soil acidification in the Netherlands is dominant in non-calcareous forest soils ( $\geq 80\%$ ), intermediate in non-calcareous agricultural soils ( $\leq 50\%$ ) and minor in calcareous soils ( $\leq 20\%$ );
- (ii)  $\text{SO}_4$  behaves conservative in Dutch forest soils, whereas N is largely retained. Despite the high N deposition, actual soil acidification, which is mainly manifested by leaching of Al associated with  $\text{SO}_4$  and  $\text{NO}_3$  leaching, is dominantly caused by S deposition;
- (iii) dissolution of Al from secondary inorganic Al compounds is the dominant buffer-mechanism in acid sandy (forest) soils. The dissolution rate of Al can be described well as a function of the secondary Al pool and the degree of undersaturation with respect to gibbsite;

- (iv) average critical N loads for forests, heathlands, ground waters and surface waters in the Netherlands generally vary between  $500 \text{ mol}_c \text{ ha}^{-1} \text{ yr}^{-1}$  ('sensitive' heathlands and surface waters) and  $3600 \text{ mol}_c \text{ ha}^{-1} \text{ yr}^{-1}$  ('insensitive' ground waters). Average critical acid loads are generally lower and range between  $400 \text{ mol}_c \text{ ha}^{-1} \text{ yr}^{-1}$  ('sensitive' ground- and surface waters) to  $1700 \text{ mol}_c \text{ ha}^{-1} \text{ yr}^{-1}$  ('insensitive' forests and ground waters);
- (v) critical loads are largely exceeded in Central and Western Europe both in N (up to  $3500 \text{ mol}_c \text{ ha}^{-1} \text{ yr}^{-1}$ ) and S (up to  $12000 \text{ mol}_c \text{ ha}^{-1} \text{ yr}^{-1}$ ). In the Netherlands largest exceedances occur in areas with intensive animal husbandry. There emission reductions of more than 80% are needed to meet the critical loads;
- (vi) long-term continuation of present atmospheric deposition causes a depletion of the pool of secondary Al compounds, both in forest soils and dune soils of the Netherlands, leading to extremely low pH values. However, reduction of atmospheric deposition levels leads to a fast improvement of the soil solution quality (decreased concentrations in  $\text{SO}_4$ ,  $\text{NO}_3$  and Al and increased pH);
- (vii) deposition scenarios including current reduction plans with respect to S and N emission lead to an improvement in the soil solution quality below forests in the Netherlands, but not in Europe.

Additional index words:

acid deposition, soil acidification, soil solution chemistry, element budgets, weathering kinetics, aluminium dissolution, critical loads, simulation models, uncertainty, sensitivity analyses, scenario analyses.

## VOORWOORD

'Dit is veel te dik.' Ik kan me voorstellen dat dit de reactie van menigeen is bij het zien van dit proefschrift. Ontegengesteld is deze dissertatie lijviger dan oorspronkelijk de bedoeling was. Die betrof het uitvoeren van literatuur-, veld- en laboratoriumonderzoek voor de ontwikkeling, toetsing en toepassing van een dynamisch bodemverzuringmodel op nationale schaal. De weerslag hiervan vindt u in de hoofdstukken 2.1, 2.2, 2.3, 3.1, 3.2, 6.2, 6.3 en 7.2. In een vroeg stadium (1986) raakte ik echter, via het International Institute of Applied Systems Analyses (IIASA), betrokken bij de ontwikkeling en toepassing van een bodemverzuringmodel op Europese schaal. Resultaten hiervan vindt u in de hoofdstukken 6.1 en 7.1. Kort daarop (1987) werd ik benaderd door het Ministerie van VROM om een inschatting te maken van gemiddelde kritische depositieniveaus voor stikstof en zwavel in Nederland. Later (1989) kwam de vraag om de variabiliteit daarvan in kaart te brengen, zowel voor Nederland als Europa. Resultaten van dit onderzoek zijn weergegeven in de hoofdstukken 4.1, 4.2, 5.1 en 5.2. Hoewel ik aanvankelijk aarzelde om de verschillende onderzoeksaspecten samen te brengen in dit proefschrift, heb ik in overleg met mijn promotor prof. dr. N. van Breemen besloten dit toch te doen. De belangrijkste beleidsvraagstukken op het gebied van de verzuring, namelijk kritische depositieniveaus en lange-termijneffecten van depositiescenario's, zijn hierdoor gebundeld en dat op meerdere schaalniveaus (Nederland en Europa). Dit voordeel vergoedt hopelijk het bezwaar van de omvang.

Met het noemen van mijn promotor ben ik toegekomen aan het dankwoord aan een reeks van personen, die bijgedragen hebben aan de totstandkoming van dit proefschrift. Na enig wikken en wegen is de stijl daarbij zowel zakelijk als persoonlijk geworden. Een zakelijk stijl (voorletters), omdat ik in een officieel stuk moeite heb met de huidige Jan, Piet en Klaas stijl. Tevens heb ik titels vermeld omdat ik het eens ben met prof. dr. B. Smalhout dat die buiten de privé-sfeer een functionele betekenis hebben. Daarnaast ook een persoonlijke stijl (voornaam) omdat die toch het best weergeeft welke dank ik voel ten opzichte van vele van mijn collega's.

Allereerst dank ik mijn promotor prof. dr. N. van Breemen voor de opbouwende kritiek op alle manuscripten. Nico, bedankt voor het vertrouwen dat je in me stelde bij de totstandkoming van dit proefschrift. Hetzelfde geldt voor mijn co-promotor dr. A. Breeuwsma. Daarnaast bedank ik je Auke voor de ruimte die je als afdelingshoofd mij gaf om het proefschrift af te ronden.

Mijn dank gaat verder uit naar alle collega's die nauw betrokken zijn geweest bij dit proefschrift als co-auteur van één of meerdere artikelen. Behalve mijn promotor en co-promotor zijn dat ir. J. Kros, mw. M.M.T. Meulenbrugge, dhr. W. Balkema, dhr. R.Ch. Sjardijn, dhr. J.C. Voogd, ir. G.J. Reinds, drs. C. van der Saal, ing. P.C. Jansen, ing. E.E.J.M. Leeters, dr. J. Klijn (Staring Centrum), dr. J.J.M. van Grinsven (RIVM, Bilthoven), dr. M. Posch en dr. J. Kämäri (Water and Environment Research Institute, Helsinki, Finland). Hans, Marjon, Wim, Ronald, Jan Cees, Gert-Jan, Caroline, Peter, Ellis, Jan en Hans, van harte bedankt voor jullie bijdrage, de prettige collegiale omgang

en de vele stimulerende discussies. I also like to thank you, Max and Juha, for your enthusiastic cooperation, together with Gert Jan, in developing and applying the SMART model on a European scale. I hope that we can extend the cooperation in new projects, since I believe that it has been very fruitful, both in a scientific and a personal context.

Zonder de overigen tekort te willen doen, wil ik een aantal mensen apart bedanken. Allereerst de twee Hansen. Hans (van Grinsven), jij was het die mij in de beginperiode bij de toenmalige Stichting voor Bodemkartering je inzichten in de verzuring toevertrouwde, zowel op het gebied van de modellering als de uitvoering van laboratorium-experimenten. Gezien het feit dat je toen nog moest promoveren op die onderwerpen, was die houding onbaatzuchtig en ik ben je daar zeer erkentelijk voor. Via jou is Hans Kros ook bij de Stichting voor Bodemkartering komen werken. Het is zonder enige overdrijving als ik stel dat dit essentieel is geweest voor het tot stand komen van een groot deel van dit proefschrift. Hans (Kros), samenwerken met jou is uiterst plezierig. Je secure en kritische instelling en je kunde in programmeren hebben in hoge mate bijgedragen aan een succesvolle toepassing van RESAM op nationale schaal. In het bijzonder wil ik ook jou, Jan Cees, bedanken voor de eindeloze stroom figuren en tabellen die je voor me hebt geproduceerd in de afgelopen jaren (slechts een beperkt deel staat in dit proefschrift). En jullie, Marjon en Wim, voor de vindingrijkheid en inzet bij de uitvoering van vele laboratorium-experimenten.

Zeer veel andere collega's, zowel binnen als buiten het Staring Centrum, hebben in meerdere of mindere mate een bijdrage geleverd aan dit proefschrift. Het is vrijwel ondoenlijk om een compleet overzicht te geven. Ik denk bijvoorbeeld aan alle collega's met wie ik iets over bodemverzuring heb gepubliceerd. Daarvoor verwijs ik liever naar Annex D. Toch wil ik een aantal mensen met name bedanken en wel allereerst collega's binnen het Staring Centrum die in een vroeger of later stadium bijgedragen hebben aan het hier beschreven verzuringsonderzoek: dhr. R. Zwijnen, dhr. J. Denneboom, dhr. C. Schuiling, ir. J.E. Groenenberg, ing. F. de Vries en ir. C.M. Hendriks. Roet, Johan, Rini, Bert Jan, Folkert en Kees, bedankt voor jullie inbreng. Daarnaast dank ik een aantal collega's buiten het Staring Centrum en wel dr. H.U. Sverdrup (University of Lund, Zweden) en dr. J.P. Hettelingh (RIVM, Bilthoven), die met mij respectievelijk een 'manual' en 'vademecum' hebben geschreven om kritische depositieniveaus in kaart te brengen; drs. A. Bakema, dr. J.W. Erisman en dr. F.A.A.M. de Leeuw (RIVM, Bilthoven), die essentiële depositiegegevens (scenario's) voor Nederland hebben toegeleverd; dhr. R. Kok (RIVM, Bilthoven), die een programma schreef om geautomatiseerde datafiles in te lezen voor de nationale toepassing van RESAM; dr. R. Leemans (RIVM, Bilthoven), dr. M. Amann en dipl. ing. W. Schöpp (IIASA, Oostenrijk), die respectievelijk neerslag-, depositie- en opnamegegevens voor bomen in Europa toeleverden; drs. H. Marseille (Ministerie van VROM, Den Haag), voor discussies over de beleidsrelevantie van het onderzoek en ir. G.J. Heij (RIVM, Bilthoven), wiens integere en kundige verwerking van de onderzoeksresultaten in de eindrapportage van het Additioneel Programma Verzuringsonderzoek respect afdwingt. Jean Paul, Aldrik, Jan Willem, Frank, Rob, Rik, Harriëtte en Bert Jan: bedankt voor jullie inbreng en medewerking. Harold, Markus and

Wolfgang: thanks for your collaboration. It is specifically you Harold, together with Jean Paul, whom I like to thank for the very fruitful (still ongoing) discussions about methods to derive critical loads on a large regional scale.

Een apart dankwoord is op zijn plaats voor collega's van de zogenaamde ondersteunende afdelingen. Zo zijn de figuren getekend door mw. D. ten Cate. Het ontwerp voor de omslag is gemaakt door dhr. M. Jansen. Veel nuttige wenken voor de lay-out zijn verder gegeven door ing. B. ten Cate. Dasja, Martin en Bram: bedankt voor jullie spontane hulp, die zonder enige twijfel de zichtbare kwaliteit van dit proefschrift heeft verhoogd. Heel in het bijzonder dank ik mw. L.C. van Liere voor de verwerking van de complete tekst van dit proefschrift. Lena, jouw bijdrage is moeilijk naar waarde te schatten en ik wil je dan ook hartelijk bedanken voor de fantastische manier waarop je alle mogelijke (en onmogelijke) correcties hebt uitgevoerd en de vele vrije uren die je er in de laatste fase aan hebt besteed.

Het Ministerie van VROM ben ik erkentelijk voor de financiering van het grootste deel van het onderzoek dat in dit proefschrift is beschreven. Ook dank ik de directie van het DLO-Staring Centrum voor de mogelijkheid die zij mij geboden heeft om dit proefschrift te schrijven.

Last, but not least dank ik mijn ouders, die mij niet alleen stimuleerden om te studeren maar die daaruit ook persoonlijk alle financiële consequenties hebben getrokken. Graag draag ik dit proefschrift dan ook aan hen op. En vanzelfsprekend aan mijn vrouw, die geconfronteerd werd met de sociale consequenties van een dissertatie. Carla, 'hij' is af. Bedankt voor je geduld, vooral in de laatste fase, en wees gerust: ik heb niet de ambitie van prof. dr. dr. dr. W.J. Ouweneel om drie proefschriften te schrijven. Zelfs geen twee.

Dit dankwoord wekt mogelijk de indruk dat het welslagen van een proefschrift voornamelijk afhangt van goede contacten met collega's. Persoonlijk heb ik echter de waarheid ervaren van het onderstaande Bijbelwoord, uit Spreuken 2 vers 6. Daardoor wordt dit dankwoord in het juiste perspectief geplaatst.

*"Want de Heere geeft wijsheid; uit Zijn mond komt kennis en verstand"*



Aan : mijn vader en moeder  
Carla

## CONTENTS

	Page
VOORWOORD	
1 INTRODUCTION	13
1.1 Background and aim	15
1.2 Modelling the impact of acid deposition on soils	17
1.3 Outline of the thesis	24
2 CAUSES, RATES AND EFFECTS OF SOIL ACIDIFICATION	27
2.1 Relations between soil acidification and element cycling	29
2.2 Relative importance of natural and man-induced acidification of soils in the Netherlands	45
2.3 Impacts of acid deposition on concentrations and fluxes of solutes in acid sandy forest soils in the Netherlands	57
3 RATES AND MECHANISMS OF CATION AND SILICA RELEASE IN ACID SANDY SOILS	83
3.1 Influence of mineral pools and mineral depletion	85
3.2 Effects of pH and aluminium concentration	107
3.3 Differences between soil horizons and soil types	129
4 AVERAGE CRITICAL LOADS FOR FORESTS, HEATHLANDS, GROUND WATER AND SURFACE WATER IN THE NETHERLANDS	153
4.1 Critical loads for nitrogen	155
4.2 Critical loads for acidity	169
5 REGIONAL VARIABILITY IN CRITICAL LOADS FOR FORESTS	189
5.1 Critical loads and their exceedance in Europe	191
5.2 Critical loads and their exceedance in the Netherlands	225
6 LONG-TERM IMPACTS OF ACID DEPOSITION ON SOME CHARACTERISTIC SOILS	263
6.1 Impacts on soils in various buffer ranges	265
6.2 Impacts on a characteristic forest soil in the Netherlands	295
6.3 Impacts on two characteristic dune soils in the Netherlands	323
7 REGIONAL VARIABILITY IN LONG-TERM IMPACTS OF ACID DEPOSITION ON SOILS	345
7.1 Impacts on forest soils in Europe	347
7.2 Impacts on forest soils in the Netherlands	375
8 GENERAL DISCUSSION AND CONCLUSIONS	405

	Page
SUMMARY	415
SAMENVATTING	423
REFERENCES	431
ANNEXES	
A Notation of symbols in the models START, MACAL, SMART and RESAM	465
B Relationships between empirical functions describing cation release	471
C Solution method of the model SMART	473
D Publications on acid deposition and soil acidification	479
CURRICULUM VITAE	487

# **Chapter 1**

## **INTRODUCTION**

### **1.1 BACKGROUND AND AIM**

### **1.2 MODELLING THE IMPACT OF ACID DEPOSITION ON SOILS**

- MODELLING APPROACH
- MODEL CHARACTERISTICS
- PROCESS DESCRIPTIONS
- MODEL EVALUATION

### **1.3 OUTLINE OF THE THESIS**

## 1.1 BACKGROUND AND AIM

Enhanced soil, ground water and surface water acidification by elevated atmospheric deposition of  $\text{SO}_x$ , ( $\text{SO}_2$  and  $\text{SO}_4$ ),  $\text{NO}_x$  ( $\text{NO}$ ,  $\text{NO}_2$  and  $\text{NO}_3$ ) and  $\text{NH}_x$  ( $\text{NH}_3$  and  $\text{NH}_4$ ) compounds, is one of the most important large scale environmental problems today. For centuries, burning of sulphur-rich coal has been recognized as a problem for human health in urban areas. However, the strong increase in the use of fossil fuel after the second World War and the long range transport of the pollution gases by high smoke stacks transformed the problem from a local scale to a regional and even continental scale. In addition to  $\text{SO}_2$  emission,  $\text{NO}_x$  ( $\text{NO}$  and  $\text{NO}_2$ ) emission (formed during internal combustion) and  $\text{NH}_3$  emission (from intensive animal husbandry) were recognized as increasingly important sources to acidic deposition in the 1980's. In the Netherlands, N compounds, especially  $\text{NH}_x$ , are presently major contributors to acid deposition (Erisman, 1991).

Acid atmospheric deposition first became recognized as a problem in the early seventies in relation to acidification of lakes and streams in Scandinavia and Northeastern America causing a decline in fish species (Likens and Bormann, 1974). Ulrich et al. (1979) were among the first to pay attention to acidification of forest soils caused by acid deposition and its potentially harmful effects on forest ecosystems. Evidence exists that the vitality of forest ecosystems in Europe is seriously endangered by changes in soil chemistry in the rootzone. Examples are a decrease in pH and base saturation, an increase in toxic Al and the unbalanced availability of base cation nutrients (Ca, Mg, K) due to excessive Al and  $\text{NH}_4$  (Roelofs et al., 1985; Roberts et al., 1989).

Although acidification of soils, such as decalcification and podzolization, is a natural process in areas with a precipitation excess, it is the present rate of soil acidification which is alarming. Current enhanced soil acidification due to elevated atmospheric deposition has been proven by input-output budgets. By measuring or estimating annual inputs of all major inorganic compounds in atmospheric deposition, and outputs by drainage and uptake, the soil acidification rate has been quantified on an annual basis (e.g. Van Breemen et al., 1988; Van Dobben et al., 1992). Recently enhanced soil acidification in Central and Northern Europe has also been proven by resampling forest soils at intervals of several decades in Sweden (Falkengren-Grerup, 1986; Falkengren-Grerup et al., 1987; Hallbäcken and Tamm, 1986), Scotland (Billet et al., 1988, 1990b), Germany (Ulrich et al., 1980; Butzke, 1981; 1988), Austria (Glatzel and Kazda, 1985) and the Netherlands (Van der Salm, 1985). These studies showed that soil pH and base saturation have decreased strongly within the rootzone of most forest soils in the past 20 to 30 years.

Soils have various mechanisms to buffer acid inputs, such as the exchange of base cations against protons and the adsorption of  $\text{SO}_4$  on Al and Fe hydroxides against hydroxyl ions (Johnson, 1984). Both buffering processes are fast and, especially cation

exchange, will prevent the occurrence of temporarily, extremely low pH values and associated high concentrations of Al. However, compared to current deposition rates, the capacity of these buffer mechanisms is limited on a long-time scale (decades or centuries). Another important mechanism which involves proton consumption is mineral weathering. Contrary to the capacity for cation exchange and  $\text{SO}_4$  adsorption, the acid neutralizing capacity (ANC) of silicate minerals is nearly infinite, but the rate (kinetics) of mineral dissolution is low and this determines the importance of this buffering process. At low base saturation (and pH), dissolution of Al from secondary Al compounds (organic Al complexes and secondary Al minerals such as (amorphous) hydroxides and imogolite) can play an important role. In this stage the overall weathering reaction (the reaction stoichiometry) of silicates and secondary Al compounds is important as it determines the absolute concentration of Al and its ratio to the concentration of base cations, which are both important parameters with respect to forest damage.

This thesis aims to answer the following research questions:

- (i) What is the relative contribution of natural soil forming processes, land use (agriculture and forestry) and acid atmospheric deposition to the acidification of soils in the Netherlands?
- (ii) What are the current impacts of atmospheric S and N deposition on the soil solution chemistry below Dutch forests, in particular on the concentrations of  $\text{SO}_4$ ,  $\text{NO}_3$ ,  $\text{NH}_4$  and Al.
- (iii) What is the role of various buffer mechanisms, such as N immobilization,  $\text{SO}_4$  adsorption, cation exchange, mineral weathering and Al dissolution, in neutralizing the acid input to Dutch forest soils?
- (iv) What are average critical deposition levels (critical loads) of N and acidity (N and S) on sensitive Dutch terrestrial and aquatic ecosystems, below which unfavourably high concentrations of Al and N ( $\text{NH}_4$  and/or  $\text{NO}_3$ ) in soil solution, ground water and surface water are avoided?
- (v) What is the regional variability in critical loads and the degree by which these loads are presently exceeded on forest soils, both on a national and European scale?
- (vi) What is the long-term impact of present atmospheric deposition levels on soils and how does the soil react on deposition changes (including the question whether soil acidification is reversible at reduced acid inputs)?
- (vii) What is the regional variability in long-term response of forest soils to deposition scenarios, both on a national and on a European scale?

To answer these questions, especially those regarding critical deposition levels and long-term soil response to atmospheric deposition (questions iv to vii), use was made of several steady-state and dynamic soil acidification models developed for this purpose. An overview of these models is given in the next section.

## 1.2 MODELLING THE IMPACT OF ACID DEPOSITION ON SOILS

### MODELLING APPROACH

The modelling approach is largely determined by the goals and objectives of the model application. In this respect, distinction can be made between research models and management models. Research models are used as a research tool to get insight into, or generate hypotheses about, system behaviour, and to direct further investigations. Management models aim to help decision makers in designing (environmental) policies (Kämäri, 1987). In contrast to research models, management models have an immediate practical application.

Examples of different modelling approaches are (Kämäri, 1987; De Vries, 1990):

- empirical (black-box) versus process-oriented (mechanistic) models
- deterministic versus stochastic models
- spatially lumped versus spatially distributed parameter models
- steady-state versus dynamic models

Two major groups of soil acidification models are those based on an empirical approach and those based on mechanistic descriptions of processes. A disadvantage of relatively simple empirical models is that they lack a theoretical basis for establishing confidence in the predictions (research aim). A disadvantage of relatively complex mechanistic models is that input data for their application on a regional scale (management aim) is generally incomplete. So, even if the model structure is correct (or at least adequately representing current knowledge), the uncertainty in the output of complex models may still be large due to because of the uncertainty of input data, such as forcing functions (source/sink terms), initial conditions of soil variables and parameter values (Hornberger et al., 1986). This dilemma between detail and reliability of information obtained (research model) and regional applicability (management model) is illustrated in Figure 1.1.

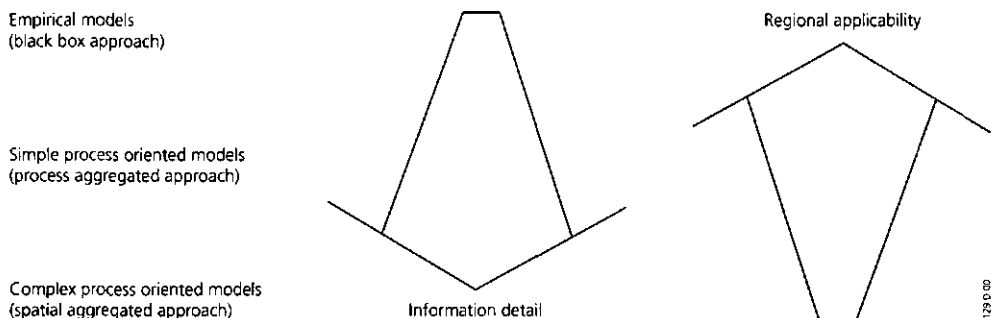


Figure 1.1 Schematic diagram illustrating the trade off between model complexity and regional applicability (after De Vries, 1987)

The desired degree of spatial resolution in model output is a factor of crucial importance when selecting the level of detail that is appropriate for both the model and its input data. In this respect, two important aspects must be considered when assessing the adequacy of process-oriented simulation models for application on a regional scale. The first aspect concerns the extent to which the spatial heterogeneity of soil properties can be lumped (spatial aggregation). For example, predicting the chemical composition of surface water may not require precise knowledge of the spatial variation in soil properties in the catchment. Consequently, insight into the hydrological and chemical response of surface water to inputs (e.g. precipitation, deposition) is generally obtained from process-oriented spatially lumped parameter models which average or lump the spatially distributed physical and chemical processes in the catchment (Cosby et al., 1985a). However, prediction of the chemical soil (solution) composition in the same catchment does not allow such a lumping procedure. The second aspect concerns the degree in which the multitude of processes that occur in soils can be represented by simple conceptualizations (process aggregation). For example, the response of soil solution chemistry to input of pollutants has to be ascertained by using a process-oriented spatially distributed parameter model, because soil types and soil horizons influence the hydrological and chemical behaviour of the soil system. In order to apply such a model on a regional scale, the various hydrological, biochemical and geochemical processes occurring in the soils must either be limited to a few key soil processes, which mainly control the gross behaviour of the soil system, or represented by simple conceptualizations. Failure to do so, leads to complex models with a high potential to explain system behaviour but with few possibilities for regional application.

All soil acidification models described here are characterized by a process-oriented deterministic approach using spatially distributed input data. They range from a relatively simple steady-state model (START) to a relatively complex long-term dynamic model (RESAM). Even though the models are process-oriented, or mechanistic, the description of processes is mainly empirical. The reason for differentiating in steady-state and dynamic models and in relatively simple and complex versions of both model types was the aim of the model and the scale at which the model is applied, respectively (see next section on model characteristics). Their major common aspect is the use of spatially distributed data to ascertain the geographic variation in soil acidification. Spatially variable input data are derived from basic land and climate characteristics such as soil type, tree species and air temperature, which are available in geographic information systems. For example, the large amount of soil data needed in the dynamic models, (e.g. contents of carbonates and secondary Al compounds, cation exchange capacity (CEC), base saturation and C/N ratios) are mainly derived by relationships or transfer functions (cf Bouma et al., 1986) with basic land and soil characteristics (e.g. parent material, soil type, organic matter content and texture). The stochastic character of input data can, however, be included in all models by a Monte Carlo approach, given a specified range of input data (e.g. Kros et al., 1993).



## MODEL CHARACTERISTICS

In this thesis four soil acidification models are described that were developed to map sensitive forest ecosystems in Europe and in The Netherlands. An overview of the major model characteristics is given in Table 1.1.

*Table 1.1 Characteristics of the soil acidification models described in this thesis*

Name	Complexity	Type	Aim	Soil layering	Application scale
START	Simple	Steady-state	Critical load assessment	one-layer	Europe
MACAL	Intermediate	Steady-state	Critical load assessment	multi-layer	The Netherlands
SMART	Intermediate	Dynamic	Scenario analyses	one-layer	Europe
RESAM	Complex	Dynamic	Scenario analyses	multi-layer	The Netherlands

The degree of process aggregation in the models increases (complexity decreases) when the research aim is less detailed (assessment of critical loads vs evaluation of deposition scenarios) and when the availability of data decreases, which occurs with an increase in the geographic area of application (Europe vs the Netherlands). Both aspects are discussed below.

### **Model type and model aim**

Steady-state models (START and MACAL) were developed to derive critical loads for total acidity (S and N). These models, assume that adsorbed and dissolved cations and anions (especially  $\text{SO}_4$ ) are in steady-state. Cation exchange and  $\text{SO}_4$  adsorption/desorption are thus not included in START and MACAL. At a given atmospheric input, they predict steady-state concentrations of relevant ions in the soil solution. A critical load is calculated as the deposition level at which environmentally critical chemical values (e.g. for Al concentration or Al/Ca ratio) are not exceeded in a steady-state situation. Processes that are considered in these models include deposition, mineral weathering, net uptake of nutrients, denitrification and leaching.

Dynamic models (SMART and RESAM) were developed to predict the time period before a critical chemical value is reached. In addition to the processes considered in steady-state models, these models also include processes that influence the acid production and consumption in a non-steady-state situation, such as cation exchange, N mineralization/immobilization and  $\text{SO}_4$  adsorption/desorption. SMART and RESAM do not include seasonal dynamics. The temporal resolution of the models is one year as they are specifically developed to evaluate long-term soil responses to deposition scenarios. As with START and MACAL, the hydrologic description in these models is very simple. Simulation of the interannual variability is included in an extended version of the RESAM model called NUCSAM (Nutrient Cycling and Soil Acidification Model;

Groenenberg et al., 1994) which is specifically developed for application (and validation) on a site scale. SMART and RESAM are part of integrated acidification simulation models that give a quantitative description of the linkages between emissions, deposition and environmental impacts such as soil acidification and effects on terrestrial and aquatic ecosystems. The integrated models under consideration are RAINS (Regional Acidification Information and Simulation model) for application on a European scale (Aicamo et al., 1990) and DAS (Dutch Acidification Simulation model) for application in the Netherlands (Olsthoorn et al., 1990).

Steady-state and dynamic models for mapping sensitive forest areas are complementary, and both are needed to get insight into the area of forests under air pollution stress. Steady-state models identify the forest areas where the present deposition exceeds the critical load. These models are thus useful to determine the final emission rate based on a final critical acidification status. Dynamic models identify the areas where critical chemical values are exceeded at a certain point in time. These models are necessary to determine an optimal emission scenario, based on the temporal evolution of the acidification indicators (e.g. Al concentration or Al/Ca ratio).

#### **Data availability and scale of model application**

The major reason for differentiating between one-layer and multi-layer models was the trade-off between the level of detail in model outputs and the availability of model inputs. Multi-layer models give insight into the spatial (vertical) variation in soil (solution) chemistry within the rootzone, whereas one-layer models only predict average concentrations in the rootzone. Since the hydrologic description in the one-layer models is simplified to the use of an annual precipitation excess draining from the rootzone, these models only predict soil solution chemistry at the bottom of the rootzone. Important acidification indicators such as the Al concentration and Al/Ca ratio, however, increase with depth due to Al mobilization, transpiration and Ca uptake. Since most fine roots, responsible for nutrient uptake, occur in the upper soil layer (0-30 cm soil depth), it is important to obtain reliable estimates for this layer by including water uptake with depth and nutrient cycling (foliar uptake, foliar exudation, litterfall, mineralization and nutrient uptake within the rootzone). However, inclusion of these processes in the model requires additional data on nutrient cycling. These data are easily available for the Netherlands but not for Europe. Consequently, the multi-layer models MACAL and RESAM, developed for application in the Netherlands, include such processes whereas the one-layer models, START and SMART, developed for application on a European scale, do not (Table 1.1). The use of one-layer models is thus limited. This aspect is thoroughly discussed in Chapter 5.

## PROCESS DESCRIPTIONS

START, MACAL, SMART and RESAM, are all based on the principle of ionic charge balance and on a strongly simplified water and solute transport description (cf Table 1.2). In all models, it is assumed that:

- a soil layer is a homogeneous compartment of constant density;
- the element input mixes completely in a soil layer;
- the annual water flux percolating through a soil layer is constant and equals the infiltration minus the transpiration.

Furthermore, N-fixation,  $\text{SO}_4$  reduction,  $\text{SO}_4$  precipitation and complexation reactions are not included, and the various process descriptions for biological and geochemical interactions are simplified to minimize input data.

Going from RESAM to START the degree of process aggregation increases by (i) ignoring several processes (e.g. nutrient cycling), (ii) simpler descriptions of processes (e.g. equilibrium equations instead of rate limited reactions) and (iii) ignoring elements (e.g. organic anions, RCOO) or lumping elements (e.g. sum of base cations, BC, instead of Ca, Mg, K and Na separately). This is illustrated in Table 1.2.

Biological processes are all described by rate-limited reactions. In most cases first-order reactions are used. Notable exceptions are the canopy interactions in MACAL and RESAM that are described by linear relationships with atmospheric deposition (cf Table 1.2). In START, MACAL and SMART, all geochemical reactions are described by equilibrium equations, except for silicate weathering which is described by a zero-order reaction (Table 1.2). In RESAM, the geochemical reactions are either described by equilibrium equations (dissociation of  $\text{CO}_2$ , cation exchange and  $\text{SO}_4$  adsorption) or first-order reactions (protonation of organic anions and weathering of carbonates, silicates and secondary Al compounds). So, unlike SMART, RESAM accounts for the effect of mineral depletion on the weathering rate. In the various models, secondary Al compounds are assumed to consist of Al hydroxides only (cf Table 1.2 and Chapter 4, 5, 6 and 7). Secondary Al compounds, extracted by Na-pyrophosphate (Mulder et al., 1989) or  $\text{NH}_4$ -oxalate (De Vries, 1994a; cf Section 3.1) do, however, consist of organic Al complexes and inorganic (mainly amorphous) Al compounds, including Al hydroxides. The limitations of the model approach are further discussed in Chapter 8.

In all model descriptions, a similar annotation was used to denote variables and parameters. A complete overview of the list of symbols is given in Annex A. A complete description of the various models is given in Section 5.1 (START), 5.2 (MACAL), 6.1 (SMART) and 6.2 (RESAM).

Table 1.2 Processes and process formulations included in START, MACAL, SMART and RESAM

Processes	START	MACAL	SMART	RESAM
<b>Hydrological processes:</b>				
Water flow	Precipitation excess	Variable flow with depth	Precipitation excess	Variable flow with depth
<b>Biological processes:</b>				
Foliar uptake	-	Proportional to total deposition	-	Proportional to total deposition
Foliar exudation	-	Proportional to H and NH <sub>4</sub> deposition	-	Proportional to H and NH <sub>4</sub> deposition
Litterfall	-	First-order reaction	-	First-order reaction
Root decay	-	-	-	First-order reaction
Mineralization/immobilization	Zero-order reaction <sup>1)</sup>	Zero-order reaction <sup>1)</sup>	Proportional to N deposition	First-order reaction
Growth uptake	Constant growth	Constant growth	Constant growth	- Constant growth - Logistic growth
Maintenance uptake	-	Forcing function <sup>2)</sup>	-	Forcing function <sup>2)</sup>
Nitrification	Proportional to net NH <sub>4</sub> input	Proportional to gross NH <sub>4</sub> input	Proportional to net NH <sub>4</sub> input	First-order reaction
Denitrification	Proportional to net NO <sub>3</sub> input	Proportional to gross NO <sub>3</sub> input	Proportional to net NO <sub>3</sub> input	First-order reaction
<b>Geochemical processes:</b>				
CO <sub>2</sub> dissociation	Equilibrium equation	Equilibrium equation	Equilibrium equation	Equilibrium equation
RCOO protonation	-	-	-	First-order reaction
Carbonate weathering	-	-	Equilibrium equation	First-order reaction
Silicate weathering	Zero-order reaction	Zero-order reaction	Zero-order reaction	First-order reaction <sup>3)</sup>
Al hydroxide weathering	Equilibrium equation	Equilibrium equation	Equilibrium equation	- First-order reaction - Elovich equation
Cation exchange	-	-	Gaines Thomas equation <sup>4)</sup>	Gaines Thomas equation <sup>4)</sup>
SO <sub>4</sub> adsorption	-	-	Langmuir equation	Langmuir equation

<sup>1)</sup> START and MACAL only include long-term net nitrogen immobilization.

<sup>2)</sup> In MACAL the maintenance uptake equals litterfall plus foliar exudation minus foliar uptake and in RESAM it equals the sum of litterfall, root decay and foliar exudation minus foliar uptake.

<sup>3)</sup> In RESAM there is also the option to include a dependence of pH on the weathering rate.

<sup>4)</sup> In SMART cation exchange is limited to H, Al and the sum of base cation (BC) whereas in RESAM it includes H, Al, NH<sub>4</sub>, Ca, Mg, K and Na

## MODEL EVALUATION

Important aspects of model evaluation are (i) validation of model results on measured data and (ii) assessment of the uncertainty in model results due to uncertainties in model inputs and model structure. According to Janssen et al. (1990), model validation can be divided in a conceptual validation (are the various model assumptions and concepts justified), an operational validation (is the model suitable for the purpose aimed at and does it produce plausible results) and a model output validation (is there a good agreement between model predictions and measured data). A conceptual validation is given in several sections describing the models (cf Section 4.2 and 6.1). Operational validation is also discussed in several model applications. Validation of model outputs on measured data, however, is not an integral part of this thesis. The only model output validation included is a comparison between cumulative frequency distributions of results of the RESAM model and soil chemistry data of 150 forest stands on acid sandy soils in the Netherlands (Section 7.2). Various other model (output) validations are presented in articles not included in this thesis (Kros et al., 1994; Van Oene and De Vries, 1994; Van der Salm et al., 1994). The MACAL model has been validated on measured soil solution chemistry data in the topsoil (0-30 cm) and subsoil (60-100 cm) of the 150 forest stands mentioned above (Kros et al., 1994). Most model parameters were fixed but several poorly known parameters (e.g. nitrification and Al dissolution parameters) were obtained by calibration. Actually, the major aim of this study was to limit the uncertainty of these parameters. The SMART and RESAM model were validated by comparing simulations with historical observations of changes in (i) soil chemistry between 1949 and 1984 for five sites in Sweden (SMART; Van Oene and De Vries, 1994) and (ii) soil solution chemistry between 1974 and 1989 in a continuously monitored spruce site in Solling, Germany (SMART and RESAM; Van der Salm et al., 1994).

It is important to note that output validation of steady-state models, such as MACAL, and of dynamic models which do not include interannual variability, such as SMART and RESAM, is problematic since soils are seldom in steady-state and since long-term time series of soil chemistry data are generally lacking. Regarding MACAL, a comparison of model results and data was, however, reasonable to good for most parameters since dynamic adsorption/desorption reactions for cations and  $\text{SO}_4$  were likely to be insignificant in the 150 forest stands (cf Section 2.3; Kros et al., 1994). Regarding SMART and RESAM, data were either too scarce (Swedish sites), or the time period of the data set was too short for a rigorous validation of the model outputs. Consequently, the question about the accuracy of the long-term soil responses estimated by the SMART and RESAM model cannot be answered satisfactorily. However, the reasonable to good agreement between measured and simulated:

- (i) changes in soil and soil solution chemistry on a site scale (Van Oene and De Vries, 1994; Van der Salm et al., 1994);

- (ii) soil interactions or ion behaviour (e.g. the relationship between (i) Al concentration and base saturation; cf Section 6.1, (ii) leaching of Al and that of  $\text{SO}_4$  plus  $\text{NO}_3$ ; cf Section 6.2 and (iii) pH and carbonate content; cf Section 6.3), and
- (iii) frequency distributions of ion concentrations on a regional scale (cf Section 7.2), imply that the SMART and RESAM model do produce plausible results.

As with (model output) validation, thorough uncertainty analyses of the various models are not included in this thesis, although such an analysis, using a Monte Carlo approach, has been performed for the RESAM model (Kros et al., 1993). However, uncertainties in the results of regional model applications, due to uncertainties in model inputs and model structure (and in critical chemical values in case of the steady-state models calculating critical loads) are evaluated for all models, based on simple sensitivity analyses (cf Section 5.1, 5.2, 7.1 and 7.2).

### 1.3 OUTLINE OF THE THESIS

The various research questions posed before (see background and aim) are dealt with in this thesis in six chapters, each consisting of two or three sections. This thesis is a compilation of papers (to be) published in international journals. A complete list of publications, dealing with the research questions mentioned, is given in Annex D.

The relative contribution of natural soil forming processes, land use and acid atmospheric deposition to the acidification of Dutch forest soils is discussed in the Sections 2.1 and 2.2. Section 2.1 gives theoretical background information about causes of soil acidification by describing relationships with element cycling. This is a prerequisite to properly estimate the importance of various proton sources. In Section 2.2 such estimates are given using original research data on natural soil acidification and (interpreted) literature data on man-induced soil acidification.

Present impacts of acid atmospheric deposition on the solution chemistry of Dutch forest soils, especially on the concentrations of  $\text{SO}_4$ ,  $\text{NO}_3$  and Al are described in Section 2.3. The role of  $\text{SO}_4$  adsorption, N immobilization and mobilization of Al and base cations in buffering acid inputs is also dealt with in this section on the basis of input-output budgets for these elements.

Rates and mechanisms of geochemical acid neutralization processes are discussed more specifically in Chapter 3. Section 3.1 describes the rates and mechanisms of cation and silica release in four representative horizons of acid sandy soils at pH 3.0. Section 3.2 deals with the influence of pH and Al concentration on release rates of cations and Si in the same four soil horizons. The influence of soil horizon and soil type on rates of cation and Si release is discussed in Section 3.3.

Average critical loads of N and S derived for on forests, heathlands, ground water and surface water in the Netherlands are given in Chapter 4. Section 4.1 deals with critical N loads, whereas Section 4.2 deals with critical loads of acidity (S and N) and their use in acidification abatement policy.

The regional variability in critical loads for forests, and the degree by which they are currently exceeded, is dealt with in Chapter 5. In Section 5.1 and 5.2 results for European and Dutch forests are reported, based on calculations with the START and MACAL model, respectively. Both sections also deal extensively with uncertainties in the results caused by uncertainties and variability in critical values of chemical criteria (e.g. Al/Ca ratio), model structure and input data.

The long-term soil response to present atmospheric deposition levels and deposition changes is described in Chapter 6. Section 6.1 describes the SMART model and its simulation of the long-term soil response in various buffer ranges going from an initially calcareous soil (carbonate buffer range) to a strongly acidified soil (aluminium buffer range). In Section 6.2 the RESAM model is described and its simulation of the long-term response of a representative acid forest soil in the Netherlands to deposition changes. Section 6.3 deals with the long-term impacts of present acid inputs on calcareous and non-calcareous dune soils in the Netherlands. Again, RESAM was used to perform such an analysis.

The regional variability in long-term responses of forest soils to deposition scenarios is dealt with in Chapter 7. In Section 7.1 and 7.2 results for European and Dutch forest soils are reported, based on calculations with the SMART and RESAM model, respectively. Uncertainties in future predictions, induced by model descriptions and uncertainties/variability in input data (especially initial conditions), are also discussed in these sections. A general discussion, including overall conclusions based on the research described in this thesis, is given in Chapter 8.

# Chapter 2

## CAUSES, RATES AND EFFECTS OF SOIL ACIDIFICATION

### 2.1 RELATION BETWEEN SOIL ACIDIFICATION AND ELEMENT CYCLING

- INTRODUCTION
- CONCEPTS OF SOIL ACIDIFICATION
- PROCESSES AFFECTING THE HYDROGEN-ION CYCLE
- THE CARBON CYCLE
- THE NITROGEN CYCLE
- THE SULPHUR CYCLE
- THE CATION CYCLE
- DISCUSSION AND CONCLUSIONS

### 2.2 RELATIVE IMPORTANCE OF NATURAL AND MAN-INDUCED ACIDIFICATION OF SOILS IN THE NETHERLANDS

- INTRODUCTION
- CAUSES OF NATURAL SOIL ACIDIFICATION
- QUANTIFICATION OF NATURAL SOIL ACIDIFICATION
- QUANTIFICATION OF MAN-INDUCED SOIL ACIDIFICATION
- DISCUSSION AND CONCLUSIONS

### 2.3 IMPACTS OF ACID DEPOSITION ON CONCENTRATIONS AND FLUXES OF SOLUTES IN ACID SANDY FOREST SOILS IN THE NETHERLANDS

- INTRODUCTION
- MATERIALS AND METHODS
- SOIL SOLUTION CHEMISTRY
- INPUT-OUTPUT BUDGETS
- DISCUSSION AND CONCLUSIONS



Section 2.1 is a slightly revised version of:

W. de Vries and A. Breeuwsma, 1987. *The relation between soil acidification and element cycling*. Water Air and Soil Pollution 35: 293-310.

Section 2.2 is a moderately revised version of:

W. de Vries and A. Breeuwsma, 1986. *Relative importance of natural and anthropogenic sources in soils in the Netherlands*. Water Air and Soil Pollution 28: 173-184.

Section 2.3 has been submitted to Geoderma as:

W. de Vries, J.J.M. van Grinsven, N. van Breemen, E.E.J.M. Leeters and P.C. Jansen. *Impact of acid atmospheric deposition on concentrations and fluxes of solutes in acid sandy forest soils in the Netherlands*.

## 2.1 RELATION BETWEEN SOIL ACIDIFICATION AND ELEMENT CYCLING

### ABSTRACT

*Controversy about the contribution of acid deposition to soil acidification partly arises from different concepts of soil acidification. Differentiating between actual and potential soil acidification is shown to be appropriate for properly identifying and quantifying the natural and anthropogenic sources of protons. Actual soil acidification is primarily manifested by leaching of cations from the soil, regulated by the mobility of major anions. Leaching of  $\text{HCO}_3^-$  and  $\text{RCOO}^-$  occurs naturally whereas leaching of  $\text{NO}_3^-$  and  $\text{SO}_4^{2-}$  is mainly caused by acid deposition. Potential soil acidification is primarily due to accumulation of atmospherically derived N and S. This potential acid threat is partly realized by mineralization processes after the removal of vegetation.*

### INTRODUCTION

In recent decades, concern has grown about the potential impact of acid deposition on land and water. The relative importance of acid deposition in soil acidification has, however, been a matter of controversy in literature. Some authors believe that the contribution of acid deposition to soil acidification in Western Europe and America is minimal compared with natural causes and land use (Rosinqvist et al., 1980; Iserman, 1983; Krug and Frink, 1983), whereas others state the opposite (Ulrich and Matzner, 1983; Driscoll and Likens, 1982; Van Breemen et al., 1983; 1984). This dissension is partly due to different concepts of soil acidification. This is, amongst others, shown by the discussion between Krug (1985) and Van Breemen et al. (1985) on the relevance of hydrogen-ion budgets. According to Krug, H budgets, as presented by Van Breemen et al. (1983, 1984), should not be used to estimate soil acidification rates, since these budgets only account for net H transformations, thus excluding the acidification induced by the accumulation of acid organic matter. This controversy shows that an unambiguous concept of soil acidification is a prerequisite in assessing the contribution of natural and man-induced proton sources to soil acidification. Another reason for the dissension is that several authors (e.g. Iserman, 1983) only considered parts of the H transfer processes in the soil.

In this section an overview is given of the relation between various H transfer processes and the cycles of major elements, i.e. C, N, S and cations. A comprehensive analyses of all major H transfer processes has also been given by Van Breemen et al. (1983), who showed that such an approach allows to identify and quantify internal and external (acid deposition-induced) proton sources. In this section, this approach is extended by subdividing internal acid production in natural and land use-induced acid production. Furthermore, the concept of soil acidification introduced by Van Breemen et al. (1983, 1984) is redefined by distinguishing actual and potential soil acidification.

## CONCEPTS OF SOIL ACIDIFICATION

The pH is generally used to indicate the acidity of the soil and it governs many ecologically important reactions. However, production of protons in the soil is only partially reflected in changes of the pH. For this reason, Van Breemen et al. (1983, 1984) defined soil acidification in terms of a capacity factor rather than an intensity factor, such as the pH. Analogous to aqueous systems, they defined soil acidification as a decreased in the acid-neutralizing capacity (ANC) of the inorganic fraction of the soil including the solution phase. ANC is defined as the sum of the basic components minus the strongly acidic components:

$$ANC_m = B_m - A_m \quad (2.1)$$

where B is basic components (the cations that contribute depend on the reference pH chosen), A is strongly acidic components (anions of strong acids) and *m* is mineral soil.

According to this definition, soil acidification or ANC decrease is thus only associated with the net removal of cations and the net accumulation of anions in the mineral soil. The organic phase was not included to simplify calculations. This leads to the statement that the transfer of cations from the mineral soil to organic matter should be considered soil acidification (Van Breemen et al., 1985). However, this is rather artificial. Organic matter is an integral part of the soil and exchangeable cations on carboxyl groups also contribute to the ANC. Furthermore, accumulation of N and S in organic matter is an increase in strongly acidic components thus decreasing the ANC. This potential source of acidification can be accounted for in the same way as the accumulation of S in the inorganic phase. Both phenomena spread the impact of acidic deposition in time. Immobilization of atmospheric N and S may lead to large proton loads after clear felling of forests by mineralization and nitrification processes (Likens et al., 1969; Vitousek et al., 1979). Precipitation or adsorption of SO<sub>4</sub> may induce H production after reduction of SO<sub>2</sub> deposition by dissolution or desorption processes (Prenzel, 1983). Consequently, soil acidification can better be defined in terms of a decrease in ANC of the total solid (mineral and organic) and solution phase of the soil.

In order to separate actual and potential acidification it is useful to differentiate between the acid-neutralizing capacity (ANC) and the base-neutralizing capacity (BNC) by defining ANC as the sum of the basic components and BNC as the sum of the acidic components of the soil:

$$ANC_s = B_m - B_o \quad (2.2)$$

$$BNC_s = A_m - A_o \quad (2.3)$$

where A is strongly and weakly acidic components, s is solid and solution phase (total soil) and o is organic phase. At present, BNC is simply used as the opposite of ANC (Krug, 1985; Van Breemen et al., 1985). Actual soil acidification is now defined as a decrease in  $ANC_s$  (the ANC of the total soil) and potential soil acidification as an increase in  $BNC_s$ . Thus, actual acidification is reflected by cation removal and potential acidification by anion retention.

Contrary to Van Breemen et al. (1983, 1984), the weakly acidic organic acids are also included in the definition of  $BNC_s$ . The exclusion of these components was criticized by Krug (1985). Although Krug and Frink (1983) did not define soil acidification, their approach suggests that it is mainly related to an increase in exchange acidity caused by the accumulation of acid organic matter. This increases the BNC of the soil, and should thus be considered potential soil acidification. This potential load will partly be realized by dissociation of H when the pH of acid forest soils is raised by liming. However, under ambient conditions this increase in BNC is irrelevant to the actual soil acidification, as indicated by Van Breemen et al. (1985).

#### PROCESSES AFFECTING THE HYDROGEN-ION CYCLE

The hydrogen-ion cycle is the most complex of all element cycles, being affected by virtually every biochemical reaction (Sollins et al., 1980; Driscoll and Likens, 1982; Van Breemen et al., 1983). Attempts to discuss H producing and H consuming processes in soil frequently become bogged down in details about isolated biochemical processes, such as bioproduction and dissociation of  $CO_2$  or nitrification, which contribute little to the understanding of soil acidification in an ecosystem. Furthermore, these processes are often considered to be the main cause of natural soil acidification (Bache, 1980; Holowaychuk and Lindsay, 1982; Isermann, 1983), thus concealing the ultimate driving force for this phenomenon.

As a general rule, it can be stated that soil acidification is caused by the uncoupling of element cycles in an ecosystem (Ulrich, 1981b, 1983a; Matzner and Ulrich, 1983). Consequently, it is vitally important to synthesize information about all relevant processes in element cycling in relation to hydrogen-ion cycling. The most important processes are given in Table 2.1. This table is modified after Van Breemen et al. (1983), who gave a comprehensive survey of the different H transfer processes in an ecosystem and their relation to soil acidification. In this context, the terms H source and H sink relate respectively to acid production and acid consumption in the soil solution.

Complete budgets of the total elemental turnover in each compartment of the soil-plant system account for all these H transfer process (Driscoll and Likens, 1982; Ulrich and Matzner, 1983; Van Breemen et al., 1983, 1984) and give insight in actual and potential soil acidification rates. Incomplete budgets, for example by ignoring processes such as

Table 2.1 *The relation between H producing and H consuming processes in the soil (modified after Van Breemen et al., 1983)*

H sources	H sinks
uptake of cations	uptake of anions
mineralization of anions	mineralization of cations
oxidation reactions	reduction reactions
dissociation of weak acids (CO <sub>2</sub> , organic acids)	association of weak acids (CO <sub>2</sub> , organic acids)
-----	-----
weathering, desorption of anions	weathering, desorption of cations
precipitation, adsorption of cations	precipitation, adsorption of anions

N turnover (Sollins et al., 1980), fluxes of anions (Likens et al., 1979) or plant uptake (Johnson et al., 1983), may lead to erroneous conclusions with respect to the rates and causes of soil acidification.

To identify and quantify natural and anthropogenic causes of soil acidification, it is appropriate to examine the cycles of major elements in more detail as shown by Reuss (1977), who gave a brief description of the most important acidity relationships in the N and S cycle. Below the cycles relating to the major anions in soil (HCO<sub>3</sub>, RCOO, NO<sub>3</sub> and SO<sub>4</sub>) will first be reviewed, i.e. the C, N and S cycles. Next, a review of the cation cycle will be given without differentiating between cations.

## THE CARBON CYCLE

The main processes within the C cycle are shown in Figure 2.1. The reaction equations of the H transfer (and H indifferent) processes are summarized in Table 2.2, together with those of the N, S and cation cycles. Formation of carbohydrates through photosynthesis (pathway 1; reaction 1A) followed by mineralization of photosynthetically formed organic matter (pathway 2a, b; reaction 1B) or by root respiration (pathway 3) are the transport mechanisms of CO<sub>2</sub> from the atmosphere to the gas phase of the soil. Some of the CO<sub>2</sub> gas returns to the atmosphere via diffusion (pathway 4). Part of the CO<sub>2</sub> remaining in the soil may dissociate in water, leading to acid production (pathway 5a, reaction 2A).

Dissociation of CO<sub>2</sub> is a very dominating proton source in calcareous soils of high pH. In non-calcareous soils with pH above 5, CO<sub>2</sub> is still an important proton source. Leaching studies in non-calcareous soils of unpolluted regions indicate that carbonic acid dominates the leaching process in temperate and tropical coniferous sites (Reuss, 1977; Johnson et al., 1977; Johnson and Cole, 1980; Cronan et al., 1978). However, in acidic soils with a pH less than 5, the acidifying effect of CO<sub>2</sub> is negligible. This can be deduced from the pK value of reaction 2B (pK = 7.81) and CO<sub>2</sub> pressures of 5-20 mbar, which are commonly occurring values in well-drained soils. Consequently, it is misleading to compare the effect

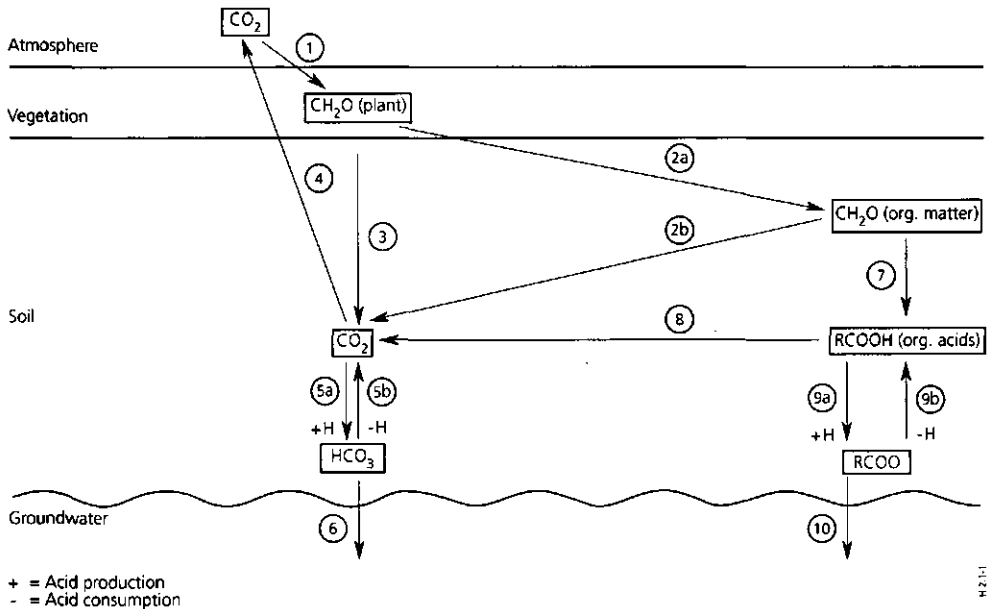


Figure 2.1 Schematic presentation of the C cycle

- |    |                                 |    |                               |
|----|---------------------------------|----|-------------------------------|
| 1  | Photosynthesis                  | 6  | Leaching of $\text{HCO}_3^-$  |
| 2a | Accumulation of organic C       | 7  | Formation of organic acids    |
| 2b | Mineralization of organic C     | 8  | Oxidation of organic acids    |
| 3  | Respiration                     | 9a | Dissociation of organic acids |
| 4  | Diffusion of $\text{CO}_2$      | 9b | Protonation of organic anions |
| 5a | Dissociation of $\text{CO}_2$   | 10 | Leaching of organic anions    |
| 5b | Protonation of $\text{HCO}_3^-$ |    |                               |

of  $\text{CO}_2$  with acid deposition without making a distinction between non-acidic and acidic soils, as done by Krug and Frink (1983).

In a natural (not anthropogenically influenced) ecosystem, further acidification results from organic acids that are intermediate by-products of the decomposition of organic matter to  $\text{CO}_2$ . Especially, under unfavourable conditions such as cold, wet climates and low nutrient status, both mineralization and humification of low-molecular organic acids are inhibited (Van Breemen and Brinkman, 1976). In such situations, organic acids play an important role in soil acidification, because they can deprotonate even at low pH values (pathway 9a, reaction 5A). Leaching studies in arctic and (sub)alpine forest soils of unpolluted regions reveal that organic anions are dominant in soil-solution chemistry (Johnson et al., 1977; Ugolini et al., 1977; Cronan et al., 1978).

Table 2.2 Reactions equations of H transfer processes in the C, N, S and cation cycles

Process from left to right	Reaction equation		Process from right to left
<b>THE CARBON CYCLE</b>			
(1A) Photosynthesis	$\text{CO}_2 + \text{H}_2\text{O}$	$\rightleftharpoons \text{CH}_2\text{O} + \text{O}_2$	Respiration (1B)
(2A) Dissociation of $\text{CO}_2$	$\text{CO}_2 + \text{H}_2\text{O}$	$\rightleftharpoons \text{HCO}_3^- + \text{H}^+$	Protonation of $\text{HCO}_3^-$ (2B)
(3) Formation of formic acid	$2\text{CH}_2\text{O} + \text{O}_2$	$\rightarrow 2\text{HCOO}^- + 2\text{H}^+$	
(4) Oxidation of formic acid	$2\text{HCOO}^- + \text{O}_2 + 2\text{H}^+$	$\rightarrow 2\text{CO}_2 + 2\text{H}_2\text{O}$	
(5A) Dissociation of organic acids	$\text{RCOOH}$	$\rightleftharpoons \text{RCOO}^- + \text{H}^+$	Protonation of organic anions (5B)
(6A) Formation of an aluminium-organic complex	$3\text{RCOOH} + \text{Al}(\text{OH})_3$	$\rightleftharpoons (\text{RCOO})_3\text{Al} + 3\text{H}_2\text{O}$	Hydrolysis of an aluminium-organic complex (6B)
<b>THE NITROGEN CYCLE</b>			
(7) Fixation of $\text{N}_2$	$4\text{ROH} + 2\text{N}_2 + 3\text{CH}_2\text{O}$	$\rightarrow 4\text{RNH}_2 + 3\text{CO}_2 + \text{H}_2\text{O}$	
(8A) Ammonification	$\text{RNH}_2 + \text{H}_2\text{O} + \text{H}^+$	$\rightleftharpoons \text{ROH} + \text{NH}_4^+$	Uptake of $\text{NH}_4^+$ (8B)
(9A) Volatilization of $\text{NH}_3$	$\text{NH}_4^+$	$\rightleftharpoons \text{NH}_3 + \text{H}^+$	Formation of $\text{NH}_4^+$ (9B)
(10) Nitrification	$\text{NH}_4^+ + 2\text{O}_2$	$\rightarrow \text{NO}_3^- + 2\text{H}^+ + \text{H}_2\text{O}$	
(11) Uptake to $\text{NO}_3^-$	$\text{ROH} + \text{NO}_3^- + \text{H}^+ + 2\text{CH}_2\text{O}$	$\rightarrow \text{RNH}_2 + 2\text{CO}_2 + 2\text{H}_2\text{O}$	
(12) Denitrification	$5\text{CH}_2\text{O} + 4\text{NO}_3^- + 4\text{H}^+$	$\rightarrow 2\text{N}_2 + 5\text{CO}_2 + 7\text{H}_2\text{O}$	
(13) Chemodenitrification	$\text{CH}_2\text{O} + 4\text{NO}_3^- + 4\text{H}^+$	$\rightarrow 4\text{NO}_2 + \text{CO}_2 + 3\text{H}_2\text{O}$	
(14) Absorption of $\text{NH}_3$	$\text{ROH} + \text{NH}_3$	$\rightarrow \text{RNH}_2 + \text{H}_2\text{O}$	
(15) Absorption of $\text{NO}_2$	$4\text{ROH} + 4\text{NO}_2 + 7\text{CH}_2\text{O}$	$\rightarrow 4\text{RNH}_2 + 7\text{CO}_2 + 5\text{H}_2\text{O}$	
(16) Oxidation of $\text{NO}_2$	$4\text{NO}_2 + \text{O}_2 + 2\text{H}_2\text{O}$	$\rightarrow 4\text{NO}_3^- + 4\text{H}^+$	
<b>THE SULPHUR CYCLE</b>			
(17) Uptake of $\text{SO}_4$	$\text{ROH} + \text{SO}_4^{2-} + 2\text{H}^+ + 2\text{CH}_2\text{O}$	$\rightarrow \text{RSH} + 2\text{CO}_2 + 3\text{H}_2\text{O}$	
(18) Mineralization of organic S	$\text{RSH} + \text{H}_2\text{O} + 2\text{O}_2$	$\rightarrow \text{ROH} + \text{SO}_4^{2-} + 2\text{H}^+$	
(19) Reduction of $\text{SO}_4$	$\text{SO}_4^{2-} + 2\text{H}^+ + 2\text{CH}_2\text{O}$	$\rightarrow \text{H}_2\text{S} + 2\text{CO}_2 + 2\text{H}_2\text{O}$	
(20) Oxidation of $\text{H}_2\text{S}$ to $\text{SO}_4$	$\text{H}_2\text{S} + 2\text{O}_2$	$\rightarrow \text{SO}_4^{2-} + 2\text{H}^+$	
(21) Reduction of $\text{Fe}_2\text{O}_3$ and $\text{SO}_4$	$2\text{Fe}_2\text{O}_3 + 8\text{SO}_4^{2-} + 16\text{H}^+ + 15\text{CH}_2\text{O}$	$\rightarrow 4\text{FeS}_2 + 15\text{CO}_2 + 23\text{H}_2\text{O}$	
(22) Oxidation of $\text{FeS}_2$	$4\text{FeS}_2 + 15\text{O}_2 + 8\text{H}_2\text{O}$	$\rightarrow 2\text{Fe}_2\text{O}_3 + 8\text{SO}_4^{2-} + 16\text{H}^+$	
(23) Absorption of $\text{H}_2\text{S}$	$\text{H}_2\text{S} + \text{ROH}$	$\rightarrow \text{RSH} + \text{H}_2\text{O}$	
(24) Oxidation of $\text{H}_2\text{S}$ to $\text{SO}_2$	$2\text{H}_2\text{S} + 3\text{O}_2$	$\rightarrow 2\text{SO}_2 + 2\text{H}_2\text{O}$	
(25) Absorption of $\text{SO}_2$	$2\text{SO}_2 + 2\text{ROH} + 3\text{CH}_2\text{O}$	$\rightarrow 2\text{RSH} + 3\text{CO}_2 + 3\text{H}_2\text{O}$	
(26) Oxidation of $\text{SO}_2$	$2\text{SO}_2 + \text{O}_2 + 2\text{H}_2\text{O}$	$\rightarrow 2\text{SO}_4^{2-} + 4\text{H}^+$	
(27A) Adsorption of $\text{SO}_4$	$(\text{OH})_2\text{ex} + \text{SO}_4^{2-} + 2\text{H}^+$	$\rightleftharpoons \text{SO}_4^{2-}\text{ex} + 2\text{H}_2\text{O}$	Desorption of $\text{SO}_4$ (27B)
(28A) Precipitation of $\text{SO}_4$	$\text{Al}(\text{OH})_3 + \text{SO}_4^{2-} + 2\text{H}^+$	$\rightleftharpoons \text{AlOHSO}_4 + 2\text{H}_2\text{O}$	Dissolution of $\text{SO}_4$ (28B)
<b>THE CATION CYCLE</b>			
(29A) Uptake of M	$\text{RCOOH} + \text{M}^+$	$\rightleftharpoons \text{RCOOM} + \text{H}^+$	Mineralization of M (29B)
(30A) Precipitation of M	$2\text{M}^+ + \text{H}_2\text{O}$	$\rightleftharpoons \text{M}_2\text{O} + 2\text{H}^+$	Weathering (30B)
(31A) Adsorption of M	$\text{M}^+ + \text{Hex}$	$\rightleftharpoons \text{M}^+\text{ex} + \text{H}^+$	Desorption of M (31B)
(32) Weathering and uptake of M	$2\text{RCOOH} + \text{M}_2\text{O}$	$\rightarrow 2\text{RCOOM} + \text{H}_2\text{O}$	
(33) Reduction of $\text{Fe}_2\text{O}_3$	$2\text{Fe}_2\text{O}_3 + \text{CH}_2\text{O} + 8\text{H}^+$	$\rightarrow 4\text{Fe}^{2+} + \text{CO}_2 + 5\text{H}_2\text{O}$	
(34) Oxidation of Fe	$4\text{Fe}^{2+} + \text{O}_2 + 4\text{H}_2\text{O}$	$\rightarrow 2\text{Fe}_2\text{O}_3 + 8\text{H}^+$	

The acid production resulting from dissociation of organic acids is mainly neutralized by weathering (and desorption) of cations (especially Al and Fe), which may form a complex with the organic anions (reaction 6A). Transport of Al and Fe as metal-organic complexes is generally accepted as an important transport mechanism of these elements in well-drained acid soils (Schnitzer and Skinner, 1963; Mokma and Buurman, 1982). Other mechanisms that may be responsible for the transport of Al, are transport in ionic form (Van Schuylenborgh and Bruggenwert, 1965) and transport as an inorganic alumino-silicate complex (Farmer et al., 1980; Childs et al., 1983). Leaching of Al and Fe rarely proceeds beyond 50-100 cm in well-drained soils. This process, called podzolization, leads to a characteristic bleached eluviation (albic) horizon and a dark brown illuviation (spodic) horizon. As mentioned before, this transfer of cations from the soil mineral phase to the soil organic phase can not be considered soil acidification in itself. However, the leaching of Al and Fe leads to acidification (ANC decrease) in the eluviation horizon and alkalization in the illuviation horizon. Net acidification over the complete soil profile occurs when the metal-organic complexes are leached to the ground water.

The actual acid production rate from dissociation of weak (carbonic and organic) acids can be quantified from the leaching for the relevant acid producing anions ( $\text{HCO}_3^-$  and/or  $\text{RCOO}^-$ ) on an annual basis:

$$\text{H production} = (\text{HCO}_3^- + \text{RCOO}^-)_{le} \quad (2.4)$$

where the subscript *le* stands for leaching (from the rootzone). The input of  $\text{HCO}_3^-$  and  $\text{RCOO}^-$  can be considered negligible. The output (leaching) of these anions can be quantified by measuring their concentration and the flux of soil water. Decalcification and/or podzolization rates can also be calculated by comparing the amount of weatherable cations (ANC) in the topsoil with the amount in the presumed parent material and estimating the time since the process started (historical approach). Values thus obtained for calcareous and podzolic soils in The Netherlands are in the same range as those obtained by input-output balances of  $\text{HCO}_3^-$  and  $\text{RCOO}^-$  (Section 2.2; De Vries and Breeuwsma, 1986).

The potential acid production by weak acids can be quantified by measuring the exchange acidity by titration. However, this does not give any information on actual H production resulting from dissociation. Consequently, it is wrong to assess the impact of acidic deposition compared to natural soil-forming processes by comparing the amount of H in deposition with the exchange acidity, as done by Krug and Frink (1983). Moreover, the amount of H in deposition is only a small proportion of the total acid load (in the Netherlands ca. 5% because of the extremely large input of  $\text{NH}_4^+$ ; Van Breemen et al., 1982).

Air pollution may have several effects on the C cycle and thus on H production. First of all, an increased acidification, due to deposition and oxidation of  $\text{SO}_x$ ,  $\text{NO}_x$  and  $\text{NH}_x$  may



decrease C mineralization (Tamm et al., 1980; Popovic, 1984) and through that the natural rate of acidification, although significant effects have not always been found (Roberts et al., 1980). Furthermore, acid deposition induced H production may decrease the dissociation of weak acids in non-calcareous soils and thereby reduce the leaching of organic ions (Krug and Frink, 1983). However, their hypothesis that protonation of organic anions in the soil solution (pathway 9b, reaction 5B) is an important buffering mechanism in acid soils is rather doubtful. First, the quantitative importance of this buffering process cannot be great, since the concentration of organic anions in the soil solution is low (Johnson et al., 1977; Ugolini et al., 1977; Cronan et al., 1978). Furthermore, the agreement of values on decalcification and podzolization rates based on an actual approach (Van Breemen et al., 1984) and a historical approach (Section 2.2; De Vries and Breeuwsma, 1986) indicate that the influence of anthropogenic activities on natural H production is small.

## THE NITROGEN CYCLE

N transformation processes, which are extremely important in regulating the hydrogen-ion cycle, can easily be mis-interpreted. Therefore, attention is focused on the net effect of N cycling on H transfer processes. The main biochemical processes in the N cycle are illustrated in Figure 2.2. Natural processes (pathways 1-8) are distinguished from processes mainly caused by acid deposition (pathways 9-20). The distinction is somewhat artificial, because all processes do occur naturally and nearly all are influenced by acid deposition. However, deposition of  $\text{NH}_3$ ,  $\text{NH}_x$  and reaction products ( $\text{NH}_4$ ,  $\text{NO}_3$ ) (pathways 9-20) is nearly negligible in unpolluted regions and as such the distinction is useful.

An important conclusion that can be drawn from Figure 2.2 is that N accumulation in biomass (organic matter, vegetation) is not accompanied by a net production or consumption of H. The principal reason for this is that N is not originally present in the soil but stems from volatile N compounds (in unpolluted regions mainly  $\text{N}_2$ ). Neither the transformation of "atmospheric" N to organic N in vegetation by fixation of  $\text{N}_2$  (pathway 1, reaction 7) nor the internal N transformation from soil organic matter to vegetation leads to a net H transfer. Mineralization of organic N to  $\text{NH}_4$  (pathway 2b, reaction 8A) results in H consumption whereas  $\text{NH}_4$  uptake (pathway 3, reaction 8B) leads to H release and the net balance is zero. If  $\text{NH}_4$  is nitrified (pathway 4, reaction 9) two H ions are produced leaving a net H balance of +1 but after  $\text{NO}_3$  uptake (pathway 6, reaction 10) the net balance is zero again. Statements that the H budget is affected by the form in which N is taken up (Ulrich et al., 1979) are therefore wrong. The same is true for calculations of the H production resulting from biomass accumulation that are based on a certain  $\text{NH}_4/\text{NO}_3$  ratio (Ulrich et al., 1979; Nilsson et al., 1982).

Research on element cycling shows that N cycling does not generally contribute to the overall H production in forest ecosystems in relatively unpolluted areas (release is balanced by uptake: closed cycle) (Johnson et al., 1977; Ugolini, et al., 1977; Cronan et al., 1978;

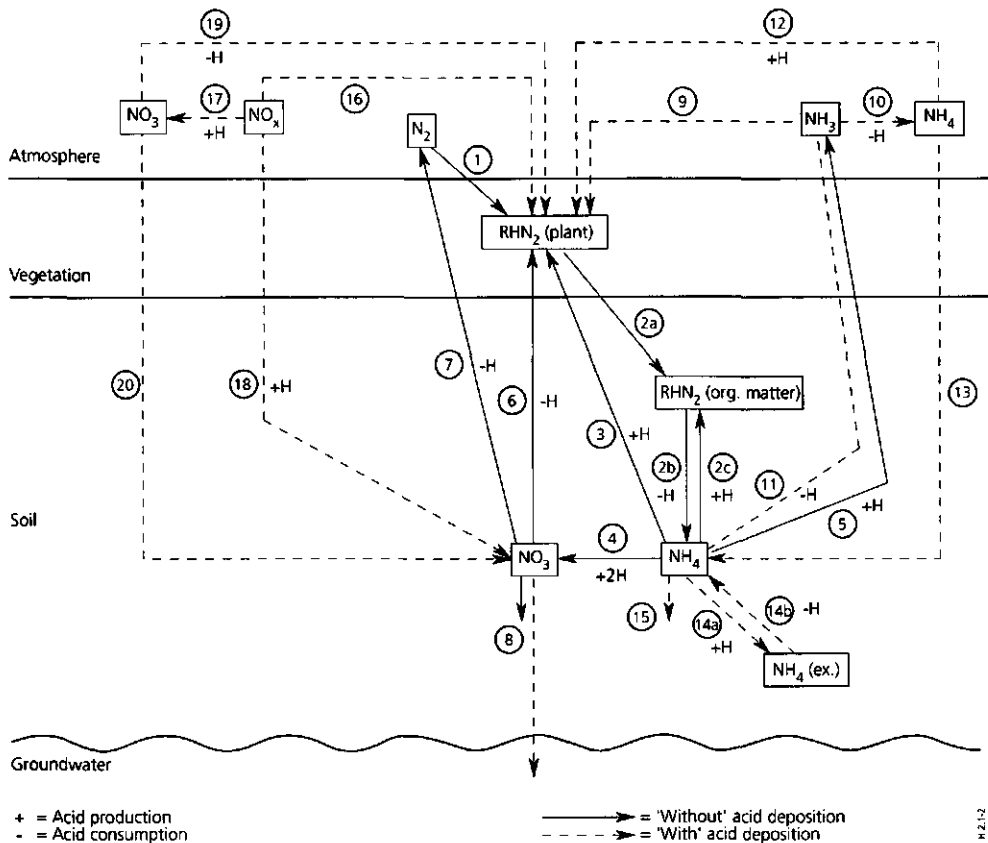


Figure 2.2 Schematic presentation of the N cycle

- |                                     |  |
|-------------------------------------|--|
| 1 N <sub>2</sub> fixation           | 11 Deposition and protonation of NH <sub>3</sub> |
| 2a Accumulation of organic N        | 12 Absorption of NH <sub>4</sub>                 |
| 2b Mineralization of organic N      | 13 Deposition of NH <sub>4</sub>                 |
| 2c N immobilization                 | 14a Adsorption of NH <sub>4</sub>                |
| 3 Uptake of NH <sub>4</sub>         | 14b Desorption of NH <sub>4</sub>                |
| 4 Nitrification                     | 15 Leaching of NH <sub>4</sub>                   |
| 5 Volatilization of NH <sub>3</sub> | 16 Absorption of NO <sub>x</sub>                 |
| 6 Uptake of NO <sub>3</sub>         | 17 Oxidation of NO <sub>x</sub>                  |
| 7 Denitrification                   | 18 Deposition and oxidation of NO <sub>x</sub>   |
| 8 Leaching of NO <sub>3</sub>       | 19 Absorption of NO <sub>3</sub>                 |
| 9 Absorption of NH <sub>3</sub>     | 20 Desorption of NO <sub>3</sub>                 |
| 10 Protonation of NH <sub>3</sub>   |  |

Bormann et al., 1977). A notable exception has to be made for N fixing stands such as red alder, where the amount of NO<sub>3</sub> produced exceeds biological demand. In this case, the natural rate of acidification resulting from an imbalance in the N cycle can be as high as 4 kmol<sub>c</sub> ha<sup>-1</sup> yr<sup>-1</sup> (Johnson et al., 1983; Van Miegroet and Cole, 1984). Furthermore, it should be noted that even if the N cycle is closed, it may have profound local effects on the acidification of soil layers, because of spatial uncoupling of the ion cycle (Ulrich, 1983a).

When the natural cycling of N is disturbed by removal of vegetation, N reactions may become extremely important in the hydrogen-ion cycle (Likens et al., 1969; Vitousek et al., 1979). In this case, mineralization and nitrification of organic N to  $\text{NO}_3$  is not balanced by uptake of  $\text{NO}_3$ . Generally, it is assumed that nitrification is inhibited in acid forest soils (Campbell and Lees, 1967; Keeney, 1980). This is true in forest soils that have N deficiency (e.g. many young soils), where  $\text{NH}_4$  released during decomposition of organic matter is readily taken up. However, leaching studies in several acid forest soils with ample N supply indicate that  $\text{NH}_4$  may be nitrified even at low pH values (Likens et al., 1969; Johnson et al., 1979; Van Breemen et al., 1983, 1984). It has therefore been suggested that availability of  $\text{NH}_4$  is a major regulator for nitrification (Johnson et al., 1979; Johnson and Cole, 1980). Acidification by removal of vegetation is manifested by the leaching of  $\text{NO}_3$  (pathway 8) with accompanying cations. In forest soils this effect is usually not important because vegetation generally regrows rapidly and clearing is not frequent. However, mineralization of N is the major source for soil acidification if biomass is removed each year, as in agricultural soils. Acidification by mineralization may also occur after a change in moisture regime from wet to dry by lowering the water table. This effect may continue for a long time.

The N cycle can also be strongly influenced by man through (potentially) acid deposition. Deposition of  $\text{NH}_x$  has a profound effect on the N cycle in areas with intensive animal husbandry, whereas  $\text{NO}_x$  is an important pollutant in areas with heavy traffic. As stated before, there is no net H transfer as long as the N compounds from the atmosphere ( $\text{NH}_x$ ,  $\text{NO}_x$ ,  $\text{N}_2$ ) are taken up by the vegetation, irrespective of the pathway and the medium (air or soil). The only important thing to know is the form ( $\text{NH}_4$  or  $\text{NO}_3$ ) in which N enters and leaves the soil. The actual acid production rate resulting from N transformations can thus be quantified by balancing the input of  $\text{NH}_4$  (H source) and  $\text{NO}_3$  (H sink) versus the output on an annual basis (Van Breemen et al., 1983):

$$\text{H production} = (\text{NH}_{4,td} - \text{NH}_{4,fb}) - (\text{NO}_{3,td} - \text{NO}_{3,fb}) \quad (2.5)$$

where the subscript *td* stands for the total deposition above the forest canopy. Eq. (2.5) represents the H production resulting from removal of  $\text{NH}_4$  (by uptake, immobilization and/or nitrification or volatilization) and the H consumption resulting from removal of  $\text{NO}_3$  (by uptake, immobilization and/or denitrification). The input of the N compounds can best be estimated by measuring wet and dry deposition above the forest canopy. Although throughfall measurements give an indication of total (wet and dry) deposition of  $\text{NH}_3$  and  $\text{NO}_x$ , this is always inaccurate because of interaction of the compounds with the canopy. The immobilization of N in organic matter forms a potential source of acidification that can be estimated from the increase in organic N in the soil. It is also possible to measure total deposition by throughfall and to calculate accumulation of organic N by subtracting uptake and output. However, this is only reasonable if denitrification can be ignored.

## THE SULPHUR CYCLE

Numerous authors have studied S cycling in forest ecosystems (Shriner and Henderson, 1978; Sollins et al., 1980; Turner et al., 1980; Meiwes and Khanna, 1981; David et al., 1982). The major biochemical processes in the S cycle are illustrated in Figure 2.3. Similar to the N cycle, a distinction is made between naturally occurring processes (pathways 1-7) and processes mainly induced by acid deposition (pathways 8-13).

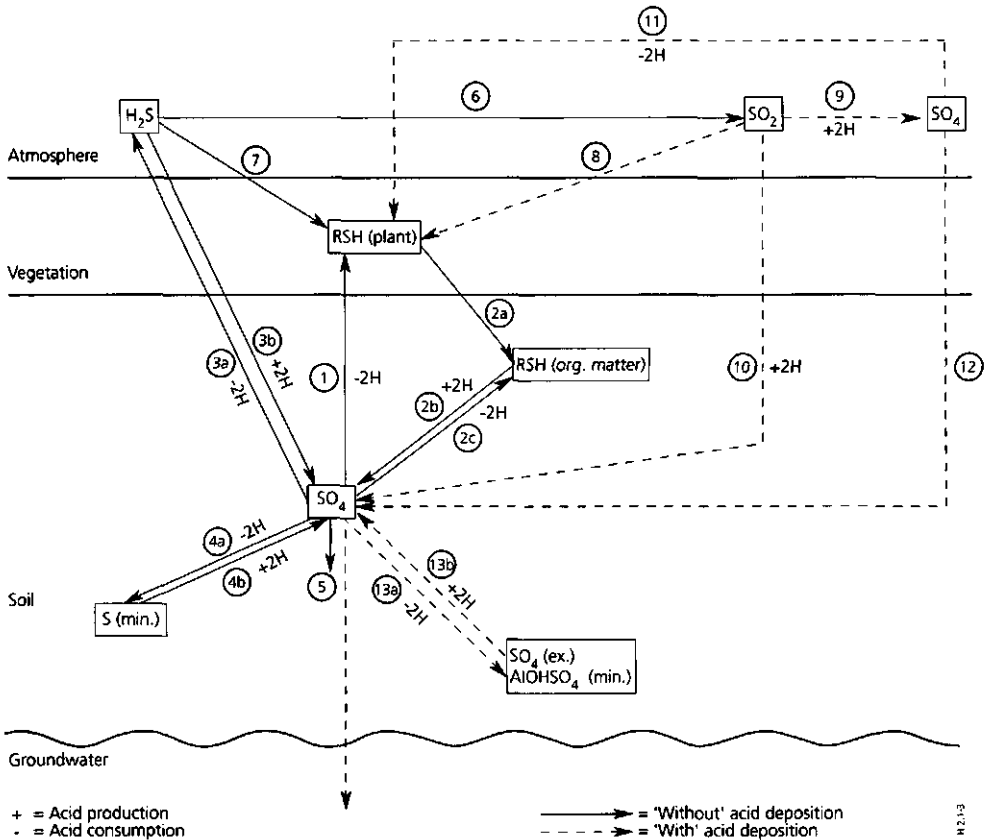


Figure 2.3 Schematic presentation of the S cycle

- |   |  |
|---|--|
| 1 Uptake of $SO_4$                        | 6 Oxidation of $H_2S$ to $SO_2$          |
| 2a Accumulation of organic S              | 7 Absorption of $H_2S$                   |
| 2b Mineralization of organic S            | 8 Absorption of $SO_2$                   |
| 2c Incorporation of $SO_4$ in organic S   | 9 Oxidation of $SO_2$                    |
| 3a Reduction of $SO_4$ to $H_2S$          | 10 Deposition and oxidation of $SO_2$    |
| 3b Oxidation of $H_2S$ to $SO_2$          | 11 Absorption of $SO_4$                  |
| 4a Reduction of $SO_4$ to $FeS$ , $FeS_2$ | 12 Deposition of $SO_4$                  |
| 4b Oxidation of $FeS$ , $FeS_2$ to $SO_4$ | 13a Adsorption (precipitation) of $SO_4$ |
| 5 Leaching of $SO_4$                      | 13b Desorption (dissolution) of $SO_4$   |

As with N, research on element cycling in relatively unpolluted areas shows that S cycling hardly contributes to the H production in a forest ecosystem (Johnson et al., 1977; Ugolini et al., 1977; Cronan et al., 1978). In these areas, the S cycle is generally closed and thus the release of  $\text{SO}_4$  by mineralization and oxidation (pathway 2b, reaction 18) resulting in proton production is balanced by  $\text{SO}_4$  uptake (pathway 1, reaction 17). A notable exception are tidal flats or seabottom sediments where conveyance of  $\text{SO}_4$  by seawater and reduction to iron sulphides (pathway 4a, reaction 21) leads to a large accumulation of S, thus increasing the BNC. This potential acid load is realized after drainage by oxidation of FeS or  $\text{FeS}_2$  to  $\text{SO}_4$  (pathway 4b, reaction 22) leading to acid sulphate soils with an extremely low pH (Van Breemen, 1975). This is, however, only of regional importance.

Uncoupling of the S cycle leads to effects that are comparable to that of N, i.e. soil acidification by leaching of  $\text{SO}_4$  (pathway 5) with accompanying cations. Contrary to N, S is originally present in most soils. Therefore, incorporation of S in vegetation could be accompanied by removal of S from the soil. However, especially in areas with  $\text{SO}_2$  pollution, S in forest vegetation most likely stems from volatile S compounds in the atmosphere. The atmosphere always contains a certain amount of  $\text{SO}_2$ , but in industrialized countries this is relatively small compared to anthropogenically derived  $\text{SO}_2$ . Analogous to N, there is no net H transfer as long as  $\text{SO}_2$  is taken up by the vegetation, irrespective of the pathway and the medium. However, the uptake of S by vegetation is considerably lower than that of N. The acidifying effect of  $\text{SO}_2$ , therefore, is usually high compared with that of  $\text{NH}_3$  and  $\text{NO}_x$  (Van Breemen et al., 1983, 1984).

Another important difference between  $\text{SO}_4$  and  $\text{NO}_3$  is that, contrary to that of  $\text{NO}_3$ , the mobility of  $\text{SO}_4$  can be affected by soil adsorption or by precipitation (pathway 13a). Adsorption of  $\text{SO}_4$  on sesquioxides (reaction 27A), can be an important buffering mechanism in podzolic soils with a sesquioxide-rich B horizon (Johnson and Cole, 1977, 1980; Johnson et al., 1980; Singh, 1980; Singh et al., 1980; Abrahamson and Stuanes, 1980; Farrel et al., 1984). Precipitation of  $\text{SO}_4$  may occur as jurbanite ( $\text{AlOHSO}_4$ ) (reaction 28A) (Van Breemen et al., 1975; Nordstrom, 1982; Prenzel, 1983; Weaver et al., 1985) or other basic Al sulphates (Singh and Brydon, 1969; Adams and Rawajfih, 1977; Nilsson and Bergkvist, 1983).

The actual H production rate caused by S transformations can be quantified by balancing the input of  $\text{SO}_2$  versus the output on an annual basis:

$$\text{H production} = -(\text{SO}_{4,\text{td}} - \text{SO}_{4,\text{le}}) \quad (2.6)$$

$\text{SO}_4$  leaching equals  $\text{SO}_4$  deposition when this compound is not taken up, reduced or retained via immobilization, precipitation or adsorption. In the case of S retention, the BNC of the soil increases (potential acidification). This potential acidification rate can be obtained as described for N.

## THE CATION CYCLE

The relevant naturally occurring processes in the cation cycle (pathways 1-4), including anthropogenic influences (pathways 5-6), are illustrated in Figure 2.4. The cation cycle is strongly correlated with the cycles of C, N and S, since the mobilities of the anions  $\text{HCO}_3^-$ ,  $\text{RCOO}^-$ ,  $\text{NO}_3^-$  and  $\text{SO}_4^{2-}$  regulate the leaching of cations (Johnson and Cole, 1980). In terms of an H budget, mineralization (pathway 2b, reaction 29B), weathering (pathway 3b, reaction 30B) and desorption of cations (pathway 3b, reaction 31B) neutralizes the acid production induced by the production of anions in mineralization and oxidation processes. Removal of cations, decreasing  $\text{ANC}_s$ , thus reflects the acid production in the soil.

The cation cycle is not completely balanced, not even in a natural forest ecosystem, since cations are leached (pathway 4) with  $\text{HCO}_3^-$  and/or  $\text{RCOO}^-$  (natural acidification). Natural leaching of cations also occurs in periodically reduced soils such as ferrolyzed soils (reactions 33 and 34) (Brinkman, 1970). However, this process is of regional importance only. When the natural cycling of cations is disturbed by removal of vegetation, release of cations is temporarily unbalanced by uptake. This leads to a decrease in  $\text{ANC}_s$  equal to the

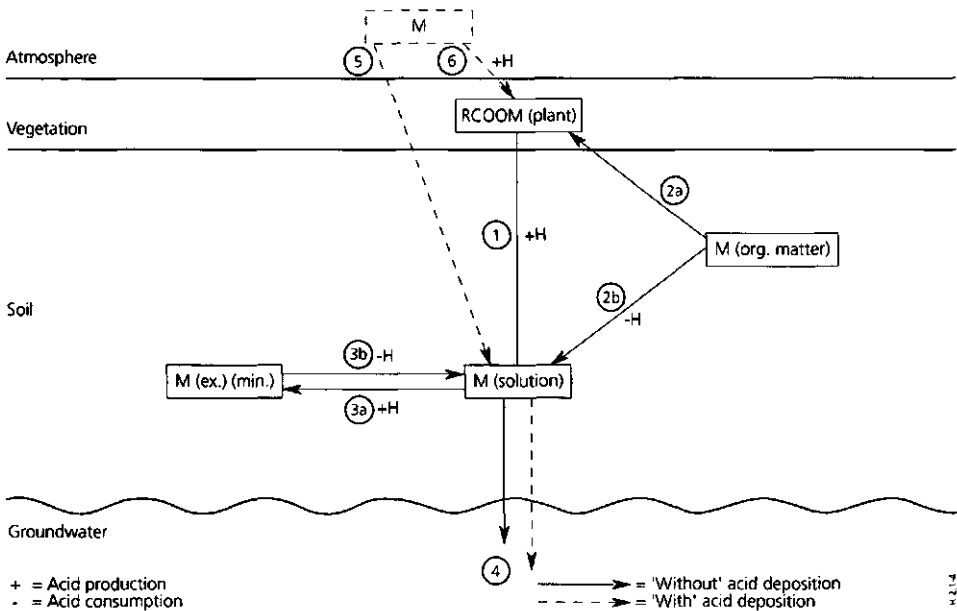


Figure 2.4 Schematic presentation of the cation cycle

- |  |                                  |
|--|----------------------------------|
| 1 Uptake of M                          | 3b Desorption (dissolution) of M |
| 2a Accumulation of M in organic matter | 4 Leaching of M                  |
| 2b Mineralization of M                 | 5 Deposition of M                |
| 3a Adsorption (precipitation) of M     | 6 Absorption of M                |

amount of mineralized cations. Furthermore, cations in vegetation are also removed permanently from the soil (no recycling), thus inducing a continuous decrease in  $ANC_s$ .

The acid consumption rate resulting from weathering and desorption of cations can be quantified by balancing the input of cations in deposition (pathways 5 and 6) against the output by leaching and correcting for net cation uptake (uptake minus litterfall) on an annual basis:

$$H \text{ consumption} = M_{le} - M_{ld} + M_{gu} \quad (2.7)$$

where the subscript *gu* stands for net uptake due to forest growth.

## DISCUSSION AND CONCLUSIONS

A synthesis of all major element cycles leads to the general conclusion that actual rates of natural and anthropogenic soil acidification can be identified by the anion that is leached from the soil profile. Conjugated bases of weak acids ( $HCO_3$ ,  $RCOO$ ) are an indication of natural soil acidification, whereas conjugated bases of strong acids ( $NO_3$ ,  $SO_4$ ) are indicative of anthropogenic soil acidification. More specifically, the following conclusions can be drawn about natural and man-induced soil acidification.

### *Natural soil acidification*

A net acid production in a natural ecosystem mostly results from dissociation of weak acids. The prerequisites for natural decalcification and podzolization are the presence of  $CO_2$  in the atmosphere and the precipitation surplus. The actual acidification rate, that is manifested by the leaching of  $HCO_3$  and/or  $RCOO$  with cations, can be quantified by measuring the output of these anions, since the input may be ignored. Additional proton sources may be present in soils with a N fixing vegetation and in special soils, such as acid sulphate soils and ferrolyzed soils. More information on natural soil acidification is given in Section 2.2 (De Vries and Breeuwsma, 1986).

### *Land use*

Removal of vegetation causes soil acidification because it implies removal of cations from the soil. In this context, the term cation stands for all cation nutrients except  $NH_4$ , because uptake of N does not contribute to soil acidification. As all anions mainly stem from the atmosphere, the acid production caused by removal of biomass can be quantified as:

$$H \text{ production} = M_{gu} \quad (2.8)$$

The acidification rate resulting from base cation removal can be estimated by measuring the growth rate and chemical composition of the vegetation. These values are indicative of

the long-term acidification induced by forestry, because production forests are always in the aggradation phase. Furthermore, removal of vegetation temporarily leads to proton production, since mineralization is not balanced by uptake. This proton production, which is the realization of a potential acid threat (increase in  $BNC_s$ ) caused by the immobilization of (atmospherically derived) N and S, can be quantified as:

$$H \text{ production} = (NO_3 + SO_4)_{mi} \quad (2.9)$$

where the subscript *mi* stands for mineralization. An indication of the actual acid production rate by mineralization can be obtained by an input-output balance for  $NO_3$  and  $SO_4$  in the organic toplayer and surface horizon, but it is difficult to distinguish between the influence of mineralization and that of acid deposition. In agricultural soils this effect is extremely important because the crops are harvested each year (cf Section 2.2; De Vries and Brèeuwsma, 1986).

#### *Acid deposition*

Atmospheric deposition of potential acid substances such as  $SO_x$ ,  $NO_y$  and  $NH_x$  (acid deposition) leads to soil acidification when the oxidation of these compounds to nitric and sulphuric acid is not balanced by reduction and/or incorporation of S and N in vegetation. The potential acidification is manifested by the accumulation of organic N and S as stated before. The actual acidification manifests itself mainly as a leaching of  $NO_3$  and  $SO_4$  with accompanying cations (in acid soils mainly Al; Cronan and Schofield, 1979; Johnson et al., 1981; David and Driscoll, 1984; Driscoll et al., 1985). An indication of the actual acid production rate caused by acid deposition can be obtained from an input-output balance of H,  $NH_4$ ,  $NO_3$  and  $SO_4$ :

$$H \text{ production} = (H_{td} - H_{le}) + (NH_{4,td} - NH_{4,le}) - (NO_{3,td} - NO_{3,le}) - (SO_{4,td} - SO_{4,le}) \quad (2.10)$$

In Dutch forest soils, the actual acidification rate (Eq. 2.10) is nearly equal to the acidification rate induced by N transformations (Eq. 2.5), since  $SO_4$  behaves as a tracer and the difference between the input and output of protons is small (cf Section 2.2 and 2.3).



## 2.2 RELATIVE IMPORTANCE OF NATURAL AND MAN-INDUCED ACIDIFICATION OF SOILS IN THE NETHERLANDS

### ABSTRACT

*Dissociation of weak acids is shown to be the main cause of natural proton (acid) production. This proton source was quantified for calcareous and non-calcareous sandy soils in the Netherlands. Estimates of proton production rates due to land use and acid deposition (man-induced sources) were made by using and interpreting literature data. It is shown that the relative contribution of the proton sources depends upon the ecosystem. Natural proton production predominates in calcareous soils, irrespective of the land use. Man-induced proton production is most important in non-calcareous soils. This is primarily caused by removal of biomass in agricultural soils and by acid deposition in forest soils.*

### INTRODUCTION

Acid production in soils results from natural soil forming processes, such as decalcification and podzolization, and anthropogenic activities, i.e. land use and acid deposition. The adverse effects of acid deposition on surface water chemistry and biota in fresh water have been recognized as a major environmental problem over vast regions of Europe and North America (Baker and Schofield, 1982; Driscoll et al., 1980; Hall et al., 1984). Furthermore, soil acidification induced by acid deposition may play a key role in the forest dieback in Western Europe (Ulrich et al., 1979; Ulrich and Matzner, 1983). However, the contribution of acid deposition to proton production in soils is still controversial. Several authors such as Rosenqvist (1980), Isermann (1983) and Krug and Frink (1983) postulate a key role of natural and land-use induced proton sources. Other investigators ascribe a dominant role to acid deposition (Ulrich et al., 1979; Driscoll and Likens, 1982; Van Breemen et al., 1984). This dissension is partly due to differences in the ecosystems that have been considered. However, the most important reason is that the former authors considered only parts of the H transfer processes that are relevant in the soil. Isermann (1983) for example only considered H producing processes, such as dissociation of CO<sub>2</sub>, nitrification, formation of a humus layer, and no H consuming processes, as required in an overall picture of the H cycle.

A comprehensive analysis of the different relevant acid producing and acid consuming processes in an ecosystem has been given by van Breemen et al. (1983) and De Vries and Breeuwsma (1987). This approach makes it possible to identify and quantify soil acidification induced by natural soil forming processes, land use and acid deposition (Section 2.1). In this section results on the relative importance of the various proton sources in different ecosystems in The Netherlands is given by comparison of own data on natural H production with literature data about man-induced (land use-induced, and acid deposition-induced) H production.

## CAUSES OF NATURAL SOIL ACIDIFICATION

The ultimate cause of proton production in the soil is the uncoupling of element cycles in an ecosystem (Ulrich, 1981b, 1983a; De Vries and Breeuwsma, 1987). In that case, the several processes within the element cycle accompanied with H production or consumption in the soil no longer counteract each other.

The main processes in the element cycles, i.e. ion uptake by the vegetation and release of ions by mineralization of organic matter, lead to acid production or acid consumption depending upon the element involved (cation or anion; Section 2.1). Furthermore, oxidation reactions accompanied by H production and reduction reactions accompanied by H consumption play a key role in the N cycle (nitrification and denitrification). In a natural ecosystem (an ecosystem that is not influenced by man), the cycles of major elements such as N and S are often closed (Bormann et al., 1977). This means that the net acid production due to the cycling of these elements is zero (cf Section 2.1).

The reasoning given above does not hold for the C cycle. Dissociation of  $\text{CO}_2$ , ultimately coming from the atmosphere, is an important proton source in calcareous soils with high pH values, where the acid production is neutralized by the weathering of Ca carbonate. Both Ca and  $\text{HCO}_3^-$  are leached by the precipitation excess. This process leads to a decrease of the acid neutralizing capacity (ANC) of the soil. Dissociation of  $\text{CO}_2$  does not occur in non-calcareous soils with pH values lower than 4.5 to 5. However, in these soils, a further decrease in pH occurs due to organic acids that can deprotonate even at low pH values. In non-calcareous non-agricultural (e.g. forest) soils with low nutrient status, oxidation of organic matter is generally limited and in this situation, organic acids can play an important role in the natural proton production in the soil. The acid production in the soil is neutralized by weathering (and desorption) of cations (mainly Al and Fe) that may form a complex with the organic anions ( $\text{RCOO}^-$ ). The overall proton production rate equals the amount of  $\text{RCOO}^-$  that is leached to the ground water (cf Section 2.1).

Natural leaching of elements due to production of  $\text{HNO}_3$  can be an important additional proton source in soils with a N fixing vegetation such as red alder (Van Miegroet and Cole, 1984). However, situations where  $\text{NO}_3^-$  is produced in excess of biological demand in forests are infrequent. Finally, successive oxidation and reduction of Fe and S gives rise to a strong acid production in periodically reduced soils such as ferrolysed soils and acid sulphate soils but this is only of regional importance (Brinkman, 1970; van Breemen, 1975).

It can thus be concluded that a net acid production in a natural ecosystem is mostly due to dissociation of weak acids. This conclusion is warranted by soil leaching studies in forest ecosystems in unpolluted regions (Johnson et al., 1977; Ugolini et al., 1977). The ultimate driving forces for natural decalcification and podzolization (acidification) are the presence of  $\text{CO}_2$  in the atmosphere and the precipitation excess. Important processes affecting the C cycle, and through that the natural H production are root respiration (especially in

calcareous soil) and accumulation of organic matter due to incomplete decomposition (especially in podzolic soils).

## QUANTIFICATION OF NATURAL SOIL ACIDIFICATION

The natural proton production can be estimated in various ways, e.g. from:

- the current production of  $\text{HCO}_3^-$  and/or  $\text{RCOO}^-$  ions;
- the decrease in acid neutralizing capacity (ANC) in the past.

### Current acidification rates

#### *Method*

The current natural proton production rate can be quantified by balancing the input versus the output for the relevant acid producing anions ( $\text{HCO}_3^-$  or  $\text{RCOO}^-$ ). This calculation is made by using the assumption that the net production of such anions implies the net production of an equivalent amount of H. The input of  $\text{HCO}_3^-$  and  $\text{RCOO}^-$  can be considered negligible. The output of these anions can be quantified by measuring their concentration and the flux of soil water. Since organic anions are not easily measured, the approach usually employed is to determine all major cations and anions and then assign the anion deficit (if any) to organic anions.

#### *Results for calcareous soils*

Values on the production of H in calcareous soils obtained by the measured leaching flux of  $\text{HCO}_3^-$  range from 7.2-12.6  $\text{kmol}_e \text{ ha}^{-1} \text{ yr}^{-1}$  (Van Breemen et al., 1984). For these soils, such values can also be estimated from the solubility of  $\text{CaCO}_3$  using the following equation:

$$\log [\text{HCO}_3^-] = -1.84 + 1/3 \log p\text{CO}_2 \quad (2.11)$$

where  $[\text{HCO}_3^-]$  is the concentration of  $\text{HCO}_3^-$  ( $\text{mol l}^{-1}$ ) and  $p\text{CO}_2$  the partial  $\text{CO}_2$  pressure (bar) in the soil. Eq. (2.11) is based on the implicit assumption that the activity of  $\text{HCO}_3^-$  equals the  $\text{HCO}_3^-$  concentration. This will lead to a slight under estimation of  $[\text{HCO}_3^-]$ . The activity coefficient for  $\text{HCO}_3^-$  is likely to be close to 0.9, assuming an ionic strength of 0.01 (cf Lindsay, 1979). The natural acidification rate by  $\text{HCO}_3^-$  leaching from the soil can be calculated by multiplying  $[\text{HCO}_3^-]$ , using Equation (2.11), with the precipitation excess. Natural acidification rates thus calculated vary between 7.5 to 20.4  $\text{kmol}_e \text{ ha}^{-1} \text{ yr}^{-1}$  with a  $\text{CO}_2$  pressure varying between 5 to 100 mbar and a precipitation excess of 300  $\text{mm yr}^{-1}$  (Table 2.3). The values given by Van Breemen et al. (1984) correspond to  $\text{CO}_2$  pressures varying between about 5 to 20 mbar, which is a commonly occurring range in well-drained soils.

**Table 2.3** *Theoretical decalcification (acidification) rates in calcareous soils as a function of the CO<sub>2</sub> pressure in the soil*

pCO <sub>2</sub> (mbar)	[HCO <sub>3</sub> ] (mol <sub>c</sub> m <sup>-3</sup> )	Proton production rate (kmol <sub>c</sub> ha <sup>-1</sup> yr <sup>-1</sup> ) <sup>1)</sup>
5	2.5	7.5
10	3.1	9.3
20	3.9	11.7
50	5.4	16.2
100	6.8	20.4

<sup>1)</sup> Precipitation excess = 300 mm yr<sup>-1</sup>

#### *Results for non-calcareous soils*

In non-calcareous soils, H production rates are far less. Johnson et al. (1977) measured HCO<sub>3</sub> concentrations between 0.1 to 0.2 mol<sub>c</sub> m<sup>-3</sup> in non-calcareous tropical soils with a pH >5. Concentrations of organic anions were generally very small. With a precipitation excess ranging between 100 to 1000 mm yr<sup>-1</sup>, H production rates vary between ca. 0.1 to 2.0 kmol<sub>c</sub> ha<sup>-1</sup> yr<sup>-1</sup> in these soils. A similar range in acidification rates can be derived from Cronan et al. (1978). In acidic podzolic soils (pH <5) HCO<sub>3</sub> is not present any more and consequently H production rates measured by the leaching of organic anions are even lower, ranging from 0.1 to 0.7 kmol<sub>c</sub> ha<sup>-1</sup> yr<sup>-1</sup> (Ulrich and Matzner, 1983; Van Breemen et al., 1984).

### **Historical acidification rates**

#### *Method*

The natural H production can also be estimated from the decrease in ANC that has taken place in the past by decalcification or podzolization. In calcareous soils, the loss of ANC is equal to the weathering of CaCO<sub>3</sub>, whereas the ANC decrease in non-calcareous soils is mainly due to the weathering of the cation acids Al and Fe and of the bases Ca, Mg, K and Na.

The weathering rate for each element can be calculated from the decrease in element amount in the (decalcified or weathered) topsoil during the period of weathering according to (after Kundler, 1959):

$$X_{we} = (\rho_o \cdot T_o \cdot ctX_o - \rho_p \cdot T_p \cdot ctX_p) \cdot f_c / t_{we} \quad (2.12)$$

where  $X_{we}$  is the weathering rate of element X (mol<sub>c</sub> ha<sup>-1</sup> yr<sup>-1</sup>),  $\rho_o$  and  $\rho_p$  are the original and present bulk density, respectively (kg m<sup>-3</sup>),  $T_o$  and  $T_p$  are the original and present thickness, respectively (m),  $ctX_o$  and  $ctX_p$  are the original and present total element content, respectively (mol<sub>c</sub> kg<sup>-1</sup>),  $t_{we}$  is the time that has passed since the weathering process started (yr) and  $f_c$  is a factor for the conversion of units from mol<sub>c</sub> m<sup>-2</sup> yr<sup>-1</sup> to mol<sub>c</sub> ha<sup>-1</sup> yr<sup>-1</sup> (10<sup>4</sup> m<sup>2</sup> ha<sup>-1</sup>).

To calculate weathering rates, it was assumed that (i) the original content of element X in the weathered (decalcified) topsoil,  $ctX_o$ , is equal to the present content of element X in the C horizon,  $ctX_{p,c}$  and (ii) there has been no loss of soil material in the weathered topsoil. In formula:

$$ctX_o = ctX_{p,c} \quad (2.13)$$

$$\rho_o \cdot T_o = \rho_p \cdot T_p \quad (2.14)$$

Combining the Eqs (2.12), (2.13) and (2.14) gives:

$$X_{we} = (\rho_p \cdot T_p \cdot (ctX_{p,c} - ctX_p)) \cdot 10 / t_{we} \quad (2.15)$$

To obtain natural acid production rates by an historical approach, the decrease of the ANC in the past was studied by measuring carbonate contents and total cation contents in complete soil profiles of two calcareous soils and six podzolic soils in the Netherlands, respectively. Since the comparison between the total amount of cations in the parent material (C horizon) and the overlying A and B horizons, relates to the mineral part of the soil, a correction for the humus content was made by multiplying the total cation content in the soil by a factor  $100/(100 - \% \text{ organic matter})$ .

#### *Results for calcareous soils*

With respect to decalcification, estimates were made for two deeply decalcified sandy soils in coastal dunes. The estimated acid production rates (Table 2.4) are considerably lower than literature data about the current leaching of  $\text{HCO}_3$  in calcareous soils. However, one should be aware that the calculated past decalcification rates are an average of fast initial decalcification rates as long as  $\text{CaCO}_3$  is present in the rootzone (high  $\text{CO}_2$  pressure) followed by slow decalcification rates below the rootzone (low  $\text{CO}_2$  pressure). Comparison of the results with the calculated decalcification rates in Table 2.3 shows good agreement for  $\text{CO}_2$  pressures varying between about 0.3 mbar (atmospheric pressure) and 5 mbar. Literature data about the past decalcification rates in the upper 25 to 30 cm of calcareous clay soils in the Netherlands vary between 60 to 90 yr for 1%  $\text{CaCO}_3$  (Edelman and de Smet, 1951). These values result in a rate of acid production of about 8 to 15  $\text{kmol}_c \text{ ha}^{-1}$

*Table 2.4 Natural decalcification (acidification) rates of two calcareous sandy soils*

Soil type	Decalcification depth (m)	$\text{CaCO}_3$ in subsoil (%)	Decalcification rate <sup>1)</sup> ( $\text{kmol}_c \text{ ha}^{-1} \text{ yr}^{-1}$ )
Albic arenosol	1.80	2.5	3.4
Humic gleysol	1.20	6.7	6.0

<sup>1)</sup> The time that has evolved since decalcification started is estimated at 4000 yr (age of the dunes)

yr<sup>-1</sup>, which agrees well with decalcification rates obtained by measuring or calculating the output of HCO<sub>3</sub>.

#### *Results for non-calcareous (podzolic) soils*

Estimates of podzolization rates were made by analysing the cationic composition of six soil profiles, namely a Carbic Podzol, three Gleyic Podzols and two Cambic Podzols (FAO, 1988). The samples were all taken in non-agricultural land (forest and heathland) where the influence of man has been slight or absent. The samples of the Carbic and Gleyic Podzols were taken in a cover-sand area with a homogeneous texture profile (Bathmen). The samples of the Cambic Podzols were taken in an ice-pushed ridge (Doorwerth) and a fluvioglacial plain (Oud Reemst) with a more heterogeneous texture profile.

The Gleyic Podzols form a hydro(topo)sequence with different depths to the water table. In the Netherlands, these depths are grouped into watertable classes. The definitions of these classes are based on the depths of the mean highest (MHW) and the mean lowest watertables (MLW) (Van Heesen, 1970). The different Gleyic Podzols are in the classes VII (MHW deeper than 80 cm), VI (MHW between 40 and 80 cm), and V (MHW shallower than 40 cm). The MLW is in all cases deeper than 120 cm. In the text, the Gleyic Podzols are distinguished by the words high (class VII), medium-high (class VI) and low (class V). The other podzols are all in class VII.

Results of the change in cation amounts in the various A, E and B horizons, as compared to the C horizon, are shown in Fig. 2.5. The values need to be interpreted with some care as they are based on the assumption that the original cationic composition of the topsoil (A, E and B horizons) was equal to the present composition in the parent material (C horizon). As far as the Cambic Podzols are concerned, this assumption is not likely as the samples are taken in ill-sorted sandy material. This is illustrated by the fact that Fe appears to be accumulated whereas Al and bases are leached in the Ah and Bh horizons of the Cambic Podzols from Oud Reemst and Doorwerth.

The mean annual soil acidification rate (Table 2.5) showed a marked increase in the order Cambic Podzols < Carbic and high Gleyic Podzols < medium-high and low Gleyic Podzols. The low weathering rate of the Cambic Podzols reflects the low degree of podzolization. The relatively high weathering rate of the medium-high and low Gleyic Podzols is probably due to the influence of the watertable. The values of the annual acid production rate caused by the weathering of base cations (BC) only, varied from about 100 to 200 mol<sub>e</sub> ha<sup>-1</sup> yr<sup>-1</sup> for the Carbic and Gleyic Podzols, respectively (values for the Cambic Podzols are questionable). Similar values have been reported in literature for these soil types. Ulrich (1981a), for example, gave values of 200 mol<sub>e</sub> ha<sup>-1</sup> yr<sup>-1</sup> for a "Calluna Podzol" and 140 mol<sub>e</sub> ha<sup>-1</sup> yr<sup>-1</sup> for a "Podzoligen Braunerde" (soils which are comparable to the Carbic and Cambic Podzols, respectively), whereas Teveldal et al. (1990) reported a value of 190 mol<sub>e</sub> ha<sup>-1</sup> yr<sup>-1</sup> for an iron-humus podzol (comparable to a Carbic Podzol).

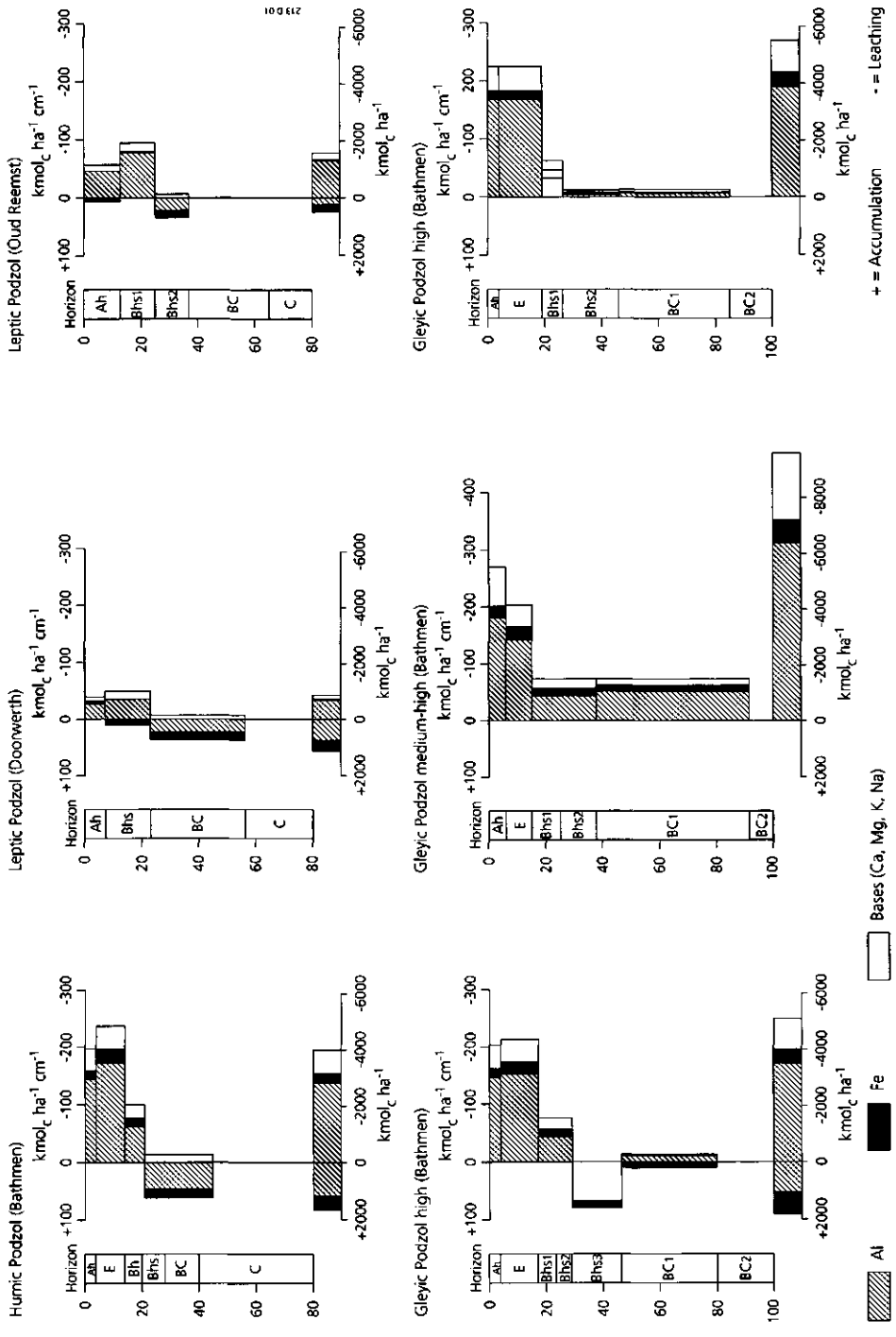


Figure 2.5 Leaching and accumulation of Al, Fe and bases (Ca, Mg, Na and K) in six podzolic soils in the Netherlands

*Table 2.5 Natural weathering (acidification) rate of six podzolic soils in the Netherlands<sup>1)</sup>*

Soil type (FAO, 1988)	Acidification (mol <sub>c</sub> ha <sup>-1</sup> yr <sup>-1</sup> ) due to leaching of:							
	Al	Fe	Ca	Mg	K	Na	Bases	Total
Carbic Podzol	154	-8	17	14	28	34	93	239
Gleyic Podzol high	239	-10	6	23	41	40	110	339
Gleyic Podzol medium-high	638	76	31	36	65	59	191	905
Gleyic Podzol low	390	49	35	32	17	33	117	556
Cambic Podzol (Doorwerth)	-7	-39	1	11	10	2	24	-22 <sup>2)</sup>
Cambic Podzol (Oud Reemst)	118	-14	4	3	18	8	33	137

<sup>1)</sup> The time that has evolved since podzolization started is estimated at 10 000 yr.

<sup>2)</sup> Negative values indicate that the original amount of elements in the topsoil has been higher than the present amount in the C horizon.

The annual acid production rates in these soils based on the weathering of Al, Fe and base cations varied from about 200 to 900 mol<sub>c</sub> ha<sup>-1</sup> yr<sup>-1</sup>. Comparison of the values with those given by van Breemen et al. (1984) for the leaching of RCOO in podzols shows good agreement. Higher values were reported by Mazzarino et al. (1983), i.e. 900 to 1900 mol<sub>c</sub> ha<sup>-1</sup> yr<sup>-1</sup>, but this may partly be explained by differences in parent material (soils with a large fraction of loess).

It should be noted that the values given in Table 2.5 are likely to be an underestimate due to the assumption that there is no loss of soil material (Eq. 2.14). The effect of this assumption can be derived by measuring the content of a mineral that is resistant to weathering, such as zirconium (Zr). Loss of soil material by weathering is reflected by an increase in the Zr content. A better estimate of the original amount of soil material can thus be derived by multiplying the present amount (cf Eq. 2.14) with the ration of the Zr content in the weathered topsoil compared to the C horizon (Olsson and Melkerud, 1991). Recent investigations in which Zr was measured in Dutch podzolic soils shows that this may have caused an underestimation of approximately 15-30%.

The ratio between Al and BC weathering (mol<sub>c</sub> mol<sub>c</sub><sup>-1</sup>) varied between 1.7 and 2.2 in the well drained Carbic and high Gleyic Podzols, and equalled 3.3 in the poorly drained Gleyic podzols. The latter value indicates nearly stoichiometric weathering of K and Na feldspar, such as microcline and albite, and of Ca aluminosilicates, such as anorthite, with stoichiometric Al/BC weathering ratios of 3.0 mol<sub>c</sub> mol<sub>c</sub><sup>-1</sup>.

## QUANTIFICATION OF MAN-INDUCED SOIL ACIDIFICATION

### *Land use*

The present proton production in the soil is strongly influenced by man via land use (removal of vegetation) and acid deposition. The three main effects of removal of vegetation are (i) removal of a cation surplus from the soil, (ii) disequilibrium between mineralization and uptake and (iii) reduction in C load to the soil. The first two effects lead



to an increase in proton production while the last one reduces the natural acid production. However, generally, the overall effect is an increased H production. This will be discussed in some detail.

- (i) Removal of biomass leads to a continuous removal of a cation surplus (i.e. a surplus of cations over anions) from the soil. In this case, the term cation surplus stands for all ions except  $\text{NH}_4$  and  $\text{NO}_3$ . N should not be taken into account, as this element is not originally present in the soil. In a non-fertilized soil, the N accumulated in biomass (organic matter, vegetation) came originally from the atmosphere. The transformation of atmospheric N ( $\text{N}_2$ ,  $\text{NO}_x$ ,  $\text{NH}_3$ ) to organic N in soil or vegetation does not result in H transfer. The form in which N is transferred is unimportant. The net effect of the mineralization and uptake is zero for both  $\text{NH}_4$  and  $\text{NO}_3$  (Section 2.1). The accumulation of a cation surplus in biomass decreases the acid-neutralizing capacity of the soil. The proton production rate due to biomass accumulation can be quantified by measuring the growth rates and chemical composition of the vegetation. Literature values about the cation surplus in the harvestable parts of several cereals (oats, barley and rye) and tuberous plants (potatoes, sugarbeet) vary from about 2 to 5  $\text{kmol}_c \text{ ha}^{-1} \text{ yr}^{-1}$  (Loman and de Willigen, 1972). For production forests, total cation uptake values vary from about 0.1 to 2.0  $\text{kmol}_c \text{ ha}^{-1} \text{ yr}^{-1}$  (Ulrich und Matzner, 1983; van Breemen et al., 1984). However, the long-term acidification rate associated with removal of plant material, has to be based on cation uptake in the harvestable parts of the tree, only. In the Netherlands, stemwood removal is common practice. Literature values about the accumulation rates of (base) cations in stems vary from about 0.3 to 0.7  $\text{kmol}_c \text{ ha}^{-1} \text{ yr}^{-1}$  (Nilsson et al., 1982; Ulrich, 1983a; cf Section 4.2 and 5.2). It should be stressed that these values are indicative of the proton production due to forestry. In a natural steady-state forest ecosystem, there is an equilibrium between uptake and mineralization. Accumulation of biomass has only occurred during a relatively short aggradation period of several hundred years. However, removal of trees causes a continuous disequilibrium between uptake and mineralization. Consequently, production forests are always in the aggradation phase.
- (ii) Biomass removal can result in a large proton production as long as the mineralization of cations and anions is not balanced by ion uptake. This is due to the fact that the amount of mineralized organic N and S (accompanied with H production) generally exceeds the amount of mineralized cations (accompanied with H consumption). H production only occurs when mineralization of organic N is followed by nitrification. It is well known that autotrophic nitrification is inhibited in acid soils (Dancer et al., 1973; Keeney, 1980). Consequently it is generally assumed that nitrification does not occur at low pH values (pH <4 to 5). However, various publications have shown that heterotrophic nitrification may still occur even at very low pH values (Strayer et al., 1981; Klein et al., 1983). Furthermore, several authors found  $\text{NO}_3$  to be the dominating anion in solutions leaching from disturbed acid forest soils (Likens et al., 1969; Hook and Kardos, 1978; Vitousek et al., 1979). Consequently nitrification in acid soils might be less inhibited as previously thought, although the importance of this process decreases at low pH values. In situations where nitrification is not inhibited, N plays a

dominant part in the acid production. Data about the H budget of a deforested ecosystem in Hubbard Brook in New Hampshire indicate an acidification rate due to mineralization processes that is equal to  $6.1 \text{ kmol}_c \text{ ha}^{-1} \text{ yr}^{-1}$  (van Breemen et al., 1984). Although the acidification due to mineralization can be significant, the effect is only temporary as the regrowth of vegetation is generally fast. Consequently, it is of minor importance in non-agricultural soils in comparison with the permanent effect of biomass accumulation. However, in agricultural soils net mineralization plays a dominant part in the acid production. Values about the liming of Dutch agricultural soils indicate that the total H production ranges from about 3 to  $14 \text{ kmol}_c \text{ ha}^{-1} \text{ yr}^{-1}$ , while the H production due to net mineralization accounts for about 1 to  $9 \text{ kmol}_c \text{ ha}^{-1} \text{ yr}^{-1}$  (Loman and de Willigen, 1972).

- (iii) Finally removal of biomass may also reduce the natural acid production by reducing the C load to soils. In calcareous soils, the decrease in  $\text{CO}_2$  pressure, and consequently in acid production rate (cf Table 2.3), can be important after removal of biomass. However, an indication of the overall effect in calcareous forest soils is not easy since biomass (trees) strongly regulates the flow of water through these soils. Literature data indicate that a decrease in  $\text{HCO}_3^-$  concentration in deforested calcareous soils may be compensated by an increase in precipitation excess (van Breemen et al., 1984b). In non-calcareous soils, the C cycle plays a far less important role in H transfer processes as discussed before. In agricultural soils, the acid production is mainly regulated by cation uptake and N mineralization. Proton production by dissociation of  $\text{CO}_2$  and/or organic acids is limited and consequently a reduction in C load only slightly reduces the H production rate. In acid forest soils, the effect will even be less, since dissociation of  $\text{CO}_2$  is limited to pH values above 4.5 to 5.0. Furthermore, the acid production due to formation and dissociation of organic acids is mainly regulated by leaf litter. Removal of trees (generally except leaves) once in about 50 to 100 yr hardly influences the C load by litterfall.

#### *Acid deposition*

The acidification due to wet and dry deposition of (potentially) acid substances (acid deposition) has been especially important in the last decades. An estimate of the mean potential acid input caused in the Netherlands is  $5.8 \text{ kmol}_c \text{ ha}^{-1} \text{ yr}^{-1}$  (Van Aalst and Diederer, 1982). This value is based on the wet deposition of H and  $\text{NH}_4$  and the dry deposition of  $\text{SO}_2$ ,  $\text{NO}_x$  and  $\text{NH}_3$ .  $\text{NH}_3$  is not counted as a base but as a (potential) acid, that should be added to  $\text{SO}_x$  and  $\text{NO}_x$  through its inherent acidifying effect in the soil via nitrification. Further in this thesis the term acid deposition is used for the deposition of potentially acid substances. In Western Europe and America the potential acid load generally ranges between 2 to  $4 \text{ kmol}_c \text{ ha}^{-1} \text{ yr}^{-1}$  (Ulrich and Matzner, 1983; van Breemen et al., 1984). The extreme values in the Netherlands are mainly due to the occurrence of intensive animal husbandry over vast areas, leading to a mean  $\text{NH}_x$  deposition of about  $2 \text{ kmol}_c \text{ ha}^{-1} \text{ yr}^{-1}$  which is about 35% of the total acid load (van Aalst en Diederer, 1982). In forests, the potential acid load can be even higher (up to  $7.5 \text{ kmol}_c \text{ ha}^{-1} \text{ yr}^{-1}$ ) due to the larger interception surface for dry deposition (van Breemen et al., 1982). However, the

actual acidification rate caused by acid deposition is less due to N retention by immobilisation and uptake and/or denitrification. An estimate can be made with an input-output balance for H, NH<sub>4</sub>, NO<sub>3</sub> and SO<sub>4</sub> (Section 2.1). Values obtained in this way vary from about 2.0 to 6.5 kmol<sub>c</sub> ha<sup>-1</sup> yr<sup>-1</sup> in Dutch forest soils (Van Breemen et al., 1983; 1984). Recent investigations even indicated acidification rates up to 10 kmol<sub>c</sub> ha<sup>-1</sup> yr<sup>-1</sup> (cf Section 2.3). It is probable that in agricultural soils in the Netherlands, values will generally be less than about 5 kmol<sub>c</sub> ha<sup>-1</sup> yr<sup>-1</sup>, since dry deposition on short vegetations, such as agricultural crops, is lower than on forests.

## DISCUSSION AND CONCLUSIONS

The ultimate cause of natural proton production is mainly the presence of CO<sub>2</sub> in the atmosphere, that induces the dissociation of weak (carbonic and organic) acids in the soil. The proton production rates are strongly influenced by photosynthesis and root respiration (especially in alkaline calcareous soils) and by production of organic acids (especially in acid podzolic soils). Current natural proton production rates in calcareous soils, obtained by an input-output balance of HCO<sub>3</sub><sup>-</sup>, and historic decalcification rates, obtained by determination of the decrease in CaCO<sub>3</sub> content in a soil profile with depth, are in the same range. Similarly, the current natural acidification rate of podzolic soils, obtained by an input-output balance of organic anions, and the historic podzolization rate, obtained by determination of Al, Fe and bases in the soil profile, are also comparable.

An overview of the acid production due to natural and man-induced proton sources in Dutch soils is given in Table 2.6. Comparison shows that natural soil acidification is dominant in calcareous soils (irrespective of land use), whereas land use (biomass removal) is most important in non-calcareous agricultural soils, and acid deposition in non-calcareous forest soils. Taking an average soil acidification rate of 1.0 kmol<sub>c</sub> ha<sup>-1</sup> yr<sup>-1</sup> due to natural causes, and land use (net removal of base cations) and an average acid production by N transformations of 4.0 kmol<sub>c</sub> ha<sup>-1</sup> yr<sup>-1</sup> (cf Table 2.6) implies an average contribution of acid deposition to forest soil acidification of about 80%. In calcareous soils and non-calcareous agricultural soils this contribution is likely to be less than 20% and 50%, respectively (cf Table 2.6).

*Table 2.6 Acidification rates due to natural causes, land use and acid deposition*

Acidification rates (kmol <sub>c</sub> ha <sup>-1</sup> yr <sup>-1</sup> )				
Natural causes		Land use		Acid deposition
calcareous soils <sup>1)</sup>	non-calcareous soils <sup>2)</sup>	forest soils	agricultural soils	
7-20	0.1-0.9	0.3-0.7	3-14	2.0-6.5

<sup>1)</sup> Dissociation of CO<sub>2</sub>

<sup>2)</sup> Dissociation of organic acids

## 2.3 IMPACTS OF ACID DEPOSITION ON CONCENTRATIONS AND FLUXES OF SOLUTES IN ACID SANDY FOREST SOILS IN THE NETHERLANDS

### ABSTRACT

*The most important impacts of acid atmospheric deposition on the soil solution chemistry of acid sandy forest soils in the Netherlands are summarized by comparing and interpreting data from soil solution monitoring studies (18 stands) and a national soil solution survey (150 stands). Major conclusions are: (i) in forest subsoils there is almost a 1:1 relationship between the concentrations of  $\text{SO}_4$  and  $\text{NO}_3$  and those of H and Al, (ii) presumed critical Al concentrations ( $0.2 \text{ mol}_c \text{ m}^{-3}$ ) and Al/Ca ratios ( $1.0 \text{ mol mol}^{-1}$ ) are generally exceeded below 20 cm soil depth whereas  $\text{NH}_4/\text{K}$  ratios sometimes exceed a presumed critical value ( $5 \text{ mol mol}^{-1}$ ) in the upper 20 cm, (iii)  $\text{SO}_4$ ,  $\text{NO}_3$ , Al and H concentrations decrease in the order: spruce forests > pine forests > deciduous forests, (iv) forest soils are invariably saturated with  $\text{SO}_4$  (leaching equals deposition), (v) there is generally a relative large retention of N although there are indications that forest soils become N-saturated at total N inputs above  $4.0 \text{ kmol}_c \text{ ha}^{-1} \text{ yr}^{-1}$ , (vi)  $\text{NH}_4$  leaching is generally negligible but may become substantial above an  $\text{NH}_4$  input of  $3.0 \text{ kmol}_c \text{ ha}^{-1} \text{ yr}^{-1}$  and (vii) Al mobilization is the major buffer mechanism neutralizing the acidity produced from N transformations. The conclusions (i), (iv) and (vi) imply that a decrease in atmospheric inputs of S and N will give a nearly equivalent decrease in (H and) Al leaching.*

### INTRODUCTION

Since the early eighties it is recognized that Dutch forests receive large inputs of  $\text{NH}_4$  and  $\text{SO}_4$  from the atmosphere (Van Breemen et al., 1982). Since then, effects of atmospheric deposition of  $\text{SO}_x$ ,  $\text{NO}_x$  and  $\text{NH}_x$  on forests have received much attention in the Netherlands. Research efforts were focused on the impacts of acid deposition on soil (solution) chemistry (e.g. Van Breemen et al., 1988; Kleijn et al., 1989; Van Dobben et al., 1992), forest vegetation (e.g. Hommel et al., 1990), forest vitality (e.g. Van den Burg et al., 1988) and the relationship between soil solution chemistry and forest vitality (e.g. Roelofs et al., 1985). Results of these studies indicated the presence of high concentrations of  $\text{NH}_4$ ,  $\text{NO}_3$  and Al in the soil solution (Kleijn et al., 1989), associated with a shift towards nitrophilous grass-species in forests (Hommel et al., 1990) and an increased (relative) deficiency of Ca, Mg and P in forests (Van den Burg et al., 1988). Based on these results, critical loads for nitrogen (N) and total acidity have been derived for Dutch forests (De Vries and Heij, 1991).

Much experimental research on the effects of acid atmospheric deposition on Dutch forests dealt with the impacts on the soil solution chemistry. Several local monitoring studies were performed in a total of eighteen forest stands. Furthermore, a one-time national survey was carried out in early spring in 150 representative forest stands across the country (Table 2.7). With respect to the monitoring studies, a distinction can be made regarding the intensity of monitoring (cf Table 2.7). Intensive soil solution monitoring (sampled fortnightly or monthly) was mainly performed to gain insight in (i) the fate of  $\text{SO}_4$ ,  $\text{NH}_4$  and  $\text{NO}_3$  in

Table 2.7 Overview of research activities related to impacts of acid atmospheric deposition on the soil solution chemistry of Dutch forest stands

Type of research	Number of sites	Measurements per year	Period	Reference
Intensive soil monitoring	10	12-24	1979-1990 <sup>1)</sup>	Van Breemen and Verstraten, 1991 <sup>2)</sup>
Extensive soil monitoring	8	4	1987-1988	Kleijn et al., 1989
Soil solution survey	150	1	1990	De Vries and Leeters, 1994

<sup>1)</sup> During this period monitoring occurred at different sites for at least two years up to seven years

<sup>2)</sup> Summarizes results from various publications (cf Table 2.8)

forest soils and (ii) the mobilization of Al and base cations (Ca, Mg, K and Na), which mainly neutralize the acid input, based on input-output budgets (Van Breemen and Verstraten, 1991). Extensive soil solution monitoring in eight Douglas fir stands was specifically carried out to study the relationship between the soil and soil solution chemistry and forest vitality characteristics such as needle loss and needle colour, and root characteristics such as root length and mycorrhizae frequency (Kleijn et al., 1989). Major aims of the one-time national survey were (i) the determination of relationships between soil solution chemistry and deposition level, stand characteristics (such as tree species) and site characteristics (such as soil type; De Vries and Leeters, 1994), (ii) predictions of the chemical composition of the soil solution on a national scale using these relationships (Leeters and De Vries, 1992) and (iii) assessment of input-output budgets as a function of tree species (De Vries and Jansen, 1994). A further objective of the national soil solution survey was to assess whether the results of (budget studies for) the monitoring sites were representative for Dutch forests. This was considered questionable since monitoring was mainly performed in stands (i) located in areas with intensive animal husbandry, (ii) occupied with Douglas fir and oak and (iii) on relatively loamy and moderately to poorly drained soils.

In this section, major results of the various studies mentioned above are summarized, focusing on SO<sub>4</sub>, NO<sub>3</sub>, NH<sub>4</sub>, Al and pH (and the ratio of NH<sub>4</sub> and Al to base cations), which are the most important indicators of soil acidification and increased N availability. Emphasis is placed on (i) the variability of these ions in time, and space (both vertically and regionally) and (ii) the behaviour of these ions in the soil, in terms of net retention or net mobilization based on input-output budgets.

## MATERIALS AND METHODS

### Characteristics of the study sites

#### *Monitoring sites*

Soil solution monitoring was carried out at eighteen sites. These sites were mostly located in the eastern and southern part of the country, light textured (sand or loamy sand), non-calcareous (except for the subsoil of two sites), moderately to deeply drained and covered

by Douglas fir, oak and Scots pine (Table 2.8). The sites were clearly biased by a large number of stands with Douglas fir (the key tree species studied within the Dutch Priority Programme on Acidification; Heij and Schneider, 1991), which only covers 6% of Dutch forests. More information on the sites is given in the literature cited in Table 2.8.

Table 2.8 Characteristics of the eighteen monitoring sites

Location	Monitoring period <sup>1)</sup>	Soil type (FAO, 1988)	Gt class <sup>2)</sup>	Tree species	Reference
Winterswijk	1979-1986 (i)	Dystric Planosol <sup>3)</sup>	V	oak/beech	Verstraten et al., 1990
Hackfort A	1981-1987 (i)	Dystric Cambisol <sup>3)</sup>	VI	oak/birch	Van Breemen et al., 1998
Hackfort B	1981-1987 (i)	Dystric Cambisol	VI	oak/birch	Van Breemen et al., 1988
Hackfort C	1981-1987 (i)	Dystric Cambisol	VI	oak/birch	Van Breemen et al., 1988
Tongbersven	1983-1987 (i)	Carbic Podzol	VIII	Scots pine	Van Dobben et al., 1992
Gerritsfles	1983-1987 (i)	Haplic Arenosol	VIII	Scots pine	Van Dobben et al., 1992
Buunderkamp	1988-1989 (i)	Fimic Anthrosol	VII	oak	De Boer and Tietema, 1990
Leuvenum	1989-1990 (i)	Haplic Arenosol	VII	Douglas fir	De Boer and Tietema, 1990
Speuld A	1988-1990 (i)	Orthic Podzol	VIII	Douglas fir	Van der Maas and Pape, 1990
Kootwijk A	1988-1990 (i)	Cambic Podzol	VII	Douglas fir	Van der Maas and Pape, 1990
Speuld B	1986-1987 (e)	Cambic Podzol	VIII	Douglas fir	Kleijn et al., 1989
Kootwijk B	1986-1987 (e)	Carbic Podzol	VII	Douglas fir	Kleijn et al., 1989
Gardereren	1986-1987 (e)	Carbic Podzol	VII	Douglas fir	Kleijn et al., 1989
Amerongen	1986-1987 (e)	Cambic Podzol	VIII	Douglas fir	Kleijn et al., 1989
Lage Vuursche	1986-1987 (e)	Gleyic Podzol	VI	Douglas fir	Kleijn et al., 1989
Ruurlo	1986-1987 (e)	Gleyic Podzol	VI	Douglas fir	Kleijn et al., 1989
Zelhem A	1986-1987 (e)	Haplic Arenosol	VI	Douglas fir	Kleijn et al., 1989
Zelhem B	1986-1987 (e)	Haplic Arenosol	VII	Douglas fir	Kleijn et al., 1989

<sup>1)</sup> (i) stands for intensively (biweekly or monthly) monitored sites and (e) for extensively (three-monthly) monitored sites.

<sup>2)</sup> Meaning for Gt class (ground water level class): V = poorly drained, VI = moderately drained, VII = well drained and VIII = very well drained.

<sup>3)</sup> These soils have calcium carbonate in the subsoil.

The pH in the humus layer and the upper mineral soil horizons (0-10 or 0-15 cm depth) at these sites was very low (close to 3.5 in H<sub>2</sub>O and to 3.0 in 0.01 M CaCl<sub>2</sub> or 1.0 M KCl). Except for the two sites with calcium carbonate at greater depth (cf Table 2.8), the pH (in H<sub>2</sub>O) in the subsoil (50-100 cm depth) was always below 4.5. Base saturation in the mineral soil (in % of the cation exchange capacity, CEC, in unbuffered extracts) was always below 20% and generally even below 10%. Both pH and base saturation indicates that all soils are in the so-called aluminium buffer range (Ulrich, 1981a).

### Survey sites

A single soil solution measurement was performed at 150 forest stands in early spring 1990. The stands were selected from about 3000 stands belonging to the Dutch forest vitality inventory. According to the frequency distribution of tree species in the Netherlands, 45 stands of *Pinus sylvestris* (Scots pine; 30%), 30 stands of *Quercus robur* (oak; 20%) and 15 stands (each 10%) of *Pinus nigra* (black pine), *Pseudotsuga menziesii* (Douglas fir), *Picea abies* (Norway spruce), *Larix leptolepis* (Japanese larch) and *Fagus sylvatica* (beech) were selected on non-calcareous sandy soils, which are most sensitive to acidification.

Furthermore, most Dutch forests (about 85%) are located on acid sandy soils. More information on the selection procedure is given in De Vries and Leeters (1994).

At each site, an indication was given of stand characteristics influencing the atmospheric input to forest soils such as tree height (Stevens, 1987) in intervals of 5 m (0-5 m, 5-10 m, 10-15 m, 15-20 m, > 20 m), canopy coverage (Draayers et al., 1992) in intervals of 25 % (< 50%, 50-75%, > 75%), distance of trees to the forest edge (Hasselrot and Grennfelt, 1987) in intervals of 20 m (< 20 m, 20-40 m, 40-60 m, 60-80 m, > 100 m) and surrounding soil use (Boumans and Beltmans, 1991), i.e. maizetields, grassland, arable land and non-agricultural land. Furthermore, soil type and ground water level class were determined. Based on the Dutch classification system, 19 soil types were distinguished which were clustered into six major soil types (cf Table 2.9). A comprehensive description of all site and stand characteristics has been given by De Vries and Leeters (1994).

The distribution of tree species over soil type is given in Table 2.9. Three forest stands (black pine, Japanese larch and oak), which appeared to occur on calcareous soils, were removed from the data set. The coniferous forest stands mainly occurred on well-drained soils whereas the deciduous stands also occurred relatively often on poorly-drained soils. Most tree species occurred on Gleyic and Carbic Podzols, especially Norway spruce and Japanese larch, and to a lesser extent on Arenosols (cf Table 2.9).

As with the soils of the (intensively) monitored sites, the pH in the humus layer and the mineral topsoil (0-30 cm) was nearly always (very) low. In both soil layers, pH-H<sub>2</sub>O varied between 3.5 and 5.0 whereas pH-KCl varied between 2.5 and 4.3. The median base saturation in the mineral layer was 6% but in some cases, especially below deciduous trees on poorly drained soils, base saturation was above 25% (De Vries and Leeters, 1994).

Table 2.9 Distribution of forest stands over non-calcareous soils for 147 survey sites

Soil type (FAO, 1988)	Drainage	Number of stands							
		Scots pine	Black pine	Douglas fir	Norway spruce	Japanese larch	Oak	Beech	Total
Haplic Arenosol <sup>1)</sup>	good	13	7	2	0	1	3	0	26
Gleyic Podzol <sup>2)</sup>	good to moderate	21	7	7	11	11	10	7	74
Cambic Podzol	good	9	0	3	0	1	2	2	17
Fimic Anthrosol	good	1	0	3	1	1	3	2	11
Umbric Gleysol <sup>3)</sup>	poor	0	0	1	3	0	7	3	14
Dystric Gleysol	moderate to poor	0	0	0	0	0	4	1	5
		44 <sup>4)</sup>	14	16 <sup>4)</sup>	15	14	29	15	147

<sup>1)</sup> Including some Gleyic Arenosols that are moderately to poorly drained

<sup>2)</sup> Including Carbic Podzols that are well-drained

<sup>3)</sup> Including soils with a high organic matter content

<sup>4)</sup> At one stand, the major tree species appeared to be Douglas fir instead of Scots pine (as expected), resulting in 16 stands of Douglas fir and 44 stands of Scots pine

## Sampling and chemical analyses of the soil solution

### *Intensive monitoring sites*

At all intensively monitored sites, soil solution was extracted by suction, either using porous ceramic cups (Winterswijk, Hackfort, Buunderkamp and Leuvenum) or porous filter plates (Tongbersven, Gerritsfles, Speuld A and Kootwijk A) that were installed at different soil depths within the upper meter of the soil profile (Van Breemen and Verstraten, 1991). Two to four replicates were used for each soil layer (four to six layers depending upon soil type). When using porous ceramic cups, soil solution was collected in a previously evacuated sample bottle, using a vacuum tank (50-80 kPa suction) to maintain matric suction (Van Breemen et al., 1988). At the 'Tongbersven' and 'Gerritsfles' sites, soil solution was sampled through porous acrylic polymer filter plates (Van Dobben et al., 1992) at a constant suction of 10 to 15 kPa, using a hanging water column. At 'Speuld A' and 'Kootwijk A', soil solution was sampled through porous polythene plates using a suction that was continuously (electronically) regulated to match the matric suction head at the depth of the porous plate (measured with a tensiometer), to collect water flux-weighted soil solution samples. Soil solution samples from cups and plates were collected biweekly (Speuld A and Kootwijk A) or monthly (all other intensively monitored sites).  $\text{NO}_3^-$ ,  $\text{SO}_4^{2-}$ ,  $\text{H}_2\text{PO}_4^-$  and Cl in the solution samples were analyzed by ion chromatography, Ca and Mg by atomic absorption spectrometry, K and Na by atomic emission spectrometry,  $\text{NH}_4^+$  and Al by spectrophotometry and pH by potentiometry.

### *Extensive monitoring sites*

At the eight Douglas fir stands, soil solution was collected by centrifugation. This was done to extract soil solution in the summer period. Both solution sampling by suction devices and by centrifugation tend to fail when the soil is dry. However, the equivalent suction that can be applied by centrifugation ( $\approx 10^3$  kPa) is much higher than by vacuum extraction ( $\approx 80$  kPa) and consequently centrifugation yields soil solution in situations where vacuum extraction fails. At each stand five replicate soil samples were taken at different depths (0-15 cm, 15-30 cm, 30-45 cm and 45-60 cm). Soil samples were taken with a Riverside auger near the same five trees in each plot. This number was sufficient to estimate the mean log-concentration of each ion within an error of 20% (Kleijn and De Vries, 1987). Soil samples were collected in June, September and December 1986 and in April 1987. A 400 g soil sample was centrifuged at 7500 rpm and the soil solution obtained was filtered over a  $0.45 \mu$  filter. Solution samples from centrifugation were analysed by inductive coupled plasma atomic emission spectrometry for Al, Ca and Mg, and by atomic absorption spectrometry for Na and K. Other ions were analysed by similar techniques as used for the solution samples from vacuum extraction.

### *Survey sites*

At the 150 forest stands, soil solution was also collected with the centrifugation method described above. The soil was sampled between 15 February and 16 May 1990. The choice of this sampling period was based on a statistical analyses of the chemical



composition of soil solution samples collected at the intensively monitored 'Hackfort' sites (Van Breemen et al., 1988). These results indicated that solute concentrations in early spring (March, April) are generally most representative for the 'flux-weighted average annual solute concentration', which is derived by division of annual solute fluxes by annual water fluxes (Table 2.10). For  $\text{SO}_4$ ,  $\text{NO}_3$  and  $\text{NH}_4$ , the correlation was, however, weak, although better than in all other months.

Soil samples were taken of the humus layer, and three mineral soil layers, i.e. 0-30 cm, 30-60 cm and 60-100 cm. Spatial variability, which is the dominant source of error in calculating input-output budgets (Van Grinsven et al., 1987), was reduced by using one composite sample, consisting of 20 subsamples, for each mineral layer. This number was based on a statistical analysis of soil solution data obtained by the centrifugation of 60 soil samples collected in 1990 from two forest stands (Speuld A and IJsselstein), at fifteen spots (situated two meters apart) at two depths (topsoil and subsoil). Results of the analyses showed that 20 subsamples reduces the margin of error of the estimated mean concentration in a mineral layer to less than 20%, except for Al and  $\text{NH}_4$  where the margin of error was close to 30% (De Vries and Leeters, 1994). This level of uncertainty was considered acceptable for this study. The sample points were chosen according to a fixed pattern in a square of 20 x 20 meters in the middle of the forest stand. Soil moisture, was withdrawn from the samples of the mineral topsoil (0-30 cm) and the mineral subsoil (60-100 cm). In diluted samples the concentrations of Si, Al, Fe, Ca, Mg, K, Na,  $\text{NH}_4$ ,  $\text{NO}_3$ , Cl,  $\text{SO}_4$  and  $\text{H}_2\text{PO}_4$  were measured using the methods described above for the extensive soil monitoring sites (cf De Vries and Leeters, 1994).

Table 2.10 Linear regression parameters in the relationship 'MOC =  $\alpha_0 + \alpha_1$  FWC' for the three 'Hackfort' sites for a six year period<sup>1)</sup>

Statistics	H		Al		Ca		$\text{SO}_4$		$\text{NO}_3$		$\text{NH}_4$	
	M <sup>2</sup>	A <sup>2</sup>	M	A	M	A	M	A	M	A	M	A
$\alpha_0$ (mol <sub>c</sub> m <sup>-3</sup> )	0.01	0.01	0.06 <sup>3)</sup>	0.12 <sup>3)</sup>	-0.04	-0.08	-0.21 <sup>3)</sup>	-0.01	0.30 <sup>3)</sup>	0.45 <sup>3)</sup>	-0.01	-0.01
$\alpha_1$	0.88	0.94	0.88	0.84	1.12	1.26	1.24	0.91	0.83	0.89	0.81	0.87
$R^2_{adj}$	0.85	0.80	0.87	0.68	0.93	0.89	0.56	0.47	0.58	0.49	0.42	0.60

<sup>1)</sup> MOC is monthly concentration and FWC is flux-weighted annual average concentration

<sup>2)</sup> M is March: number of observations is 82, A is April: number of observations is 67

<sup>3)</sup> Significant at  $\alpha = 0.05$

## Calculation of Input-output budgets

### Monitoring sites

At each monitoring site atmospheric inputs of  $\text{SO}_4$ ,  $\text{NO}_3$ ,  $\text{NH}_4$ , base cations and Cl were estimated from fortnightly (Speuld A and Kootwijk A) or monthly (all other sites) measurements of the amount and chemical composition of bulk deposition and throughfall water, as described in Van Breemen and Verstraten (1991). The procedure to calculate

total deposition from bulk deposition and throughfall has been given by Van der Maas and Pape (1990).

Solute output fluxes at the ten intensively monitored sites were calculated by multiplying observed soil water concentrations with simulated unsaturated soil water fluxes. Soil water fluxes were simulated using the SWIF model (Tiktak and Bouten, 1992) for Winterswijk, Buunderkamp, Leuvenum, Speuld A and Kootwijk A, or the SWATRE model (Belmans et al., 1983, Van Grinsven et al., 1987) for Hackfort, Tongbersven and Gerritsfles. Output fluxes from the system were mainly calculated at 90 or 100 cm depth. At 'Winterswijk', the only calculated catchment involved, output fluxes were also measured directly by gauging stream output. Calculated biweekly or monthly solute fluxes were added to obtain annual solute fluxes.

Soil solution at the eight extensively monitored (Douglas fir) sites was sampled only four times within one year, which in principle is not sufficient to calculate annual solute (output) fluxes. Based on the results in Table 2.10 we did, however, assume that the average concentrations in April are equal to the flux-weighted annual average concentration (further denoted as annual average concentration). The output fluxes for the Douglas fir sites were thus calculated by multiplying the annual precipitation excess (precipitation minus actual evapotranspiration) from the system (estimated with SWATRE; Reurslag et al., 1990) with solute concentrations in April. The precipitation excess was, however, adjusted such that the Cl output from the subsoil (layer of 45-60 cm) equalled the measured throughfall flux of Cl (Cl-corrected precipitation excess). This approach is based on the assumption that the deviation of monthly concentrations from the annual average concentration is equal for all elements in the subsoil, and mainly determined by hydrology.

### Survey sites

Atmospheric deposition levels on the 147 survey sites were derived from estimates with the model DEADM (Erisman, 1991; Draayers and Erisman, 1993) for a 5 km x 5 km grid. To account for the effect of scavenging of dry deposition by forests, total deposition values on the gridcells where the forests are situated were multiplied by filtering factors (Table 2.11).

Table 2.11 Forest filtering factors for  $SO_4$ ,  $NH_4$  and  $NO_3$  for spruce -, pine - and deciduous forests in the Netherlands

Forest type	Filtering factors <sup>1)</sup>		
	$SO_4$	$NH_4$	$NO_3$
Spruce	1.6	1.5	1.0
Pine	1.4	1.3	0.85
Deciduous	1.15	1.1	0.7

<sup>1)</sup> Derived from a comparison of throughfall data below spruce -, pine - and deciduous forests at 42 sites in the Netherlands (Erisman, 1990; Houdijk, 1990) and total deposition estimates with the TREND model using 1985 emission data (cf De Vries, 1991).

Bulk deposition of base cations (Ca, Mg, K, Na) and Cl was estimated by interpolating data from 22 weatherstations in the Netherlands during the period 1978-1986 (KNMI/RIVM, 1988). Total base cation deposition was derived by multiplying bulk deposition values with average throughfall/bulk deposition ratios for Na of 2.0 for deciduous tree species (including Japanese larch), 2.5 for pine trees and 3.0 for spruce trees (based on measured ratios in 42 forests; De Vries, 1991).

Output fluxes from the 147 forest stands were calculated by multiplying solute concentrations in March to May (sampling period) in the subsoil (60-100 cm) with a Cl-corrected precipitation excess. The annual precipitation excess was first calculated by subtracting estimated values for the annual sum of interception, soil evaporation and transpiration from yearly precipitation values that were derived by interpolation from 280 weatherstations. Details on the procedure are given in De Vries and Jansen (1994). The precipitation excess was corrected, so that the median Cl leaching from each tree species equalled the median Cl deposition (De Vries and Jansen, 1994). Corrected values of the precipitation excess of deciduous tree species (including Japanese larch) were much lower than the original values (Table 2.12), indicating that the measured solute concentrations below deciduous tree species were greater than annual average solute concentrations.

*Table 2.12 Original and Cl-corrected median annual precipitation excesses for the seven tree species at the 147 survey sites*

Tree species	Precipitation excess (mm yr <sup>-1</sup> )		
	Original <sup>1)</sup>	Corrected <sup>2)</sup>	Correction
Scots pine	216	222	-6
Black pine	225	185	40
Norway spruce	93	106	-9
Douglas fir	122	131	-13
Japanese larch	276	121	155
Oak	230	130	100
Beech	271	156	115

<sup>1)</sup> Calculated by subtracting estimates values for annual evapotranspiration from annual precipitation

<sup>2)</sup> Calculated so that median Cl deposition equals median Cl leaching for each tree species

## SOIL SOLUTION CHEMISTRY

### Relations between soil acidity and acid anions

The most pronounced reflections of atmospheric deposition of S and N on the solution chemistry of Dutch acid sandy soils are the high SO<sub>4</sub> and NO<sub>3</sub> concentrations in the soil solution and concomitantly high concentrations of acidity (H+Al). In the monitoring plots there was a clear linear relationship between the H+Al concentration and the concentration

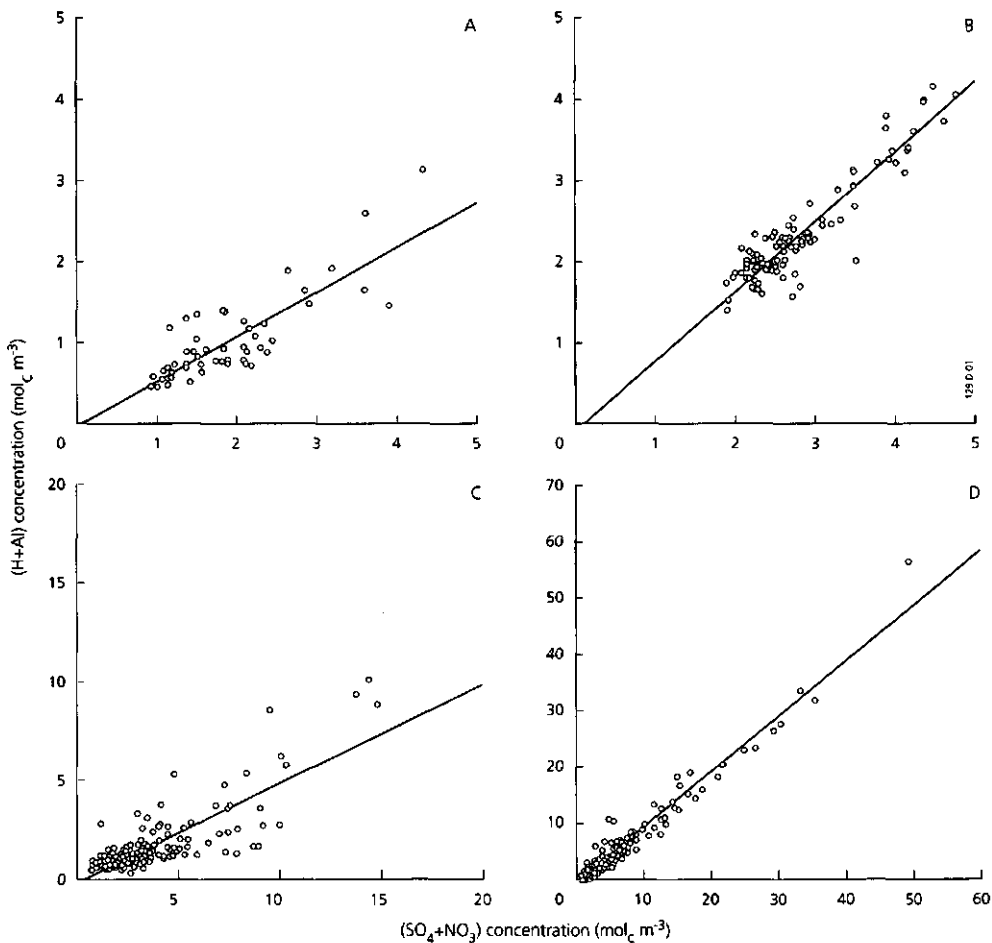


Figure 2.6 Relationship between the H+Al concentration and the  $\text{SO}_4 + \text{NO}_3$  concentration for the intensively monitored site 'Hackfort B' at 10 cm depth (A) and 90 cm depth (B) and for eight extensively monitored Douglas fir sites at 15 cm depth (C) and 60 cm depth (D).

of  $\text{SO}_4 + \text{NO}_3$ , as illustrated for the intensively monitored 'Hackfort' site (studied during the longest time period) and the eight extensively monitored Douglas fir sites (Fig. 2.6).

Highest solute concentrations were found at the Douglas fir sites. This is partly caused by higher rainfall interception by Douglas fir (38% of precipitation; Kleijn et al., 1989) compared to the deciduous trees at the Hackfort site (19-21%; Van Breemen et al., 1988). An increase in rainfall interception by 10% can cause an increase of concentration of a conservative ion (eg. Cl) by 20 to 40%, depending on the ratio of precipitation and

drainage. Furthermore, acid atmospheric deposition on the Douglas fir stands was slightly higher (6.2-10.7 kmol<sub>c</sub> ha<sup>-1</sup> yr<sup>-1</sup>; Kleijn et al., 1989) than on the oak stand at Hackfort B (7.0 kmol<sub>c</sub> ha<sup>-1</sup> yr<sup>-1</sup>; Van Breemen et al., 1988). Higher concentrations under the extensively monitored Douglas fir sites were, however, also due to methodological differences. First, the centrifugation method used at these sites allows soil solution collection at lower soil water potentials compared to suction cups, used in Hackfort. Very high concentrations (occasionally above 15 mol<sub>c</sub> m<sup>-3</sup>) in the summer period (June, September) were thus measured at the extensively monitored Douglas fir sites, whereas there were no soil solution measurements with suction cups in this period. Second, concentrations in a centrifugate are generally somewhat higher than in a suction cup although the difference is nearly always less than 25% (Verhagen and Diederer, 1991).

Results of linear regression analyses for various monitoring and survey sites (Table 2.13), show that the concentration of H+Al got closer to the concentration of SO<sub>4</sub>+NO<sub>3</sub> ( $\alpha_1 \approx 1$ ) with increasing depth for nearly all sites. Moreover, the linearity of the relationship increased with increasing depth as shown by an increasing value for the adjusted coefficient of determination ( $R^2_{adj}$ ). A 1:1 relationship between [H+Al] and [SO<sub>4</sub>+NO<sub>3</sub>] in the soil layers below the rootzone, indicates that external inputs of N and S to the soil (corrected for N and S retention in the soil), will cause mobilization and leaching of equivalent amounts of H and Al. Lower values of the  $\alpha_1$  and of  $R^2_{adj}$  in the upper soil layers are mainly caused by a variable production of base cations (BC) and NO<sub>3</sub>, induced by mineralization and nitrification of plant litter. In the soil survey sites, the value of  $\alpha_1$  in the subsoil was much less than one (0.66) and  $R^2_{adj}$  was also relatively low (0.75; cf Table 2.13). In these sites BC concentrations were generally quite high, which may partly be due to the fact that concentrations do not really represent annual average values (see Discussion).

Table 2.13 Linear regression parameters in the relationship:  
 $[H+Al] = \alpha_0 + \alpha_1 [SO_4+NO_3]$  for various sites and depths.

Sites	Depth (cm)	$\alpha_0$ (mol <sub>c</sub> m <sup>-3</sup> )	$\alpha_1$	$R^2_{adj}$
Hackfort B <sup>1)</sup>	10	-0.02	0.54	0.69
	90	-0.12	0.86	0.83
Tongbersven <sup>1)</sup>	12	0.27	0.15	0.27
	57	0.45	0.70	0.66
Gerritsfles <sup>1)</sup>	10	-0.58	0.89	0.92
	100	-0.11	0.97	0.96
Douglas fir <sup>2)</sup> sites (n=8)	0-15	-0.13	0.50	0.67
	15-30	-0.46	0.83	0.81
	30-45	-0.28	0.86	0.88
	45-60	-0.65	0.99	0.96
Survey sites (n=147)	0-30	0.08	0.54	0.77
	60-100	-0.16	0.66	0.75

<sup>1)</sup> Intensively monitored sites

<sup>2)</sup> Extensively monitored sites

In all sites the value of the intercept ( $\alpha_0$ ) was negative, except for 'Tongbersven' and the topsoil of the soil survey sites. A negative intercept suggests that no Al will be leached, when there is no leaching of  $\text{SO}_4$  or  $\text{NO}_3$ . As substantial leaching of  $\text{SO}_4$  and  $\text{NO}_3$  in forest soil results from elevated atmospheric inputs of N and S, the leaching of Al should decrease strongly if loadings of N and S are (will be) reduced to preindustrial levels. The positive intercept at Tongbersven may be due to podzolization, i.e. mobilization of Al by organic anions, but the value of  $R^2_{adj}$  was rather poor for this site, especially in the topsoil.

In all monitoring sites with a non-calcareous subsoil (16 out of 18 sites), the annual average Al concentration largely exceeded the drinking water standard ( $0.2 \text{ mg l}^{-1} \approx 0.02 \text{ mol}_c \text{ m}^{-3}$ ) in the subsoil. The annual average  $\text{NO}_3$  concentration exceeded the EG drinking water standard for  $\text{NO}_3$  ( $50 \text{ mg l}^{-1} \approx 0.8 \text{ mol}_c \text{ m}^{-3}$ ) in 14 sites and the Dutch target value ( $0.4 \text{ mol}_c \text{ m}^{-3}$ ) in 16 sites. In the non-calcareous survey sites (147) the drinking water standards in the subsoil were exceeded everywhere for Al and in 31% of the cases for  $\text{NO}_3$ , whereas 55% of the sites exceeded the target value for  $\text{NO}_3$  (cf Fig. 2.7). An Al concentration of  $0.2 \text{ mol}_c \text{ m}^{-3}$ , which is considered critical with respect to effects of roots (De Vries, 1993; cf Section 4.2), was exceeded in 80% of the sites. However, Al and  $\text{NO}_3$  concentrations measured at the survey sites may deviate from annual average values.

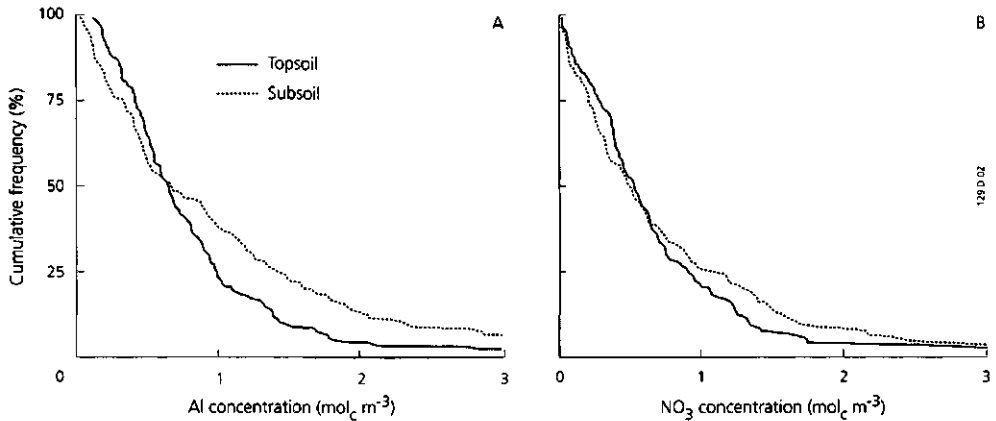


Figure 2.7 Inverse cumulative frequency distributions of Al (A) and  $\text{NO}_3$  (B) in the topsoil (0-30 cm) and subsoil (60-100 cm) of 147 survey sites.

## Variability with depth and time

### Variation with depth

Concentrations of solutes generally vary with depth as illustrated for the 'Hackfort B' and 'Tongbersven' site (Figure 2.8).

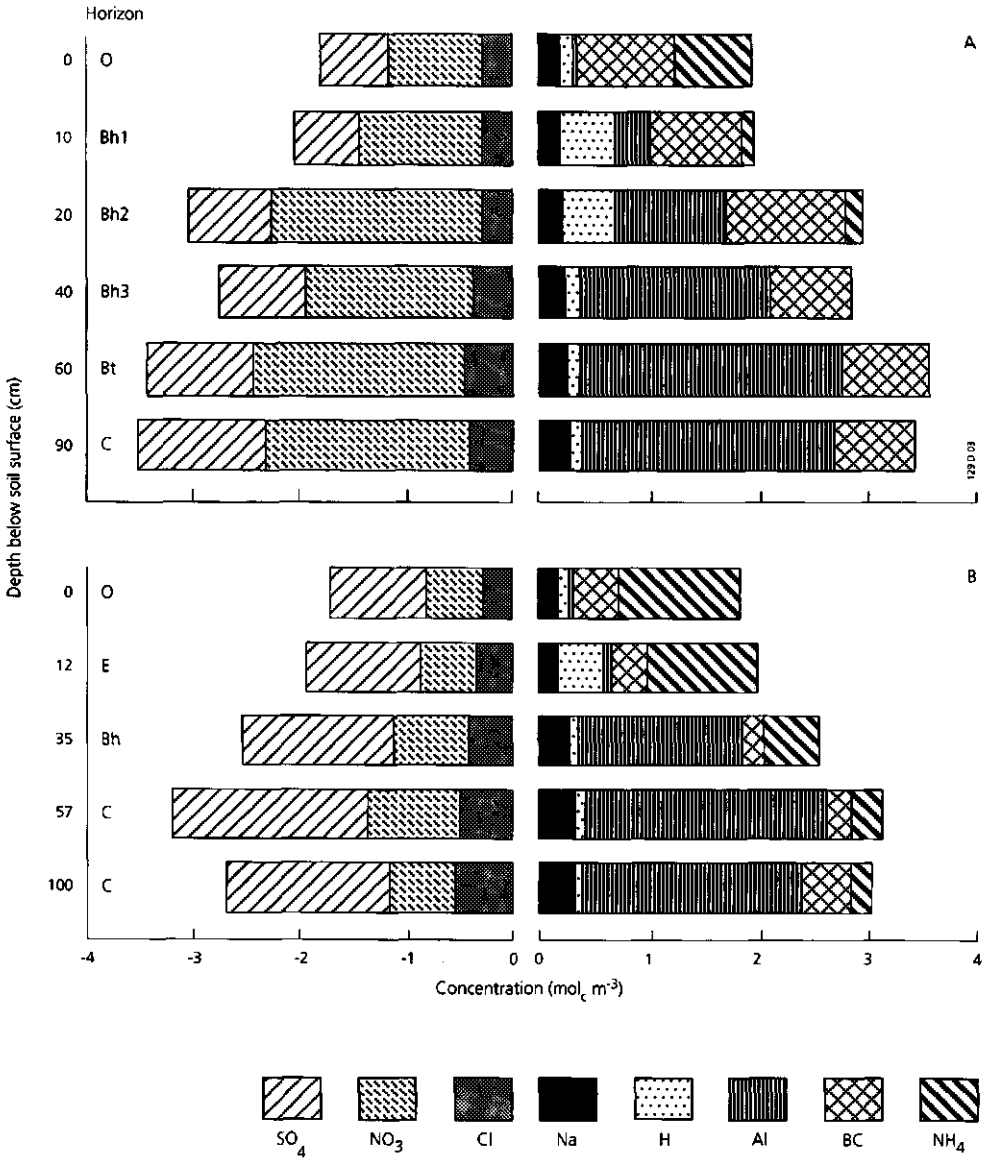


Figure 2.8 Mean annual flux-weighted solute concentration in the intensively monitored sites 'Hackfort B' (A) and 'Tongbersven' (B) during the years 1984-1987.

The concentration gradients depended on vegetation cover and soil type. At 'Hackfort B', annual average concentrations of Cl steadily increased with depth, resulting from a nearly linear increase in cumulative water uptake with depth and the conservative behaviour of Cl (Fig. 2.8A). Similar patterns were observed for  $\text{SO}_4$  and Na, indicating that sorption, weathering and element cycling hardly affects  $\text{SO}_4$  and Na concentrations at this site. Concentrations of K, Ca and Mg slowly decreased with depth as a result of ongoing root uptake of cation inputs (by mineralization and throughfall) at the soil surface.  $\text{NH}_4$  concentrations steadily decreased within the upper 40 cm, of the soil profile. While the decrease in  $\text{NH}_4$  concentration with depth is partly caused by root uptake (and possible cation exchange), the simultaneous increase in  $\text{NO}_3$  concentrations in 'Hackfort B' indicates the occurrence of nitrification as well. Annual average concentrations for Al strongly increased between 0 and 40 cm depth, while proton concentrations decreased in spite of increased nitrification. This phenomenon is caused by the dissolution of solid Al phases, including organically bound Al and amorphous Al hydroxides (Mulder et al., 1989; cf Section 3.1, 3.2 and 3.3). The main soil processes responsible for the observed concentration gradients between 0 and 40 cm depth are thus water and nutrient uptake, nitrification and dissolution of Al (Van Breemen et al., 1988).

The presence of more explicit soil horizons in a Carbic Podzol (Tongbersven) as compared to a Dystric Cambisol (Hackfort B) was reflected in the evolution of soil solution chemistry with depth (Fig. 2.8B). The presence of a strongly leached E horizon in the Carbic Podzol (Tongbersven) apparently limits both nitrification and Al dissolution, causing persistence of high concentrations of  $\text{NH}_4$  and H. In the B horizon, the concentration of H strongly decreased, while that of Al strongly increased. Substantial concentrations of  $\text{NH}_4$  were maintained down to 1 m depth (Fig. 2.8B).

Critical levels for Al and  $\text{NH}_4$  in soil solution related to effects on forest vitality (e.g. decreased root uptake) are mostly indicated in terms of molar Al/Ca and  $\text{NH}_4/\text{K}$  ratios, which are regarded as indicators of potential reduction of nutrient uptake by roots. Both ratios showed strong gradients with depth, as illustrated for five intensively monitored sites (Fig. 2.9). The Al/Ca ratios, based on annual average Al and Ca concentrations, for the sites 'Hackfort A, B, C' and 'Tongbersven' were below an assumed critical value of 1.0 (De Vries, 1993; cf Section 4.2) up to a depth of 20 cm, which is the predominant zone of root activity. At the Douglas fir sites, sampled with the centrifugation method, the Al/Ca ratios in April 1987 were somewhat higher than the annual average values of the intensively monitored sites, and invariably above the critical value of 1.0. When applying the Al/Ca ratio as a practical criterium for evaluating measures to reduce soil acidification, a soil layer of 0 to 30 cm seems to be appropriate, considering the dominant occurrence of fine roots in this layer (Grier et al., 1981; Persson, 1983). At 30 cm depth, Al/Ca ratios in all soil monitoring sites were above the critical value.



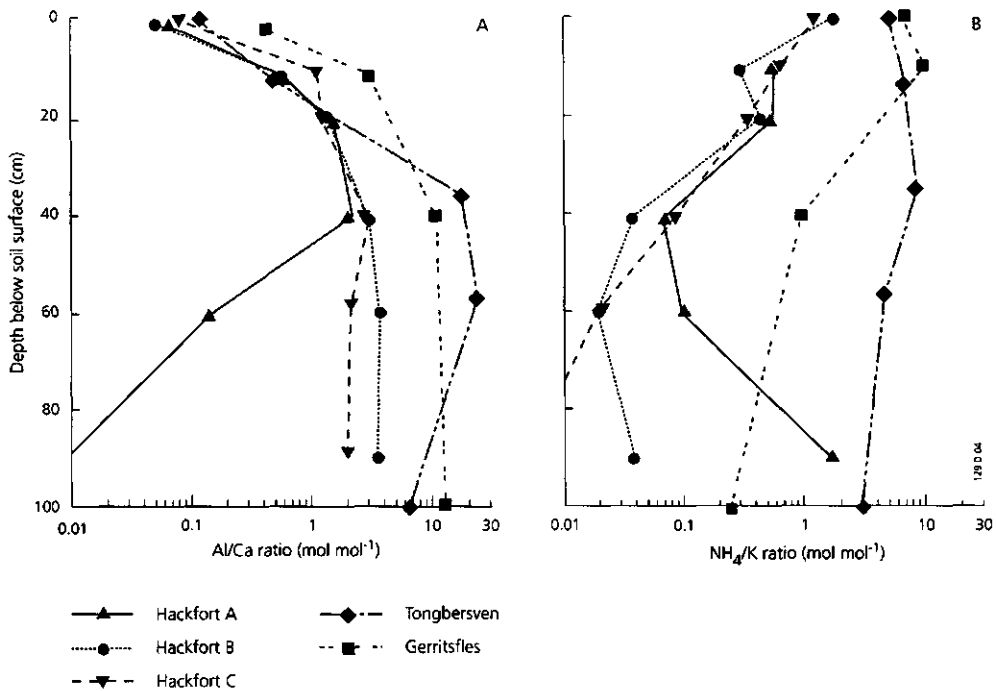


Figure 2.9 Molar Al/Ca ratios (A) and molar  $\text{NH}_4/\text{K}$  ratios (B) in soil solution in five intensively monitored sites

In contrast to Al/Ca ratios,  $\text{NH}_4/\text{K}$  ratios tended to decrease, and so become more favourable for biota, with increasing depth. Molar  $\text{NH}_4/\text{K}$  ratios in the sites 'Tongbersven' and 'Gerritsfles A' (Scots pine) were above an assumed the critical value of 5 (De Vries, 1993; cf Section 4.1) in the upper 30 cm of the soil. The same trend was observed at the Douglas fir sites at 'Lage Vuursche', 'Ruurlo' and 'Zelhem' (data not shown).

Values for the molar Al/Ca and  $\text{NH}_4/\text{K}$  ratio in the survey sites were generally lower than those at the monitoring sites. In the forest topsoil (0-30 cm depth), the critical Al/Ca ratio of 1.0 was exceeded in 57% of the 147 survey sites, whereas only 4% of the survey sites exceeded the critical  $\text{NH}_4/\text{K}$  ratio of 5 (Fig. 2.10). The relatively low Al/Ca ratios were mainly a result of a high Ca concentration. This may partly be the result of a high Ca input from the atmosphere due to strong filtering of base cations by the forest canopy, especially near forest edges (Draayers et al., 1992). Compared to the monitoring sites, the soil survey sites were generally located close to agricultural areas (55% at a distance less than 100 m). Liming and fertilization of the forests in the past may have played a role as well. The most important explanation for the apparent difference between Al/Ca ratios in (intensive) soil monitoring sites and soil survey sites might, however, be the different methodology to obtain soil solution (see Discussion).

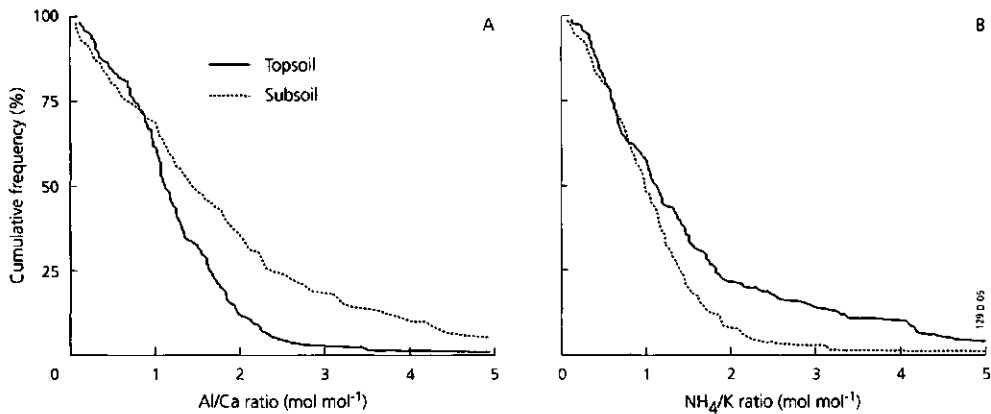


Figure 2.10 Inverse cumulative frequency distributions of the molar Al/Ca ratio (A) and  $\text{NH}_4^+/\text{K}$  ratio (B) in the topsoil (0-30 cm) and subsoil (60-100 cm) of 147 survey sites

#### Variation in time

Another problem when comparing actual soil solution concentrations and ratios with critical values is temporal (interannual) variation. Interannual variation is mainly caused by increased biological activity in the growing season, causing increased transpiration, mineralization/nitrification and nutrient uptake by roots. As the effect of enhanced transpiration and mineralization on soil solution concentrations is to some extent counteracted by nutrient uptake, the change in soil solution composition over the year can not easily be predicted, particularly for  $\text{NH}_4^+$  and  $\text{NO}_3^-$  (Van Breemen et al., 1987).

Molar Al/Ca ratios can vary by a factor of five within the year (Fig. 2.11). For 'Tongbersven' the Al/Ca ratio fluctuated around the critical value. In general highest Al/Ca ratios were found between June and September, which is the period of highest biological activity (water uptake), causing a strong increase in Al concentrations in this period (Mulder et al., 1987). Unfortunately this is also the period when sampling of soil solution often fails, due to low soil water contents. This complicates the establishment of 'safe' Al/Ca ratios on the basis of a comparison of data on soil solution chemistry and forest effects in the field. At present, critical values are mainly based on laboratory experiments (e.g. Rost-Siebert, 1983). Seasonal patterns of the  $\text{NH}_4^+/\text{K}$  ratios were less explicit than for Al/Ca ratios (data not shown). This is obvious because, in contrast to Ca and Al, variations in  $\text{NH}_4^+$  and K are determined by the same processes, i.e. mineralization and root uptake.

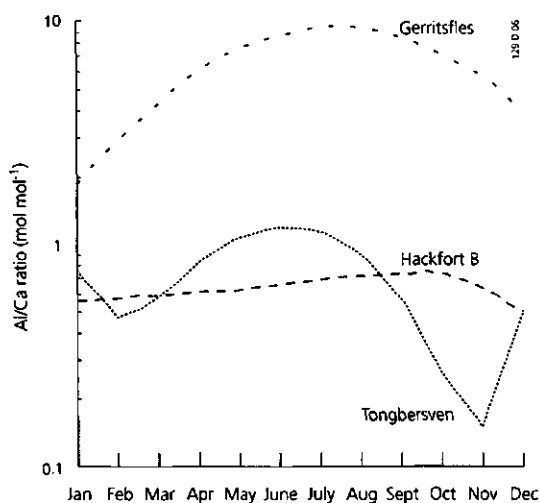


Figure 2.11 The mean seasonal variation of the molar Al/Ca ratio between 1983 and 1987 for 'Hackfort B', 'Tongbersven' and 'Gerritsfles' at 10 cm depth

## Regional variability

### *Influence of tree species and stand characteristics*

The various soil solution parameters in the 147 soil survey sites were largely influenced by tree species (Table 2.14). Lowest pH values and highest concentrations in Al, SO<sub>4</sub> and NO<sub>3</sub> occurred below Norway spruce and Douglas fir. The reverse was true for oak and beech, whereas Japanese larch, Scots pine and black pine occupied an intermediate position. The increase in solute concentrations between tree species, going from deciduous forest to pine forests to spruce forests, is most probably caused by increased dry deposition (Draayers and Erisman, 1993) and evapotranspiration (De Vries and Jansen, 1994). Table 2.14 also shows that SO<sub>4</sub> concentrations were higher than NO<sub>3</sub> concentrations indicating, that atmospheric inputs of S (still) dominate those of N in soil acidification and Al mobilization.

Table 2.14 Median values of important soil solution parameters in the mineral topsoil (0-30 cm) for each tree species in 147 survey sites

Tree species	pH	Concentrations (mol <sub>e</sub> m <sup>-3</sup> )			Ratios (mol <sub>e</sub> mol <sup>-1</sup> )	
		Al	SO <sub>4</sub>	NO <sub>3</sub>	NH <sub>4</sub> /K	Al/Ca
Scots pine	3.61	0.70	0.97	0.47	1.01	1.07
Black pine	3.69	0.62	0.80	0.27	1.19	1.27
Douglas fir	3.41	1.56	2.19	1.07	2.56	1.34
Norway spruce	3.43	1.09	2.02	0.49	2.52	1.42
Japanese larch	3.60	0.74	1.02	0.62	1.67	1.17
Oak	3.69	0.41	0.85	0.57	0.53	0.63
Beech	3.77	0.44	0.63	0.20	0.64	1.17
All species	3.60	0.64	0.99	0.53	1.13	1.09

Table 2.15 Median values of important soil solution parameters in the mineral topsoil (0-30 cm) as a function of tree height and canopy coverage in 147 survey sites

Stand characteristic	pH	Element concentrations (mol <sub>c</sub> .m <sup>-3</sup> )			Ratios (mol.mol <sup>-1</sup> )	
		Al	SO <sub>4</sub>	NO <sub>3</sub>	NH <sub>4</sub> /K	Al/Ca
Tree height (m)						
< 5	3.78	0.19	0.35	0.21	0.80	0.99
5-10	3.73	0.40	0.73	0.31	1.04	0.83
10-15	3.59	0.67	1.0	0.54	1.13	1.14
15-20	3.59	0.73	1.0	0.58	1.45	1.22
> 20	3.60	0.78	1.0	0.53	1.21	1.07
Canopy coverage (%)						
< 50	3.64	0.52	0.83	0.44	0.78	1.15
50-75	3.58	0.63	1.01	0.54	1.45	1.08
> 75	3.64	0.72	1.25	0.63	1.93	1.08

Stand characteristics that mainly influenced the soil solution chemistry were tree height and canopy coverage (Table 2.15). Concentrations of Al, SO<sub>4</sub> and NO<sub>3</sub> increased with increasing tree height and canopy coverage. This is most likely due to an increase in atmospheric S and N deposition with an increase in tree height (Stevens, 1987) and canopy coverage (Draayers et al., 1992). Compared to these parameters, the influence of the distance of the tree to the nearest forest edge appeared to be small for Al and SO<sub>4</sub>. NO<sub>3</sub> concentrations, however, clearly increased in forest stands close to agricultural land (data not shown).

#### Predictions on a regional scale

Relationships between soil solution parameters and stand characteristics were derived by multiple linear regression analysis. Relative good relationships ( $R^2_{adj} > 0.5$ ) were found between the SO<sub>4</sub> and Al concentration and the tree species, tree height and acid atmospheric deposition. Even tree species and tree height alone already explained more than 40% of the variation in SO<sub>4</sub> and Al concentration in the forest topsoil (Table 2.16).

Table 2.16 Regression coefficients in 'ion concentration =  $\alpha_0$  ·  $\alpha_1$  (tree species) ·  $\alpha_2$  (tree height)' for the topsoil (0-30 cm) of 147 survey sites

Ion	$\alpha_0$ <sup>1)</sup> (mol <sub>c</sub> .m <sup>-3</sup> )	$\alpha_1$ <sup>2)</sup>							$\alpha_2$ <sup>3)</sup>				$R^2_{adj}$
		DF	NS	BP	JL	OA	BE	>20m	15-20	10-15	5-10		
SO <sub>4</sub>	0.41	2.48	2.34	1.02	1.04	1.08	0.67	2.48	2.29	2.39	1.60	0.40	
Al	0.28	2.46	1.95	1.08	1.22	0.65	0.73	2.20	2.44	2.48	1.48	0.43	

<sup>1)</sup> The values of  $\alpha_0$  are related to a Scots pine with a tree height < 5 m. The effect of other tree species and tree heights is related to this reference site.

<sup>2)</sup> DF is Douglas fir, NS is Norway spruce, BP is black pine, JL is Japanese larch, OA is oak and BE is beech (for Scots pine  $\alpha_1$  equals 1)

<sup>3)</sup> For a tree height < 5 m,  $\alpha_2$  equals 1

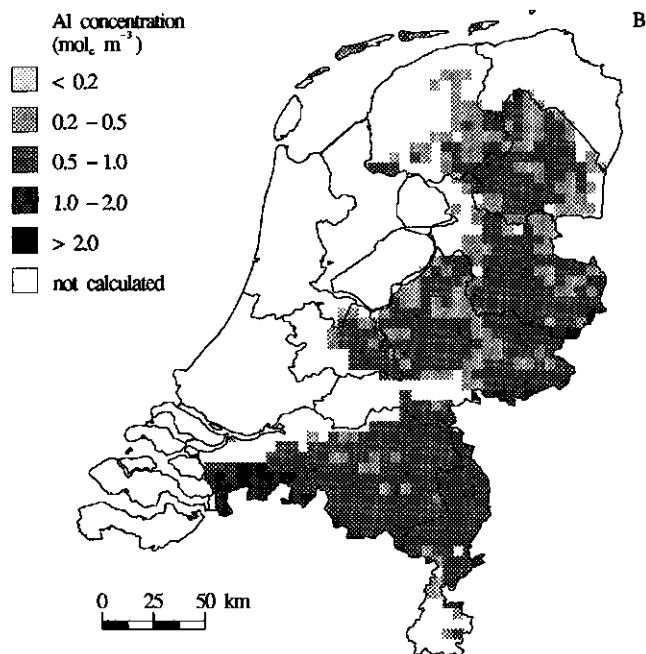
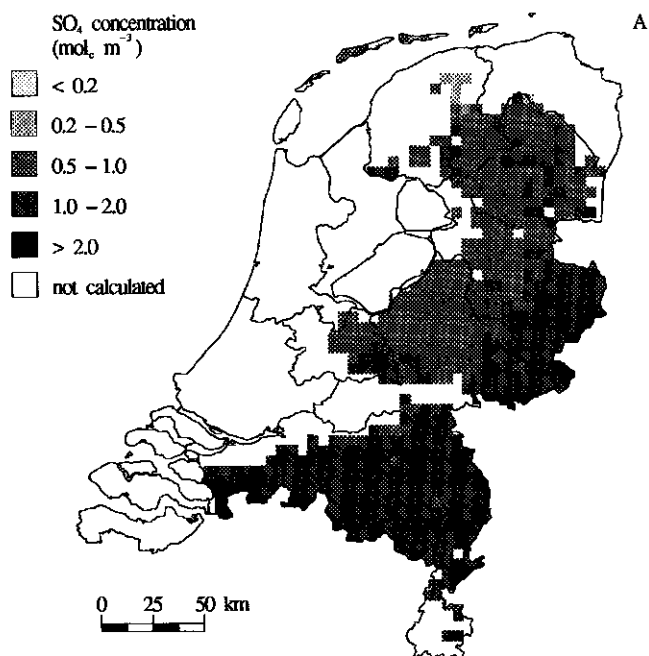


Figure 2.12 Maps of the predicted median SO<sub>4</sub> (A) and Al concentration (B) in the topsoil (0-30 cm) of non-calcareous sandy forest soils in the Netherlands

In case of  $\text{NO}_3$ , the distance of trees to the forest edge was a significant variable. The influence of canopy coverage appeared to be less important. However, it should be noted that there is a relationship between this characteristic and the tree species. For example, the canopy coverage of Douglas fir and Norway spruce is larger than for the other coniferous trees, and furthermore the canopy coverage is often larger with increasing tree height.

The relationships that were found between Al and  $\text{SO}_4$  concentration in non-calcareous forest soils on one hand and the tree species, tree height and atmospheric deposition of  $\text{SO}_4$  and  $\text{NH}_4$  on the other hand were used to produce Al and  $\text{SO}_4$  concentration maps at a grid resolution of 5 km x 5 km (Fig. 2.12). Data on tree species and the age of the stands were derived from a forest data base (the 4<sup>th</sup> Forest Inventory; CBS, 1985) with a resolution of 500 m x 500 m. Tree height was estimated indirectly from the stand age and the underlying soil type (La Bastide and Faber, 1972). Information on the areal distribution of tree species and soil types in each grid was derived by overlaying the forest data base with a soil data base with soil type information in a 100 m x 100 m grid. Atmospheric deposition data on a 5 km x 5 km grid were derived from estimates with the model DEADM for 1990 (Erisman, 1991).

Predicted median soil solution concentrations generally varied from 0.5 to 2.0 mol<sub>c</sub> m<sup>-3</sup> for  $\text{SO}_4$  and from 0.5 to 1.0 mol<sub>c</sub> m<sup>-3</sup> for Al. Highest  $\text{SO}_4$  concentrations were predicted in the southern and eastern part of the Netherlands (median values from 1.0 to 2.0 mol<sub>c</sub> m<sup>-3</sup>). Although  $\text{SO}_4$  and Al concentrations did increase going from the northern to the southern part of the Netherlands, in response to increased deposition in that direction, the predicted difference was rather small. This is due to the large influence of tree species on  $\text{SO}_4$  and Al concentrations. In the northern part (the province of Drenthe), Norway spruce is a dominant tree species, which has a large filtering capacity, while Scots pine is more dominant in the south.

## INPUT-OUTPUT BUDGETS

### Sulphur and nitrogen budgets

#### *Monitoring sites*

Input-output budgets for S and N give insight in the capacity of the soil to retain both elements, by e.g. sorption (S) or incorporation in organic matter (N). Comparison of atmospheric inputs and drainage outputs of  $\text{SO}_4$  for the eighteen soil monitoring sites show that all soils are essentially saturated with  $\text{SO}_4$  (Fig. 2.13A). The  $\text{SO}_4$  saturated character of Dutch forest soils must be attributed to high levels of atmospheric S deposition in combination with relatively low  $\text{SO}_4$  sorption capacities.  $\text{SO}_4$  will be particularly sorbed by Al and Fe oxides, of which the investigated soils contain relatively small fractions (1-3%).

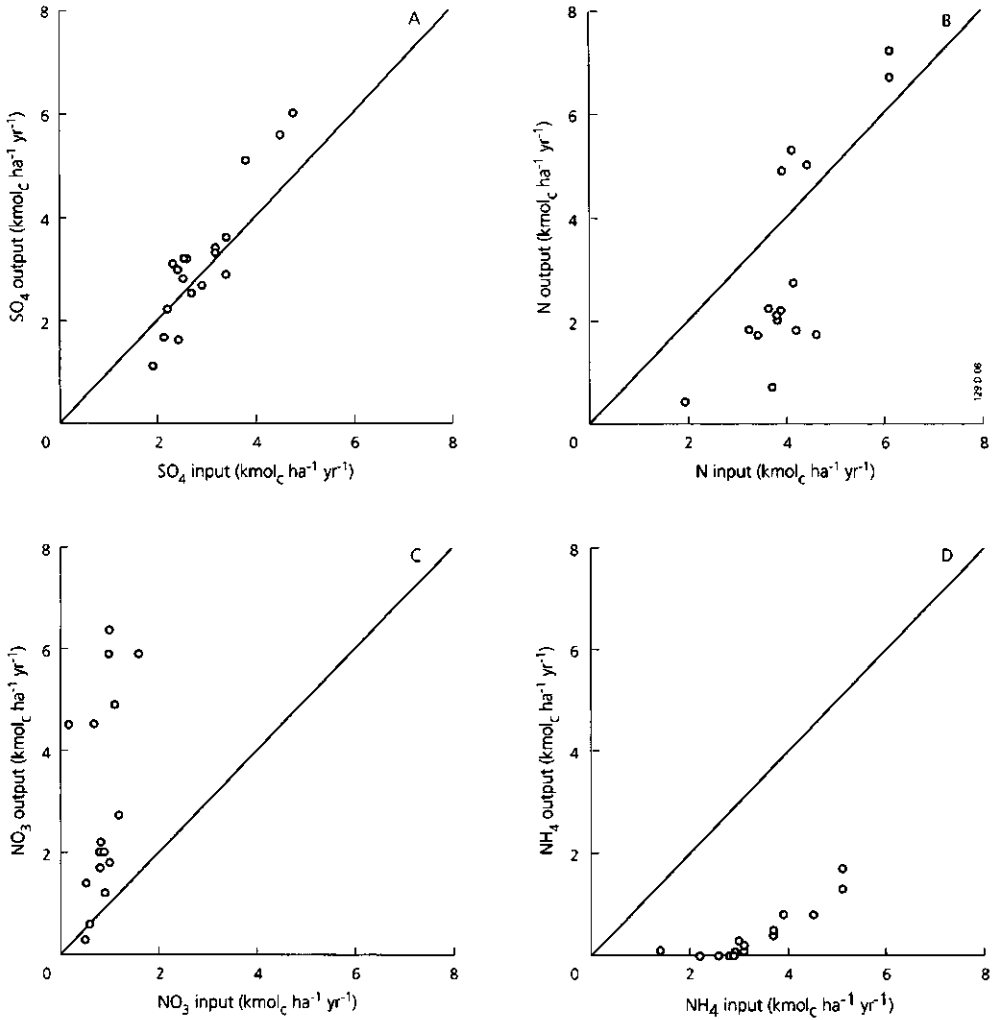


Figure 2.13 Relationship between mean annual input and output fluxes of SO<sub>4</sub> (A), N (B), NO<sub>3</sub> (C) and NH<sub>4</sub> (D) for eighteen monitoring sites

Comparison of atmospheric inputs and drainage outputs of N gave a different picture. Leaching of N (Fig. 2.13B) occurred mainly in the form of NO<sub>3</sub> (cf Fig. 2.13C and 2.13D) in all sites. Up to an external N-input of about 4 kmol ha<sup>-1</sup> yr<sup>-1</sup>, a rather constant amount of 1.5 kmol N (20 kg) was retained annually in the ecosystems (Fig. 2.13B). This amount agrees well with values of net N immobilization reported for the 'Hackfort' sites (Van Breemen and Van Dijk, 1988). At external N inputs higher than 4 kmol ha<sup>-1</sup> yr<sup>-1</sup>, data for five sites suggest that ecosystems may shift rather abruptly to a state of N-saturation (N-output exceeds the

N-input). However, the reliability of the leaching data is questionable since they refer to four extensively monitored Douglas fir sites and only one intensively monitored site (Hackfort A). A state of consistent net N mobilisation indicates that the net uptake of N in stems and branches is reduced, and that the N pool in leaf-, root- and/or microbial biomass is not maintained. So both the vegetation and the decomposing soil microbes may be affected by excessive external loadings of N. In this situation mineralization and nitrification of organic N also contribute to soil acidification. Sites showing N-saturation also leached appreciable amounts of  $\text{NH}_4$  (Fig. 2.13D). At  $\text{NH}_4$  inputs below  $3 \text{ kmol}_c \text{ ha}^{-1} \text{ yr}^{-1}$ ,  $\text{NH}_4$  leaching was nearly negligible (the combined effect of  $\text{NH}_4$  uptake and nitrification) but for  $\text{NH}_4$  inputs above  $3 \text{ kmol}_c \text{ ha}^{-1} \text{ yr}^{-1}$  leaching of  $\text{NH}_4$  increased with increasing input. Again, the  $\text{NH}_4$  leaching data refer to four extensively monitored Douglas fir sites, thus being less reliable.

### Survey sites

Inverse cumulative frequency distributions of the output/input ratio of S and N of the 147 survey sites (Fig. 2.14) show a large variation, which is strongly induced by the uncertainty in the leaching and deposition estimates. This is especially true for the leaching fluxes, since the assumption that  $\text{SO}_4$ ,  $\text{NH}_4$  and  $\text{NO}_3$  concentrations in spring equals the annual average concentrations of these ions will not hold at many sites (cf Table 2.10). However, the figure does show that on average  $\text{SO}_4$  behaves conservatively (median leaching / deposition ratio is nearly 1.0) whereas N is strongly retained in the soil. Only in 2% of the cases the estimated leaching / deposition ratio for N exceeded 1.0 indicating N saturation. The variation in deposition of  $\text{SO}_4$  and  $\text{NO}_3$  was small and of  $\text{NH}_4$  large, whereas the opposite was true for leaching.

Median values of the input and output fluxes and the net budgets of the separate tree species (Table 2.17) show that  $\text{SO}_4$  behaved conservative for nearly each tree species.

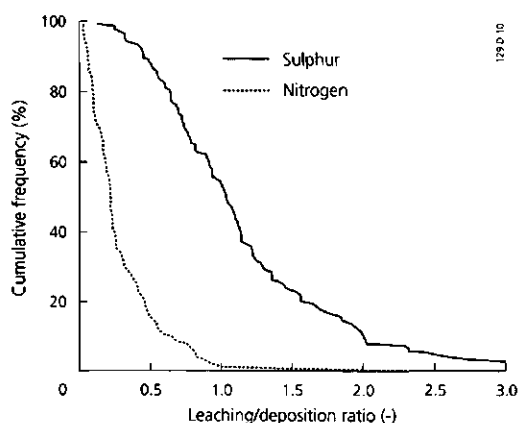


Figure 2.14 Inverse cumulative frequency distributions of the leaching/deposition ratio of S and N for 147 survey sites



Table 2.17 Median annual deposition (in), leaching (out) and their difference (in-out) of SO<sub>4</sub> and N for each tree species in the 147 survey sites

Tree species	SO <sub>4</sub> budget (mol <sub>c</sub> ha <sup>-1</sup> yr <sup>-1</sup> )			N budget (mol <sub>c</sub> ha <sup>-1</sup> yr <sup>-1</sup> )		
	in	out	in-out	in	out	in-out
Scotch pine	2013	2001	12	4092	892	3200
Black pine	1926	1924	2	4954	1157	3797
Douglas fir	2646	2493	153	5034	1885	3149
Norway spruce	1798	1822	-24	4510	453	4057
Japanese larch	1286	1024	244	3206	651	2555
Oak	1283	1771	-488	3428	462	2966
Beech	1403	1415	-12	3473	347	3126
All species	1744	1773	-29	4159	834	3325

Median N leaching, however, was reduced by 80% compared to median N deposition. Differences in N leaching between the tree species were, however, considerable. Compared to the input by deposition, median N retention was smallest for Douglas fir (63%) and greatest for Norway spruce (90%). The contribution of NO<sub>3</sub> to N deposition was relatively small, but median leaching of NO<sub>3</sub> (700 mol<sub>c</sub> ha<sup>-1</sup> yr<sup>-1</sup>) almost equalled median NO<sub>3</sub> deposition (971 mol<sub>c</sub> ha<sup>-1</sup> yr<sup>-1</sup>). Apparently, nitrification compensates for NO<sub>3</sub> loss by uptake and denitrification. NH<sub>4</sub> contributed most to N deposition (median value is 3188 mol<sub>c</sub> ha<sup>-1</sup> yr<sup>-1</sup>), but hardly to N leaching (median value is 134 mol<sub>c</sub> ha<sup>-1</sup> yr<sup>-1</sup>). Nearly all NH<sub>4</sub> was removed by immobilization, nitrification and (preferential) NH<sub>4</sub> uptake.

## Aluminum and base cation mobilization

### Monitoring sites

The strong relation that was found between atmospheric deposition of NH<sub>x</sub>, NO<sub>x</sub> and SO<sub>x</sub> on the one hand and leaching of Al on the other hand at the eighteen monitoring sites (Fig. 2.15) confirms that Al mobilization is the dominant buffer mechanism in acid sandy soils. The proton production associated with leaching of SO<sub>4</sub> and NO<sub>3</sub> (corrected for NH<sub>4</sub>) at these sites (Fig. 2.15B) nearly equalled the production of protons in the soil by N-transformations (Fig. 2.15A). The latter value is equal to the sum of the net consumption (input-output) of NH<sub>4</sub> and the net production (output-input) of NO<sub>3</sub> and includes proton production from external and internal sources of N (Van Breemen et al., 1988; cf Section 2.1). The larger part of the proton production was neutralized by mobilization of Al, except for the sites 'Winterswijk' and 'Hackfort A' which have calcareous subsoils. Proton production which was not neutralized by Al was either leached as free protons or neutralized by mobilization of base cations. Several authors, such as Mulder et al. (1989), Van der Salm and Verstraten (1994) and De Vries (1994a, b) found evidence that most Al is mobilized from a relatively small pool of secondary Al compounds. This pool is rapidly depleted at the present rates of Al mobilization, thus increasing leaching of protons in the future (De Vries and Kros, 1989; cf Section 6.3).

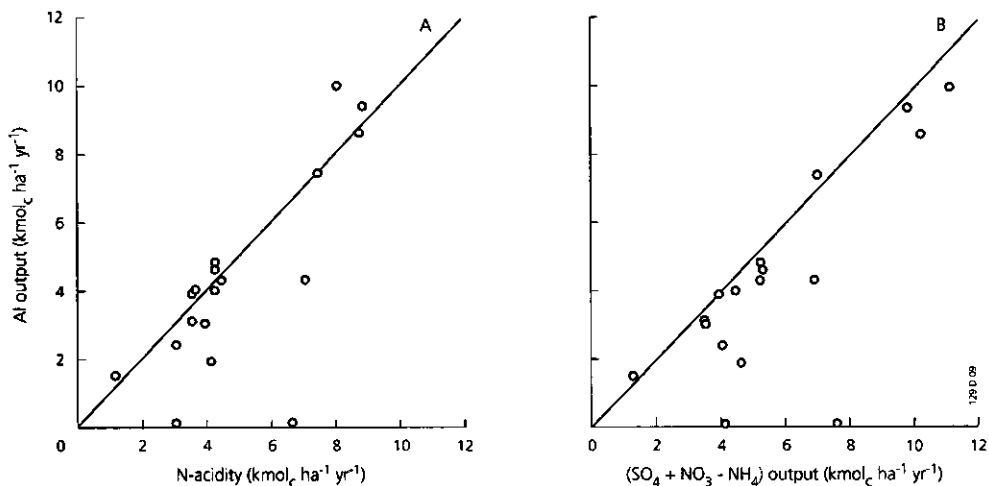


Figure 2.15 Relationships between mean output fluxes of Al and annual proton production from N-transformations (A) and output fluxes of  $SO_4 + NO_3 - NH_4$  (B) at eighteen soil monitoring sites

### Survey sites

Since atmospheric deposition of Al is negligible, Al leaching is entirely due to Al mobilization. At the survey sites, Al mobilization generally decreased going from spruce trees (Douglas fir and Norway spruce) to pine trees (Scots pine and black pine) to deciduous trees (oak and beech; Table 2.18). Although the absolute Al mobilization at the survey sites was much less than at the monitoring sites (cf Table 2.18 and Figure 2.15), the relative contribution of Al mobilization in the total cation release was about equal, i.e. 82%.

Table 2.18 Median Al and BC mobilization fluxes in the rootzone for each tree species in 147 survey sites

Tree species	Mobilization ( $mol_c \text{ ha}^{-1} \text{ yr}^{-1}$ )	
	Al	BC
Scotch pine	1042	358
Black pine	1273	219
Douglas fir	2284	76
Norway spruce	1533	411
Japanese larch	897	176
Oak	422	882
Beech	523	80
All species	976	221

The estimated median value for BC mobilization at all survey sites was much less than Al mobilization, even though the median BC concentration at the soil survey sites was much larger than that of Al. This is because we assumed that a large amount of the base cations originated from dry deposition (cf Section on calculation of input-output budgets). The

overall median value ( $221 \text{ mol}_e \text{ ha}^{-1} \text{ yr}^{-1}$ ) was similar to the estimated average weathering rate of acid sandy forest soils in the Netherlands ( $200 \text{ mol}_e \text{ ha}^{-1} \text{ yr}^{-1}$ ; De Vries, 1993). The large estimated mobilization of base cations (mainly Ca) at the oak stands (Table 2.18) is likely to be an overestimate. Some locations with oaks have high water tables with probable influences of ground water seepage. Another, explanation is an underestimation of Ca (and Mg) input, since nearly all oak stands border agricultural land with relatively high dust inputs.

## DISCUSSION AND CONCLUSIONS

The soil solution data, presented in this section, represent the chemical soil solution composition of acid forest soils in the Netherlands, exposed to moderate or high loadings of atmospheric S and N. The data suggest that acidification rates in the monitoring sites are larger than in the survey sites. This is reflected by larger leaching fluxes (concentrations) of  $\text{SO}_4$ ,  $\text{NO}_3$  and Al, whereas the reverse is true for base cations. One conclusion might be that the monitoring sites are not representative for Dutch forests and are biased towards higher acidification rates, due to the relative large number of sites occupied with Douglas fir (11 out of 18 sites). Atmospheric deposition on these tree species is higher than on pine trees and deciduous trees (Draayers et al., 1992). The difference in average  $\text{SO}_4$  deposition on the monitoring sites ( $2950 \text{ mol}_e \text{ ha}^{-1} \text{ yr}^{-1}$ ; cf Fig. 2.13A) and the survey sites ( $1750 \text{ mol}_e \text{ ha}^{-1} \text{ yr}^{-1}$ ; cf Table 2.17) also points in this direction, although this may partly be due to decreasing  $\text{SO}_4$  deposition during the last decade (monitoring sites were investigated between 1979 and 1990 and survey sites in 1990).

The relative large difference in concentrations and fluxes of solutes in monitoring and survey sites, however, may also be strongly influenced by differences in sampling soil solution. First of all, measured concentrations in the survey sites in March and April are only an approximation of the flux-weighted annual average concentration. For  $\text{SO}_4$ ,  $\text{NO}_3$  and  $\text{NH}_4$ , correlations between concentrations in these months and annual average concentrations appear to be rather weak ( $R^2_{adj}$  between 0.42 and 0.60; cf Table 2.10). For Al and Ca, the correlation is better but here the regression coefficients ( $\alpha_1$ ) indicate that measured Ca concentrations in March and April are likely to be higher than the annual average Ca concentration ( $\alpha_1 > 1$ ) whereas the opposite is true for Al ( $\alpha_1 < 1$ ; cf Table 2.10). Secondly, centrifuge soil solutions deviate from lysimeter soil solutions. For example, Ca concentrations in soil solution obtained by centrifugation (soil survey sites) are generally higher than Ca concentrations in soil solution obtained by suction cups, whereas the opposite is true for Al (Zabowski and Ugolini, 1990; Verhagen and Diederer, 1991). These artefacts, introduced by differences in sampling technique may account for the calculated lower Al/Ca ratios in early spring in the survey sites as compared to the annual average Al/Ca ratio in the (intensively) monitored sites.

Finally, the use of a Cl-corrected precipitation excess, to correct for concentration deviations from annual average values, may cause errors in leaching estimates, especially in forest-soil combinations with a short soil water residence time in the rootzone. Unlike  $\text{SO}_4$  and  $\text{NO}_3$ , Cl deposition is highly variable over the year and high Cl concentrations measured in the subsoil in spring may have partly been caused by a considerable Cl deposition at the very beginning of 1990. Soil water residence times for the various tree species, that were calculated by dividing an estimated moisture content in the rootzone (mm) by an estimated precipitation excess ( $\text{mm yr}^{-1}$ ), were generally longer than one year for the coniferous trees and less than one year for deciduous trees (De Vries and Jansen, 1994). The correction in precipitation excess for deciduous trees (cf Table 2.12) may thus be too large causing an underestimation in leaching fluxes. However, combining the original precipitation excesses with measured  $\text{SO}_4$  concentrations is certainly not correct. This would result in a large removal of  $\text{SO}_4$  from soils below deciduous trees (including Japanese larch), which is very unlikely (cf De Vries and Jansen, 1994).

Despite the various uncertainties in results for the survey sites, the following conclusions can be drawn regarding concentrations and fluxes of soil solutes in Dutch acid sandy forest soils:

- (i) High levels of atmospheric deposition of S and N cause soil solutions to be dominated by  $\text{SO}_4$ ,  $\text{NO}_3$  and Al. In absence of calcareous subsoils, Al concentrations always exceeded the EC drinking water standard of  $0.2 \text{ mg l}^{-1}$ , irrespective of soil and vegetation type. The drinking water standard of  $\text{NO}_3$  ( $50 \text{ mg l}^{-1}$ ) was also exceeded in part of the investigated sites.
- (ii) There is an increasing linearity and proportionality between the concentration of H+Al and that of  $\text{SO}_4$ + $\text{NO}_3$  with increasing depth. In most monitoring sites, almost perfect 1:1 relationships were found near 1 m depth.
- (iii) Soil solution chemistry shows strong gradients with depth, in particular in podzolic soils where nitrification and Al mobilization is subdued above the B-horizon. In all monitoring sites molar Al/Ca ratios increased with depth, and generally exceeded an assumed critical value of 1.0 below 20 cm depth. Molar  $\text{NH}_4$ /K ratios decreased with depth and generally exceeded an assumed critical value of 5 in the upper 20 cm, which is the zone of predominant biological activity. Both Al/Ca ratios and  $\text{NH}_4$ /K ratios were highest between June and September, when biological activity is highest.
- (iv) The regional variation in soil solution chemistry strongly depends on tree species and, to a lesser extent, on tree height and deposition level. Concentrations of H, Al,  $\text{SO}_4$  and  $\text{NO}_3$  decrease in the order spruce forest (Norway spruce, Douglas fir) > pine forests (Scots pine, black pine) > deciduous forests (oak, beech).
- (v) Soils are invariably saturated with  $\text{SO}_4$ . In all monitoring sites,  $\text{SO}_4$  leaching equalled  $\text{SO}_4$  deposition. Furthermore, median values for  $\text{SO}_4$  leaching and  $\text{SO}_4$  deposition were equal for all tree species included in the survey sites.
- (vi) There is still a relatively large N (even a nearly complete  $\text{NH}_4$ ) retention in most soils. This can be derived from the results of the survey sites, which indicate that N saturation and appreciable  $\text{NH}_4$  leaching hardly occurs. Results from monitoring

studies, which indicate that forest soils become abruptly saturated with N above an N loading of  $4 \text{ kmol ha}^{-1} \text{ yr}^{-1}$ , and that  $\text{NH}_4$  leaching becomes proportional to  $\text{NH}_4$  loadings above  $\text{NH}_4$  inputs of  $3 \text{ kmol}_c \text{ ha}^{-1} \text{ yr}^{-1}$ , are likely biased by, relatively unreliable, high estimates for the leaching of  $\text{NO}_3$  and  $\text{NH}_4$  in four extensively monitored Douglas fir sites.

- (vii) Al mobilization is the major buffer mechanism in acid sandy soils. Even in the survey sites where Al mobilization was considerably lower than in the monitoring sites, which is mainly due to a lower  $\text{SO}_4$  deposition and a larger retention of N, it still accounts for 80% of the cation release (the remaining 20% refers to base cation mobilization).

In conclusion, we can say that the results indicate that a decrease in S and N deposition will cause an equivalent decrease in concentrations and fluxes of H and Al in acid forest soils.

# Chapter 3

## RATES AND MECHANISMS OF CATION AND SILICA RELEASE IN ACID SANDY SOILS

### 3.1 INFLUENCE OF MINERAL POOLS AND MINERAL DEPLETION

- INTRODUCTION
- MATERIALS AND METHODS
- RESULTS AND DISCUSSION
- CONCLUSIONS

### 3.2 EFFECTS OF pH AND ALUMINIUM CONCENTRATION

- INTRODUCTION
- MATERIALS AND METHODS
- RESULTS AND DISCUSSION
- CONCLUSIONS

### 3.3 DIFFERENCES BETWEEN SOIL TYPES AND SOIL HORIZONS

- INTRODUCTION
- MATERIALS AND METHODS
- RESULTS AND DISCUSSION
- CONCLUSIONS

Chapter 3 has been submitted to Geoderma as:

W. de Vries. *Rates and mechanisms of cation and silica release in acid sandy soils: 1. Influence of mineral pools and mineral depletion.*

W. de Vries. *Rates and mechanisms of cation and silica release in acid sandy soils: 2. Effects of pH and aluminium concentration.*

W. de Vries, M.M.T. Meulenbrugge, W. Balkema, J.C.H. Voogd and R.C. Sjardijn. *Rates and mechanisms of cation and silica release in acid sandy soils: 3. Differences between soil horizons and soil types.*

### 3.1 INFLUENCE OF MINERAL POOLS AND MINERAL DEPLETION

#### ABSTRACT

*Rates and mechanisms of cation and silica release at pH 3.0 were studied in four mineral horizons, i.e. an (A+B)<sub>p</sub>, Bh, BCs and C horizon, of three acid sandy forest soils. One-year batch experiments were performed at nearly constant ionic strength and temperature (20°C). Exchangeable cation contents were measured before and after the experiment to distinguish between weathering (dissolution) and cation exchange. Furthermore, a sequential extraction of Al by lanthanum chloride, ammonium oxalate and dithionite-citrate-bicarbonate was performed before and after the experiment to gain insight in the contribution of various solid-phase pools of Al to total Al release. Results showed that (i) Al dissolution is the dominant acid neutralizing mechanism in all horizons, exceeding Fe and BC release by a factor 10-50, (ii) Si release is high in the BCs horizon, indicating a readily dissolving pool of secondary aluminosilicates, (iii) Al release rates decrease exponentially with cumulative Al release (depletion of Al pool), (iv) inorganic secondary Al compounds are the dominant source of Al release although organically complexed Al may play an important role in the (A+B)<sub>p</sub> and Bh horizon and (v) cation exchange plays a relative important role in base cation release in the (A+B)<sub>p</sub> and Bh horizon but not in the BCs and C horizon.*

#### INTRODUCTION

Elevated deposition rates of SO<sub>x</sub>, NO<sub>x</sub> and NH<sub>x</sub> in the Netherlands have caused high Al concentrations and low pH values in the soil solution of non-calcareous sandy forest soils (Heij et al., 1991). Toxic effects of Al and H on roots (e.g. Boxman and Van Dijk, 1988) may be an important factor for a decrease in forest vitality. To predict changes in soil and soil solution, especially Al, chemistry in response to changes in acid inputs, various dynamic soil acidification models have been developed in the Netherlands, including SMART (Section 6.1; De Vries et al., 1989b) and RESAM (Section 6.2; De Vries et al., 1994b). Key processes in these models are geochemical interactions, i.e. base cation weathering from silicates, cation exchange and dissolution of Al from secondary compounds (e.g. Al hydroxides). Insight in the rates and mechanisms of cation release in response to acid inputs is therefore of utmost importance to simulate changes in soil (solution) chemistry.

Previous laboratory studies on cation release have mainly focused on weathering of pure minerals, to present theories on weathering mechanisms such as the surface precipitate hypothesis (e.g. Wollast, 1967; Helgeson, 1971), the leached layer hypothesis (e.g. Busenberg and Clemency, 1976) and the surface reaction hypothesis (e.g. Lasaga, 1983; Helgeson et al., 1984; Velbel, 1986). Recently, laboratory studies on whole soil samples have also been performed to derive insight in the dissolution kinetics of Al and base cations (e.g. Van Grinsven et al., 1986; 1992) and in the contribution of various solid-phase pools of Al to Al release rates (e.g. Dahlgren and Walker, 1993; Van der Salm and Verstraten, 1994) of acid sandy soils. However, a systematic analyses of



both rates and mechanisms of cation release in all major horizons of sandy soils, including the effect of pH, Al concentration and Al depletion on the dissolution kinetics of Al is still lacking.

In this Chapter results are given of cation and silica (Si) release rates from various pools (silicates, adsorption complex, reactive Al pools) in all major soil horizons of acid sandy soils in the Netherlands. Results are based on batch and column experiments. Emphasis is given to the dynamics of Al release which is the dominant process in these soils. Four major features of the experiments conducted are:

- (i) Sample pretreatment was limited to sieving and air drying (which hardly influences the results; Dahlgren and Walker, 1993) and stirring was very mild in the batch experiments, to minimize the discrepancy between laboratory and field weathering (dissolution) rates (cf Van Grinsven and Van Riemsdijk, 1992).
- (ii) Both pH and Al concentration were kept (nearly) constant in all experiments; and
- (iii) Batch experiments were conducted during one year to obtain detectable rates of base cation weathering.
- (iv) Pools of exchangeable cations and reactive Al and Fe compounds were measured before and after the experiment.

Until now hardly any experiment fulfills all these four conditions. Especially the time period of batch experiments is generally much shorter, causing inaccurate estimates of the release of Al compounds from various sources (e.g. Van Grinsven et al., 1992).

In this section, results are given of cation and Si release in four major soil horizons, measured in batch experiments at pH 3.0. Studied soil horizons are an (A+B)<sub>p</sub>, Bh, BCs and C horizon of three acid podzolic soils in the Netherlands. In Section 3.2, the influence of pH and Al concentration on cation and Si release rates in these soil horizons is described. In Section 3.3, differences in cation and Si release between soil types and soil horizons are described in more detail.

The objective of the study presented in this section was to gain insight in:

- (i) rates of cation and Si release from the various horizons as a function of time and mineral depletion.
- (ii) the contribution of weathering and cation exchange to the total release of base cations.
- (iii) the contribution of various solid-phase pools of Al to the total Al release.

## **MATERIALS AND METHODS**

### **Soil samples and basic chemical analyses**

Soil samples were taken from acid sandy soils at three forested sites in the Netherlands (Kootwijk, Ugchelen and Lijnt Erp), i.e. two Carbic podzols (FAO, 1988) or Typic

Haplohumods (USDA, 1975) and one Gleyic Podzol (FAO, 1988) or Typic Haplaquod (USDA, 1975). Further in this section, the soils will be identified by their name in the FAO classification. The samples were selected from a total of 63 (De Vries et al., 1994g; Section 3.3), because of their large reactive Al pool, thus allowing reliable estimates of Al depletion from various sources. Information on soil characteristics of the samples used is given in Table 3.1. All samples were sieved over 2 mm mesh width, to remove stones and roots, and air dried before storage.

Table 3.1 Basic physical and chemical characteristics of the soil samples studied

Location	Soil type (FAO, 1988)	Soil horizon	Soil depth (cm)	Bulk density (kg m <sup>-3</sup> )	pH- KCl	Organic matter (%)	Particle size distribution (%)		
							<2 $\mu$	2-50 $\mu$	>50 $\mu$
Kootwijk	Carbic Podzol	(A+B)p	0-15	1190	3.6	6.8	3.1	7.6	89.3
Ugchelen	Carbic Podzol	Bh	20-27	1110	3.7	11.1	0.8	15.7	82.5
Ugchelen	Carbic Podzol	BCs	37-52	1550	4.0	0.6	0.3	2.2	97.5
Lijnt Erp	Gleyic Podzol	C	65-80	1640	4.4	0.2	0.5	2.0	97.5

To gain insight in the various pools of cations, total contents were measured by destruction with concentrated HF (Langmyhr and Paus, 1968), whereas adsorbed contents were determined in a 0.01 N silver thiourea (AgTu) extract (Pleysier and Juo, 1980) except for NH<sub>4</sub>, which was measured in a 1 N KCl extract (Coleman et al., 1959). Concentrations of the various cations were determined with an Inductively Coupled Plasma Emission Spectrometer (ICP; Al, Fe, Ca and Mg), an Atomic Absorption Spectrometer (AAS; K and Na) and a Flow Injection Analyser (FIA; NH<sub>4</sub>). The exchangeable proton content was calculated by subtraction of the sum of all exchangeable cations (Al, Fe, Mn, NH<sub>4</sub>, Ca, Mg, K and Na) from the effective CEC, that was derived from the silver consumption. Exchangeable cation contents generally decreased going from the (A+B)p to the C horizon, whereas the total cation contents generally increased in that direction (Table 3.2). In all samples exchangeable base cation contents were extremely low (the base saturation was less than 10%).

Table 3.2 Total and exchangeable cation contents of the soil samples studied

Element	Total content (mmol <sub>e</sub> kg <sup>-1</sup> )				Exchangeable content (mmol <sub>e</sub> kg <sup>-1</sup> )			
	(A+B)p	Bh	BCs	C	(A+B)p	Bh	BCs	C
H					8.3	8.9	5.4	0.01
Al	1401	1630	1573	1972	24	36	4.8	1.25
Fe	285	318	178	182	2.2	1.1	0.15	0.05
Ca	35	72	105	90	1.57	0.52	0.00	0.03
Mg	28	18	35	20	0.34	0.24	0.01	0.01
K	325	120	156	271	0.24	0.46	0.00	0.05
Na	207	71	120	183	0.25	0.22	0.00	0.05
Total <sup>1)</sup>	2281	2229	2167	2637	37	48	10.4	1.40

<sup>1)</sup> Sum of all cations, which equals the acid neutralizing capacity (ANC) when total contents are considered and the cation exchange capacity (CEC) when exchangeable cations are considered

## Secondary aluminium and iron compounds

Total Al and Fe includes Al and Fe in primary minerals (silicates) and in secondary compounds. More information on the secondary Al and Fe pools was obtained by a sequential extraction with lanthanum chloride (organically complexed Al and Fe; Bloom et al., 1979a); ammonium oxalate (amorphous secondary Al and Fe minerals; Schwertmann, 1964) and dithionite-citrate-bicarbonate (crystalline secondary Al and Fe minerals; Mehra and Jackson, 1960).

Pools of secondary Al and Fe compounds decreased according to: Bh horizon > (A+B)p ≈ BCs horizon > C horizon (Table 3.3). Compared to the total content of Al, the pool of secondary Al compounds is quite limited, especially in the C horizon. Unlike Al, the pool of secondary Fe compounds is quite comparable to total Fe, especially in the (A+B)p and Bh horizon (cf Table 3.2 and 3.3).

Table 3.3 Pools of secondary Al and Fe compounds in the soil samples studied

Pools	Al content (mmol <sub>c</sub> kg <sup>-1</sup> )				Fe content (mmol <sub>c</sub> kg <sup>-1</sup> )			
	(A+B)p	Bh	BCs	C	(A+B)p	Bh	BCs	C
Organic <sup>1)</sup>	78	106	11	5.4	6.3	1.4	0.30	1.8
Amorphous <sup>1)</sup>	209	515	241	103	210	214	20	38
Crystalline <sup>1)</sup>	11	31	13	7.0	38	29	20	7.7
Secondary <sup>2)</sup>	298	652	265	115	254	244	40	48
Reactive <sup>3)</sup>	322	688	270	117	258	246	40	48

<sup>1)</sup> Indicative terms, since the specificity of the various extraction methods in extracting these pools is unknown. Organic stands for the pool of Al extracted with lanthanum chloride minus silver thiourea, amorphous for Al in oxalate minus Al in lanthanum chloride and crystalline for Al in dithionite minus Al in oxalate

<sup>2)</sup> Sum of organic, amorphous and crystalline secondary Al and Fe compounds. Further denoted as secondary Al and Fe pool.

<sup>3)</sup> Sum of exchangeable Al and Fe (see Table 3.2) and secondary Al and Fe compounds. Further denoted as reactive Al and Fe pool.

The various methods that were used to determine organic, amorphous and crystalline secondary Al and Fe compounds are operationally defined and their specificity in extracting the various pools is not exactly known. This holds specifically for Al. Regarding organically complexed Al, extraction by pyrophosphate (McKeague, 1967) is often used, but this extractant most likely overestimates this Al pool, especially in the lower B and C horizons (Childs et al., 1983). This can also be derived by comparing the complexing capacity of organic carbon with the amount of pyrophosphate extractable Al, or Al+Fe, per kg carbon for the soil samples studied (Table 3.4). The amount of Al extracted with pyrophosphate approached or exceeded the amount of Al extracted with oxalate in all horizons, except for the BCs horizon. The negligible difference in Al extracted by pyrophosphate and oxalate has often been reported in literature for A and B horizons of podzolic soils (Mokma and Buurman, 1982; Van Grinsven et al., 1992; Dahlgren and Walker, 1993).

Table 3.4 Extracted Al and Al+Fe in lanthanum chloride (LaCl<sub>3</sub>) and sodium pyrophosphate per kg organic carbon in the soil samples studied<sup>1)</sup>

Soil horizon	Extracted Al (mol <sub>c</sub> kg <sup>-1</sup> C) <sup>2)</sup>		Extracted Al and Fe (mol <sub>c</sub> kg <sup>-1</sup> C) <sup>2)</sup>	
	LaCl <sub>3</sub>	pyrophosphate <sup>3)</sup>	LaCl <sub>3</sub>	pyrophosphate <sup>3)</sup>
(A+B)p	3.0	7.7 (8.4)	3.2	11 (16)
Bh	2.6	12 (12)	2.6	15 (16)
BCs	5.5	39 (86)	5.4	42 (93)
C	6.7	107 (109)	8.5	143 (149)

<sup>1)</sup> The organic carbon content was calculated as 50% of the organic matter content (Table 3.1). The complexing capacity of organic carbon is ca. 11 mol<sub>c</sub> kg<sup>-1</sup>

<sup>2)</sup> Includes exchangeable Al or Al and Fe

<sup>3)</sup> Values in brackets refer to oxalate-extractable Al or Al and Fe

The capacity of organic carbon to complex metals on carboxyl groups, the primary binding sites of humic substances, varies from ca. 4 mol<sub>c</sub> kg<sup>-1</sup> in A horizons to 8 mol<sub>c</sub> kg<sup>-1</sup> in B and C horizons. These values can be derived from (i) relationships between the CEC at pH 8 and the organic carbon content (Helling et al., 1964; Kalisz and Stone, 1980; Mokma and Buurman, 1982) and (ii) the concentration of carboxyl groups in fulvic and humic acids (ca. 14 and 5 mol<sub>c</sub> kg<sup>-1</sup> C, respectively; Stevenson, 1982; Wesemael and Verstraten, 1993) multiplied by the fraction of fulvic and humic acids in soil organic carbon (ca. 30% in A horizons; Wesemael and Verstraten, 1993 to ca. 80% in B horizons; Stevenson, 1982). Including the complexing capacity of weakly acidic phenolic groups, titratable up to pH 11, the binding capacity of organic carbon might be as high as 11 mol<sub>c</sub> kg<sup>-1</sup> (De Wit et al., 1993). These authors calculated a maximum negative charge of carboxylic and phenolic groups of 6-11 mol<sub>c</sub> kg<sup>-1</sup> C, based on 11 proton titration datasets for humic substances. Unlike lanthanum chloride, the measured amounts of Al and certainly of Al+Fe, per kg C in sodium pyrophosphate exceeded a maximum capacity of 11 mol<sub>c</sub> kg<sup>-1</sup> C in the Bh, BCs and C horizon (Table 3.4). Values for the lower BCs and C horizon are, however, quite unreliable because of the uncertainty in the extremely low organic C content. Nevertheless, it is clear that pyrophosphate overestimates the pool of organically complexed Al in soil horizons, at greater depth.

In most literature (e.g. Mokma and Buurman, 1982; Dahlgren and Walker, 1993), sodium pyrophosphate is assumed to extract Al and Fe below the maximum complexing capacity of organic matter, based on the calculation of a maximum molar (Al+Fe)/C ratio of 0.16 by Higashi et al. (1981). However, this value is far too high. First, Higashi et al. (1981) took a maximum complexing capacity of organic matter of 14 mol<sub>c</sub> kg<sup>-1</sup> C (which is very high) and furthermore, they assumed that every cation (Al, Fe) is bound to only one carboxyl group. However, the prevalent Al and Fe form in the solution of podzol A and B horizons, with a pH below 4, is Al<sup>3+</sup> and Fe<sup>3+</sup>. Consequently, binding of one mol Al or Fe needs a negative charge of three mol<sub>c</sub> of carboxylic and phenolic groups, assuming that the organic pool is uncharged. This means that the maximum molar (Al+Fe)/C ratio does not exceed 0.05 (using a complexing capacity of 11 mol<sub>c</sub> kg<sup>-1</sup> C).

## Batch experiments at constant pH levels

To study the influence of mineral depletion on cation release rates, batch experiments were conducted during one-year at a constant temperature of 20°C at pH 3.0. First a 75 ml mixture of sulphuric and nitric acid at pH 3.0, containing the most important cations (Al, Ca, Mg), was added to 7.5 g of soil in a 100 ml plastic container. Based on results of the soil solution chemistry of Dutch forest soils (cf Section 2.3), concentrations of the various ions were set equal to 1.5 mol<sub>c</sub> m<sup>-3</sup> for SO<sub>4</sub>, NO<sub>3</sub> and Al, 0.3 mol<sub>c</sub> m<sup>-3</sup> for Ca and 0.2 mol<sub>c</sub> m<sup>-3</sup> for Mg. The proton activity equalled 1.0 mol<sub>c</sub> m<sup>-3</sup> (pH 3.0). The total cation concentration, including H, thus equalled ca. 3.0 mol<sub>c</sub> m<sup>-3</sup>. During the experiment the samples were gently shaken. Since the experiments are very time consuming, they were not conducted in replicate. Replicates of batch experiments at pH 3.0 with eight other soil samples gave a reproduction of acid neutralization and Al release rates within 10% (cf Section 3.3).

The pH and the total cation concentration (ionic strength) were kept constant by intermittent titration with an H<sub>2</sub>SO<sub>4</sub>-HNO<sub>3</sub> mixture, with a concentration of 3.0 mol<sub>c</sub> m<sup>-3</sup> that equals the concentration of all cations added initially to the solution. Concentrations of SO<sub>4</sub> and NO<sub>3</sub> in solution thus hardly changed during the experiment. Since Al mobilization was the dominant source of cation release, changes in the concentration of Al during the experiment were also small. The time intervals at which pH was measured, and titrated to the desired value of 3.0, increased from hours during the first day of the experiment (i.e. after 0.25, 0.50, 0.75, 1, 2, 3, 4, 5, 6 and 24 hours), to days up to the seventh day, to weeks up to the end of the experiment (52 weeks). Generally, the pH did not increase more than 0.1 pH unit during these time intervals, except for the first day. The pH was measured with an NH<sub>4</sub>Cl (instead of KCl) electrode to avoid K release from the electrode.

The acid neutralization rate was calculated from the amount of H added to maintain the pH at the desired level. The cation and silica release rates were calculated by measuring the concentration of Si, Al, Fe, Ca, Mg (ICP), K and Na (AAS) in solution in each 25 ml aliquot after 25 ml of acid mixture had been added. The number of aliquots varied between 14 and 29 depending on the soil horizon. Concentrations of NH<sub>4</sub>, SO<sub>4</sub>, NO<sub>3</sub> and Cl were also measured (FIA) to gain insight in the possible interactions of these ions with the soil (e.g. mineralization, denitrification or SO<sub>4</sub> adsorption). Furthermore, the possible mobilization of organic anions was investigated, by assuming that the difference in the concentration of all cations minus all anions (anion deficit) equals the concentration of organic anions (RCOO). By measuring the exchangeable cation contents and the various solid phase pools of Al and Fe before and after the experiment (cf section on soil samples and chemical analysis), insight was gained in the contribution of (i) cation exchange and weathering to the total cation release rate and (ii) dissolution of organically complexed Al and of amorphous and crystalline secondary Al compounds to the total Al dissolution rate.

## Computational procedures

The release rate of each cation X during a given time interval,  $\Delta t$ , was calculated as:

$$RR_{X,t} = \frac{(V_t - V_{t-1}) \cdot [X]_t + V_{t-1} \cdot ([X]_t - [X]_{t-1})}{A_s \cdot \Delta t} \quad (3.1)$$

where  $RR_{X,t}$  is the release rate of cation X at time  $t$  ( $\text{mmol}_c \text{ kg}^{-1} \text{ d}^{-1}$ ),  $V_t$  and  $V_{t-1}$  are the solution volumes ( $\text{m}^3$ ) at time  $t$  (in days;  $d$ ) and time  $t-1$  respectively,  $[X]_t$  and  $[X]_{t-1}$  are the concentrations of ion X at  $t$  and  $t-1$ , respectively ( $\text{mol}_c \text{ m}^{-3}$ ),  $A_s$  is the amount of soil (kg) and  $\Delta t$  is the time interval between  $t$  and  $t-1$ . The first term in the numerator of Eq. (3.1) equals the amount of cations in the 25 ml aliquot whereas the second term equals the change in cation amount in the plastic container.

The cumulative release of each cation X, i.e. the integral of the release rate over time, was fitted as a function of time by various empirical equations, i.e. an empirical three parameter model (Eq. 3.2), a double logarithmic equation (Eq. 3.3) and a single logarithmic equation (Eq. 3.4):

$$CR_{X,t} = \frac{\alpha_1 \cdot t}{\alpha_2 + t} + \alpha_3 \cdot t \quad (3.2)$$

$$\log CR_{X,t} = \log \alpha_4 + \alpha_5 \log t \quad (3.3)$$

$$CR_{X,t} = \alpha_6 + \alpha_7 \ln t \quad (3.4)$$

where  $CR_{X,t}$  is the cumulative release of cation X at time  $t$  ( $\text{mmol}_c \text{ kg}^{-1}$ ),  $t$  is time ( $d$ ),  $\alpha_1$ ,  $\alpha_4$  and  $\alpha_6$  are capacity parameters, ( $\alpha_4$  and  $\alpha_6$  give the cumulative cation release at  $t$  is one day:  $\text{mmol}_c \text{ kg}^{-1}$ );  $\alpha_2$  is a time parameter ( $d$ ) and  $\alpha_3$ ,  $\alpha_5$  and  $\alpha_7$  are rate parameters. The three parameter model (Van Grinsven and Van Riemsdijk, 1992) was applied to distinguish between a fast reacting pool ( $\alpha_1$ ) with a non-linear dissolution behaviour (with a half-life time  $\alpha_2$ ) and a linear long-term release (weathering) rate  $\alpha_3$ . Values for  $\alpha_1$ ,  $\alpha_2$  and  $\alpha_3$  were derived by minimizing the sum of squares of deviations between model results and experimental data for the cumulative cation release, using a non-linear curve fitting programme (Freyer, 1990).

Parameters in the double and single logarithmic equations, were estimated by linear regression analysis. Both equations can be derived from the relationship:

$$RR_{X,t} = \alpha_8 \cdot t^{\alpha_9} \quad (3.5a) \quad \text{or} \quad \log RR_{X,t} = \log \alpha_8 + \alpha_9 \log t \quad (3.5b)$$

where  $\alpha_8$  and  $\alpha_9$  are parameters. Eq. (3.3) can be derived from Eq. (3.5a) by integration and logarithmization, whereas Eq. (3.4) can be derived by integrating Eq. (3.5a) for the specific situation that  $\alpha_9$  is - 1. The equations were applied to investigate whether diffusion through the mineral surface influences initial (base) cation release. In that case  $\alpha_9 = 0.5$  ( $\alpha_9 = -0.5$ ; Wollast, 1967).

The release rate of each cation X was also fitted as a function of the cumulative release, i.e. the depletion of the solid-phase pool of that cation, by a double and a single logarithmic equation according to:

$$\log RR_{X,t} = \log \alpha_{10} + \alpha_{11} \log CR_{X,t} \quad (3.6)$$

$$\ln RR_{X,t} = \ln \alpha_{12} + \alpha_{13} CR_{X,t} \quad (3.7)$$

where  $\alpha_{10}$  and  $\alpha_{12}$  are rate parameters ( $\text{mmol}_c \text{ kg}^{-1} \text{ d}^{-1}$ ) and  $\alpha_{11}$  and  $\alpha_{13}$  are time parameters. The major use of Eq. (3.6) and (3.7) is the practical application in soil acidification modelling, as it gives an empirical relation between the release rate and the solid-phase pool (depletion) of a cation X. Again, Eq. (3.6) and (3.7) can both be derived from Eq. (3.5a) as shown in Annex B. The single logarithmic equation (3.7) refers to the specific situation that  $\alpha_9$  is - 1. This so called Elovich equation has often been used to describe P sorption behaviour on secondary Al compounds (e.g. Van Riemsdijk and De Haan, 1981; Schoumans et al., 1987; Van der Zee and Van Riemsdijk, 1988; in that case, both  $RR$  and  $CR$  are negative since P adsorption rate decreases exponentially with the cumulative P adsorption).

## RESULTS AND DISCUSSION

### Annual cation and silica release

Cumulative release of cations during one-year batch experiments invariably showed that Al dissolution is the dominant source of cation release (ca. 90%) and acid neutralization in the various soil horizons (Table 3.5). In the BCs and C horizon the total cation release corresponded well with the rate of proton consumption (differences of ca. 2%). However, in the (A+B)<sub>p</sub> and Bh horizon the total cation release was clearly larger than the proton consumption rate, especially in the Bh horizon where Al release alone already exceeded the acid neutralization rate in terms of charge (Table 3.5). In calculating Al release rates, the charge of Al was, however, assumed to be three. The effective charge of Al species in the (A+B)<sub>p</sub> and Bh horizon was, however, less than

Table 3.5 Annual cation release and acid neutralization at pH 3.0 for the soil samples studied

Soil horizon	Annual release (mmol <sub>c</sub> kg <sup>-1</sup> )							Proton consumption (mmol <sub>c</sub> kg <sup>-1</sup> )
	Al	Fe	Ca	Mg	K	Na	Cations <sup>1)</sup>	
(A+B)p	123	8.5	1.71	1.10	1.63	1.42	137	125
Bh	256	16.6	1.21	0.41	4.24 <sup>2)</sup>	4.46 <sup>2)</sup>	283	238
BCs	223	2.7	0.93	0.59	1.86	1.52	231	236
C	102	8.1	0.25	0.03	1.47	2.58	114	116

<sup>1)</sup> Cations stand for the sum of Al, Fe, Ca, Mg, K and Na

<sup>2)</sup> These release rates are anomalous (too high) compared to values at lower pH values (cf Table 3.15; Section 3.2)

three due to complexation of Al by apparently mobilized organic anions. Effects of hydrolysis can be neglected at pH 3.0. Calculated mobilization rates of organic anions, derived from the measured anion deficit during the experiment, equalled 14 and 51 mmol<sub>c</sub> kg<sup>-1</sup> yr<sup>-1</sup> for the (A+B)p and Bh horizon, respectively. After correction for complexation by organic anions, the equivalent total cation release of the (A+B)p and Bh horizon equalled 123 and 232 mmol<sub>c</sub> kg<sup>-1</sup> yr<sup>-1</sup>, respectively, which is within 5% of the proton consumption rate.

At pH 3.0 annual Fe release was generally higher than the annual release of all base cations, except for the BCs horizon. However, compared to Al, Fe release at pH 3.0 very low. Interactions of SO<sub>4</sub> and NO<sub>3</sub> with the soil appeared to be small. Data suggested SO<sub>4</sub> release (desorption) in all horizons, varying between 0.1 and 4.2 mmol<sub>c</sub> kg<sup>-1</sup> yr<sup>-1</sup>, and NO<sub>3</sub> removal (denitrification) in the (A+B)p, Bh and C horizon (8.6 - 9.3 mmol<sub>c</sub> kg<sup>-1</sup> yr<sup>-1</sup>). In the BCs horizon, however, NO<sub>3</sub> release was observed (1.8 mmol<sub>c</sub> kg<sup>-1</sup> yr<sup>-1</sup>). Since both SO<sub>4</sub> and NO<sub>3</sub> are added in the experiments, these values are quite inaccurate and interpretation in terms of processes is doubtful.

In comparison to the observed release of base cations, Al release was far too large to be explained by congruent dissolution of primary alumino-silicates, such as K and Na feldspars (the dominating Al silicates in these soils), anorthite and chlorite. The measured annual Al/BC ratio (mol<sub>c</sub> mol<sub>c</sub><sup>-1</sup>), where BC stands for Ca+Mg+K+Na, equalled 21, 25, 45 and 23 for the (A+B)p, Bh, BCs and C horizon respectively, which is ca. 10-20 times as high as the Al/BC ratio at congruent weathering (cf Table 3.6). Furthermore, Al dissolution from primary minerals may even be less than the values estimated from congruent dissolution, since observed annual Si release in the (A+B)p, Bh and C horizon was lower than annual Si release estimated from stoichiometric weathering (Table 3.6). Precipitation of Si was unlikely, because Si concentrations, which ranged from 0.05 mol m<sup>-3</sup> (Bh horizon) to 0.28 mol m<sup>-3</sup> (BCs horizon) at the end of the experiment, were undersaturated with respect to quartz (Si = 10<sup>-3.1</sup> mol l<sup>-1</sup> = 0.79 mol m<sup>-3</sup>; Lindsay, 1979). Van Grinsven et al. (1988), who observed a similar phenomenon in column experiments with acid sandy soils, suggested that the relatively low Si release rate might be due to incongruent dissolution of primary silicates and formation of secondary alumino-silicates.



Table 3.6 Measured and estimated annual Al and Si dissolution in one-year batch experiments at pH 3.0

Soil Horizon	Al dissolution (mmol <sub>c</sub> kg <sup>-1</sup> )		Si dissolution (mmol <sub>c</sub> kg <sup>-1</sup> )		Al/Si dissolution ratio (mol <sub>c</sub> mol <sub>c</sub> <sup>-1</sup> ) <sup>1)</sup>	
	measured <sup>2)</sup>	estimated <sup>3)</sup>	measured <sup>2)</sup>	estimated <sup>3)</sup>	measured	estimated
(A+B)p	128	9.5	12	37	1.1 (14)	0.34 (0.45)
Bh	273	29	12	108	23 (30)	0.26 (0.34)
BCs	224	14	101	54	2.2 (2.9)	0.29 (0.39)
C	104	13	36	51	2.9 (3.9)	0.26 (0.35)

<sup>1)</sup> Values in brackets are molar release rates

<sup>2)</sup> Measured Al dissolution equals measured total Al release minus Al exchange during the experiment, whereas measured Si dissolution equals measured Si release

<sup>3)</sup> Estimated annual Al and Si dissolution was based on the measured annual BC dissolution, assuming congruent weathering of alkali feldspars (K and Na), anorthite (Ca) and chlorite (Mg). BC release by cation exchange was subtracted from annual BC release to derive annual BC dissolution (cf Section on mechanisms of cation release). In calculating the dissolution rates a charge of three was used for Al and of four for Si (Si is released as uncharged H<sub>4</sub>SiO<sub>4</sub>).

Preferential mobilisation of Al and BC over Si at low pH values has also been observed in weathering experiments with pure Albite (Chou and Wollast, 1985) and an alkali feldspar (Holdren and Speyer, 1985). For both minerals, stoichiometric release of Al and Si was observed at pH values above 5.5-6.0. Non-stoichiometric release at lower pH values was attributed to the formation of a Si enriched layer on the mineral surface and not by precipitation of a secondary aluminosilicate (Chou and Wollast, 1985; Holdren and Speyer, 1985). This mechanism is more likely, considering Si release in the BCs horizon. Unlike, the other three horizons, observed Si release in the BCs horizon was larger than the estimated Si release. This implies dissolution of Si from a secondary aluminosilicate pool.

The large observed Al release implies that secondary Al compounds are the major source of Al release. The ratio of observed annual Al release to the reactive Al pool (cf Table 3.3 and 3.6) increased from 0.35-0.37 in the (A+B)p and Bh horizon to 0.83-0.87 in the BCs and C horizon, respectively. Considering the average molar Al/Si release ratio of 2.9, the secondary Al pool in the BCs horizon might consist of allophane or imogolite which has been determined in B horizons of podzols (Farmer et al., 1980; Childs et al., 1983; Dahlgren and Ugolini, 1991). Quantification of Al and Si in the amorphous fraction of a BCs horizon of a Carbic Podzol in Ughelen, located near the soil profile studied here, however, showed that this pool most likely consist of amorphous secondary Al silicates. The average molar Al/Si ratio, estimated with Scanning Electron Microscopy - Energy Dispersive X-ray Analysis (SEM-EDXRA) in a thin section of the soil, was 2.1 (n=15; Bisdom and Boersma, 1994), which nearly equals the molar Al/Si ratio of imogolite (2.0). However, molar Al/Si ratios varied between 1.6 and 4.0 depending on the type of amorphous material (values were, for example, lower in decomposed plant fragments than in fine mass on sand grains). It is therefore more likely that an amorphous aluminosilicate of variable composition governs both Al and Si

release in the BCs horizon. Such a mechanism was also suggested by Weaver and Bloom (1977) for highly weathered Oxisols.

During the experiment, the stoichiometry of Al, Fe, BC and Si release changed due to depletion of secondary Al compounds, as illustrated for the Bh and C horizon (Fig. 3.1). The Al/BC release ratio generally increased with cumulative Al release. This was due to very fast initial BC release, followed by slow long term BC release. The Al/Fe and Al/Si release ratio decreased with cumulative Al release. The decrease in Al/Fe ratio implies that Al pools are depleted faster than the Fe pools. The larger initial Al release, compared to Si release, implies that non-silicate pools of Al are more rapidly depleted than Al silicates (cf next section on release rates with time).

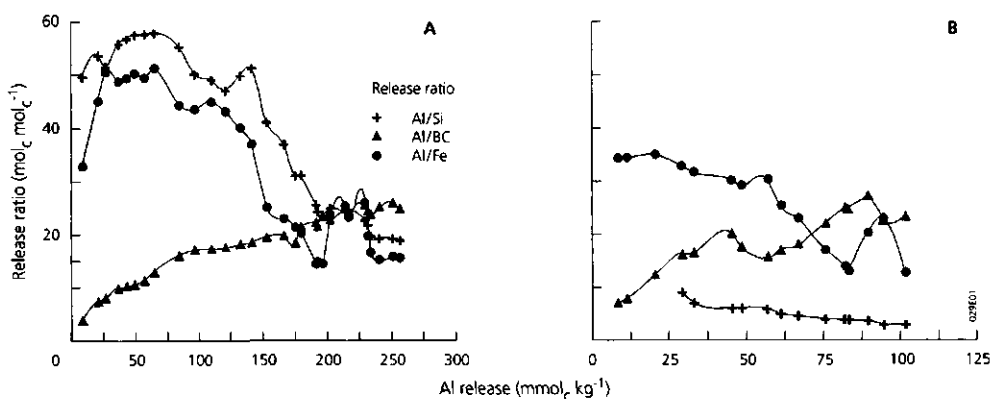


Figure 3.1 Release ratios of Al to Si, Fe and BC as a function of cumulative Al release at pH 3.0 for the Bh horizon (A) and the C horizon (B). Release ratios are given in mol<sub>c</sub> mol<sub>c</sub><sup>-1</sup> since BC includes Ca, Mg, K and Na with different charges

## Rates of aluminium, base cation and silica release with time

### Cumulative release

The cumulative release of Al, BC and Si during the experiment could be fitted quite well with the empirical three parameter model (Eq. 3.2) for all soil samples studied (Fig. 3.2). The fit of Al and Si release from the BCs horizon was less good due to the (unexplained) anomalous behaviour of Al and Si between 40 and 100 days. This behaviour was not found at other pH levels (cf Section 3.2). Fitted values for  $\alpha_1$ ,  $\alpha_2$  and  $\alpha_3$  (Table 3.7) clearly illustrate the difference in behaviour between Al, BC and Si.

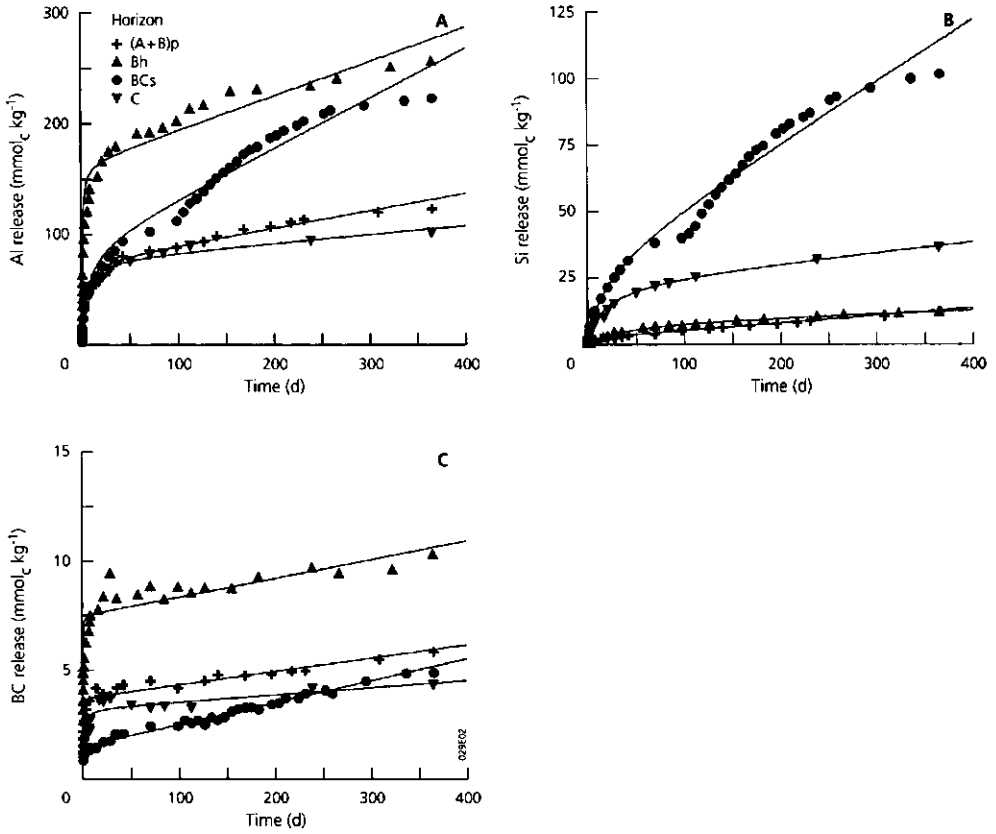


Figure 3.2 Measured and predicted cumulative release of Al (A), Si (B) and BC (C) with time at pH 3.0 for the soil samples studied. Experimental data are denoted by symbols, whereas solid lines are the predictions made with an empirical three parameter model (Eq. 3.2)

Table 3.7 Values of the fitted parameters  $\alpha_1$ ,  $\alpha_2$  and  $\alpha_3$  in the empirical relationship between cumulative release of Al, BC and Si versus time (Eq. 3.2) at pH 3.0 for the soil samples studied

Soil horizon	$\alpha_1$ (mmol <sub>c</sub> kg <sup>-1</sup> )			$\alpha_2$ (d)			$\alpha_3$ (mmol <sub>c</sub> kg <sup>-1</sup> yr <sup>-1</sup> )			$R^2_{adj}$ <sup>1)</sup>		
	Al	BC	Si	Al	BC	Si	Al	BC	Si	Al	BC	Si
(A+B)p	75	3.7	1.6	3.1	1.4	2.3	56	2.2	10.4	0.98	0.91	0.99
Bh	163	7.5	8.5	0.7	0.09	46	112	3.1	4.5	0.96	0.90	0.99
BCs	91	1.5	31	6.8	0.03	20	163 <sup>2)</sup>	3.7	83 <sup>2)</sup>	0.98	0.98	0.98
C	77	3.2	23	4.3	1.0	19	28	1.2	14	0.98	0.80	0.99

<sup>1)</sup>  $R^2_{adj}$  is the adjusted coefficient of determination

<sup>2)</sup> Likely to be an overestimate due to the anomalous Al and Si release between 40 and 100 days (cf Fig. 3.2)

Values of the non-linear dissolution capacity,  $\alpha_1$ , for Al were always lower than the reactive Al pool (exchangeable Al and secondary Al compounds) and ranged from 23% to 67% of that pool going from the (A+B)p to the C horizon (cf Table 3.3 and 3.7). Unlike Al, values of  $\alpha_1$  for BC were always larger than the exchangeable BC pool, although  $\alpha_1$  in the (A+B)p horizon approximated the pool size (cf Table 3.2 and 3.7). Most likely, high values of  $\alpha_1$  are due to a very fast exchange of H against (alkali) cations on the mineral surface at the start of the experiment, induced by the low pH (Wollast, 1967; Busenberg and Clemency, 1976). Under field circumstances, this phenomenon is unlikely since the pH will not (rapidly) drop to a value of 3.0 in these highly buffered soil horizons. In the field situation, it is therefore unlikely that the reactive BC pool is much larger than the exchangeable BC pool. The occurrence of fast exchange of H against BC is supported by values of  $\alpha_2$ , i.e. the half-life time of the most reactive pool. These values ranged from less than one day to nearly one week for Al and from less than one hour to ca. one day for BC (Table 3.7). This implies a much faster depletion rate of the reactive non-linear pool of BC than of Al. Depletion of the reactive non-linear Al pool was, however, faster than that of Si, except for the (A+B)p horizon (Table 3.7). This implies that non-silicate pools of Al are more rapidly depleted than Al silicates (cf Fig. 3.1).

Comparison of the pool of secondary Al compounds (Table 3.3) corrected for the depletion of a fast reacting Al pool ( $\alpha_1$ ; Table 3.7) and the long-term Al dissolution rate ( $\alpha_3$ ; Table 3.7) indicates that this pool can be totally depleted approximately 5 years in the (A+B)p and the Bh horizon, and within 1.5 year in the BCs and C horizon. The estimated time periods might be too low since Al depletion may cause a constant decrease in Al release rate with time. Using Al release rates obtained with the double logarithmic equation (Eq. 3.3), the time to deplete the Al pool increased to 10-15 years for the (A+B)p and Bh horizon and to 2 years for the BCs and C horizon. (Values of  $F^2_{adj}$  for the fits were 0.97, 0.96, 0.90 and 0.95 for the (A+B)p, Bh, BCs and C horizon, respectively). Fits of the cumulative Al release with a single logarithmic equation (Eq. 3.4) lead to even larger time periods for Al depletion. This is illustrated for the Bh and C horizon in Fig. 3.3. Even though the adjusted coefficients of determination,  $F^2_{adj}$ , were nearly equal for the double and single logarithmic equations (Table 3.8), the single logarithmic equation gave much better predictions of Al release with time on a non-

Table 3.8 Intercept and slopes of double and single logarithmic equations for the cumulative Al release ( $\text{mmol}_e \text{ kg}^{-1}$ ) with time (d) at pH 3.0 for the Bh and C horizon

Soil horizon	N <sup>1)</sup>	Double logarithmic equation (Eq. 3.3)			Single logarithmic equation (Eq. 3.4)		
		intercept ( $\log \alpha_4$ )	slope ( $\alpha_5$ )	$F^2_{adj}$	intercept ( $\alpha_6$ )	slope ( $\alpha_7$ )	$R^2_{adj}$
Bh	30	1.46	0.26	0.93	17.9	24.4	0.98
C	16	0.88	0.32	0.96	-14.8	12.6	0.98

<sup>1)</sup> N = number of measurements

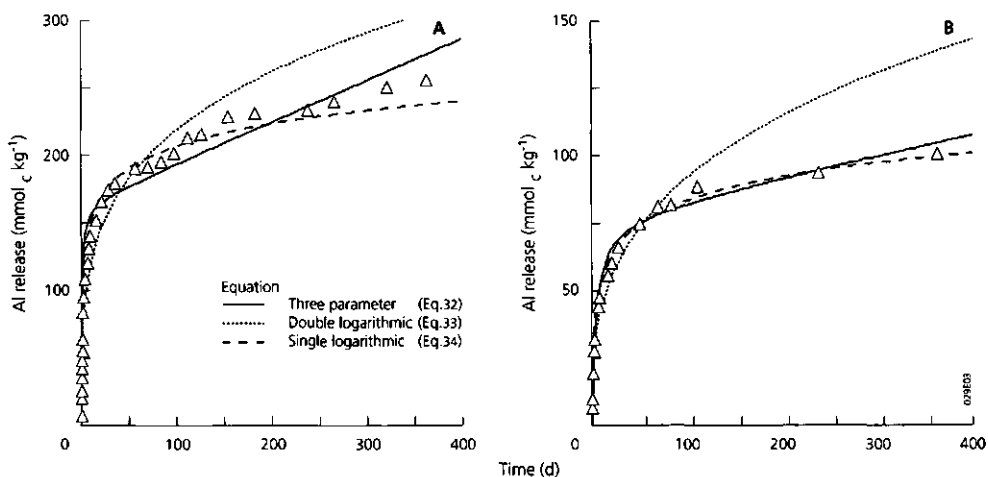


Figure 3.3 Measured and predicted cumulative Al release at pH 3.0 with three different equations for the Bh (A) and C horizon (B)

logarithmic scale (Fig. 3.3). Using this equation, the time period to deplete the secondary Al pool was approximately 4 years for the C horizon but more than 100 years for the Bh horizon.

#### Long-term release rates

An estimate of the long-term release rate for Al, Si and BC can be derived from the  $\alpha_3$  value in the three parameter model (Table 3.7). Release rates predicted at one year with Eq. (3.5b) appeared to be ca. 30-60% lower than the values derived with Eq. (3.2). Except for the Bh horizon, however, the Al/Si and Al/BC ratio predicted with both equations hardly differed (Table 3.9). The long-term Al/Si ratio in the BCs and C horizon was lower than the annual Al/Si ratio (Table 3.6) and approached a value of 2.0. As with the ratio of annual Al to BC release, the long-term release rate of Al was, however,

Table 3.9 Long-term release (weathering) rates of Al and BC for the soil samples studied as predicted with two different equations

Soil Horizon	Release rate ( $\text{mmol}_c \text{ kg}^{-1} \text{ yr}^{-1}$ )						Release ratio			
	Al		BC		Si		Al/BC ( $\text{mol}_c \text{ mol}_c^{-1}$ )		Al/Si ( $\text{mol mol}^{-1}$ )	
	Eq. 3.2	Eq. 3.5b	Eq. 3.2	Eq. 3.5b	Eq. 3.2	Eq. 3.5b	Eq. 3.2	Eq. 3.5b	Eq. 3.2	Eq. 3.5b
(A+B)p	56	32	2.2	1.2	10.4	5.7	25	25	7.2	7.5
Bh	112	38	3.1	2.1	4.5	4.5	36	18	33	11.3
BCs	163	101	3.7	2.5	83	63	44	40	2.6	2.1
C	28	20	1.2	0.8	14	23 <sup>1)</sup>	23	25	2.7	1.2 <sup>1)</sup>

<sup>1)</sup> These values are unreliable since the fit of Si release rate with time (Eq. 3.5) was bad ( $F^2_{adj} = 0.24$ )

approximately 10-30 times as large as that of BC (cf Table 3.9). This indicates that, even on a long-term, dissolution of secondary Al compounds is the major source of Al.

Release rates of Al and BC were described quite well with Eq. (3.5b): Values of  $F_{adj}^2$  varied between 0.90 and 0.97 for Al and between 0.80 and 0.93 for BC. Predictions were also reasonable for Si ( $0.61 < F_{adj}^2 < 0.88$ ) except for the C horizon ( $F_{adj}^2$  is 0.24). In several experiments with pure minerals (Wollast, 1967; Busenberg and Clemency, 1976; Chou and Wollast, 1985), the value of  $\alpha_s$  (Eq. 3.5) during the initial period (up to 20 days) was found to be ca. -0.5. Based on this behaviour, it was assumed that the initial rate limitation of silicate weathering is determined by diffusion of cations through a surface precipitate (e.g. Wollast, 1967) or a leached layer (e.g. Busenberg and Clemency, 1976). In the experiments described here, values of  $\alpha_s$  for Si also ranged around -0.5 ( $-0.66 < \alpha_s < -0.44$ ). Values of  $\alpha_s$  for Al and BC were, however, close to -1 for the (A+B)p, Bh and C horizon, i.e. between -0.83 and -0.94 for Al and between -0.91 and -0.99 for BC. Only in the BCs horizon  $\alpha_s$  was close to -0.5 (-0.66 for Al and -0.74 for BC). The deviation of  $\alpha_s$  from -0.5 implies that initial cation release is not so much governed by diffusion through the mineral surface but by fast exchange reactions (BC and Al) and dissolution reactions (Al).

Long-term BC release rates of ca. 1-2 mmol<sub>c</sub> kg<sup>-1</sup> yr<sup>-1</sup> (see Table 3.8; Eq. 3.5b) are similar to values obtained for sandy soils in unstirred batch experiments (Van Grinsven et al., 1988). Using the values for soil thickness and bulk density given in Table 3.1, the long-term BC release rate in kmol<sub>c</sub> ha<sup>-1</sup> yr<sup>-1</sup> equals 2.1, 1.6, 4.2 and 2.0 for the (A+B)p, Bh, BCs and C horizon respectively. Summing up to 1 meter, the release rate is more than 10 kmol<sub>c</sub> ha<sup>-1</sup> yr<sup>-1</sup>, which is approximately 50 times as large as the estimated average field weathering rate for BC in sandy soils (cf Section 2.2 and 4.2). Possible explanations for the discrepancy between field and laboratory weathering rates are the lower pH value (pH 3.0) the more efficient contact between solution and solids and the higher temperature (20 °C) in the laboratory experiments. Temperature effects explain an increase in weathering rate by a factor two to four (Wesselink, pers. comm.) whereas the difference in pH value between the laboratory (pH 3.0) and field circumstances (pH 3.5-4.5) may increase the weathering rate by a factor of four to six (cf Section 3.2).

### **Effect of Al depletion on Al release rates**

The strong decrease in Al release rate with time can be caused by approaching chemical equilibrium with (secondary) inorganic and organic Al compounds and by a decreasing pool of reactive Al. During the experiments, solutions were always undersaturated with respect to secondary Al minerals such as gibbsite, kaolinite, basaluminite, jurbanite and imogolite. The degree of undersaturation with respect to Al hydroxides and Al hydroxy sulphates (gibbsite, basaluminite and jurbanite) hardly changed since concentration changes in Al and SO<sub>4</sub> were low. The maximum change in

Al concentration during the experiment was always less than 35% (from 1.5 mol<sub>c</sub> m<sup>-3</sup> to 2.0 mol<sub>c</sub> m<sup>-3</sup>), except for the Bh horizon, where release of organically complexed Al was large. SO<sub>4</sub> concentration changes were within 10%. Mineral saturation indices, calculated as the logarithmic ratio of the ionic activity product and the solubility product of a mineral phase, varied during the experiment between -2.57 and -2.45 for synthetic gibbsite, between -9.85 and -9.38 for basaluminite and between -0.54 and -0.44 for jurbanite. Activity coefficients were calculated with the Debye-Hückel equation, whereas equilibrium constants for the various minerals were taken from Mulder et al. (1987). For Al silicates (kaolinite, imogolite), changes in saturation indices were larger since Si concentrations increased with time. However, values remained far below 0 during the whole experiment and increased from -6.20 to -4.64 for kaolinite and from -7.02 to -5.41 for imogolite. These results indicate that changes in mineral saturation are not a plausible cause for a decrease in Al release rate with time.

The strong decrease in Al release during the first week may also be due to fast initial exchange of organically bound Al against protons, followed by slow release of Al from inorganic (primary and secondary) Al pools in a situation where adsorbed and dissolved Al and H are in equilibrium. The importance of soil organic matter in controlling the solubility of Al through complexation reactions has been stressed by various authors (Bloom et al., 1979b; Cronan et al., 1986; Mulder et al., 1989; Mulder en Stein, 1994). In the (A+B)p and Bh horizon, with a relative large pool of organically complexed Al, this mechanism may play an important role. The estimated fast reacting Al pool,  $\alpha_1$ , in the (A+B)p and Bh horizon is 75 and 163 mmol<sub>c</sub> kg<sup>-1</sup> yr<sup>-1</sup>, respectively (Table 3.6) whereas the pool of organically bound Al, estimated with LaCl<sub>3</sub>, equals 78 and 106 mmol<sub>c</sub> kg<sup>-1</sup> yr<sup>-1</sup> (Table 3.3). In the BCs and C horizon,  $\alpha_1$  values for Al are, however, much higher than lanthanum chloride-extractable Al. In these horizons, rate-limited dissolution of inorganic secondary Al compounds must be the dominating mechanism. The higher value for  $\alpha_2$  in the BCs and C horizon as compared to the Bh horizon, and to a lesser extent in the (A+B)p horizon, may also point to a different reaction mechanism.

Rate-limited Al dissolution implies that the decrease in Al release rate with time can be explained by a decrease in reactive Al pool. This hypothesis is supported by the strong decrease in Al release rate during the experiment as a function of the cumulative Al release (Table 3.10). As with the equations describing cumulative Al release against time, the single logarithmic (Elovich) equation (Eq. 3.7) described the Al release rate (slightly) better than the double logarithmic equation (Eq. 3.6), except for the BCs horizon (cf the values for  $F_{adj}^2$  in Table 3.10). This is consistent with the relative large deviation of the value  $\alpha_9$  in Eq. (3.5b) from -1 for this horizon (see before).

Eq. (3.7) was used to calculate the relation between the relative decrease in Al release rate and the relative depletion of the reactive Al pool, assuming that Al is only released from that pool (cf the section on mechanisms of cation release). Results (Table 3.11) showed that a relative decrease of 10% in the reactive Al pool of the (A+B)p and Bh

Table 3.10 Intercept and slopes of double and single logarithmic equations for the Al release rate ( $\text{mmol}_e \text{ kg}^{-1} \text{ d}^{-1}$ ) against cumulative Al release ( $\text{mmol}_e \text{ kg}^{-1}$ ) for the soil samples studied

Soil horizon	N <sup>1)</sup>	Double logarithmic equation (Eq. 3.6)			Single logarithmic equation (Eq. 3.7)		
		intercept	slope	R <sup>2</sup> <sub>adj</sub>	intercept	slope	R <sup>2</sup> <sub>adj</sub>
(A+B)p	22	4.38	-2.51	0.92	4.18	-0.059	0.93
Bh	30	7.24	-3.24	0.84	6.87	-0.038	0.94
BCs	36	3.13	-1.56	0.87	2.83	-0.021	0.75
C	16	0.88	-2.73	0.87	4.34	-0.073	0.95

<sup>1)</sup> N = number of measurements

horizon caused a decrease in Al release rate of ca. 90%. In the BCs and C horizon a relative decrease of ca. 41% and 27%, respectively was needed for the same reduction in Al release rate (cf Table 3.10). The difference in Al release kinetics between the upper and lower horizons might be due to the different contribution of organically complexed Al to the secondary Al pool (Table 3.3; cf Van der Salm and Verstraten, 1994). The extreme reduction in Al release rate with cumulative Al release in the (A+B)p and Bh horizon may be caused by approaching equilibrium with organically bound Al during the first day, whereas the long-term release in these horizons may be due to rate-limited dissolution of inorganic secondary Al compounds. Most likely, the latter mechanism mainly governs Al release in the BCs and C horizon from the start of the experiment (cf section on mechanism of cation release).

For BC, the release rate was not as well correlated with the cumulative release as for Al, especially in the BCs and C horizon. Unlike Al, the effect of BC depletion on the long-term BC release rate is likely to be small. Even though BC release was much faster in the laboratory than the field situation, it would still take more than one hundred years in the laboratory to deplete the total BC pool (cf Table 3.2 and 3.7).

Table 3.11 Relationship between the relative decrease in Al release rate and relative depletion of reactive Al for the soil samples studied

Soil horizon	Relative decrease in Al release rate <sup>1)</sup> at a relative Al depletion of		
	10%	20%	50%
(A+B)p	88%	98%	>99%
Bh	93%	99%	>99%
BCs	43%	68%	94%
C	57%	82%	99%

<sup>1)</sup> The initial release rate of Al, was determined from the intercept of Eq. (3.7) (cf Table 3.9). The Al release rate at a given value of Al depletion (cumulative Al release) was estimated from the slope of Eq. (3.7) (cf Table 3.9)



### Mechanisms of cation release

Base cation release was completely dominated by mineral weathering in the lower BCs and C horizon (measurements in these horizons even indicated a slight BC adsorption; cf Table 3.12). In the (A+B)p and Bh horizon, however, desorption of cations, especially of Ca and Mg, was an important contribution to the total release of Ca and Mg (39-85% for Ca and 27-54% for Mg respectively; see Table 3.12). The contribution of K and Na desorption to total K and Na release was relatively low in these horizons (< 10-15%).

Table 3.12 Weathering and desorption of base cations during one year at pH 3.0 for the soil samples studied

Soil horizon	Annual base cation release (mmol <sub>c</sub> kg <sup>-1</sup> )									
	Ca		Mg		K		Na		BC	
	weath.	des.	weath.	des.	weath.	des.	weath.	des.	weath.	des.
(A+B)p	0.26	1.45	0.80	0.30	1.48	0.15	1.26	0.16	3.80	2.06
Bh	0.74	0.47	0.19	0.22	3.83	0.41	4.45	0.01	9.21	1.11
BCs	0.95	-0.02	0.62	-0.03	1.92	-0.06	1.53	-0.01	5.02	-0.12
C	0.27	-0.02	0.04	-0.01	1.48	-0.01	2.57	0.01	4.36	-0.03

The change in various solid-phase Al pools, estimated by sequential removal with various extractants (cf materials and methods), indicated that Al release is dominated by dissolution of Al from amorphous secondary compounds in all soil samples studied. The ratio of Al release from amorphous secondary compounds to Al release in solution approached, or even exceeded 1.0 (Table 3.13). In the (A+B)p horizon the contribution of amorphous secondary compounds to the release from the reactive Al pool was lower (65%) than in the BCs and C horizon (ca. 98%; cf Table 3.13). In the Bh horizon the contribution was 91% but this value is likely to be overestimated, since the estimated release of organically complexed Al in this horizon (24 mmol<sub>c</sub> kg<sup>-1</sup> yr<sup>-1</sup>) is lower than the release of organic anions in water (51 mmol<sub>c</sub> kg<sup>-1</sup> yr<sup>-1</sup>; cf section on annual cation and silica release). The depletion of the pool of amorphous secondary Al compounds was also lower in the (A+B)p and Bh horizon (ca. 60%) than in the BCs and C horizon (ca. 90%; cf Table 3.13 and Table 3.3).

The interpretation of secondary Al pools responsible for Al release, however, strongly depends on the specificity of the extractants used. Van Grinsven et al. (1992) and Van der Salm and Verstraten (1994) concluded that dissolution of amorphous secondary Al minerals, indicated as Al oxides, dominate Al release. This was based on the amount of, and the decrease in ammonium oxalate-extractable Al, respectively. By contrast, Mulder et al. (1989) and Dahlgren and Walker (1993) concluded that organic Al complexes dominate Al release in the E, B and C horizons of acid sandy soils. This implies that exchange of H against Al in organic matter (cf Bloom et al., 1979b; Cronan et al., 1986) is the most important Al release mechanism. This was based on the decrease in, and the amount of pyrophosphate-extractable Al, respectively. As shown before, use of

Table 3.13 Al release mechanisms in one-year batch experiments at pH 3.0 for the soil samples studied

Mechanisms <sup>1)</sup>	Annual Al release (mmol <sub>c</sub> kg <sup>-1</sup> )			
	(A+B)p	Bh	BCs	C
Desorption	-5.1	-17	-0.7	-3.3
Release of complexed Al <sup>2)</sup>	38 (116)	24 (364)	5.8 (101)	3.3 (93)
Release from:				
- amorphous compounds	125	324	224	92
- crystalline compounds	34	22	8.5	3.3
	+	+	+	+
Release from reactive pool	192	353	238	95
Release in solution	123	256	223	102
Difference <sup>3)</sup>	-69	-97	-15	7

<sup>1)</sup> Calculated as the difference in Al contents before and after the experiment in a sequential extraction with silver thiourea (desorption), lanthanum chloride (release of complexed Al), ammonium oxalate (dissolution of amorphous secondary Al minerals) and dithionite/citrate/bicarbonate) dissolution of crystalline secondary Al minerals)

<sup>2)</sup> Values in brackets refer to the measured decrease in pyrophosphate-extractable Al. Except for the BCs horizon, the decrease in the pyrophosphate-extractable pool was nearly equal to the calculated total release from the reactive Al pool.

<sup>3)</sup> Difference between measured Al release in solution and total Al release from the reactive pool. In the upper (A+B)p and Bh horizon the amount of Al released from solid-phase pools is substantially larger than the amount released in solution. The same phenomenon was found at all other pH levels (De Vries, 1994b; Section 3.2). Possibly, reactive Al in the (A+B)p and Bh horizon is released in colloidal form and retained on the filter paper

sodium pyrophosphate causes an overestimation of the pool of organically bound Al, at least in BCs and C horizons. This does, however, not imply that lanthanum chloride is a good extractant for organically bound Al. Especially in the (A+B)p and Bh horizon this is questionable. First of all, the larger release of organic anions (organically complexed Al) in solution than the decrease in lanthanum chloride-extractable Al, indicates an underestimation of the organic Al pool in these horizons with LaCl<sub>3</sub>. Furthermore, Al extracted with LaCl<sub>3</sub> in organic soil layers, such as the forest floor and peat soils, appears to be only half the amount extracted with pyrophosphate (DLO Winand Staring Centre, unpublished data). Assuming that the estimated release of organic Al by LaCl<sub>3</sub> is underestimated by a factor 2, this mechanism may even dominate Al release in the (A+B)p horizon (cf Table 3.13). A more distinct determination of the various solid-phase Al pools is thus needed to warrant the conclusion that either rate-limited dissolution of inorganic Al compounds or equilibrium reactions with organic Al complexes mainly governs Al release in the upper (A+B)p horizon.

Recently, Mulder and Stein (1994) claimed to provide new evidence for the dominating influence of complexation reactions with soil organic matter on Al solubility. First of all, they observed a positive correlation between log Al + 3 pH in soil solution and the molar ratio of pyrophosphate-extractable Al to total organic C in the soil solid phase, using data from different soil layers in three Dutch forest soils. This pattern might indicate that Al solubility increases with increasing Al saturation of the organic complexation sites, as suggested by Mulder and Stein (1994). However, this is likely to be coincidence. Larger

values for both Al + 3 pH and the molar Al/C ratio were found at greater depth. This can be expected because of (i) an increase in acid neutralization by cumulative Al mobilization with depth (increases log Al + 3 pH) and (ii) a decrease in organic carbon with depth (increases the molar Al/C ratio). Furthermore, samples at a depth below 20 cm had a molar Al/C ratio varying between 0.08 and 0.14, exceeding a theoretical maximum value of 0.05. Al compounds at these depths are thus largely inorganic.

In trend analyses of soil solution concentrations over a six year period, Mulder and Stein (1994) also observed that undersaturation with respect to gibbsite was always largest in the summer period, when water retention times are largest and soil temperatures are highest. This seems to contradict the rate-limited dissolution of inorganic Al compounds. However, in summer ion concentrations are much higher than in winter, due to a decrease in water fluxes and water contents. Unless the dissolution rate of Al largely increases with an increase in soil temperature and water retention, this hydrologic aspect causes an increased undersaturation with respect to gibbsite, since the equilibrium Al concentration increases with the third power of the H concentration.

Another aspect that should be taken into consideration is the occurrence of, sometimes extreme, hydrophobicity in most sandy soils in the Netherlands during the summer period. Water drop penetration time tests showed that more than 75% of the cropland and grassland topsoils in the Netherlands are slightly to extremely water-repellent, whereas more than 95% of the topsoils in forests and nature reserves are strongly to extremely water-repellent (Dekker 1988; Dekker and Jungerius, 1990; Hendricks et al., 1993). This phenomenon, which causes a strong decrease in the area and time of contact between solution and solid, may strongly affect the release of Al in the summer. Both hydrologic aspects imply that an increase in undersaturation with respect to gibbsite during the summer period is very well possible in a situation of rate-limited Al dissolution.

## CONCLUSIONS

Major results of the one-year batch experiments presented before are (cf the objectives of the study):

- (i) Al dissolution is the dominant acid neutralizing mechanism in all investigated horizons of acid sandy soils. Annual release of Si, Fe and base cations (in mmol, kg<sup>-1</sup> yr<sup>-1</sup>) was 10-50 times lower than Al release, except for Si release in the BCs and C horizon (ca. 2-3 times lower). Cumulative Al release with time could be described well with an empirical three parameter model and by a linear relationship with the (natural) logarithm of time. The Al release rate could be described well by a linear relationship with the natural logarithm of the cumulative Al release (depletion of Al pool).

- (ii) The pool of secondary Al compounds is the major source of Al release. In the (A+B)p and Bh horizon, however, the depletion of that pool during the experiment was much lower (less than 40%) than in the BCs and C horizon (more than 80%). In the BCs and C horizon, dissolution of inorganic secondary compounds (most likely aluminosilicates) dominated Al release. In the (A+B)p and Bh horizon, release of organically complexed Al played a relative important role, but even in these horizons dissolution of secondary Al minerals seems to dominate Al release.
- (iii) Desorption of base cations (BC) plays a relative important role in BC release (ca. 10-35%) in the upper soil horizons ((A+B)p and Bh horizon), whereas the influence is negligible in the lower soil horizons (BCs and C horizon).

The dominating influence of Al release on acid neutralization rates in acid sandy soils is consistent with results of laboratory experiments reported earlier (Mulder et al., 1989; Van Grinsven et al; 1992; Dahlgren and Walker, 1993; Van der Salm and Verstraten, 1994). The description of cumulative Al release and Al release rates and the depletion of a pool of secondary Al compounds also confirms results published by several of these authors. The interpretation of the solid-phase pool of Al that dominates Al release is, however, controversial. Results reported here show that organic Al compounds play a minor role in the lower BCs and C horizon. In the upper (A+B)p and Bh horizon, the relative importance of secondary organic and inorganic Al compounds in long-term Al release remains unclear because of the lack of specificity of extractants for the different Al pools.

## 3.2 EFFECTS OF pH AND Al CONCENTRATION

### ABSTRACT

*The influence of pH (five levels between 2.3 and 4.0) and Al concentration (five levels between 0.5 and 99 mol<sub>c</sub> m<sup>-3</sup>) on cation and Si release rates was studied in an (A+B)<sub>p</sub>, Bh, BCs and C horizon of acid sandy forest soils by means of one-year batch - and one-week column experiments, respectively. During the experiments pH and Al concentration remained nearly constant. Results showed that the effect of pH on release rates decreased going from Mg > Fe > Si = Al > Ca = K = Na. The Al concentration level affected Al and Fe release in all horizons and the release of Si and Ca in the lower BCs and C horizon. The effect of Al was, however, much smaller than that of pH. Cumulative release of cations and Si could be described as a function of the proton or Al activity and reaction time. The combined effect of pH and Al depletion was described well as a function of the degree of undersaturation with gibbsite and the pool of secondary Al compounds. The combined effect of Al activity and Al depletion was, however, described less satisfactory with this model. Secondary amorphous Al compounds were the dominant source of Al release at all pH levels considered.*

### INTRODUCTION

Models are commonly used to predict changes in soil chemical status in response to acid atmospheric deposition (e.g. De Vries et al., 1989b; 1994b). An adequate model should at least describe the effects of pH and mineral depletion on the release rates of base cations (BC) and Al. Especially for Al dissolution, an adequate description is needed, since this buffering process is most important in acid sandy soils with a low base saturation (Mulder et al., 1989; Van Grinsven et al., 1992; Van der Salm and Verstraten, 1994; De Vries, 1994a), which are the dominant forest soils in the Netherlands. Information on the effects of pH, mineral saturation and depletion of pools of reactive Al on the Al dissolution rate is a prerequisite for a proper simulation of changes in Al chemistry (cf Van Grinsven et al., 1992).

In Section 3.1 (De Vries, 1994a), rates and mechanisms of cation and silica (Si) release were studied in four mineral soil horizons of podzolic soils, i.e. an (A+B)<sub>p</sub>, Bh, BCs and C horizon, at one pH level (pH 3.0). Results showed that the pool of oxalate-extractable Al is the dominant source of Al release and that depletion of that pool causes an exponential decrease in Al release rate. This section deals with a study of the effect of pH and Al concentration on the release of cations and Si in the same four mineral soil horizons, using batch and column experiments. The major objective of this study was to derive and test empirical descriptions of effects of pH and Al concentration (activity) on

- (i) cumulative release and release rates of Al, Fe, Bc and Si, in combination with effects of reaction time
- (ii) release rates of Al in combination with effects of depletion of secondary Al compounds
- (iii) release mechanisms of Al, Fe and base cations

Emphasis is placed on an empirical description of the effects of pH, Al activity and Al depletion on Al release rates, to be used in soil acidification modelling (cf Section 6.2 and 7.2).

## MATERIALS AND METHODS

Information on the various soil samples studied is given in Section 3.1. All samples have a low pH-KCl (3.6-4.4) and a low clay content (<4%; cf Table 3.1), a low base saturation (< 10%; cf Table 3.2) and a relatively large pool of secondary Al compounds (115-652 mmol<sub>c</sub> kg<sup>-1</sup>; cf Table 3.3).

### Batch experiments at different pH levels

To study the influence of pH on cation release rates, one-year batch experiments were conducted at a constant temperature of 20°C at five constant pH levels. The pH range studied for each sample depended on the initial pH and varied over one pH unit, as shown in Table 3.14.

*Table 3.14 Constant pH levels at which batch experiments were conducted during one-year (indicated with +)*

Soil horizon	Initial pH	pH level							
		2.3	2.5	2.7	3.0	3.3	3.5	3.7	4.0
(A+B)p	3.6	+	+	+	+	+			
Bhe	3.7		+	+	+	+	+		
BCs	4.0		+	+	+	+	+		
C	4.4				+	+	+	+	+

First a 75 ml mixture of sulphuric and nitric acid with a given pH, containing the most important cations (Al, Ca, Mg), was added to 7.5 g of soil in a 100 ml plastic container. Concentrations of the various ions were set equal to 1.5 mol<sub>c</sub> m<sup>-3</sup> for SO<sub>4</sub> and Al, 0.3 mol<sub>c</sub> m<sup>-3</sup> for Ca, 0.2 mol<sub>c</sub> m<sup>-3</sup> for Mg, X mol<sub>c</sub> m<sup>-3</sup> for H and 0.5+X mol<sub>c</sub> m<sup>-3</sup> for NO<sub>3</sub>, where X varied between ca. 0.1 (pH 4.0) and ca. 5 (pH 2.3). During the experiment the samples were gently shaken. The pH and the Al concentration were kept nearly constant by intermittent titration with an H<sub>2</sub>SO<sub>4</sub>-HNO<sub>3</sub> mixture with an equivalent concentration that was equal to the equivalent concentration of all cations (including H) added initially to the solution (2.0 + X mol<sub>c</sub> m<sup>-3</sup>; cf Section 3.1). Concentrations of Si, Al, Fe, Ca, Mg, K and Na were measured in 25 ml aliquots, that were sampled after 25 ml of acid mixture had been added. Concentrations of NH<sub>4</sub>, SO<sub>4</sub>, NO<sub>3</sub> and Cl were not measured except for the batch experiments at pH 3.0, since interactions with these ions generally appeared to be small (cf Section 3.1). More information on the batch experiments is given in Section 3.1 (De Vries, 1994a).

## Column experiments at different Al concentrations

To determine whether Al release is controlled by the concentration of dissolved Al, one-week column experiments were conducted at a constant temperature of 20°C and a constant pH of 3.0 and at (nearly) constant Al concentrations of 0.5, 2.0, 5.0, 9.0 and 99 mol<sub>c</sub> m<sup>-3</sup>. First a 100 ml HNO<sub>3</sub> solution, containing Al as the only cation, was added to a plastic container of 150 ml with an overflow at 100 ml. This solution, which contained ca. 1.0 mol<sub>c</sub> m<sup>-3</sup> H (pH=3.0), X mol<sub>c</sub> m<sup>-3</sup> Al and 1.0 + X mol<sub>c</sub> m<sup>-3</sup> NO<sub>3</sub> (where X varied between 0.5 and 99; see above), was recirculated through a small column of packed soil at a constant upward flow rate of 10 ml min<sup>-1</sup> by means of a peristaltic pump. The columns were ca. 4.0 cm high and 2.2 cm in diameter, contained about 20 g soil and were enclosed between ca. 2.0 cm thick layers of inert glasswool, to obtain homogeneous throughflow. The glasswool was covered with 0.45 μ filterpaper to prevent loss of fine particles. The solution was kept at pH 3.0 with an automatic titrator (Radiometer PHM 82 standard pH meter, TTT 80 titrator and ABU 80 autoburette). The titration solution contained HNO<sub>3</sub> with an electrolyte level equal to that of all cations (H and Al) added initially to the solution (1+X mol<sub>c</sub> m<sup>-3</sup>). The pH of the solution leaving the soil column was also measured. The proton consumption was recorded every 5 minutes. The experimental setup is illustrated in Fig. 3.4.

In the plastic container, the solution was stirred continuously. The stirred solution which left the overflow, after addition of titration solution, was transferred to a measuring cylinder. The volume of these cylinders was 100 ml or 1000 ml, depending on the Al concentration level. The total amount of solution passing the overflow varied from less than ten ml at Al concentrations of 99 mol<sub>c</sub> m<sup>-3</sup> to nearly 9 l at Al concentrations of 0.5 mol<sub>c</sub> m<sup>-3</sup>. The large increase in solution volume collected at lower Al concentration levels was mainly due to a decrease in H concentration of the titration solution (from

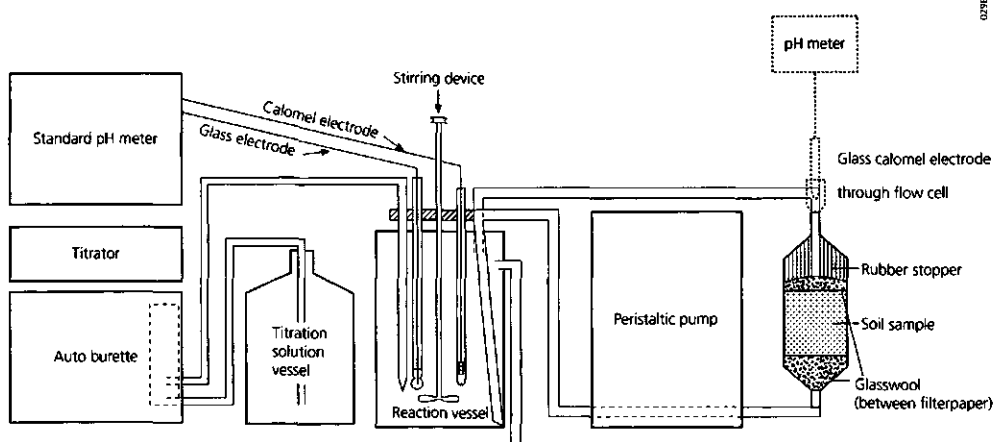


Figure 3.4 Schematic overview of the experimental setup of column experiments at constant pH

100 to 1.5 mol<sub>c</sub> m<sup>-3</sup>). Measuring cylinders were initially replaced after 25, 50 or 100 ml of solution was added, depending on the Al concentration level. Overnight, all incoming solution was collected. During the first day of the experiment, this could amount to ca. one l at low Al concentrations. Concentrations of Si, Al, Fe, Ca and Mg were measured with ICP and K and Na with AAS. At the end of the experiment, the concentration of cations and Si was also measured in the stirred solution in the plastic container. Rates of cation and Si release during a given time interval were calculated with Eq. 3.1 (Section 3.1). As with the batch experiments, exchangeable cations and solid-phase pools of Al and Fe were measured before and after the experiment.

### Hypothetical models for cation release

#### *Base cations*

Until the mid-seventies, the rate of mineral weathering was generally believed to be limited by diffusion of reactants through a layer of secondary precipitates (e.g. Helgeson, 1971) or leached material (e.g. Busenberg and Clemency, 1976) covering the mineral surface. At present the prevailing hypothesis is that the rate of mineral weathering is limited by detachment of an activated complex (at specific sites) on the mineral surface (e.g. Aagaard and Helgeson, 1982). According to the latter hypothesis (the transition state theory), the rate of mineral dissolution can be described as a function of the proton activity and the degree of undersaturation with the reacting material. Far from equilibrium, the last term is, however, negligible (Aagaard and Helgeson, 1982). In sandy soils, base cation release is likely dominated by weathering from primary Al silicates, such as feldspars, anorthite and chlorite, that are far from equilibrium with dissolved cations. It was hypothesized that mineral weathering in these soils is governed by proton activity. Depletion of the reactive minerals may also influence the weathering rate, but the change in base cation pool during one-year batch experiments is generally very small (cf Section 3.1). To describe the fast initial decrease in base cation release rates (which may be due to a fast decrease of the exchange between H and base cations at the mineral surface), the influence of reaction time was, however, included in the model according to:

$$CR_{X,t} = \beta_1 \cdot (H)^{\beta_2} \cdot t^{\beta_3} \quad (3.8)$$

where  $CR_{X,t}$  is the cumulative release of cation X at time t (mmol<sub>c</sub> kg<sup>-1</sup>), t is time (d), (H) is the proton activity,  $\beta_1$  is a rate constant and  $\beta_2$  and  $\beta_3$  are exponents. At a fixed proton activity, Eq. (3.8) becomes equal to Eq. 3.5a (Section 3.1).

According to Van der Zee et al. (1989) there is a functional relationship between the conversion of solid-phase particles by element release and the integral of concentration over time (the so-called exposure variable) for reactions whose rates are controlled by



reactant diffusion, a first-order chemical reaction or a combination of both. Generally, the conversion of solid-phase compounds is related to the cumulative element release in water. This holds specifically for cumulative Al release, and the conversion of secondary Al compounds (Section 3.1). According to this hypothesis, the exponents  $\beta_2$  and  $\beta_3$  should not differ significantly. Eq. (3.8) thus simplifies to:

$$CR_{X,t} = \beta_1 ((H) \cdot t)^{\beta_2} \quad (3.9)$$

An important consequence of the use of an exposure variable  $((H) \cdot t)$  is that information on cation release rates after long reaction times and at low proton activities, or high pH values, may be assessed with short duration experiments at high proton activities, or low pH values (concentration - time scaling; cf Van der Zee, 1989).

To describe the effect of proton activity on cation release, the observed cumulative release with time was used (cf Eq. 3.8). Observed release rates with time became extremely low, and thus inaccurate, in the course of the experiment. Release rates can, however, be derived by differentiating Eq. (3.8) according to:

$$RR_{X,t} = \beta_1^* \cdot (H)^{\beta_2} \cdot t^{\beta_2} \quad (3.10)$$

where  $RR_{X,t}$  is the release rate of cation X at time t ( $\text{mmol}_c \text{ kg}^{-1} \text{ d}^{-1}$ ).  $\beta_1^*$  equals  $\beta_1 \cdot \beta_3$  and  $\beta_3^*$  equals  $\beta_3 - 1$ . At a given time t the effect of pH and cation release rate can be described by a simple power-type relationship according to (see Aagaard and Helgeson, 1982; Van Grinsven et al., 1992; Dahlgren and Walker, 1993):

$$RR_X = \beta_4 \cdot (H)^{\beta_4} \quad (3.11)$$

To allow intercomparison of the effect of pH, the various equations were not only applied to the release of base cations but also to Al, Fe and Si release. Combined effects of Al activity and time on the release of cations or Si were described with similar equations as those given for proton activity and time. In Eq. (3.9), however, the reciprocal Al activity was used, since a lower Al activity will increase the release rate of Al and possibly that of Si and other cations.

### Aluminium

Unlike base cations, there is a clear relationship between the release rate of Al and mineral depletion (depletion of secondary Al compounds). The logarithmic Al release rate was found to decrease linearly with the cumulative release of Al, which mainly stems from secondary Al compounds (Section 3.1). Furthermore, secondary Al compounds in acid sandy soils are much closer to equilibrium than primary Al silicates. It is thus very well possible that the influence of proton and Al activity on Al release

rates is caused by a change in the degree of undersaturation with the secondary Al compound. It was therefore hypothesized that the combined effect of proton or Al activity and Al depletion on the (logarithmic) Al release rate can be described by the degree of undersaturation with respect to -, and the pool of secondary Al compounds according to:

$$\ln \left( \frac{RR_{Al,t}}{(Al)_e - (Al)} \right) = \ln \beta_5 + \beta_6 \cdot Al_{sc,t} \quad (3.12a)$$

or (cf Eq. 6.53 in Section 6.2):

$$RR_{Al,t} = \beta_5 \cdot e^{\beta_6 \cdot Al_{sc,t}} \cdot ((Al)_e - (Al)) \quad (3.12b)$$

where  $(Al)_e$  is the activity of Al in equilibrium with the secondary Al compounds ( $\text{mol}_c \text{ m}^{-3}$ ),  $Al_{sc,t}$  is the pool of secondary Al compounds at time  $t$  ( $\text{mmol}_c \text{ kg}^{-1}$ ) and where  $\beta_5$  ( $\text{l kg}^{-1} \text{ d}^{-1}$ ) and  $\beta_6$  ( $\text{kg mmol}_c^{-1}$ ) are rate and capacity constants, respectively. The pool of secondary Al compounds with time, further denoted as secondary Al pool, was calculated by subtracting the cumulative Al release, corrected for Al exchange measured at the end of the experiment. To eliminate differences in the initial secondary Al pool of the various horizons, the logarithmic Al release rate, scaled by the degree of undersaturation, was also described as a function of the depletion fraction of that pool:

$$\ln \left( \frac{RR_{Al,t}}{(Al)_e - (Al)} \right) = \ln \beta_5 + \beta_7 \cdot \left( 1 - \frac{Al_{sc,t}}{Al_{sc,t_0}} \right) \quad (3.13)$$

where  $Al_{sc,t_0}$  is the secondary Al pool at the start of the experiment ( $t_0$ ). Based on results of an 'equilibrium study' between Al and pH in three Bs horizons of podzolic soils (Dahlgren and Walker, 1993), the equilibrium Al activity was assumed to be regulated by Al hydroxides with an equilibrium constant,  $KAl_{ox}$ , equal to that of synthetic gibbsite.  $(Al)_e$  was thus calculated as:

$$(Al)_e = KAl_{ox} \cdot (H)^3 \quad (3.14)$$

with  $\log KAl_{ox} = 8.1$ . Actually, Dahlgren and Walker (1993), observed an exponent of 2.7 instead of 3.0. Even though gibbsite is hardly detected in acid sandy soils, the equilibrium constant for the dissolution of this mineral often yields a reasonable prediction of the Al activity in the subsoil of acid sandy soils (e.g. Nilsson and Bergkvist, 1983; Driscoll et al., 1985; Mulder and Van Breemen, 1987).

The degree of undersaturation with respect to 'gibbsite' is determined both by the actual Al activity and the equilibrium Al activity, which in turn is influenced by the pH (Eq. 3.14). Consequently, the Eqs. (3.12) and (3.13) can be used to describe the effect of different levels of both pH and Al activity on the Al release rate. We also investigated whether fits improved when the degree of undersaturation in the Eqs. (3.12) and (3.13) was represented according to  $((Al)_e - (Al)) / (Al)_e$ . This description is nearly equal to  $1 - Q/K$  where  $Q$  is the ionic activity product of gibbsite (the product of  $(Al)$  and  $(H)^3$ ) and  $K$  is  $KAl_{ox}$ , described according to Eq. (3.14). Such a description was used by Van Grinsven et al. (1986) to account for the effect of changes in Al activity. At a constant pH, the different descriptions for the degree of undersaturation do not affect the fit since  $(Al)_e$  is constant.

## RESULTS AND DISCUSSION

### Cumulative cation and silica release

#### Effects of pH

Cumulative release of cations and Si during one year significantly increased with decreasing pH for all soil samples studied. As an example, results are given for the Bh horizon (Table 3.15).

Table 3.15 Annual release of cations and silica from the Bh horizon in batch experiments at five pH levels

pH level	Annual release (mmol <sub>e</sub> kg <sup>-1</sup> )								Proton consumption (mmol <sub>e</sub> kg <sup>-1</sup> )
	Si <sup>1)</sup>	Al	Fe	Ca	Mg	K	Na	Cations <sup>2)</sup>	
2.5	29	469	37	3.13	1.28	3.06	2.61	516	470
2.7	17	398	30	2.69	0.88	2.67	2.08	436	370
3.0	12	256	17	1.21	0.41	4.24 <sup>3)</sup>	4.46 <sup>3)</sup>	278	238
3.3	6.1	113	4.3	1.28	0.29	1.37	0.94	122	105
3.5	4.2	43	0.23	0.46	0.23	0.83	0.51	47	42

<sup>1)</sup> For Si a charge of 4 was used

<sup>2)</sup> Cations stands for the sum of Al, Fe, Ca, Mg, K and Na

<sup>3)</sup> Anomalous values

The effect of pH on the dissolution rate of the various cations and Si could be described well with a power-type relationship (Eq. 3.11). Except for Ca and Mg in the C horizon, values of  $R^2_{adj}$  which give an indication of the goodness of fit, varied between 0.76 and 0.97. Values for the exponent  $\beta_2$  (Table 3.16) generally decreased according to  $Mg > Fe > Al \approx Si > Ca \approx K \approx Na$ . There were, however, striking differences between the various horizons. In the BCs horizon, for example, the effect of pH on the release rate was larger for Si than for Al and the annual Al/Si release ratio (mol mol<sup>-1</sup>) decreased from 3.9 at pH 3.5 to 2.4 at pH 2.5. In the C horizon, however, the annual Al/Si ratio stayed rather constant, i.e. 4.2 at pH 4.0 and 3.7 at pH 3.0. The constant, or even

Table 3.16 Values for the exponent  $\beta_2$  in the relationship  $CR_x = \beta_2 \cdot (H)^{\beta_2}$  for the soil samples studied<sup>1)</sup>

Soil horizon	$\beta_2$ value						
	Al	Fe	Ca	Mg	K	Na	Si
(A+B)p	0.72	1.31	1.22	0.93	0.71	0.72	0.93
Bh	1.00	1.38	0.48	2.01	0.73	0.75	0.81
BCs	0.62	1.33	0.64	2.31	0.56	0.52	0.79
C	1.63 <sup>2)</sup>	0.70 <sup>3)</sup>	- <sup>3)</sup>	- <sup>3)</sup>	0.71	1.45	1.20

<sup>1)</sup>  $CR_x$  is the cumulative dissolution of element X during a one-year batch experiment ( $\text{mmol}_e \text{ kg}^{-1} \text{ yr}^{-1}$ ), which was calculated by subtracting annual release by cation exchange from total annual cation release

<sup>2)</sup> This large value is strongly influenced by the nearly negligible Al release at the highest pH level.

<sup>3)</sup> Statistically insignificant

decreasing, Al/Si ratio at lower pH values supports the hypothesis made earlier (De Vries, 1994a; Section 3.1) that the secondary Al pool in the BCs and C horizon largely consists of secondary aluminosilicates.

Values of  $\beta_2$  calculated for Al are in the range reported in literature (0.3-1.2; Stumm and Furrer, 1986; Bloom and Erich, 1987; Van Grinsven et al., 1992; Dahlgren and Walker, 1993), except for the C horizon ( $\beta_2 = 1.63$ ). However, exclusion of the highest pH level (pH 4.0), where Al release was nearly negligible gave a  $\beta_2$  value of 0.84 for this horizon. The relative low value for the BCs horizon was due to depletion of the pool of reactive Al, i.e. secondary Al compounds including exchangeable Al (Table 3.3; Section 3.1), after one year at pH values below 3.0. Below pH 3.0, the ratio of annual Al release to the reactive Al pool approached 1.0 in that horizon. In the other horizons, total Al depletion was not yet observed (Fig. 3.5A).

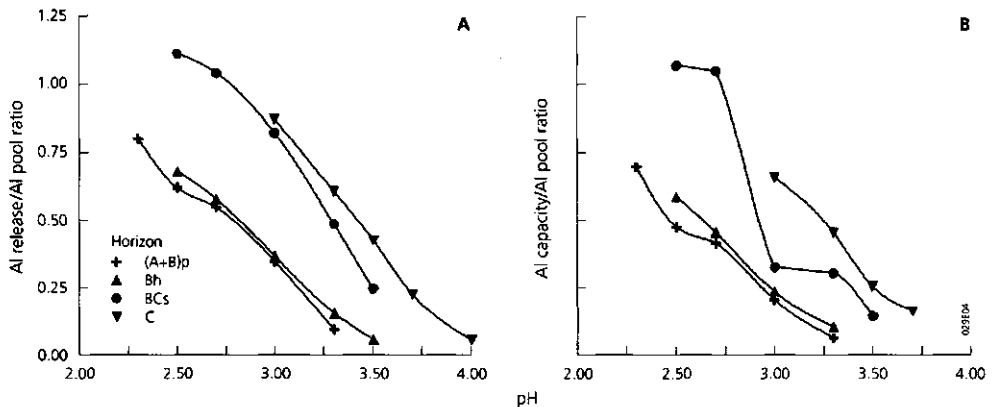


Figure 3.5 The ratio of annual Al release (A) and the non-linear Al dissolution capacity (B) to the reactive Al pool as a function of pH level for the soil samples studied

In the BCs horizon, the ratio of the calculated non-linear dissolution capacity  $\alpha_1$  (Eq. 3.2; Section 3.1) to the reactive Al pool also approached 1.0 below pH 3.0 (Fig. 3.5B). At sufficiently low pH values, the value of  $\alpha_1$  in the empirical three parameter model thus appeared to coincide with the reactive Al pool. The half-life time of this pool decreased significantly with a decrease in pH (ca. 20 days at pH 3.5 to ca. 6 days at pH 2.5). A similar decrease in half-life time was found for the Bh and C horizon. This indicates that rate-limited dissolution of inorganic Al compounds dominates the release of Al in the Bh, BCs and C horizon. In the (A+B)p horizon, however, the half-life time varied between ca. 1.0 and 3.5, nearly independent of the pH level. This indicates that release of Al in this horizon is dominated by equilibrium reactions between protons and organically bound Al (cf Section 3.1).

The strong effect of pH on Fe release is likely influenced by the stronger depletion of secondary Al compounds at lower pH values. At a given rate of Al depletion (cumulative Al release), Fe release rates were hardly influenced by pH. This is illustrated in Figure 3.6 for the (A+B)p and Bh horizon, where Fe release is relatively large (in accordance with the large pool of secondary Fe compounds; cf Table 3.3 in Section 3.1). Fe release became more important in these horizons at a larger Al depletion, irrespective of the pH (Fig. 3.6).

$\beta_2$  values calculated for Mg are slightly above those given by Van Grinsven et al (1988), who reported a range between 0.7 and 1.7.  $\beta_2$  values for Ca, K and Na are also higher than those reported by Van Grinsven et al. (1988). These authors observed no pH effects on Ca and Na release, except below pH 3.0. The calculated values for  $\beta_2$  in this study were, however, strongly influenced by the large increase in base cation release at pH values of 3.0 (C horizon) and lower (other horizons).

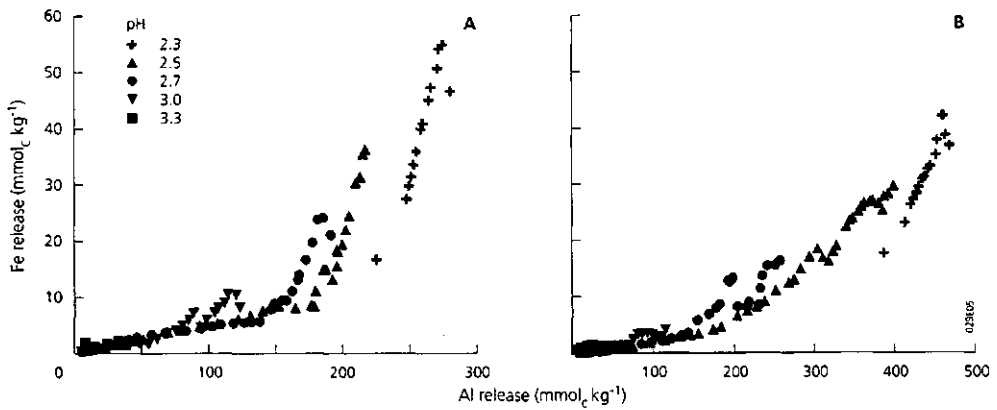


Figure 3.6 Cumulative Fe release in the (A+B)p horizon (A) and Bh horizon (B) as a function of cumulative Al release at five pH levels

### Effects of Al concentration

An increase in Al concentration level significantly decreased Al release rates in all soil horizons. In the BCs and C horizon, where secondary Al silicates are the major source of Al release, Si release decreased even more strongly with increasing Al concentration (Fig. 3.7). Si release in the (A+B)p and Bh horizon only decreased when the Al concentration increased from 0.5 to 2.0 mol<sub>c</sub> m<sup>-3</sup>, indicating that (secondary) Al silicates also play a minor role in Al release from these horizons. Fe release also decreased significantly in all soil horizons with an increase in Al concentration from 0.5 to 9.0 mol<sub>c</sub> m<sup>-3</sup>. At the highest Al concentration, Fe release increased again in the (A+B)p and Bh horizon, which was partly due to exchange of Al against Fe. The increase in Fe release with decreasing Al concentration is likely due to Al depletion.

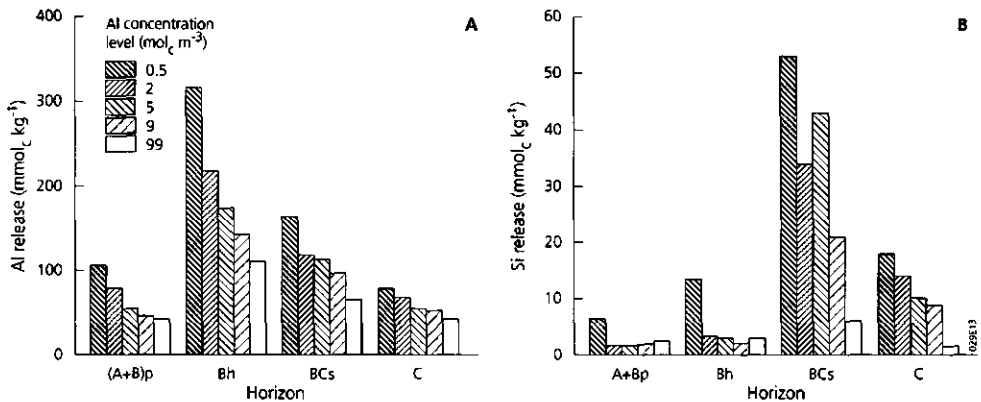


Figure 3.7 Release of Al (A) and Si (B) in column experiments during one week as a function of Al concentration level for the soil samples studied

In the BCs and C horizon, release rates of Ca, and to a lesser extent those of Mg, K and Na, decreased significantly with an increase in Al concentration. In these horizons, cation release is hardly influenced by cation exchange and release rates nearly equal weathering rates (Section 3.1; cf section on effects of pH and Al concentration on cation release mechanisms). The observed decrease in BC release with an increase in Al concentration in the lower BCs and C horizon implies that dissolved Al limits the rate of Al and BC weathering from primary Al silicates. This effect has also been observed in laboratory studies with pure minerals, such as albite (Chou and Wollast, 1985), K feldspar (Wollast, 1967; Fung et al., 1980) and anorthite (Sverdrup, 1990). It has also been implemented in a model that calculates weathering rates from information on the mineralogical composition of soils (Sverdrup and Warfvinge, 1988a).

Cumulative Al release could be described very well as a power of the Al activity. This equation also gave reasonable to good predictions of Si, Fe and Ca release in the BCs and C horizon (Table 3.17). Values for the exponent  $\beta_9$  were comparable for the BCs

Table 3.17 Values for the exponent  $\beta_9$  and the adjusted coefficient of determination,  $R^2_{adj}$ , in the relationship  $CR_x = \beta_9 \cdot (Al)^{\beta_9}$  for the BCs and C horizon

Soil horizon	$\beta_9$ value				$R^2_{adj}$			
	Al	Si	Fe	Ca	Al	Si	Fe	Ca
BCs	-0.25	-0.58	-0.57	-0.17	0.97	0.75	0.92	0.47
C	-0.18	-0.68	-0.57	-0.28	0.95	0.87	0.99	0.99

<sup>1)</sup>  $CR_x$  is the cumulative release of element X during a one-week column experiment ( $\text{mmol}_c \text{ kg}^{-1} \text{ wk}^{-1}$ ), and (Al) is the Al activity ( $\text{mol}_c \text{ m}^{-3}$ ) at the beginning of the experiment (the value of (Al) hardly changed with time)

and C horizon for all elements.  $\beta_9$  values for Al in the (A+B)p and Bh horizon equalled -0.26 and -0.28 ( $R^2_{adj}$  was 0.93 and 0.99, respectively), which is comparable to the BCs and C horizon. Comparison with Table 3.16 shows that the effect of proton activity on Al release rates is much larger than the effect of Al activity.

### Cation and silica release rates with time

#### Effects of pH

For all soil horizons and at all pH levels (except for pH 4.0 in the C horizon), rates of cation release with time could be described reasonably well by a double logarithmic equation (Section 3.1; Eq. 3.5b). Fits were best for Al ( $R^2_{adj} > 0.90$ ). Values of  $R^2_{adj}$  for Fe, BC and Si generally ranged between 0.60 and 0.90. For Al, the ratio of log release rate to log time (the exponent in the relation between release rate and time; Section 3.1; Eq. 3.5a) mostly approached a value of -1, as illustrated for the Bh horizon (Fig. 3.8A; Table 3.18). For the other cations, the slope generally ranged between -0.5 and -1 as illustrated for Fe release in the Bh horizon (Fig. 3.8B; Table 3.18).

The change in the (log) release rate of Al with (log) time (the slope in Table 3.18) increased with decreasing pH. The reverse was found for the Fe release rate, although the uncertainty in the slope was relatively large at high pH values. Again, this illustrates that a faster depletion of secondary Al compounds (at lower pH values) counteracts the effect of pH on Al release rates at longer reaction times, whereas Al depletion stimulates Fe release. Based on the intercept and slope in the double logarithmic equation for Al at pH 2.5 and at pH 3.5 (cf Table 3.18), it can be calculated that Al release rates in the Bh horizon are equal for both pH values after ca. 19 years (i.e.  $7.67 \cdot 10^{-3} \text{ mmol}_c \text{ kg}^{-1} \text{ d}^{-1}$  or  $2.8 \text{ mmol}_c \text{ kg}^{-1} \text{ yr}^{-1}$ ). At pH 2.5, however, the reactive Al pool ( $688 \text{ mmol}_c \text{ kg}^{-1}$ ) will be depleted by more than 90% after 19 years, whereas it will have decreased by only ca. 10% at pH 3.5 (assuming that cumulative Al release is equal to the decrease in reactive Al pool; cf Section 3.1). Unlike Al, calculated Fe release rates at pH 2.5 are more than 100 times larger than those at pH 3.5 after ca. 19 years.

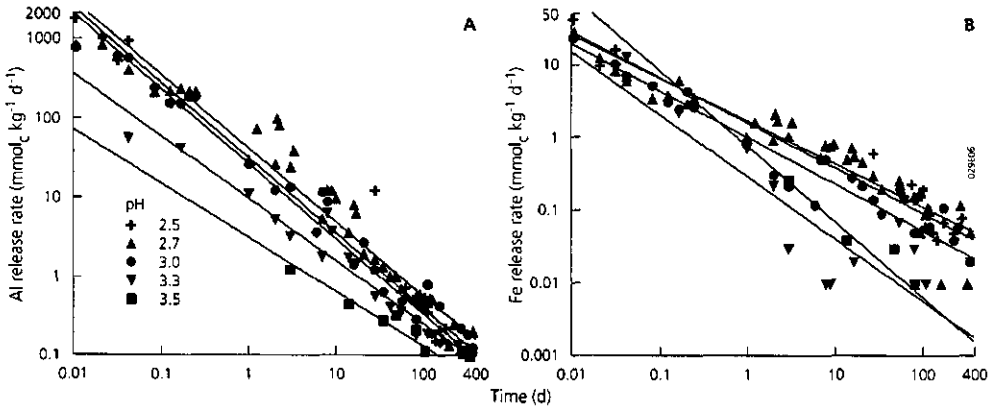


Figure 3.8 Measured and predicted release rates of Al (A) and Fe (B) with time at five pH levels for the Bh horizon. Experimental data are denoted by symbols, whereas solid lines are the predictions made with a double logarithmic model (Table 3.18)

Table 3.18 Intercepts and slopes of a double logarithmic equation (Eq. 3.5b; Section 3.1) for the release rate of Al and Fe ( $\text{mmol}_c \text{kg}^{-1} \text{d}^{-1}$ ) against time (d) at five pH levels for the Bh horizon

pH level	Al release rate			Fe release rate		
	intercept ( $\log \alpha_8$ )	slope ( $\alpha_9$ )	$R^2_{adj}$	intercept ( $\log \alpha_8$ )	slope ( $\alpha_9$ )	$R^2_{adj}$
2.5	1.50 (0.09)	-0.94 (0.04)	0.96	0.23 (0.07)	-0.58 (0.04)	0.95
2.7	1.62 (0.05)	-0.92 (0.03)	0.95	0.20 (0.07)	-0.62 (0.03)	0.84
3.0	1.42 (0.06)	-0.94 (0.04)	0.96	0.01 (0.07)	-0.64 (0.05)	0.89
3.3	0.99 (0.07)	-0.78 (0.04)	0.95	-0.53 (0.23)	-0.85 (0.14)	0.71
3.5	0.50 (0.13)	-0.67 (0.07)	0.93	-0.11 (0.25)	-1.03 (0.15)	0.92

<sup>1)</sup> Values between brackets denote the standard deviation

The combined effect of proton activity (pH) and time on cumulative Si release was described reasonably well with the concentration-time scaling principle (Eq. 3.9), with a value of 0.5 for the exponent  $\beta_2$  ( $0.82 < R^2_{adj} < 0.94$ ). This is illustrated for the Bh horizon in Figure 3.9. A similar result was found by Van der Zee et al. (1989) who argued that experimental data confirming such a relation can either be due to diffusion-controlled kinetics (e.g. Wollast, 1967; Helgeson, 1971) or to a first-order surface reaction (e.g. Helgeson et al., 1984). Even though cumulative BC release was described less well with Eq. (3.9), as compared to Si, the description did not improve significantly when different exponents were used for H and t (cf Eq. 3.8), except for Mg, K and Na in the C horizon. Values of  $R^2_{adj}$  generally varied between 0.5 and 0.8. The description of cumulative Al release, however, improved significantly ( $0.85 < R^2_{adj} < 0.94$ ) when different exponents were used for H and t (Eq. 3.8) as compared to the concentration-time scaling principle ( $0.64 < R^2_{adj} < 0.78$ ). Exponents for H ( $\beta_2$ ) varied between 0.77 and 1.28 (cf Table 3.16) whereas exponents for t ( $\beta_3$ ) varied between 0.29 and 0.46.



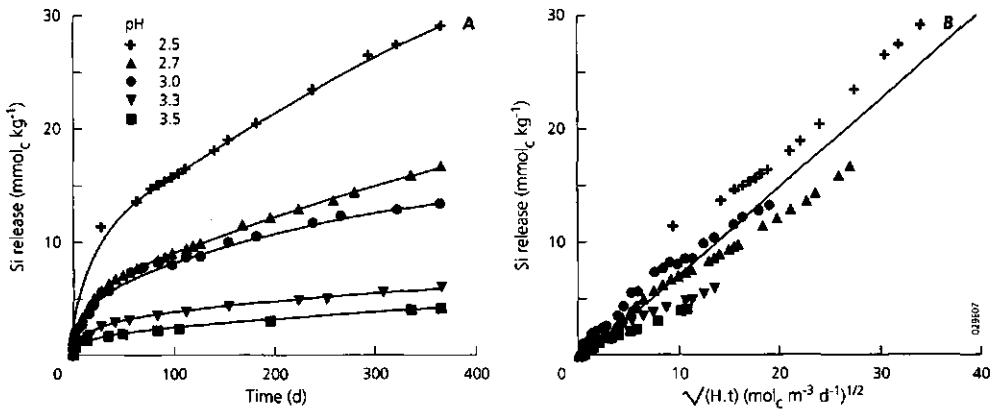


Figure 3.9 Cumulative Si release of as a function of time at five pH levels (A) and as a function of the square root of proton activity and time (B) for the Bh horizon. Experimental data are denoted by symbols. The solid line in Fig. 3.9B is the prediction made with Eq. (3.9)

Concentration-time scaling thus appeared to be of limited value in describing Al release, in contrast to results given by Van der Zee et al. (1989). The exponents for H and  $t$  in the description of cumulative Fe release also differed significantly. Exponents for H varied between 0.89 and 1.26 (cf Table 3.16) whereas exponents for  $t$  varied between 0.35 and 0.53. Presumably, release of Al and Fe from secondary Al and Fe compounds is neither limited by surface reactions nor by reactant diffusion. Especially in the upper (A+B)p and Bh horizon, the rapid decrease in Al (and Fe) release rate ( $\beta_3 < 0.5$ ) may be influenced by approaching equilibrium with organic Al compounds (cf Section 3.1).

#### pH, mineral saturation and Al release rates

The strong effect of pH on Al release rates with time can be caused by approaching equilibrium with secondary Al minerals at higher pH. At a given pH level the degree of undersaturation with respect to Al hydroxides (gibbsite) and Al hydroxy sulphates (jurbanite, basaluminite) hardly changed during the experiments, since concentrations of Al and  $\text{SO}_4$  changed little (cf Section 3.1). However, the degree of undersaturation with respect to these minerals, was less in experiments with higher pH levels (Fig. 3.10).

Figure 3.10 shows that the variation in degree of undersaturation was very small at each of the eight pH levels considered (cf Table 3.13), except for pH 3.3 ( $2\text{pH} + \text{pSO}_4 \approx 10$ ). Going from batch experiments at pH 2.3 ( $2\text{pH} + \text{pSO}_4 \approx 8$ ) to pH 4.0 ( $2\text{pH} + \text{pSO}_4 \approx 11.5$ ), however, the degree of undersaturation strongly decreased with respect to gibbsite and basaluminite but only slightly with respect to jurbanite. The occurrence of points along the jurbanite solubility line is generally found in systems where Al and  $\text{SO}_4$  dominate the soil solution (such as acid forest soils) and is not any proof for the existence of this mineral in acid sandy soils. It is even unlikely that jurbanite governs Al release, since saturation with respect to jurbanite and a considerable annual Al release

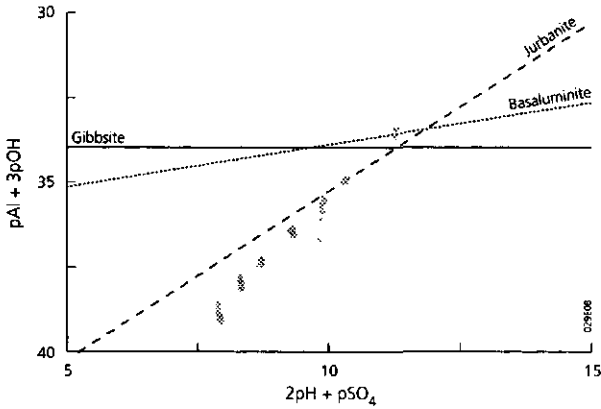


Figure 3.10  $pAl+3pOH$  as a function of  $2pH+pSO_4$  for solutions from batch experiments with the four soil horizons studied at eight pH levels (after Van Breemen, 1973). Experimental data are denoted by dotted points, whereas solid lines represent the solubility diagrams for synthetic gibbsite, basaluminite and jurbanite (see Table 3.19 for the equilibrium relationship used)

(43-69  $mmol_c kg^{-1}$ ) occurred simultaneously in batch experiments near pH 3.5 ( $2pH + pSO_4 \approx 10$ ) with the Bh, BCs and C horizons (cf Mulder et al., 1988).

Saturation indices (Table 3.19;  $SI = 0$  indicates equilibrium,  $SI > 0$  oversaturation and  $SI < 0$  undersaturation with respect to the solubility of the mineral considered) indicated that saturation of the solution with respect to secondary Al minerals, other than jurbanite, hardly ever occurred. The only exception was the batch experiment with the C horizon at pH 4.0, where solutions were slightly oversaturated with respect to synthetic gibbsite and kaolinite and nearly saturated with respect to imogolite (Fig. 3.11B; Table

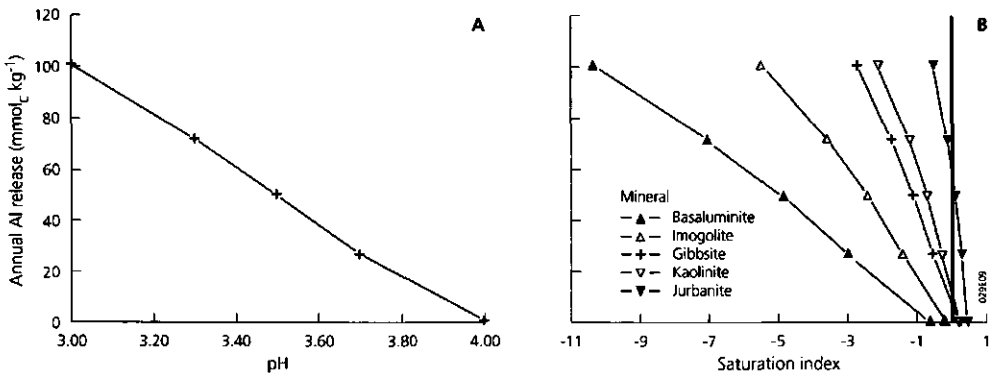


Figure 3.11 Annual Al release in the C horizon as a function of pH level (A) and saturation index with respect to various secondary Al minerals at the end of the batch experiments (B)

Table 3.19 Saturation indices in solutions from the soil samples studied at the end of batch experiments at the lowest and highest pH level considered

Secondary Al mineral	Saturation indices <sup>1)</sup>							
	Lowest pH value <sup>2)</sup>				Highest pH value <sup>3)</sup>			
	(A+B)p	Bh	BCs	C	(A+B)p	Bh	BCs	C
Synthetic gibbsite	-4.9	-4.2	-4.3	-2.7	-1.7	-1.1	-1.2	0.18
Natural gibbsite	-5.6	-4.8	-5.0	-3.4	-2.4	-1.8	-1.8	-0.49
Basaluminite	-17.5	-15.1	-15.7	-10.4	-6.8	-4.8	-5.0	-0.67
Jurbanite	-1.3	-1.0	-1.1	-0.54	-0.07	0.13	0.05	0.43
Kaolinite	-5.0	-3.8	-3.5	-2.2	-2.5	-1.1	-0.61	0.19
Imogolite	-10.5	-8.5	-8.4	-5.5	-4.8	-2.8	-2.4	-0.22

1) Saturation indices, SI, were calculated as  $SI = \log Q_p - \log K_p$ , where  $Q_p$  is the ionic activity product and  $K_p$  is the solubility product for the solid phase p. Activity corrections were made with the Debye-Hückel equation. Equilibrium relationships at 25°C (298°K) that were used are:  $\log Al - 3 \log H = 8.11$  (synthetic gibbsite);  $\log Al - 3 \log H = 8.77$  (natural gibbsite);  $4 \log Al + 4 \log SO_4 - 10 \log H = 22.70$  (basaluminite);  $\log Al + \log SO_4 - \log H = -3.23$  (jurbanite);  $\log Al + \log H_2SiO_4 - 3 \log H = 3.30$  (kaolinite) and  $2 \log Al + \log H_2SiO_4 - 6 \log H = 12.00$  (imogolite). Temperature corrections to 20°C (293°K) were made with the Van 't Hoff equation

2) Lowest pH values equalled 2.3 for the (A+B)p horizon, 2.5 for the Bh and BCs horizon and 3.0 for the C horizon (cf Table 3.14)

3) Highest pH values equalled 3.3 for the (A+B)p horizon, 3.5 for the Bh and BCs horizon and 4.0 for the C horizon (cf Table 3.14)

3.19). In this experiment, annual release of Al was indeed nearly negligible (Fig. 3.11A). Al regulation by kaolinite is unlikely in view of the negligible clay content in the C horizon and the large Al/BC release ratio at low pH values (cf Table 3.1 and 3.5; Section 3.1). Considering this result, the hypothesis that Al hydroxides, with a pK value equal to that of gibbsite, govern Al release was not rejected. Most likely, secondary Al silicates play, however, a more dominant role in the lower BCs and C horizon.

#### Effects of Al concentration

As with the batch experiments, Al release rates with time could be described well ( $0.90 < R^2_{adj} < 0.99$ ) by a double logarithmic equation (Eq. 3.5b). Fits were made with Al release rates, that were estimated as the difference between H consumption rates and the sum of Fe and BC release rates. This was done because Al concentration measurements were only very few in column experiments at high Al concentration levels, whereas proton consumption, which nearly equals Al release (cf Section 3.1), was recorded every five minutes. Unlike the batch experiments, the exponent in the relation between Al release rate and time (cf Eq. 3.5a) generally ranged around -0.5 ( $-0.39 < \alpha_9 < -0.58$ ). It is, however, unlikely that proton diffusion is the rate-limiting step in the column experiments. Limitation of proton transport from the solution to the mineral by a stagnant water film at the interface of the reaction surface and bulk solution, (cf Van Grinsven and Van Riemsdijk, 1992) is not plausible at the extremely fast through-flow of titration solution ( $10 \text{ ml min}^{-1}$ ) in these experiments.

The combined effect of Al activity and time on cumulative release of Al, Si and Fe was described well with Eq. (3.8) with (Al) instead of (H) in the equation. Values of  $R^2_{adj}$  were generally comparable for Al, Fe and Si ( $0.89 < R^2_{adj} < 0.96$ ), except for the (A+B)p horizon where Al release was fitted much better ( $R^2_{adj} = 0.89$ ) than Si release ( $R^2_{adj} < 0.62$ ). Exponents for (Al) for the BCs and C horizon equalled 0.16 and 0.18 for Al, 0.37 and 0.45 for Si and 0.41 and 0.42 for Fe, respectively (cf Table 3.17). Similar exponents were found in the (A+B)p and Bh horizon, except for the effect of (Al) on Fe release (exponents near 0.1). The description of Al release in the various horizons decreased significantly when a similar exponent (0.5) for H and  $t$  was used ( $R^2_{adj}$  was 0.74 and 0.68 in the BCs and C horizon, respectively; cf Table 3.17). Again, concentration-time scaling did not give an adequate description of Al release. The same was found for BC release, which was already described poorly as a function of Al activity and time ( $0.39 < R^2_{adj} < 0.86$ ). However, the description decreased significantly when a similar exponent was used for H and  $t$ .

Rates of Al release in the column experiments were higher than in the batch experiments under similar conditions for pH (3.0) and Al concentration (near  $2.0 \text{ mol}_e \text{ m}^{-3}$ ), as illustrated in Table 3.20. Compared to the batch experiments, Al release in the column experiments was twice as high in the (A+B)p, Bh and BCs horizon during the first week, whereas rates were quite comparable in the C horizon. Measured (batch experiments) and extrapolated (column experiments) Al release after 1 year hardly differed, except for the Bh horizon, because of the effect of Al depletion. One explanation for the larger (initial) release rates in the column experiments is that the pH was continuously kept at pH 3.0, whereas the pH initially (first day) increased up to 3.5 in the batch experiments. Furthermore, the contact between titration solution and soil samples (reactive Al pool) is more efficient in the column experiments, than in the batch experiments, where the suspension was hardly stirred.

Table 3.20 Al release in batch and column experiments at pH 3.0 and an Al concentration near  $2.0 \text{ mol}_e \text{ m}^{-3}$  for the soil samples studied

Soil horizon	Al release ( $\text{mmol}_e \text{ kg}^{-1}$ )					
	1 day		1 week		1 year	
	batch	column <sup>1)</sup>	batch	column	batch	column <sup>2)</sup>
(A+B)p	24	39	48	80	123	136
Bhe	84	114	132	219	256	359
BCs	25	25	53	119	222	221
C	20	26	45	68	101	124

<sup>1)</sup> Calculated as H consumption minus Fe and BC release, since measurements of Al were too few during the first day for an accurate estimate

<sup>2)</sup> Based on extrapolation of Al release to 1 year with a single logarithmic equation

## Al depletion and Al release rates

### Effects of pH

The Al release rate decreased exponentially as a function of cumulative Al release at all pH levels and for all soil samples studied, as illustrated for the (A+B)p and Bh horizon (Fig. 3.12). Fits with a single logarithmic equation (Eq. 3.7; Section 3.1) were good ( $0.88 < R^2_{adj} < 0.97$ ) (cf Fig. 3.12), except for two experiments (pH 2.7 and pH 3.0) with the BCs horizon ( $0.75 < R^2_{adj} < 0.79$ ), where Al release was quite anomalous between 40 and 100 days (cf Section 3.1).

The effect of pH on the ratio of log Al release rate to cumulative Al release (the slope in Fig. 3.12) was opposite to the ratio of log Al release rate to log time (the slope in Fig. 3.8A). In most soil horizons the effect of pH on Al release rate increased with an increase in cumulative Al release, as illustrated in Table 3.21. The exponent  $\beta_2$  for Al (Eq. 3.11) was much higher at a given cumulative Al release (depletion of secondary Al compounds) than at a given time (cf Table 3.16 and 3.21). The average value approached 3. This is the value of the exponent that is used to calculate the equilibrium Al activity as a function of H activity, assuming that 'gibbsite' governs the dissolution of Al (Eq. 3.14).

The combined effect of Al depletion and pH on Al release rate could be described well as a function of the secondary Al pool and the degree of undersaturation with respect to gibbsite (Fig. 3.13A; Table 3.22). Even fits of the logarithmic Al release rate against the pool of secondary Al compounds and pH were slightly worse ( $0.77 < R^2_{adj} < 0.91$ ) than those with Eq. (3.12a) (cf Table 3.22). The pH effect was, however, not described well

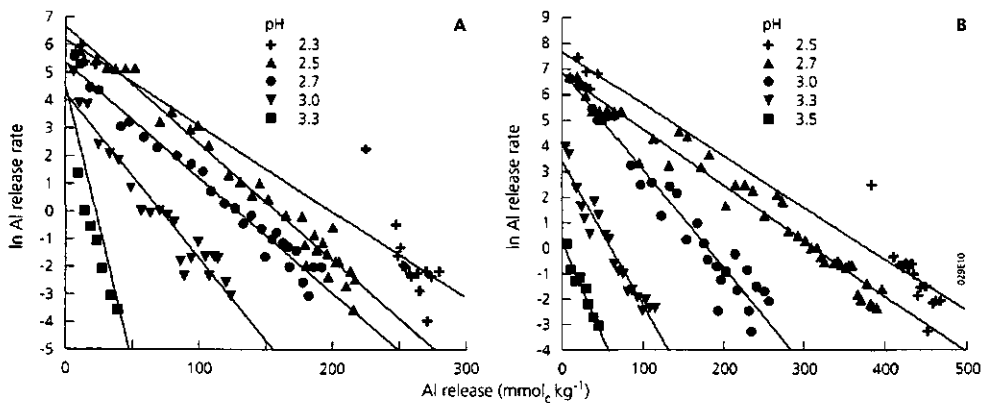


Figure 3.12 Measured and predicted logarithmic Al release rates at five pH levels as a function of cumulative Al release for the (A+B)p horizon (A) and the Bh horizon (B). The Al release rate is given in  $\text{mmol}_c \text{kg}^{-1} \text{d}^{-1}$ . Experimental data are denoted by symbols, whereas solid lines are the predictions made with a single logarithmic equation (Eq. 3.7; Section 3.1)

**Table 3.21** Values for the exponent  $\beta_2$  in the relationship between Al release rate and proton activity (Eq. 3.11) at a cumulative Al release of 25 and 100 mmol<sub>c</sub> kg<sup>-1</sup> for the soil samples studied

Soil horizon	Al release = 25 mmol <sub>c</sub> kg <sup>-1</sup>			Al release = 100 mmol <sub>c</sub> kg <sup>-1</sup>		
	N <sup>1)</sup>	$\beta_2$	$F^2_{adj}$	N	$\beta_2$	$F^2_{adj}$
(A+B)p	5	2.8	0.92	4 <sup>2)</sup>	3.4	0.79
Bh	5	4.3	0.84	4 <sup>2)</sup>	4.1	0.85
BCs	5	1.7	0.80	4 <sup>2)</sup>	2.8	0.87
C	4	3.4	1.00	1 <sup>3)</sup>	-	-

<sup>1)</sup> N is the number of data points

<sup>2)</sup> Al depletion up to 100 mmol<sub>c</sub> kg<sup>-1</sup> did not occur at the highest pH values, i.e. pH 3.3 ((A+B)p horizon) and pH 3.5 (Bh and BCs horizon)

<sup>3)</sup> A value of  $\beta_2$  could not be derived since Al depletion of 100 mmol<sub>c</sub> kg<sup>-1</sup> only occurred at one pH level (pH 3.0) in this horizon

( $0.23 < F^2_{adj} < 0.50$ ) when the degree of undersaturation was expressed as  $((Al_s) - (Al)) / (Al_s)$ . The decrease in Al release rate with a relative depletion of the secondary Al pool was faster in the upper (A+B)p and Bh horizon than in the lower BCs and C horizon (Fig. 3.13B; cf. the product of  $\beta_6$  and  $Al_{sc}$  in Table 3.22). This difference in Al behaviour between the horizons was also illustrated in De Vries (1994a) for batch experiments at pH 3.0 (Table 3.10; Section 3.1).

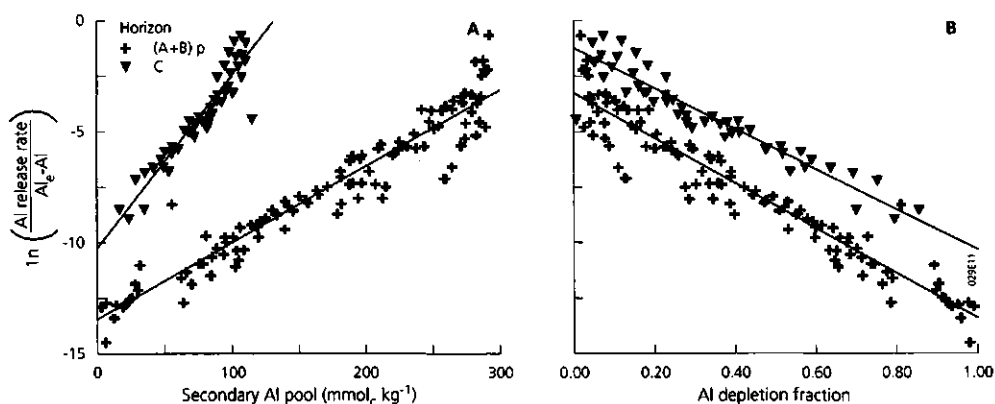


**Figure 3.13** The logarithmic Al release rate, scaled by the degree of undersaturation with respect to gibbsite, as a function of the secondary Al pool (A) and the depletion fraction of the secondary Al pool (B) for the (A+B)p and the C horizon. The Al release rate is given in mmol<sub>c</sub> kg<sup>-1</sup> d<sup>-1</sup>. Experimental data are denoted by symbols, whereas solid lines are the predictions made with Eq. (3.12a) (A) and Eq. (3.13) (B)

#### Effects of Al concentration

As with the batch experiments, the logarithmic Al release rate measured in the column experiments could be described very well as a linear function of cumulative Al release

**Table 3.22** Values for the parameters  $\beta_5$  and  $\beta_6$  in the relationship between Al release rate versus the secondary Al pool and the degree of undersaturation (Eq. 3.12a) for the soil samples studied. Values are estimated from batch experiments

Soil horizon	$\beta_5^{(1)}$ ( $\text{m}^3 \text{ kg}^{-1} \text{ yr}^{-1}$ )	$\beta_6^{(1)}$ ( $\text{kg} \cdot \text{mmol}_c^{-1}$ )	$\beta_6 \cdot \text{Al}_{sc}$	$F^2_{adj}$
(A+B)p	$5.5 \cdot 10^{-7}$	0.034	10.2	0.92
Bh	$1.4 \cdot 10^{-7}$	0.020	13.3	0.86
BCs	$3.1 \cdot 10^{-5}$	0.026	6.8	0.85
C	$1.3 \cdot 10^{-5}$	0.078	9.0	0.85

<sup>1)</sup> In the dynamic model RESAM (De Vries et al., 1994b), Eq. (3.12b) is used to describe the effects of both pH and Al concentration on the Al release rate (Eq. 6.53; Section 6.2). There  $\beta_5$  is denoted as  $kEI_1$  and  $\beta_6$  as  $kEI_2$  (Elovich constants). Furthermore, the pool of secondary Al compounds,  $\text{Al}_{sc}$ , is denoted as  $\text{Al}_{ox}$  which stands for oxalate extractable Al

(Eq. 3.7; Section 3.1) for all horizons at all Al activity levels ( $0.87 < F^2_{adj} < 1.00$ ). The combined effect of Al activity and Al depletion (cumulative Al release) was, however, not described so well by fitting the logarithmic Al release rate, scaled by the degree of undersaturation with gibbsite, against the secondary Al pool (Eq. 3.12a). Values for  $F^2_{adj}$  varied between 0.47 and 0.64 (Table 3.23). The values for  $\beta_5$  derived from the column experiments were higher than from the batch experiments, whereas the reverse was true for  $\beta_6$ , although the differences were small for the (A+B)p horizon (cf Table 3.22 and 3.23). The reliability of the values is, however, small considering the (lack of) fit. The measured effect of a change in Al concentration from 0.5 to 99  $\text{mol}_c \text{ m}^{-3}$  (a change in Al activity from ca. 0.35 to 13.5  $\text{mol}_c \text{ m}^{-3}$ ) was much larger than predicted by Eq. (3.12a). Such a change hardly affects the degree of undersaturation ( $(\text{Al}_a) - (\text{Al})$ ) since the value of  $(\text{Al}_a)$  at pH 3.0 equals 300  $\text{mol}_c \text{ m}^{-3}$  (using  $K\text{Al}_{ox}$  is  $10^{8.0} \text{ mol}^2 \text{ l}^2$ ).

The lack of fit of Eq. (3.12a) for column experiments at different Al concentration levels may point to control of Al solubility by organically bound Al. In the BCs and C horizon this is, however, very unlikely. In these horizons (secondary) Al silicates largely govern Al release (see before). The description of the Al release rate with Eq. (3.12a) was, however, just as bad in the lower BCs and C horizon as in the upper (A+B)p and Bh horizon. Describing the Al concentration effect by the degree of undersaturation with

**Table 3.23** Values for the parameters  $\beta_5$  and  $\beta_6$  in the relationship between Al release rate versus the secondary Al pool and the degree of undersaturation (Eq. 3.12a) for the soil samples studied. Values are estimated from column experiments at various Al concentration levels

Soil horizon	$\beta_5$ ( $\text{m}^3 \text{ kg}^{-1} \text{ yr}^{-1}$ )	$\beta_6$ ( $\text{kg} \text{ mmol}_c^{-1}$ )	$\beta_6 \cdot \text{Al}_{sc}$	$F^2_{adj}$
(A+B)p	$7.5 \cdot 10^{-6}$	0.033	9.8	0.55
Bh	$2.5 \cdot 10^{-4}$	0.011	7.4	0.64
BCs	$3.3 \cdot 10^{-3}$	0.012	3.1	0.62
C	$2.6 \cdot 10^{-3}$	0.024	2.8	0.47

Al release rate against the Al activity and the secondary Al pool also only slightly improved the description ( $0.45 < R^2_{adj} < 0.82$ ). Unlike pH, it seems that the combined effect of Al activity and Al depletion on the Al release rate can not be described well, neither as a function of the undersaturation with gibbsite nor by a simple empirical relation with Al activity.

**Effects of pH and Al concentration on cation release mechanisms**

*Base cations*

In the BCs and C horizon, with a nearly negligible base saturation (Table 3.2; Section 3.1), exchange of base cations played a negligible role compared to weathering. In the (A+B)p and Bh horizon, however, desorption of base cations was relatively important, especially at the higher pH levels (Fig. 3.14). Ca desorption dominated Ca release in the (A+B)p horizon above pH 2.5, whereas Mg desorption dominated Mg release in the Bh horizon above pH 3.0. At the higher pH levels, where both desorption and release were small, results are less reliable. This is illustrated by a contribution of Ca desorption to total Ca release above 100% at pH 3.3 in the (A+B)p horizon (Fig. 3.14A). The increased contribution of BC desorption to BC release with increasing pH is because BC desorption stays nearly constant at all pH levels, whereas BC weathering decreases. In the (A+B)p horizon, for example, Ca desorption approached the initial exchangeable Ca content ( $1.57 \text{ mmol}_c \text{ kg}^{-1}$ ; cf Table 3.2 of Section 3.1) at all pH levels. Values varied between  $1.45$  and  $1.57 \text{ mmol}_c \text{ kg}^{-1} \text{ yr}^{-1}$ , whereas Ca release decreased from  $3.28 \text{ mmol}_c \text{ kg}^{-1} \text{ yr}^{-1}$  at pH 2.3 to  $1.30 \text{ mmol}_c \text{ kg}^{-1} \text{ yr}^{-1}$  at pH 3.3.

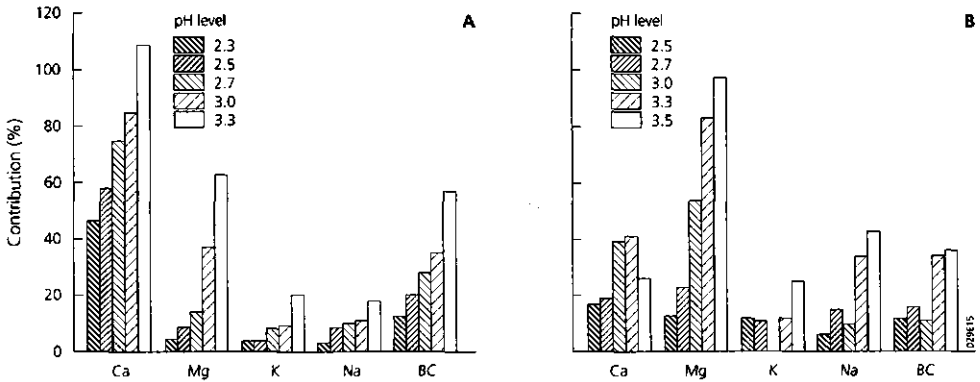


Figure 3.14 Contribution of desorption to the annual release of base cations in the (A+B)p horizon (A) and Bh horizon (B) at the various pH levels considered



### *Aluminium and iron*

Both Al and Fe exchange were nearly negligible in the BCs and C horizon. Al exchange, i.e. adsorption or desorption, in the (A+B)p and Bh horizon was still small compared to total Al release ( $< \pm 8\%$ ), even though absolute Al desorption could be large (up to  $16.8 \text{ mmol}_c \text{ kg}^{-1} \text{ yr}^{-1}$  in the (A+B)p horizon at pH 2.3). Fe adsorption in these horizons was, however, relatively large and varied mostly between 20 and 40% of the Fe release in water. So, Fe weathering was ca. 20 to 40% higher than Fe release in water.

Al and Fe release from the various secondary Al and Fe pools (cf Table 3.3; Section 3.1) was strongly dominated ( $> 80\%$ ) by dissolution from amorphous secondary compounds at nearly all pH and Al concentration levels, except for Al release in the (A+B)p horizon. This could be derived from the difference in Al and Fe contents before and after the batch and column experiments in a sequential extraction with lanthanum chloride (indicates release of organically bound Al and Fe), ammonium oxalate (indicates dissolution of amorphous secondary Al and Fe compounds) and sodium dithionite (indicates dissolution of crystalline secondary compounds). This procedure may, however, overestimate the contribution of amorphous Al and Fe compounds, especially in the (A+B)p and Bh horizons, since the pool of organically bound Al and Fe is likely to be underestimated with  $\text{LaCl}_3$  (cf De Vries, 1994a; Section 3.1). For the BCs and C horizon, no estimates were made about the contribution of various Fe pools, since the differences between these pools before and after the experiment were too small.

The contribution of inorganic amorphous secondary Al compounds to the total release of Al from the secondary Al pool was nearly independent of the pH level and varied between 54-65% in the (A+B)p horizon, 80-88% in the Bh horizon, 93-97% in the BCs horizon and 93-100% in the C horizon. The remaining contribution was mainly organically bound Al. Inorganic amorphous Al compounds were also the major source ( $> 80\%$ ) of Al release in the Bh, BCs and C horizon at the various Al concentration levels. In the (A+B)p horizon, however, the contribution of amorphous Al compounds to Al release decreased from 73% at an Al concentration of  $0.5 \text{ mol}_c \text{ m}^{-3}$  to 31% at an Al concentration of  $99 \text{ mol}_c \text{ m}^{-3}$ . At the highest Al concentration level, release of organically bound Al was dominant (64%). The different impact of Al concentration on the release of organically bound Al in the upper (A+B)p and Bh horizon, with a relative large organic Al pool, is illustrated in Table 3.24.

Release of organically bound Al slightly decreased with a rise in Al concentration level in the (A+B)p horizon, whereas it strongly decreased with increasing Al concentration in the Bh horizon. The pool of organically bound Al in that horizon even increased at high Al concentrations (negative depletion). At the same time, the pool of inorganic Al compounds still decreased. The latter finding illustrates that release of Al from inorganic compounds can continue as long as mineral saturation is not yet attained, while exchange of H against organically bound Al is limited or even reversed.

**Table 3.24** *Relative depletion of organic and inorganic secondary Al compounds in the (A+B)p and Bh horizon at five Al concentration levels*

Soil horizon	Secondary Al pool	Depletion (%)				
		Al concentration level (mol <sub>c</sub> m <sup>-3</sup> )				
		0.5	2.0	5.0	9.0	99
(A+B)p	Organic	46	50	43	41	39
	Inorganic	45	40	34	21	7
Bh	Organic	18	13	-10	-3	-11
	Inorganic	69	57	45	42	28

## CONCLUSIONS

Major results of the experiments performed are (cf the objectives of the study):

- (i) Cumulative release of cations and Si can be described well as a function of a power of the proton or Al activity and a power of time. A clear effect of Al activity on Si and base cation release was only found in the BCs and C horizon, where weathering of secondary and primary Al silicates governs the release of Si and BC respectively. The effect of a decrease in pH on the element release decreased going from Mg > Fe > Si ≈ Al > Ca ≈ K ≈ Na. The effect of Al activity on Al release was much lower than the effect of proton activity. Cumulative release of Si was also described quite well as a function of the product of proton or Al activity and time. Cumulative Al, Fe and BC release was, however, not described well by scaling the proton or Al activity against time. Concentration time-scaling thus seems of limited use in describing cumulative cation release with time.
- (ii) The combined effect of pH and Al depletion on the Al release rate can be described well as a function of the degree of undersaturation with respect to gibbsite and the pool of secondary Al compounds. This offers a good perspective for the modelling of Al release in response to acid inputs. The description of the combined effect of Al activity and Al depletion with this function is, however, less good. In the (A+B)p and Bh horizon this may (partly) be caused by a relative large impact of organically bound Al on Al release. A dominating influence of exchange of H against organically complexed Al is, however, unlikely in the BCs and C horizon.
- (iii) Release of Na and K is dominated by weathering in all horizons, whereas desorption plays an important role in the release of Ca and Mg in the upper (A+B)p and Bh horizon. Release of Al and Fe is dominated by dissolution from secondary amorphous Al and Fe compounds at all pH and Al concentration levels considered. The only exception was the (A+B)p horizon where release of organically bound Al dominated at very high Al concentrations.

### 3.3 DIFFERENCES BETWEEN SOIL HORIZONS AND SOIL TYPES

#### ABSTRACT

*The influence of soil type and soil horizon on rates and mechanisms of silica and cation release of acid sandy soils was studied in one-year batch experiments at various pH levels. A total of 63 soil samples was investigated, including Ah, Aan, (A+B)p, (A+C)p, E, Bh, Bhs, BCs, C and D horizons of Cambic, Carbic and Gleyic Podzols, Fimic Anthrosols, Umbric Gleysols and Haplic Arenosols. Al dissolution from secondary Al compounds was the dominant acid neutralizing mechanism in all horizons, except for the Aan horizon, where base cation (BC) desorption played a dominant role. BC desorption also dominated in an Ah horizon with an extremely large organic matter content, whereas BC weathering played a major role in two C horizons of dune soils. Effects of pH on Al release with time could be described well as a function of the (relative depletion of the) pool of secondary Al compounds and the degree of undersaturation with respect to gibbsite. Relative Al depletion during the one-year experiments increased with a relative decrease of organically bound Al in the secondary Al pool. Values ranged from ca. 20% in A horizons to ca. 90% in C horizons at pH 3.0.*

#### INTRODUCTION

In two previous sections results have been given of the effect of mineral (Al) depletion, pH and Al concentration on the rates and mechanisms of cation and silica release in four mineral soil horizons (Section 3.1 and 3.2; De Vries, 1994a, b). Emphasis was given to an empirical description of Al release, which was the dominating buffer mechanism in all soil horizons. Results showed that the Al release rate can be described as a function of the pool of secondary Al compounds and the degree of undersaturation with respect to gibbsite. This description was used in a Regional Soil Acidification Model, RESAM, that was developed to predict long-term impacts of acid deposition on solid-phase and soil solution chemistry of acid sandy forest soils in the Netherlands (De Vries et al., 1994b, Section 6.2). Application of RESAM on a national scale requires insight in the cation release kinetics in the various horizons of Dutch sandy soils. Soil samples studied in Section 3.1 and 3.2 represented only a part of the relevant soil horizons in acid sandy forest soils in the Netherlands. Furthermore, the pool of secondary Al compounds, was relatively large in these samples, to allow reliable measurements of the effect of Al depletion, Al concentration and pH.

In this section, results are given of one-year batch experiments on the kinetics of cation (especially Al) and Si release in all relevant mineral horizons of acid sandy soils in the Netherlands. A total of 63 soil samples was investigated, including Ah, Aan, (A+B)p, (A+C)p, E, Bh, Bhs, BCs and D horizons of Cambic, Carbic and Gleyic Podzols, Fimic Anthrosols, Umbric Gleysols and Haplic Arenosols, (classification according to FAO,

1988). All experiments were conducted at pH 3.0 to allow comparison between the various horizons at one pH level. Furthermore, the influence of pH level on Al and base cation (BC) release rates was investigated in 26 soil samples. The major aim of this study was to gain insight in the differences between major soil horizons in various sandy soils with respect to:

- (i) the relative importance of cation exchange, especially BC desorption, and mineral weathering, especially Al release, in the neutralization of acid inputs.
- (ii) Al release from organic Al complexes and from secondary inorganic Al compounds
- (iii) Al release kinetics in relation to the pool of secondary Al compounds and the degree of undersaturation with respect to gibbsite.

Emphasis was placed on the derivation of dissolution rate constants for Al in the various horizons of different soil types, to be used in regional applications of RESAM (cf Section 7.2; De Vries et al., 1994c).

## MATERIALS AND METHODS

### **Soil samples and basic physical and chemical characteristics**

Samples of mineral soil horizons were taken from 32 different sites at 15 locations. Sites were mainly located in the central, most densely forested, part of the Netherlands (Fig. 3.15). All sites were forested except for Putten and Diessen, where anthropogenically influenced Aa horizons of Fimic Anthrosols were sampled in agricultural land. Unlike the forested soils, the base saturation of these agricultural soils was high ( $\approx 90\%$ ). Samples from agricultural soils were included to study the relationship between Al release and base saturation. Samples of organic soil horizons were not included in the study as they were considered irrelevant for the long-term buffering of soils against acid inputs. James and Riha (1986) claimed that pH buffering in organic horizons (humus layers) of acid forest soils is extremely important, because of the relative large pool of base cations in this layer. However, this is only true in laboratory experiments with an (infinitely) high H/BC ratio in the titration solution (the titration solution generally contains only protons and no base cations). However, in the field situation, a constant supply of base cations by litterfall and mineralisation and by foliar exudation prevents a large base cation release from the adsorption complex, even at low pH.

A total number of 63 samples was investigated including Cambic Podzols (14 samples), Carbic Podzols (16 samples), Gleyic Podzols (16 samples), Fimic Anthrosols (6 samples), Umbric Gleysols (3 samples) and Haplic Arenosols (8 samples, including one sample from a mineralogically identical Gleyic Arenosol). Most of the samples were Ah horizons (15 samples), B horizons (16 samples, i.e. 3 Bh, 6 Bhs and 7 BCs horizons) and C horizons (14 samples, including one AC horizon). Remaining soil samples

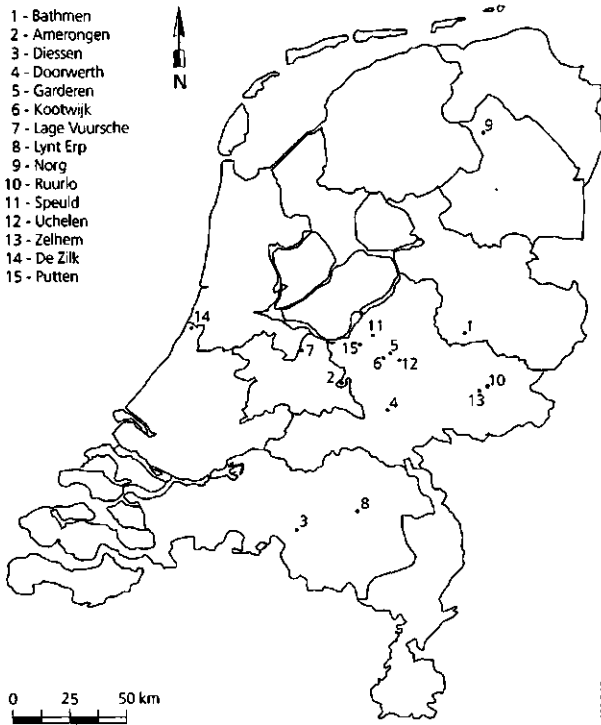


Figure 3.15 Sites where the soil samples were taken

included (i) upper soil horizons that were anthropogenically influenced by ages of organic manure input (Aan horizon; 6 samples) and by plowing in the forest between 1920 and 1940 ((A+B)p horizons; 5 samples and (A+C)p horizons; 3 samples), (ii) strongly leached E horizons from Carbic Podzols (2 samples) and (iii) boulder clay, that often underlies the parent material of podzolic soils in the northern part of the Netherlands from ca. 50 cm onwards (D horizons; 2 samples).

All samples were sieved over 2 mm mesh width, to remove stones and roots, and air dried before storage. Basic characteristics of the soil samples used are given in Table 3.25. Values for pH-KCl in soils from the forested sites varied between 2.7 in Ah horizons to 4.7 in C horizons. pH-KCl values in the Aan horizons of Fimic Anthrosoils, taken in agricultural soils, were slightly higher and varied between 4.0 and 5.2. Organic matter contents varied from ca. 2-10% in the upper A and B horizons to less than 0.5% in the C horizon. One Ah horizon, i.e. a Gleyic Podzol at Norg (cf Table 3.25), had an extremely large organic matter content (53%), indicating that it more closely resembles the H horizon of an organic layer. All samples were coarse-textured with a clay content below 8%, except for the two boulder clay samples with a slightly higher clay content.

Table 3.25 Basic physical and chemical characteristics of the soil samples studied

Location	Soil type (FAO, 1988)	Soil horizon	Soil depth (cm)	Bulk density (kg m <sup>-3</sup> )	pH- KCl	Organic matter (%)	Particle size distribution (%)		
							<2 $\mu$	2-50 $\mu$	>50 $\mu$
Norg 1	Gleyic Podzol	Ah(H)	0-8	460	2.7	53.0	2.3	62.4	35.3
Norg 2	Cambic Podzol	Ah	0-8	1090	2.7	11.0	1.9	24.5	73.6
Norg 3	Carbic Podzol	Ah	0-18	1270	3.3	5.6	1.5	14.3	84.2
Bathmen 1	Gleyic Arenosol	Ah	0-11	1500	3.7	2.3	6.1	16.7	77.2
Bathmen 2	Gleyic Podzol	Ah	0-4	1250	2.8	6.6	2.8	12.7	84.5
Speuld 1	Cambic Podzol	Ah	0-15	1250	3.2	4.4	5.2	12.6	82.2
Speuld 2	Cambic Podzol <sup>1)</sup>	Ah	0-7	1160	2.9	8.7	2.5	12.6	84.9
Ugchelen 1	Carbic Podzol	Ah	0-10	1130	2.9	9.5	1.2	12.8	86.0
Ugchelen 2	Carbic Podzol	Ah	0-6	1230	2.9	6.6	0.5	8.9	90.6
Amerongen	Cambic Podzol	Ah	0-15	1160	3.4	4.7	5.5	8.9	85.6
Doorwerth 1	Cambic Podzol <sup>1)</sup>	Ah	0-6	1000	2.9	13.6	4.9	18.8	76.3
De Zilk 1	Haplic Arenosol	Ah	0-7	1400	3.8	2.3	2.1	1.0	96.9
De Zilk 2	Umbric Gleysol	Ah	6-16	1100	3.6	7.6	2.2	13.5	84.3
Lynt-Erp 1	Gleyic Podzol	Ah	15-18	1380	3.5	4.0	0.2	8.0	91.8
Lynt-Erp 2	Umbric Gleysol	Ah	0-18	1560	3.4	5.9	4.7	14.3	81.0
Putten 1	Fimic Anthrosol	Aan	0-25	1270	4.8	3.0	2.5	11.5	86.0
Putten 1	Fimic Anthrosol	Aan	25-60	1330	4.0	2.3	2.6	10.8	86.6
Putten 2	Fimic Anthrosol	Aan	0-25	1270	5.2	2.5	2.0	10.5	87.5
Putten 2	Fimic Anthrosol	Aan	25-60	1390	4.1	1.5	2.3	10.1	87.6
Diessen 1	Fimic Anthrosol	Aan	0-25	1340	4.4	3.7	2.2	11.9	85.9
Diessen 2	Fimic Anthrosol	Aan	0-25	1300	5.2	5.3	3.3	14.8	81.9
Ruurlo	Gleyic Podzol	(A+B)p	0-15	1310	2.9	6.5	3.0	9.9	87.1
Ruurlo	Gleyic Podzol	(A+B)p	15-30	1240	3.4	6.2	4.1	11.0	84.9
Garderen	Carbic Podzol	(A+B)p	0-15	1260	3.4	5.8	2.7	6.5	90.8
Kootwijk	Carbic Podzol	(A+B)p	0-15	1190	3.7	6.8	3.1	7.6	89.3
Kootwijk	Carbic Podzol	(A+B)p	15-30	1400	4.1	4.3	3.3	7.5	89.2
Lage Vuursche	Gleyic Podzol	(A+C)p	0-15	1250	3.4	3.7	2.2	2.1	95.7
Zelhem 1	Haplic Arenosol	(A+C)p	0-15	1230	3.8	2.6	3.3	9.4	87.3
Zelhem 2	Haplic Arenosol	(A+C)p	0-15	1370	3.6	3.3	1.7	3.7	94.6
Bathmen 3	Carbic Podzol	E	4-9	1500	3.2	0.8	1.6	9.9	88.5
Ugchelen 2	Carbic Podzol	E	6-20	1430	3.1	2.6	1.0	4.3	94.7
Norg 3	Cambic Podzol	Bhs	45-60	1470	4.1	1.3	2.9	17.5	79.6
Bathmen 2	Gleyic Podzol	Bhs	19-26	1320	3.3	4.2	4.1	14.5	81.4
Speuld 2	Cambic Podzol <sup>1)</sup>	Bhs	40-50	1480	4.3	1.3	2.2	7.7	90.1
Doorwerth 1	Cambic Podzol <sup>1)</sup>	Bhs	12-23	1400	3.3	3.1	7.2	15.3	77.5
Lynt-Erp 1	Gleyic Podzol	Bhs	25-32	1260	3.5	6.9	1.5	12.3	86.2
Lynt-Erp 3	Gleyic Podzol	Bhs	29-40	1390	3.3	3.3	0.9	6.5	92.6
Norg 1	Carbic Podzol	Bh	25-34	1200	3.7	8.5	1.6	13.8	84.6
Bathmen 3	Carbic Podzol	Bh	17-21	1260	3.5	6.7	2.9	9.1	88.0
Ugchelen 2	Carbic Podzol	Bh	20-27	1130	3.7	11.1	0.8	16.5	82.7
Norg 2	Gleyic Podzol	BCs	28-53	1490	4.3	2.2	2.4	14.8	82.8
Bathmen 2	Gleyic Podzol	BCs	46-65	1540	4.4	0.8	2.5	4.0	93.5
Bathmen 3	Carbic Podzol	BCs	29-45	1500	4.4	1.4	4.4	7.8	87.8
Speuld 2	Cambic Podzol <sup>1)</sup>	BCs	50-62	1560	4.4	0.6	1.8	6.2	92.0
Ugchelen 2	Carbic Podzol	BCs	37-82	1550	4.4	0.6	0.3	2.5	97.2
Doorwerth 1	Cambic Podzol <sup>1)</sup>	BCs	23-38	1420	4.0	2.6	6.6	14.7	78.7
Doorwerth 2	Cambic Podzol <sup>1)</sup>	BCs	55-82	1560	4.3	0.5	1.3	4.7	94.0
Norg 1	Carbic Podzol	C	87-120	1660	4.7	0.1	0.7	0.9	98.4
Norg 3	Cambic Podzol	C	81-120	1640	4.4	0.2	1.6	8.4	90.0
Norg 5	Haplic Arenosol	C	60-120	1660	4.7	0.1	5.3	3.3	91.4
Norg 6	Haplic Arenosol	C	60-120	1600	4.6	0.6	1.2	3.5	95.3
Bathmen 2	Gleyic Podzol	C	130-150	1730	4.3	0.2	3.9	8.1	88.0
Bathmen 3	Carbic Podzol	C	80-100	1640	4.6	0.2	2.0	5.3	92.7

Table 3.25 continued

Location	Soil type (FAO, 1988)	Soil horizon	Soil depth (cm)	Bulk density (kg m <sup>-3</sup> )	pH- KCl	Organic matter (%)	Particle size distribution (%)		
							<2 $\mu$	2-50 $\mu$	>50 $\mu$
Speuld 2	Cambic Podzol <sup>1)</sup>	C	78-90	1660	4.6	0.1	0.3	1.1	98.6
Ugchelen 2	Carbic Podzol	C	78-90	1660	4.7	0.1	0.5	2.5	97.0
Doorwerth 1	Cambic Podzol <sup>1)</sup>	C	75-100	1650	4.5	0.1	4.5	6.5	89.0
De Zilk 1	Haplic Arenosol	AC	7-15	1680	4.2	0.6	2.3	0.6	97.1
De Zilk 1	Haplic Arenosol	C	20-25	1510	4.3	0.2	2.0	0.5	97.5
De Zilk 2	Umbric Gleysol	C	108-125	1380	4.5	1.0	0.2	0.8	99.0
Lynt-Erp 1	Gleyic Podzol	C	65-80	1640	4.4	0.2	0.5	1.9	97.6
Lynt-Erp 4	Gleyic Podzol	C	68-85	1690	4.4	0.2	1.0	1.8	97.2
Norg 2	Gleyic Podzol	Dg	53-120	1680	4.3	1.2	8.9	20.4	70.7
Norg 4	Gleyic Podzol	Dg	73-120	1680	4.5	0.8	10.5	17.8	71.7

<sup>1)</sup> Coarse sandy soils

The loam content was always less than 20% except for the organic rich Ah (H) horizon and the two D horizons.

### Batch experiments and computational procedures

Rates of proton consumption, in combination with cation and Si release rates were studied for all soil samples in one-year batch experiments at 20°C and pH 3.0. The effect of pH on proton consumption and cation release rates was studied in 26 soil samples (cf Table 3.26). Information on the batch experiments conducted is given in Section 3.1 and 3.2 (De Vries, 1994a, b). Since the experiments were very time consuming, they were not conducted in replicate. To test reproducibility, batch

Table 3.26 Number of batch experiments that were conducted at different pH levels for the soil horizons studied

Soil horizon	Number of experiments							
	pH 2.3	pH 2.5	pH 2.7	pH 3.0 <sup>1)</sup>	pH 3.3	pH 3.5	pH 3.7	pH 4.0
Ah		7	6	15 (7)				
Aan				6 (0)				
(A+B)p	<sup>1)</sup>	3	5	5 (5)	3			
(A+C)p		3	3	3 (3)				
E		1	1	2 (1)				
Bhs		1	2	3 (2)	2	1		
Bh		<sup>1)</sup>	2	6 (2)	2	<sup>1)</sup>		
BCs		<sup>1)</sup>	2	7 (2)	2	<sup>1)</sup>		
C				14 (3)	3	<sup>1)</sup>	3	<sup>1)</sup>
D				2 (1)	1	1	1	1
All	1	17	21	63 (26)	14	5	4	2

<sup>1)</sup> Values in brackets denote samples that were investigated at different pH levels

<sup>2)</sup> Experiments with an (A+B)p, Bh, BCs and C horizon at five pH levels described in detail before (De Vries 1994a, b; Section 3.1 and 3.2)

experiments at pH 3.0 with eight soil samples (2 Ah, 3 Bh(s) and 3 C horizons) were duplicated. Rates of acid neutralization and of Al release were reproducible within 10%. Cumulative release of base cations, however, sometimes differed by a factor of two.

The acid neutralization rate was calculated from the amount of H added to maintain the pH at the desired level. The silica and cation release rate was calculated by measuring the concentration of Si, Al, Fe, Ca, Mg (ICP), K and Na (AAS) in solution in a 25 ml aliquot after 25 ml of acid mixture had been added (cf Eq. 3.1; Section 3.1). In 28 of the batch experiments at pH 3.0, concentrations of  $\text{NH}_4$ ,  $\text{NO}_3$ ,  $\text{SO}_4$  and Cl were also measured (FIA) to gain insight in the possible interactions of these anions with the soil (e.g. mineralization or  $\text{SO}_4$  adsorption). Since interactions with  $\text{NH}_4$ ,  $\text{NO}_3$ ,  $\text{SO}_4$  and Cl were generally small, these analyses were not performed at other pH levels.

To gain insight in the contribution of cation exchange and weathering to cation release, adsorbed cation contents were determined in a 0.01 N silverthiourea (AgTu) extract (Pleysier and Juo, 1980) (except for  $\text{NH}_4$ , which was measured in a 1 N KCl extract; Coleman et al., 1959) before and after the batch experiments. Total cation contents were only measured before the experiment, after destruction with concentrated HF (Langmyhr and Paus, 1968). Insight in the contribution of organic Al complexes and of secondary amorphous and crystalline Al minerals to Al dissolution was derived by a sequential extraction with lanthanum chloride (organically complexed Al; Bloom et al., 1979a); ammonium oxalate (amorphous secondary Al minerals; Schwertmann, 1964) and dithionite-citrate-bicarbonate (crystalline secondary Al minerals; Mehra and Jackson, 1960) before and after the experiment (cf Section 3.1).

Long-term release rates for cations and Si in the various experiments were derived by fitting cumulative release with time with an empirical three parameter model (Eq. 3.2; Section 3.1). The influence of pH on cation and Si release was described by a linear relationship with a power of the proton activity (Eq. 3.11; Section 3.2). The combined effect of pH and Al depletion on Al release rates was described by fitting the logarithmic Al release rate, scaled by the degree of undersaturation with respect to gibbsite, to the fractional amount of secondary Al compounds according to (cf Eq. 3.12 and Eq. 3.13 of Section 3.2):

$$\ln \left( \frac{RR_{Al,t}}{(A)_e - (Al)} \right) = \ln \gamma_1 + \gamma_2 \cdot Al_{sc,t} / Al_{sc,t_0} \quad (3.15)$$

where  $RR_{Al,t}$  is the Al release rate at time  $t$  ( $\text{mmol}_c \text{ kg}^{-1} \text{ d}^{-1}$ ),  $(A)_e$  and  $(Al)$  are the activity of Al in equilibrium with gibbsite and the actual Al activity, respectively ( $\text{mol}_c \text{ m}^{-3}$ ),  $Al_{sc(t)}$  and  $Al_{sc(t_0)}$  are the secondary Al pools at a given time  $t$  and at the start of the experiment  $t_0$ , respectively ( $\text{mmol}_c \text{ kg}^{-1}$ ) and where  $\gamma_1$  ( $\text{l kg}^{-1} \text{ d}^{-1}$ ) and  $\gamma_2$  are rate constants.  $\gamma_1$  gives insight in the Al release rate when the secondary Al pool is totally depleted (assuming that Eq. (3.15) still holds in that situation), whereas the sum of  $\gamma_1$  and  $\gamma_2$  (or more



precisely  $e^{\ln r^{1+\tau^2}}$ ) gives information on the Al release rate at the beginning of the experiment (No Al depletion). The pool of secondary Al compounds at a given time  $t$  was scaled to the initial secondary Al pool to combine the various experiments, conducted for each soil horizon, in the statistical analyses.

## RESULTS AND DISCUSSION

### Buffer characteristics

Solid-phase characteristics that mainly determine the capacity of the soil to neutralize acid inputs are the total and exchangeable pools of cations and the pools of secondary Al compounds. Average total cation contents in the various soil horizons (Table 3.27) were highest in the (A+C)p horizon and in the D horizons (boulder clay) and lowest in the E horizon. Differences between the other horizons were comparatively small.

Table 3.27 Average total cation contents of the soil horizons studied

Soil horizon	N <sup>1)</sup>	Total contents (mmol <sub>c</sub> kg <sup>-1</sup> )							
		Al	Fe	Ca	Mg	K	Na	BC <sup>2)</sup>	All <sup>3)</sup>
Ah	15	1423	276	46	33	247	202	528	2228
Aan	6	1201	223	67	34	312	230	644	2068
(A+B)p	5	1566	223	34	30	307	207	578	2367
(A+C)p	3	3529	397	85	91	302	291	769	4694
E	2	640	50	39	7	153	86	286	975
Bhs	6	1442	196	27	28	240	165	460	2099
Bh	3	1408	183	41	17	173	110	340	1931
BCs	7	1804	246	52	45	211	153	461	2511
C	14	1539	161	52	47	322	254	675	2376
D	2	3812	802	70	187	348	147	752	5366

<sup>1)</sup> N is the number of soil samples studied

<sup>2)</sup> BC is base cations (Ca+Mg+K+Na)

<sup>3)</sup> Al+Fe+Ca+Mg+K+Na, which equals the acid neutralizing capacity (ANC)

Total K and Na contents were much higher than those of Ca and Mg, indicating the dominance of K and Na feldspars in these soils. The stoichiometric ratio of Al to K and Al to Na in feldspars is 3 mol<sub>c</sub> mol<sub>c</sub><sup>-1</sup>. Total contents of Al, K and Na reasonably confirm this. A better indication of the contents of Al and BC in primary silicates can be derived by subtracting contents of secondary Al compounds (Table 3.29) and exchangeable BC (Table 3.28) from the total Al and BC contents, respectively. Al/BC ratios (mol<sub>c</sub> mol<sub>c</sub><sup>-1</sup>) in primary minerals, thus derived, varied between 2.1 and 3.3 in the various horizons, except for the (A+C)p and D horizon which had much higher ratios (4.4 and 4.8 mol<sub>c</sub> mol<sub>c</sub><sup>-1</sup>, respectively). In the D horizon, this indicates the relative large contribution of clay minerals such as illite and kaolinite to the total Al content.

Average contents of exchangeable cations (Table 3.28) were highest in the Bh horizon and lowest in the C horizon. In most horizons the average base saturation varied between 5 and 10%. Much higher values were found in the Aan horizons, where the base saturation varied between 75 and 95% (agricultural soils). The average base saturation in the Ah and C horizon was also higher than 10%, i.e. 19% and 28%, respectively. In the Ah horizon, however, the average value was influenced by the high base saturation (40%) of the sample with an extremely large organic matter content (resembles an H horizon). The relatively high base saturation in the C horizon was caused by samples from two dune soils (De Zilk), i.e. a Haplic Arenosol and an Umbric Gleysol (cf Table 3.25) with a base saturation of 85% and 73%, respectively. Excluding these horizons gave an average base saturation (of 13% for Ah horizons and) of 8% for C horizons.

Table 3.28 Average exchangeable cation contents of the soil horizons studied

Soil horizon	N	Exchangeable contents (mmol. kg <sup>-1</sup> )									Base saturation (%)
		H	Al	Fe	Ca	Mg	K	Na	BC	All	
Ah	15	15	16	6.4	5.4	1.8	1.1	1.0	9.2	49	19 <sup>1)</sup>
Aan	6	0.3	1.4	0.7	19	5.2	5.1	0.8	29.8	33	90
(A+B)p	5	15	25	1.7	1.7	0.4	0.4	0.3	2.8	46	6
(A+C)p	3	6.5	16	1.7	1.9	0.5	0.3	0.3	2.9	28	10
E	2	5.3	6.2	0.9	0.8	0.2	0.1	0.0	1.1	15	7
Bhs	6	6.5	27	1.2	0.8	0.2	0.3	0.3	1.6	38	4
Bh	1	12	43	1.7	2.3	0.3	0.3	0.5	3.5	60	6
BCs	7	1.1	4.3	0.1	0.1	0.0	0.1	0.1	0.4	7.3	5
C	14	0.4	2.6	0.1	1.2	0.2	0.1	0.1	1.6	5.8	28 <sup>2)</sup>
D	2	6.1	22	0.2	0.5	0.6	0.8	0.3	2.1	30	7

<sup>1)</sup> H+Al+Fe+Ca+Mg+K+Na, which equals the cation exchange capacity (CEC)

<sup>2)</sup> Exclusion of an Ah(H) horizon with an extremely large organic matter content gave an average base saturation of 13%

<sup>3)</sup> Exclusion of two samples of dune soils, which contained shell fragments, gave an average base saturation of 8%

Average contents of secondary Al compounds (Table 3.29) were highest in the B horizons (especially the Bh horizon) and lowest in the E horizons. Values for the upper Ah and Aan horizons were comparable to the lower C horizons, but in the Ah horizon the contribution of organically complexed Al to the secondary Al pool was larger than in the Aan and C horizon. The average contribution of secondary Al compounds to total Al contents (cf Table 3.27 and 3.29) was low, except for the Bh horizon (32%). Values for the other horizons varied between 3 and 6% for the Ah, Aan, (A+C)p, E, C and D horizon and between 13% and 16% for the (A+B)p, Bhs and BCs horizon. Average contents of secondary compounds for Fe were ca. twice as high as those for Al in the Ah, Aan and D horizon, and ca. twice to three times as low in the (A+B)p, (A+C)p, E, Bhs, BCs and C horizon (cf Table 3.29).

Table 3.29 Average contents of secondary Al compounds of the soil horizons studied

Soil horizon	N	Al pools (mmol <sub>c</sub> kg <sup>-1</sup> )				
		organic	amorphous	crystalline	secondary	reactive <sup>1)</sup>
Ah	15	17	28	9.5	54	70 (131)
Aan	6	10	49	9.1	69	70 (138)
(A+B)p	5	50	150	16	215	240 (117)
(A+C)p	3	22	83	12	117	133 (57)
E	2	8.3	9.2	4.2	22	28 (9)
Bhs	6	42	129	14	184	205 (113)
Bh	3	113	314	18	445	490 (124)
BCs	7	15	249	26	290	294 (103)
C	14	6.0	56	7.4	69	72 (38)
D	2	10	73	66	149	171 (343)

<sup>1)</sup> Reactive Al includes exchangeable Al and secondary Al compounds. Values in brackets indicate the pool of reactive Fe compounds

### Cation and silica release at pH 3.0

#### Annual release and stoichiometry

Release of Al was the dominant cause of acid neutralization in the various soil horizons, except for the Aan horizons where BC release dominated the buffering (Table 3.30). Average annual Al and BC release rates in the Ah horizon were nearly equal. The average annual BC release in this horizon, however, was strongly influenced by a large value (49 mmol<sub>c</sub> kg<sup>-1</sup>) for the Ah (H) horizon with an organic matter content of 53%. BC release in this sample was mainly due to fast (< 1 d) exchange of protons against a large pool of exchangeable base cations (6 mmol<sub>c</sub> kg<sup>-1</sup>). Similar results were found by Nätscher and Schwertmann (1991) for organic horizons. Excluding this organic soil sample gave an average BC release of 6.7 mmol<sub>c</sub> kg<sup>-1</sup> yr<sup>-1</sup> for the Ah horizon, which was less than the annual average Al release (cf Table 3.30). Average annual release rates for Fe were always less than those for BC, except for the Bh horizon, where both rates were nearly similar. Compared to Al, Fe release was very low. The ratio of observed Fe release to the reactive Fe pool was always below 0.10 (cf Table 3.28 and 3.29). For Al this ratio was always higher than 0.10. The annual Al release as a fraction of the reactive Al pool increased according to Ah (0.13) < Aan (0.22) < Bh (0.31) < Bhs (0.33) < (A+B)p (0.45) < (A+C)p (0.46) < D (0.54) < BCs (0.66) < C horizon (0.96).

The standard deviation in cation release (relative to the average annual release) was generally larger for Al and Fe than for BC, except for the C horizon. The large standard deviation in BC release in the C horizon was mainly due to high BC weathering rates in two samples of dune soils with shell fragments (Haplic Arenosol and Umbric Gleysol at De Zilk; cf Table 3.25). These samples also contributed strongly to the standard deviation in Al release. Annual Al release in the coastal dune soils was much lower (ca. 10-16 mmol<sub>c</sub> kg<sup>-1</sup>) than in the inland soils, because of their small pool of oxalate-extractable Al (ca. 6-18 mmol<sub>c</sub> kg<sup>-1</sup>; cf Table 3.30).

**Table 3.30** Average annual cation release and acid neutralization at pH 3.0 for nine soil horizons studied<sup>1)</sup>

Soil horizon	N	Annual release rate (mmol <sub>c</sub> kg <sup>-1</sup> ) <sup>2)</sup>				Proton consumption (mmol <sub>c</sub> kg <sup>-1</sup> )
		Al <sup>3)</sup>	Fe	BC	Cations	
Ah	12 <sup>1)</sup>	9.4 (230)	3.4 (101)	10.3 <sup>4)</sup> (125)	23 (110)	30 (92)
Aan	6	16 (62)	2.9 (52)	47 (58)	65 (53)	71 (45)
(A+B)p	4 <sup>1)</sup>	108 (58)	5.0 (70)	5.3 (10)	118 (56)	104 (63)
(A+C)p	3	61 (104)	3.5 (85)	5.8 (8)	70 (92)	60 (89)
Bhs	6	68 (98)	2.5 (131)	3.3 (44)	73 (94)	80 (81)
Bh	3	150 (63)	7.7 (101)	7.6 (32)	165 (63)	148 (53)
BCs	7	194 (56)	3.9 (59)	4.5 (31)	202 (55)	196 (56)
C	14	69 (49)	3.1 (63)	10.2 <sup>5)</sup> (111)	83 (36)	94 (30)
D	2	93 (36)	3.2 (104)	5.2 (21)	102 (36)	104 (35)

<sup>1)</sup> No acid neutralization was observed at pH 3.0 in three Ah horizons, one (A+B)p horizon and the two E horizons. These experiments were excluded in calculating average values

<sup>2)</sup> Values in brackets indicate the standard deviation in percent of the average annual release rate

<sup>3)</sup> In calculating Al release rates, the charge of Al was assumed to be three. This was too high in the (A+B)p and Bh horizons due to complexation of Al with organic anions

<sup>4)</sup> Exclusion of the Ah horizon with an extremely high organic matter content gave an average value of 6.7 mmol<sub>c</sub> kg<sup>-1</sup>

<sup>5)</sup> Exclusion of two C horizons from dune soils, in which shell fragments occurred, gave an average annual Al release of 79 mmol<sub>c</sub> kg<sup>-1</sup> and an average annual BC release of 7.1 mmol<sub>c</sub> kg<sup>-1</sup>

Average annual cation release rates generally corresponded well with the average annual acid neutralization rate. In the (A+B)p, (A+C)p and Bh horizons, however, cation release rates clearly exceeded the acid neutralization rates (Table 3.30). This can mainly be attributed to mobilization of organic anions (derived from the measured anion deficit during the experiment), most of which form complexes with Al (Section 3.1). In contrast, average annual acid neutralization rates were (slightly) higher than cation release rates in the Ah, Aan, Bhs and C horizon. This was mainly due to the removal of NO<sub>3</sub> (denitrification) measured in most of the experiments. The average NO<sub>3</sub> removal rate measured in ten C horizons, for example, equalled 8.8 mmol<sub>c</sub> kg<sup>-1</sup> yr<sup>-1</sup>, which is nearly equal to the difference between the average annual rate of acid neutralization and cation release in this horizon (11 mmol<sub>c</sub> kg<sup>-1</sup> yr<sup>-1</sup>; cf Table 3.30). In the Ah horizons, the difference in acid neutralization and release of Al, Fe and BC was mainly caused by release of NH<sub>4</sub> and removal of NO<sub>3</sub> (both 36 mmol<sub>c</sub> kg<sup>-1</sup> yr<sup>-1</sup>) in the soil sample with an organic matter content of 53%. Similar results were found by Nätscher and Schwertmann (1991) for organic horizons. Most likely, this effect is caused by mineralization and denitrification, respectively.

Except for the upper Ah and Aan horizons, observed annual Al dissolution rates (Al release corrected for Al exchange) were much larger than estimated annual Al dissolution rates, assuming congruent weathering of base cations (BC) and Al from alkali feldspars (the dominating Al silicates; cf Table 3.27), anorthite (Ca) and chlorite (Mg) (Table 3.31). Annual BC weathering was calculated by subtracting BC release by cation exchange from total BC release (cf section on cation release mechanisms). This result implies that dissolution of secondary Al compounds plays a major role in acid

neutralization in most soil horizons. In the Ah horizon, congruent Al dissolution from primary minerals can explain the observed Al release. In the Aan horizons, however, Al (and Si) release estimated from silicate weathering exceeded the observed value(s). Presumably, the samples from these horizons contained a large non-silicate pool of base cations, that dissolves rapidly (see further).

Unlike Al, observed annual Si dissolution (release) rates were general lower than estimated values, except for the Bhs, BCs and D horizon (Table 3.31). In the latter horizons, dissolution of Si from a secondary aluminosilicate pool seems to occur (cf Section 3.1). Average molar Al/Si release ratios in these horizons were 4.2 (Bhs horizon), 3.7 (BCs horizon) and 1.8 (D horizon). Values for the (A+C)p and C horizon were 2.6 and 2.4, respectively. These ratios are comparable to molar Al/Si ratios in the amorphous fractions of Bhs, Bh, BCs and C horizons, estimated recently with SEM-EDXRA in thin sections of soil horizons from a Cambic, Carbic and Gleyic Podzol. Molar Al/Si ratios in the amorphous fractions generally varied between ca. 1.0 and 3.0 (Bisdorn and Boersma, 1994; cf Section 3.1). It suggests that secondary aluminosilicates may play an important role in Al dissolution in lower soil horizons.

*Table 3.31 Average annual dissolution of Al and Si for the soil horizons studied as measured in batch experiments at pH 3.0 and as estimated assuming congruent weathering of primary Al silicates<sup>1)</sup>*

Soil horizon	N	Al dissolution (mmol <sub>c</sub> kg <sup>-1</sup> )		Si dissolution (mmol <sub>c</sub> kg <sup>-1</sup> )	
		measured	estimated <sup>2)</sup>	measured	estimated <sup>2)</sup>
Ah	12	6.4 (302)	5.2 (167)	17 (54)	20 (166)
Aan	6	20 (63)	52 (51)	16 (54)	204 (51)
(A+B)p	4	109 (64)	7.0 (34)	13 (25)	27 (34)
(A+C)p	3	57 (110)	8.9 (48)	29 (59)	34 (48)
Bhs	6	66 (104)	2.3 (210)	21 (94)	9.4 (198)
Bh	3	155 (67)	8.3 (90)	7.1 (78)	33 (89)
BCs	7	196 (56)	8.2 (35)	71 (84)	32 (35)
C	14	70 (49)	20 <sup>3)</sup> (123)	39 (30)	78 <sup>3)</sup> (124)
D	2	89 (41)	7.4 (3)	66 (4)	29 (2)

<sup>1)</sup> Values in brackets indicate the standard deviation in percent of the average annual dissolution rate

<sup>2)</sup> In calculating the dissolution rates a charge of three was used for Al and of four for Si (Si is released as uncharged H<sub>4</sub>SiO<sub>4</sub>)

<sup>3)</sup> These relative large values are influenced by high BC weathering rates in two dune soils with shell fragments. Excluding these samples gave average values of 13 and 49 mmol<sub>c</sub> kg<sup>-1</sup> for annual Al and Si dissolution, respectively

#### *Release rates with time*

The cumulative release of Al, BC and Si with time could be fitted quite well with an empirical three parameter model (Section 3.1; Eq. 3.2) in all experiments where those elements were released in substantial amounts. The model, of course, failed in samples which hardly buffered at pH 3.0 (mainly Ah horizons). The three parameter model gives insight in the capacity,  $\alpha_1$ , and the half-life time,  $\alpha_2$ , of a fast reacting pool, with non-

linear dissolution behaviour, and in the long-term release rate,  $\alpha_3$ , from a slowly reacting pool, with linear dissolution behaviour (cf Section 3.1).

Average fitted values for  $\alpha_1$ ,  $\alpha_2$  and  $\alpha_3$  (Table 3.32) illustrate the different release kinetics of Al, BC and Si. In most soil horizons, the average non-linear dissolution capacity,  $\alpha_1$ , was much lower (ca. three to ten times) than the reactive pool of Al, except for the C horizon, where values were quite comparable (cf Table 3.29 and 3.32). The standard deviation of  $\alpha_1$  mostly ranged between 40 and 80% of the average value, according to the standard deviation in the reactive Al pool (not shown in the Tables 3.29 and 3.32). Unlike Al, average values of  $\alpha_1$  for BC generally approached or even exceeded the reactive exchangeable BC pool (cf Table 3.28 and 3.32). The excess was (relatively) large in the Aan horizon (see further). In all soil horizons, the half-life time,  $\alpha_2$ , of the fast reactive pool  $\alpha_1$  was higher for Al than for Si. This implies that (secondary) non-silicate pools of Al are more rapidly depleted than (secondary) Al silicates. The much lower values of  $\alpha_2$  for BC indicate the occurrence of fast exchange of H against BC. These results all confirm the conclusions that were drawn earlier for (A+B)p, Bh, BCs and C horizons on the basis of one year batch experiments with four soil samples (Section 3.1).

Table 3.32 Average fitted values of the parameters  $\alpha_1$ ,  $\alpha_2$  and  $\alpha_3$  in the empirical relationship between cumulative release of Al, BC and Si versus time (Eq. 3.2) at pH 3.0 for the soil horizons studied

Soil horizon	N <sup>1)</sup>	$\alpha_1$ (mmol <sub>c</sub> kg <sup>-1</sup> )			$\alpha_2$ (d)			$\alpha_3$ (mmol <sub>c</sub> kg <sup>-1</sup> yr <sup>-1</sup> )			$F^2_{adj}$		
		Al	BC	Si	Al	BC	Si	Al	BC	Si	Al	BC	Si
Ah	4 <sup>2)</sup>	17	6.0	13	2.2	0.04	86	16	2.7	13	0.98	0.91	0.99
Aan	5	13	47	6.0	3.8	0.04	18	10	5.7	11	0.88	0.94	0.99
(A+B)p	4	65	3.2	2.5	3.1	0.12	9.1	50	2.1	11	0.98	0.92	0.99
(A+C)p	2	51	3.1	17	3.9	0.11	21	36	2.4	22	0.99	0.97	0.99
Bhs	3	67	2.4	17	0.82	0.05	18	50	1.8	17	0.97	0.97	0.99
Bh	2	116	6.1	4.1	0.38	0.06	11	81	2.0	5.3	0.97	0.94	0.99
BCs	7	89	1.8	24	8.7	0.01	32	121	2.9	54	0.98	0.95	0.99
C	10 <sup>2)</sup>	51	2.8	19	2.6	0.18	14	28	5.0	24	0.97	0.87	0.98
D	2	43	2.9	17	1.0	0.02	4.8	52	2.5	4.8	0.98	0.86	0.99

<sup>1)</sup> To allow comparison of values for Al, Si and BC, all samples were excluded where one or more of these elements could not be fitted well with Eq. (3.2) ( $F^2_{adj} < 0.5$ ). This caused the exclusion of 10 Ah horizons, 1 Aan horizon, 1 (A+B)p and 1 (A+C)p horizon, 2 E horizons, 4 Bhs horizons and 2 C horizons. In most cases lack of fit was due to nearly negligible release of cations at pH 3.0 (most Ah and Bhs horizons and the two E horizons)

<sup>2)</sup> The Ah(H) horizon with an extremely high content of organic matter and two samples from dune soils in which shell fragments occurred were not included in the calculation of average values because of their different behaviour (high BC - and low Al release rates)

Average long term release rates,  $\alpha_3$ , for Al were comparable to those of Si in the Ah, Aan, C and D horizons, whereas  $\alpha_3$  values for Al exceeded those of Si by a factor of two to four in the (A+B)p, (A+C)p, Bhs and BCs horizons. Dissolution of aluminosilicates thus seems to play an important role in long-term Al release from nearly all soil horizons. Only in the Bh horizon, long-term Al release remained much larger (more than

ten times) than long-term Si release. Considering the molar Al/Si release ratio of ca. 1.5 to 4.0 (except for the Bh horizon), it is likely that secondary Al silicates are the primary source of Si and Al in most horizons (the molar Al/Si ratio in primary Al silicates generally equals 0.33). The importance of secondary Al pools in the lower B and C horizons, even in the long run, is supported by the estimated long-term Al/BC release ratio. The average long-term Al release rate in these horizons was approximately 10-30 times as large as that of BC. Long-term Al/BC release ratios in the Ah and Aan horizons were relatively low (ca. 2.5; cf the average values of  $\alpha_3$  for Al and BC in Table 3.32). Long-term release rates of BC were comparable for the various horizons (ca. 2-3 mmol<sub>c</sub> kg<sup>-1</sup> yr<sup>-1</sup>), except for the Aan and C horizons where values were about twice as high.

The anthropogenic Aan horizons from agricultural soils, the Ah(H) horizon with a high organic matter content and two C horizons from dune soils behaved completely different than the acid mineral horizons from forest soils, because of their high initial base saturation. Initially, Al in solution was adsorbed in these horizons, causing a strong decrease in dissolved Al, and acid inputs were mainly neutralized by exchange of H and BC. The calculated non-linear dissolution capacity of base cations, however, exceeded the initial pool of exchangeable base cations, except for the Ah(H) horizon (cf Table 3.33).

The change in exchangeable BC content in the Ah horizon, however, approached the non-linear dissolution capacity. This horizon still contained a relative large amount of base cations at the end of the experiment (17 mmol<sub>c</sub> kg<sup>-1</sup>) because of its comparatively low affinity for protons and its high CEC (154 mmol<sub>c</sub> kg<sup>-1</sup>). In the C horizons, the larger release of BC compared to the exchangeable pool can be explained by fast dissolution of the Ca from shell fragments. For the Aan horizons, the explanation is less clear. Presumably, these horizons from agricultural soils contain a relatively large pool of rapidly dissolvable salts.

*Table 3.33 The calculated non-linear dissolution capacity and the measured initial content of base cations of eight samples with a high initial base saturation*

Horizon	Location	Depth (cm)	Non-linear dissolution capacity for BC <sup>1)</sup> (mmol <sub>c</sub> kg <sup>-1</sup> )	Initial exchangeable BC content <sup>2)</sup> (mmol <sub>c</sub> kg <sup>-1</sup> )
Ah(H)	Norg	0-8	33	61
Aan	Putten 1	0-25	47	30
	Putten 2	0-25	53	32
	Putten 2	25-60	16	10
	Diessen 1	0-25	39	25
	Diessen 2	0-25	82	65
C	De Zilk 1	20-25	34	11
	De Zilk 2	108-125	12	5

<sup>1)</sup> The half life time,  $\alpha_2$ , of this pool was less than 2.5 hours except for one C horizon (De Zilk 2), where  $\alpha_2$  equalled ca. 8 days

<sup>2)</sup> The exchangeable BC content at the end of the experiment was negligible (< 1 mmol<sub>c</sub> kg<sup>-1</sup>), except for the Ah(H) horizon (17 mmol<sub>c</sub> kg<sup>-1</sup>)

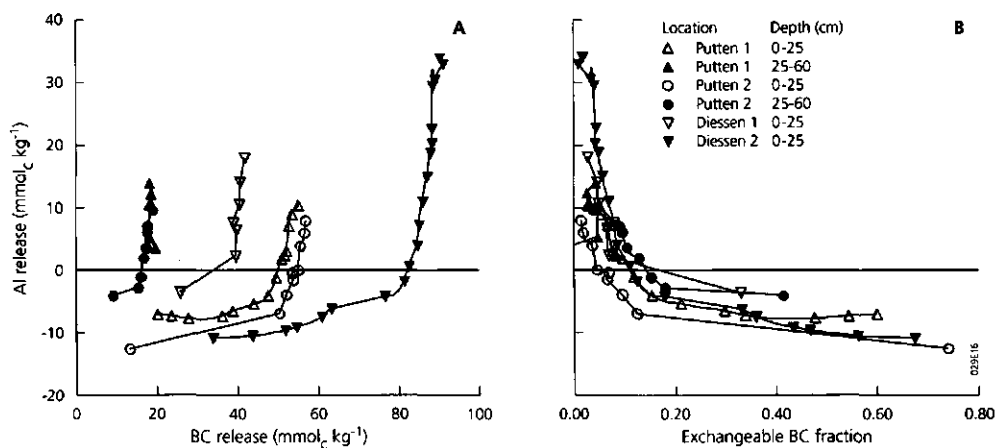


Figure 3.16 The relationship between measured Al release and measured BC release (A) and estimated base saturation (B) in six Aan horizons of Fimic Anthrosols

The BC release at which net Al release was zero approached or slightly exceeded the initial exchangeable BC content in the various Aan horizons (cf Fig. 3.16A and Table 3.33). This implies that net Al release occurred at a very low base saturation in all Aan horizons, as illustrated in Fig. 3.16B. The relationship between Al release and base saturation was calculated by assuming a constant ratio between weathering and exchange of BC, as measured at the end of the end of experiment (cf Table 3.34). A clear increase in Al concentration (Al release) started at a base saturation between ca. 10 and 20%, whereas net Al release started at a base saturation between ca. 5 and 15%. The estimated relationships between dissolved Al and base saturation are consistent with field data and model results (cf Section 6.1; De Vries et al., 1989b), which also show that dissolved Al increases significantly at a base saturation below 20%.

#### Cation release mechanisms

Annual release of base cations was dominated by cation exchange in the Ah and Aan horizon, whereas mineral weathering was the primary cause in all other horizons (Table 3.34). The relative contribution of the various cations in annual BC desorption generally decreased according to  $Ca > Mg > K > Na$  in all soil horizons. Average values for all soil samples (57) were 62% for Ca, 18% for Mg 15% for K and 5% for Na. The relative contribution of these cations to annual BC weathering generally decreased according to  $K > Na > Ca \approx Mg$ . Average contributions in all soil samples except for the Aan horizons (6 samples) were 35% for K, 26% for Na, 20% for Ca and 19% for Mg. In the Aan horizons, Ca weathering was dominant (75% of total BC weathering). Ca weathering also dominated in the C horizon of a dune soil in which shell fragments occurred (63% of total BC weathering).



**Table 3.34** Average annual weathering and desorption of base cations at pH 3.0 in the soil horizons studied

Process	Annual base cation release (mmol <sub>e</sub> kg <sup>-1</sup> )								
	Ah	Aan	(A+B)p	(A+C)p	Bhs	Bh	BCs	C	D
Weathering	2.9	18	3.2	3.1	2.0	5.8	4.3	8.8 <sup>1)</sup>	3.6
Desorption	7.4 <sup>2)</sup>	29	2.1	2.7	1.3	1.8	0.2	1.4	1.6
Total	10.3	47	5.3	5.8	3.3	7.6	4.5	10.2	5.2

<sup>1)</sup> This value is influenced by large base cation weathering rates (up to 33 mmol<sub>e</sub> kg<sup>-1</sup> yr<sup>-1</sup>) in two dune soils in which shell fragments occurred (Haplic Arenosol and Umbric Gleysols at De Zilk; cf Table 3.25). Excluding these samples gave an average value of 6.8 mmol<sub>e</sub> kg<sup>-1</sup>

<sup>2)</sup> Excluding the Ah(H) horizon with a large organic matter content gave an average value of 4.1 mmol<sub>e</sub> kg<sup>-1</sup>

Al release from the reactive Al pool was dominated by dissolution of amorphous secondary compounds in all soil horizons, assuming that extraction with LaCl<sub>3</sub> gives a reliable estimate of the pool of organically bound Al (Fig. 3.17). The average contribution of amorphous inorganic Al compounds (oxalate minus lanthanum chloride-extractable Al) to the release of secondary Al compounds increased going from the Ah horizon (59%) to the BCs and C horizon (87%). The contribution of organically bound Al (lanthanum chloride minus silver thiourea-extractable Al) decreased in the same direction (47% in the Ah horizon and 4% in the BCs horizon). The contribution of crystalline Al compounds (dithionite minus oxalate-extractable Al) was small (< 8%), except for the Aan horizon (19%) and the D horizon (25%). The observed larger release of Al from secondary Al compounds, as compared to measured Al dissolution may be due to retention of polymers of organically complexed Al on the filter paper.

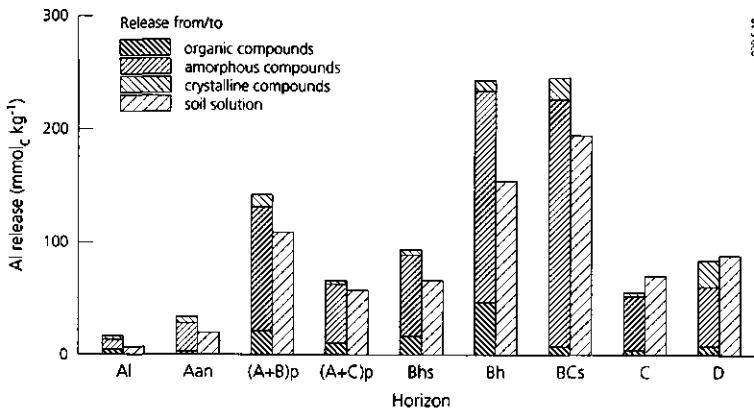


**Figure 3.17** Average Al release from secondary Al compounds as compared to measured Al dissolution (including Al exchange)

The large contribution of amorphous inorganic Al compounds to the release of secondary Al compounds is partly due to their large contribution to the secondary Al pool (cf Table 3.29). However, the release rate scaled to the pool of the different secondary Al compounds was also largest for the amorphous inorganic compounds, except for the Ah and Aan horizon. In the Ah horizon the depletion fraction of organic Al was highest, whereas the depletion fraction of the inorganic crystalline Al pool was largest in the Aan horizon (cf Table 3.35). The average depletion of the secondary Al pool in all soil horizons was 54%, i.e. 42% of the organic Al pool, 60% of the inorganic amorphous Al pool and 31% of the inorganic crystalline Al pool. Results also indicated a weak but significant relationship between the depletion fraction of secondary Al compounds and the contribution of organically complexed Al to the secondary Al pool (organic Al fraction; Fig. 3.18).

**Table 3.35** Average depletion fraction of secondary Al compounds in one-year batch experiments in the soil horizons studied

Secondary Al pool	Depletion fraction								
	Ah	Aan	(A+B)p	(A+C)p	Bhs	Bh	BCs	C	D
organic	0.29	0.21	0.26	0.44	0.45	0.41	0.47	0.61	0.64
amorphous	0.26	0.52	0.59	0.51	0.51	0.58	0.89	0.82	0.69
crystalline	0.13	0.70	0.51	0.24	0.37	0.49	0.70	0.00	0.30

The decrease in Al release at an increased contribution of organically bound Al may be caused by a change in the dominating Al release mechanism. In samples with a high content of organically bound Al, such as Ah horizons, initial Al release may be

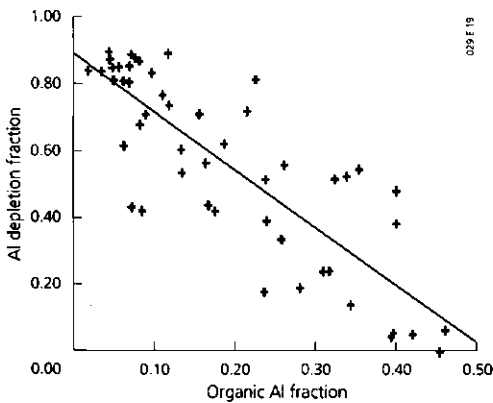


**Figure 3.18** The depletion fraction of secondary Al compounds in one-year batch experiments as a function of the organic Al fraction in the secondary Al pool. Symbols denote the experimental data whereas the solid line is derived by linear regression analyses (Al depletion fraction is  $0.92 - 2.09$  organic Al fraction;  $R^2_{adj}$  is 0.68)

dominated by exchange of H against complexed Al until an equilibrium is approached. In the equilibrium situation, Al release may be due to slow release of primary and or secondary Al silicates. Considering the long-term Al/BC release ratio of 2.5 mol<sub>c</sub> mol<sub>c</sub><sup>-1</sup>, dissolution of primary silicates seems to dominate in this horizon. In samples with a low content of organically bound Al, such as BCs and C horizons, both initial and long-term Al release is likely dominated by rate-limited dissolution of inorganic secondary Al compounds (mainly Al silicates). For these compounds, an equilibrium situation is never approached (cf Section 3.1).

One argument against the interpretation above might be that the pool of inorganically complexed Al, as determined by LaCl<sub>3</sub>, is generally not even dominant in the Ah horizon. (cf Table 3.29). However, most likely this extractant underestimates the organic Al pool in the upper A and B horizons. When Na pyrophosphate would have been used as an extractant for organic Al, the contribution of organically bound Al would have been much higher. In A and B horizons, pyrophosphate-extractable Al generally approaches oxalate-extractable Al (cf Section 3.1; Mokma and Buurman, 1982). Pyrophosphate was not used since it likely overestimates the organic Al pool, especially in the lower soil horizons. This can be derived from the ratio of pyrophosphate-extractable Al or Al and Fe, to organic C, which often exceeds a maximum complexing capacity of 11 mol<sub>c</sub> kg<sup>-1</sup> C. (Section 3.1). However, in the uppermost Ah and E horizons the amount of oxalate-extractable Al (which is assumed to equal the amount of pyrophosphate-extractable Al) per kg carbon remained always below the maximum complexing capacity of organic matter. This was also the case in several Aan, (A+B)p and (A+C)p horizons. In the three Bh horizons oxalate-extractable Al and Fe only slightly exceeded the maximum complexing capacity (Table 3.36). Most likely, the contribution of organic Al compounds as estimated from LaCl<sub>3</sub>-extractable Al, is too low in the upper A and B horizons. The observed larger Al release from amorphous secondary compounds as compared to measured Al release in solution in these horizons also points in this direction (Fig. 3.17; cf Table 3.13 in Section 3.1).

Table 3.36 *Extracted Al and Al+Fe in ammonium oxalate per kg organic carbon in the soil horizons studied*

Soil horizon	N	Extracted Al (mol <sub>c</sub> kg <sup>-1</sup> C)			Extracted Al+Fe (mol <sub>c</sub> kg <sup>-1</sup> C)		
		min	mean	max	min	mean	max
Ah	15	0.5	2.0	5.2	0.8	4.1	9.2
Aan	6	3.1	4.3	6.3	7.1	10	16
(A+B)p	5	2.4	8.0	14	2.9	11	20
(A+C)p	3	4.2	8.3	16	5.4	10	18
E	2	2.6	2.7	2.8	3.5	3.5	3.5
Bhs	6	5.7	17	40	7.9	23	52
Bh	3	9.1	11	12	11	13	16
BCs	7	15	53	92	22	62	105
C	14	1.1 <sup>1)</sup>	82	213	6.1	96	232
D	2	20	21	23	31	32	33

<sup>1)</sup> Exceptional value for a dune soil with an extremely low oxalate-extractable Al content

## pH effects on cation and silica release

### Annual release rates

Annual release rates of cations and Si increased with decreasing pH in nearly all the 26 soil samples studied. The effect of pH on the dissolution rate could generally be described well with a power-type relationship (Section 3.2; Eq 3.11). It should, however, be noted that most experiments were only conducted at three pH levels. Values for the exponent  $\beta_2$  generally decreased in the order  $Al \approx Fe \approx Mg > Si > K \approx Na \approx Ca$  (Table 3.37). However, there were clear differences between and within the various horizons.

Table 3.37 Average values for the exponent  $\beta_2$  in the relationship  $CR_x = \beta_1(H)^{\beta_2}$  for eight soil horizons of acid sandy soils<sup>1)</sup>

Soil horizon	Number of samples <sup>2)</sup>	pH range	$\beta_2$ value						
			Al	Fe	Ca	Mg	K	Na	Si
Ah	4	2.5-3.0	1.13	1.82	0.86	1.42	1.22	0.82	0.76
(A+B)p	4	2.3-3.3	1.85	1.41	0.99	1.52	0.91	0.75	1.20
(A+C)p	3	2.5-3.0	0.92	1.34	0.79	1.25	1.44	1.03	0.87
Bhs	2	2.5-3.5	0.47	1.21	1.27	1.56	0.89	0.76	1.28
Bh	2	2.5-3.5	1.23	1.32	1.27	2.01	0.82	0.75	0.88
BCs	2	2.5-3.5	0.59	1.17	0.63	2.46	0.67	0.59	0.82
C	3	3.0-4.0	1.15	1.02	0.19	1.36	0.91	1.18	1.08
D	1	3.0-4.0	1.51	1.33	0.60	0.87	-. <sup>3)</sup>	0.87	1.14

<sup>1)</sup>  $CR_x$  is the annual dissolution rate ( $\text{mmol}_c \text{ kg}^{-1}$ ), which was calculated by subtracting cation release by cation exchange from total cation release

<sup>2)</sup> In calculating the average exponent  $\beta_2$ , all samples with less than three data points (pH levels) were excluded. This requirement led to the exclusion of three Ah horizons, one (A+B)p horizon and the only E horizon because acid neutralization was negligible at the highest pH level studied (3.0 for Ah and E horizons and 3.3 for (A+B)p horizons)

<sup>3)</sup> Statistically insignificant value. The value of  $R^2_{adj}$  for the samples included varied mostly between 0.65 and 1.00

The average standard deviation of  $\beta_2$  ranged between 31% of the average value for Na up to 91% of the average value for Al. The estimated average values for  $\beta_2$  are generally higher than those reported in the literature for Al (e.g. Van Grinsven et al., 1992; Dalhgren and Walker, 1993) and BC (e.g. Van Grinsven et al., 1988). Estimated values for the exponent  $\beta_2$  for base cations suggest that the use of a standard value of 0.5 in several models (e.g. Chen et al., 1983; Van Grinsven et al., 1987) is too low for (extremely) acid sandy soils. For K, Na and Ca the average value approaches 0.85 and for Mg a value of 1.5 would be better.

### Al depletion and Al release rates

In all soil samples with a substantial release of Al, (only part of the Ah and Bhs samples) the Al release rate decreased exponentially as a function of cumulative Al release at all pH levels studied. For most horizons, the combined effect of pH and Al depletion could be described well as a function of the secondary Al pool and the degree

of undersaturation with respect to gibbsite (Eq. 3.15). Results (Table 3.38) show a markedly different behaviour of Al in the various soil horizons. To give an indication of the scatter of datapoints around the fitted curve, results for major soil horizons are illustrated in Fig 3.19.

**Table 3.38** Values for the parameters  $\gamma_1$  and  $\gamma_2$  in the relationship between Al release rate versus the secondary Al fraction (secondary Al pool as a fraction of the initial content) and the degree of undersaturation with gibbsite (Eq. 3.15) for the nine soil horizons studied<sup>1)</sup>

Soil horizon	Number of samples	Number of pH levels	$\ln \gamma_1$	$\gamma_2$	$\gamma_1$ ( $10^{-7} \text{ m}^3$ $\text{kg}^{-1} \text{ yr}^{-1}$ )	$e^{\ln \gamma_1 + \gamma_2}$ ( $10^{-3} \text{ m}^3$ $\text{kg}^{-1} \text{ yr}^{-1}$ )	$R^2_{adj}$
Ah	6	3	-16.2	11.4	0.35	3.0	0.68
Aan	6	1	-11.5	4.2	39	0.26	0.23
(A+B)p	5	2-5	-13.2	10.8	6.8	33	0.81
(A+C)p	3	3	-12.9	8.6	8.8	4.8	0.60
Bhs	4	1-3	-10.9	9.1	70	64	0.67
Bh	3	3-5	-13.2	12.3	6.5	143	0.84
BCs	7	1-5	-9.5	7.3	262	40	0.77
C	13	1-3	-10.8	9.8	78	144	0.89
D	2	1-5	-15.1	14.5	1.0	202	0.67

<sup>1)</sup> Al least four data points per sample were required to be included in the statistical analyses. This caused the exclusion of nine Ah horizons, the two E horizons, two Bhs horizons and one C horizon (a dune soil with shell fragments). In these horizons Al release was very low or negligible at the pH level(s) studied

At the beginning of the experiment (at zero Al depletion), Al release rates were high in the Bh, C and D horizons, low in the Ah, Aan and (A+C)p horizons and intermediate in the (A+B)p, Bhs and BCs horizons (cf the values for  $\ln \gamma_1 + \gamma_2$  in Table 3.38). The extremely low initial Al release rates in the Aan horizons are, of course, due to the initial large release of base cations by exchange against protons, as shown before. Consequently the coefficient of determination for this horizon was very low ( $R^2_{adj}$  is 0.23) and the standard deviation in the estimated values was high. Predicted Al release rates at complete Al depletion were highest for the Aan, Bhs, BCs and C horizons, lowest for the Ah and D horizons, and intermediate for the (A+B)p, (A+C)p and Bh horizons (cf the values for  $\ln \gamma_1$  in Table 3.38). The most remarkable difference in Al release at negligible and complete Al depletion was found for the D horizon. However, unlike the other soil horizons, complete Al depletion was not approached in this horizon for any of the experiments (the lowest secondary Al fraction was 0.37). Extrapolation to complete Al depletion is thus doubtful.

For a given degree of undersaturation and Al depletion, Al release rates can be estimated with Eq 3.15, using the values for  $\ln \gamma_1$  and  $\gamma_2$  given in Table 3.38. Results thus obtained for major soil horizons, assuming a pH level of 3.0 (the dominant pH level studied), illustrate the marked differences between upper and lower soil horizons (Table 3.39) In nearly all soil horizons, the range in Al depletion during the experiments varied between 10% and 90%. To avoid dubious extrapolation of Al release rates to 0% and

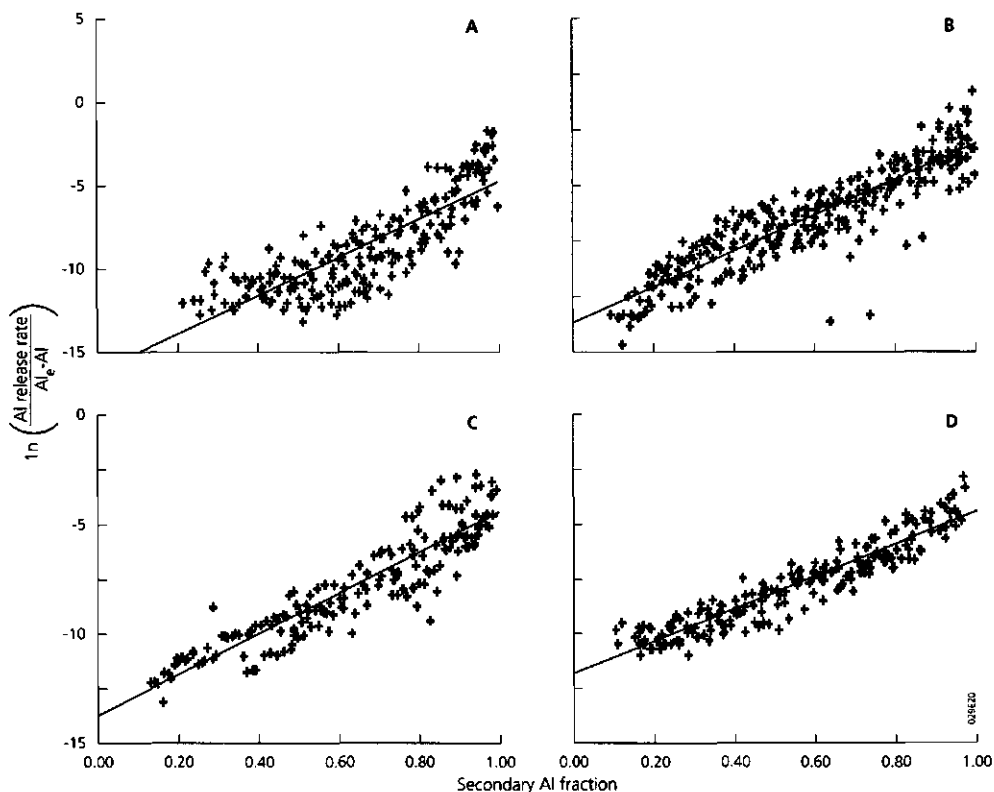


Figure 3.19 The logarithmic Al release rate, scaled by the degree of undersaturation with respect to gibbsite, as a function of the secondary Al fraction for the Ah horizon (A), (A+B)p horizon (B), Bh horizon (C) and C horizon (D). The Al release rate is given in  $\text{mmol}_c \text{ kg}^{-1} \text{ d}^{-1}$ . Experimental data are denoted by symbols, whereas solid lines are the predictions made with Eq. 3.15 (cf Table 3.38 for information on the rate constants  $\gamma_1$  and  $\gamma_2$ )

Table 3.39 Predicted Al release rates at pH 3.0 in four major soil horizons as a function of Al depletion<sup>1)</sup>

Soil horizon	Al release rate ( $\text{mmol}_c \text{ kg}^{-1} \text{ yr}^{-1}$ ) at an Al depletion of					
	10%		50%		90%	
Ah	286	(286)	3.0	(3.0)	0.03	(0.03)
(A+B)p	3351	(405)	45	(5.4)	0.59	(0.07)
Bh	12926	(347)	94	(2.5)	0.69	(0.02)
C	15018	(45)	298	(1.0)	5.9	(0.02)

<sup>1)</sup> Values in brackets are calculations for pH levels commonly encountered in the field, i.e. 3.0 for the Ah horizon, 3.3 for the (A+B)p horizon, 3.5 for the Bh horizon and 3.7 for the C horizon

100% depletion, these values were used as an indication of (nearly) negligible and (nearly) complete Al depletion.

The predicted Al release rates at (nearly) complete Al depletion at pH 3.0 ranged from 0.03 mmol<sub>c</sub> kg<sup>-1</sup> yr<sup>-1</sup> in the Ah horizon to 5.9 mmol<sub>c</sub> kg<sup>-1</sup> yr<sup>-1</sup> in the C horizon. These release rates can be attributed to weathering from primary silicates. Multiplying those values with an average bulk density of 1400 kg m<sup>-3</sup> gives an Al release rate varying between 0.42 and 83 kmol<sub>c</sub> ha<sup>-1</sup> yr<sup>-1</sup> m<sup>-1</sup>. With the exception of the Ah horizon, these values are still 1-2 orders of magnitude higher than Al release rates from primary minerals than can be expected under field circumstances. This deviation is most likely due to differences in pH (and temperature) between the laboratory and the field.

The predicted Al release rates near the pH occurring in the field situation was much lower for the (A+B)p, Bh and C horizon (cf the values in brackets in Table 3.39). Using the average bulk density of 1400 kg m<sup>-3</sup> leads to Al release rates of 0.42, 0.98, 0.28 and 0.28 kmol<sub>c</sub> ha<sup>-1</sup> yr<sup>-1</sup> m<sup>-1</sup> for the Ah, (A+B)p, Bh and C horizon, respectively, at an Al depletion of 90%. These values are similar to Al weathering rates from primary minerals in the field situation (De Vries and Breeuwsma, 1986). Considering an average field weathering rate for base cations in acid sandy soils of 0.1-0.2 kmol<sub>c</sub> ha<sup>-1</sup> yr<sup>-1</sup> m<sup>-1</sup> and an equivalent stoichiometric Al/BC weathering ratio of ca 2-3 (cf section 2.2 and 4.2), the average rate of Al release from primary minerals in the field most likely ranges between 0.2 and 0.9 kmol<sub>c</sub> ha<sup>-1</sup> yr<sup>-1</sup> m<sup>-1</sup>. The agreement between Al weathering rates from primary silicates measured in the field and those estimated from laboratory experiments may, however, be coincidence. Extrapolation of Eq. (3.15) to complete Al depletion is theoretically doubtful. Most likely, the pH effect on the Al release from primary Al silicates can not be described by the degree of undersaturation with gibbsite. On the other hand, Eq. (3.15) appears to fit measured Al release up to nearly total Al depletion, thus allowing the use of Eq. (3.15) to describe pH effects on Al release rates for this situation.

#### *Effects of soil type on Al release rates.*

In the previous section, several samples from different soil types were included in the statistical analyses for each soil horizon. Sometimes, this caused a marked decrease in the goodness of fit (the value of  $R^2_{adj}$ ) of Eq. (3.15). For example, the outliers in the relationship between Al release rate and secondary Al fraction in the (A+B)p horizon (cf Fig 3.19B) were due to one sample of a Gleyic Podzol. Relationships that were derived for specific combinations of soil horizons and soil types generally gave a better fit. For example, values of  $R^2_{adj}$  for each combination of Ah horizon and soil type ranged between 0.71 and 0.83, whereas the value of  $R^2_{adj}$  for the Ah horizon equalled 0.68 (cf Table 3.38 and 3.40).

The influence of soil type on the release of Al was much larger in the Ah and Bh(s) horizons than in the C horizon (Table 3.40). This can be expected since the parent

Table 3.40 Values for the parameters  $\gamma_1$  and  $\gamma_2$  in the relationship between Al release rate versus secondary Al fraction and the degree of unsaturation with gibbsite (Eq. 3.15) for Ah, Bh(s) and C horizons from different soil types

Soil type	Ah horizon			Bh(s) horizon			C horizon		
	$\ln \gamma_1$	$\gamma_2$	$R^2_{adj}$	$\ln \gamma_1$	$\gamma_2$	$R^2_{adj}$	$\ln \gamma_1$	$\gamma_2$	$R^2_{adj}$
Cambic Podzol	-16.0	11.6	0.78	-10.8	9.5	0.83	-11.0	9.8	0.89
Carbic Podzol	-	-	-	-13.2	12.3	0.84	-10.0	8.1	0.83
Gleyic Podzol	-28.1	26.5	0.83	-23.1	22.4	0.63	-10.5	9.8	0.90
Umbric Gleysol	-22.1	18.3	0.71	-	-	-	-	-	-
Haplic Arenosol <sup>1)</sup>	-15.0	11.3	0.83	-	-	-	-11.6	11.3	0.95

<sup>1)</sup> Includes a Gleyic Arenosol in the Ah horizon.

material of these acid sandy soils is generally quite comparable. Note, however, that the Al release rate is fitted as a function of the secondary Al fraction. Even in the C horizon there were marked differences in Al release rate with time due to differences in the initial content of secondary Al compounds.

## CONCLUSIONS

Major results of the experiments performed are (cf the objectives of the study):

- (i) Al release from secondary Al compounds is the dominant buffer mechanisms in all mineral horizons of acid sandy forest soils, although cation exchange is nearly of equal importance the Ah horizon. In the field situation, however, exchange of protons against base cations in Ah horizons (and in organic horizons) is likely to be less important, because of a relative large BC input in this horizon, induced by mineralization and throughfall. In mineral soils with a high base saturation (Aan horizons of Fimic Anthrosols in agricultural land), BC release by cation exchange dominates the neutralization of acid inputs, up to a base saturation of ca. 20%.
- (ii) In upper Ah horizons with a high content of organically bound Al, initial fast release is most likely dominated by exchange of H against complexed Al, followed by rate-limited slow release of (primary and secondary) Al silicates. In lower BCs, C and D horizons, both (fast) initial and (slow) long-term release is most likely dominated by rate-limited dissolution of inorganic secondary Al silicates. In (A+B)<sub>p</sub>, (A+C)<sub>p</sub>, Bhs and Bh horizons, rate limited dissolution of inorganic Al compounds seems to dominate Al release, but equilibrium reactions between protons and organically bound Al may play an equally important role as well.
- (iii) In all horizons of acid sandy forest soils, Al release kinetics was described well as a function of the pool of secondary Al compounds and the degree of undersaturation with respect to gibbsite. Even though it is unlikely that gibbsite governs Al solubility and even though it is questionable that rate-limited Al dissolution dominates initial Al release in upper Ah horizons (see above), this empirical model is of practical use in soil acidification modelling. Predicted Al



release rates at a pH of 3.0 were lowest in the upper Ah horizon, intermediate in the (A+B)<sub>p</sub>, (A+C)<sub>p</sub>, B<sub>hs</sub> and B<sub>h</sub> horizons and highest in the lower BCs and C horizon. Predicted Al release rates at actual pH values at complete Al depletion approached field estimates of Al weathering by primary minerals.

# Chapter 4

## AVERAGE CRITICAL LOADS FOR FORESTS, HEATHLANDS, GROUND WATER AND SURFACE WATER IN THE NETHERLANDS

### 4.1 CRITICAL LOADS FOR NITROGEN

- INTRODUCTION
- METHODS, CRITERIA AND MODELS TO DERIVE CRITICAL NITROGEN LOADS
- EMPIRICAL DATA
- MODEL RESULTS
- DISCUSSION AND CONCLUSIONS

### 4.2 CRITICAL LOADS FOR ACIDITY

- INTRODUCTION
- CRITERIA AND MODELS TO DERIVE CRITICAL ACID LOADS
- MODEL RESULTS
- DISCUSSION AND CONCLUSIONS

Chapter 4 is a strongly revised version of:

W. de Vries, 1993. *Average critical loads for nitrogen and sulfur and its use in acidification abatement policy in the Netherlands*. *Water Air and Soil Pollution* 68: 399-434.

## 4.1 CRITICAL LOADS FOR NITROGEN

### ABSTRACT

Effects due to an excess input of N include vegetation changes in forests, heathlands and surface waters, forest damage and nitrate pollution of ground water. Critical loads (deposition levels) for N on terrestrial and aquatic ecosystems in the Netherlands related to these effects have been derived by empirical data and steady-state nitrogen models. Critical loads of N generally vary between 500 and 2000 mol<sub>c</sub> ha<sup>-1</sup> yr<sup>-1</sup>. Empirical data and model results for critical N loads related to vegetation changes and nutrient imbalances appear to be comparable. Application of a steady-state nitrogen model on European forests shows that the area exceeding critical N loads, related to vegetation changes, is about 50%. The uncertainty in critical loads can be large. This is mainly due to uncertainties in the long term acceptable immobilization rate of N and in the chemical criteria that are used.

### INTRODUCTION

In terrestrial ecosystems where N is a growth-limiting factor, an extra input of N will lead primarily to increased production. A further increase in N input will cause a change in ecosystem composition. Species adapted to live in a N-poor environment will be replaced by species adapted to a N-rich environment. Today, vegetation changes threaten the wild flora of most European countries (Ellenberg, 1985). The most susceptible ecosystems are oligotrophic wetlands, heathlands with a high proportion of lichen cover, and low meadow vegetation types without any addition of fertilizers. The most obvious phenomenon in the Netherlands during the last decades was the expansion of the grasses *Molinia caerulea* and *Deschampsia flexuosa* in heathlands at the expense of the heather species *Calluna vulgaris* and *Erica tetralix* (Heil and Diemont, 1983; Roelofs, 1986). A comparative field study by Roelofs et al. (1983) showed that this expansion is related to the N status of the soil. The N levels in grass-dominated heathlands appeared to be much higher than in heather-dominated heathlands whereas the pH showed hardly any difference. The increased N availability in forests also affects the herb layer towards a shift in nitrophilous species (Van Breemen and Van Dijk, 1988; Hommel et al., 1990). Furthermore, nitrophilous epiphytic lichens are becoming increasingly abundant (Van Dobben, 1987).

A continuous high input of N, such as in the Netherlands, leads to a situation where other growth factors, such as other nutrients and water, may become limiting for the growth of forest. The relation between water shortage and N surplus can be explained by the fact that a high N input favours growth of canopy biomass, whereas root growth is relatively unaffected. The increase in canopy biomass will lead to a higher demand for water and therefore to an increased risk of water shortage. It also causes an increased demand of base cation nutrients (Ca, Mg, K) whereas the availability of these cations is reduced by increased dissolved levels of NH<sub>4</sub>. A recent inventory of the needle

composition of 150 forest stands in the Netherlands revealed that most forests (more than 60%) suffer from (a relative) Mg and P deficiency due to high N contents (Hendriks et al., 1994). Nihlgård (1985) hypothesized that N surplus also affects mycorrhizal functions, causing relative deficiencies of K, Mg, and P. High N levels in needles and buds are also correlated with early budbreak and increased sensitivity to natural stress factors such as frost (Aronsson, 1980) and attacks by fungi (Roelofs et al., 1985). Finally, a high N input may lead to nutrient imbalances both in needles and in the soil (Roelofs et al., 1985; Van den Burg et al., 1988).

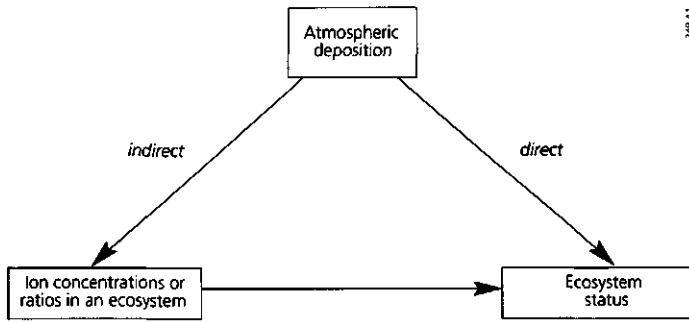
Apart from vegetation changes in forests and heathlands and decreased vitalities of forests, an excess input of N causes various other effects such as vegetation changes in oligotrophic surface waters (Schuurkes et al., 1987) and pollution of ground water due to  $\text{NO}_3$  leaching (Boumans and Beltman, 1991). In the Netherlands, high N inputs have caused eutrophication problems in almost all small oligotrophic surface waters (Schuurkes et al., 1987). Furthermore, high  $\text{NO}_3$  concentrations in ground water do often occur in the Netherlands, especially in areas with intensive animal husbandry.  $\text{NO}_3$  concentrations in shallow ground water underneath forests range between 0 and 200 mg  $\text{l}^{-1}$  (Boumans and Beltman, 1991), often exceeding the current EC drinking water standard of 50 mg  $\text{l}^{-1}$ . This is harmful in areas where ground water is used for water supply.

In this section, an overview is given of various methods to derive critical N loads, together with its application for forests, heathlands, ground waters and surface waters in the Netherlands. Regarding the methods used, a distinction is made between an empirical approach and a model approach. Critical N loads derived by an empirical approach are based on literature data. Emphasis is given to the model approach, by describing the models developed and their application on the various ecosystems.

## METHODS, CRITERIA AND MODELS TO DERIVE CRITICAL NITROGEN LOADS

### Methods

Critical loads for ecosystems can be derived in a direct and an indirect way as indicated in Fig. 4.1. Critical loads can be derived directly from the relationship between atmospheric deposition and effects on "specified sensitive elements" within an ecosystem (ecosystem status) by correlative or experimental research. For example, increased N loads may lead to changes from heathlands to grasslands. Critical N loads can be estimated by comparing the N deposition on grass dominated and heather dominated heathlands, or by experimental investigation of the biomass development of grasses as a function of N input.



249 A1

**Figure 4.1** Research methods to derive critical loads for N and S (each arrow indicates a relationship that can be assessed by correlative research, process research and/or model research).

Critical loads can also be derived indirectly from critical values for ion concentrations or ion ratios in the ecosystem, based on dose response relationships between these chemical criteria and the ecosystem status (Figure 4.1). In the Netherlands, critical loads have mostly been derived in an indirect way, because a direct assessment generally leads to an overestimation, since effects on ecosystems may occur before harmful effects are visible. In this respect, steady-state nitrogen models were developed, calculating critical loads from critical chemical ion concentrations and/or ratios.

### Criteria

An overview of the criteria that were used to assess critical N loads for various ecosystems in the Netherlands is given in Table 4.1.

#### *Nitrate concentrations*

A critical  $\text{NO}_3$  concentration related to vegetation changes in forests, heathlands and surface waters is difficult to assess. In the Netherlands, a target value of  $2.2 \text{ mg l}^{-1}$  ( $0.16 \text{ mol}_c \text{ m}^{-3}$ ) of total N is used to avoid algal growth in surface waters (VW, 1989). Values related to vegetation changes in terrestrial ecosystems will depend on the species considered. Preliminary experiences from the Swedish Forest Survey Programme suggest increasing values for changes going from lichens < cranberries < blueberries < grasses < herbs (Warfvinge et al., 1992a). Suggested values for changes in lichens are as low as  $0.02 \text{ mol}_c \text{ m}^{-3}$ . A similar value was used by Rosén (1990) on the basis of  $\text{NO}_3$  concentrations in stream water of nearly unpolluted forested areas in Sweden. However, such a low value was not used for the Netherlands where lichens hardly occur in forests. Here a rather arbitrary value of  $0.1 \text{ mol}_c \text{ m}^{-3}$  was used (based on the value suggested by Warfvinge et al., 1992a for changes from grasses to herbs).

Table 4.1 Critical chemical values used for various N parameters

Ecosystem	Effects	Criteria			
		Compartment	Parameter	Unit	Value
Forest	Vegetation changes	Soil solution	NO <sub>3</sub>	(mol <sub>c</sub> m <sup>-3</sup> )	0.1
	Nutrient imbalances	Soil solution	NH <sub>4</sub> /K	(mol mol <sup>-1</sup> )	5
		Soil solution	NH <sub>4</sub> /Mg	(mol mol <sup>-1</sup> )	10
	Increased susceptibility <sup>1)</sup>	Leaves	N	(%)	1.8
Heathland	Vegetation changes	Soil solution	NO <sub>3</sub>	(mol <sub>c</sub> m <sup>-3</sup> )	0.1
Surface water	Vegetation changes		N	(mol <sub>c</sub> m <sup>-3</sup> )	0.16
Ground water	Nitrate pollution		NO <sub>3</sub>	((mol <sub>c</sub> m <sup>-3</sup> )	0.8 <sup>2)</sup>

<sup>1)</sup> Refers to frost damage, pests and diseases

<sup>2)</sup> Target value in the Netherlands is 0.4 mol<sub>c</sub> m<sup>-3</sup>

Critical NO<sub>3</sub> concentrations for ground water were derived from the EC drinking water standards of 50 mg l<sup>-1</sup>, (approximately 0.8 mol<sub>c</sub> m<sup>-3</sup>). For NO<sub>3</sub>, a target value of 25 mg l<sup>-1</sup> (0.4 mol<sub>c</sub> m<sup>-3</sup>), used in the Netherlands, was also employed to derive critical loads for N (cf Table 4.1).

#### Ammonium / base cation ratios

Roelofs et al. (1985) were among the first who postulated that increased NH<sub>4</sub> concentrations and ratios of NH<sub>4</sub> to K and Mg are an important cause of decreasing forest vitality in the Netherlands. They found a reasonable correlation between the ratios of NH<sub>4</sub> to K and Mg in the topsoil and the vitality of coniferous trees. The accumulation of NH<sub>4</sub> in the soil, induced by the deposition of NH<sub>3</sub> and NH<sub>4</sub>, appeared to inhibit the growth of ectomycorrhizae, which play an important role in nutrient uptake by many coniferous trees (Boxman et al., 1986). Imbalanced nutrient concentrations in the soil solution thus cause K and Mg deficiencies, resulting in chlorotic yellow-brown needles. Boxman and Van Dijk (1988) found a strong decrease in the uptake of Ca and Mg at an increasing NH<sub>4</sub>/K molratio in a laboratory experiment with two-year-old Corsican pines. Using these data Boxman et al. (1988) proposed a critical NH<sub>4</sub>/K ratio of 5.

#### Nitrogen contents

For most coniferous tree species, a N content in the needles of 1.6 to 2.0% is considered optimal for growth. Above 2.5%, forest growth even decreases irrespective of the ratio to other nutrients (Van den Burg et al., 1988). At these levels the sensitivity to frost and fungal diseases increases too. In a fertilization experiment in Sweden, it was found that frost damage to the needles of Scots pine strongly increased above an N content of 1.8% (Aronsson, 1980). At this N level, the occurrence of fungal diseases such as *Sphaeropsis sapinea* and *Brunchorstia pinea* also appears to increase. This can be derived from correlative field research in the Netherlands about the N content in needles of Corsican pine and Scots pine and the occurrence of these fungal diseases (Roelofs et al., 1985; Boxman and Van Dijk, 1988; Van den Burg et al., 1988). In this context, Van den Burg et al. (1988) suggested critical levels of 1.6 and 1.8% for

Corsican pine and Scots pine, respectively. Based on these results, an N content of 1.8% in needles was considered to be critical.

## Steady-state models

### Total nitrogen

Critical loads of total N for terrestrial and aquatic ecosystems were derived with a simple model of the N balance. The complete N balance including all N fluxes (in mol<sub>c</sub> ha<sup>-1</sup> yr<sup>-1</sup>) in an ecosystem reads:

$$N_{td} + N_{fi} = N_{gu} + N_{im} + N_{de} + N_{ad} + N_{le} \quad (4.1)$$

where the subscript *td* refers to total deposition, *fi* to fixation, *gu* to growth uptake, *im* to net immobilization, *de* to denitrification, *ad* to adsorption and *le* to leaching. Adsorption of N was neglected as this process only plays a temporary role. However, even in the short term adsorption of N can be neglected since (i) N mainly occurs as NO<sub>3</sub> except for the topsoil and (ii) the preference of the adsorption complex for NH<sub>4</sub> is low in (acid) sandy soils. N fixation can be considered negligible in most forest and heathland ecosystems (Granhall and Lindberg, 1980) except for N-fixing species, such as red alder (Van Miegroet and Cole, 1984). In most (Dutch) forest soils, N below the root zone (at 1m depth) is dominated by NO<sub>3</sub> (Heij et al., 1991) and therefore it is reasonable to assume that NH<sub>4</sub> leaching is negligible (N<sub>le</sub> equals NO<sub>3,le</sub>). By assuming N fixation, N adsorption and NH<sub>4</sub> leaching to be negligible, Eq. (4.1) can be written as:

$$N_{td} = N_{gu} + N_{im} + N_{de} + NO_{3,le} \quad (4.2)$$

Denitrification was described as a fraction of the net N input (Breeuwsma et al., 1991):

$$N_{de} = fr_{de} \cdot (N_{td} - N_{gu} - N_{im}) \quad (4.3)$$

From Eqs. (4.2) and (4.3) a critical N load, N<sub>td(crit)</sub>, was derived according to:

$$N_{td(crit)} = N_{gu} + N_{im(crit)} + \frac{fr_{de}}{(1 - fr_{de})} \cdot NO_{3,le(crit)} + NO_{3,le(crit)} \quad (4.4)$$

where N<sub>im(crit)</sub> stands for a critical (long-term acceptable) level of N immobilization and NO<sub>3,le(crit)</sub> for a critical level of NO<sub>3</sub> leaching. The third term in the right hand side of Eq. (4.4) stands for the denitrification rate at critical N loads. In wet forest- and heathland soils, deep ground water and surface waters denitrification is generally not negligible and should be accounted for. However, in well-drained forest and heathland



soils, denitrification is (nearly) negligible (Klemetsson and Svensson, 1988) and for these systems (including phreatic ground water) Eq. (4.4) simplifies to:

$$N_{td}(\text{crit}) = N_{gu} + N_{im}(\text{crit}) + \text{NO}_{3,e}(\text{crit}) \quad (4.5)$$

### Ammonia

Critical loads of  $\text{NH}_3\text{-N}$  for terrestrial ecosystems were derived with a simple model including the major  $\text{NH}_4$  and K inputs to the system. The ratio of  $\text{NH}_4$  to K in the soil solution, which is the criterium for deriving a critical  $\text{NH}_3\text{-N}$  load, is determined by system inputs (in  $\text{mol}_e \text{ ha}^{-1} \text{ yr}^{-1}$ ) according to:

$$R_{\text{NH}_4\text{K}} = (\text{NH}_{4,tf} + \text{NH}_{4,mi} - \text{NH}_{4,ni} - \text{NH}_{4,ru}) / (\text{K}_{tf} + \text{K}_{mi} + \text{K}_{we} - \text{K}_{ru}) \quad (4.6)$$

where  $R_{\text{NH}_4\text{K}}$  is the  $\text{NH}_4/\text{K}$  ratio, the subscript *tf* stands for throughfall, *mi* for mineralization, *ni* for nitrification, *ru* for root uptake and *we* for weathering. In calculating a critical load, the model was simplified by assuming that (i) throughfall of  $\text{NH}_4$  and total deposition of  $\text{NH}_3$  are equal, (ii) mineralization of  $\text{NH}_4$  and K is equal to the N and K input by litterfall (steady-state situation), (iii) root uptake does not affect the  $\text{NH}_4/\text{K}$  molratio and (iv) weathering of K is negligible. Eq. (4.6) thus simplifies to:

$$R_{\text{NH}_4\text{K}} = \text{NH}_{3,td} + \text{NH}_{lf} - \text{NH}_{4,ni} / \text{K}_{lf} + \text{K}_{lf} \quad (4.7)$$

where *lf* stands for litterfall. Nitrification of  $\text{NH}_4$  was described as a fraction of the  $\text{NH}_4$  input according to:

$$\text{NH}_{4,ni} = fr_{ni} \cdot (\text{NH}_{3,td} + \text{N}_{lf}) \quad (4.8)$$

where  $fr_{ni}$  is a nitrification fraction. Combination of Eqs. (4.7) and (4.8) gives:

$$R_{\text{NH}_4\text{K}} = (1 - fr_{ni}) \cdot (\text{NH}_{3,td} + \text{N}_{lf}) / (1 - fr_{ni}) \quad (4.9)$$

Defining a critical  $\text{NH}_4/\text{K}$  ratio,  $R_{\text{NH}_4\text{K}}(\text{crit})$ , a critical  $\text{NH}_3\text{-N}$  load,  $\text{NH}_{3,td}(\text{crit})$ , was derived according to:

$$\text{NH}_{3,td}(\text{crit}) = R_{\text{NH}_4\text{K}}(\text{crit}) \cdot (\text{K}_{lf} + \text{K}_{lf}) - (1 - fr_{ni}) \cdot \text{N}_{lf} / (1 - fr_{ni}) \quad (4.10)$$

## EMPIRICAL DATA

An overview of empirical data for critical N loads on terrestrial and aquatic ecosystems in the Netherlands is given in Table 4.2. Values are discussed below.

Table 4.2 Empirical data of critical N loads ( $\text{mol}_c \text{ ha}^{-1} \text{ yr}^{-1}$ ) for various effects in forests, heathlands and surface waters

Critical N-load	Ecosystem	Effects	Reference	
700-1400	Forest	Vegetation changes	Correlation with N deposition and species diversity	Tyler (1987)
3000	Forest	Increased susceptibility	Correlation between N deposition and N content in needles	Van den Burg et al. (1988)
800	Forest	Nutrient imbalances (most sensitive systems)	Precipitation experiment	Boxman et al. (1988)
850-1400	Heathland	Change to grassland	Precipitation experiment	Roelofs (1986)
500-700	Heathland	Decreased species diversity	Correlation with N deposition	Schneider and Bresser (1988)
1400	Surface water	Change to nitrophilous species	Precipitation experiment	Schuurkes et al. (1987)
500 <sup>1)</sup>	Surface water	Decreased species diversity	Correlation with N deposition	Arts (1990)

<sup>1)</sup> Refers to oligotrophic surface waters in the Netherlands with low denitrification and N immobilization

### Vegetation changes

Critical N loads related to vegetation changes in heathlands were derived from Roelofs (1986) who performed one year precipitation experiments with  $\text{NH}_4$  on small heathland systems in a greenhouse. Results showed that the biomass development of grasses increases strongly at a deposition rate above  $1400 \text{ mol}_c \text{ ha}^{-1} \text{ yr}^{-1}$ . More detailed experiments showed that the increase already started at a deposition rate of  $850 \text{ mol}_c \text{ ha}^{-1} \text{ yr}^{-1}$  or  $12 \text{ kg ha}^{-1} \text{ yr}^{-1}$  (Roelofs, Catholic University of Nijmegen, pers. comm.).

However, since vegetation change is a slow process, it is necessary to consider that the effects of the present deposition have not yet occurred in many ecosystems. Taking into account the effect of N accumulation and the slow response of ecosystems, the upper limit for the long term critical load is probably lower. A decrease in species diversity in heathlands occurs already between  $500$  and  $700 \text{ mol}_c \text{ ha}^{-1} \text{ yr}^{-1}$  (Schneider and Bresser, 1988). In forest ecosystems changes in forest undergrowth (Tyler, 1987) were found to occur when the deposition exceeds  $1400 \text{ mol}_c \text{ ha}^{-1} \text{ yr}^{-1}$  or  $20 \text{ kg ha}^{-1} \text{ yr}^{-1}$ .

A critical N load related to vegetation changes in oligotrophic, poorly buffered pools and lakes in the Netherlands was derived from empirical data by Schuurkes et al. (1987) and Arts (1990). Schuurkes et al. (1987) treated small-scale soft water ecosystems in a greenhouse with water containing  $(\text{NH}_4)_2 \text{SO}_4$ . From those experiments, they derived a critical N load (given as  $\text{NH}_4$ ) of  $1400 \text{ mol}_c \text{ ha}^{-1} \text{ yr}^{-1}$ . This was based on the observed luxuriant growth of acid-tolerant nitrophilous macrophyte species which formed dense mats, suppressing the submerged development and growth of typical macrophytes of oligotrophic soft waters. From historical data for N deposition and species decline in surface waters given by Arts (1990) a critical N load of  $500 \text{ mol}_c \text{ ha}^{-1} \text{ yr}^{-1}$  was derived.

### **Effects on forest vitality**

A critical N load related to increased susceptibility to frost damage and fungal diseases was derived from field data by Van den Burg et al. (1988), which show that an N content of 1.8% in needles of Scots pine is associated with an N deposition of approximately  $3000 \text{ mol}_c \text{ ha}^{-1} \text{ yr}^{-1}$ . However, this value should be considered an overestimate, since the same concentration can be reached by exposure to lower inputs over a longer period. By mathematical modeling, Van Grinsven et al. (1991) simulated an N content in needles of Douglas fir close to 1.8% at an N deposition level near  $1500 \text{ mol}_c \text{ ha}^{-1} \text{ yr}^{-1}$  in a 40-yr period. This period nearly equals the average rotation period of a coniferous tree in the Netherlands.

Critical loads of  $\text{NH}_3$  related to nutrient imbalances were derived from Boxman et al. (1988) based on experimental field data. They measured a molar  $\text{NH}_4/\text{K}$  ratio near 5 at an artificially induced  $\text{NH}_4$  input of  $800 \text{ mol}_c \text{ ha}^{-1} \text{ yr}^{-1}$ , in soils with a very low nitrification rate. However, it is likely that empirical data lead to an under-estimation of critical  $\text{NH}_3$  loads because the present N/K ratio in needles is enhanced compared to the situation at critical loads.

## **MODEL RESULTS**

### **Vegetation changes**

Critical N loads related to vegetation changes in forests and heathlands were also derived by using the steady-state N balance model described before (Eq. 4.5). The use of Eq. (4.5) is based on the idea that any N input exceeding the net uptake by forest growth, critical long term immobilization and natural leaching of N finally leads to vegetation changes.

#### *N uptake*

The average annual net uptake of N in forests is equal to the amount of N that is

removed by harvesting divided by the rotation period. This depends upon tree species, forestry practice (stemwood removal or whole-tree harvesting), and site quality. With respect to harvesting, stemwood removal is common in the Netherlands. Average annual N uptake data of Dutch forests are given in Table 4.3.

Table 4.3 Average annual N uptake in stemwood and distribution of Dutch forests on low-, medium- and high-quality sites (total forest area is 332 500 ha)

Site quality	N uptake ( $\text{mol}_c \text{ ha}^{-1} \text{ yr}^{-1}$ )		Distribution (%)	
	Coniferous forest	Deciduous forest	Coniferous forest	Deciduous forest
low	230	320	31.5	11.8
medium	350	460	23.2	13.8
high	480	630	5.3	14.4

The values given in Table 4.3 are based on a literature review on growth data and N contents in stemwood by De Vries et al. (1990) for the most common tree species in the Netherlands, i.e. *Pinus sylvestris* (Scots pine), *Pinus nigra* (Black pine), *Pseudotsuga menziessi* (Douglas fir), *Picea abies* (Norway spruce), *Larix leptolepis* (Japanese larch), *Quercus robur* (Oak) and *Fagus sylvatica* (Beech). It was assumed that these values are not influenced by the present high N deposition. The growth data were derived from yield tables, published before the large increase in  $\text{NH}_3$  emissions in the Netherlands, whereas the N contents are taken from sites with a relatively low N deposition such as Scandinavian forests. At present, the net N uptake in stemwood in the Netherlands can be much higher than the values given above due to increased N contents in stems and possibly by increased growth rates as well. For example, De Visser (1986) estimated an N uptake near  $1000 \text{ mol}_c \text{ ha}^{-1} \text{ yr}^{-1}$  for an oak forest on a relatively rich forest soil in the Netherlands. However, use of such values was considered unacceptable for a long term critical load derivation, since the high uptake at this site is associated with a largely increased  $\text{NO}_3$  leaching rate (Van Breemen et al., 1986). However, use of increased uptake rates in response to N deposition is important in dynamic model applications to assess acceptable interim loads (De Vries, 1991).

Using the data given in Table 4.3, area-weighted, average N uptake rates of 300 and  $500 \text{ mol}_c \text{ ha}^{-1} \text{ yr}^{-1}$  were used for coniferous and deciduous forests respectively. For heathlands the average annual N uptake was calculated to be in the same order of magnitude. Assuming a net increase of  $750 \text{ kg ha}^{-1} \text{ yr}^{-1}$  (Gimingham, 1972) and a N content of  $0.8 \text{ mol}_c \text{ kg}^{-1}$  in the green parts (33%) and  $0.4 \text{ mol}_c \text{ kg}^{-1}$  in the woody parts (67%) (Heil and Diamond, 1983) resulted in a net uptake of  $400 \text{ mol}_c \text{ ha}^{-1} \text{ yr}^{-1}$ .

#### N immobilization

The long term critical net N-immobilization in stable organic N-compounds in the soil (stable forms of humus) was derived from the accumulation of N in soils since the

period of soil formation. Data on present N amounts in the rootzone of 150 forest soils in the Netherlands indicate an average N amount of  $400 \text{ kmol}_c \text{ ha}^{-1} \text{ yr}^{-1}$  (De Vries and Leeters, 1994). Most Dutch forest soils are podzols with an assumed soil formation period of 10 000 yr. This leads to a long term immobilization rate of approximately  $40 \text{ mol}_c \text{ ha}^{-1} \text{ yr}^{-1}$ , which was neglected.

One could argue that the amount of  $\text{NO}_3\text{-N}$  leached after harvesting should also be immobilized during the rotation period to avoid N deficiencies. Data about the increased leaching rate of  $\text{NO}_3$  in a deforested ecosystem in southern Sweden equalled about  $700 \text{ mol}_c \text{ ha}^{-1} \text{ yr}^{-1}$  (Wiklander et al., 1991). However, the effect lasted for less than five years since the regrowth of vegetation was very fast. A review of more than 40 studies on the effects of forest harvesting on  $\text{NO}_3\text{-N}$  losses showed that in most cases  $\text{NO}_3$  concentrations in clear-cut and control forests are comparable within five years (Vitousek and Melillo, 1979). Their data also indicate that the overall N loss from the soil organic matter after harvesting is generally less than  $4 \text{ kmol}_c \text{ ha}^{-1}$ . Taking an average rotation period of 80 years, this implies an average yearly immobilization leaching rate of  $50 \text{ mol}_c \text{ ha}^{-1} \text{ yr}^{-1}$ . This amount was also neglected.

In the short term (the coming decades), N accumulation in the humus layer of forests and heathlands may be higher. For Dutch forests this is due to the fact that most of them are in their first or second generation phase succeeding heathlands. Consequently the litter layer is generally not yet in equilibrium with litterfall. Data given by Van den Burg and Schoenfeld (1988) for first- and second-generation forests of Japanese larch, Douglas fir, and Norway spruce indicate an organic matter accumulation in the humus layer between  $500$  and  $1500 \text{ kg ha}^{-1} \text{ yr}^{-1}$  for stand ages between 20 and 60 yr. The average N content of the litter layer was approximately  $1.0 \text{ mol}_c \text{ kg}^{-1}$  (Van den Burg and Schoenfeld, 1988), leading to an N accumulation rate of  $500$  to  $1500 \text{ mol}_c \text{ ha}^{-1} \text{ yr}^{-1}$ . Their data also indicate that the accumulation is not yet finished. Similarly, Turner (1975) found an average humus accumulation rate of  $550 \text{ kg ha}^{-1} \text{ yr}^{-1}$  underneath stands of Douglas fir varying between 9 and 50 yr. Short term accumulation of N can also occur because of an increase in the N content of the litter layer. Berendse (1988) thus reported an N accumulation rate of approximately  $2000 \text{ mol}_c \text{ ha}^{-1} \text{ yr}^{-1}$  for Dutch heathlands. As with increased N uptake, short term N accumulation should not be included in deriving a long term critical load, but it is important for assessing short term interim loads.

#### *Nitrate leaching*

Critical  $\text{NO}_3$  leaching rates were derived by multiplying the critical  $\text{NO}_3$  concentration of  $0.1 \text{ mol}_c \text{ m}^{-3}$  with the precipitation excess (precipitation minus actual evapotranspiration where actual evapotranspiration stands for the sum of interception evaporation by the forest canopy, actual soil evaporation and actual transpiration (water uptake) in the rootzone). Average values used for the precipitation excess underneath coniferous forest, deciduous forests and heathlands in the Netherlands were 200, 300 and 400 mm

yr<sup>-1</sup>, respectively, leading to critical NO<sub>3</sub> leaching rates of 200, 300 and 400 mol<sub>c</sub> ha<sup>-1</sup> yr<sup>-1</sup>, respectively.

The precipitation excesses for forests were based on an annual precipitation of 780 mm yr<sup>-1</sup>, which is a 30-yr average value in the Netherlands, interception evaporations of 33 and 20% of the annual precipitation for coniferous forests (Calder and Newson, 1979; Hiege, 1985) and deciduous forests (Leyton et al., 1967; Tietema and Verstraten, 1988), respectively, and an average annual transpiration of 325 mm yr<sup>-1</sup> for all tree species (Roberts, 1983). Soil evaporation was considered negligible. Similar values for the precipitation excess underneath forests in the Netherlands are given by Ter Hoeve (1978), De Laat (1985) and De Visser and De Vries (1989) based on lysimeter experiments and model calculations respectively. The precipitation excess underneath heathlands was based on model calculations with an annual precipitation of 780 mm yr<sup>-1</sup> (De Visser and De Vries, 1989).

#### *Critical loads*

Adding the average values for uptake and natural leaching results in critical N loads as given in Table 4.4. The critical loads thus derived might be too low since the effect of increased N availability on the vegetation is not included in this simple model approach. In an overview on the effects of atmospheric deposition on heathlands, Van Dobben (1991) mentioned a critical load of 700 to 1100 mol<sub>c</sub> ha<sup>-1</sup> yr<sup>-1</sup> based on competition models for grasses and heather.

*Table 4.4 Model estimates of critical N loads for coniferous forests, deciduous forests and heathlands related to the occurrence of vegetation changes*

Land use	Critical N load (mol <sub>c</sub> ha <sup>-1</sup> yr <sup>-1</sup> )		
	Uptake	Leaching	Total
Coniferous forest	300	200	500
Deciduous forest	500	300	800
Heathland	400	400	800

#### **Nutrient imbalances in forests**

Critical loads of NH<sub>3</sub> related to nutrient imbalances in forests were derived with Eq. (4.10) using a critical molar NH<sub>4</sub>/K ratio of 5. The problem in using Eq. (4.10) is that throughfall and litterfall data for N and K, which are necessary to derive a critical NH<sub>4</sub> load, strongly depend on the deposition level of NH<sub>4</sub>. This affects the K exudation rate and the N/K ratios in needles. The average K input by throughfall varies between approximately 250 mol ha<sup>-1</sup> yr<sup>-1</sup> in relatively unpolluted areas (Berdén et al., 1987) and 500 mol ha<sup>-1</sup> yr<sup>-1</sup> in polluted areas, such as the Netherlands (Houdijk, 1990). Data given by Van den Burg and Kiewiet (1989) show that the present average molar N/K ratio in

needles of Scots pine, Corsican pine and Douglas fir in the Netherlands, is approximately 10. However, this ratio was approximately 5 in most coniferous trees in the Netherlands at the beginning of 1960 when the N load was much lower. The difference is mainly due to an increase in N content in the last decades. Furthermore, the K input by litterfall also decreases with an increasing N deposition, by causing an absolute decrease in K content, but this effect is relatively small (Van den Burg and Kiewit, 1989). A reasonable average value for K in litterfall equals  $500 \text{ mol}_c \text{ ha}^{-1} \text{ yr}^{-1}$  (De Vries, 1988). Finally, the nitrification fraction varies from site to site. Tietema and Verstraten (1988) reported a nitrification percentage of 50 ( $fr_{ni} = 0.5$ ) for the topsoil of an acid sandy forest soil but lower values are likely to occur as well (Boxman et al., 1988).

An overview of critical loads of  $\text{NH}_3$  calculated for varying input data is given in Table 4.5. The first and second combination of data on N/K ratio in needles and K input by litterfall and throughfall in Table 4.5 are assumed to be indicative for the present situation and the situation at critical loads (see above). Use of the input data presently found are likely to give an underestimate of the critical load of  $\text{NH}_3\text{-N}$ . Table 4.5 shows that the critical  $\text{NH}_3\text{-N}$  load increases significantly with an increase in nitrification fraction. Using the data that are likely to occur at critical loads leads to a minimum value of  $1250 \text{ mol}_c \text{ ha}^{-1} \text{ yr}^{-1}$  for soils with a negligible nitrification rate. However, this value is likely to be an underestimate since nitrification will never be inhibited completely.

Table 4.5 Model estimates of critical loads for  $\text{NH}_3\text{-N}$  as a function of the N/K ratio in needles, the K input in throughfall and the nitrification fraction.

N/K ratio in needles ( $\text{mol mol}^{-1}$ )	K input by litterfall ( $\text{mol}_c \text{ ha}^{-1} \text{ yr}^{-1}$ )	K input by throughfall ( $\text{mol}_c \text{ ha}^{-1} \text{ yr}^{-1}$ )	Critical $\text{NH}_3\text{-N}$ load ( $\text{mol}_c \text{ ha}^{-1} \text{ yr}^{-1}$ )			
			$fr_{ni}=0$	$fr_{ni}=0.1$	$fr_{ni}=0.3$	$fr_{ni}=0.5$
10	500	500	0	550	1800	5000
5	500	250	1250	1650	2850	5000

### Ground water pollution

A critical N load in relation to pollution of phreatic ground water underneath well-drained forests and heathlands was also derived by applying Eq. (4.5). For N uptake, an average value of 300, 400 and  $500 \text{ mol}_c \text{ ha}^{-1} \text{ yr}^{-1}$  was used for coniferous forests, heathlands and deciduous forests and long-term N immobilisation was neglected as given before. Critical  $\text{NO}_3$  leaching fluxes were derived by multiplying critical  $\text{NO}_3$  concentrations of  $25 \text{ mg l}^{-1}$  ( $0.4 \text{ mol}_c \text{ m}^{-3}$ ) and  $50 \text{ mg l}^{-1}$  ( $0.8 \text{ mol}_c \text{ m}^{-3}$ ; Table 4.1), with the precipitation excesses given before, i.e. 200, 300 and  $400 \text{ mm yr}^{-1}$  for coniferous forests, deciduous forests and heathlands, respectively. Adding these N leaching fluxes to the net uptake of N lead to critical loads as mentioned in Table 4.6.

**Table 4.6** Model estimates of critical N loads for phreatic ground water underneath well-drained forests and heathlands in the Netherlands for different critical  $\text{NO}_3$  concentrations

Land use	Critical N load ( $\text{mol}_c \text{ ha}^{-1} \text{ yr}^{-1}$ )		
	uptake	leaching <sup>1)</sup>	total
Coniferous forest	300	800 (0.4)	1100
	300	1600 (0.8)	1900
Deciduous forest	500	1200 (0.4)	1700
	500	2400 (0.8)	2900
Heathland	400	1600 (0.4)	2000
	400	3200 (0.8)	3600

<sup>1)</sup> Values between brackets denote the critical  $\text{NO}_3$  concentration used in  $\text{mol}_c \text{ m}^{-3}$

The critical N loads given in Table 4.6 are not related to deep ground water, which is used for drinking water. Here the effect of denitrification should be accounted for. However, the values given in Table 4.6 can be used as a worst case option by neglecting denitrification in the saturated zone.

## DISCUSSION AND CONCLUSIONS

An overview of the various critical N loads based on empirical data and on results from modelling approaches (Eqs. 4.5 and 4.10) shows that a critical N load below  $1000 \text{ mol}_c \text{ ha}^{-1} \text{ yr}^{-1}$  will present most effects on terrestrial and aquatic ecosystems in the Netherlands (Table 4.7).

**Table 4.7** Average critical N loads for terrestrial and aquatic ecosystems in the Netherlands

Effects	Critical N load ( $\text{mol}_c \text{ ha}^{-1} \text{ yr}^{-1}$ )			
	Coniferous forests	Deciduous forests	Heathlands	Surface waters
Vegetation changes <sup>1)</sup>	500-1400	800-1400	800-1400	500-1400
Frost damage <sup>2)</sup>	1500-3000			
Nutrient imbalances <sup>3)</sup>	800-1250			
Ground water pollution <sup>4)</sup>	900-1500	1700-2900	2000-3600	

<sup>1)</sup> The first value is derived by applying Eq. (4.5), whereas the second value is based on experimental data.

<sup>2)</sup> Empirical data

<sup>3)</sup> The first value is based on experimental data, whereas the second value is derived by applying Eq. (4.10) (both values only refer to  $\text{NH}_3\text{-N}$ ).

<sup>4)</sup> Both values are derived by applying Eq. (4.5) but the first values refers to a critical  $\text{NO}_3$  concentration of  $25 \text{ mg l}^{-1}$  ( $0.4 \text{ mol}_c \text{ m}^{-3}$ ) and the second value to  $50 \text{ mg l}^{-1}$  ( $0.8 \text{ mol}_c \text{ m}^{-3}$ ).

Uncertainties in empirical data on critical N loads are related to the occurrence of time lags. Harmful effects on ecosystems may already occur before they are visible.



Uncertainties in critical N loads derived by steady state models are determined by the uncertainty in critical chemical values, model structure and data. The choice of the critical  $\text{NO}_3$  concentration and  $\text{NH}_4/\text{K}$  ratio strongly affects the critical N and  $\text{NH}_3$  loads. In this context, the uncertainty in critical N loads on forests will be larger than the critical N load related to  $\text{NO}_3$  leaching to ground water since  $50 \text{ mg l}^{-1}$  of  $\text{NO}_3$  is an accepted critical value for drinking water, whereas the criteria for forest damage are very uncertain. Uncertainties induced by the model structure are related to modeling assumptions. For example, the assumption that N fixation and denitrification can be neglected is reasonable for nearly all well-drained forests and heathlands in the Netherlands, but it will cause a large error in wetlands. The same is true when deriving critical loads in areas with a complex hydrology including seepage or surface runoff. Uncertainties in the (long-term) average data are most likely quite small. However, for deep ground water, the uncertainty in critical N loads can be substantial due to uncertainties about the occurrence and rate of denitrification in the saturated zone. Use of the values derived for phreatic ground water might be a substantial underestimate of the critical loads that are relevant at the depth of ground water extraction.

The aforementioned critical loads formed the basis for the assessment of target loads used in the Dutch acidification policy. A target acid load of  $1400 \text{ mol}_e \text{ ha}^{-1} \text{ yr}^{-1}$  has been set for the year 2010 with an N input below  $1000 \text{ mol}_e \text{ ha}^{-1} \text{ yr}^{-1}$  (cf Section 4.2). At these levels, nearly all effects on terrestrial ecosystems are prevented or considerably decreased. Vegetation changes might still occur in the long term at an N load of  $1000 \text{ mol}_e \text{ ha}^{-1} \text{ yr}^{-1}$  (cf Table 4.6). However, this effect will also be slowed down considerably compared to the present N input in the Netherlands, which is equal to  $3000 \text{ mol}_e \text{ ha}^{-1} \text{ yr}^{-1}$  on average (Erisman et al., 1987) up to  $10.000 \text{ mol}_e \text{ ha}^{-1} \text{ yr}^{-1}$  in areas with intensive animal husbandry (Houdijk, 1990).

## 4.2 CRITICAL LOADS FOR ACIDITY

### ABSTRACT

*Atmospheric deposition of N and S on terrestrial and aquatic ecosystems causes effects induced by eutrophication and acidification, such as forest damage, ground water pollution, and loss of fish populations due to Al mobilization. Critical loads (deposition levels) for total acidity (S and N) on terrestrial and aquatic ecosystems in the Netherlands related to these effects were mainly derived by a steady-state acidification model. Average critical loads varied between 300 to 500 mol<sub>c</sub> ha<sup>-1</sup> yr<sup>-1</sup> for phreatic ground waters and surface waters and between 1100 to 1400 mol<sub>c</sub> ha<sup>-1</sup> yr<sup>-1</sup> for forests. On the basis of the various critical loads a deposition target for total acidity of 1400 mol<sub>c</sub> ha<sup>-1</sup> yr<sup>-1</sup> has been set in the Netherlands from which the N input should be less than 1000 mol<sub>c</sub> ha<sup>-1</sup> yr<sup>-1</sup>. This level, to be reached in the year 2010, implies an emission reduction of 80-90% in SO<sub>2</sub>, NO<sub>x</sub> and NH<sub>3</sub> in the Netherlands and of about 30% in neighbouring countries compared to 1980 emissions.*

### INTRODUCTION

At present soil, ground water, and surface water in large areas of Europe and North America are undergoing accelerated acidification due to deposition of S and N compounds. The major changes in water chemistry are increases in SO<sub>4</sub>, NO<sub>3</sub> and Al concentrations and decreases in pH and alkalinity values. Effects of acid (N and S) deposition on non-agricultural areas in the Netherlands include:

- (i) nutrient deficiencies in forest ecosystems induced by leaching of base cations (mainly Ca and Mg) and inhibition of the uptake of these elements due to Al mobilization in the soil (Heij et al., 1991);
- (ii) pollution of ground water for drinking water supply due to increased hardness and increased concentrations of Al mobilized from the soil (Boumans and Van Grinsven, 1991); and
- (iii) loss of fish populations caused by a decrease in pH and an increase in labile Al in surface waters (Arts, 1988).

Apart from acidification, an excess input of N also causes various other effects in the Netherlands such as vegetation changes in forests (Hommel et al., 1990), heathlands (Heil and Diamond, 1983) and oligotrophic surface waters (Schuurkes et al., 1991), decreased vitalities of forests, caused by an increased susceptibility to natural stress factors such as frost and diseases (Roelofs et al., 1985; Heij et al., 1991) and pollution of ground water due to NO<sub>3</sub> leaching (Boumans and Beltman, 1991) (cf Section 4.1).

Political decisions on emission reductions require scientific determinations of those deposition levels (loads) of SO<sub>2</sub>, NO<sub>x</sub> and NH<sub>3</sub> which cause adverse environmental effects. Information on these, so called, critical loads constitutes an important basis for the development and adaptation of the Netherlands' "Acidification abatement policy".

The most general definition of a critical load is: "quantitative estimate of an exposure to one or more pollutants below which significant harmful effects on specified sensitive elements of the environment do not occur according to our present knowledge" (Article 1, Paragraph 7 of the draft NO<sub>x</sub> protocol EB Air/WG.3/16, Annex). Another definition is: "the maximum deposition of acidifying compounds that will not cause chemical changes leading to long term harmful effects on ecosystem structure and function" (Nilsson and Grennfelt, 1988). In deriving critical loads, a long term (i.e. decades) perspective has to be considered, as most of the effects are results of accumulated depositions. The term 'critical load' should not be confused with 'target load', which is related to political decisions. The critical load is an inherent property of an ecosystem, whereas the target load is less restrictive and also implies other factors, such as economical (cost benefit) or emotional considerations.

In this section, an overview is given of criteria and models to derive critical acid loads (S and N), together with its application for forests, heathlands, ground waters and surface waters in the Netherlands. Furthermore, the political conclusions drawn in the Netherlands, in defining target loads to be reached within the coming decades, are discussed.

## CRITERIA AND MODELS TO DERIVE CRITICAL ACID LOADS

### Criteria

Critical loads can be derived directly from the relationship between atmospheric deposition and effects on "specified sensitive elements" within an ecosystem (ecosystem status) by correlative or experimental research (cf Section 4.1; De Vries, 1993). For example, critical acid loads related to the decline of fish species can be estimated by experimental investigation of the fish decline as a function of the acid input. However, in forest ecosystems, such a clear relationship does not exist between tree mortality and acid atmospheric deposition. Here, critical loads can only be derived indirectly from critical values for ion concentrations or ion ratios in the ecosystem. Critical chemical values can be derived from effects influencing forest vitality, such as decreased mycorrhizal frequency, root damage or inhibited nutrient uptake. A discussion of the various criteria is given below. An overview of the criteria that were used to assess critical acid loads is given in Table 4.8.

#### *Forest soils*

Ulrich and his coworkers (e.g. Ulrich and Matzner, 1983) were among the first who postulated the hypothesis that increased Al concentration and Al/Ca ratio in the soil solution is a major cause of forest dieback by damaging the root system of tree species. Tolerance to Al toxicity has generally been related to root and/or shoot growth, and sometimes to the degree of mortality. The sensitivity of a tree to Al varies as a function

**Table 4.8** Critical values used for pH, Al concentration and Al/Ca ratio to derive critical acid loads for forests, ground waters and surface waters

Criteria	Unit	Forest	Ground water (soil solution)	Surface water
pH	-	- <sup>1)</sup>	6.0	5.3 (6.0) <sup>2)</sup>
[Al] <sup>3)</sup>	mol <sub>c</sub> m <sup>-3</sup>	0.2	0.02	0.003
Al/Ca	mol mol <sup>-1</sup>	1.0 <sup>4)</sup>	-	-

<sup>1)</sup> No criteria available. However, the value can be related to a critical (inorganic) Al concentration

<sup>2)</sup> For waters receiving acid peakflow from meltwater

<sup>3)</sup> Refers to inorganic Al; 1 mol<sub>c</sub> m<sup>-3</sup> = 9 mg l<sup>-1</sup>

<sup>4)</sup> The equivalent Al/Ca ratio is thus 1.5 mol<sub>c</sub> mol<sub>c</sub><sup>-1</sup>

of solution pH, Al speciation, Ca concentration, overall ionic strength, the form of inorganic N (NH<sub>4</sub> or NO<sub>3</sub>), mycorrhizal interactions, soil moisture etc. Consequently, a wide range of Al toxicity thresholds for various tree species has been reported in the literature varying between less than 1.5 and more than 30 mg l<sup>-1</sup> (e.g. McCormack and Steiner, 1978; Steiner et al., 1980; Ryan et al., 1986a, b; Thornton et al., 1987; Smit et al., 1987; Joslin and Wolfe, 1988, 1989; Keltjens and Van Loenen, 1989). Results are all based on experiments with seedlings either grown in water cultures or in a greenhouse. Overall research findings of the ALBIOS (Al in the Biosphere) project carried out in eastern North America and northern Europe indicate that red spruce is the most sensitive tree species. Statistically significant biomass reductions started to occur near 2 mg l<sup>-1</sup> of inorganic Al which is toxic to roots. Moderately sensitive species include sugar maple, Douglas fir, spruce and European beech whereas Scots pine, oak and birch are relatively insensitive to Al (Cronan et al., 1989).

As with Al, a wide range in toxicity thresholds for the Al/Ca ratio have been reported. Based on the greenhouse experiments of Rost-Siebert (1983), Ulrich and Matzner (1983) proposed critical molar Al/Ca ratios of 1.0 for spruce and 10 for birch. A correlative field study between soil solution chemistry and forest vitality (Roelofs et al., 1985) yielded a critical molar Al/Ca ratio for black pine of 1.0 which is similar to that for spruce. Furthermore, laboratory experiments with two-year old black pine trees showed a strong decrease in Ca and Mg uptake at Al/Ca ratios above 1 (Boxman and Van Dijk, 1988). Based on the data given above, an inorganic Al concentration of 0.2 mol<sub>c</sub> m<sup>-3</sup> (about 2 mg l<sup>-1</sup>) and a molar Al/Ca ratio of 1.0 were used as critical values for the rootzone (cf Table 4.8).

#### *Ground water and surface water*

A critical pH of 6.0 in ground water was taken from the literature (Sverdrup et al., 1990a). A critical Al concentration for ground water was derived from the EC drinking-water standards of 0.2 mg l<sup>-1</sup> (approximately 0.02 mol<sub>c</sub> m<sup>-3</sup>). The critical pH of 5.3 and a critical Al concentration of 0.003 mol<sub>c</sub> m<sup>-3</sup> in surface water (cf Table 4.8) is based on Hultberg (1988). Application of these criteria still allows episodic effects on fish for situations with non-equilibrium conditions between pH and dissolved inorganic Al. These

effects can occur in lakes and rivers with a pH between 5.3 and 6.0 receiving acid peakflow from meltwater with a high labile Al concentration. The water in the mixing zone may show oversaturated concentrations of dissolved inorganic Al and will therefore be toxic to fish and other aquatic organisms, even at high pH values. In these waters a criterion of pH 6.0 (cf Table 4.8) is more suitable (Hultberg, 1988).

## Steady-state model

### Model derivation

Steady-state models are useful to derive critical loads of N (cf Section 4.1; De Vries, 1993) and total acidity (S and N). These models do not include processes that influence acid production and consumption during a finite time scale such as cation exchange, mineralization/immobilization of  $\text{NH}_4$ ,  $\text{SO}_4$  and base cations, and adsorption/desorption of  $\text{NH}_4$  and  $\text{SO}_4$  (Sverdrup et al., 1990; De Vries, 1991). They include only processes that influence acid production and consumption during infinite time such as weathering and net uptake, and predict directly the concentration of relevant ions in the soil solution (e.g. Al,  $\text{NH}_4$ , pH etc.) in a final equilibrium situation. Here a simple steady-state model is described that was used to derive critical loads of total acidity for terrestrial ecosystems on well-drained non-calcareous sandy soils. These conditions are required to allow for the various assumptions that have been made. Most Dutch forests and heathlands (more than 70%) occur on these soils.

The acidification model described is a steady-state mass balance model for the fluxes of N, S and base cations through an ecosystem. A steady-state situation with respect to soil acidification implies a constant pool of exchangeable base cations (BC). Consequently the following mass balance (in  $\text{mol}_c \text{ ha}^{-1} \text{ yr}^{-1}$ ) should hold:

$$\text{BC}_{le}^* = \text{BC}_{td}^* + \text{BC}_{we} - \text{BC}_{gu} \quad (4.11)$$

where the subscripts *we* and *gu* stand for weathering and growth uptake and where  $\text{BC}_{le}^*$  and  $\text{BC}_{td}^*$  stands for leaching and total deposition of base cations corrected for Cl ( $\text{BC}^*$  is Ca+Mg+K+Na-Cl). In the Netherlands Cl is mainly balanced by Na, Mg and K. Consequently, the value of  $\text{BC}_{td}^*$  is generally quite close to the deposition of Ca.

Charge balance of ions in the soil leachate requires that:

$$\text{H}_{le} + \text{Al}_{le} + \text{BC}_{le}^* + \text{NH}_{4,le} = \text{SO}_{4,le} + \text{NO}_{3,le} + \text{HCO}_{3,le} + \text{RCOO}_{le} \quad (4.12)$$

where  $\text{RCOO}_{le}$  is the leaching of the sum of all organic anions. It is assumed that concentrations of OH and  $\text{CO}_3$  are negligible. Defining the acidity of the soil solution, *Ac*, as:

$$[Ac] = [H] - [Al] - [HCO_3] - [RCOO] \quad (4.13)$$

(where [ ] denotes the concentration in mol<sub>c</sub> m<sup>-3</sup>) and combining Eqs. (4.12) and (4.13) gives:

$$SO_{4,le} + NO_{3,le} = BC_{le}^* - NH_{4,le} + AC_{le} \quad (4.14)$$

Leaching of ammonium (NH<sub>4,le</sub>) can be neglected in almost all forest ecosystems due to (preferential) uptake and/or complete nitrification within the root zone (Van Breemen and Verstraten, 1991). Using this assumption and combining the Eqs. (4.11) and (4.14) leads to:

$$SO_{4,le} + NO_{3,le} = BC_{td}^* + BC_{we} - BC_{gu} + AC_{le} \quad (4.15)$$

From Eq. (4.15), a critical load for the sum of S and N can be derived by defining a critical acidity leaching and linking the leaching of SO<sub>4</sub> and NO<sub>3</sub> to the deposition of these compounds by means of a mass balance. The N balance reads (cf Section 4.1):

$$N_{le} = N_{td} + N_{fi} - N_{gu} - N_{im} - N_{de} - N_{ad} \quad (4.16)$$

where the subscript *fi* refers to fixation, *im* to net immobilization, *de* to denitrification and *ad* to adsorption. By assuming N fixation, N adsorption and NH<sub>4</sub> leaching to be negligible (cf Section 4.1), Eq. (4.16) can be written as:

$$NO_{3,le} = N_{td} - N_{gu} - N_{im} - N_{de} \quad (4.17)$$

The S balance reads:

$$S_{le} = S_{td} - S_{gu} - S_{im} - S_{re} - S_{ad} \quad (4.18)$$

where the subscript *re* refers to reduction. An overview of S cycling in forests by Johnson (1984) suggests that the net (growth) uptake, immobilization, and reduction of SO<sub>4</sub> are generally insignificant. SO<sub>4</sub> adsorption occurs especially in Fe- and Al-oxide rich subsurface horizons (Johnson et al., 1979, 1982; Johnson and Todd, 1983). However, when deriving a long term critical load, the effect of adsorption must be neglected, since this phenomenon is only of temporary importance (several decades). Even in the short term, SO<sub>4</sub> adsorption is negligible in most Dutch forest soils (Van Breemen et al., 1986; Van Breemen and Verstraten, 1991). The same is true for most

European forest ecosystems, as shown by various budget studies given in Berdén et al. (1987). Using the various assumptions given before, Eq. (4.18) simplifies to:

$$S_{le} = S_{td} \quad (4.19)$$

Since S is completely oxidized in the soil profile,  $S_{le}$  equals  $SO_{4,le}$ . Combining Eqs. (4.15), (4.17) and (4.19) leads to:

$$S_{td} + N_{td} = BC_{td}^* + BC_{we} - BC_{gu} + N_{gu} + N_{im} + N_{de} + Ac_{le} \quad (4.20)$$

In the Netherlands, deposition of total acidity,  $Ac_{td}$ , is defined as the sum of S and N deposition minus the Cl-corrected bulk (wet) deposition of base cations:

$$Ac_{td} = S_{td} + N_{td} - BC_{wd}^* \quad (4.21)$$

where the subscript *wd* stands for wet deposition. This implies that  $NH_3$  is counted as an acid and not as a base. This is based on the assumption that leaching of  $NH_4$  from the soil is negligible. The total Cl-corrected deposition of base cations equals:

$$BC_{td}^* = BC_{wd}^* + BC_{dd}^* \quad (4.22)$$

where the subscript *dd* stands for dry deposition. From the Eqs. (4.20), (4.21) and (4.22) a critical load for total acidity,  $Ac_{td}(crit)$ , can be derived according to:

$$(Ac)_{td}(crit) = BC_{dd}^* + BC_{we} - BC_{gu} + N_{gu} + N_{im}(crit) + N_{de}(crit) + Ac_{le}(crit) \quad (4.23)$$

where  $Ac_{le}(crit)$  is a critical level of acidity leaching. Although the steady-state model described above was developed for application to forest soils, it can also be used to derive critical loads for deep ground water and surface water. In surface waters, alkalinity generation by  $SO_4$  reduction should also be accounted for (Schindler, 1986; Shaffer et al., 1988).

For well-drained forest and heathland soils denitrification can be neglected (Klemetsson and Svensson, 1988) and Eq. (4.23) simplifies to:

$$Ac_{td}(crit) = BC_{dd}^* + BC_{we} - BC_{gu} + N_{gu} + N_{im}(crit) + Ac_{le}(crit) \quad (4.24)$$

Apart from denitrification, differences in critical acid loads for forest soils, ground waters and surface waters in the same area are mainly due to differences in the weathering

rate and the critical acidity leaching flux. The areal weathering rate, expressed in  $\text{mol}_c \text{ ha}^{-1} \text{ yr}^{-1}$ , is determined by the parent material and the considered depth of the soil profile. This depth equals the average thickness of the root zone for forest soils, the unsaturated zone for phreatic ground water, depth to ground water extraction for deep ground water and the thickness of the catchment for surface water (Sverdrup et al., 1990). The difference in critical acidity leaching for the various receptors is due to different criteria for the pH and Al concentration (cf Table 4.8). These concentrations determine the value of the acidity (cf Eq. 4.13). A further discussion on the calculation of the critical acidity leaching term is given below.

#### *Calculation of the critical acidity leaching*

The critical acidity leaching flux (in  $\text{mol}_c \text{ ha}^{-1} \text{ yr}^{-1}$ ) is equal to (cf Eq. 4.13):

$$Ac_{le}(\text{crit}) = PE \cdot ([H] + [Al] - [HCO_3] - [RCOO])(\text{crit}) \quad (4.25)$$

where  $PE$  is the precipitation excess from the system ( $\text{m}^3 \text{ ha}^{-1} \text{ yr}^{-1}$ ). The criteria given in Table 4.8 for  $[Al]$  refer to the inorganic Al concentration which is toxic to roots. Assuming that organic anions are completely bound by Al, Eq. (4.25) simplifies to:

$$Ac_{le}(\text{crit}) = PE \cdot ([H] + [Al_i] - [HCO_3])(\text{crit}) \quad (4.26)$$

where  $[Al_i]$  is the inorganic Al concentration ( $\text{mol}_c \text{ m}^{-3}$ ). In ground water and surface water, the critical pH is above 5 (cf Table 4.8) and consequently  $[HCO_3]$  can not be neglected. The  $HCO_3$  concentration in these systems can be derived as:

$$[HCO_3] = KCO_2 \cdot pCO_2 / [H] \quad (4.27)$$

where  $KCO_2$  is the product of the first dissociation constant of  $H_2CO_3$  and Henry's law constant ( $\text{mol}^2 \text{ l}^{-2} \text{ bar}^{-1}$ ) and  $pCO_2$  is the partial  $CO_2$  pressure in the soil (bar). In forest soils, a critical pH is not given (cf Table 4.8). However, the 'critical' H-concentration or pH can be related to the critical Al concentration assuming an equilibrium with Al hydroxides:

$$[H](\text{crit}) = ([Al_i](\text{crit}) / KAl_{ox})^{1/3} \quad (4.28)$$

or

$$pH(\text{crit}) = (\log KAl_{ox} - \log [Al_i](\text{crit})) / 3 \quad (4.29)$$



where  $KAl_{ox}$  is the equilibrium constant for Al hydroxide dissolution ( $\text{mol}^{-2} \text{l}^2$ ) and  $[Al]_i(\text{crit})$  is the critical inorganic Al concentration ( $\text{mol l}^{-1}$ ). The Eqs. (4.28) and (4.29) are based on the assumption that the concentration and the activity of inorganic Al are equal. This assumption was made because of the large uncertainty in the critical value of  $[Al]_i$ . Taking  $[Al]_i(\text{crit})$  equal to  $0.2 \text{ mol}_c \text{ m}^{-3}$  (cf Table 4.8), i.e.  $6.67 \cdot 10^{-5} \text{ mol l}^{-1}$  and using a value of  $\log KAl_{ox}$  of 8.0 (based on H and Al concentrations in the subsoil of eight forest soils; Kleijn et al., 1989; cf Section 2.3), leads to a pH near 4.0. At this pH level,  $\text{HCO}_3^-$  can be neglected and Eq. (4.26) simplifies to:

$$Ac_{le}(\text{crit}) = PE \cdot ([H] + [Al]_i(\text{crit})) \quad (4.30)$$

Instead of directly using  $[Al]_i(\text{crit})$  for forest soils from Table 4.8 (Al concentration criterion) the value can also be calculated indirectly from the critical Al/Ca ratio (Al/Ca ratio criterion) according to:

$$[Al]_i(\text{crit}) = RAICa(\text{crit}) \cdot BC_{le}^* / PE \quad (4.31)$$

where  $RAICa(\text{crit})$  is the critical Al/Ca ratio and  $BC_{le}^*$  is the leaching flux of base cations, corrected for Cl input, as defined in Eq. (4.11). Eq. (4.31) is based on the assumption that this flux is equal to the leaching flux of Ca.

Finally,  $[Al]_i(\text{crit})$  for forest soils can also be calculated indirectly by aiming at a negligible depletion of secondary Al compounds (Al depletion criterion). This is based on the idea that using an alkalinity limit based on a critical Al concentration or Al/Ca ratio may imply that the accepted rate of Al leaching is greater than the rate of Al mobilization by weathering of primary minerals. The remaining part of Al has to be supplied from secondary Al compounds. This causes depletion of these compounds, which might induce an increase in Fe buffering which in turn leads to a decrease in the availability of phosphate (De Vries and Kros, 1989). Negligible depletion of secondary Al compounds is achieved when Al leaching equals mobilization of Al from primary minerals.  $[Al]_i(\text{crit})$  can thus be calculated as

$$[Al]_i(\text{crit}) = r \cdot BC_{we} / PE \quad (4.32)$$

where  $r$  is the equivalent stoichiometric ratio of Al to BC in the congruent weathering of silicates (primary minerals).

#### *The relation between acidification and eutrophication*

The critical Al concentration and Al/Ca ratio were used to derive a critical acid (N+S) load. Separate critical N loads have also been derived independent of the acidification

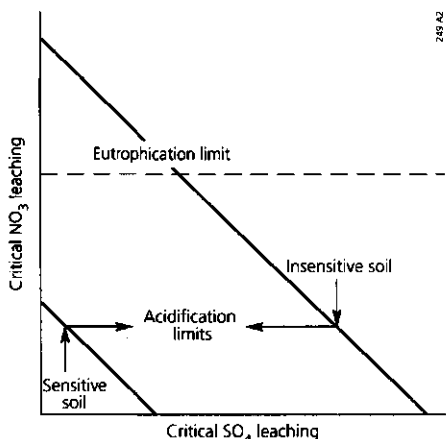


Figure 4.2 The relation between critical SO<sub>4</sub> and NO<sub>3</sub> leaching for given acidification limits.

aspect using values for a critical NO<sub>3</sub> concentration (cf Section 4.1). However, there is a relationship between the two critical loads as shown in Figure 4.2.

From the viewpoint of eutrophication, the critical level of NO<sub>3</sub> leaching is determined by the critical NO<sub>3</sub> concentration in soil water, ground water (drinking water) or surface water (cf Eq. 4.5 and 4.17). However, from the viewpoint of acidification, the critical NO<sub>3</sub> leaching level is determined by the critical acidity leaching flux and the SO<sub>4</sub> leaching level (Eq. 4.15). The limit for NO<sub>3</sub> leaching related to eutrophication can be higher or lower than the limit related to acidification (cf Fig. 4.2).

## MODEL RESULTS

### Forest ecosystems

Effects of increased concentrations of SO<sub>4</sub> and NO<sub>3</sub> in the soil solution of forest in the Netherlands include (Heij et al., 1991; Van Breemen and Verstraten, 1991):

- a decrease in the availability of mineral nutrients due to leaching of Ca and Mg and precipitation of P, which may cause nutrient deficiencies and
- increased concentrations of H<sup>+</sup> (a decreased pH), and Al, which may have toxic effects on roots and soil organisms.

Critical acid loads were derived in relation to the latter effect by applying Eq. (4.24) while using the various criteria for acidity leaching given in the Eqs. (4.30), (4.31) and (4.32). Data used for the net input of base cations by dry deposition, weathering and growth uptake and for acidity leaching and the critical loads thus derived are discussed in the following sections.

### *Dry deposition*

Data on dry deposition of base cations were derived from data on wet deposition according to:

$$BC_{dd}^* = f_{dd} \cdot BC_{wd}^* \quad (4.33)$$

where  $f_{dd}$  is a dry deposition factor.  $f_{dd}$  was derived from the difference in throughfall and bulk (wet) deposition of Na at 42 sites (Van Breemen et al., 1986; Ivens et al., 1988; Kleijn et al., 1989; Houdijk, 1990; Van Dobben et al., 1992) according to:

$$f_{dd} = (Na_{tf} - Na_{wd}) / Na_{wd} \quad (4.34)$$

Average values thus derived for coniferous and deciduous forests equalled 1.5 and 0.75 respectively. Data on wet deposition were based on 14 weatherstations during the period 1978-1985 (KNMI/RIVM, 1985). An average value for the seasalt corrected base cation input in the eastern part of the Netherlands, where most forests occur, equalled  $200 \text{ mol}_c \text{ ha}^{-1} \text{ yr}^{-1}$ . Multiplying the values for  $f_{dd}$  and  $BC_{wd}^*$  leads to a dry deposition of  $BC^*$  equal to  $300 \text{ mol}_c \text{ ha}^{-1} \text{ yr}^{-1}$  for coniferous forests and  $150 \text{ mol}_c \text{ ha}^{-1} \text{ yr}^{-1}$  for deciduous forests. Total deposition values were equal to 500 and  $350 \text{ mol}_c \text{ ha}^{-1} \text{ yr}^{-1}$  for coniferous and deciduous forests, respectively.

### *Weathering*

Weathering rates of non-calcareous sandy soils in the Netherlands were estimated from the depletion of base cations in the soil profile by chemical analyses of different soil horizons including the parent material (Section 2.2) and from input-output budgets based on hydrochemical monitoring (Van Breemen et al., 1986; Mulder et al., 1988). The first approach gives the average weathering rate over the period of soil formation (e.g. podzolization), whereas the second approach gives an estimate of the current weathering rate. The main problem with respect to profile analysis is the difficulty of identifying the parent mineral matrix (April and Newton, 1985; De Vries and Breeuwsma, 1986). The weakness in the approach of watershed budget studies is the relatively poor accuracy of the estimate due to the occurrence of cation exchange. An overview of methods available to determine weathering rates is given in Sverdrup et al. (1990).

An overview of weathering rates based on these approaches is given in Table 4.9. Most data are related to podzols and Udipsamments which are the most common forest soils in the Netherlands. Values of current weathering rates based on input-output budgets of base cations were somewhat higher than weathering rates based on soil profile analysis indicating a small effect of acid load on base cation weathering. Data reported by April and Newton (1985) and Fölster (1985) also indicate that the current weathering rate is somewhat enhanced by an increased acid load. However, it should be noted that the high value for the Dystric Cambisol at Hackfort B ( $700 \text{ mol}_c \text{ ha}^{-1} \text{ yr}^{-1}$ ) is due to the high

**Table 4.9** Weathering rates of base cations in the root zone of non-calcareous sandy soils in the Netherlands

Weathering rate (mol <sub>c</sub> ha <sup>-1</sup> yr <sup>-1</sup> )	Location	Soil type (FAO, 1988)	Method	Reference
110	Bathmen	Gleyic Podzol high <sup>1)</sup>	Profile analysis	De Vries and Breeuwsma, 1986
190	Bathmen	Gleyic Podzol medium <sup>1)</sup>	Profile analysis	De Vries and Breeuwsma, 1986
120	Bathmen	Gleyic Podzol low <sup>1)</sup>	Profile analysis	De Vries and Breeuwsma, 1986
90	Bathmen	Carbic Podzol	Profile analysis	De Vries and Breeuwsma, 1986
150	Ugchelen	Carbic Podzol	Profile analysis	De Vries, Unpublished data
100	Tongbersven	Gleyic Podzol	Budget	Mulder et al., 1988
300	Hasselsven	Gleyic Podzol	Budget	Mulder et al., 1988
400	Gerritsfles	Haplic Arenosol	Budget	Mulder et al., 1988
700	Hackfort B	Dystric Cambisol	Budget	Van Breemen et al., 1986
400	Hackfort C	Dystric Cambisol	Budget	Van Breemen et al., 1986

<sup>1)</sup> The terms high, medium and low refer to the drainage conditions (cf Section 2.2)

total base cation content of this soil type, which is not representative for Dutch forest soils. Neglecting this value an average weathering rate of 200 mol<sub>c</sub> ha<sup>-1</sup> yr<sup>-1</sup> was derived for the root zone of acid sandy forest soils (cf Table 4.9).

### Growth uptake

The average uptake of N and the base cations Ca, Mg and K in stemwood was calculated by multiplying the average growth rate over the rotation period with the element content in stems, since stemwood removal is the common practice in the Netherlands. The results given in Table 4.10 are based on a literature review on growth data and element contents in stemwood by De Vries et al. (1990). It was assumed that the growth rates and N contents were not influenced by the present high N deposition (cf Section 4.1). Using the data given in Table 4.10, area-weighted average annual N uptake rates of 300 and 500 mol<sub>c</sub> ha<sup>-1</sup> yr<sup>-1</sup> were derived for coniferous and deciduous

**Table 4.10** Average annual N uptake, BC uptake and distribution of Dutch forests on low-, medium- and high-quality sites (total forest is 332 500 ha)

Site quality	N uptake (mol <sub>c</sub> ha <sup>-1</sup> yr <sup>-1</sup> )		BC uptake (mol <sub>c</sub> ha <sup>-1</sup> yr <sup>-1</sup> )		Distribution (%)	
	Coniferous forest	Deciduous forest	Coniferous forest	Deciduous forest	Coniferous forest	Deciduous forest
low	230	320	210	230	31.5	11.8
medium	350	460	330	340	23.2	13.8
high	480	630	450	460	5.3	14.4

forests, respectively. Average BC uptake rates thus derived equalled 300 and 350 mol<sub>c</sub> ha<sup>-1</sup> yr<sup>-1</sup> for coniferous and deciduous forests, respectively.

#### *Critical acidity leaching*

Critical acidity leaching fluxes were derived by applying Eq. (4.30) (critical Al concentration), Eq. (4.31) (critical Al/Ca ratio) and Eq. (4.32) (no Al depletion from hydroxides). The critical Al leaching rate was calculated by:

- multiplying the critical Al concentration of 0.2 mol<sub>c</sub> m<sup>-3</sup> (Table 4.8) with precipitation excesses of 200 and 300 mm yr<sup>-1</sup> for coniferous and deciduous forests (Al concentration criterion; cf Eq. 4.30);
- multiplying the critical equivalent Al/Ca ratio of 1.5 (Table 4.8) with base cation leaching rates of 400 and 200 mol<sub>c</sub> ha<sup>-1</sup> yr<sup>-1</sup> for coniferous and deciduous forests. Base cation leaching rates were calculated according to Eq. (4.11) using the data on total deposition, weathering and growth uptake of base cations given before (Al/Ca ratio criterion; cf Eqs. 4.30 and 4.31); and
- multiplying a stoichiometric weathering ratio of Al to BC of 2.5 (cf Section 2.2; Sverdrup et al., 1990) with a weathering rate of 200 mol<sub>c</sub> ha<sup>-1</sup> (Al depletion criterion; cf Eqs. 4.30 and 4.32).

The critical H leaching rate was calculated by multiplying the previously given precipitation excesses of 200 mm yr<sup>-1</sup> and 300 mm yr<sup>-1</sup> for coniferous and deciduous forests (Section 4.1) with a critical H concentration of 0.1 mol<sub>c</sub> m<sup>-3</sup>. The latter value was derived with Eq. (4.28), taking [Al<sub>i</sub>](crit) equal to 0.2 mol<sub>c</sub> m<sup>-3</sup> and log KAl<sub>ox</sub> equal to 8.0. This leads to a critical H leaching rate of 200 mol<sub>c</sub> ha<sup>-1</sup> yr<sup>-1</sup> for coniferous forests and 300 mol<sub>c</sub> ha<sup>-1</sup> yr<sup>-1</sup> for deciduous forests. Values of [Al<sub>i</sub>](crit) are somewhat higher and lower, respectively, when the concentration is calculated from the Al/Ca criterion (Eq. 4.31) and the Al depletion criterion (Eq. 4.32) but this hardly affects the H concentration. Log KAl<sub>ox</sub> was derived from soil solution data of forest soils below Douglas stands at 60 cm soil depth (Kleijn et al., 1989). A log KAl<sub>ox</sub> value of 8.0 is nearly equal to the equilibrium constant of synthetic gibbsite (log K = 8.11). In the literature Al hydroxide is sometimes referred to as gibbsite, because field studies indicated that the dissolution constant for this mineral yield a reasonable prediction of Al in the subsoil (Mulder et al., 1987; Cronan et al., 1986). However, the dissolution of Al in acid sandy soils is mainly confined to amorphous secondary Al compounds (De Vries et al., 1994a, b; Section 3.1 and 3.2).

#### *Critical acid loads*

An overview of the average critical acid loads derived, including the data used for dry deposition weathering, uptake and acidity leaching, is given in Table 4.11. The critical acid load was calculated by adding the various input terms except for BC uptake which is subtracted (Eq. 4.24). Results in Table 4.11 show that the influence of the criterion on the calculated critical load was quite small. Values varied between 1100 and 1400 mol<sub>c</sub> ha<sup>-1</sup> yr<sup>-1</sup> both for coniferous and deciduous forests.

Table 4.11 Average critical acid loads for Dutch forest ecosystems for three acidity leaching criteria

Criterion	Forest type	Critical acid load ( $\text{mol}_c \text{ ha}^{-1} \text{ yr}^{-1}$ )						
		$\text{BC}_{dd}^*$	$\text{BC}_{wo}$	$\text{BC}_{up}$	$\text{N}_{up}$	$\text{H}_{le}(\text{crit})$	$\text{Al}_{le}(\text{crit})$	Total
Al concentration	Coniferous	300	200	300	300	200	400	1100
	Deciduous	150	200	350	500	300	600	1400
Al/Ca ratio	Coniferous	300	200	300	300	200	600	1400
	Deciduous	150	200	350	500	300	300	1100
Al depletion	Coniferous	300	200	300	300	200	500	1200
	Deciduous	150	200	350	500	300	500	1300

## Ground water

Acidification of ground water is a serious problem below forest soils in the Netherlands especially in areas with sensitive, shallow aquifers with high permeability (Appelo, 1982; Mulder et al., 1990; Boumans and Van Grinsven, 1991). Acidic ground water affected by anthropogenic acidification shows a decreased pH and increased concentration of Al harmful to health, which may finally appear in drinking water.

As with forests soils, a long term critical load to protect the quality of phreatic ground water below forest soils, used in private wells, was assessed by using Eq. (4.24). Data used for the dry deposition and uptake of base cations and for N uptake were equal to those given before for forests (cf Table 4.11). The average areal weathering rate for the unsaturated zone depends on its thickness. A weathering rate of  $400 \text{ mol}_c \text{ ha}^{-1} \text{ yr}^{-1}$  was used. This was based on an average depth to ground water of 2 m (Steur et al., 1985) and an average weathering rate in the unsaturated zone of  $200 \text{ mol}_c \text{ ha}^{-1} \text{ yr}^{-1} \text{ m}^{-1}$  (cf Table 4.9).

The critical acidity for ground water is quite different from that for forest. Relating the criteria to drinking water quality, the Al concentration should be lower than  $0.02 \text{ mol}_c \text{ m}^{-3}$ , whereas the pH should preferably be above 6.0 (cf Table 4.8). This implies that the acidity value should even be negative (positive alkalinity) due to the availability of  $\text{HCO}_3^-$  in this pH range. The  $\text{HCO}_3^-$  concentration can be derived from Eq. (4.27). Taking  $\log K_{\text{CO}_2}$  at -7.8 and assuming an average  $p\text{CO}_2$  of 10 mbar leads to a critical acidity of  $-0.14 \text{ mol}_c \text{ m}^{-3}$ . A similar value was given by Sverdrup et al (1990). Multiplying this value by the precipitation excess leads to a critical acidity leaching of approximately  $-200 \text{ mol}_c \text{ ha}^{-1} \text{ yr}^{-1}$  below coniferous forests and  $-400 \text{ mol}_c \text{ ha}^{-1} \text{ yr}^{-1}$  below deciduous forests. This leads to critical loads varying between 300 and  $500 \text{ mol}_c \text{ ha}^{-1} \text{ yr}^{-1}$  for phreatic ground water below deciduous and coniferous forests.

An overview of the average critical acid loads derived, including the input data used is given in Table 4.12. Critical acid loads for deep ground water extracted for public water supply are relevant for sandy sediments which have been decalcified to a large depth,

such as the endmoraines of the 'Veluwe' area in the Netherlands. The values given above could be used as a worst case option for deep ground water by neglecting weathering in the saturated zone. However, this is clearly an underestimate.

An indication of the weathering rate in the saturated zone can be derived from the amount of the Al hydroxides in the sandy sediments and the time period since the start of the holocene. This is based on the assumption that Al hydroxides (secondary minerals) have been formed due to weathering of Al from silicates (primary minerals), which in turn is related to base cation weathering from silicates. Using an average value of  $60 \text{ mol}_c \text{ kg}^{-1}$  for the content of Al hydroxides in sandy sediments (data from the Netherlands Soil Information System), an average bulk density of  $1600 \text{ kg m}^{-3}$ , a time period since the start of the weathering of 10 000 yr and a stoichiometric ratio of Al to BC weathering of 2.5 leads to a base cation weathering rate near  $40 \text{ mol}_c \text{ ha}^{-1} \text{ yr}^{-1} \text{ m}^{-1}$ . This is only 20% of the value derived before for the rootzone of non-calcareous sandy soils (cf Table 4.12). Most likely, this is due to the higher pH values in the saturated zone compared to the rootzone. In the Netherlands, ground water used for public water supply is, extracted at an average depth of about 32 m (Heij, pers. comm.). This implies a weathering rate of  $1200 \text{ mol}_c \text{ ha}^{-1} \text{ yr}^{-1}$  in the saturated zone and a critical acid load of about  $1600 \text{ mol}_c \text{ ha}^{-1} \text{ yr}^{-1}$ .

Table 4.12 Average critical acid loads for phreatic ground water below forests

Forest	Critical acid load ( $\text{mol}_c \text{ ha}^{-1} \text{ yr}^{-1}$ )					Total
	$\text{BC}_{\text{dd}}^*$	$\text{BC}_{\text{wo}}$	$\text{BC}_{\text{up}}$	$N_{\text{up}}$	$\text{Ac}_{\text{ia}}(\text{crit})$	
Coniferous	300	400	300	300	200	500
Deciduous	150	400	350	500	400	300

## Surface water

In the Netherlands, acidification of surface water has become an increasing environmental problem. Particularly the small shallow heathland pools with originally sandy sediments, characteristic for the pleistocene regions in the middle, eastern and southern part of the country, have been acidified recently. During the last few decades, acidification has been observed in at least 55% of these waters (Leuven et al., 1986; Arts, 1988). This acidification (and eutrophication) is accompanied by a strong decline in species diversity (Roelofs, 1983; Arts, 1988). The effects of acid deposition on surface water chemistry are similar to ground water, i.e. decreases in pH and acidity and increases in the concentrations of  $\text{SO}_4$ ,  $\text{NO}_3$ , base cations, and Al. Potential deleterious impacts include loss of fish populations and other aquatic biota, and changes in species diversity of macrophytes and phytoplankton.

In-lake alkalinity generation is the only neutralizing mechanism of the poorly buffered pools and lakes in the Netherlands, since these shallow aquatic systems are hydrologically isolated. In this respect,  $\text{NO}_3$  and  $\text{SO}_4$  reduction and N retention in lake sediments are the processes of potentially greatest importance (Schindler, 1986; Schuurkes et al., 1988). Shaffer et al. (1988) give data on in-lake acidity generation for 20 watersheds in Europe and North America varying between 200 and 2400  $\text{mol}_c \text{ ha}^{-1} \text{ yr}^{-1}$  with an average value of 900  $\text{mol}_c \text{ ha}^{-1} \text{ yr}^{-1}$ . However, this refers to alkaline waters with an organic layer. In Dutch shallow poorly-buffered pools these processes will be limited by the very low organic matter contents and the oxic state of the mineral sandy sediments (Schuurkes et al., 1987). Base cation weathering and N uptake by macrophytes and algae is also very low in this type of sediment. From these considerations, it can be deduced that the critical acid load for surface waters will be low. This is confirmed by empirical data from Schuurkes et al. (1987), who treated small-scale soft water systems in a greenhouse with water containing sulphuric acid. The critical acid load appeared to be as low as 250 to 400  $\text{mol}_c \text{ ha}^{-1} \text{ yr}^{-1}$ , which is much lower than the critical N load of 1400  $\text{mol}_c \text{ ha}^{-1} \text{ yr}^{-1}$  for surface waters (cf Section 4.1). This result agreed well with recent historical data on acidification of soft water systems in the Netherlands (Arts, 1988).

Although the critical load given above is low, it is of a similar order of magnitude as various estimates derived for sensitive lakes in Canada, USA and Scandinavia (Table 4.13), even though these lakes are generally not hydrologically isolated and the acid input is also neutralized by alkalinity production within the catchment.

Table 4.13 Estimated average critical acid loads for sensitive surface waters in the Netherlands, Scandinavia, Switzerland, Canada and the USA<sup>1)</sup>

Critical load ( $\text{mol}_c \text{ ha}^{-1} \text{ yr}^{-1}$ )	Country	Reference
350	The Netherlands	Schuurkes et al. (1987)
150	Sweden	Dickson (1986)
400	- shallow soils - glacial till	
400	Norway	
400	- precipitation 2000 mm	Henriksen et al. (1986),
200	- precipitation 1000 mm	Henriksen and Brakke (1988)
350	Switzerland	Schnoor and Stumm (1987)
340	Eastern U.S.A.	Henriksen and Brakke (1988)
600	- Adirondacks, New York	
350	- Catskills/Poconos	
570	- Southern New England	
380	- Central New England	
620	- Maine	
200	- Northwestern Minnesota	
310	- Upper Peninsula of Michigan	
750	- Upper Great Lakes area	
	White Oak, Run,	Wright et al. (1988)
		Virginia, USA

<sup>1)</sup> Applies to catchments where base cation weathering rates are very low



Critical acid loads do not vary significantly and generally fall within the range of 150 to 500 mol<sub>c</sub> ha<sup>-1</sup> yr<sup>-1</sup>. The estimates in Table 4.13 were generally based on an empirical method relating the sensitivity to depositions of Ca and Mg (neutralizing the S input) and to concentrations of Ca and Mg in surface water, which reflects the acid neutralization in the catchment by weathering and cation exchange (Henriksen and Brakke, 1988). Furthermore, critical loads were also based on results from process-oriented dynamic models (Dickson, 1986; Wright et al., 1988). Most of the estimates aim at keeping the pH above 5.3 (cf Table 4.8) in the most sensitive lakes in the areas.

Note that the critical loads in Table 4.13 are all related to S only, since NO<sub>3</sub> is not yet a problem in most countries, although the concentrations have markedly increased in many surface waters during the last decade. In a survey of 1000 lakes in Norway, the NO<sub>3</sub> concentrations had almost doubled in the lakes receiving the highest deposition (Henriksen, 1988).

## DISCUSSION AND CONCLUSIONS

### **Uncertainties in critical load derivations**

The uncertainty in the average critical load values derived before can be large and is mainly determined by the uncertainty in critical chemical values set for the receptor, calculation methods and data.

#### *Critical chemical values*

Uncertainties in critical chemical values for a given receptor partly reflect our lack of knowledge regarding the effect of acid deposition and are partly due to a natural range in sensitivity. This uncertainty can be very large, especially for critical acid loads on forests (soils) since the range in Al toxicity appears to be very large for different tree species. A change in critical Al concentration directly influences the critical load by the critical acidity leaching term. Apart from the values used for the critical Al concentration and Al/Ca ratio, average annual values, as used in the steady-state model (Eq. 4.24), may be less relevant. According to Ulrich (1981b, 1983a), the toxic effect of Al is mainly due to acidification pushes occurring in spring (and summer) because of mineralization and nitrification. For ground water and surface water the uncertainty in acceptable acidity leaching is less, since the range of critical chemical levels for alkalinity is lower.

#### *Calculation methods*

Uncertainties in the calculation methods relate to the assumptions that have been made to simplify the "real world" such as aggregated process descriptions and temporal and spatial aggregation within the model. Unlike the uncertainty in critical chemical values and data, it is difficult to quantify the uncertainty due to modeling assumptions. In this

context, it is important to note that the use of a one layer model will most likely cause an underprediction of critical acid loads. The annual average water flux at 30 cm depth is higher than the precipitation excess, thus affecting the critical acidity leaching (cf Section 5.2; De Vries et al., 1994d).

### Data

Uncertainties in data are due to lack of knowledge, including measurement errors, and spatial variability. The values that have been used for deposition, weathering, uptake and precipitation excess are (long term) averages. The uncertainty for the critical load at a specific location may be in the order of 50% due to spatial variability in these data. Especially for deep ground water, the uncertainty in critical acid loads can be substantial due to uncertainties about the occurrence and rate of denitrification and weathering in the saturated zone.

### Critical loads and target loads

An overview of the critical acid loads derived in the previous sections is given in Table 4.14. Comparison of the critical acid loads with the critical N loads given in Section 4.1 (Table 4.7) shows that critical acid loads are generally more stringent than critical N loads. This applies especially to shallow ground water (drinking water) and surface water since the allowable Al concentrations in water are very small. Terrestrial vegetations can stand higher Al concentration than fish and aquatic vegetations.

The aforementioned critical loads formed the basis for the assessment of target loads used in the Dutch acidification policy. The level at which all detrimental effects are prevented (a critical acid load of  $400 \text{ mol}_c \text{ ha}^{-1} \text{ yr}^{-1}$ ) require such extreme emission reductions (> 90%) in the Netherlands and in Europe, that it will not be possible to approach this level. For this reason another guiding principle of environmental policy in the Netherlands influenced the target loads, i.e. the attainment of sustainable development. This stands for development that meets the needs of the present without compromising the ability of future generations to meet their own needs. With regard to

Table 4.14 Average critical acid loads for terrestrial and aquatic ecosystems in the Netherlands

Effects	Criteria	Unit	Critical acid loads ( $\text{mol}_c \text{ ha}^{-1} \text{ yr}^{-1}$ )		
			Coniferous forests	Deciduous forests	Surface waters
Root damage	Al < 0.2	$\text{mol}_c \text{ m}^{-3}$	1100	1400	
	Al/Ca < 1.0	$\text{mol mol}^{-1}$	1400	1100	
Al depletion	$\Delta\text{Al}(\text{OH})_3=0$		1200	1300	
Al leaching	Al < 0.02	$\text{mol}_c \text{ m}^{-3}$	500 <sup>1)</sup>	300 <sup>1)</sup>	
Fish dieback	Al < 0.003	$\text{mol}_c \text{ m}^{-3}$			400

<sup>1)</sup> This refers to phreatic ground water. For ground water used for the preparation of drinking water, a critical acid load of  $1600 \text{ mol}_c \text{ ha}^{-1} \text{ yr}^{-1}$  can be used

acidification policy this principle has been translated into the attainment of environmental quality such that important terrestrial ecosystems (forests and heathlands) can survive without drastic measures and ground water satisfies the standards for the preparation of drinking water. To achieve these objectives, a target acid load of  $1400 \text{ mol}_e \text{ ha}^{-1} \text{ yr}^{-1}$  has been set for the year 2010. At this level, nearly all effects on terrestrial ecosystems are prevented or considerably decreased. However, increased Al concentrations in phreatic ground water and surface waters (heathland pools) will not be prevented (cf Table 4.14). To ensure that the target load of  $1400 \text{ mol}_e \text{ ha}^{-1} \text{ yr}^{-1}$  will be realized, a time path containing interim targets for the years 1994 and 2000 has been set as shown in Table 4.15.

*Table 4.15 Actual situation and objectives of the Netherlands acidification abatement policy*

	Year	Acid deposition ( $\text{mol}_e \text{ ha}^{-1} \text{ yr}^{-1}$ )
Actual situation	1980	6800
	1988	4800
Target values	1994	4000
	2000	2400
	2010	1400

The target loads presented in Table 4.15 provided the basis for the development and adoption of the Netherlands' 'Acidification abatement policy'. The Dutch government presented this policy in 1989 in National Environmental Policy Plan (NEPP)<sup>\*</sup> elaborated it more fully in the Netherlands Acidification Abatement Plan<sup>\*\*</sup> during the same year and updated the measures in the so called NEPP-plus<sup>\*\*\*</sup>. To attain the target loads presented in Table 4.15, objectives for emission reductions were formulated for the Netherlands as given in Table 4.16. The Acidification Abatement Plan presented packages of measures with which these emission reductions can be attained.

*Table 4.16 Objectives for the reduction of emissions in the Netherlands using 1980 emission data*

Year	Reduction (%)		
	$\text{NH}_3$	$\text{NO}_x$	$\text{SO}_2$
1994	30	20	60
2000	70	50	80
2010	80-90	80-90	80-90

\* *Parliamentary Documents II, 1988/89, 21137, nrs. 1-2, issued to Dutch Parliament May 25th, 1989*

\*\* *Parliamentary Documents II, 1988/89, 18225, nr. 31, issued to Dutch Parliament July 20th, 1989*

\*\*\* *Parliamentary Documents II, 1989/90, 21137, nr. 20, issued to Dutch Parliament June 14th, 1990*

Average critical loads, as derived in this Chapter, have played a major role in the acidification abatement policy of the Netherlands. A logical follow-up is the derivation of critical load maps. The derivation of such maps for Europe and for the Netherlands is reported in the next Chapter. These maps may form an important basis for an international strategy for the abatement of acidifying substances.

# **Chapter 5**

## **REGIONAL VARIABILITY IN CRITICAL LOADS FOR FORESTS**

### **5.1 CRITICAL LOADS AND THEIR EXCEEDANCE ON FORESTS IN EUROPE**

- INTRODUCTION
- THE MODEL START
- APPLICATION METHODOLOGY AND INPUT DATA
- RESULTS
- UNCERTAINTIES
- CONCLUSIONS

### **5.2 CRITICAL LOADS AND THEIR EXCEEDANCE ON FORESTS IN THE NETHERLANDS**

- INTRODUCTION
- THE MODEL MACAL
- APPLICATION METHODOLOGY AND INPUT DATA
- RESULTS
- UNCERTAINTIES
- CONCLUSIONS

Section 5.1 is a slightly revised version of:

W. de Vries, G.J. Reinds and M. Posch, 1994. *Assessment of critical loads and their exceedance on European forests using a one-layer steady-state model*. Water Air and Soil Pollution 72: 357-394.

Section 5.2 is a slightly revised version of:

W. de Vries, G.J. Reinds and M. Posch, 1994. *Assessment of critical loads and their exceedance on Dutch forests using a multi-layer steady-state model*. Water Air and Soil Pollution 76 (in press).

## 5.1 CRITICAL LOADS AND THEIR EXCEEDANCE ON FORESTS IN EUROPE

### ABSTRACT

*Critical loads for N, S and total acidity, and amounts by which they are exceeded by present atmospheric loads, were derived for coniferous and deciduous forests in Europe using the one-layer steady-state model START. Results indicated that present acid loads exceed critical values in approximately 45% of the forested area, i.e. 52% of all coniferous forests and 33% of all deciduous forests. The area where critical loads are exceeded was nearly equal for N (50%) and S (52%). However, the maximum exceedances were much higher for S (up to 12000 mol<sub>c</sub> ha<sup>-1</sup> yr<sup>-1</sup> in former Czechoslovakia, Poland and Germany) than for N (up to 3500 mol<sub>c</sub> ha<sup>-1</sup> yr<sup>-1</sup> in the Netherlands, Belgium and Germany). Furthermore, the critical N loads derived refer to the risk of increased vegetation changes. Higher values, i.e. lower exceedances, were found for N when it was related to an increased risk in forest vitality decline. The uncertainty in the area where critical loads are exceeded was estimated to be about ± 50% of the given value. This is mainly due to uncertainties in the chemical criteria that have been used. However, despite the uncertainties involved it is clear that large exceedances in critical N and S loads occur in Western and Central Europe. This coincides with the area where a decline in forest vitality has been reported.*

### INTRODUCTION

The vitality of forests in Europe has become a subject of wide public and political discussion since the beginning of the eighties due to the extensive forest damage observed in rural areas of Central Europe (Schütt et al., 1983; Lammel, 1984). Since that time, forest vitality characteristics, i.e. needle loss and needle discoloration, are monitored throughout the whole of Europe. Acid deposition affects the vitality of forest ecosystems both by direct effects on the forest canopy and by indirect soil mediated effects on the roots. A recent literature review by Roberts et al. (1989) suggests that direct effects of gaseous air pollutants, such as SO<sub>x</sub>, NO<sub>x</sub> and O<sub>3</sub>, play only a minor role in the declining vitality of forests in Europe. The indirect effects caused by soil acidification and N accumulation are likely to be more important. They concluded that spruce decline in Central Europe mainly results from foliar Mg deficiency. This deficiency is likely to be due to (i) an increased Mg demand due to faster tree growth caused by an increased N input and (ii) a decreased Mg uptake due to damage to roots and mycorrhizae, caused by the mobilization of Al in the soil in response to S and N inputs. Still, the relationship between forest vitality and air pollution is not clear due to a large number of natural stress factors such as unsuitable soil conditions, seasalt deposition, drought, frost, pests and fungal diseases. However, numerous studies, both in the laboratory and in the field, have shown that nutrient imbalances resulting from high concentrations of Al and N (NH<sub>4</sub>) as compared to (divalent) base cations (BC) such as Ca and Mg, have a negative influence on root elongation and root uptake (cf Sverdrup et al., 1990; Heij et al., 1991 and De Vries, 1991 for summarizing overviews). Such unfavourable conditions (sometimes called predisposing stress) do increase the

vulnerability of forest stands to frost and drought and to insect and pathogen damage (sometimes called triggering stress).

Information on critical deposition levels (loads) for N and S are a prerequisite for political decisions on emission reductions. An overview of average critical loads on forests, based on critical values for the Al concentration and Al/BC ratio, is given in De Vries and Gregor (1991). To gain more insight in the magnitude and the spatial variation in critical loads, the Working Group on Effects of the UN-ECE Executive Body on Long Range Transboundary Air Pollution has installed a Task Force on Mapping. This Task Force is assisted by a Co-ordination Centre on Effects (CCE). The Task Force and the Co-ordination Centre have produced a Manual on Mapping Critical Loads (Sverdrup et al., 1990) and a Mapping Vademecum (Hettelingh and De Vries, 1992) respectively, containing guidelines for the preparation of critical load maps. At present, such maps have been produced by most European countries and results are summarized in Hettelingh et al. (1991). The maps cannot be compared directly since they are based on different receptors (surface waters and forest soils), methods (qualitative and quantitative) and criteria used by different countries (cf De Vries et al., 1991).

This section provides an overview of the variation in critical loads for European forest soils and the amounts by which they are exceeded. The multi-stress theory (e.g. Heij et al, 1991) described above implies that critical loads for N, S and acidity on forests can not be derived in an empirical way. Consequently, in this study critical loads were derived indirectly from critical values for  $\text{NO}_3$  and Al concentrations and Al/BC ratios in soil water, which are important indicators for eutrophication and acidification, using the one-layer steady-state model START, provided with a uniform set of criteria and input data. Attention is also given to the effect of the uncertainty in criteria, modeling assumptions and data on the results. The criteria that were used to calculate critical loads are summarized in Table 5.1 (cf Table 4.1 and 4.8).

Critical values for the Al concentrations and Al/BC ratios were based on effects influencing the forest vitality, such as decreased mycorrhizal frequency, root damage and inhibited nutrient uptake. The critical  $\text{NO}_3$  concentration was related to effects on the forest vegetation (cf Chapter 4).

*Table 5.1 Critical chemical values that were used to calculate critical loads for acidity and nitrogen in Europe*

Critical load	Criterion	Unit	Value
Acidity <sup>1)</sup>	Al concentration	$\text{mol}_e \text{ m}^{-3}$	0.2
	Al/BC ratio	$\text{mol mol}^{-1}$	1.0
Nitrogen	$\text{NO}_3$ concentration	$\text{mol}_e \text{ m}^{-3}$	0.1

<sup>1)</sup> Critical loads were calculated by using the minimum of two criteria



## THE MODEL START

### Modelling approach

START is the steady-state version of the model SMART (Simulation Model for Acidification's Regional Trends) described in Section 6.1 (De Vries et al., 1989b). It calculates the soil solution concentration at the bottom of the rootzone at equilibrium for a given deposition rate. The rooting zone is represented as one homogeneous compartment. The model is based on the assumption that dynamic processes such as cation exchange, adsorption/desorption of  $\text{SO}_4$  and  $\text{NH}_4$  and mineralization/-immobilization dynamics of N, S and BC are unimportant for the assessment of a long-term critical load. Further assumptions in START are: (i) negligible N fixation and (ii) negligible net uptake, reduction and precipitation of  $\text{SO}_4$ . A justification for these assumptions is given in Chapter 4 (cf De Vries, 1991a; 1993). The reason for using such a relatively simple model is because of the general lack of input data for the application of relatively complex multi-layer models on a European scale. A more thorough discussion on the aspect of model complexity versus regional applicability is given in Chapter 1 (cf De Vries, 1990).

### Basic process formulations

The governing equation in START is a charge balance equation:

$$[\text{H}] + [\text{Al}] + [\text{BC}^+] + [\text{NH}_4] = [\text{NO}_3] + [\text{SO}_4] + [\text{HCO}_3] \quad (5.1)$$

where [ ] denotes the concentration in the soil solution in  $\text{mol}_c \text{ m}^{-3}$ .  $[\text{Al}]$  is the inorganic Al concentration which is assumed to equal the total Al concentration minus the concentration of organic anions,  $\text{RCOO}$ , (consequently  $\text{RCOO}$  is neglected) and  $[\text{BC}^+]$  is the Cl-corrected BC concentration ( $\text{Ca}+\text{Mg}+\text{K}+\text{Na}-\text{Cl}$ ) which is assumed to be equal to  $\text{Ca}+\text{Mg}$ .

For  $X = \text{SO}_4, \text{BC}^+, \text{NH}_4$  and  $\text{NO}_3$ , the concentration is calculated according to:

$$[\text{X}] = (\text{X}_{td} + \text{X}_{int}) / \text{PE} \quad (5.2)$$

where  $\text{X}_{td}$  is the total deposition flux of ion X to the soil and  $\text{X}_{int}$  is the sum of all interaction fluxes for ion X in the soil (both in  $\text{mol}_c \text{ ha}^{-1} \text{ yr}^{-1}$ ) and where  $\text{PE}$  is the precipitation excess (the amount of soil water draining from the rootzone), i.e. precipitation minus actual evapotranspiration ( $\text{m}^3 \text{ ha}^{-1} \text{ yr}^{-1}$ ). The sum of the total deposition flux and the interaction fluxes is equal to the leaching flux of ion X. Direct surface runoff has been neglected. This may cause an underestimate of the precipitation excess in areas with steep slopes.

The Al concentration and  $\text{HCO}_3^-$  concentration are both computed from an equilibrium with  $[\text{H}^+]$  according to:

$$[\text{Al}] = K_{\text{Al}_{\text{ox}}} \cdot [\text{H}^+]^3 \quad (5.3)$$

$$[\text{HCO}_3^-] = K_{\text{CO}_2} \cdot p_{\text{CO}_2} / [\text{H}^+] \quad (5.4)$$

where  $K_{\text{Al}_{\text{ox}}}$  is the equilibrium constant for Al hydroxide dissolution ( $\text{mol}^{-2} \text{l}^2$ ),  $K_{\text{CO}_2}$  is the product of the first dissociation constant of  $\text{H}_2\text{CO}_3$  and Henry's law constant for the equilibrium between  $\text{CO}_2$  in soil water and soil air ( $\text{mol}^2 \text{l}^{-2} \text{bar}^{-1}$ ) and  $p_{\text{CO}_2}$  is the partial  $\text{CO}_2$  pressure (bar). For given values of  $X_{\text{int}}$ , combination of Eqs. (5.1) to (5.4) gives one unknown,  $[\text{H}^+]$ , which is solved by an iterative procedure (Brent's method described in Press et al., 1986).

### Description of interaction fluxes

A description of interaction fluxes for  $\text{BC}^+$ ,  $\text{NH}_4$  and  $\text{NO}_3^-$  (for  $\text{SO}_4$  the interaction flux equals zero) in START is given in Table 5.2. Apart from growth uptake, which affects all ions,  $\text{BC}^+$  fluxes are influenced by weathering, whereas interaction of N compounds

Table 5.2 Description of interaction fluxes in the START model<sup>1)</sup>

$$\text{BC}_{\text{int}}^+ = \text{BC}_{\text{we}} - \text{BC}_{\text{gu}} \quad (5.5)$$

$$\text{NH}_{4,\text{int}} = -\text{NH}_{4,\text{gu}} - \text{NH}_{4,\text{ni}} - \text{NH}_{4,\text{im}}(\text{crit}) \quad (5.6)$$

$$\text{NO}_{3,\text{int}} = -\text{NO}_{3,\text{gu}} + \text{NH}_{4,\text{ni}} - \text{NO}_{3,\text{im}}(\text{crit}) - \text{NO}_{3,\text{de}} \quad (5.7)$$

$$\text{NH}_{4,\text{gu}} = N_{\text{gu}} \cdot \text{NH}_{4,\text{td}} / N_{\text{td}} \quad (5.8)$$

$$\text{NO}_{3,\text{gu}} = N_{\text{gu}} \cdot \text{NO}_{3,\text{td}} / N_{\text{td}} \quad (5.9)$$

$$\text{NH}_{4,\text{ni}} = fr_{\text{ni}} \cdot (\text{NH}_{4,\text{td}} - \text{NH}_{4,\text{gu}} - \text{NH}_{4,\text{im}}(\text{crit})) \quad (5.10)$$

$$\text{NO}_{3,\text{de}} = fr_{\text{de}} \cdot (\text{NO}_{3,\text{td}} + \text{NH}_{4,\text{ni}} - \text{NO}_{3,\text{gu}} - \text{NO}_{3,\text{im}}(\text{crit})) \quad (5.11)$$

$$\text{NH}_{4,\text{im}}(\text{crit}) = N_{\text{im}}(\text{crit}) \cdot \text{NH}_{4,\text{td}} / N_{\text{td}} \quad (5.12)$$

$$\text{NO}_{3,\text{im}}(\text{crit}) = N_{\text{im}}(\text{crit}) \cdot \text{NO}_{3,\text{td}} / N_{\text{td}} \quad (5.13)$$

<sup>1)</sup> The subscript *int* stands for interaction, *we* for weathering, *gu* for growth uptake (net uptake needed for forest growth), *ni* for nitrification, *de* for denitrification, *im(crit)* for the critical steady-state immobilization rate, *td* for total deposition, and *fr<sub>ni</sub>* and *fr<sub>de</sub>* are dimensionless nitrification and denitrification fractions, respectively

<sup>2)</sup> N equals  $\text{NH}_4 + \text{NO}_3$

includes nitrification, denitrification and immobilization (cf Eq. 5.5 - 5.7). The preference of  $\text{NH}_4$  over  $\text{NO}_3$  uptake is implicitly accounted for in START since the effect of nitrification on the  $\text{NH}_4$  availability is not included in the uptake calculations (cf Eq. 5.8 and 5.9). Nitrification and denitrification are described in START as a fraction of the net  $\text{NH}_4$  input and  $\text{NO}_3$  input, respectively, i.e. after uptake and immobilization have taken place (cf Eqs. 5.10 and 5.11). This implies that, N transformations do not affect the uptake and immobilization rate of N. N transformations are assumed to occur deeper in the soil profile than uptake and immobilization that mainly occur at the soil surface or even above the soil (foliar uptake).

In START, the leaching fluxes of the various ions, i.e. the sum of the total deposition flux and the interaction fluxes, are directly calculated according to (De Vries, 1991):

$$\text{SO}_{4,le} = \text{SO}_{4,td} \quad (5.14)$$

$$\text{BC}_{le} = \text{BC}_{td}^* + \text{BC}_{we} - \text{BC}_{gu} \quad (5.15)$$

$$\text{NH}_{4,le} = (1 - fr_{ni}) \cdot \text{NH}_{4,td} \cdot \left( \frac{N_{td} - N_{gu} - N_{im}(\text{crit})}{N_{td}} \right) \quad (5.16)$$

$$\text{NO}_{3,le} = (1 - fr_{de}) \cdot (\text{NO}_{3,td} + fr_{ni} \cdot \text{NH}_{4,td}) \cdot \left( \frac{N_{td} - N_{gu} - N_{im}(\text{crit})}{N_{td}} \right) \quad (5.17)$$

where the subscript *le* stands for leaching.

### Calculation of critical acid loads

Acid loads, or loads of potential acidity, were defined as the sum of S and N loads that are not counteracted by seasalt corrected base cation loads (cf Section 4.2). Critical acid loads were derived with START by substituting a critical Al concentration in the charge balance equation (Eq. 5.1). This equation can thus be rewritten as:

$$([\text{SO}_4] + [\text{NO}_3] - [\text{NH}_4])(\text{crit}) = [\text{BC}^+] + [\text{Ac}](\text{crit}) \quad (5.18)$$

where  $[\text{Ac}](\text{crit})$  stands for the critical acidity concentration ( $\text{mol}_e \text{ m}^{-3}$ ) which is defined as (cf Section 4.2; Eq 4.26):

$$[\text{Ac}](\text{crit}) = ([\text{Al}] + [\text{H}] - [\text{HCO}_3])(\text{crit}) \quad (5.19)$$

The concentrations of  $\text{SO}_4$ ,  $\text{NO}_3$ ,  $\text{NH}_4$  and  $\text{BC}^+$  are determined by Eq. (5.2) together with the equations describing the leaching fluxes (Eq. 5.14 - 5.17). The value of  $[\text{Al}]_i(\text{crit})$  determines the critical H and  $\text{HCO}_3$  concentration according to Eqs. (5.3) and (5.4). The critical inorganic Al concentration is calculated as the minimum of two values: one

assigned directly and one indirectly through a critical equivalent Al/BC ratio,  $RA/BC(\text{crit})$ , according to (cf Table 5.1 for the values used):

$$[Al](\text{crit}) = RA/BC(\text{crit}) \cdot [BC] \quad (5.20)$$

There is also the possibility to calculate the critical Al concentration indirectly from the requirement that depletion of Al hydroxides is negligible in order to avoid very low pH values (Section 4.2; Eq. 4.32). However, this criterion was not used in this study since there is no direct link with this phenomenon and effects on forest vitality.

When nitrification in the rooting zone is not complete, a critical acid load cannot be calculated directly because N transformation processes are a function of the N deposition (cf Eqs. 5.10 and 5.11). The unknown values in the combined set of equations (Eqs. 5.2 - 5.4 and 5.14 - 5.20) are the deposition of  $NH_4$ ,  $NO_3$  and  $SO_4$  at critical load. In order to obtain these three values it is assumed that the ratios of  $NH_4$  and of  $NO_3$  to total N and the ratio of N to S at critical load are equal to the present ratios. This leads to one equation with one unknown, i.e. the critical acid load, which is solved iteratively. It should be realized that the critical acid load thus calculated, changes when the ratio of S to N deposition changes, because of changes in the nitrification and denitrification rate.

When nitrification is assumed to be complete, a direct solution is possible since the  $NH_4$  concentration becomes zero. Multiplying Eq. (5.18) with the precipitation excess,  $PE$ , gives

$$(SO_{4,le} + NO_{3,le} - NH_{4,le})(\text{crit}) = BC_{le}^* + Ac_{le}(\text{crit}) \quad (5.21)$$

Combining Eq. (5.21) with Eqs. (5.14) - (5.17), with  $fr_{ni} = 1$ , gives the critical load for S and N,  $(S_{td} + N_{td})(\text{crit})$ :

$$(S_{td} + N_{td})(\text{crit}) = BC_{td}^* + BC_{we} - BC_{gu} + N_{gu} + N_{im}(\text{crit}) + N_{de}(\text{crit}) + Ac_{le}(\text{crit}) \quad (5.22)$$

where  $N_{de}(\text{crit})$  is the denitrification rate at critical load, which is described as (cf Eq. 5.10 and 5.11 with  $fr_n=1$ ):

$$N_{de}(\text{crit}) = fr_{de} \cdot (N_{td}(\text{crit}) - N_{gu} - N_{im}(\text{crit})) \quad (5.23)$$

where  $N_{td}(\text{crit})$  is the critical N load. A critical load for S and N is thus derived by requiring that it does not exceed the net input of base cations ( $BC_{td}^* + BC_{we} - BC_{gu}$ ) plus the net uptake, reduction and critical immobilization of N plus a critical leaching rate of acidity. The excess deposition of base cations not counteracted by chloride ( $BC_{td}^*$ ) is subtracted from the S and N deposition ( $S_{td} + N_{td}$ ) to calculate a critical acid load,  $Ac_{le}(\text{crit})$ :

$$Ac_{td}(\text{crit}) = BC_{we} - BC_{gu} + N_{gu} + N_{im}(\text{crit}) + N_{de}(\text{crit}) + Ac_{le}(\text{crit}) \quad (5.24)$$

This so called steady-state mass balance (SMB) model (cf Section 4.2; Eq. 4.23) has been widely used to calculate critical acid loads for forest soils in Europe on the basis of critical values for the Al concentration and/or Al/BC ratio (Hettelingh et al., 1991).

### The relation between critical loads for nitrogen, sulphur and total acidity

Independent from acidification, an upper limit is set on the N deposition by the eutrophication aspect according to (Schulze et al., 1989; De Vries, 1993):

$$N_{td}(\text{crit}) = N_{gu} + N_{im}(\text{crit}) + N_{de}(\text{crit}) + NO_{3,le}(\text{crit}) \quad (5.25)$$

where  $NO_{3,le}(\text{crit})$  is a critical level of  $NO_3$ -N leaching related to eutrophication (vegetation changes). The model is based on the assumption that any N input above net N uptake by forest growth, denitrification and a critical rate of N immobilization and  $NO_3$ -N leaching will finally lead to unacceptable high N contents in soil organic matter, thus causing vegetation changes in forests. Furthermore, the model assumes that nitrification is complete within the rooting zone.

Combination of Eqs. (5.23) and (5.25) yields (cf Section 4.1; Eq. 4.4):

$$N_{td}(\text{crit}) = N_{gu} + N_{im}(\text{crit}) + \frac{fr_{de}}{1 - fr_{de}} \cdot NO_{3,le}(\text{crit}) + NO_{3,le}(\text{crit}) \quad (5.26)$$

The denitrification flux at critical load in Eq (5.23) is defined in Eq. (5.26) by the critical  $NO_3$ -N leaching level and a denitrification fraction. For high values of  $fr_{de}$ , the critical N load can become higher than the present N load. In that situation a potential denitrification rate is calculated. In systems with complete denitrification ( $fr_{de}=1$ ) the critical N load thus becomes infinite since potential denitrification is infinite. As with alkalinity leaching, the critical  $NO_3$  leaching level is determined by the precipitation excess and a critical  $NO_3$  concentration (cf Table 5.1 for the value used).

A critical S load was calculated by combining the Eqs. (5.22) and (5.25) according to:

$$S_{td}(\text{crit}) = BC_{td}^* + BC_{we} - BC_{gu} + Ac_{le}(\text{crit}) - NO_{3,le}(\text{crit}) \quad (5.27)$$

As with the critical acid load, the value of  $BC_{td}^*$  can also be subtracted from the S deposition to obtain the acidifying part of it. However, Eq. (5.27) was used to derive critical S loads as these values can be compared directly with S deposition (scenarios).

## APPLICATION METHODOLOGY AND INPUT DATA

### Application methodology

To limit the number of calculations with START, areas were defined in which the deposition was assumed to be reasonably constant (deposition areas). Within these areas, critical loads were calculated for all major combinations of tree species and soil type (receptors). For the deposition areas, a gridcell system of 1.0° longitude x 0.5° latitude was used since reasonable deposition estimates exist at this scale. In this gridcell the length in the south-north direction is 56 km and the width in the east-west direction varies between 38 to 91 km, depending on the latitude (approximately 50 to 60 km in Central Europe). Regarding the receptors, a distinction was made between 2 tree species (coniferous and deciduous trees) and 80 soil types, which were distinguished on the basis of the 1 : 5 000 000 FAO-UNESCO Soil Map of the World (FAO, 1981). The number of mapping units on this map is more than 300. This large number is because the code of a mapping unit contains four items: the dominant soil unit, the associated soil unit, the dominant texture class and the dominant slope class. In this study the associated soil unit was not considered. Texture classes have been defined as: 1 (coarse): clay content less than 18%, 2 (medium): clay content between 18 and 35% and 3 (fine): clay content above 35%. When two texture classes occur within one mapping unit, this is indicated as 1/2, 2/3 or 1/3. Slope classes have been defined as: *a* (even): slope less than 8%, *b* (undulating): slope between 8 and 30% and *c* (steep): slope above 30%. Several slope classes may occur within one mapping unit, and this is indicated as *ab* or *bc*.

The areal distribution of soils was obtained by estimating the fraction of each mapping unit (soil type, texture class and slope class) within each gridcell using the FAO-UNESCO soil map. Gridcells contained one to seven mapping units (the mean number was 2.2). The areal distribution of forests was obtained by estimating the fraction of coniferous and deciduous forests in each gridcell using aeronautic maps. Since the soil and forest information was derived from different sources, the distribution of soil - forest type combinations was not known. To obtain this distribution it has been assumed that forests are mainly located in areas with steep slopes and poor soils (low weathering rates and coarse texture). The area of forest-soil combinations in each gridcell was estimated by the following allocation procedure: (i) forests were first allocated on soils with steep slopes (slope classes *c* and *bc*); (ii) if there was still forest left they were allocated to non-calcareous coarse textured soils followed by peat soils, calcareous coarse textured soils, non-calcareous medium and fine textured soils and finally to calcareous medium and fine textured soils. The total number of forest-soil combinations, i.e. the total number of START calculations, equalled 4670.

In Europe 28.5% of the total land area consists of forests. About 65% are coniferous forests and 35% deciduous forests. Forest percentages in the various countries vary

from less than 1% in Ireland to more than 60% in Finland (cf De Vries et al., 1992a). An overview of the most important forest soils, covering more than 1% of the forested area in Europe, is given in Table 5.3. This Table also gives information on the forest coverage of these soil types assuming that forests are evenly distributed over the soil types, i.e. proportional to their area. The difference between the proportional distribution and the forest allocation described above was very small.

Most forests are located on Podzols (nearly 40%), especially in the Nordic countries, and to a lesser extent on Podzoluvisols and Cambisols (more than 15%) and luvisols (about 10%). The occurrence of forests on all other soil types is less than 15% (cf Table 5.3). Most forest soils are non-calcareous (91.2%). The distribution of these soils over sand (texture class 1 and 1/2), clay (texture class 2, 3 and 2/3) and peat is 58.8%, 27.7% and 3.7%, respectively.

Table 5.3 Dominant forest soils in Europe, as a percentage of the total forest area

Soil type (FAO, 1981)	Area (%)	
	assumed distribution	proportional distribution
Orthic Podzol	33.8	31.4
Eutric Podzoluvisol	12.6	12.7
Dystric Cambisol	9.4	8.6
Eutric Cambisol	6.4	5.8
Gleyic Luvisol	4.9	4.5
Orthic Luvisol	3.6	4.1
Dystric Histosol	3.5	4.5
Dystric Podzoluvisol	3.3	3.6
Calcic Cambisol	2.7	3.1
Rendzina	2.5	2.9
Leptic Podzol	2.2	1.5
Chromic Luvisol	1.4	2.1
Gleyic Podzol	1.2	1.1
Lithosol-Ranker	1.1	0.5
Humic Cambisol	1.1	0.9
	$\Sigma = 89.7$	$\Sigma = 87.3$

### Assessment of Input data

Input data for START are the atmospheric deposition of  $SO_4$ ,  $NO_3$ ,  $NH_4$  and BC, growth uptake of N and BC, BC weathering, N transformation rates, precipitation and evapotranspiration. These data were derived as a function of location and the combination of tree species and soil type as shown in Table 5.4. To obtain the data mentioned in Table 5.4 for all forest ecosystems within all gridcells, we used or derived transfer functions (relationships) with available data on basic land and climate characteristics, such as tree species, soil type, elevation, and temperature.

Table 5.4 Influence of location, tree species and soil type accounted for in the assessment of input data for START<sup>1)</sup>

Data related to	Location	Tree species	Soil type
Atmospheric deposition	x	x	x
Weathering	x	-	x
Growth uptake	x	x	-
N transformations	-	-	x
Al dissolution	-	-	x
Precipitation	x		
Evapotranspiration	x	x	x

<sup>1)</sup> x means that the influence was taken into account, whereas - means that an influence might exist, but this was not accounted for

### Sulphur and nitrogen deposition

Total deposition estimates for SO<sub>x</sub>, NO<sub>x</sub> and NH<sub>x</sub> on each gridcell were derived from emission deposition matrices from the RAINS model (Alcamo et al., 1990). These matrices are based on EMEP model calculations for a gridcell of 150 km x 150 km, that have been calibrated on available monitoring data on wet deposition and air pollutant concentrations from the EMEP network (Iversen et al., 1989).

Filtering of dry deposition by coniferous and deciduous forest stands was included by relating the total deposition on coniferous and deciduous forests,  $td_c$  and  $td_d$ , to the total average deposition on a gridcell,  $td_g$ , according to:

$$td_c = ff_c \cdot td_g \quad (5.28)$$

$$td_d = ff_d \cdot td_g \quad (5.29)$$

where  $ff_c$  and  $ff_d$  are filtering factors for coniferous and deciduous forests, respectively. In all calculations, it was assumed that there is a constant ratio between the forest filtering factors  $ff_c$  and  $ff_d$ :

$$ff_c = R_{cd} \cdot ff_d \quad (5.30)$$

Applying the above corrections for the deposition on forests, two additional assumptions were made: (i) the total deposition on a gridcell is correct which means that the deposition on open land is reduced accordingly, and (ii) the total deposition on open land is at least as high as the wet deposition on the gridcell. When the last condition was not met,  $ff_d$  was recalculated according to (De Vries et al., 1992a):

$$ff_d = \frac{1 - fr_{c,o} \cdot (wd_g / td_g)}{fr_{c,c} \cdot R_{cd} + fr_{c,d}} \quad (5.31)$$



where  $fr_{c,o}$ ,  $fr_{c,c}$  and  $fr_{c,d}$  are the coverage fractions of coniferous forests, deciduous forests and open land respectively, ( $fr_{c,o} = 1 - fr_{c,c} - fr_{c,d}$ ) and  $wd_g$  is the wet deposition on a gridcell. Values used for  $ff_d$  were 1.0 for  $SO_2$ , 0.7 for  $NO_x$  and 1.2 for  $NH_3$  whereas  $R_{cd}$  was put equal to 1.6 for all elements, based on Ivens et al. (1989), who compared throughfall data for  $SO_4$ ,  $NO_3$  and  $NH_4$  at 47 sites in Europe with total deposition estimates using the EMEP model.

#### Base cation deposition

The CI-corrected bulk deposition (wet deposition and a small part of dry deposition) of base cations was derived from 65 monitoring stations in Europe (Pedersen et al., 1990). Gridcell values were derived by interpolating between the five nearest stations according to:

$$BC_{wd,i}^* = \sum_{j=1}^5 \frac{BC_{wd,j}^*}{r_{i,j}} / \sum_{j=1}^5 \frac{1}{r_{i,j}} \quad (5.32)$$

where  $BC_{wd,i}^*$  and  $BC_{wd,j}^*$  are the wet (bulk) deposition of base cations in gridcell  $i$  and at station  $j$ , respectively, and  $r_{i,j}$  is the distance of the centre of gridcell  $i$  to station  $j$ .

The influence of dry deposition on the total deposition has been accounted for by multiplying the wet (bulk) deposition according to:

$$BC_{td}^* = (1 + f_{dd}) \cdot BC_{wd}^* \quad (5.33)$$

where  $f_{dd}$  is a dry deposition factor. Eq. (5.33) is based on the assumption that dry deposition is linearly related to wet deposition. The value of  $f_{dd}$  was derived from the ratio of Na in bulk deposition and throughfall (Ulrich, 1983b; Bredemeier, 1988) using results of a literature survey by Ivens et al. (1989) for 47 sites in Europe. Median values for  $f_{dd}$  thus derived were 0.6 for deciduous forests and 1.1 for coniferous forests. However, these data are based on results in areas which are sparsely occupied by forests. It is to be expected that  $f_{dd}$  will decrease with an increase in the forested areas within a gridcell, since dry deposition of base cations increases at forest edges nearby agricultural land (Draaijers et al., 1992). For the application on Europe, this effect was accounted for by a linear relationship between  $f_{dd}$  and the coverage fraction of open land,  $fr_{c,o}$ , according to:

$$f_{dd} = \alpha \cdot fr_{c,o} \quad (5.34)$$

where  $\alpha$  was 0.6 for deciduous forests and 1.1 for coniferous forests (see above).

#### Base cation weathering

The base cation weathering rate was estimated from the dominant parent material class and texture class of the dominant soil unit within each mapping unit (Table 5.5). The

assumed dominant parent material class for each soil type on the FAO soil map of Europe below forests has been given by De Vries (1991). The precipitation rate was considered irrelevant for the weathering rate, which might lead to an underestimate in areas with a large precipitation excess. The assumption that texture class has a dominating influence on the weathering rate was based on a linear relationship between weathering rate and clay content (Sverdrup et al., 1990). However, there is a strong correlation between parent material and texture. Parent material class 1 is mainly associated with texture class 1 and 1/2 while parent material class 2 is mainly correlated with texture class 2 and 2/3.

The weathering rates in Table 5.5 were derived from results of the weathering model PROFILE that has been developed to estimate field weathering rates based on the soil mineralogy (Sverdrup and Warfvinge, 1988a, b). The major inputs to this model are reaction rate coefficients of minerals and rocks, derived from laboratory studies. Using this information, Sverdrup and Warfvinge (1988a, b) established weathering rate classes (approximately 0-500; 500-1000; 1000-1500; 1500-2000 and 2000-2500 and 2500-3000 mol<sub>c</sub> ha<sup>-1</sup> yr<sup>-1</sup> m<sup>-1</sup>) on the basis of the mineralogy that controls the weathering rates. These weathering rate classes were used to assign a weathering rate to European forest soils. Within each weathering class, mean values were used in Table 5.5. Multiplying these values with an assumed standard soil depth of 0.5 m gave weathering rates of 125, 375, 625, 875, 1125, 1375 mol<sub>c</sub> ha<sup>-1</sup> yr<sup>-1</sup>. The percentage of forest soils to which these weathering rates were assigned was 20.4%, 40.9%, 21.1%, 6.7%, 1.5% and 0.5%, respectively. The remaining 8.9% were calcareous soils.

*Table 5.5 Weathering rates used for the various combinations of parent material class and texture class (indicated by 1, 1/2, etc.) that occur below forests*

Parent material class	Weathering rate (mol <sub>c</sub> ha <sup>-1</sup> yr <sup>-1</sup> m <sup>-1</sup> )					
	1	1/2	1/3	2	2/3	3
Acidic <sup>1)</sup>	250	750		1250	1750	
Intermediate <sup>2)</sup>	750	1250	1750	1750	2250	2750
Basic <sup>3)</sup>	750	1250		2250	2750	

<sup>1)</sup> Acidic : Sand (stone), gravel, granite, quartzine, gneiss (schist, shale, greywacke, glacial till) Schist, shale, greywacke and glacial till are put in brackets since soil types containing these parent materials can be converted to the acidic or intermediate parent material class, depending on the other parent materials available.

<sup>2)</sup> Intermediate : Gronodiorite, loess, fluvial and marine sediment (schist, shale, greywacke, glacial till)

<sup>3)</sup> Basic : Gabbro, basalt, dolomite, volcanic deposits.

The weathering rates thus assigned were corrected for the effect of temperature according to (Sverdrup, 1990):

$$BC_{we}(T) = BC_{we}(T_0) \cdot e^{(A/T_0 - A/T)} \quad (5.35)$$

where  $BC_{we}(T)$  is the weathering rate at the local mean annual temperature  $T$  (K),  $BC_{we}(T_o)$  is the average weathering rate defined in Table 5.5 for each combination of soil type and texture class at a reference temperature  $T_o$  (K) and  $A$  is a pre-exponential temperature factor (K). For  $A$  a value of 3600 K has been taken (Sverdrup, 1990).

The reference temperature was calculated for each weathering rate class as the weighted average of the mean annual air temperatures of all soil types in a given weathering rate class. The weighting factor was the percent coverage of the soil type in each gridcell. Reference temperatures (in °C) in the weathering rate classes 1 to 6 equalled 4.3, 2.6, 6.5, 8.3, 8.5 and 8.8 respectively. Low temperatures were associated with low weathering rate classes, which mainly occur in northern Europe. The temperature correction procedure given above implies that the weathering rates given in Table 5.5 are average values which decrease and increase with a lower and higher temperature respectively.

For calcareous soils an arbitrary high weathering rate of  $10\,000 \text{ mol}_c \text{ ha}^{-1} \text{ yr}^{-1}$  was used to avoid any exceedance of critical acid loads on these soils. Note, however, that direct effects of  $\text{SO}_2$  can not be neglected at these loads. Taking a critical annual concentration level for  $\text{SO}_2$  of  $20 \mu\text{g m}^{-3}$  (De Vries and Gregor, 1991) and multiplying this with a dry deposition velocity of  $1.3 \text{ cm s}^{-1}$  (Van Aalst and Erisman, 1991) leads to an annual dry deposition flux of  $5100 \text{ mol}_c \text{ ha}^{-1} \text{ yr}^{-1}$ . Assuming a ratio of wet to dry deposition of 1:2, gives an annual total (critical) load of  $7700 \text{ mol}_c \text{ ha}^{-1} \text{ yr}^{-1}$ , which is less than the value assigned for calcareous soils.

#### *Growth uptake*

The average annual uptake of N and base cations in stems and branches, was derived by multiplying the annual increase in biomass with the element contents in the various compartments according to:

$$X_{gu} = k_{gr} \cdot \rho_{st} \cdot (ctX_{st} + R_{br,st} \cdot ctX_{br}) \quad (5.36)$$

where  $X_{gu}$  is the net uptake flux of element X ( $\text{mol}_c \text{ ha}^{-1} \text{ yr}^{-1}$ ),  $k_{gr}$  is the annual average stem growth rate constant ( $\text{m}^3 \text{ ha}^{-1} \text{ yr}^{-1}$ ),  $\rho_{st}$  is the density of stemwood ( $\text{kg m}^{-3}$ ),  $ctX_{st}$  is the content of element X in stems ( $\text{mol}_c \text{ kg}^{-1}$ ),  $ctX_{br}$  is the content of element X in branches ( $\text{mol}_c \text{ kg}^{-1}$ ) and  $R_{br,st}$  is the branch to stem ratio ( $\text{kg kg}^{-1}$ ). The contribution of branches was included assuming that whole-tree harvesting (stems and branches) is practised.

Data on average stem growth rates in Europe for coniferous and deciduous forests in each gridcell were derived from a literature compilation by Nilsson and Sallnäs (in press). For the boreal forests area, the growth rate was calculated from a relationship with the temperature according to (Kauppi and Posch, 1988):

$$k_{gr} = k_{gr,max} / (1 + e^{-a \cdot ETS + b}) \quad (5.37)$$

where  $k_{gr,max}$  is the maximum growth rate constant ( $m^3 \text{ ha}^{-1} \text{ yr}^{-1}$ ),  $ETS$  is the effective temperature sum, i.e. the annual sum of daily temperatures above  $5^\circ\text{C}$ , and  $a$  and  $b$  are constants. Values used for  $k_{gr,max}$ ,  $a$  and  $b$  were  $6.0 \text{ m}^3 \text{ ha}^{-1} \text{ yr}^{-1}$ ,  $0.005 \text{ }^\circ\text{C}^{-1}$  and 5, respectively (Kauppi and Posch, 1988).

Average values used for the density of stemwood and the branch to stem ratio were  $500 \text{ kg m}^{-3}$  and  $0.15 \text{ kg kg}^{-1}$  for coniferous forests and  $700 \text{ kg m}^{-3}$  and  $0.20 \text{ kg kg}^{-1}$  for deciduous forests respectively (Kimmins et al., 1985; De Vries et al., 1990). Data for the element contents in stems and branches were computed, according to:

$$ctX = ctX_{min} + \beta \cdot (ctX_{max} - ctX_{min}) \quad (5.38)$$

where  $ctX_{min}$  and  $ctX_{max}$  are the minimum and maximum contents ( $\text{mol}_c \text{ kg}^{-1}$ ) of element  $X$  in stems or branches and  $\beta$  is a fraction ( $0 \leq \beta \leq 1$ ), varying linearly with the latitude between  $55^\circ \text{ N}$  and  $65^\circ \text{ N}$ , based on data given in Rosén (1990). For  $X = \text{N}$ ,  $\text{Mg}$  and  $\text{K}$ ,  $\beta$  was set to 0 for latitude  $\geq 65^\circ$  and to 1 for latitude  $\leq 55^\circ$ . For  $X = \text{Ca}$ ,  $\beta$  was set to 1 for latitude  $\geq 65^\circ$  and 0 for latitude  $\leq 55^\circ$ . Element contents of  $\text{N}$ ,  $\text{Mg}$  and  $\text{K}$  in stems and branches of boreal forests (above latitude  $55^\circ$ ) were thus taken lower than in Central and Southern European forests (below latitude  $55^\circ$ ) whereas the opposite was done for  $\text{Ca}$ . Values used for the minimum and maximum element contents show that latitude mainly affects the element content in branchwood (Table 5.6).

Table 5.6 Minimum and maximum values of nitrogen and base cation contents in stems and branches of coniferous and deciduous forests in Europe<sup>1)</sup>

Forest type	Compartment	Minimum contents (%)				Maximum contents (%)			
		N	Ca	Mg	K	N	Ca	Mg	K
Coniferous	Stems	0.10	0.08	0.02	0.05	0.10	0.16	0.02	0.05
	Branches	0.20	0.30	0.03	0.10	0.40	0.60	0.05	0.25
Deciduous	Stems	0.15	0.13	0.04	0.10	0.15	0.21	0.04	0.10
	Branches	0.20	0.45	0.03	0.05	0.40	0.75	0.05	0.20

<sup>1)</sup> The minimum values for  $\text{Ca}$  and maximum values of  $\text{N}$ ,  $\text{Mg}$  and  $\text{K}$  apply to all forests below latitude  $55^\circ$  (based on data by Kimmins et al., 1985).

<sup>2)</sup>  $\text{N}$  contents were taken from sites with a relatively low  $\text{N}$  deposition (Scandinavian forests). In areas with a high  $\text{N}$  deposition, such as the Netherlands, the  $\text{N}$  content increases leading to higher  $\text{N}$  uptake values (De Vries, 1993). However, this is associated with an increased  $\text{NO}_3$  leaching rate. Actually, one should use the  $\text{N}$  content at critical load that is likely to be relatively low. Apart from  $\text{N}$  contents, growth rates are also affected by  $\text{N}$  deposition. In several areas, growth rates might be very low due to  $\text{N}$  deficiency, thus decreasing the calculated critical load value. Actually, growth rates should also be used that can be realized at critical  $\text{N}$  loads.

### *Nitrogen transformations and aluminium dissolution*

N transformations include immobilization, nitrification and denitrification. The rate of net immobilization of stable organic N compounds in the soil (stable forms of humus) is low. An estimate of the long-term N immobilization rate from the total amount of soil nitrogen divided by the period of soil formation is generally less than  $50 \text{ mol}_e \text{ ha}^{-1} \text{ yr}^{-1}$  (Section 4.1). The actual accumulated amount may be higher on the short term (the harvesting period). This is important for the assessment of interim target loads by dynamic models. However, in deriving a long-term critical load, this short-term accumulation was neglected (cf Section 4.1).

The nitrification fraction ( $fr_{ni}$ ) was set to 1.0. This was based on the low  $\text{NH}_4$  concentrations below the rootzone of forests, even in the Netherlands with a high input of  $\text{NH}_4$  (Heij et al., 1991). This implies that critical acid loads were calculated according to Eq. (5.24). Denitrification fractions were related to soil type on the basis of data given by Breeuwsma et al. (1991) for peat, clay and sandy soils in the Netherlands. Values used were 0.8 for peat soils, 0.7 for clay soils (texture classes 2, 3 and 2/3), 0.5 for sandy soils (texture classes 1 and 1/2) with gleyic features and 0.1 for sandy soils without gleyic features. In deeply drained sandy forest soils, denitrification appears to be nearly negligible (Klemetsson and Svensson, 1988).

The parameter governing Al dissolution, i.e.  $KAl_{ox}$ , was set at  $10^8 \text{ mol}^{-2} \text{ l}^2$  for mineral soils (based on Heij et al., 1991) and at  $10^6 \text{ mol}^{-2} \text{ l}^2$  for peat soils (based on Wood, 1989).

### *Precipitation and evapotranspiration*

Data used for the average precipitation in each gridcell were interpolated values from selected records of average monthly precipitation during the period 1930-1960 from 1678 weather stations in Europe (Leemans and Cramer, 1991). Data for the average evapotranspiration (a lumped expression for the sum of interception evaporation, soil evaporation and transpiration) of forests in a gridcell were based on results of a simple hydrologic model (Cramer and Prentice, 1988). The influence of forest type on evapotranspiration was accounted for by assuming that the average actual evapotranspiration for forests in a gridcell ( $E_f$ ), is correct, whereas differences between coniferous and deciduous forests are caused by interception evaporation only. The sum of soil evaporation, and transpiration, denoted as  $E'_p$  was thus assumed independent of tree species, which is a reasonable assumption (Roberts, 1983). On a gridcell basis, this value was calculated as

$$E'_f = E_f - E_{i,f} \quad (5.39)$$

where  $E_{i,f}$  is the average interception for forests in a gridcell, calculated as:

$$E_{i,f} = (f_c \cdot E_{i,c} + f_d \cdot E_{i,d}) / (f_c + f_d) \quad (5.40)$$

where  $E_{i,c}$  and  $E_{i,d}$  are the interception evaporation values for coniferous forests and deciduous forests, respectively. The evapotranspiration for each receptor was calculated by adding  $E_{i,c}$  and  $E_{i,d}$  respectively to  $E_r$ . Based on data given by Calder and Newson (1979), interception evaporation was described as a function of precipitation ( $P$ ) according to:

$$E_{i,c} = 1.75 \cdot P^{0.75} \quad \text{and} \quad E_{i,d} = 1.0 \cdot P^{0.75} \quad (5.41)$$

The values of 1.75 for coniferous forests and 1.0 for deciduous forests were based on Mitscherlich and Moll (1970) and Van Grinsven et al. (1987), respectively. The maximum annual interception evaporation over Europe equalled 680 and 390 mm yr<sup>-1</sup> for coniferous and deciduous forests respectively, at a maximum precipitation rate of 2850 mm yr<sup>-1</sup>. Interception data for high rainfall areas in Scotland are consistent with these values (Cape and Lightowlers, 1988).

## RESULTS

### Calculated model inputs

Cumulative frequency distributions of model inputs used for the calculation of critical loads show that present loads of  $BC_{td}^*$  were almost everywhere less than 1500 mol<sub>c</sub> ha<sup>-1</sup> yr<sup>-1</sup> (Fig. 5.1A). Values appeared to be higher for deciduous than for coniferous forests. The above mentioned lower input of base cations by dry deposition on deciduous forests was more than compensated because a relative large proportion of these forests is located in Southern Europe (cf Table 5.1). Maps of the present loads of  $BC_{td}^*$  showed a clear decrease from Southern to Northern Europe caused by a decrease in inputs of Saharian dust (De Vries et al., 1992a).

Nearly all non-calcareous soils had weathering rates below 1500 mol<sub>c</sub> ha<sup>-1</sup> yr<sup>-1</sup> (Fig. 5.1B). The range is mainly determined by the allocation of weathering rates to soils (Table 5.5). The median value for all soils was about 500 mol<sub>c</sub> ha<sup>-1</sup> yr<sup>-1</sup>. Values were somewhat higher below deciduous forests, which generally occur on richer soils. A map of the median weathering rates in each 1.0° x 0.5° longitude-latitude gridcell over Europe (De Vries et al., 1992a) showed a clear decrease in weathering rate from Southern to Northern Europe. Values below 500 mol<sub>c</sub> ha<sup>-1</sup> yr<sup>-1</sup> mainly occurred in Scandinavia, Scotland, Poland, the Netherlands and Northern Germany, i.e. the area with podzolic soil types. Almost all values for N and BC uptake were below 1000 mol<sub>c</sub> ha<sup>-1</sup> yr<sup>-1</sup> (Fig. 5.1C and 5.1D). Uptake rates for deciduous forests were nearly twice as high as coniferous forests due to both higher growth rates and higher N and BC contents (cf Table 5.6).

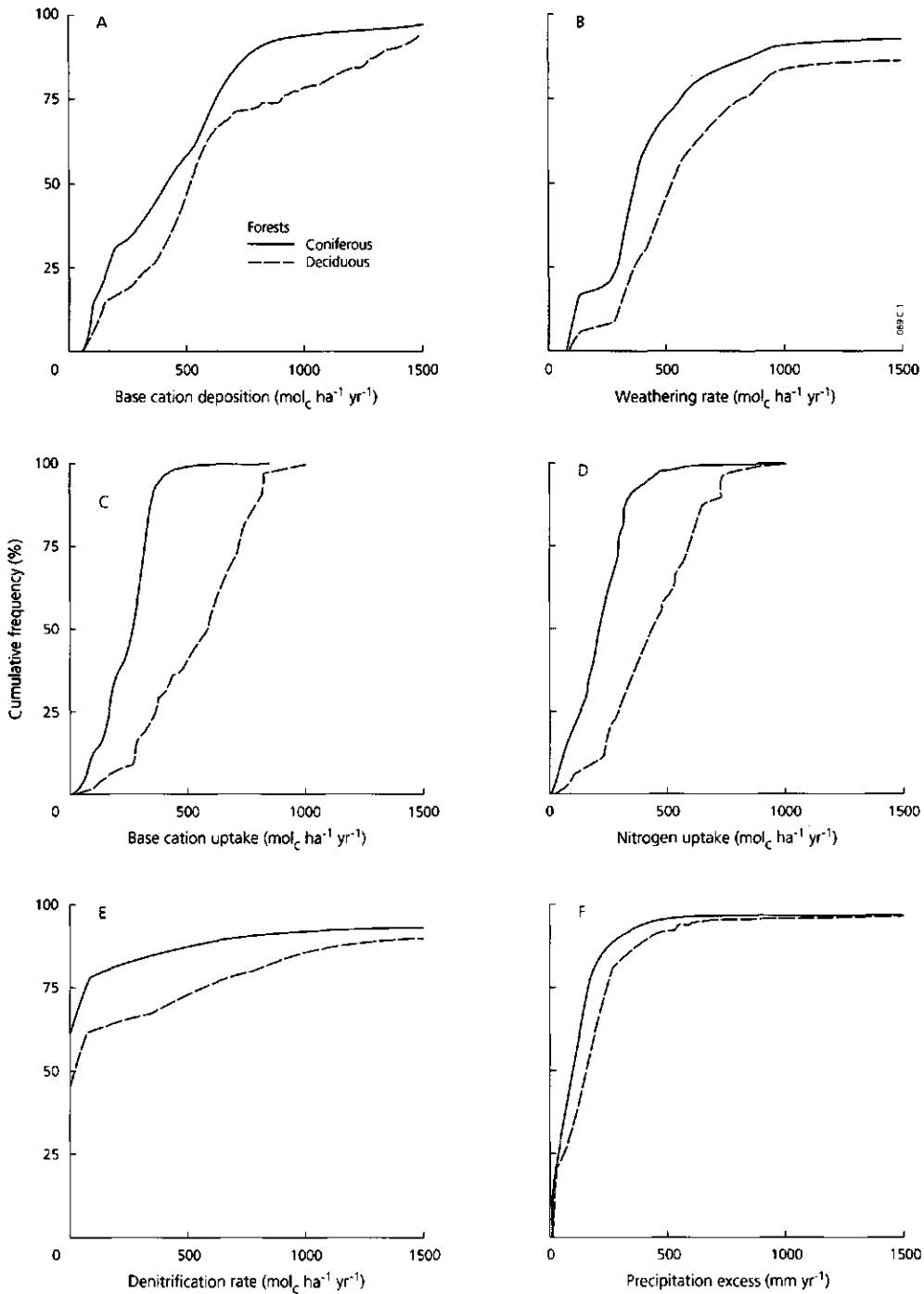


Figure 5.1 Cumulative frequency distributions of the Cl-corrected base cation deposition (A), base cation weathering (B), base cation uptake (C), N uptake (D), denitrification rate at critical N load (E) and precipitation excess (F) for coniferous and deciduous forests in Europe

Furthermore, BC uptake appeared to be somewhat higher than N uptake. Median values for all forests were about  $350 \text{ mol}_c \text{ ha}^{-1} \text{ yr}^{-1}$  for BC uptake and  $300 \text{ mol}_c \text{ ha}^{-1} \text{ yr}^{-1}$  for N uptake. This implies that forest uptake causes some acidification, but the overall effect is small. Maps of the N and BC uptake (De Vries et al., 1992a), showed a clear decrease in uptake rate in the boreal forests in Scandinavia. Extremely low values (below  $100 \text{ mol}_c \text{ ha}^{-1} \text{ yr}^{-1}$ ) occurred in the northern parts of Norway, Sweden and Finland and the Alps.

In nearly 50% of all forest soils denitrification (at critical N load) appeared to be negligible (Fig. 5.1E). In the other 50% most values remained below  $1500 \text{ mol}_c \text{ ha}^{-1} \text{ yr}^{-1}$ . Medium to high values occurred in clay and peat soils, respectively. The variation in denitrification rates was strongly determined by the distribution of forests over these soil types. However, it should be stressed that the actual denitrification rate in clay and peat soils will generally be lower, since present N loads for these soils are mostly below critical N loads. In Northern and Central Europe, where deeply drained podzolic soils dominate, values were generally low. Since coniferous forests dominate in the north, denitrification below these forests was less than for deciduous forests (cf Figure 5.1E). In Southern Europe, where clay soils are relatively more abundant, values were generally higher. However, high values also occurred in the north, for example Finland, in areas with peat soils (De Vries et al., 1992a). The calculated distribution of European forests over sand, clay and peat was 62.7%, 33.6% and 3.7%, respectively. Only a small part of the sandy soils had gleyic features (13.2%).

The precipitation excess was generally less than  $500 \text{ mm yr}^{-1}$  (Fig. 5.1F). Median values were about 150 to  $200 \text{ mm yr}^{-1}$  for coniferous and deciduous forests respectively. A map of the precipitation excess below coniferous and deciduous forests in Europe showed that values vary mostly between 50 and  $200 \text{ mm yr}^{-1}$  in the Northern, Eastern and Southern European countries with a precipitation rate below  $700 \text{ mm yr}^{-1}$ . In Central Europe most values ranged between 100 and  $300 \text{ mm yr}^{-1}$ . Values above  $1000 \text{ mm yr}^{-1}$  mainly occurred in Norway and Scotland but also in the Swiss and Austrian Alps (De Vries et al., 1992a).

### **Present loads and critical loads**

Cumulative frequency distributions of present loads and critical loads for N, S and acidity for coniferous and deciduous forests in Europe are shown in Figure 5.2. Present loads of N and S were generally below  $2000 \text{ mol}_c \text{ ha}^{-1} \text{ yr}^{-1}$  (cf Figs. 5.2A and 2C). The higher loads on coniferous forests, compared to deciduous forests, reflect the effect of forest filtering. Median values for N and S on all forests were about 550 and  $840 \text{ mol}_c \text{ ha}^{-1} \text{ yr}^{-1}$ . High N loads up to  $4000 \text{ mol}_c \text{ ha}^{-1} \text{ yr}^{-1}$  occurred in the Netherlands, Belgium and Germany. Extremely high S loads up to  $13000 \text{ mol}_c \text{ ha}^{-1} \text{ yr}^{-1}$  occurred in Czechoslovakia, Poland and Germany. Relatively low loads, both in N and S, occurred



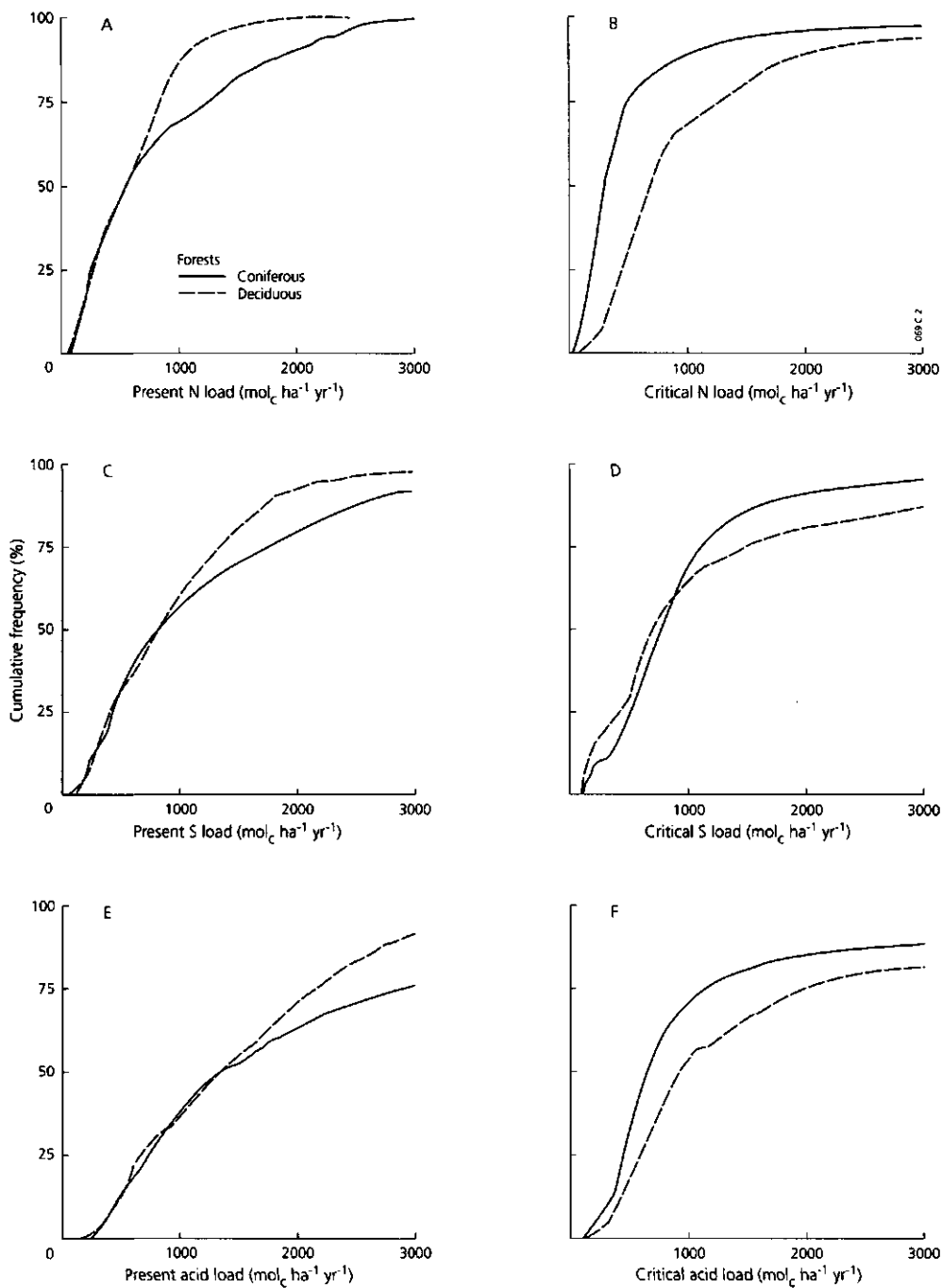


Figure 5.2 Cumulative frequency distributions of the present load and critical load of N (A and B), S (C and D) and acidity (E and F) on coniferous and deciduous forests in Europe

in the Nordic countries. Present loads of potential acidity were generally less than 3000 mol<sub>c</sub> ha<sup>-1</sup> yr<sup>-1</sup> (Fig. 5.2E). As with N and S, the load of potential acidity was higher on coniferous than on deciduous forests. High loads occur in Central Europe and the UK, with extreme inputs in Czechoslovakia, Poland and Germany caused by SO<sub>2</sub> pollution. In Southern Europe values became close to zero. This implies that the input of base cations (corrected for seasalt) is nearly equal to the input of S and N (cf Fig. 5.2E).

As with the present loads, most values for the critical loads of N and S were below 2000 mol<sub>c</sub> ha<sup>-1</sup> yr<sup>-1</sup> (cf Figs. 5.2B, 5.2D). Median values for all forests were 480 mol<sub>c</sub> ha<sup>-1</sup> yr<sup>-1</sup> for N and 770 mol<sub>c</sub> ha<sup>-1</sup> yr<sup>-1</sup> for S. Critical N loads were higher for deciduous forests because of higher values for N uptake (cf Fig. 5.1D) and denitrification (cf Fig. 5.1E). At the same location, critical S loads were higher for coniferous forests, due to higher values of dry deposition of BC and lower values of BC uptake (cf Fig. 5.1C) causing less acidification due to forest growth. This appeared to compensate the lower values for BC weathering (cf Fig. 5.1B). However, because a relatively large proportion of deciduous forests is located in Southern Europe, with a large deposition of base cations, this effect is hidden in Figure 5.2D. As with the present loads, critical acid loads were generally below 3000 mol<sub>c</sub> ha<sup>-1</sup> yr<sup>-1</sup>, except for calcareous soils. Values were higher for deciduous forests (Fig. 5.2F) which was mainly due to higher values for weathering, denitrification and acidity leaching. Acidity leaching was higher since the precipitation excess was higher below deciduous forests (cf Fig. 5.1F).

Critical loads for N, S and acidity varied substantially over Europe. The values were generally higher in Southern Europe. Lower values generally occurred in Scandinavia, USSR, Poland, Germany and the Netherlands (Table 5.7). For some countries (Netherlands and Denmark), the critical acid load appeared to be lower than the critical nitrogen load. This means that in these countries the critical load of acidity associated to S became negative. The positive critical S load given in Table 5.7 refers to the total S input (cf Eq. 5.27) which is partly (or completely) neutralized by base cation input from the atmosphere.

### **Exceedances of critical loads**

Results of the excess of present loads over critical loads for N, S and acidity on coniferous and deciduous forests in Europe are shown in Figure 5.3 by inverse cumulative frequency distributions, which directly give insight in the forested area above a given excess load. In relative large areas in Europe present loads exceeded critical loads but the excess was mostly less than 3000 mol<sub>c</sub> ha<sup>-1</sup> yr<sup>-1</sup>. For N, the excess was much higher on coniferous than on deciduous forests (Fig. 5.3A), due to both higher present loads (Fig. 5.2A) and lower critical loads (Fig. 5.2B). For S the excess was much smaller (Fig. 5.3B) since both present and critical S loads did not deviate that much for both forest types (cf Figs. 5.2C and 5.2D). The forested area where critical

**Table 5.7** Median values for the critical loads of N, S and acidity for forests in the European countries

Country	Critical load (mol <sub>c</sub> ha <sup>-1</sup> yr <sup>-1</sup> )		
	N	S	Acid
Albania	3165	7230	8800
Austria	1430	2755	3020
Belgium	1315	960	1600
Bulgaria	460	2265	1465
Czechoslovakia (former)	725	1160	1220
Denmark	620	790	555
Finland	380	670	750
France	775	1110	1485
Germany	905	955	1245
Greece	820	6720	5690
Hungary	770	2310	1920
Ireland	2430	1475	3120
Italy	1485	1855	2220
Luxembourg	1840	955	2130
Netherlands	555	220	540
Norway	470	345	670
Poland	320	675	305
Portugal	1080	1385	2375
Romania	750	1070	775
Spain	560	1300	1810
Sweden	305	405	580
Switzerland	975	1665	2115
UK	865	620	1235
USSR <sup>1)</sup> (former)	425	780	725
Yugoslavia (former)	845	2480	2190
Europe	480	770	805

<sup>1)</sup> Refers to the European part including Estonia, Latvia and Lithuania

loads are exceeded was nearly equal for N and S, i.e. 50% for N (63% of all conifers and 30% of all deciduous forests) and 52% for S (53% of all conifers and 49% of all deciduous forests). For total acidity, the forested area where critical loads are exceeded equalled 45% (52% of all conifers and 33% of all deciduous forests; Fig. 5.3C).

Quite unexpectedly the area where critical N loads are exceeded appeared to be large. Note, however, that the calculated critical N loads relate to the occurrence of vegetation changes in forests. Rosén (1990) indeed found a good correlation between the exceedance of critical N loads, calculated according to Eq. (5.25), and the occurrence of vegetation changes in Swedish forests. However, N loads affecting forest vitality, appear to be much higher. Average critical loads derived for Dutch forest soils related to these effects are about 1500 to 3000 mol<sub>c</sub> ha<sup>-1</sup> yr<sup>-1</sup> (cf Section 4.1; De Vries, 1993). These loads even violated the acidity criterion. The calculation of critical N loads related to effects on forests can thus better be related to the inherent acidifying effect. Application of acidification criteria strongly affects the area where critical loads for N are exceeded. This aspect is elaborated in the section on uncertainties.

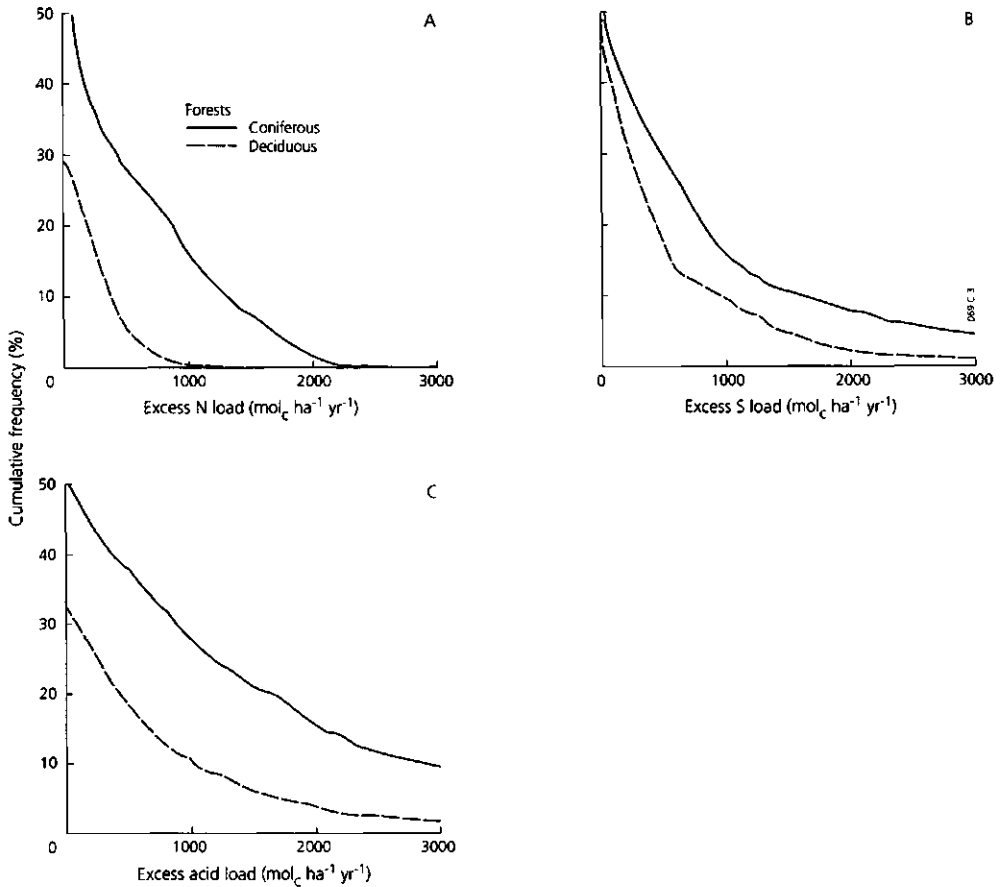


Figure 5.3 Inverse cumulative frequency distributions of the amount by which critical loads of N (A), S (B) and acidity (C) are exceeded on coniferous and deciduous forests in Europe.

Maps of the forested area where critical loads for N and acidity are exceeded showed that an exceedance in critical loads occurred nearly all over Europe except for the Northern part of Norway, Sweden and Finland and large parts of Scotland, Ireland, Portugal, Spain, Italy, Greece and Albania (Fig. 5.4). Critical acid loads were exceeded in more than 85% of the forested area in Denmark, the Netherlands, Belgium, Luxembourg, Germany, Poland, former Czechoslovakia and Romania. In most Mediterranean countries, the area where critical acid loads are exceeded appeared to be relatively low (less than 15 to 35%) i.e. in Spain, Portugal, Italy, former Yugoslavia and Bulgaria. The same was true for most of the Nordic countries, i.e. Norway, Sweden (except for the southern part) and Finland. Exceedances were almost negligible (less than 5%) in Albania, Greece and Ireland.

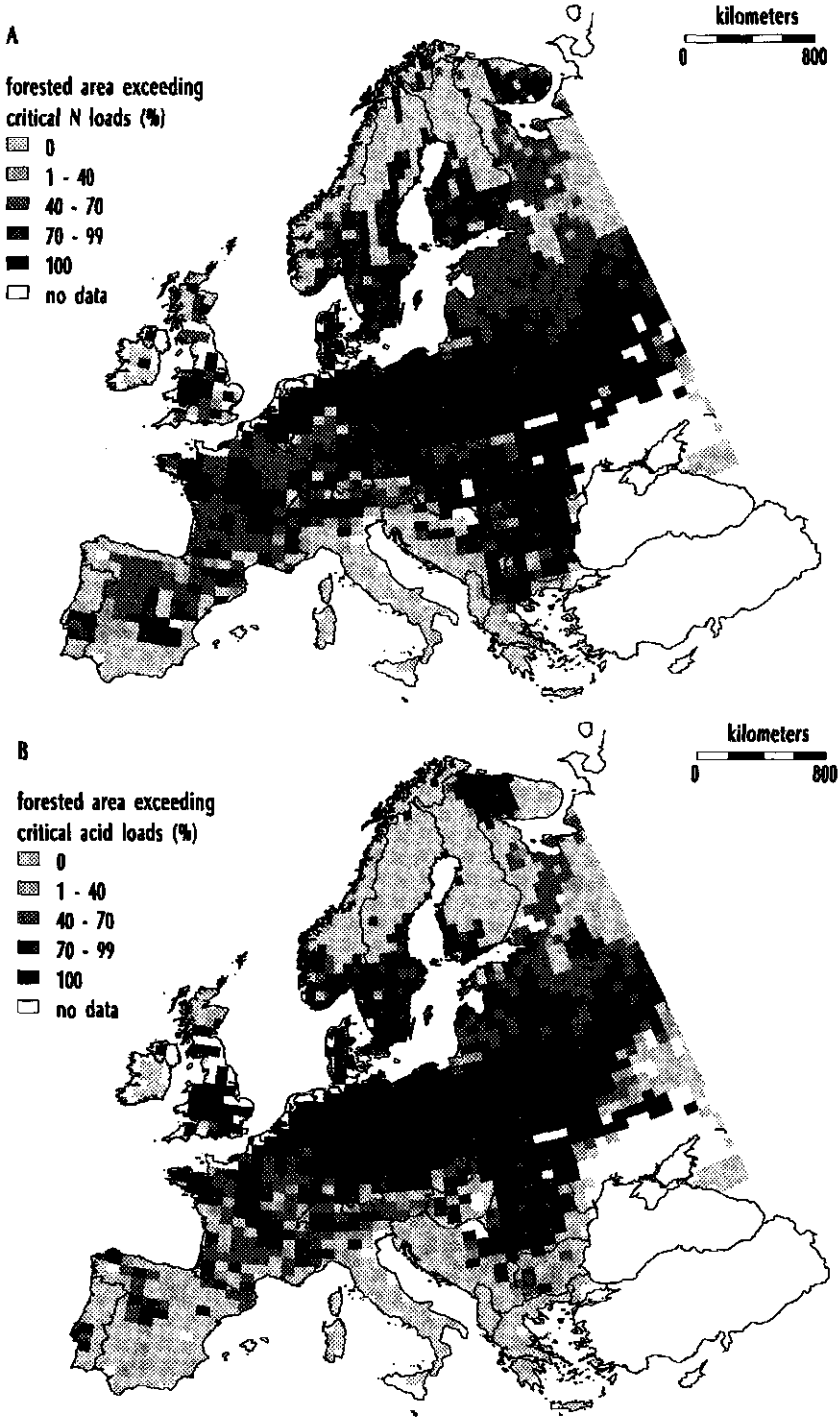


Figure 5.4 Geographic distribution of the forested area in Europe exceeding critical loads for N (A) and acidity (B)

The variation in the excess of present loads over critical loads of N and acidity in Europe is shown in Figure 5.5. Large exceedances (more than 2000 mol<sub>c</sub> ha<sup>-1</sup> yr<sup>-1</sup>) in critical loads in more than 50% of the forested area were mainly restricted to Central and Western Europe, i.e. the Netherlands, Belgium, Germany, Poland and former Czechoslovakia. Relative large exceedances in critical loads of N and acidity also occurred in the former USSR and in parts of the UK, Romania and France. Maximum exceedances in critical loads for N and S were close to present loads, i.e. up to 3500 mol<sub>c</sub> ha<sup>-1</sup> yr<sup>-1</sup> for N in the Netherlands, Belgium and Germany and up to 12000 mol<sub>c</sub> ha<sup>-1</sup> yr<sup>-1</sup> for S in former Czechoslovakia, Poland and Germany (cf Section on present loads).

In areas where critical acid loads are exceeded, the critical Al concentration of 0.2 mol<sub>c</sub> m<sup>-3</sup> and/or the critical Al/BC ratio of 1.0 mol mol<sup>-1</sup> is exceeded in a steady-state situation. A prediction of both soil solution parameters at steady-state in European forest soils was made with the START model using present deposition rates. Maps of the median values of the Al concentration and Al/BC ratio in each 1.0° x 0.5° longitude-latitude gridcell are given in Figure 5.6. Comparison with the map of the median values for the exceedance in critical acid loads (Fig. 5.5B) shows a striking similarity with that for the Al concentration (Fig. 5.6A). This implies that the Al concentration criterion is generally most limiting.

## UNCERTAINTIES

The uncertainty in critical loads derived above can be large. This is mainly determined by the uncertainty in critical chemical values, model structure and input data (Sverdrup et al., 1990; De Vries, 1991). The discussion below is limited to effects on the area where critical loads are exceeded.

### Uncertainties in critical chemical values

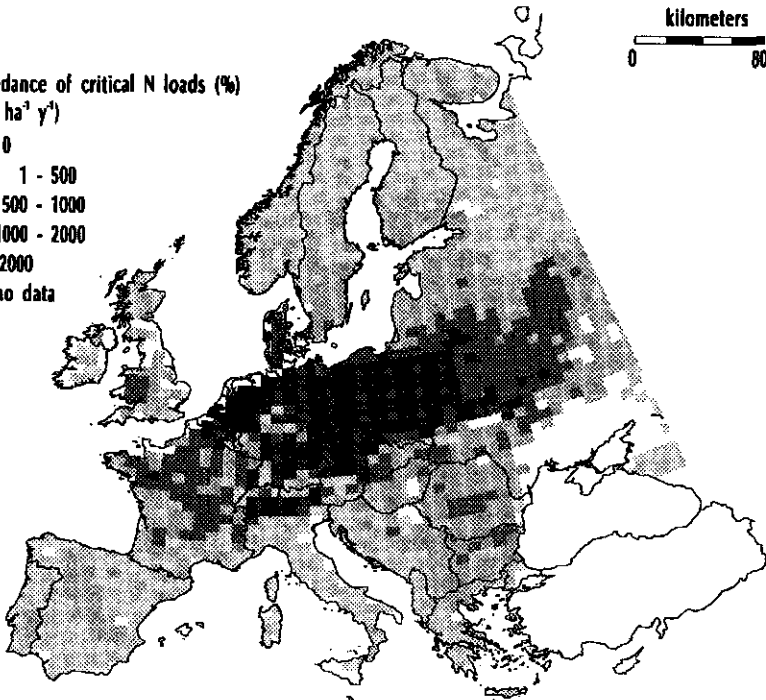
#### *Critical Al concentration and critical Al/BC ratio*

In calculating a critical acid load, a certain rate of Al and H leaching is accepted. However, Al mobilization hardly occurs in peat soils. So, here a critical pH should be defined. Furthermore, in mineral soils leaching of Al occurs at relatively low base saturation levels, generally below 25% (De Vries et al., 1989b). This implies that the pool of exchangeable base cations in soils with high levels of base saturation is gradually depleted, at a given critical load, until a new state of equilibrium is reached, in which the base saturation and soluble Al concentration or Al/BC ratio remains constant. It is implicitly assumed that this new state of equilibrium poses no threat to trees when the Al concentration and Al/BC ratio stay below critical values. For acid forest soils, such as podzols, this seems a reasonable approach since the base saturation is already low. However, one may argue that a strong depletion of exchangeable base cations and

A

exceedance of critical N loads (%)  
(mol. ha<sup>-1</sup> y<sup>-1</sup>)

- 0
- 1 - 500
- 500 - 1000
- 1000 - 2000
- >2000
- no data



B

exceedance of critical acid loads (%)  
(mol. ha<sup>-1</sup> y<sup>-1</sup>)

- 0
- 1 - 1000
- 1000 - 2000
- 2000 - 3000
- >3000
- no data

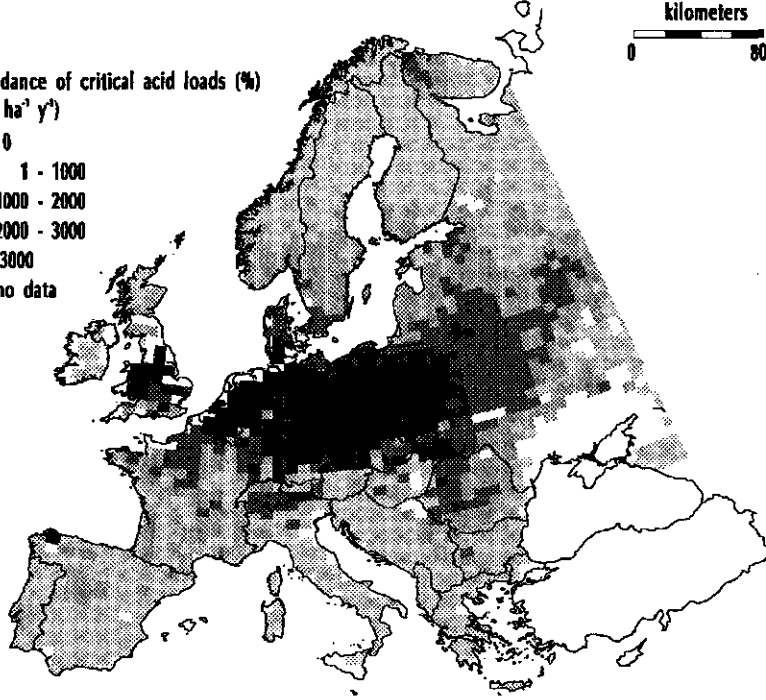


Figure 5.5 Geographic distribution of median values for the exceedance of critical loads for N (A) and acidity (B) on European forests

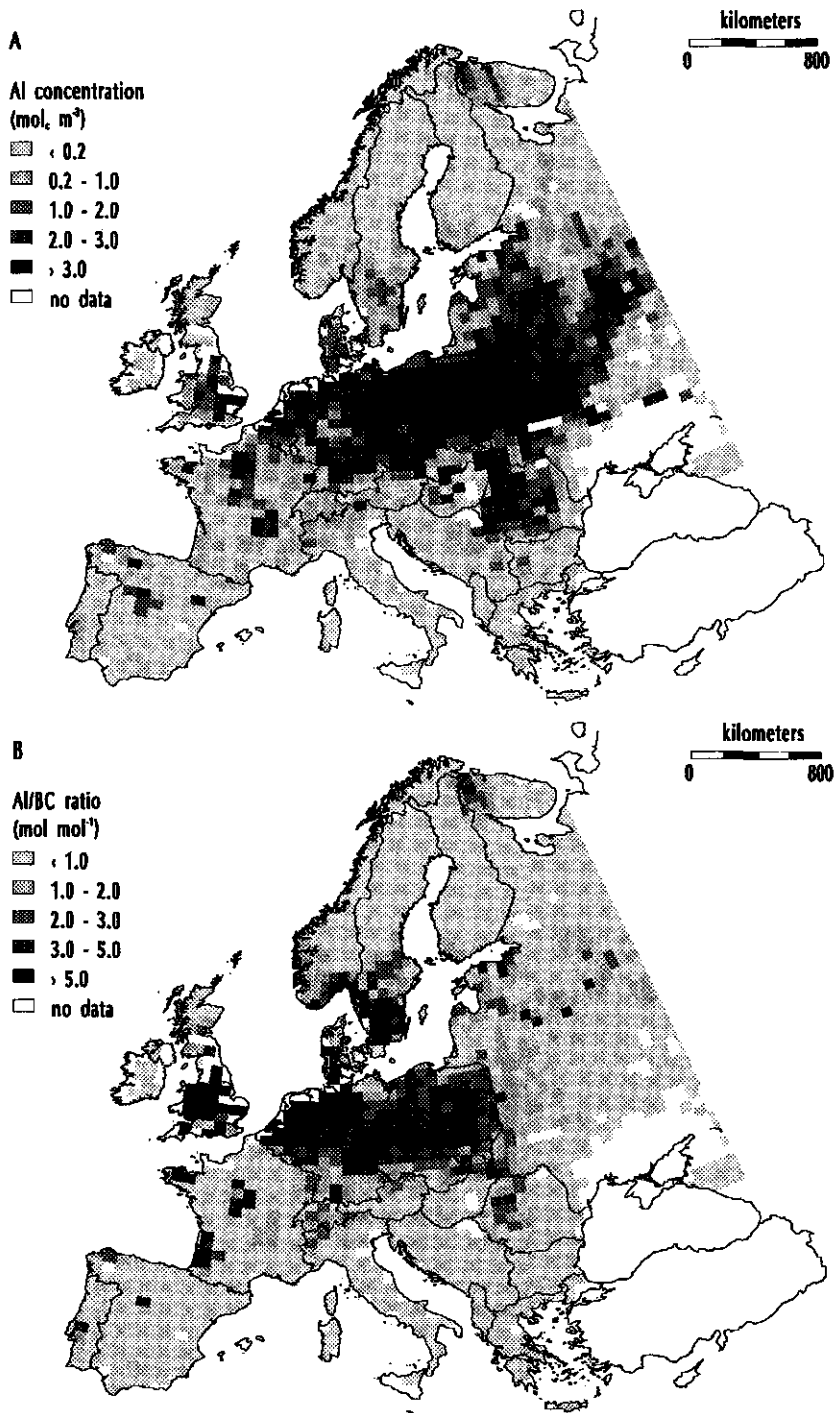


Figure 5.6 Geographic distribution of median values for the Al concentration (A) and Al/BC ratio (B) in European forest soils, as predicted by the START model



a consequent drop in pH to a value near 4 should be avoided in slightly acid mineral soils (soils with a pH > 5). Taking this viewpoint, the Al concentration has to be nearly negligible in these soils.

Even when a certain Al leaching is accepted, uncertainties in critical values for the Al concentration and Al/BC ratio are large. This is due to a lack of knowledge about the effects of Al in the field situation and a natural range in the sensitivity of various tree species for Al toxicity (De Vries, 1991). Note also that we used critical annual average values whereas the temporal variation can be large, with peak values in the summer. The influence of the criteria used for the Al concentration and Al/BC ratio on the area where critical acid loads are exceeded can directly be derived from the inverse cumulative frequency distributions of Al concentrations (Fig. 5.7A) and Al/BC ratios (Fig. 5.7B), which were calculated by using present deposition values.

Assuming a critical value for the Al concentration or Al/BC ratio close to zero resulted in an area where critical acid loads are exceeded of 71%. However, application of this criterion is not relevant for acid forest soils such as podzols, which cover a large part of central and northern Europe (cf Table 5.3). The forested area where a critical Al concentration of  $0.2 \text{ mol}_c \text{ m}^{-3}$  is exceeded equalled 43%. However, this area strongly decreased with an increase in Al concentration, especially in the range between 0.2 and  $1.0 \text{ mol}_c \text{ m}^{-3}$ , i.e. from 43% to 24% (cf Fig. 5.7A). The area where a critical Al/BC ratio of 1.0 is exceeded was 30%, i.e. 36% of all conifers and 19% of all deciduous forests (cf Fig. 5.7B). This implies that the Al concentration criterion is more stringent than the Al/BC ratio criterion. The decrease in the area where a critical value is exceeded was very large in the range between 0 and  $1.0 \text{ mol mol}^{-1}$  (from 71% to 30%) and much less

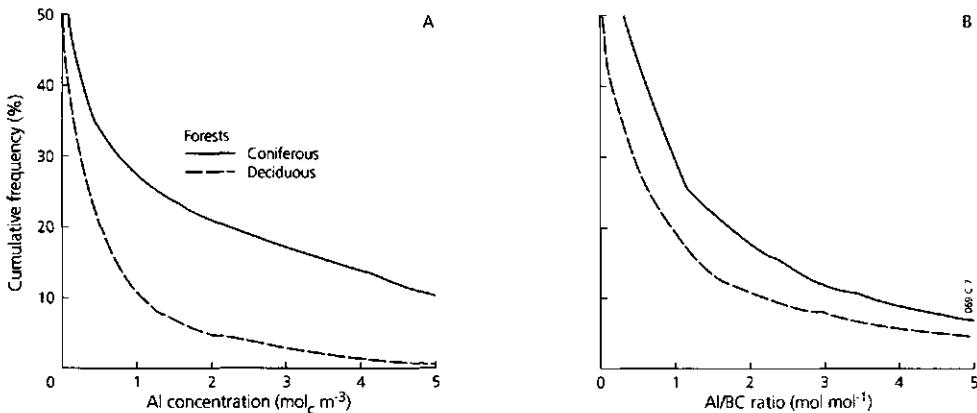


Figure 5.7 Inverse cumulative frequency distributions of the Al concentration (A) and Al/BC ratio (B) below coniferous and deciduous forests in Europe.

above this value, although an increase of the Al/BC ratio to 2.0 mol mol<sup>-1</sup> still caused a decrease in the exceedance area up to 16%. However, even in this situation, large exceedances, i.e. above 50% were still calculated for the highly polluted countries in Western and Central Europe.

#### *Critical N concentration*

The choice of the critical N concentration strongly affects the critical loads of N and S (cf Eqs. 5.26 and 5.27). The uncertainty in this criterion is likely to be large. However, one can argue that at complete nitrification (NO<sub>3</sub> concentration equals N concentration) the upper limit is determined by the critical acidity concentration (the critical S load is then determined by the net base cation input; cf Eq. 5.27), whereas the lower limit is zero (close to natural leaching). Results of a sensitivity analysis in which the critical NO<sub>3</sub> concentration was varied between these values, show that the variation in the NO<sub>3</sub> concentration criterion had a large effect on the area where critical loads are exceeded, especially regarding N (Table 5.8).

*Table 5.8 Influence of the critical nitrate concentration on the percentage of coniferous and deciduous forests in Europe where critical loads for N and S are exceeded*

Forest type	Area where critical N loads are exceeded (%)			Area where critical S loads are exceeded (%)		
	[NO <sub>3</sub> ] <sub>(crit)</sub>			[NO <sub>3</sub> ] <sub>(crit)</sub>		
	0.1 <sup>1)</sup>	0	[Ac] <sub>(crit)</sub> <sup>2)</sup>	0.1 <sup>1)</sup>	0	[Ac] <sub>(crit)</sub> <sup>2)</sup>
Coniferous	63	99	36	53	44	72
Deciduous	30	57	17	49	35	69
All	50	84	29	52	41	71

<sup>1)</sup> Standard run

<sup>2)</sup> The critical NO<sub>3</sub> concentration is taken equal to the critical acidity concentration

### **Uncertainties in model structure**

#### *Homogeneity in the rootzone*

Uncertainties in model structure refer to the assumptions in the model. An important assumption in the START model is the assumed homogeneity of the rootzone both in a horizontal and vertical direction. In a horizontal direction, large variations in soil solution chemistry do occur due to the occurrence of stemflow, differences in canopy coverage, preferred hydrological pathways etc. (e.g. Kleijn et al., 1989).

Unlike the stochastic variation in space and time within the rootzone, there is also a systematic change in soil solution chemistry with depth. Use of a one-layer model such as START implies that the critical Al concentration and Al/BC ratio used refers to the situation at the bottom of the rootzone, whereas most roots occur in the topsoil. Values

for the Al concentration and Al/BC ratio generally increase with depth due to Al mobilization, BC uptake and transpiration. An indication of these effects on the critical acid loads was derived by calculating the Al concentration and Al/BC ratio in the middle of the rootzone (here a depth of 25 cm) with START, assuming a uniform weathering, uptake and transpiration with depth. Furthermore, the value for  $KAI_{ox}$  was adapted to  $10^7 \text{ mol}^{-2} \text{ l}^2$  based on soil solution measurements in the topsoil of 150 forest stands in the Netherlands (Heij et al., 1991).

Figure 5.8 shows that the depth considered had a considerable effect on the frequency distribution of the Al concentration. The area where a critical Al concentration of  $0.2 \text{ mol}_c \text{ m}^{-3}$  is exceeded at a depth of 25 cm was calculated at 25% compared to 43% at the bottom of the rootzone (cf Fig. 5.8A). The effect on the Al/BC ratio was much less (Fig. 5.8B), since the decrease in water flux due to transpiration also caused an increase in the BC concentration. However, the Al/BC ratio thus derived is not reliable since the effect of BC cycling by litterfall and mineralization was not included. This will be illustrated in Section 5.2 (De Vries et al., 1994d) where the application of the multi-layer model MACAL for the Netherlands is described.

#### Description of denitrification

Another aspect related to the model structure is the way in which denitrification is included. First of all, use of Eq. (5.26) implies that denitrification is a function of the critical, rather arbitrarily selected,  $\text{NO}_3$  concentration. Secondly, the assumption that N immobilization is a faster process than denitrification (cf Eq. 5.23) implies that any increase in the deposition level of N will first cause an increase in the rate of N immobilization which will also be a function of N deposition (unless the system is N saturated). Using a critical N immobilization rate equal to zero, this implies that the N

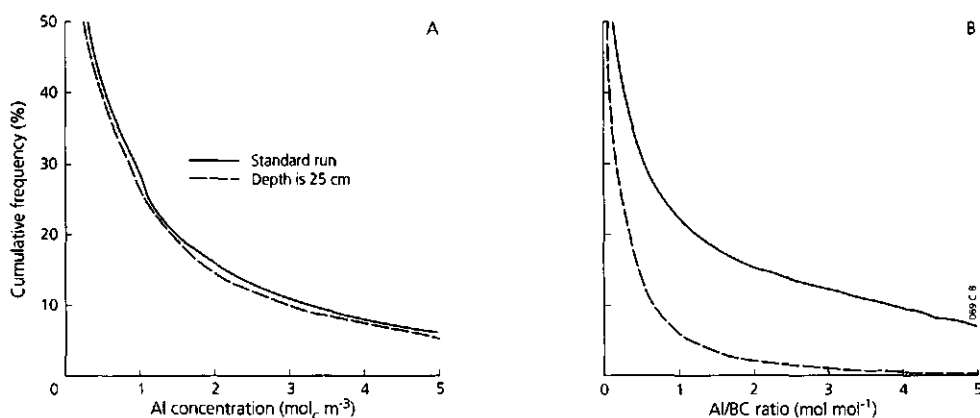


Figure 5.8 Inverse cumulative frequency distributions of the Al concentration (A) and Al/BC ratio (B) in European forest soils at two different depths.

input should not be higher than N uptake and a 'natural' leaching rate. In this situation, denitrification is also negligible. Consequently, we investigated the effect of neglecting denitrification on the critical N load and the area where critical N loads are exceeded. In fact, the maps that have been produced until now by various countries are mostly based on the SMB model excluding denitrification (Hettelingh et al., 1991; cf Section 4.1; Eq. 4.5). Results are shown in Figure 5.9. Neglecting denitrification increased the forested area where deposition exceeds critical N loads from 50% to 61%. However, denitrification most probably does affect the N immobilization rate appreciably. When one assumes that denitrification is a faster process than N immobilization, the values calculated in this report still hold. In reality both processes occur simultaneously thus influencing each other.

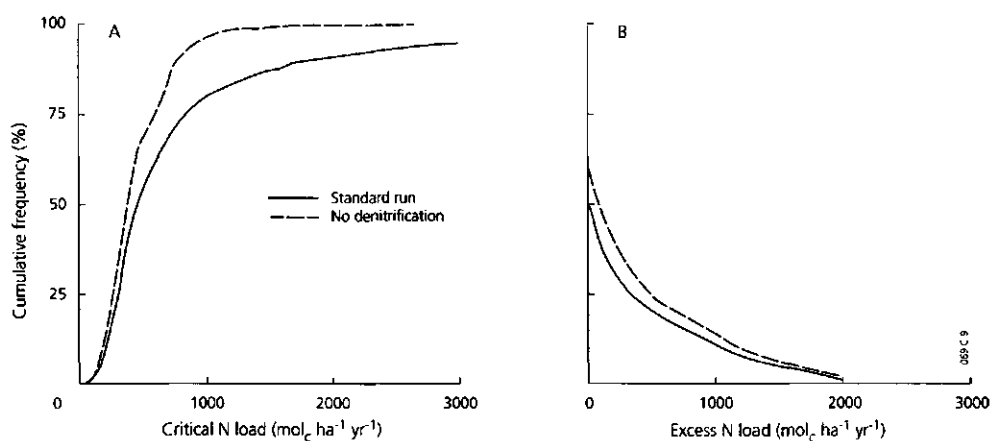


Figure 5.9 Cumulative frequency distributions of the critical N load (A) and the amount by which it is exceeded (B) including and excluding the effect of denitrification

#### Impacts of hydrologic processes

Another uncertainty in the model is the neglect of surface runoff in areas with steep slopes. This applies especially to areas with slope class c (slope above 30%), and to a lesser extent to areas with slope class b (slope between 8 and 30%) which mainly occur in southern and eastern Europe including Austria and Switzerland (ca. 33% of all forest in Europe). Surface runoff will decrease the precipitation excess, thus decreasing the critical load. However, surface runoff also contains N and S compounds. Consequently, the effect of neglecting this process is likely to be small since the present load is also decreased. A similar reasoning holds for the neglect of bypass flow in clay soils and hydrophobic soils.

A final important uncertainty related to model structure is the calculated increase in critical load with an increased precipitation excess. Using a semi-quantitative method,

Kuylenstierna and Chadwick (1989) assumed that an increase in the precipitation excess causes a decrease in the critical acid load for European forest soils. The rationale behind their approach is that the exchangeable base cation pool of soils is depleted more rapidly in areas with a high precipitation excess. The rationale behind the SMB and START model is that it is acceptable that an ecosystem comes in the Al buffer range as long as the Al concentration and Al/BC ratio remain below critical values. Consequently, an increased precipitation excess increases the critical load due to dilution of the mobilised Al. The effect is less pronounced when the Al/BC ratio criterion is used, since BC is diluted as well. However, even then an increased precipitation excess causes an increase in critical load due to a larger rate of H leaching.

The difference between the results of both methods becomes striking in high rainfall areas such as the Norwegian coast, Scotland and the Alpine region. The high critical loads calculated for these areas with the START (SMB) model might be questionable since a strong dilution of base cations may cause a decreased uptake, irrespective of the toxicity effect of Al. In other words, the high leaching rates of base cations in high rainfall areas may cause base cation deficiencies, since the available pool is too small to match the demand of the vegetation. However, this is not an acidification problem, and forest fertilizing is likely to be more effective in these areas than deposition reductions.

In this context, it is also important to note that Sumner et al. (1986) proposed to use the  $(Al/BC)^{3/2}$  ratio as a meaningful parameter for rooting performance. A similar index was proposed by Sverdrup et al. (1992), by assuming that root uptake is governed by an adsorption mechanism, analogous to competitive ion exchange between Al and BC. Using the  $(Al/BC)^{3/2}$  ratio, an increase in precipitation excess above 500 mm yr<sup>-1</sup> hardly affects the rate of acidity leaching.

## **Uncertainties in Input data**

### *Model inputs*

Comparison between model inputs used in this study and values derived in various individual countries (e.g. weathering rates in Sweden, Olsson et al., 1991; precipitation excesses in the Netherlands, De Vries et al., 1992b) indicated that the overall uncertainty in model inputs is less than 50%, although it can be more than 100% at specific sites. Except for the uncertainty in the weathering rate estimate itself, the uncertainty (reliability) of the soil map may also be significant. Furthermore, the depth of the rootzone can be lower than 50 cm, e.g. in lithosols. However, these soils only occupy a small fraction of the forested area in Europe (cf Table 5.3).

Effects of a 50% change in model inputs on the area where critical acid loads are exceeded (Table 5.9) show that a change in weathering rate and in precipitation excess seriously affected this area. An increase in the weathering rate and the precipitation

Table 5.9 Influence of model input variation on the percentage of the forested area in Europe where critical acid loads are exceeded

Forest type	Area where critical acid loads are exceeded (%)								
	Standard run	Weathering		Uptake		Drainage		log $KAl_{ox}$	
		-50%	+50%	-50%	+50%	-50%	+50%	-1	+1
Coniferous	52	66	45	50	54	63	46	48	53
Deciduous	33	41	26	32	33	40	28	29	35
All	45	57	38	44	46	55	40	41	48

excess (drainage rate) increases the critical acid load, by an increase in either the acid neutralization in the system or acid leaching from the system (cf Eq. 5.24), thus decreasing the area where critical acid loads are exceeded. The effect of a change in the Al hydroxide constant by a factor 10 was small. (The standard value used was  $10^8 \text{ mol}^2 \text{ l}^2$ ). An increase in this value causes a decrease in the critical H concentration (cf Eq. 5.3), thus decreasing the critical acid load. The effect of a 50% change in growth rate (uptake rate) appeared to be negligible. The decrease in critical acid load caused by an increased base cation uptake was almost completely compensated by an increased N uptake.

Results of variations in important model inputs differed for the various European countries. In several highly polluted countries, such as the Netherlands and Poland, effects were small. In several other countries such as France and Hungary, effects were substantial (De Vries et al., 1992a).

Although a change in growth rate hardly affected the critical acid load, it did affect the separate critical loads for N and S. An increased growth rate increases the critical N load (cf Eq. 5.26), whereas the critical S load decreases (cf Eq. 5.27). The area where critical N and S loads are exceeded appeared to vary between 36% and 62% for N and between 40% and 64% for S for a 50% variation in uptake rate. Again, effects appeared to be small in highly polluted countries, such as the Netherlands and Poland, whereas drastic changes occurred in several other countries such as Finland, Ireland and Romania (De Vries et al., 1992a).

An important uncertainty in the assessment is the neglect of N immobilization. This is related to the long time period considered. Accepting a 10% change in N amount (C/N ratio) during a 100 yr period would lead to an immobilization rate of about  $400 \text{ mol}_c \text{ ha}^{-1} \text{ yr}^{-1}$  in Dutch forest soils (cf Section 4.1). Using this rate the area where critical N loads are exceeded would decrease to 23%, i.e. 32% of all coniferous and 9% of all deciduous forests (cf Fig. 5.3A).

#### Filter factors

The area where critical loads are exceeded is also influenced by the filtering factors for

SO<sub>x</sub>, NO<sub>x</sub>, NH<sub>x</sub> and base cations, since they affect the present loads. Actually, for base cations, the term 'dry deposition factor' is used. However, assuming that total deposition on open land is equal to bulk deposition, this factor can also be seen as a filtering factor. The effect of neglecting enhanced deposition of S, N and base cations by (forest filtering of) dry deposition was investigated by assuming that the filtering factors for SO<sub>x</sub>, NO<sub>x</sub> and NH<sub>x</sub> are 1 and that the dry deposition factor for base cations is zero. Results are given in Table 5.10.

*Table 5.10 Influence of neglecting the effect of forest filtering on the percentage of coniferous and deciduous forests where critical loads for N, S and acidity are exceeded*

Forest type	Area where critical loads are exceeded (%)					
	N		S		Acidity	
	Standard run	No filtering	Standard run	No filtering	Standard run	No filtering
Coniferous	63	49	53	47	52	44
Deciduous	30	31	49	62	33	42
All	50	43	51	53	45	43

Table 5.10 shows that the overall effect of neglecting forest filtering on the forested area where critical acid loads are exceeded was very small, i.e. only 2%. Neglecting the effect of forest filtering appeared to decrease the area of coniferous forests in which critical loads are exceeded, whereas the opposite was true for deciduous forests, especially with respect to S. This is because the filtering factor for SO<sub>x</sub> on deciduous forests was assumed to be 1.0 in the standard run, whereas the filtering factor for base cations was 1.6. Consequently, the decreased filtering by deciduous forests only refers to the dry deposition of base cations, thus decreasing the critical S load and increasing its excess. In coniferous forests, with a standard filtering factor for SO<sub>x</sub> of 1.6, the decrease in base cation input was more than compensated by a decrease in S input.

## CONCLUSIONS

The comparison of present loads and critical loads for N, S and acidity presented in this Section indicated large exceedances in Western and Central Europe, i.e. the Netherlands, Belgium, Germany, Poland and former Czechoslovakia. In these countries the exceedance for N and S was generally more than 2000 mol<sub>c</sub> ha<sup>-1</sup> yr<sup>-1</sup> up to 3500 mol<sub>c</sub> ha<sup>-1</sup> yr<sup>-1</sup> for N (Netherlands, Belgium, Germany) and 12000 mol<sub>c</sub> ha<sup>-1</sup> yr<sup>-1</sup> for S (former Czechoslovakia, Poland and Germany). Large exceedances were also calculated for parts of the UK, France, Romania and the former USSR.

The area where critical N and S loads are exceeded was calculated to be nearly equal (50% vs 52% respectively). However, the critical N loads calculated relate to vegetation changes in forests. Much larger critical N loads and smaller areas exceeding these loads (up to 29%) were obtained when the critical  $\text{NO}_3$  concentration in the soil solution was related to its inherent acidifying effect, affecting forest vitality. Except for the critical  $\text{NO}_3$  concentration, the uncertainty in the area where critical N loads are exceeded is also significantly influenced by the uncertainty in N immobilization rate and to a lesser extent in N uptake and the way in which denitrification is included. Sensitivity analysis showed a range between 23% and 62%.

The forested area where critical acid loads are exceeded was estimated at 45%. Sensitivity analysis showed that this area is much more influenced by the uncertainty in the critical chemical values for Al and Al/BC, and the soil depth where they are applied (a range between 16% and 71%), than by the uncertainty in model inputs (a range between 38% and 57%). However, although the estimated uncertainty in the area where critical loads are exceeded was large (generally about  $\pm 50\%$  of the average estimated value for N, S and acidity), it is clear that present loads in Western and Central Europe exceed the critical values in large areas.

For a correct interpretation of critical loads, it should be emphasized that an exceedance does not necessarily cause a visible effect on forests, due to the complex interactions in these ecosystems. They mainly have a signal function. However, an exceedance of the critical loads involves a certain risk to the health of forests which increases with the magnitude and the duration of the exceedance. Consequently, the calculated large exceedances in Western and Central Europe do not imply the dieback of these forests, but it certainly means that the health of these forests is endangered. This is in accordance with the reports on declining forest vitality in this area.



## 5.2 CRITICAL LOADS AND THEIR EXCEEDANCE ON FORESTS IN THE NETHERLANDS

### ABSTRACT

*Critical acid loads for Dutch forests were derived using a multi-layer steady-state model that includes canopy interactions, nutrient cycling, mineral weathering and N transformations. Values were calculated for combinations of 12 tree species and 23 soil types for a 10 km x 10 km grid. Critical acid loads thus derived increased with decreasing soil depth. Nearly 90% of the values varied approximately between 1500 and 4000 mol<sub>c</sub> ha<sup>-1</sup> yr<sup>-1</sup> at 10 cm soil depth and between 750 and 2000 mol<sub>c</sub> ha<sup>-1</sup> yr<sup>-1</sup> at the bottom of the rootzone. Separate critical loads calculated for N and S at the bottom of the rootzone varied between approximately 300 and 1000 mol<sub>c</sub> ha<sup>-1</sup> yr<sup>-1</sup> for N and between 150 and 1250 mol<sub>c</sub> ha<sup>-1</sup> yr<sup>-1</sup> for S. Using deposition data of 1990, a median reduction of the deposition by approximately 75% was calculated to achieve the critical loads at the bottom of the rootzone. The overall uncertainty in this value was estimated to be about 10%, although it can be much larger for specific soil types such as clay and peat soils. For N a larger reduction deposition percentage was calculated than for S, especially for coniferous forests with a high present N input.*

### INTRODUCTION

Acid deposition affects the vitality of forest ecosystems both by direct effects on the forest canopy and by indirect soil mediated effects on the roots. Recent information suggests that direct effects of gaseous air pollutants, such as SO<sub>2</sub>, NO<sub>x</sub>, NH<sub>3</sub> and O<sub>3</sub>, only play a minor role in the declining vitality of Dutch forests (Heij et al., 1991). Critical concentration levels of these gases, related to short-term and long-term exposure (cf De Vries and Gregor, 1991) are rarely exceeded. Indirect effects, i.e. nutrient imbalances caused by soil acidification and N accumulation, are likely to be more important (Heij et al., 1991).

Recent investigations in 150 Dutch forest stands, i.e. Scots pine (45), black pine (15), Douglas fir (15), Norway spruce (15), Japanese larch (15), oak (30) and beech (15) showed that the leaves and needles of these three species are characterized by a high N content and a (relative) deficiency of Mg and P (Hendriks et al., 1994). The decrease in forest vitality due to (relative) deficiencies in cation nutrients such as Mg, is considered to be at least partly caused by the mobilization of Al in soils in response to S and N inputs (Heij et al., 1991). In this context critical Al concentrations and Al/Ca ratios have been derived (Section 4.2; De Vries, 1993). A strong decrease in pH in response to depletion of secondary Al compounds may also play a role (Houdijk, 1993a). Furthermore, elevated N inputs increases the N content of foliage and soil humus, which in turn may lead to an increased susceptibility to fungal diseases, drought and frost (Boxman et al., 1986; Van den Burg et al., 1988) and to vegetation changes (Hommel et al., 1990).

Average critical loads for N and acidity for forests on non-calcareous sandy soils, are given in Section 4.1 and 4.2, respectively (cf De Vries, 1988; 1993). These results formed an important basis for the Dutch 'Acidification Abatement Policy'. However, this generic policy is not oriented towards specific regions, such as areas with intensive animal husbandry where present N loads are very high, or areas with forests on clay and peat soils, where critical N loads are likely to be higher. To develop additional regional policy measures, information is needed on the variation in critical loads for Dutch forest soils and the amounts by which they are exceeded. Such information was provided by De Vries et al. (1992b) using the one-layer steady-state mass balance model (SMB), model described in Section 4.2 (Eq. 4.23). Critical acid loads for forest soils in the Netherlands were derived with this model, requiring that both a critical Al concentration and Al/Ca ratio are not exceeded up to the bottom of the rootzone (to avoid root damage) and that depletion of secondary Al compounds does not occur (to avoid a strong pH decrease; cf Section 4.2). A similar approach was used in deriving critical acid loads for forest soils in Europe (Section 5.1; De Vries et al., 1994e). However, since most fine roots are concentrated in the topsoil (0-30 cm below the soil surface), it is more realistic to apply these criteria for that layer. Values for the Al concentration and Al/Ca ratio are generally lower in the topsoil than at the bottom of the rootzone because of variations in nutrient (Ca) cycling, transpiration and Al-mobilization with depth. So including effects of water uptake and nutrient cycling (foliar uptake, foliar exudation, litterfall, mineralization and root uptake) may be crucial to obtain realistic critical loads related to the forest topsoil.

This section provides an overview of the variation in critical acid loads derived by the multi-layer model MACAL (Model to Assess a Critical Acid Load). The criteria that were used to calculate critical loads are summarized in Table 5.11. The major aim of this study was to assess the effect of the soil depth considered on the estimated critical load. Emphasis is given on the difference between critical acid loads related to the forest topsoil, which are most relevant, and values related to the bottom of the rootzone, which are used in all critical load studies until now. Further important aims are a description of (i) the variation in critical loads and its exceedance as affected by tree species and soil type and (ii) the influence of uncertainties in critical chemical values, model structure and input data on the resulting critical acid loads. After a description of

*Table 5.11 Critical chemical values that were used to calculate critical loads for acidity and nitrogen in the Netherlands*

Critical load	Criterion	Unit	Value
Acidity <sup>1)</sup>	Al concentration	mol <sub>c</sub> m <sup>-3</sup>	0.2
	Al/Ca ratio	mol mol <sup>-1</sup>	1
	Al depletion <sup>2)</sup>	mol <sub>c</sub> ha <sup>-1</sup> yr <sup>-1</sup>	0
Nitrogen	NO <sub>3</sub> concentration	mol <sub>c</sub> m <sup>-3</sup>	0.1

<sup>1)</sup> Critical loads were calculated by using the minimum of three criteria

<sup>2)</sup> Stands for depletion of secondary Al compounds

the model, the application methodology, input data and the results obtained, attention is thus given to the uncertainties in critical load values.

## THE MACAL MODEL

### Modelling approach and basic process formulations

#### *Modelling approach*

MACAL predicts ionic concentrations at steady-state and thus only includes processes influencing acid production and consumption during infinite time. This implies that dynamic processes such as cation exchange, adsorption/-desorption of  $\text{SO}_4$  and  $\text{NH}_4$  and mineralization/immobilization dynamics of N, S and base cations (BC) are not considered in the assessment of a long-term critical load. Further assumptions in MACAL are: (i) negligible N fixation and (ii) negligible, reduction and precipitation of  $\text{SO}_4$ . A justification of these assumptions is given in Section 4.1 (N fixation) and Section 4.2 ( $\text{SO}_4$  interactions), respectively. Instead of defining discrete soil layers, ionic concentrations can be calculated at any given depth by using continuous functions for the various processes occurring in the rootzone. For given critical Al concentrations or Al/Ca ratios, MACAL can derive a critical acid load at any given depth. When  $\text{NH}_4$  leaching from the rootzone is negligible, the critical load value at the bottom of the rootzone calculated by MACAL is equal to the value derived by the SMB model (see further).

#### *Basic process formulations*

MACAL is based on the charge balance principle according to (cf Section 5.1; Eq. 5.1):

$$[\text{H}] + [\text{Al}_i] + [\text{Ca}] + [\text{Mg}] + [\text{K}] + [\text{Na}] + [\text{NH}_4] = [\text{NO}_3] + [\text{SO}_4] + [\text{Cl}] + [\text{HCO}_3] \quad (5.42)$$

As with START, the inorganic Al concentration,  $[\text{Al}_i]$ , is assumed to equal the total Al concentration minus the concentration of organic anions (RCOO) and consequently, RCOO has been neglected.

For X is Ca, Mg, K, Na,  $\text{NH}_4$ ,  $\text{NO}_3$ ,  $\text{SO}_4$  and Cl, the concentration at each depth z is calculated as (cf Section 5.1; Eq. 5.2):

$$[\text{X}](z) = \frac{X_{in} + X_{in}(z)}{P - E_i - E_s - E_f(z)} \quad (5.43)$$

where  $X_{in}$  is the sum of all input fluxes to the soil, and  $X_{in}(z)$  is the cumulative sum of all interaction fluxes in the soil at depth z (both in  $\text{mol}_c \text{ ha}^{-1} \text{ yr}^{-1}$ ) and where P is precipitation,  $E_i$  is interception evaporation,  $E_s$  is actual soil evaporation and  $E_f(z)$  is the

cumulative transpiration at depth  $z$  (all in  $\text{m}^3 \text{ha}^{-1} \text{yr}^{-1}$ ). The sum of the input and the cumulative interaction fluxes at depth  $z$  is equal to the leaching flux at this depth. The difference between precipitation and the various evapotranspiration terms is equal to the water flux at depth  $z$ .

The Al concentration at depth  $z$  is calculated by assuming equilibrium with Al hydroxides according to (cf Section 5.1; Eq. 5.3):

$$[\text{Al}_i](z) = K\text{Al}_{\text{ox}}(z) \cdot ([\text{H}](z))^3 \tag{5.44}$$

where  $K\text{Al}_{\text{ox}}(z)$  is calculated as:

$$K\text{Al}_{\text{ox}}(z) = 10^{\alpha + \beta \log(z/T_{rz})} \tag{5.45}$$

where  $T_{rz}$  is the thickness of the rootzone (m) and where  $\alpha$  and  $\beta$  are constants, which determine the dissolution constant at the bottom of the root zone ( $\alpha$ ) and the change in this constant within the rootzone ( $\beta$ ). This relationship is based on soil solution data from 40 sites at 4 depths in acid sandy forest soils (Kleijn et al., 1989).

The  $\text{HCO}_3^-$  concentration at each depth is calculated as (cf Section 5.1; Eq. 5.4):

$$[\text{HCO}_3^-](z) = K\text{CO}_2(z) \cdot p\text{CO}_2 / [\text{H}](z) \tag{5.46}$$

Combination of Eqs. (5.42) to (5.46) for given values for  $X_{in}$  and  $X_{int}(z)$  (see below) yields one unknown i.e.  $[\text{H}](z)$ , which is solved iteratively.

## Description of input and interaction fluxes

### Input fluxes

Input fluxes in MACAL are throughfall, i.e. deposition corrected for the effects of nutrient uptake or exudation by the forest canopy, and mineralization. Since MACAL is a steady state model, mineralization is put equal to litterfall except for N. The amount of N that is mineralized is set equal to the N input by litterfall minus a long-term N immobilization rate, which is assumed to occur above the mineral soil. This is accounted for in the  $\text{NH}_4$  input, since N is mineralized in the form of  $\text{NH}_4$ . The input fluxes of BC (Base cations, i.e. Ca, Mg, K, Na),  $\text{SO}_4$ ,  $\text{NH}_4$  and  $\text{NO}_3$  ( $\text{mol}_c \text{ha}^{-1} \text{yr}^{-1}$ ) are calculated as:

$$\text{BC}_{in} = \text{BC}_{ld} + \text{BC}_{lf} + \text{BC}_{fe} \tag{5.47}$$

$$SO_{4,in} = SO_{4,td} + SO_{lf} - SO_{4,fu} \quad (5.48)$$

$$NH_{4,in} = NH_{4,td} + N_{lf} - NH_{4,fu} - N_{im} \quad (5.49)$$

$$NO_{3,in} = NO_{3,td} - NO_{3,fu} \quad (5.50)$$

where the subscript *td* stands for total deposition, *fe* for foliar exudation, *fu* for foliar uptake, *lf* for litterfall and *im* for immobilization. Input fluxes of Na and Cl are set equal to the total deposition assuming a negligible effect of canopy interactions and litterfall (mineralization) for these ions. The total input flux of H is calculated from the charge balance equation (Eq. 5.42).

Foliar uptake of  $NH_4$ ,  $NO_3$ ,  $SO_4$  and H is described as a linear function of total deposition. The sum of foliar exudation of Ca, Mg and K is set equal to the sum of foliar uptake of  $NH_4$  and H, assuming complete cation exchange (Roelofs et al., 1985; Ulrich, 1983). It has been assumed that H and  $NH_4$  in deposition are taken up with equal preference during exchange with base cations from the forest canopy. The foliar exudation flux of each individual base cation,  $BC_{fe}$ , is calculated as:

$$BC_{fe} = frBC_{fe} \cdot (H_{fu} + NH_{4,fu}) \quad (5.51)$$

where  $frBC_{fe}$  is the foliar exudation fraction of Ca, Mg or K (-). The sum of  $frCa_{fe}$ ,  $frMg_{fe}$  and  $frK_{fe}$  equals 1.

The litterfall of N ( $NH_4$ ), Ca, Mg, K and S ( $mol_c \text{ ha}^{-1} \text{ yr}^{-1}$ ) is described as the product of a litterfall rate constant ( $yr^{-1}$ ), the amount of leaves or needles ( $kg \text{ ha}^{-1}$ ) and the element content of X in leaves ( $mol_c \text{ kg}^{-1}$ ). For N, the effect of reallocation is included. Reallocation of N from the older needles to younger needles generally takes place before litterfall. However, at high N contents reallocation hardly occurs (Oterdoom et al., 1987). Consequently, the reallocation fraction,  $fr_{re}$ , is described as a function of the N content according to:

$$fr_{re} = fr_{re,max} \cdot \left( \frac{ctN_{lv,max} - ctN_{lv}}{ctN_{lv,max} - ctN_{lv,min}} \right) \quad (5.52)$$

where  $ctN_{lv,max}$  is a maximum N content in leaves (%) above which no reallocation occurs and  $ctN_{lv,min}$  is a minimum N content in leaves below which maximum reallocation takes place. Based on data by Van den Burg et al. (1988) and Van den Burg and Kiewit (1989), the N content in leaves,  $ctN_{lv}$ , is also calculated as a linear function of the N deposition in a deposition range between 1500 and 7000  $mol_c \text{ ha}^{-1} \text{ yr}^{-1}$ .

### Interaction fluxes

The interaction fluxes for Ca, Mg, K, Na, SO<sub>4</sub>, NH<sub>4</sub> and NO<sub>3</sub> accounted for in MACAL are base cation weathering, root uptake, nitrification and denitrification. Interaction fluxes at depth  $z$  (mol<sub>c</sub> ha<sup>-1</sup> yr<sup>-1</sup>) are described according to:

$$BC_{int}(z) = BC_{we}(z) - BC_{ru}(z) \quad (5.53)$$

$$SO_{4,int}(z) = -SO_{4,ru}(z) \quad (5.54)$$

$$NH_{4,int}(z) = -NH_{4,ni}(z) - NH_{4,ru}(z) \quad (5.55)$$

$$NO_{3,int}(z) = NH_{4,ni}(z) - NO_{3,ru}(z) - NO_{3,de}(z) \quad (5.56)$$

where the subscript *we* stands for weathering, *ru* for root uptake, *ni* for nitrification and *de* for denitrification. The cumulative base cation weathering flux at depth  $z$ , BC<sub>we</sub>( $z$ ) (mol<sub>c</sub> ha<sup>-1</sup> yr<sup>-1</sup>), is described as:

$$BC_{we}(z) = fr_{we,rz}(z) \cdot BC_{we,rz} \quad (5.57)$$

with

$$fr_{we,rz}(z) = \left( 1 - \left( \frac{T_{rz} - z}{T_{rz}} \right)^{we_{exp}} \right) \cdot T_{rz} \quad \text{for } z \leq T_{rz} \quad (5.58)$$

where BC<sub>we,rz</sub> is the weathering flux per meter soil in the rootzone (mol<sub>c</sub> ha<sup>-1</sup> yr<sup>-1</sup> m<sup>-1</sup>),  $fr_{we,rz}(z)$  is the weathering fraction in the rootzone at depth  $z$  (m),  $we_{exp}$  is a dimensionless weathering exponent. At the bottom of the rootzone, ( $z = T_{rz}$ ),  $fr_{we,rz}(z)$  equals  $T_{rz}$ .

The root uptake of the base cations Ca, Mg and K (for Na, root uptake has been neglected) and of SO<sub>4</sub>, NH<sub>4</sub> and NO<sub>3</sub> consists of net uptake for forest growth and maintenance uptake to resupply these nutrients, released by litterfall and foliar exudation, to the forest canopy. The cumulative root uptake fluxes for BC, SO<sub>4</sub>, NH<sub>4</sub> and NO<sub>3</sub> at each depth  $z$  within the rootzone (mol<sub>c</sub> ha<sup>-1</sup> yr<sup>-1</sup>) are thus described as:

$$BC_{ru}(z) = fr_{ru}(z) \cdot (BC_{fl} + BC_{le} + BC_{gu}) \quad (5.59)$$

$$SO_{4,ru}(z) = fr_{ru}(z) \cdot (S_{if} - SO_{4,tu}) \quad (5.60)$$

$$NH_{4,ru}(z) = fr_{ru}(z) \cdot (N_{if} - N_{tu} + N_{gu}) \cdot (NH_{4,in} / N_{in}) \quad (5.61)$$

$$NO_{3,ru}(z) = fr_{ru}(z) \cdot (N_{if} - N_{tu} + N_{gu}) \cdot (NO_{3,in} / N_{in}) \quad (5.62)$$

with:

$$fr_{ru}(z) = fr_{ru,hl} + \left( 1 - \left( \frac{T_{rz} - z}{T_{rz}} \right)^{ru_{exp}} \right) \cdot (1 - fr_{ru,hl}) \quad \text{for } z \leq T_{rz} \quad (5.63)$$

where  $gu$  stands for growth uptake, and  $N$  for  $NH_4$  plus  $NO_3$ , and where  $fr_{ru}(z)$  is the cumulative root uptake fraction in the rootzone at depth  $z$  (-),  $fr_{ru,hl}$  is the root uptake fraction in the humus layer above the mineral soil and  $ru_{exp}$  is a dimensionless root uptake exponent. For  $ru_{exp} = 1$  the uptake pattern is uniform, for  $ru_{exp} = 2$  it is linear, for  $ru_{exp} = 3$  it is quadratic etc. The value of  $ru_{exp}$  is influenced by the root distribution with depth. The water uptake pattern is described similarly:

$$E_r(z) = fr_{ru}(z) \cdot E_t \quad (5.64)$$

where  $E_r(z)$  is the cumulative transpiration (water uptake by roots) at depth  $z$ . At  $z$  is  $T_{rz}$ ,  $fr_{ru}(z)$  equals 1 and root uptake is at its maximum.

Nitrification and denitrification are described according to:

$$NH_{4,nl}(z) = fr_{ni,hl} \cdot NH_{4,in} + fr_{nl}(z) \cdot \left( (1 - fr_{ni,hl}) \cdot NH_{4,in} - NH_{4,ru} \right) \quad (5.65)$$

$$NO_{3,de}(z) = fr_{de}(z) \cdot (NO_{3,in} + NH_{4,nl}(z) - NO_{3,ru}) \quad (5.66)$$

with

$$fr_{nl}(z) = \left( 1 - \left( \frac{T_{ni} - z}{T_{ni}} \right)^{ni_{exp}} \right) \cdot fr_{ni,max} \quad \text{for } z \leq T_{ni} \quad (5.67)$$

$$fr_{de}(z) = \left( 1 - \left( \frac{T_{de} - z}{T_{de}} \right)^{de_{exp}} \right) \cdot fr_{de,max} \quad \text{for } z \leq T_{de} \quad (5.68)$$

where  $NH_{4,ni}(z)$  and  $NO_{3,de}(z)$  are the cumulative nitrification and denitrification flux at depth  $z$  ( $mol_c ha^{-1} yr^{-1}$ ),  $fr_{ni,hl}$  is the nitrification fraction in the humus layer,  $fr_{ni,max}$  and  $fr_{de,max}$  are the maximum nitrification and denitrification fraction,  $T_{ni}$  and  $T_{de}$  are the thicknesses of the zones where nitrification and denitrification occur and  $ni_{exp}$  and  $de_{exp}$  are dimensionless nitrification and denitrification exponents, respectively. Below  $z$  is  $T_{ni}$  and  $T_{de}$  respectively, the values of  $fr_{ni}(z)$  and  $fr_{de}(z)$  are set equal to  $fr_{ni,max}$  and  $fr_{de,max}$  respectively.

### Calculation of critical loads for acidity, nitrogen and sulphur

#### Critical loads within the rootzone

In the Netherlands, the total deposition of acidity is defined as:

$$Ac_{td} = SO_{x,td} + NO_{x,td} + NH_{x,td} - BC_{wd}^* \quad (5.69)$$

where  $Ac_{td}$ ,  $SO_{x,td}$ ,  $NO_{x,td}$  and  $NH_{x,td}$  stand for the total deposition of acidity,  $SO_x$ ,  $NO_x$  and  $NH_x$  respectively and  $BC_{wd}^*$  for the Cl-corrected wet (bulk) deposition of base cations (all in  $mol_c ha^{-1} yr^{-1}$ ; cf Section 4.2; Eq. 4.21). The critical load of acidity at a given depth  $z$  cannot be derived directly since the deposition of  $SO_4$ ,  $NH_4$  and/or  $NO_3$  influences foliar uptake, foliar exudation, litterfall, nitrification and denitrification, which in turn affects the concentration of Al and the molar Al/Ca ratio. The critical load is thus obtained in MACAL by solving the Eqs. (5.42)-(5.68), while substituting a critical value for  $[Al]$  in Eq. (5.42). The critical inorganic Al concentration,  $[Al](crit)$ , was calculated such that both a critical Al concentration and Al/Ca ratio was not violated and depletion of secondary Al compounds did not occur (cf Table 5.11). The minimum of three values was thus taken (cf Section 4.2; De Vries, 1993); i.e. (i) a value assigned directly, (ii) a value derived from a critical equivalent Al/Ca ratio,  $RAICa(crit)$ , according to:

$$[Al](z)(crit) = RAICa(crit) \cdot [Ca](z) \quad (5.70)$$

and (iii) a value determined by the requirement that leached Al can be replenished by Al weathering from silicates,  $Al_{we}(z)$ , to avoid depletion of secondary Al compounds:

$$[Al](z)(crit) = Al_{we}(z) / (P - E_i - E_s - E_f(z)) \quad (5.71)$$

where  $Al_{we}(z)$  is the cumulative Al weathering flux from silicates at depth  $z$  ( $mol_c ha^{-1} yr^{-1}$ ) which is related to base cation weathering according to:



$$Al_{we}(z) = 3 \cdot Ca_{we}(z) + 0.6 \cdot Mg_{we}(z) + 3 \cdot K_{we}(z) + 3 \cdot Na_{we}(z) \quad (5.72)$$

The stoichiometric equivalent ratios of Al to BC weathering used in Eq. (5.72) have been based on the assumption that mineral soils mainly contain Al silicates, such as anorthite, chlorite, microcline and albite. Microcline and albite are commonly present in the sandy soils in the Netherlands, but the assumption that Ca originates from anorthite and Mg from chlorite is poorly supported by field data. There are various minerals containing Ca and Mg but their nature and contribution to the release of Ca and Mg is difficult to determine (cf Section 2.2 for Al/BC weathering ratios).

The critical Al concentration determines the concentrations of H and HCO<sub>3</sub> through Eqs. (5.44) and (5.46). The concentrations of all other ions are determined by Eq. (5.43) in combination with the equations describing the various input and interaction fluxes (Eqs. 5.47 to 5.68). The only unknown values in this combined set of equations is the deposition of NH<sub>4</sub> (NH<sub>x</sub>), NO<sub>3</sub> (NO<sub>x</sub>) and SO<sub>4</sub> (SO<sub>x</sub>) at critical load. MACAL has two options to calculate these three values.

In the first option the critical N load refers to the acidifying effect of N, i.e. its potential to mobilize Al above a critical value, together with S deposition. Using this option, the critical loads are calculated by assuming that the ratios of NH<sub>4</sub> (and NO<sub>3</sub>) to total N deposition and the ratio of N to S deposition at critical loads are equal to the present deposition ratios. This leads to one equation with one unknown, i.e. the critical S load at depth z, which is solved iteratively. The 'critical' N load at depth z, N<sub>td</sub>(crit)(z), is calculated according to:

$$N_{td}(z)(crit) = RNS_{td} \cdot S_{td}(z)(crit) \quad (5.73)$$

where RNS<sub>td</sub> is the ratio of the present N to S deposition. The critical acid load, Ac<sub>td</sub>(z)(crit), is calculated as (cf Eq. 5.69):

$$Ac_{td}(z)(crit) = S_{td}(z)(crit) + N_{td}(z)(crit) - BC_{wd}^* \quad (5.74)$$

In the second option, which was used in this study, the critical load for N refers to the eutrophying effect of N, i.e. the adverse effects of N accumulation. This critical N load, N<sub>td</sub>(z)(crit), is calculated independent of the soil depth considered, according to (cf Section 5.1; Eq. 5.25):

$$N_{td}(crit) = N_{gu} + N_{im}(crit) + N_{de}(crit) + NO_{3,le}(crit) \quad (5.75)$$

where  $\text{NO}_{3,le}(\text{crit})$  is a critical  $\text{NO}_3$  leaching rate below the rootzone, that has been calculated as:

$$\text{NO}_{3,le}(\text{crit}) = PE \cdot [\text{NO}_3](\text{crit}) \quad (5.76)$$

where  $[\text{NO}_3](\text{crit})$  is a critical  $\text{NO}_3$  concentration, and where  $PE$  is the precipitation excess, calculated as:

$$PE = P - E_i - E_s - E_t \quad (5.77)$$

Eq. (5.75) is based on the assumption that any N input above the sum of net N uptake by trees, N removal by denitrification, a long-term critical rate of N immobilization and  $\text{NO}_3$ -N leaching will lead to increased N contents in soil organic matter that will cause unwanted vegetation changes. Using Eq. (5.75) for  $N_{td}(\text{crit})$  and assuming that the ratio of  $\text{NH}_4$  (and  $\text{NO}_3$ ) to total N deposition at critical loads equals the present deposition ratio, the critical S load at depth  $z$  is solved iteratively. Again, the critical acid load is calculated according to Eq. (5.74).

#### *Critical loads at the bottom of the rootzone*

When the soil depth ( $z$ ) is equal to the thickness of the rootzone ( $z = T_{rz}$ ), the effect of nutrient cycling and canopy interactions can be neglected (cf Eqs. 5.47 to 5.50 with Eqs. 5.59 to 5.62, with  $fr_{ru}(z) = 1$ ). When moreover nitrification at this depth is assumed to be complete, the  $\text{NH}_4$  concentration becomes zero (cf Eq. 5.43, 5.55 and 5.65 with  $fr_{ni}(z) = 1$ ) and the  $\text{NO}_3$  concentration equals (cf Eqs. 5.43, 5.56 and 5.65 with  $fr_{ni}(z) = 1$  and  $fr_{ru}(z) = 1$ ):

$$[\text{NO}_3] = (N_{in} - N_{ru} - N_{de}) / PE \quad (5.78)$$

where  $N_{ru}$  is the sum of  $\text{NH}_4$  and  $\text{NO}_3$  uptake by roots as defined in the Eqs. (5.61) and (5.62) and  $N_{de}$  equals  $\text{NO}_{3,de}$  defined in Eq. (5.66) (with  $fr_{de}(z) = fr_{de}$ ). In this situation the critical load of acidity can be calculated directly. Combination of Eq. (5.78) with the Eqs. (5.49), (5.50), (5.61) and (5.62) with  $fr_{ru}(z) = 1$  gives:

$$[\text{NO}_3] = (N_{td} - N_{gu} - N_{de} - N_{im}(\text{crit})) / PE \quad (5.79)$$

Similarly, the concentration of  $\text{SO}_4$  (cf Eq. 5.43, 5.48 and 5.60 with  $fr_{ru}(z) = 1$ ) and of BC (cf Eqs. 5.43, 5.47, 5.53, 5.57 and 5.59 with  $fr_{ru}(z) = 1$  and  $fr_{we,rz}(z) = T_{rz}$ ) equals:

$$[\text{SO}_4] = (\text{SO}_{4,td}) / PE \quad (5.80)$$

$$[BC] = (BC_{td} + BC_{we} - BC_{gu}) / PE \quad (5.81)$$

Combination of Eqs. (5.42), (5.79), (5.80) and (5.81) and defining acidity leaching,  $Ac_{le}$ , ( $\text{mol}_c \text{ ha}^{-1} \text{ yr}^{-1}$ ) according to (cf Eq. 5.19):

$$[Ac] = ([Al_i] + [H] - [HCO_3]) \cdot PE \quad (5.82)$$

gives

$$S_{td} + N_{td} = BC_{td}^* + BC_{we} - BC_{gu} + N_{gu} + N_{im} + N_{de} + Ac_{le} \quad (5.83)$$

where  $BC^*$  stands for the sum of Ca, Mg, K and Na minus Cl.

A critical acid load can be derived by defining a critical value for acidity and N immobilization and subtracting the seasalt corrected wet deposition of base cations from the total deposition in the right hand side of Eq. (5.83) (cf Eq. 5.69) according to (Section 4.2; Eq. 5.24):

$$Ac_{td}(\text{crit}) = BC_{dd}^* + BC_{we} - BC_{gu} + N_{gu} + N_{im}(\text{crit}) + N_{de}(\text{crit}) + Ac_{le}(\text{crit}) \quad (5.84)$$

where  $BC_{dd}^*$  is the seasalt corrected dry deposition of base cations. At the depth of the rootzone a separate critical load for S,  $S_{td}(\text{crit})$ , is also calculated according to (cf Eqs. 5.75 and 5.83):

$$S_{td}(\text{crit}) = BC_{td}^* - BC_{gu} + BC_{we} + Ac_{le}(\text{crit}) - NO_{3,le}(\text{crit}) \quad (5.85)$$

## APPLICATION METHODOLOGY AND INPUT DATA

### Application methodology

To limit the number of calculations with MACAL, areas were defined in which the deposition was assumed to be constant. Within each so-called deposition area, critical loads were calculated for all major combinations of tree species (12) and soil types (23). For the deposition area a 10 km x 10 km gridcell was used, because reasonable deposition estimates exist at this scale. Tree species included were *Pinus sylvestris* (Scots pine; 38.2%), *Pinus nigra* (black pine; 5.9%), *Pseudotsuga menziesii* (Douglas fir; 5.5%), *Picea abies* (Norway spruce; 5.1%), *Larix leptolepis* (Japanese larch; 5.7%), *Quercus robur* (oak; 17.4%), *Fagus sylvatica* (beech; 4.1%), *Populus spec* (poplar; 4.6%), *Salix spec* (willow; 2.4%), *Betula pendula* (birch; 7.4%), *Fraxinus nigra* (ash;

1.9%) and *Alnus glutinosa* (black alder; 1.9%). Soil types were differentiated in 18 non-calcareous sandy soils (cf Table 5.12), calcareous sandy soils, loess soils, non-calcareous clay soils, calcareous clay soils and peat soils on the basis of a recent 1 : 250 000 soil map of the Netherlands (Steur et al., 1986).

Information on the area (distribution) of each specific forest-soil combination in each gridcell containing forest (434) was derived by overlaying the digitized 1 : 250 000 soil map, with a spatial resolution of 100 m x 100 m, and a data base with tree species information, with a spatial resolution of 500 x 500 m (CBS, 1985). The total number of forest soil combinations for all grids, i.e. the total number of MACAL calculations, equalled 17102. The number of forest/soil combinations (calculations) in a grid varied between 1 and 125. An overview of the percentage of coniferous - and deciduous forests on the various soil types in the Netherlands thus derived is given in Table 5.12.

Nearly all coniferous forests are located on non-calcareous sandy soils, whereas about 34% of the different deciduous forests is located on other soils as well (Table 5.12). The non-calcareous sandy soils included, which cover about 85% of the Dutch forested area, are dominated by Podzols, followed by Arenosols (Table 5.13).

Table 5.12 Forest coverage on sand, loess, clay, peat and calcareous soils in the Netherlands as a percentage of the total forested area<sup>1)</sup>

Soil type		Coverage (%)		
General	FAO (1988)	Coniferous forests	Deciduous forests	All forests
Sand <sup>2)</sup>	Podzols <sup>3)</sup>	57.9	26.9	84.8
Peat	Histosols	0.4	3.1	3.5
Loess	Luvissols	0.4	1.1	1.5
Clay <sup>2)</sup>	Eutric Fluvisols	0.5	3.3	3.8
Calcareous <sup>4)</sup>	Calcaric Fluvisols	0.8	5.6	6.4
		$\Sigma=60.0$	$\Sigma=40.0$	$\Sigma=100.0$

<sup>1)</sup> The total forested area in the Netherlands is about 320 000 ha, which is approximately 9.5% of the total area of the Netherlands.

<sup>2)</sup> Refers to non-calcareous soils.

<sup>3)</sup> Including Gleysols, Arenosols and Anthrosols.

<sup>4)</sup> Refers to sandy soils (2.2%) and clay soils (4.2%).

For all the non-calcareous sandy soil types a distinction was made between fine and coarse sandy variants (cf Table 5.13), to account for differences in weathering and transpiration rate.

*Table 5.13 Forest coverage on non-calcareous sandy forest soils in the Netherlands as a percentage of the total forested area<sup>1)</sup>*

Soil type FAO (1988)	Coverage (%)		
	fine sand	coarse sand	All
Cambic Podzol	2.7	8.7	11.4
Gleyic Podzol	14.9	0.3	15.2
Carbic Podzol	11.3	8.3	19.6
Fimic Anthrosol <sup>2)</sup>	7.5	0.7	8.2
Umbric Gleysol	4.1	0.1	4.2
Gleyic Arenosol	0.5	0.1	0.6
Haplic Arenosol	13.1	1.1	14.2
Associations <sup>3)</sup>	11.2	0.2	11.4
	$\Sigma=65.3$	$\Sigma=19.5$	$\Sigma=84.8$

<sup>1)</sup> The total forested area in the Netherlands is about 320 000 ha, which is approximately 9.5% of the total area of the Netherlands.

<sup>2)</sup> Including podzols with an anthropogenic humus layer (no suitable equivalent in the FAO classification).

<sup>3)</sup> Associations are included in the calculations by considering the dominant soil type.

### Assessment of input data

Input data for the MACAL model can be divided in system inputs and parameters. These data were derived as a function of location (deposition area) and receptor (the combination of tree species and soil type) as shown in Table 5.14.

*Table 5.14 Influence of location, tree species and soil type accounted for in the assessment of input data for MACAL<sup>1)</sup>*

Data related to	Location	Tree species	Soil type
Atmospheric deposition	x	x	
Canopy interactions	x	x	
Litterfall	-	x	-
Weathering	-	-	x
Growth uptake	-	x	x
Nitrogen transformations	-		x
Al dissolution			x
Precipitation	x		
Evapotranspiration	x	x	x

<sup>1)</sup> x means that the influence was taken into account, whereas - means that an influence does exist but the effect was either considered negligible or information was too scarce to include the effect

Data for all forest/soil combinations within all gridcells, were derived by using or deriving relationships (transfer functions) with basic land characteristics, such as tree species and soil type, which were available in geographic information systems.

### *Sulfur and nitrogen deposition*

Total deposition estimates for  $\text{SO}_x$ ,  $\text{NO}_x$  and  $\text{NH}_x$  for each gridcell for the year 1990 were derived by linear interpolation between the years 1985 and 1994 for which data were calculated with the deposition model TREND (Schutter and De Leeuw, 1991). The influence of tree species on atmospheric deposition was included by multiplying the deposition on the gridcell by filtering factors for spruce forests (Douglas fir and Norway spruce), pine forests (Scots pine and black pine) and deciduous forests including Japanese larch (see Section 2.3; Table 2.11). Since we assumed that the total deposition on a gridcell is correct, use of the forest filtering factors implied that the deposition on open land was less than average value for a gridcell. When the total deposition on open land became less than the (wet) bulk deposition, new values for these filtering factors were calculated according to a procedure described in De Vries (1991). This only occurred in a few densely forested gridcells in the central part of the Netherlands.

### *Base cation deposition*

Bulk deposition data for base cations and Cl were derived from 22 monitoring-stations for the period 1978-1985 (KNMI-RIVM, 1985) using inverse distance interpolation to obtain values for each gridcell (De Vries, 1991). However, bulk deposition only includes wet deposition (and a very small part of dry deposition). The influence of dry deposition on the total deposition was calculated by multiplying the bulk (wet) deposition by a dry deposition factor (cf Eq. 5.33), assuming that dry deposition is linearly related to wet deposition. Values used for this factor, derived from a comparison of Na in throughfall and bulk deposition (cf Bredemeier, 1988) for 42 forested sites in the Netherlands, were about 2.0 for spruce forests, 1.5 for pine forests and 1.0 for deciduous forests (De Vries, 1991).

### *Foliar uptake and foliar exudation*

Foliar uptake fractions for H and  $\text{NH}_4$  were calculated from total deposition of H and  $\text{NH}_4$  and foliar exudation of Ca, Mg and K according to:

$$frH_{fu} = frNH_{4,fu} = \frac{Ca_{fe} + Mg_{fe} + K_{fe}}{H_{td} + NH_{4,td}} \quad (5.86)$$

The foliar exudation of Ca, Mg and K was calculated from the difference between throughfall and total deposition for the 42 sites mentioned earlier. The total deposition of  $\text{NH}_4$  and H was based on the throughfall data of the ions on these sites. This is most likely an underestimate due to foliar uptake. Foliar uptake fractions for  $\text{SO}_4$  and  $\text{NO}_3$  were also derived from bulk and throughfall data using a procedure described in Van der Maas and Pape (1991). Foliar exudation fractions for Ca, Mg and K were calculated by dividing the Ca, Mg or K exudation by the total exudation of these cations. Values thus derived are given in Table 5.15.

**Table 5.15 Foliar uptake and foliar exudation fractions for coniferous and deciduous forests in the Netherlands**

Forest type	Foliar uptake fraction (-)			Foliar exudation fraction (-)		
	NH <sub>4</sub>	NO <sub>3</sub>	SO <sub>4</sub>	Ca	Mg	K
Coniferous	0.30	0.05	0.10	0.24	0.13	0.63
Deciduous	0.30	0.05	0.10	0.18	0.16	0.66

### Litterfall

Data used for the parameters influencing the N and BC fluxes in litterfall, are given in Table 5.16. The average biomass and litterfall rate constants were based on literature compilations by Kimmins et al. (1985) and De Vries et al. (1990) respectively. The Ca, Mg and K element contents in foliage were based on inventories of nearly 200 forest stands in the Netherlands in 1990 (Hendriks et al., 1994; Eelerwoude Ingenieursbureau, 1991).

Data for the minimum and maximum N contents were derived from Rodin and Bazilevich (1967), Kimmins et al. (1985) and De Vries et al. (1990). The maximum reallocation fraction of N was put to 0.36 based on Turner (1975). Due to limited data availability, the S content in foliage was set at 0.2% for all tree species (cf De Vries et al., 1990).

**Table 5.16 Average values used for biomass, turnover constants and element contents in foliage of the considered tree species**

Tree species	Leaf Biomass (kg ha <sup>-1</sup> )	Litterfall rate constant (yr <sup>-1</sup> )	Element content in foliage (%) <sup>1)</sup>				
			N <sup>2)</sup>		Ca	Mg	K
			min	max			
Scots pine	5500	0.55	1.0 (1.5)	3.5	0.24	0.07	0.60
black pine	7250	0.35	1.0 (1.5)	2.5	0.12	0.08	0.59
Douglas fir	10850	0.28	1.0 (1.5)	3.5	0.40	0.14	0.61
Norway spruce	16600	0.20	1.5 (2.5)	3.5	0.27	0.08	0.54
Japanese larch	4350	1.0	1.5 (2.5)	3.5	0.42	0.18	0.79
oak	3300	1.0	1.5 (2.5)	3.5	0.49	0.15	0.92
beech	2850	1.0	1.5 (2.5)	3.5	0.52	0.11	0.72
poplar	4000	1.0	1.5 (2.5)	3.5	1.17	0.21	1.07
willow	3500	1.0	1.5 (2.5)	3.5	1.07	0.21	0.85
birch	2500	1.0	1.5 (2.5)	3.5	0.98	0.25	0.93
ash	2500	1.0	1.5 (2.5)	3.5	0.81	0.28	0.97
black Alder	4000	1.0	1.5 (2.5)	3.5	0.98	0.23	1.15

<sup>1)</sup> In order to get values in mol<sub>c</sub> kg<sup>-1</sup>, the data on elements contents have to be divided by 1.4 for N, 2.0 for Ca, 1.2 for Mg and 3.9 for K

<sup>2)</sup> Values in brackets are the minimum N contents below which maximum reallocation occurs. Maximum N contents where reallocation is neglected were set equal to the absolute maximum values

### Base cation weathering

Mineral weathering rates of base cations were related to the rootzone which had a thickness varying between 60 and 80 cm depending upon soil type. Values for the non-calcareous sandy soils included in the regional application were derived on the basis of one-year batch experiments that were scaled to field data by dividing them by a factor 50. The value of 50 was based on a comparison of laboratory and field weathering rates, estimated by the depletion of base cations, in one soil profile (Hootsmans and Van Uffelen, 1991, cf Section 2.2 and Section 3.1). More information on the discrepancy between weathering rates derived in the field and in the laboratory has been given in Van Grinsven and Van Riemsdijk (1992). An overview of weathering rates thus derived is given in Table 5.17. The median value for the total base cation weathering rate in the rootzone of non-calcareous sandy forest soils in the Netherlands equalled  $200 \text{ mol}_c \text{ ha}^{-1} \text{ yr}^{-1}$  (cf Section 2.2 and 4.2). 5 and 95 percentile values were 180 and  $450 \text{ mol}_c \text{ ha}^{-1} \text{ yr}^{-1}$ , respectively.

Table 5.17 Average weathering rates in the rootzone used for the non-calcareous acid sandy forest soils of major importance in the Netherlands

Soil type (FAO, 1988)	Thickness rootzone (cm)	Weathering rate ( $\text{mol}_c \text{ ha}^{-1} \text{ yr}^{-1}$ ) <sup>1)</sup>				
		Ca	Mg	K	Na	Total
Cambic Podzol		45	20	75	80	220
Gleyic Podzol		50	95	20	35	200
Carbic Podzol		80	165	45	60	350
Fimic Anthrosol		215	225	80	60	580
Umbric Gleysol		40	310	45	75	450
Gleyic Arenosol		60	40	25	35	160
Haplic Arenosol		80	55	40	45	220

<sup>1)</sup> Values refer to fine sandy soils (cf Table 5.13). For coarse sandy variants weathering rates were assumed to be 75% of these values. This was based on results from, batch experiments on samples from fine and coarse sandy Cambic Podzols (Section 3.3; De Vries et al., 1994g).

Base cation weathering rates used for peat ( $200 \text{ mol}_c \text{ ha}^{-1} \text{ yr}^{-1}$ ) and loess soils ( $500 \text{ mol}_c \text{ ha}^{-1} \text{ yr}^{-1}$ ) were derived from literature information (Van Breemen et al., 1984 and Weterings, 1989). For clay soils, no data were available. Here rather arbitrary weathering rate of  $1000 \text{ mol}_c \text{ ha}^{-1} \text{ yr}^{-1}$  was taken, assuming that clay soils have a higher weathering rate than loess soils. For calcareous soils a weathering rate of  $10\,000 \text{ mol}_c \text{ ha}^{-1} \text{ yr}^{-1}$  was used (Van Breemen et al., 1984; De Vries and Breeuwsma, 1986) which avoids any exceedance of critical acid loads on these soils. Note, however, that direct effects of  $\text{SO}_2$  can not be neglected at these loads (Section 5.1). The weathering exponent (cf Eq. 5.58) was set to 1 for all soil types assuming uniform weathering with depth.

### Root uptake

Root uptake consists of maintenance uptake and growth uptake. For maintenance uptake no additional data are needed in MACAL as it is set equal to litterfall corrected



for foliar uptake (N, S) or foliar exudation (Ca, Mg, K; cf Eq 5.59 - 5.62). Growth uptake was calculated as the average annual element uptake in stems, since only the removal of stems is practiced in the Netherlands. Values for each tree species were derived by multiplying the annual average growth rate, with the density of stems and the element content in stems as given in Table 5.18.

The root uptake fraction in the humus layer was set to zero except for  $\text{NH}_4$ . For this element, we used a value of 0.3 for coniferous forests and 0.5 for deciduous forests based on data from Tietema and Verstraten (1991). The root uptake exponent was set to 2 (linear pattern) in agreement with most rooting patterns.

Table 5.18 Average values used for the growth rates, density of stems and element contents in stems of the considered tree species

Tree species	Growth rate ( $\text{m}^3 \text{ha}^{-1} \text{yr}^{-1}$ ) <sup>1)</sup>				Stem density <sup>2)</sup> ( $\text{kg m}^{-3}$ )	Stem content (%) <sup>3)</sup>			
	good	medium	low	average <sup>2)</sup>		N	Ca	Mg	K
Scots pine	7.1	5.5	3.1	6.3	510	0.12	0.09	0.02	0.05
Black pine	10.6	7.6	5.0	9.2	510	0.08	0.06	0.02	0.05
Douglas fir	14.7	11.1	6.6	10.9	530	0.11	0.07	0.01	0.04
Norway spruce	13.6	8.9	5.0	7.9	460	0.12	0.14	0.02	0.07
Japanese larch	14.0	10.9	5.7	10.3	550	0.12	0.06	0.01	0.04
Oak	8.0	6.0	4.0	6.3	700	0.17	0.10	0.02	0.13
Beech	7.0	5.0	3.0	5.1	700	0.14	0.11	0.03	0.10
Poplar	19.7	14.0	10.8	17.4	450	0.08	0.15	0.02	0.08
Willow	14.8	11.9	6.7	14.2	450	0.24	0.09	0.03	0.07
Birch	8.0	6.0	4.0	6.0	650	0.15	0.17	0.03	0.08
Ash	8.0	5.0	3.0	7.0	580	0.25	0.08	0.03	0.13
Black Alder	8.5	5.0	4.5	7.7	530	0.24	0.09	0.03	0.07

<sup>1)</sup> A suitability class (good, medium or low) was defined for each combination of tree species and soil type (Schütz and Van Tol, 1981), which, in turn, was related to an average growth rate. Growth rates for each suitability class were derived from La Bastide and Faber (1972) for Scots pine, black pine, Douglas fir, Norway spruce, Japanese larch and oak; from Hamilton and Cristie (1971) for beech, birch and ash; from Faber and Thiemens (1975) for poplar and willow and from Van den Burg (1978) for black alder.

<sup>2)</sup> Calculated by weighing the growth rate with the area of the various tree species on the different suitability classes (soil type dependent). A recent investigation on the (average) growth rates of Dutch forests gave nearly similar values except for beech for which the average actual value appeared to be much higher, i.e.  $12.8 \text{ m}^3 \text{ha}^{-1} \text{yr}^{-1}$  (Begeleidingsgroep Houtoogststatistiek, 1991, internal report).

<sup>3)</sup> Based on literature compilations by Kimmins et al. (1985) and De Vries et al. (1990). Due to limited data availability the S content in stems was set at 0.01% for all tree species (cf De Vries et al., 1990)

#### Nitrogen transformations and aluminium dissolution

An overview of the various parameters describing N and Al dynamics is given in Table 5.19. Most data were derived indirectly from available literature. For example, most nitrification parameters were derived from various publications by Tietema that give information on nitrification rates in humus layers (Tietema, 1992) and mineral topsoils

Table 5.19 Values used for parameters describing N transformations and Al dissolution

Process	Parameter	Unit	Value	Derivation
Nitrification	$fr_{ni,hl}$	-	0.4 <sup>1)</sup>	Via Tietema (1992)
	$fr_{ni,max}$	-	1.0 <sup>2)</sup>	Via Heij et al. (1991)
	$D_{ni}$	cm	30	Via Tietema et al. (1992)
	$ni_{exp}$	-	3	Via Tietema et al. (1992)
Denitrification	$fr_{de,max}$	-	0.1-0.8	Via Breeuwsma et al. (1992)
	$D_{de}$	cm	60-80	Assumption <sup>4)</sup>
	$de_{exp}$	-	2	Via Tietema and Verstraten (1992)
Al dissolution	$\alpha$	-	8.0	Via Kleijn et al. (1989)
	$\beta$	-	1.0	Via Kleijn et al. (1989)

1) Implies that 40% of the  $NH_4$  input is nitrified above the mineral soil

2) Implies that no  $NH_4$  is leached from the rootzone, which is reasonable in view of available data (Heij et al., 1991)

3) Denitrification fractions given in Breeuwsma et al. (1991) for agricultural soils were corrected for the more acid circumstances in forest soils. Values used were 0.8 for peat soils (Histosols), 0.7 for clay soils (Fluvisols), 0.6 for Humic Gleysols, 0.5 for Gleyic Arenosols, 0.3 for Gleyic Podzols and 0.1 for Loess soils (Luvisols) and all other sandy soils.

4) The denitrification depth was set equal to the thickness of the root zone of each soil type which varied between 60 and 80 cm.

(Tietema et al., 1992) of Dutch forest soils (cf Table 5.19). Similarly, the value of  $z$  for the denitrification exponent, which implies that most denitrification occurs in the organicrich topsoil, was based on Tietema and Verstraten (1991). The long-term N immobilization rate, which is generally less than  $50 \text{ mol}_c \text{ ha}^{-1} \text{ yr}^{-1}$  (De Vries, 1993), was neglected. One could argue that the amount of  $NO_3$ -N leached due to harvesting should also be immobilized during the rotation period to avoid N deficiencies. However, since this amount is also mostly less than  $50 \text{ mol}_c \text{ ha}^{-1} \text{ yr}^{-1}$  it was also neglected (Section 4.1).

#### Precipitation and evapotranspiration

Precipitation data were derived from weather stations from the Royal Netherlands Meteorological Institute (KNMI). Selected records of precipitation normals from 280 stations over the period 1950-1980 were interpolated to each  $10 \text{ km} \times 10 \text{ km}$  grid. Details on the interpolation procedure have been given in Hootsmans and Van Uffelen, 1991). Most values ranged between 700 and  $900 \text{ mm yr}^{-1}$ .

Interception evaporation was calculated as a fraction of the precipitation. This fraction decreases with increasing precipitation. However, the precipitation range in the Netherlands was considered too small to warrant inclusion of this effect. Average interception fractions used were 0.45 for Norway spruce; 0.40 for Douglas fir; 0.30 for Scots Pine, black pine and beech; 0.25 for Japanese larch, poplar and ash and 0.20 for oak, willow, birch and black alder. Data were based on Kleijn et al (1989; Douglas fir), Tietema and Verstraten, 1988; oak) and a literature compilation by Hiege (1985; Norway spruce, Scots pine, Japanese larch, beech, poplar and birch). Values for black pine, ash, willow and black alder were assumed equal to tree species with comparable

physical tree characteristics such as canopy storage capacity (Hendriks, SC-DLO, pers. comm.). Interception values thus derived varied mostly between 150 mm yr<sup>-1</sup> for deciduous forests up to 350 mm yr<sup>-1</sup> for Norway spruce.

Soil evaporation and transpiration data for Scots pine, Douglas fir and oak on the sandy soils considered were calculated with the simulation model SWATRE (Belmans et al., 1983), using a hydrological year with average rainfall of 780 mm yr<sup>-1</sup> in the period 1950-1980 (De Visser and De Vries, 1989). Transpiration data for the Haplic Luvisols (loess soils) were put equal to that of fine sandy Cambic Podzols. For the Fluvisols (clay soils) and Histosols (peat soils) potential transpiration values were taken. Transpiration values for black pine were put equal to that of Scots pine, whereas values for Japanese larch, beech, poplar, willow, birch, ash and black alder were put equal to that of oak. Norway spruce was assumed to transpire 10% more than Douglas fir (Hendriks, 1991, SC-DLO, pers. comm.). Results on transpiration (Table 5.20) show that nearly all values ranged between 250 and 350 mm yr<sup>-1</sup> except for wet soils (Umbric gleysols, Eutric Fluvisols and Histosols). This is in accordance with data from Roberts (1983) who found that the actual transpiration of forests in most European countries equals approximately 300 mm yr<sup>-1</sup>, independent of tree species and soil type. The average soil evaporation value equalled 50 mm yr<sup>-1</sup>. The range in precipitation excesses thus derived varied mostly between 50 and 250 mm yr<sup>-1</sup> for coniferous forests and between 150 and 300 mm yr<sup>-1</sup> for deciduous forests. Median values were nearly similar for both types of forest, because the lower interception evaporation of deciduous forests was partly compensated by the higher transpiration, due to their higher occurrence on clay and peat soils (cf Table 5.12) and on wet sandy soils.

Table 5.20 Average transpiration rates of pine, spruce and deciduous forests as used in this study

Soil type (FAO, 1988)	Transpiration rate (mm yr <sup>-1</sup> )		
	Pine	Spruce	Deciduous
Cambic Podzol <sup>1)</sup>	282	306	326
Gleyic Podzol <sup>1)</sup>	342	375	383
Carbic Podzol <sup>1)</sup>	298	329	340
Fimic Anthrosol <sup>1)</sup>	294	323	337
Umbric Gleysol <sup>1)</sup>	373	378	383
Gleyic Arenosol <sup>1)</sup>	285	275	2)
Haplic Arenosol <sup>1)</sup>	298	329	340
Haplic Luvisol	282	306	326
Eutric Fluvisol	378	417	397
Histosol <sup>3)</sup>	378	417	397

<sup>1)</sup> Values refer to fine sandy soils. For the course textured variants, transpiration was assumed to be 60 mm yr<sup>-1</sup> less (based on model simulations for coarse and fine sandy variants for the Cambic and Carbic Podzol and the Haplic Arenosol).

<sup>2)</sup> This combination hardly exists and was not included in the calculations

<sup>3)</sup> Includes Eutric and Dystric Histosols

## RESULTS

Critical loads for acidity, N and S and amounts by which they are exceeded presented in this section nearly all refer to non-calcareous forest soils in the Netherlands, since the critical acid loads of calcareous soils were completely determined by the (arbitrary) high weathering rate of  $10\,000\text{ mol}_c\text{ ha}^{-1}\text{ yr}^{-1}$ . For acidity, results are given for three depths below the soil surface, i.e. at 10 cm (intensively rooted uppermost layer), 30 cm (forest topsoil containing most of the fine roots) and the bottom of the rootzone. For N and S values always refer to the bottom of the rootzone since calculated N loads do not vary with depth (cf Eq. 5.75). The presented variation in critical acid loads with depth thus equally applies to critical S loads (cf Eq. 5.74).

### Critical loads

#### Acidity

Critical acid loads for non-calcareous forest soils calculated with MACAL were influenced by tree species, soil depth and soil type. Regarding tree species values were higher for deciduous forests, although the influence of tree species appeared to decrease at greater depth (Fig. 5.10). Greater differences between both forest types at shallow soil depth were mainly caused by a higher acidity leaching rate for deciduous forests. Results from MACAL at the bottom of the rootzone were equal to those obtained with the simple mass balance equation (Eq. 5.84). Critical acid loads decreased with increasing soil depth (Fig. 5.10) because the Al concentration and Al/Ca ratio increased with depth due to increased Al mobilization and increased cumulative uptake of water

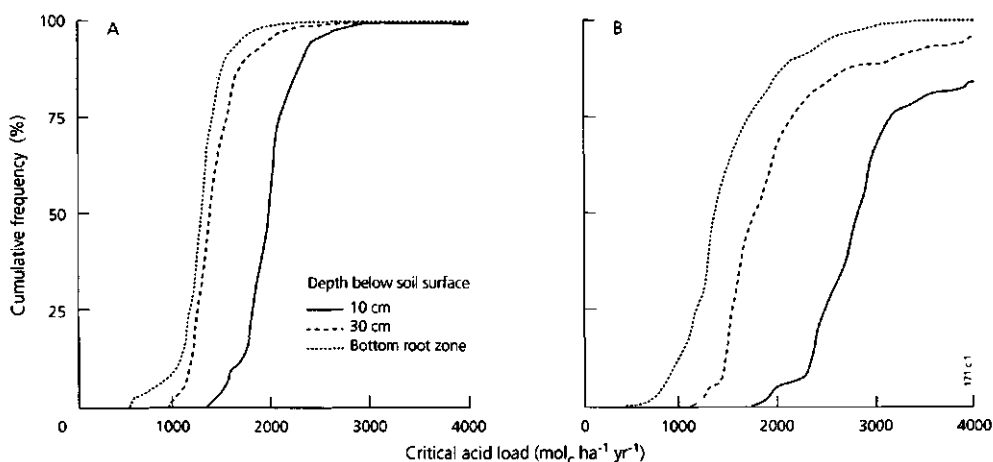


Figure 5.10 Cumulative frequency distributions of critical acid loads at three soil depths for coniferous forests (A) and deciduous forests (B) on non-calcareous soils in the Netherlands.

and Ca. However, the critical Al concentration used also included the requirement that Al only stems from primary minerals (Section 2.3; Eq. 5.72). Use of the latter criterion strongly limited the critical acid load at shallow soil depths (cf Discussion). Consequently, the differences between critical acid loads at 30 cm and at the bottom of the rootzone were small.

Critical loads strongly depended on soil type and increased in the direction sand < peat < loess < clay (Table 5.21). Especially for sandy soils, which are the dominant soils below Dutch forests (84.8%; cf Table 5.12), the difference between critical acid loads at 30 cm and at the bottom of the rootzone appeared to be small (cf Table 5.21). The median value for the critical acid load for non-calcareous sandy soils at the bottom of the rootzone ( $1295 \text{ mol}_c \text{ ha}^{-1} \text{ yr}^{-1}$ ) is in the range of average critical loads given in Section 4.2 ( $1100\text{-}1400 \text{ mol}_c \text{ ha}^{-1} \text{ yr}^{-1}$ ; cf Table 4.11). This value avoids nearly any exceedance in critical Al concentration in the forest topsoil, i.e. above 30 cm (cf Fig. 5.10 and Table 5.21).

Table 5.21 5, 50 and 95 percentile values of critical acid loads for non-calcareous forest soils in the Netherlands at three depths below soil surface

Soil type	Critical acid load ( $\text{mol}_c \text{ ha}^{-1} \text{ yr}^{-1}$ )								
	10 cm depth			30 cm depth			bottom rootzone <sup>1)</sup>		
	5%	50%	95%	5%	50%	95%	5%	50%	95%
Sand	1560	2070	3180	1120	1465	2150	735	1285	1795
Peat	1975	2955	4455	1500	2020	2780	1160	1795	2480
Loess	2390	3735	6160	1940	2895	4410	810	1785	2420
Clay	2685	4120	5960	2590	3605	4405	1260	2370	2930
All	1570	2155	4210	1125	1490	2775	745	1295	2090

<sup>1)</sup> Varies between 60 cm and 80 cm

At the bottom of the rootzone, the differences in critical acid loads between different soil types can easily be explained by the differences in the various model inputs in Eq. (5.84), as given in Table 5.22.

Table 5.22 Median values of input data for non-calcareous Dutch forest soils in the Netherlands.

Soil type	Model input data ( $\text{mol}_c \text{ ha}^{-1} \text{ yr}^{-1}$ ) <sup>1)</sup>					
	$BC_{dd}$	$BC_{we}$	$BC_{gu}$	$N_{gu}$	$N_{de}$	$Ac_{le}(\text{crit})$
Sand	250	200	270	310	35	645
Peat	220	200	395	420	815	460
Loess	460	500	440	540	25	690
Clay	210	1000	395	505	430	520
All	245	200	270	310	35	630

<sup>1)</sup> *dd* is dry deposition, *we* is weathering, *gu* is growth uptake, *de* is denitrification and *le* is leaching

Table 5.22 shows that the uptake of nitrogen (proton sink) was largely compensated by base cation uptake (proton source), resulting in a small effect of uptake on the critical acid load. In non-calcareous sandy soils and loess soils, the critical acidity leaching was the most important proton sink. In loess soils the dry deposition and the weathering of base cations was also important. The large input of base cations (mainly Ca) on loess soils in the southern part of the Netherlands is due to the proximity of limestone quarries. For clay soils, BC weathering was the most important proton sink, whereas denitrification was the most important cause of proton removal in peat soils.

#### *Nitrogen and sulphur*

Cumulative frequency distributions of critical loads for N and S for Dutch forests (Fig. 5.11) show that critical N loads were higher for deciduous forests than for coniferous forests (Fig. 5.11A) whereas the critical S loads for deciduous forests were lower (Fig. 5.11B).

The higher critical N loads for deciduous forests were mainly caused by higher values for N uptake and denitrification whereas the lower critical S loads were mainly due to a lower input of base cations by (dry) deposition and a higher BC uptake (cf Table 5.23). Dry deposition of BC was higher for coniferous forest, because of higher values for dry deposition factors, whereas uptake of N and BC was less due to lower growth rates of coniferous forests. Values for weathering and denitrification were generally lower for coniferous forests because these forests are mainly located on very poor, well drained soils. Leaching rates were also mostly lower for coniferous forests because of lower

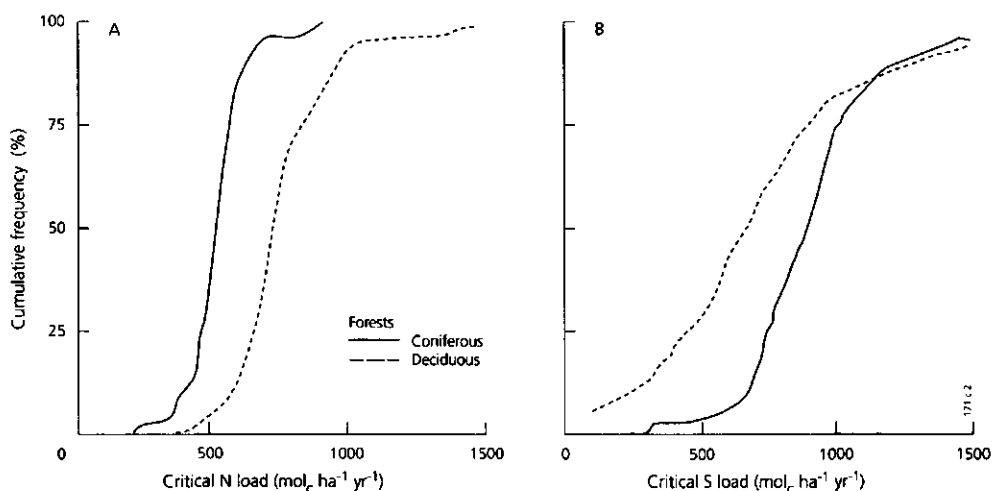


Figure 5.11 Cumulative frequency distributions of critical loads for N (A) and S (B) for coniferous and deciduous forests in the Netherlands

Table 5.23 Median values of input data for coniferous and deciduous forests in the Netherlands

Forest type	Model input data ( $\text{mol}_c \text{ ha}^{-1} \text{ yr}^{-1}$ ) <sup>1)</sup>						
	$\text{BC}_{dd}$	$\text{BC}_{we}$	$\text{BC}_{gu}$	$\text{N}_{gu}$	$\text{N}_{de}$	$\text{NO}_{3,le}(\text{crit})$	$\text{Ac}_{le}(\text{crit})$
Coniferous	310	200	240	310	30	230	670
Deciduous	175	200	370	550	85	235	590
All	245	200	270	310	35	230	630

<sup>1)</sup> *dd* is dry deposition, *we* is weathering, *gu* is growth uptake, *de* is denitrification and *le* is leaching

precipitation excesses, although median values for leaching of  $\text{NO}_3$  and acidity hardly differed.

The critical N loads increased in the direction sand < loess < clay < peat (Table 5.24). The relatively high critical N loads for clay and peat soils, are due to their (potential) anaerobic conditions that favour denitrification (cf Table 5.22). The critical N loads for calcareous soils were nearly equal to those for clay soils since most calcareous forest soils in the Netherlands are clay soils. The critical loads for S increased in the direction peat < sand < clay and loess. The low values for peat were due to a low weathering rate and a low critical acidity leaching rate caused by a low precipitation excess. The relative high critical S loads for loess soils were due high BC deposition levels on these soils (cf Table 5.22).

Table 5.24 5, 50 and 95 percentile values of critical loads for N and S at the bottom of the rootzone for non-calcareous forest soils in the Netherlands

Soil type	Critical load value ( $\text{mol}_c \text{ ha}^{-1} \text{ yr}^{-1}$ )					
	N <sup>1)</sup>			S		
	5%	50%	95%	5%	50%	95%
Sand	430	615	970	305	820	1340
Peat	760	1510	2265	100	415	985
Loess	545	810	1065	375	1305	2130
Clay	590	1140	1880	350	1345	1920
All	435	635	1410	270	825	1460

<sup>1)</sup> based on the "eutrophication criterion" ( $\text{NO}_3$  concentration below  $0.1 \text{ mol}_c \text{ m}^{-3}$ )

## Exceedances of critical loads

### Acidity

The calculated amounts by which critical acid loads are exceeded by actual atmospheric deposition are presented in Figure 5.12 as inverse cumulative frequency distributions, which directly give information on the percentage of forest above a certain excess load. Both absolute excess loads (Fig. 5.12A) and reduction percentages needed to meet the

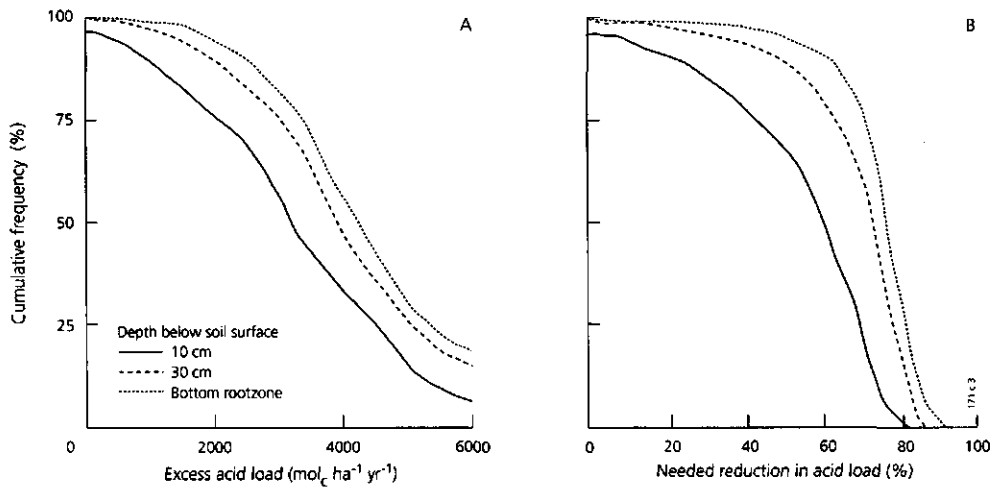


Figure 5.12 Cumulative frequency distributions of the amount by which critical acid loads at three soil depths are exceeded, expressed as an absolute amount (A) and as a percentage that is needed to reduce the present loads in order to meet the critical load (B).

critical acid loads (Fig. 5.12B), increased with increasing soil depths according to the decrease in critical acid loads with depth (cf Fig. 5.10). As with critical acid loads, the differences in reduction percentages at 30 cm depth and at the bottom of the rootzone were small. Median values at both depths were 73% and 76% respectively, whereas the median reduction percentage at 10 cm depth was 60%.

The calculated exceedances were higher for coniferous forests than for deciduous forests, as illustrated in Table 5.25 for the bottom of the rootzone. This is mainly because of larger actual deposition on conifers, since critical acid loads for both forest types at this depth are quite similar (cf Fig. 5.10).

The necessary reduction in present acid loads is related to the exceedance of the critical Al concentration, which is the minimum value of three criteria (Table 5.11). Results of MACAL for  $[Al]$  and Al/Ca (criterion 1 and 2) using present acid loads showed an increase with soil depth (Fig. 5.13). As stated before this is because of the increased cumulative Al mobilization, water uptake and Ca uptake with soil depth. At 10 cm depth, present acid loads caused a relatively small exceedance of the critical Al concentration of  $0.2 \text{ mol}_c \text{ m}^{-3}$  in 60% of the forested area (Fig. 5.13A) and of the critical Al/Ca ratio of 1.0 in less than 20% of the forested area (Fig. 5.13B). This is in accordance with measurements at this soil depth (Van Breemen and Verstraten, 1991). So, no great reductions in acid loads are needed to meet the critical Al/Ca ratio and Al concentration at 10 cm soil depth. However, the critical Al concentration related to Al depletion in the forest topsoil (criterion 3) was mostly much lower than  $0.2 \text{ mol}_c \text{ m}^{-3}$ . This criterion completely determined the critical acid loads and their exceedance at



*Table 5.25 5, 50 and 95 percentile values for the absolute and relative amounts by which critical acid loads at the bottom of the rootzone are exceeded in non-calcareous forest soils in the Netherlands*

Forest type	Excess in critical acid load ( $\text{mol}_c \text{ ha}^{-1} \text{ yr}^{-1}$ )			Needed reduction in acid load (%)		
	5%	50%	95%	5%	50%	95%
Coniferous	3305	4925	6915	69	78	88
Deciduous	1625	3440	5275	43	71	86
All	2010	4230	6625	54	76	87

shallow soil depth (cf Section 5.1). Consequently, the influence of soil depth on excess acid loads was much less than on Al concentration and Al/Ca ratio (cf Fig. 5.12 and Fig. 5.13).

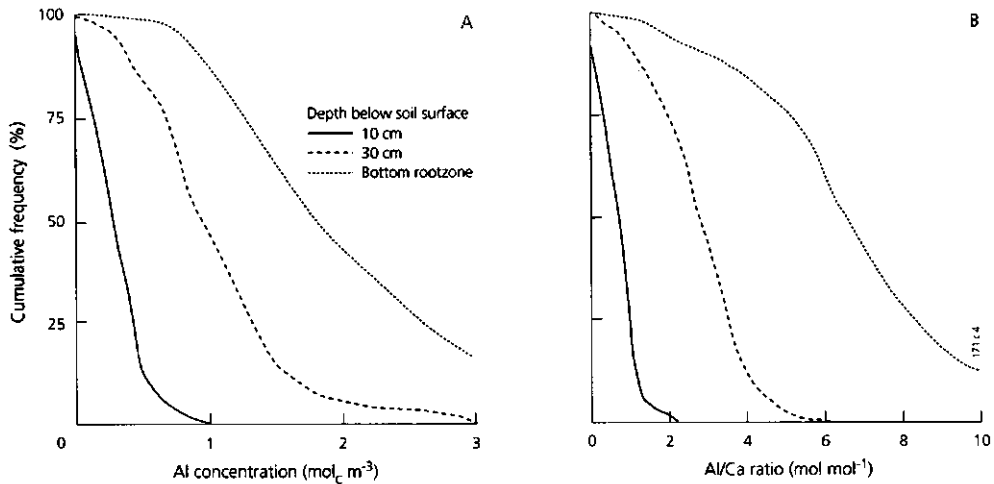


*Figure 5.13 Inverse cumulative frequency distributions of the Al concentration (A) and Al/Ca ratio (B) in non-calcareous forest soils at three soil depths below soil surface.*

Although Al depletion does not lead to direct effects on roots, it may eventually cause pH values below 3.0 at present deposition values in the Netherlands (derived from a MACAL run with  $\text{KAl}_{\text{ox}}$  is zero), with clear negative effects on trees (Houdijk, 1993a).

The geographic distributions of median acid reduction percentages that are needed to meet critical acid loads at 30 cm below soil surface (Fig. 5.14A) and at the bottom of the rootzone (Fig. 5.14B) were nearly similar. Figure 5.14 shows that high reduction percentages are needed for non-calcareous sandy soils in the central, eastern and southern part of the Netherlands. Less reduction is needed for clay and peat soils in the western and northern part. Here values even approached zero for calcareous (clay) soils.

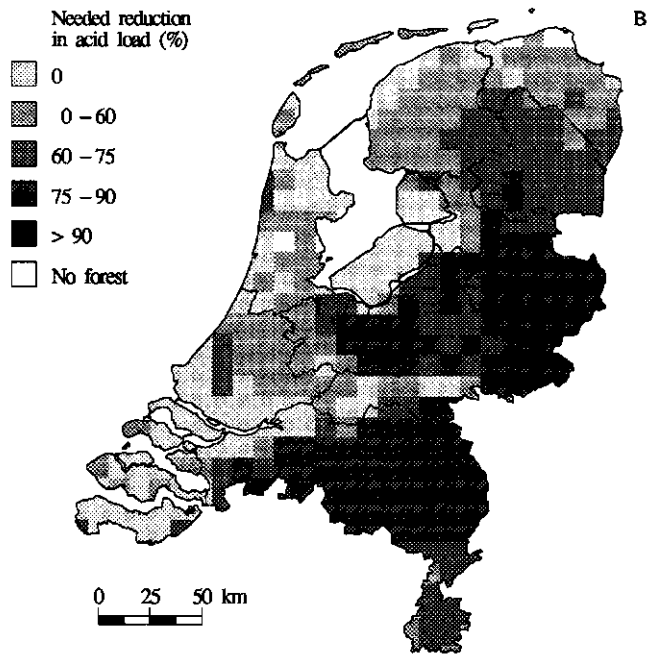
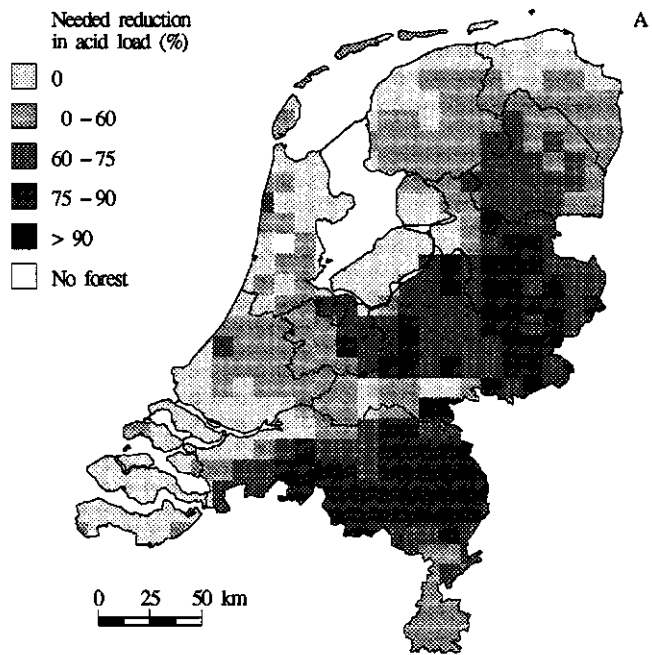


Figure 5.14 Geographic distribution of median values for reduction percentages that are needed to meet the critical acid loads at 30 cm below soil surface (A) and at the bottom of the rootzone (B)

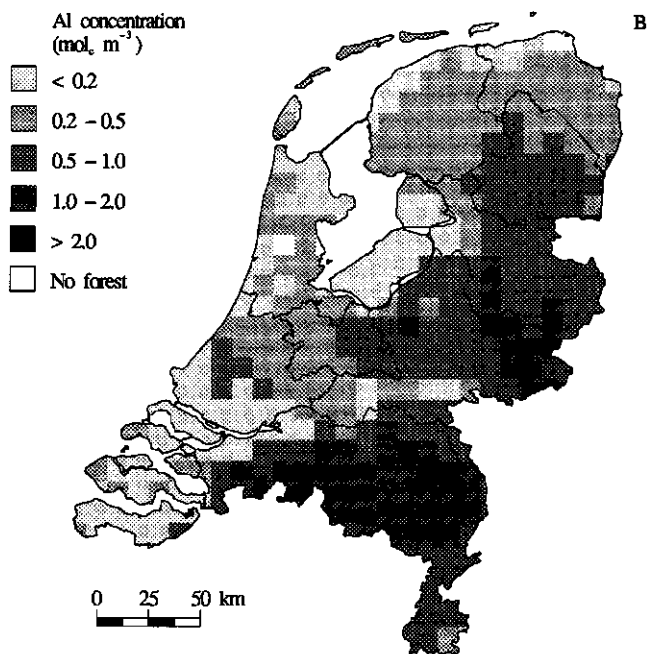
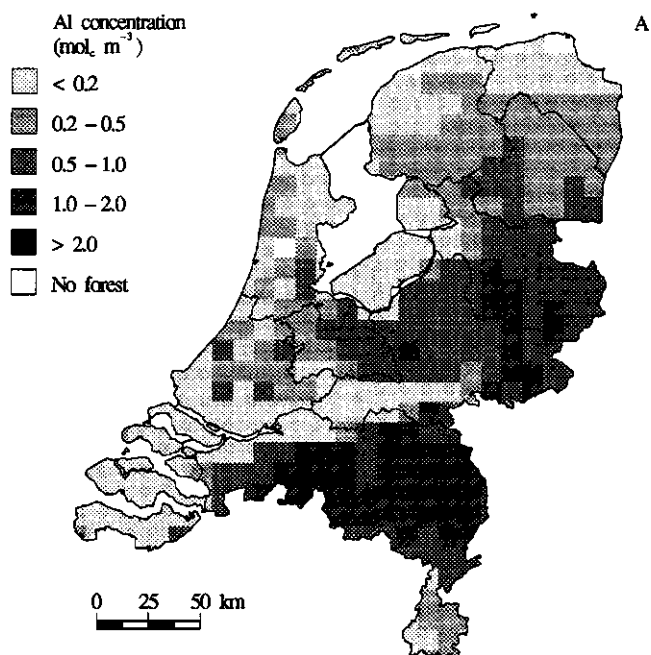


Figure 5.15 Geographic distribution of median values for the Al concentration at 30 cm below soil surface (A) and at the bottom of the rootzone (B)

The geographic pattern was also influenced by the present acid loads which had a somewhat similar pattern due to the occurrence of intensive animal husbandry in the central, eastern and southern part of the Netherlands. In these areas, where high reduction percentages are needed, the calculated AI concentrations largely exceeded the critical value of  $0.2 \text{ mol}_e \text{ m}^{-3}$ , especially at the bottom of the rootzone (Fig. 5.15).

#### *Nitrogen and sulphur*

As with acidity the amounts by which critical loads for N and S are exceeded was influenced by tree species and soil type. The calculated exceedance of critical N loads was higher for coniferous- than for deciduous forests (Fig. 5.16A). This is due to both a lower critical N load (cf Fig. 5.11A) and a higher present N load caused by more efficient filtering of dry deposition. Compared to N, the influence of tree species on the excess in S loads was much lower (Fig. 5.16B). This is because the higher present load of S on coniferous forests, caused by forest filtering, was partly compensated by a higher critical S load (cf Fig. 5.11B). The amounts by which critical loads are exceeded were higher for N than for S, due to the high input of  $\text{NH}_x$  in the Netherlands from intensive animal husbandry.

Reduction percentages needed to meet the median critical loads at the bottom of the rootzone were 79% for N and 62% for S. As with acidity, high median reduction

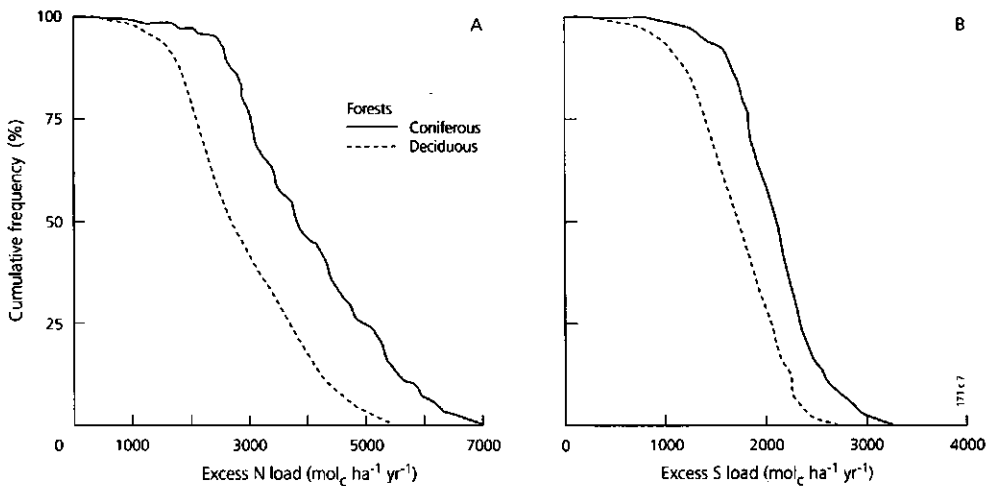


Figure 5.16 Cumulative frequency distributions of the amount by which critical loads for N (A) and S (B) at the bottom of the rootzone are exceeded on coniferous and deciduous forests in the Netherlands

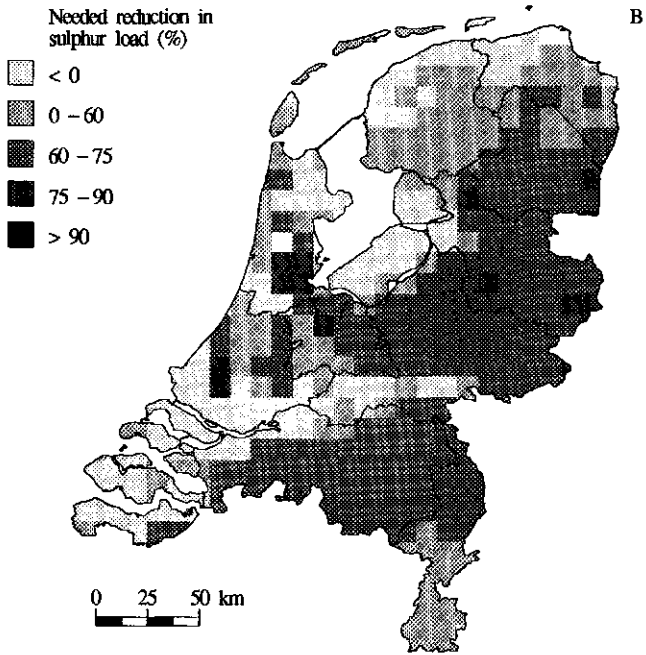
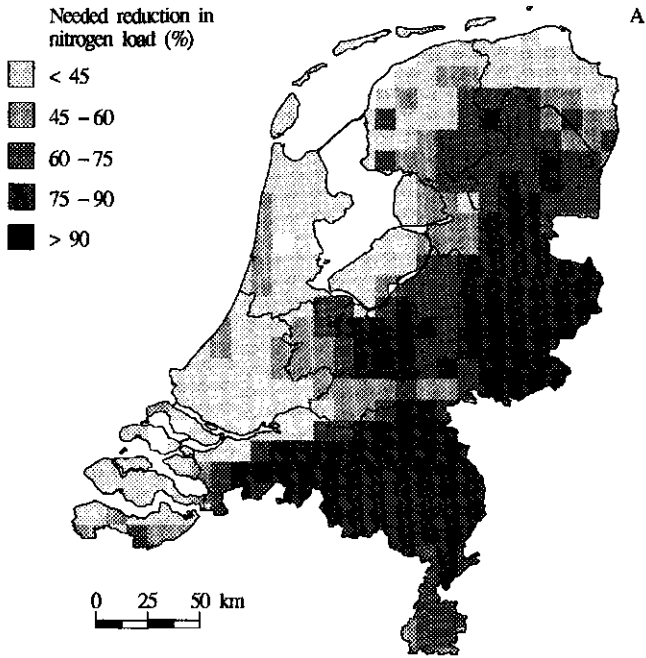


Figure 5.17 Geographic distribution of median values for reduction percentages needed to meet the critical loads for N (A) and S (B)

percentages for N and S, exceeding 75%, mainly occurred in the central, eastern and southern part of the country (cf Fig. 5.17). Very large values for N, exceeding 90%, occurred in areas with intensive animal husbandry (not shown in Fig. 5.17 where only median values are given). Nearly 90% of all Dutch forests are located in these areas, mainly on non-calcareous sandy soils. In the western and northern part of the Netherlands, the exceedance in critical N loads was less (Fig. 5.17A) due to a lower deposition of N and higher critical N loads for the calcareous and non-calcareous clay soils and peat soils occurring there. The lowest excess in critical N loads occurred on calcareous soils i.e. a median reduction percentage of 35%. Regarding S, the excess was relatively high on peat soils (a median reduction percentage of 75%) but relatively low on clay soils (a median reduction percentage of 36%) occurring in the western and northern part of the Netherlands. As with acidity, reduction percentages for S even equalled zero in a large number of gridcells in these areas, because the clay soils are often calcareous (Fig. 5.17B; cf Fig. 5.14B).

## UNCERTAINTIES

Uncertainties in critical load values are mainly determined by the uncertainty in critical chemical values, model structure and input data. The discussion below is mainly limited to uncertainties in critical acid loads and their exceedance at various depths.

### Critical chemical values

#### *Choice of critical values*

The uncertainty in critical acid loads related to direct toxic effects of Al can be large because of great uncertainties in critical values for the Al concentration and Al/Ca ratio. This is due to a lack of knowledge about the effects of Al in the field situation and a natural range in the sensitivity of various tree species for Al toxicity. For example, Keltjens and Van Loenen (1989) found that negative effects for Al only occurred above a concentration of  $1.0 \text{ mol}_c \text{ m}^{-3}$  for seedlings of Douglas fir and Japanese larch, whereas no effects were found for Scots pine, oak and birch up to  $3.3 \text{ mol}_c \text{ m}^{-3}$ . More information on the differences found in literature has been given by De Vries (1991).

The inverse cumulative frequency distributions of the Al concentration (Fig. 5.13A) and Al/Ca ratio (Fig. 5.13B), at present atmospheric deposition levels, directly give information on the influence of the critical values used for these parameters on the area exceeding critical acid loads. Assuming a value for  $[Al](crit)$  or  $RAI/Ca(crit)$  equal to zero results in 100% exceedance at all depths. Note, that this critical value for Al is needed to prevent BC depletion in soils with a high base saturation. Using the standard critical value for Al, exchangeable bases are gradually depleted in these soils until a new steady-state base saturation remains, whereby Al mobilization is such that the Al

concentration and Al/Ca ratio stay at or below critical levels. One may want to avoid such a decrease in base saturation. This argument plays a role for clay soils with a relative high base saturation (generally above 50%) and for peat soils where Al mobilization hardly occurs. However, the forest coverage on these soils is very low in the Netherlands (cf Table 5.12). Most Dutch forests occur on non-calcareous sandy soils with a low base saturation and Al mobilization as the dominant buffermechanism (Section 2.3). Compared to a negligible Al concentration, use of the standard values ( $[Al](crit) = 0.2 \text{ mol}_c \text{ m}^{-3}$  and  $RAICa(crit) = 1$ ) only gives a substantial decrease in the area exceeding critical loads at 10 cm depth. Increase of the critical Al concentration by a factor five ( $Al = 1.0 \text{ mol}_c \text{ m}^{-3}$  and  $Al/Ca = 5 \text{ mol mol}^{-1}$ ) strongly decreases this area both at 10 and 30 cm depth to nearly negligible values. However, at the depth of the rootzone, the predicted area exceeding critical loads is still substantial (cf Fig. 5.13).

### Choice of criteria

The influence of the value used for  $Al(crit)$  and  $RAICa(crit)$  on critical acid loads was (almost) completely reduced when the Al hydroxide depletion criterion was included in the calculation. Figure 5.18 shows that at shallow soil depths, i.e. above 30 cm, the critical acid load was fully determined by the Al depletion criterion (cf Fig. 5.18A). The fixed critical Al concentration or the Al depletion criterion mostly determined the critical acid load at the bottom of the rootzone (cf Fig. 5.18B). At the bottom of the rootzone, median values for the critical Al concentration differed little between the various criteria, i.e.  $0.24 \text{ mol}_c \text{ m}^{-3}$  from the critical Al/Ca ratio and  $0.21 \text{ mol}_c \text{ m}^{-3}$  to prevent Al depletion, which is nearly similar to the fixed critical Al concentration of  $0.20 \text{ mol}_c \text{ m}^{-3}$  (cf Table 5.26).

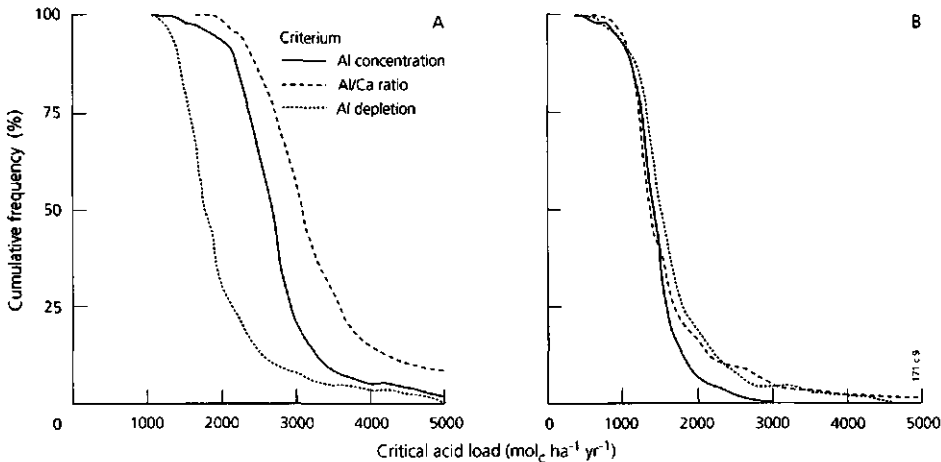


Figure 5.18 Cumulative frequency distributions of critical acid loads at 30 cm depth below soil surface (A) and at the bottom of the rootzone (B) for three critical Al concentration criteria

Table 5.26 5, 50 and 95 percentile values of critical Al concentrations calculated indirectly from a critical Al/Ca ratio and from the criterion of negligible Al depletion

Depth below soil surface (cm)	Critical Al concentration					
	Al/Ca ratio criterion			Al depletion criterion		
	5%	50%	95%	5%	50%	95%
10	0.28	0.37	0.70	0.01	0.02	0.04
20	0.22	0.32	0.64	0.03	0.04	0.09
30	0.18	0.29	0.63	0.04	0.06	0.16
40	0.14	0.26	0.66	0.07	0.09	0.25
50	0.11	0.25	0.72	0.09	0.13	0.37
BRZ <sup>1)</sup>	0.09	0.24	0.90	0.11	0.21	0.96

<sup>1)</sup> BRZ is bottom of rootzone: varies between 60 and 80 cm

The effect of both the choice of critical values and of criteria is further illustrated in Table 5.27. Results are presented as a relative increase compared to the median value derived with the standard run (using  $[Al_i](crit)$  is  $0.2 \text{ mol}_c \text{ m}^{-3}$ ,  $RAICa(crit)$  is 1.0 and  $\Delta Al_{ox}$  is 0; cf Table 5.21).

Accepting depletion of Al hydroxides, use of the standard critical Al concentration or Al/Ca ratio already increased the median critical acid loads substantially at shallow soil depths (cf Fig. 5.18A). An increase in critical values by a factor of two and five had also a tremendous effect on critical acid loads, even at the bottom of the rootzone. However, when the Al hydroxide depletion criterion was included, hardly any difference was found between the standard values and a twofold and fivefold increase in  $[Al_i](crit)$  and  $RAICa(crit)$  (Table 5.27) because the critical load value was then fully determined by the criterion of a negligible depletion of Al-hydroxides. The critical acid load related to this criterion only, mostly ranged between 1000 and 2500  $\text{mol}_c \text{ ha}^{-1} \text{ yr}^{-1}$  at the bottom of the

Table 5.27 Changes in median critical acid load of non-calcareous forest soils at different depths below soil surface due to different critical Al concentrations and Al/Ca ratios

Criteria	Value	Increase in critical acid load (%)					
		Without $\Delta Al_{ox}=0$ <sup>1)</sup>			With $\Delta Al_{ox}=0$ <sup>2)</sup>		
		10 cm	30 cm	BRZ	10 cm	30 cm	BRZ <sup>3)</sup>
$[Al_i](crit)$	$0.2 \text{ mol}_c \text{ m}^{-3}$	87	49	10	0	0	0
	$0.4 \text{ mol}_c \text{ m}^{-3}$	165	112	53	0	0	5
	$1.0 \text{ mol}_c \text{ m}^{-3}$	380	290	173	0	0	7
$RAICa(crit)$	$1.0 \text{ mol mol}^{-1}$	154	73	15	0	0	0
	$2.0 \text{ mol mol}^{-1}$	321	167	68	0	0	6
	$5.0 \text{ mol mol}^{-1}$	240	487	213	0	0	7

<sup>1)</sup> Depletion of Al hydroxides was accepted in calculating these results

<sup>2)</sup> Depletion of Al hydroxides was not accepted in calculating these results

<sup>3)</sup> When the uncertainty in the stoichiometry of Al weathering from primary minerals was included the uncertainty increased up to 23%.



rootzone with a median value of  $1385 \text{ mol}_c \text{ ha}^{-1} \text{ yr}^{-1}$ . Compared to a median value of  $1295 \text{ mol}_c \text{ ha}^{-1} \text{ yr}^{-1}$  found with the standard run (cf Table 5.21) this is only an increase of 7% (cf Table 5.27).

The uncertainty in the Al depletion criterion is relatively small since the stoichiometric Al/BC ratios in silicates vary little, except for Mg. For this element a value of 0.6 was used for the equivalent ratio of Al to Mg weathering, taking chlorite as a standard mineral. However, Mg also occurs in clay minerals such as illite and montmorillonite with much higher Al/Mg ratios. A sensitivity analysis in which a value of 3 was used for this ratio only showed a small increase in critical acid load, i.e. a median value of  $1595 \text{ mol}_c \text{ ha}^{-1} \text{ yr}^{-1}$  at the depth of the rootzone. Compared to the standard run value ( $1295 \text{ mol}_c \text{ ha}^{-1} \text{ yr}^{-1}$ ) this is only an increase of 23%. The median acid reduction percentage equalled 70%, which is 6% less than the value derived with the standard run (cf Table 5.25).

## Model structure

### *Neglection of dynamic processes*

Uncertainties caused by the model structure are due to the assumptions made. The most important assumption in MACAL is that dynamic soil processes such as cation exchange,  $\text{SO}_4$  adsorption and N immobilization can be ignored. This is based on the idea that a critical load should protect the soil for an infinite time period. However, a time perspective of one rotation period (about 100 year) may be more realistic (Nillson, 1986). Over a century, dynamic processes may be important in neutralizing the acid input. Strictly speaking, setting a definite time period implies the assessment of target loads.

The importance of cation exchange related to proton buffering depends on the actual and critical base saturation. A base saturation of 20% can be seen as a critical value, since the occurrence of dissolved Al is mostly negligible above this value (De Vries et al., 1989b). Nearly all non-calcareous sandy forest soils in the Netherlands have a base saturation below a critical value of about 20% (De Vries et al., 1992c). Recent information on loess soils below forests suggests that the base saturation mostly ranges around 20% (DLO Winand Staring Centre, 1994, yet unpublished data). Hardly any information is yet available for clay soils below Dutch forests. However, the base saturation is likely to be high in these soils as they have a relative high weathering rate. Assuming a bulk density of  $1400 \text{ kg m}^{-3}$ , a cation exchange capacity (CEC) of  $100 \text{ mmol}_c \text{ kg}^{-1}$  (at pH is 6.5) and a base saturation of 70% gives a readily exchangeable base cation amount (up to 20%) of  $350 \text{ kmol}_c \text{ ha}^{-1}$  for a soil depth of 50 cm. This implies an acid neutralization rate of  $3500 \text{ mol}_c \text{ ha}^{-1} \text{ yr}^{-1}$  for a 100 yr period.

In peat soils, cation exchange can also play a very important role during a long time period, especially in Eutric Histosols. In the Netherlands Eutric Histosols do have a high clay content (about 30%), a relatively low organic matter content (about 30%) and a high base saturation (at least 50%). Using a CEC of  $600 \text{ mmol}_c \text{ kg}^{-1}$  (at pH is 6.5), a bulk density of  $700 \text{ kg m}^{-3}$  and a base saturation of 50% for these soils (De Vries et al., 1989a) gives a buffer capacity of  $630 \text{ kmol}_c \text{ ha}^{-1}$  (up to 20% base saturation) for a soil depth of 50 cm. Consequently, these soils are strongly buffered against a change in base saturation. Furthermore, the input of Ca via seepage of bicarbonate rich ground water induces an additional buffer mechanism in these soils.

In Dystric Histosols in the Netherlands Ca input via ground water does not occur. Consequently, the base saturation is much lower than in Eutric Histosols. However, in these soils, Al mobilization hardly occurs since the mineral soil (clay) content is almost negligible. For these soils it might be better to define a critical pH which in turn is related to a critical base saturation. A base saturation (pH) that is slightly higher than the critical value already implies a substantial buffer capacity since the CEC of these soils is very high (about  $1200 \text{ mmol}_c \text{ kg}^{-1}$  at pH is 6.5). Using a bulk density of  $200 \text{ kg m}^{-3}$  (Van Wallenburg, 1988) gives a CEC of  $1200 \text{ kmol}_c \text{ ha}^{-1}$  for a soil depth of 50 cm. A difference of only 5% between the actual and critical base saturation already amounts to a buffer capacity of  $60 \text{ kmol}_c \text{ ha}^{-1}$ , i.e.  $600 \text{ mol}_c \text{ ha}^{-1} \text{ yr}^{-1}$  for a 100 yr period.

The role of N immobilization can also be important in a 100 yr period. The average total N amount in non-calcareous sandy forest soils in the Netherlands is about  $400 \text{ kmol}_c \text{ ha}^{-1}$ . Accepting for example a 10% increase in this amount during 100 yr period implies an N immobilization rate of  $400 \text{ mol}_c \text{ ha}^{-1} \text{ yr}^{-1}$ . S adsorption can safely be neglected in Dutch forest soils since they are nearly always  $\text{SO}_4$  saturated (Van Breemen and Verstraten, 1991).

Note that critical (target) loads may also become lower when dynamic processes are considered. When a critical Al concentration or Al/Ca ratio must be reached within a certain time period in strongly acidified N and S saturated soils, the occurrence of Ca-adsorption (versus H and Al), N mobilization and  $\text{SO}_4$  desorption may induce a temporary proton source (Warfvinge et al., 1992b).

#### *Description of N transformations*

The relative simple description of N transformation processes induces another uncertainty. The well-known effects of environmental variables such as temperature, moisture content and pH on N transformation rates, as reported in literature (Witkamp and Van Drift, 1961; Moore, 1986; Emmer and Tietema, 1990) are not explicitly accounted for. Furthermore, in MACAL a certain sequence is assumed in the occurrence of N transformations, i.e. mineralization/-immobilization followed by root uptake, nitrification and denitrification. Actually, if N immobilization occurs before denitrification any input in excess of N uptake and leaching will first lead to N immobilization. In a non-

equilibrium situation, i.e. when the system is not N saturated, N immobilization will be a function of the net N input. Requiring a negligible N immobilization rate implies that the net N input should not be higher than the net N uptake and a natural N leaching rate. In this situation denitrification becomes negligible as well. Neglecting denitrification has a substantial effect on the critical load of peat and clay soils (cf Table 5.22). However, the effect on sandy soils, which cover nearly 85% of the forested area is almost negligible except for wet soils such as Umbric Gleysols and Gleyic Arenosols.

#### *Calculation of reduction percentages*

Except for the bottom of the rootzone, the critical acid loads at different soil depths, presented in this section, are based on the assumption that the relative contributions of  $\text{NH}_4$  and  $\text{NO}_3$  to total N deposition at critical loads equal the present values. This is only true when planned emission reduction percentages are equal for  $\text{NH}_4$  and  $\text{NO}_3$ , which is not the case in the Netherlands. However, compared to other uncertainties, this aspect is of minor importance. MACAL results (not presented here) showed that a possible change in the future  $\text{NH}_4$  (and  $\text{NO}_3$ ) to N deposition ratio hardly affected calculated critical acid loads and their exceedance. It is, however, important to realize that the calculation of exceedances of critical loads is not straightforward anymore when the critical loads depend on a deposition ratio. The exceedance of total acidity (N and S) not necessarily equals the reduction required. A thorough discussion of this aspect is given by Posch et al. (1993a).

To a certain extent, the problem described above also applies to critical N and S loads at the bottom of the rootzone. In this paper critical N and S loads are calculated such that critical values related to eutrophication ( $\text{NO}_3$  concentration) and acidification (Al concentration, Al/Ca ratio) are both just not violated. The critical N load is the absolute upper value, but lower N loads and higher S loads are equally acceptable as long as the Al parameters stay at critical values. However, the increase in N reduction percentage (lower critical N loads) will be larger than the decrease in S reduction percentage (higher critical S loads) since denitrification decreases at a lower N deposition (cf Eq. 5.66). Again, this aspect is thoroughly discussed by Posch et al. (1993a).

#### **Input data**

The critical acid load calculated with MACAL is determined by a large number of model inputs (cf Table 5.14). A sensitivity analysis for all parameters (not given) showed that the model output was most sensitive for a change in the parameters regulating nitrification, Al dissolution and root uptake. The linear correlation coefficient was used as a statistical criterion to evaluate the sensitivity of each parameter (Kros et al., 1993). Results of an uncertainty analysis in which these parameters were varied between their likely minimum and maximum (Table 5.28) showed that the nitrification fraction in the humus layer,  $fr_{ni,hl}$  was the most important parameter at shallow soil depth (especially at

**Table 5.28** Changes in median values for critical acid loads for non-calcareous forest soils in the Netherlands at different depths below soil surface due to a change in important model parameters.

Parameter <sup>1)</sup>	Variation	Change in critical acid loads (%)			Change in needed reduction in acid load (%)		
		10 cm	30 cm	BRZ	10 cm	30 cm	BRZ
$fr_{ni,h}$	-0.2	-30	-16	0	-13	-4	0
	+0.2	+31	+16	0	+13	+4	0
$fr_{ni,max}$	-0.5	+5	+10	+10	-2	-2	-2
$fr_{ru,h}$	-0.1	-5	-3	0	-2	-1	0
	+0.1	+5	+3	0	+3	+1	0
$\alpha$	-1.0	-12	-11	-9	-11	-4	-4
	+1.0	+27	+24	+19	+5	+3	+2
$\beta$	-1.0	-9	-4	0	-8	-2	0
	+1.0	+22	+7	0	+5	+2	0

<sup>1)</sup>  $fr_{ni,h}$  is nitrification fraction in the humus layer,  $fr_{ni}$  is total nitrification fraction,  $fr_{ru,h}$  is root uptake fraction in the humus layer and  $\alpha$  and  $\beta$  are Al dissolution parameters.

10 cm) followed by the Al dissolution parameters  $\alpha$  and  $\beta$ . The influence of a change in the root uptake fraction in the humus layer,  $fr_{ru,h}$  appeared to be low. At the bottom of the rootzone the critical acid load was not influenced by the various parameters except for the total nitrification fraction,  $fr_{ni}$  and the Al dissolution parameter  $\alpha$  which influences the critical acidity leaching. However, the effect was small.

Assuming complete nitrification, the critical acid load at the depth of the rootzone is only influenced by base cation deposition, base cation weathering, forest growth, precipitation excess and the Al dissolution constant (cf Eq. 5.84). A sensitivity analysis, in which these model inputs (except  $KAl_{ox}$ ; cf the influence of  $\alpha$  in Table 5.28) were varied by plus or minus 50% caused a relatively low decrease or increase (less than 25%) in critical acid loads at the bottom of the rootzone (Table 5.29). A 50% variation is also a reasonable indication of the overall uncertainty of these model inputs although it might be somewhat lower for the precipitation excess and somewhat larger for the weathering rate. Effects of model input variation on critical loads for N and S (results not given) were somewhat higher, i.e. 15 to 30% and 20 to 50%, respectively. One reason for the larger effect on S is that a variation in the deposition and weathering of base cations only affects the critical S load. Furthermore, an increased growth increases the critical N loads by increased N uptake (cf Eq. 5.75), whereas it decreases the critical S loads because of increased BC uptake (cf Eq. 5.85). The overall effect on the critical acid load (cf Eq. 5.84) is, however, low as discussed before.

A 50% change in the input data hardly affected the reduction percentages that are needed to meet 5%, 50% or 95% of the critical acid loads (Table 5.29). Even a model run in which simultaneously BC deposition, BC weathering and the precipitation excess was increased by 50%,  $KAl_{ox}$  was decreased to  $10^7 \text{ mol}^{-2} \text{ l}^2$  ( $\alpha = -1.0$ ) and the stoichiometric ratio of Al to Mg weathering was set to 3 (cf Eq. 5.72) still gave a median acid reduction percentage of 65% (a change of -11%; cf Table 5.25).

*Table 5.29 5, 50 and 95 percentile values of changes in critical acid loads at the bottom of the rootzone and reduction percentages for acidity, for non-calcareous forest soils in the Netherlands, due to a 50% change in model input parameters*

Model input	Variation (%)	Change in critical acid loads (%)			Change in needed reduction in acid load (%)		
		5%	50%	95%	5%	50%	95%
BC deposition	-50	-8	-10	-9	+4	+3	+2
	+50	+21	+10	+9	-5	-2	-2
BC weathering	-50	-9	-9	-9	+5	+3	+1
	+50	+12	+10	+12	-6	-2	-1
Growth rate	-50	-20	0	-2	+1	0	-1
	+50	+5	+2	+3	-2	0	0
Precipitation excess	-50	-15	-22	-24	+10	+6	+3
	+50	+13	+10	+19	-8	-2	-2

## CONCLUSIONS

The most important outcome, related to the major aim of this study (cf Introduction), is that critical acid loads increase strongly going from the bottom of the rootzone to shallower soil depths, when critical chemical values for Al are only related to direct toxic effects (Al concentration and Al/Ca ratio). However, since critical acid loads were calculated by also including a criterion related to long term indirect effects (the criterion that Al depletion should be avoided), the overall effect of soil depth appeared to be limited. Especially for non-calcareous sandy soils (85% of Dutch forest soils), the difference between critical acid loads related to 30 cm soil depth and the bottom of the rootzone was small. This implies that results obtained with a one-layer Simple Mass Balance (SMB) model are reasonable for these soil types. For loess, clay and peat soils, the critical acid loads obtained with an SMB model are likely to be an underestimate.

Another important outcome, related to the second aim of the study, is that critical acid loads (related to the bottom of the rootzone) are hardly influenced by tree species, whereas they strongly depend on soil type. Regarding tree species, the larger N uptake of deciduous trees was compensated by a larger BC uptake and a lower BC input by dry deposition. These differences, however, caused a higher critical N load and a lower critical S load of deciduous trees compared to coniferous trees. Regarding soil types, values increased in the direction sand < peat < loess < clay, which was mainly caused by differences in denitrification (especially with respect to peat soils) and base cation weathering (especially with respect to clay soils). Since coniferous forests have a larger filtering capacity than deciduous forests, the excess loads of both N and S on conifers were higher than on deciduous trees.

In accordance with the distribution of soil types (affects critical loads) and atmospheric deposition of N and S (present loads), large exceedances in critical loads of N, S and

acidity on Dutch forests were calculated in the central, eastern and southern part of the Netherlands, especially in areas with intensive animal husbandry. Median values for critical loads of N, S and acidity calculated at the bottom of the rootzone for forests on non-calcareous soils equalled 635, 825 and 1295 mol<sub>c</sub> ha<sup>-1</sup> yr<sup>-1</sup> respectively (cf Table 5.21 and 5.24). Median values for the amounts by which these critical loads are exceeded were 2525, 1370 and 4230 mol<sub>c</sub> ha<sup>-1</sup> yr<sup>-1</sup> respectively (cf Fig. 5.16 and Table 5.25). The calculated percentages by which present atmospheric deposition need to be reduced to meet the median critical loads were 79% for N, 62% for S and 76% for total acidity (cf Table 5.25).

Important conclusions related to the reliability of critical acid loads (the final aim of this study) are that:

- (i) The uncertainty in critical chemical values for the Al concentration and Al/Ca ratio has a large influence on the critical acid loads. However, the effects are relatively small when considering the necessity to avoid Al depletion, since that criterion appeared to be very stringent. Consequently, the overall uncertainty was less than 25%. This hardly affected the median acid reduction percentage needed (a decrease of 6%, i.e. 70% instead of 76%).
- (ii) The uncertainty in critical loads for N, S and acidity for clay and peat soils is likely to be large due to great uncertainties associated with the model assumptions. However, these soils only cover a small part of the forested area of the Netherlands (< 7.5%). Consequently, this hardly affects the overall reduction in S, N and acid loads that is needed to meet the critical values, although it is important for a regional approach in N and S emission abatement.
- (iii) The effect of uncertain model inputs on the acid reduction percentage needed is small. Uncertainty analysis showed that even in a situation of systematic underestimation of the model inputs a reduction percentage of 65% was needed to meet the critical acid loads at the depth of the rootzone for 50% of the Dutch forests.

In summary, critical acid loads are largely exceeded on Dutch forest soils and, despite uncertainties involved in its derivation, significant emission reductions are needed to attain a long-term sustainable forest ecosystem.

# Chapter 6

## LONG-TERM IMPACTS OF ACID DEPOSITION ON SOME CHARACTERISTIC SOILS

### 6.1 IMPACTS ON SOILS IN VARIOUS BUFFER RANGES

- INTRODUCTION
- THE MODEL SMART
- SCENARIOS AND DATA
- MODEL BEHAVIOUR IN VARIOUS BUFFER RANGES
- SCENARIO ANALYSIS
- CONCLUDING REMARKS

### 6.2 IMPACTS ON A CHARACTERISTIC FOREST SOIL IN THE NETHERLANDS

- INTRODUCTION
- THE MODEL RESAM
- SCENARIO AND DATA
- RESULTS
- DISCUSSION AND CONCLUSIONS

### 6.3 IMPACTS ON TWO CHARACTERISTIC DUNE SOILS IN THE NETHERLANDS

- INTRODUCTION
- STUDY AREA
- METHODS AND DATA
- RESULTS
- DISCUSSION AND CONCLUSIONS

Section 6.1 is a slightly revised version of:

W. de Vries, M. Posch and J. Kämäri, 1989. *Simulation of the long-term soil response to acid deposition in various buffer ranges*. *Water Air and Soil Pollution* 48: 349-390.

Section 6.2 is a slightly revised version of:

W. de Vries, J. Kros and C. van der Salm, 1994. *Modelling the impact of acid deposition and nutrient cycling in forest soils*. *Ecological Modelling* (in press).

Section 6.3 is a slightly revised version of:

W. de Vries, J. Klijn and J. Kros, 1994. *Simulation of the long-term impact of atmospheric deposition on dune ecosystems in the Netherlands*. *Journal of Applied Ecology* 31: 59-73.



## 6.1 IMPACTS ON SOILS IN VARIOUS BUFFER RANGES

### ABSTRACT

*A soil acidification model has been developed to estimate long-term chemical changes in soil and soil water in response to changes in atmospheric deposition. Its major outputs include base saturation, pH and the molar Al/BC ratio, where BC stands for divalent base cations. Apart from net uptake and N transformations, the processes accounted for are restricted to geochemical interactions, i.e. weathering of carbonates, silicates and Al hydroxides, cation exchange and CO<sub>2</sub> equilibria. First, the model's behaviour in the different buffer ranges between pH 7 and pH 3 was evaluated by analysing the response of an initially calcareous soil of 50 cm depth to a constant high acid load (5000 mol<sub>c</sub> ha<sup>-1</sup> yr<sup>-1</sup>) over a period of 500 years. In calcareous soils weathering was fast and the pH remained high (near 7) until the carbonates were exhausted. Results indicated a time lag of about 100 years for each percent CaCO<sub>3</sub> before the pH starts to drop. In non-calcareous soils the response in the range between pH 7 and pH 4 mainly depended on the initial amount of exchangeable base cations. A decrease in base saturation, by exchange of BC against H and Al, caused a strong increase in the Al/BC ratio near pH 4. A further decrease in pH to values near 3 occurred when the pool of secondary Al compounds was exhausted. The analyses showed that this could occur in acid soils within several decades. The buffer mechanisms in the various pH ranges are discussed in relation to Ulrich's concept of buffer ranges. Secondly, the impact of various deposition scenarios on non-calcareous soils was analysed for a time period of 100 years. The results indicated that the time lag between reductions in deposition and a decrease in the Al/BC ratio is short. However, substantial reductions, up to a final deposition level of 1000 mol<sub>c</sub> ha<sup>-1</sup> yr<sup>-1</sup>, were needed to get Al/BC ratios below a critical value of 1.0.*

### INTRODUCTION

Information on the long-term effects of acid deposition on soils is important for the formulation of policies for emission reductions. In this respect models provide an important tool to assist decision-makers in evaluating the effectiveness of abatement strategies. Consequently, at the International Institute for Applied Systems Analysis (IIASA) a Regional Acidification Information and Simulation model (RAINS) has been developed that analyses environmental impacts on a European scale for different emission scenarios. Predictions are based on quantitative descriptions of the linkages between emissions, deposition and environmental impacts such as soil acidification and the effects on terrestrial and aquatic ecosystems (Alcamo et al., 1987; 1990). A diagram illustrating the framework and procedure for using RAINS is shown in Figure 6.1.

Within the overall framework of the RAINS model the soil acidification model forms an important link between atmospheric deposition and effects on forests, surface waters and ground water. The RAINS soil model, predicting pH as a function of sulphur deposition, was described by Kauppi et al. (1986). This model was based on the concept of buffer ranges as introduced by Ulrich (1981a).

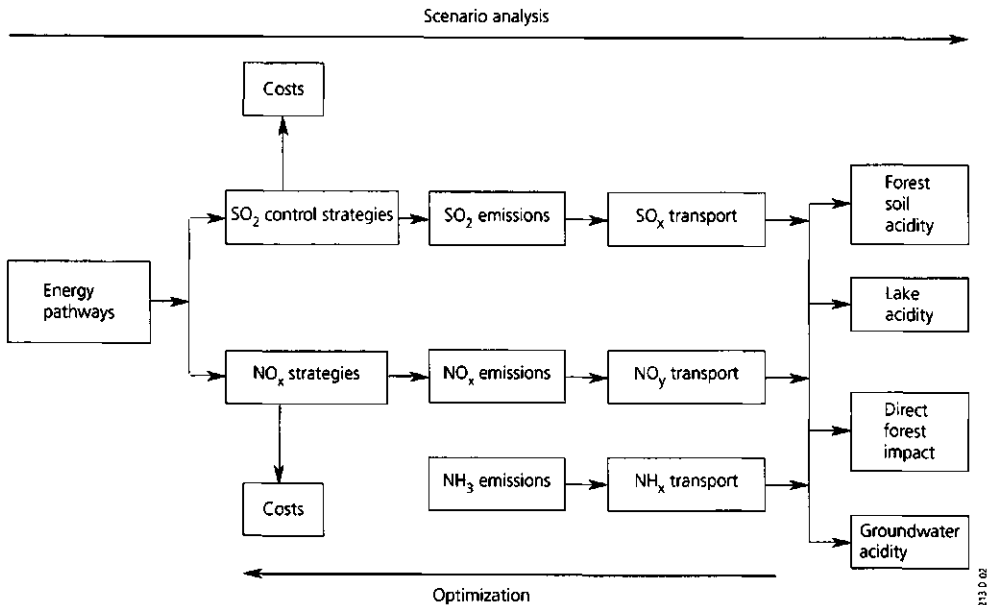


Figure 6.1 Schematic diagram of the RAINS model

In this section a new RAINS soil model, called SMART (Simulation Model for Acidification's Regional Trends), is described which includes the effects of natural soil acidification resulting from the dissociation of CO<sub>2</sub> and the impact of the deposition of SO<sub>x</sub>, NO<sub>y</sub> and NH<sub>x</sub>. Apart from pH, the model also predicts concentrations of major ions of the soil solution, i.e. Al, BC, NH<sub>4</sub>, NO<sub>3</sub>, SO<sub>4</sub> and HCO<sub>3</sub>, because the ratios of Al and/or NH<sub>4</sub> to divalent base cations (represented by BC) are more indicative and sensitive parameters of potential forest damage than pH. Furthermore, changes in the solid phase, i.e. the Ca carbonate content, content of secondary Al compounds (represented as Al hydroxide content) and base saturation are predicted with SMART. Agricultural soils have not been included, because normal farming practices such as fertilization, liming and cropping have much greater effects on soil acidity than acidic deposition.

This section focuses on the behaviour of SMART by analysing the long-term impact of various deposition scenarios on representative forest soils. Special emphasis is put on the model's behaviour in the different buffer ranges and the sensitivity of the model output to variations in model input, initial conditions and model parameters. In Section 7.1 (cf De Vries et al., 1994f) the application of SMART to Europe is described, focusing on the derivation of data for such a large-scale application.

## THE MODEL SMART

### Modelling approach

The objectives of the application of the model strongly determine which approaches are chosen for the modelling (cf Chapter 1). At present, the models for predicting the long-term effects of acid deposition on soils and surface waters are generally process-oriented, although empirical relationships are included, (e.g. Reuss, 1980; Arp, 1983; Chen et al., 1983; Cosby et al., 1985a,b; Bloom and Grigal, 1985; De Vries and Kros, 1989a, b). They have mostly been developed as research tools to elucidate responses of soils and surface waters to acid deposition. The reason for developing the SMART model is that most of these models either require a large amount of input data, and are therefore not very appropriate for application at a large regional scale, or do not describe the behaviour of soils in the complete pH range. A notable exception is the model by Bloom and Grigal (1985), but this model does not clearly separate between inputs of  $\text{SO}_2$ ,  $\text{NO}_x$  and  $\text{NH}_3$  and furthermore it uses empirical relationships that were established for soils in the north-eastern United States.

In order to be able to use the SMART model both as a research tool and a management tool (cf Chapter 1) the model is:

- process-oriented: to get insight in system's behaviour;
- simple: to minimize input data requirements for applications at a regional scale;
- dynamic: to analyse the long-term behaviour of soils; and
- spatially distributed: to predict the geographical extent of soil acidification.

A special feature of the model is that the spatial distribution of data with respect to soil types is taken into account by using soil maps and relating model parameters to soil survey data using transfer functions (De Vries, 1990).

The transfer of protons in the soil is influenced by many reactions (Section 2.1; De Vries and Breeuwsma, 1987). In order to minimize input data requirements, when applying SMART for predicting temporal and geographical patterns of forest soil acidification in Europe, the following assumptions have been made:

- The soil solution chemistry depends solely on the net element input from the atmosphere and the geochemical interactions (weathering and cation exchange) in the soil. Apart from the net uptake of N and BC in harvested plants and the net N immobilization in the forest floor, the influence of the nutrient cycle (foliar exudation, foliar uptake, litterfall, mineralization and root uptake) is not taken into account. This affects model predictions in the root zone (the uppermost 25 to 50 cm). Consequently, in a regional soil acidification model (RESAM) developed for the Netherlands, nutrient cycling processes have been included (Section 6.2; De Vries et al., 1994b). However, the data required for this model are not available on a European scale. Furthermore, runoff and leachate concentrations that are important for surface water and ground water quality, respectively, are almost unaffected by excluding the influence of the nutrient cycle.

- S output is in equilibrium with S input. Uptake, immobilization, reduction and adsorption of S were assumed to be negligible. As for adsorption; soils that are rich in hydrous oxide minerals can strongly adsorb  $\text{SO}_4$ , thus reducing cation leaching from soils (Johnson, 1980). However, element budget studies in northern and western Europe (e.g. Rosén, 1982; van Breemen et al., 1984; Nilsson, 1985) indicate that  $\text{SO}_4$  adsorption is generally negligible.
- Biological fixation of N and denitrification are negligible. Both assumptions are reasonable for most forest ecosystems (Klemetson and Svensson, 1988). Notable exceptions are red alder, which has a high rate of N fixation (van Miegroet and Cole, 1984) and extremely wet forest soils, which have a high rate of denitrification (Tietema and Verstraten, 1989).
- In acid forest soils ( $\text{pH} < 4.5$ ), natural soil acidification is neglected. Organic acids can have an appreciable impact in these soils, but the Al that is mobilized by these acids is detoxified by humic ligands (Ulrich and Matzner, 1983). The formation, complexation and protonation of organic acids has therefore been ignored in the model.
- The weathering rate of base cations from silicates is independent of the soil pH. This is based on a thermodynamic analysis of laboratory experiments, which shows that the weathering rate of pure feldspar minerals is pH independent when the pH varies between 3 and 8 (Helgeson et al., 1984). At low pH, this assumption is not really warranted any more (Section 3.2; De Vries, 1994b).
- The soil is considered as a homogeneous compartment of constant density. However, it is possible to divide the soil into several layers if this is considered important. In this study the soil depth equals the thickness of the rootzone, since most biogeochemical interactions occur in this zone.
- The water flow is stationary on a yearly basis, which equals the time step of the model. The reason for this time step is the focus on long-term effects. Seasonal, monthly or even daily fluctuations in soil water chemistry are potentially very important, but the model is developed for predicting trends in water flux-weighted annual average concentrations.
- The water flux percolating from the rootzone equals the precipitation excess. This implies that (i) forests obtain all their water from the rootzone and (ii) surface runoff is neglected. This first assumption is reasonable, but the second assumption is only justified in relatively flat areas. However, surface runoff also contains N and S compounds and consequently the effect on ion concentrations might be relatively small.
- The element input mixes completely within the considered soil compartment. This is a reasonable assumption for most forest soils which are well drained and poorly structured (sands, loamy sands and sandy loams). However, in well structured soils with channels and cracks this assumption does not hold. The same is true for hydrophobic soils with preferential flow patterns. Furthermore, it may not be the case in strongly undulating landscapes with surface runoff.

## Model concept

By incorporating the charge balance principle (Reuss et al., 1986) the model structure is based on the anion mobility concept. Figure 6.2 shows the model structure in a relation diagram. State variables depict the quantities of chemical constituents in minerals (carbonates, silicates and hydroxides) and on the exchange complex, as well as the ion concentrations in the soil solution.

Rate variables depict the processes that influence state variables. This includes the net input of elements (deposition minus net uptake and net immobilization) and water (precipitation minus evapotranspiration) and various neutralizing reactions, i.e. the dissolution (weathering) of carbonates, silicates and/or Al hydroxides, and cation exchange.

Table 6.1 shows, which ions are included in which processes. The concentrations of  $\text{SO}_4$ ,  $\text{NO}_3$  and  $\text{NH}_4$  are completely determined by the net element input; the Al concentration is controlled by chemical interaction with the soil (weathering and cation exchange) and the concentration of BC is regulated by both net element input and soil interaction.

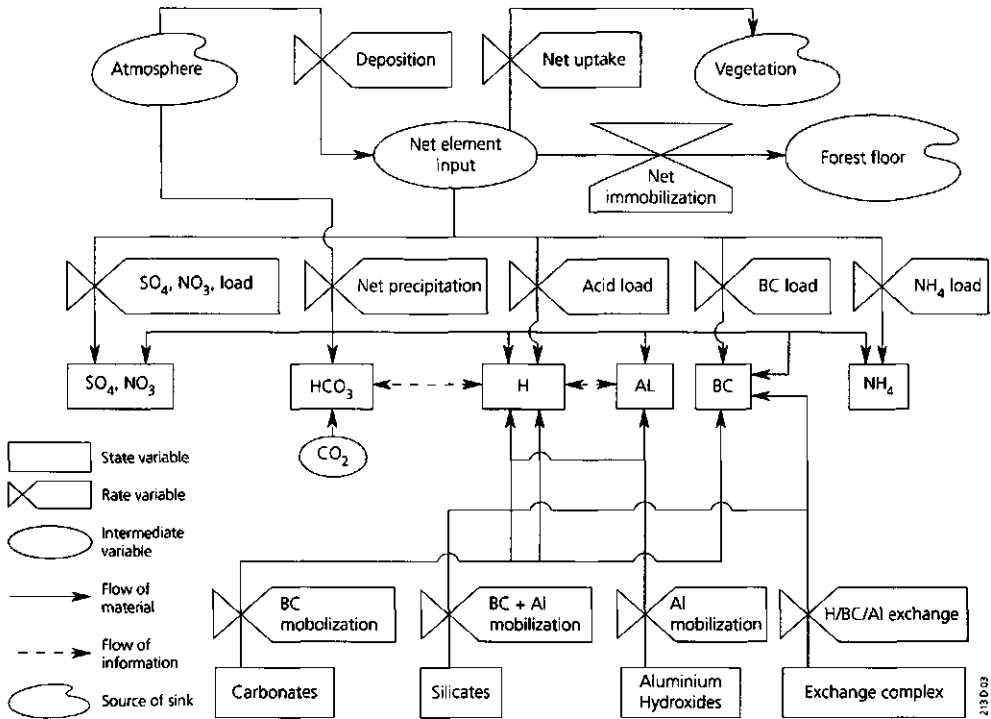


Figure 6.2 Relation diagram of the model SMART

Table 6.1 Overview of the ions involved in the process description included in SMART  
 ("+" = ion included in the respective process, "-" = ion not included)

Process	Equation	H	Al	BC	NH <sub>4</sub>	NO <sub>3</sub>	SO <sub>4</sub>	HCO <sub>3</sub>
Atmospheric deposition	Rate limited	+	-	+	+	+	+	-
Growth uptake	Rate limited	+	-	+	+	+	-	-
N immobilization	Rate limited	+	-	-	+	+	-	-
Nitrification	Rate limited	+	-	-	+	+	-	-
Denitrification	Rate limited	+	-	-	-	+	-	-
Silicate weathering	Rate limited	+	+	+	-	-	-	-
CO <sub>2</sub> dissociation/association	Equilibrium	+	-	-	-	-	-	+
Carbonate weathering	Equilibrium	+	-	+	-	-	-	-
Al hydroxide weathering	Equilibrium	+	+	-	-	-	-	-
Cation exchange	Equilibrium	+ <sup>1)</sup>	+	+	-	-	-	-

<sup>1)</sup> H is explicitly included in the cation exchange reactions. In all other reactions, H is implicitly included through a charge balance equation

The HCO<sub>3</sub> concentration is based on an equilibrium with the CO<sub>2</sub> pressure and the pH. The precipitation excess affects all ion concentrations.

Apart from silicate weathering all neutralization reactions are described by equilibrium reactions. The equilibrium reactions included play a role in specific buffer ranges as defined by Ulrich (1981a, 1983c). In calcareous and slightly acid soils (pH > 5), acidity is generated in the soil water by the formation of bicarbonate from dissolved CO<sub>2</sub> and water according to:



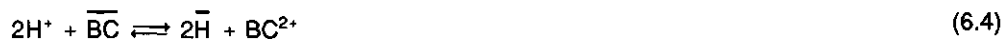
In calcareous soils the free hydrogen ion produced by this mechanism and by acid input is neutralized by the dissolution of calcite (carbonate buffer range) according to:



Combination of equations (6.1) and (6.2) gives:



In non-calcareous soils the hydrogen ions can be neutralized by exchange with divalent cations (exchange buffer range) according to:



where the bar denotes the adsorbed phase. Organic matter has an especially high affinity for hydrogen ions, leading to a strong decrease of the effective cation exchange capacity (CEC) with the pH of the soil solution (Helling et al., 1964).

Upon further acidification, a decrease in base saturation will allow H to react with Al in the soil (aluminium buffer range). This starts to become important below pH values of about 4.5 (Ulrich, 1981a). In the model it is assumed that the concentration of Al in soil water is in equilibrium with some solid phase of  $\text{Al}(\text{OH})_3$  (secondary Al compounds) according to:



In this pH range, cation exchange will not be limited to H/BC exchange, because the exchange sites of the soil matrix have a high affinity for Al, leading to Al/BC exchange according to



However, the amount of secondary Al compounds is not infinite and can be exhausted in the topsoil in the near future in areas with high acid deposition rates (Mulder et al., 1989). When this happens, secondary Fe compounds may start interacting with H (iron buffer range). In (acid) sandy soils, which are the dominant forest soil types in Europe (cf Section 5.1; Table 5.3) the mobilization rate of Fe is, however, small (cf Section 3.1; 3.3). Fe release has therefore been ignored in the model. In this stage of acidification the Al concentration depends solely on congruent weathering from primary silicates, while there will temporarily be a strong buffering of H by H/Al exchange according to



## Process formulations

### *Basic principles*

Since the SMART model is based on the charge balance principle, the basic process formulations are close to those of other models based on this principle, such as the Birkenes model (Christoffersen et al., 1982), the MAGIC model (Cosby et al., 1985a,b) the ILWAS model (Chen et al., 1983) and the model by Reuss and co-workers (Reuss, 1980, 1983; Reuss and Johnson, 1985).

SMART consists of a set of mass balance equations, which describe the soil input-output relationships for the cations (Al, BC,  $\text{NH}_4$ ) and strong acid anions ( $\text{SO}_4$ ,  $\text{NO}_3$ ), and a set of equilibrium equations, which describe the equilibrium soil processes. An explicit mass

balance for the ions H and  $\text{HCO}_3$  is not necessary, because the sources and sinks of these ions (dissociation of water and of  $\text{CO}_2$ , respectively) are not related to the soil-solid phase. Their concentration is determined by equilibrium equations and the concentration of the other ions by the charge balance principle (cf Section 5.1; Eq. 5.1)

$$[\text{H}] + [\text{Al}_i] + [\text{BC}^*] + [\text{NH}_4] = [\text{NO}_3] + [\text{SO}_4] + [\text{HCO}_3] \quad (6.8)$$

where  $[\text{Al}_i]$  is the inorganic Al concentration ( $\text{mol}_c \text{ m}^{-3}$ ) and  $[\text{BC}^*]$  is the Cl-corrected base cation concentration ( $\text{Ca}+\text{Mg}+\text{K}+\text{Na}-\text{Cl}$ ;  $\text{mol}_c \text{ m}^{-3}$ ), which is assumed to equal the concentration of the divalent base cations  $\text{Ca}+\text{Mg}$  (cf Section 5.1).

*Mass balance equations:*

For each of the cations (Al, BC,  $\text{NH}_4$ ) and anions ( $\text{SO}_4$ ,  $\text{NO}_3$ ) considered in the model, a mass balance equation is given by

$$\frac{dX_{tot}}{dt} = X_{td} + X_{int} - PE \cdot [X] \quad (6.9)$$

where  $X_{tot}$  is the total amount of ion X in the soil ( $\text{mol}_c \text{ ha}^{-1}$ ),  $X_{td}$  is the total deposition of ion X to the soil,  $X_{int}$  is the net interaction of ion X in the soil ( $\text{mol}_c \text{ ha}^{-1} \text{ yr}^{-1}$ ),  $[X]$  is the equivalent concentration of ion X in soil water ( $\text{mol}_c \text{ m}^{-3}$ ) and  $PE$  is the precipitation excess (precipitation minus evapotranspiration;  $\text{m}^3 \text{ ha}^{-1} \text{ yr}^{-1}$ ).

The total amount of  $\text{SO}_4$ ,  $\text{NO}_3$  and  $\text{NH}_4$  is given by

$$X_{tot} = \theta_{rz} \cdot f_c \cdot T_{rz} \cdot [X] \quad (6.10)$$

where  $\theta_{rz}$  is volumetric water content in the rootzone ( $\text{m}^3 \text{ m}^{-3}$ ),  $T_{rz}$  is the thickness of the rootzone (m) and  $f_c$  is a factor for the conversion from  $\text{mol}_c \text{ m}^{-2} \text{ yr}^{-1}$  to  $\text{mol}_c \text{ ha}^{-1} \text{ yr}^{-1}$  ( $10^4 \text{ m}^2 \text{ ha}^{-1}$ ). The strong acid anions  $\text{SO}_4$  and  $\text{NO}_3$  do not have an adsorbed phase in the model.  $\text{SO}_4$  adsorption is assumed to be negligible, whereas  $\text{NO}_3$  adsorption is insignificant for almost all soil types. Furthermore, the adsorption of  $\text{NH}_4$  is also ignored, because of the low preference of the exchange complex for this ion in the acid sandy soils, on which most of the forested areas in Europe occur. This can be derived from the fact that acid forest soils in the Netherlands hardly contain  $\text{NH}_4$  on the adsorption complex although the concentration of this element in the soil solution can be high, especially in the topsoil, because of the extremely high  $\text{NH}_3$  deposition on the forests in this country (Kleijn et al., 1989). For clay soils, this assumption is not valid, because fixation of  $\text{NH}_4$  may play a significant role but the forested area on clay soils is small.



In calcareous soils the total BC amount in the soil is defined as the sum of the amount in the soil solution and in the carbonates (silicate weathering and cation exchange are neglected in these soils):

$$BC_{tot} = \theta_{rz} \cdot f_c \cdot T_{rz} \cdot [BC] + \rho_{rz} \cdot f_c \cdot T_{rz} \cdot ctCa_{cb} \quad (6.11)$$

where  $\rho_{rz}$  is the bulk density of the soil ( $\text{kg m}^{-3}$ ) and  $ctCa_{cb}$  is the content of carbonates in the soil ( $\text{mol}_c \text{kg}^{-1}$ ). In non-calcareous soils the total BC amount is defined as the sum of the amount in the soil solution and at the exchange complex:

$$BC_{tot} = \theta_{rz} \cdot f_c \cdot T_{rz} \cdot [BC] + \rho_{rz} \cdot f_c \cdot T_{rz} \cdot frBC_{ac} \cdot CEC \quad (6.12)$$

where  $frBC_{ac}$  is the exchangeable BC fraction and  $CEC$  is the cation exchange capacity of the soil ( $\text{mol}_c \text{kg}^{-1}$ ).

The total Al amount is defined as the sum of the amount in soil water, at the exchange complex and in secondary Al compounds (further denoted as Al hydroxides):

$$Al_{tot} = \theta_{rz} \cdot f_c \cdot T_{rz} \cdot [Al] + \rho_{rz} \cdot f_c \cdot T_{rz} \cdot ( frAl_{ac} \cdot CEC + ctAl_{ox} ) \quad (6.13)$$

where  $frAl_{ac}$  is the exchangeable Al fraction and  $ctAl_{ox}$  is the content of Al hydroxides ( $\text{mol}_c \text{kg}^{-1}$ ). In the various surface water acidification models, such as ILWAS (Chen et al., 1983) and MAGIC (Cosby et al., 1985a,b) the Al hydroxide amount is assumed to be infinite, but this is not the case in a long-term perspective (De Vries and Kros, 1989; Mulder et al., 1989). When the amount of Al hydroxides is depleted ( $ctAl_{ox} = 0$ ),  $Al_{tot}$  only refers to the amount in soil water and at the exchange complex.

The input to the soil system is given by atmospheric deposition. The rate-limited interaction fluxes included in SMART (cf Table 6.1) are equal to those described in the START model (Section 5.1). The sum of the total deposition flux and interaction fluxes, which equals the leaching flux in a steady-state situation, equals (cf Section 5.1; Eq. 5.14 - 5.17):

$$SO_{4,td} + SO_{4,int} = SO_{4,ld} \quad (6.14)$$

$$NH_{4,td} + NH_{4,int} = (1 - fr_{nl}) \cdot NH_{4,td} \cdot \left( \frac{N_{td} - N_{im} - N_{gu}}{N_{td}} \right) \quad (6.15)$$

$$\text{NO}_{3,td} + \text{NO}_{3,int} = (1 - fr_{de}) \cdot (\text{NO}_{3,td} + fr_{ni} \cdot \text{NH}_{4,td}) \cdot \left( \frac{N_{td} - N_{im} - N_{gu}}{N_{td}} \right) \quad (6.16)$$

$$\text{BC}_{td}^* + \text{BC}_{int} = \text{BC}_{td}^* + \text{BC}_{we} + \text{BC}_{ex} - \text{BC}_{gu} \quad (6.17)$$

$$\text{Al}_{td} + \text{Al}_{int} = \text{Al}_{we} + \text{Al}_{ex} \quad (6.18)$$

where  $fr_{ni}$  and  $fr_{de}$  are dimensionless nitrification and denitrification fractions, respectively. Al weathering is related to BC weathering according to:

$$\text{Al}_{we} = r \cdot \text{BC}_{we} \quad (6.19)$$

where  $r$  is the stoichiometric equivalent ratio of Al to BC in the congruent weathering of silicates.

*Equilibrium equations:*

The dissociation of  $\text{CO}_2$  (cf Eq. 6.1) and the dissolution of Ca carbonate (cf Eq. 6.3) and of Al hydroxide (cf Eq. 6.5) are calculated as:

$$[\text{HCO}_3] = (K\text{CO}_2 \cdot p\text{CO}_2) / [\text{H}] \quad (6.20)$$

$$[\text{Ca}] \cdot [\text{HCO}_3]^2 = K\text{Ca}_{cb} \cdot p\text{CO}_2 \quad (6.21)$$

$$[\text{Al}] = K\text{Al}_{ox} \cdot [\text{H}]^3 \quad (6.22)$$

where  $K\text{CO}_2$  is the product of Henry's law constant for the equilibrium between  $\text{CO}_2$  in soil water and soil air, and the first dissociation constant of  $\text{H}_2\text{CO}_3$  ( $\text{mol}^2 \text{l}^{-2} \text{bar}^{-1}$ ),  $p\text{CO}_2$  is the partial  $\text{CO}_2$  pressure in the soil (bar),  $K\text{Ca}_{cb}$  is the equilibrium constant for Ca carbonate dissolution ( $\text{mol}^3 \text{l}^{-3} \text{bar}^{-1}$ ) and  $K\text{Al}_{ox}$  is the equilibrium constant for Al hydroxide dissolution ( $\text{mol}^2 \text{l}^2$ ). In calcareous soils Ca is set equal to BC.

The various exchange reactions (cf Eqs. 6.4, 6.6 and 6.7) are described by Gaines-Thomas equations (Gaines and Thomas, 1953) using concentrations instead of activities:

$$\frac{fr_{ac}^2}{fr_{BC_{ac}}} = K\text{H}_{ex} \frac{[\text{H}]^2}{[\text{BC}]} \quad (6.23)$$

$$\frac{frAl_{ac}^2}{frBC_{ac}^3} = KAl_{ex} \frac{[Al]_d^2}{[BC]^3} \quad (6.24)$$

where  $KH_{ex}$  and  $KAl_{ex}$  are the Gaines-Thomas selectivity constants for H/BC exchange and Al/BC exchange, respectively. The description of the exchange between H and Al is obtained by combining Eqs. (6.23) and (6.24). Since the exchange complex is assumed to comprise H, Al and BC only, charge balance requires that

$$frH_{ac} + frAl_{ac} + frBC_{ac} = 1 \quad (6.25)$$

The mathematical procedure for solving this set of mass balance and equilibrium equations as well as the initialization procedures are described in Annex C.

### Model comparison

As stated before, the formulations for most biogeochemical processes in SMART are comparable to models such as MAGIC, Birkenes and ILWAS, that have been developed to simulate streamwater chemistry. These models also include key soil processes occurring within the catchment, such as weathering and cation exchange. A general review and critique of surface water acidification models has been given before by Reuss et al. (1986) and Kämäri (1987). Apart from process-oriented charge balance models such as MAGIC, Birkenes and ILWAS, these reviews are also concerned with empirical charge balance models (Wright and Henriksen, 1983) and models in which the geochemical buffer-processes in the soil are lumped in adsorption isotherms (Arp, 1983) or kinetic expressions (Schnoor et al., 1986).

In order to justify the introduction of a new process-oriented charge balance model, i.e. SMART, a comparison is made between the processes and process formulations included in SMART and other models based on the charge balance principle (MAGIC, Birkenes and ILWAS). The models are compared in relation to the processes and process formulations included (cf Table 6.2), the assumptions made and the goals that are aimed at. Regarding the models MAGIC and ILWAS, a more detailed comparison with respect to the process formulations included has been made by Eary et al. (1989).

#### *Hydrological processes*

There are quite important differences in modelling philosophy between Birkenes and ILWAS on one hand and SMART and MAGIC on the other hand, influencing the description of hydrological processes. The Birkenes model was originally developed to describe observed streamwater chemistry in the acidified Birkenes catchment in southernmost Norway (Christophersen et al., 1982). In this catchment, streamwater chemistry is highly dependent upon the flow regime. Since the model was aimed at explaining observed short-

Table 6.2 Processes and process formulations included in SMART, MAGIC, Birkenes and ILWAS

Process	SMART	MAGIC	Birkenes	ILWAS
<u>Hydrological processes:</u>				
	Annual precipitation excess	Annual streamflow fluxes <sup>1)</sup>	Hydrologic submodel	Hydrologic submodel
<u>Biochemical processes:</u>				
Foliar uptake	-	-	-	Proportional to dry deposition
Foliar exudation	-	-	-	Proportional to leaf composition
Litterfall	-	-	-	Model input
Mineralization/immobilization	Zero-order reaction <sup>2)</sup> (NH <sub>4</sub> ,NO <sub>3</sub> )	Zero-order reaction <sup>2)</sup> (NH <sub>4</sub> ,NO <sub>3</sub> ,SO <sub>4</sub> Ca,Mg,K,Na)	Empirical equation (SO <sub>4</sub> ,BC)	First-order reaction (NH <sub>4</sub> ,SO <sub>4</sub> , Ca,Mg,K,Na)
Net uptake	Zero-order reaction <sup>2)</sup>	Zero-order reaction <sup>2)</sup>	-	Zero-order reaction <sup>2)</sup>
Maintenance uptake	-	-	-	Forcing function
Nitrification	Proportional to NH <sub>4</sub> input	Zero-order reaction <sup>2)</sup>	-	Michaelis Menten kinetics
Denitrification	Proportional to NO <sub>3</sub> input	-	-	-
CO <sub>2</sub> -production/exchange	-	-	-	+
<u>Geochemical processes:</u>				
Carbonic acid chemistry	Equilibrium <sup>-3)</sup>	Equilibria	Equilibria <sup>-4)</sup>	Equilibria
Organic acid chemistry	-	Equilibria	-	Equilibria
Carbonate weathering	Equilibrium	-	-	-
Silicate weathering	Zero-order reaction <sup>2)</sup>	Zero-order reaction <sup>2)</sup>	Zero-order reaction	First-order pH dependent reaction
Al hydroxide weathering	Equilibrium	Equilibrium	Equilibrium	Rate-limited
Al complexation	-	Equilibria (OH,F,SO <sub>4</sub> )	-	Equilibria (OH,F,SO <sub>4</sub> )
Cation exchange	Gaines Thomas (H,Al,BC) <sup>-3)</sup>	Gaines Thomas (Al,Ca,Mg,K,Na)	Gapon, Kerr (H,BC)	Gapon, Kerr (H,NH <sub>4</sub> ,Ca,Mg,K,Na)
Anion retention	-	Langmuir (SO <sub>4</sub> )	Linear (SO <sub>4</sub> )	Linear (SO <sub>4</sub> ,H <sub>2</sub> PO <sub>4</sub> ,RCOO)

<sup>1)</sup> The newest version of MAGIC also contains a hydrological submodel (Eary et al., 1989).

<sup>2)</sup> Specified by net removal/release fluxes.

<sup>3)</sup> A newer version of SMART also contains organic acid equilibria and SO<sub>4</sub> adsorption using a Langmuir equation (Posch et al., 1993).

<sup>4)</sup> A newer version of Birkenes contains an empirical equation for RCOO (Rustad et al., 1986).

term trends, a separate two-compartment hydrological submodel has been developed, simulating evapotranspiration, quick flow in the upper compartment and base flow in the lower compartment.

In the original Birkenes model snowmelt was not simulated, and predictions were only related to the summer half-year (Christophersen et al., 1982), but in more recent versions, a snow reservoir has been included (e.g. Rustad et al., 1986). As with the Birkenes model ILWAS is also based on the philosophy that confidence in a model must be established by

the ability to reproduce short-term dynamics, since long-term calibration data are not available. Consequently, ILWAS also contains a separate hydrologic submodel simulating the various hydrological processes such as snowmelt, evapotranspiration, partially saturated flow (quickflow in the upper compartment of the Birkenes model) and saturated subsurface flow (baseflow in the lower compartment of the Birkenes model). At present, use of the Birkenes model is limited to short-term applications, since it does not contain a mass balance for exchangeable cations, whereas ILWAS can also be used for long-term predictions.

Contrary to Birkenes and ILWAS, the main objective of SMART and MAGIC is to develop a heuristic tool to obtain a conceptual understanding of the long-term responses of soils and catchments, to acid deposition, in order to answer series of "what if" questions by policy makers (scenario modelling). Furthermore, both SMART and MAGIC are based on the assumption that a satisfactory description of the long-term chemical behaviour of soils and catchments can be obtained by a lumped sum representation of the chemical reactions in one homogeneous soil compartment. As far as MAGIC is concerned this implies that the routing of water within the catchment is of less importance. The original MAGIC model thus lacks a detailed hydrologic submodel. However, the newest version of MAGIC is a two compartment model that runs in conjunction with TOPMODEL (Hornberger et al., 1985), which is a surface hydrology code that provides the hydrologic parameters required to run MAGIC II (Eary et al., 1989). Since SMART is only meant to predict soil acidification, a separate hydrological model has not been included.

#### *Biochemical processes*

Regarding biochemical processes there is a major difference between ILWAS, the most complex and detailed acidification model, and the other models. In ILWAS all major biochemical processes affecting soil water (and streamwater) chemistry, i.e.: (i) Canopy interactions (foliar uptake and foliar exudation), (ii) Nutrient cycling (litterfall, mineralization and maintenance uptake), (iii) N dynamics (N mineralization/immobilization, nitrification and denitrification) and (iv) CO<sub>2</sub> dynamics (production and exchange), are explicitly included. In SMART and MAGIC, canopy interactions, litterfall and maintenance uptake and CO<sub>2</sub> dynamics are not simulated, whereas the other processes are generally included by simple zero-order reactions (model input). Birkenes only contains an empirical equation for the mineralization of SO<sub>4</sub> as far as biochemical processes are concerned.

As with hydrology, the differences between the biochemical process descriptions in the models can be explained by the goals that are aimed at. ILWAS is meant to reproduce short-term dynamics which necessitates the explicit inclusion of biochemical processes. The same is true for Birkenes, but this model was originally developed for a specific acid catchment where HCO<sub>3</sub> and NO<sub>3</sub> hardly played a role. Consequently N and CO<sub>2</sub> dynamics has not been included in this model. Attention has here been focused on SO<sub>4</sub> which is the major driving anion. SMART and MAGIC have been developed to reproduce long-term changes, which are mainly determined by geochemical interactions such as weathering and

cation exchange. Consequently, biochemical interactions, such as fluxes due to interactions with the vegetation, simply have to be specified.

### *Geochemical processes*

Regarding geochemical processes, ILWAS is again the most detailed model. However, generally spoken the similarity between the models on this point is rather striking. All models do include the effects of CO<sub>2</sub> dissociation, silicate weathering, Al hydroxide weathering and cation exchange. Apart from ILWAS, all models describe weathering of silicates and Al hydroxides as a zero-order reaction (fixed amount per year) and an equilibrium reaction with Al hydroxide (gibbsite) respectively. In ILWAS, both processes are described by first-order reactions (rate-limited), influenced by the pH and the Al concentration respectively. Cation exchange is either described by Gaines-Thomas equations (SMART and MAGIC) or by Gapon and Kerr equations (Birkenes and ILWAS). However the major difference between the models in this respect is the inclusion of different cations in the exchange equations. In SMART and Birkenes, the divalent base cations Ca and Mg are lumped (BC) whereas the monovalent base cations Na and K are excluded, since these ions hardly occur on the exchange complex of most soils. In MAGIC and ILWAS all base cations are included explicitly. Adsorption of NH<sub>4</sub> is only considered in ILWAS. Regarding the acid cations, Birkenes and ILWAS includes H, MAGIC includes Al but SMART is the only model which includes them both. In our view, this is important since H/Al exchange may play an important role in strongly acidified soils.

Apart from the inclusion of both H and Al in exchange reactions, the major difference between SMART and other models is the inclusion of carbonate weathering, whereas SO<sub>4</sub> adsorption and complexation reactions of Al with RCOO, OH, F and SO<sub>4</sub> are neglected. Furthermore, SMART contains a mass balance for both carbonates and Al hydroxides. Due to these characteristics, SMART is the only model to date, as far as we know, which is able to simulate soil behaviour in all buffer ranges.

## SCENARIOS AND DATA

The input data of the SMART model are summarized in Table 6.3. They have been divided into source/sink terms or system inputs, initial conditions of variables and parameters. System inputs are the atmospheric deposition and the net interaction fluxes (weathering, growth uptake and immobilization) of S, N and BC and the precipitation excess.

### **Deposition scenarios**

The major driving variables (source terms) are the atmospheric deposition of SO<sub>x</sub>, NO<sub>x</sub> and NH<sub>x</sub>. In order to demonstrate the model's behaviour, four deposition scenarios were simulated. The deposition levels limiting the various scenarios are given in Table 6.4; Figure 6.3 shows the trends in total deposition level for each scenario.

Table 6.3 System inputs, variables and parameters of SMART

SYSTEM INPUTS	
Atmospheric deposition	: $SO_{x,td}$ $NO_{x,td}$ $NH_{x,td}$ $BC_{td}^+$
Net removal and release in soils	: $N_{gu}$ $N_{im}$ $BC_{gu}$ $BC_{wo}$
Precipitation excess	: $PE$
VARIABLES	
Ion amounts in solid phases	: $ctCa_{cb}$ $ctAl_{ox}$
Exchangeable cation fractions	: $frH_{ac}$ $frAl_{ac}$ $frBC_{ac}$
Ion concentrations in solution	: $[H]$ $[Al]$ $[BC]$ $[NH_4]$ $[SO_4]$ $[NO_3]$ $[HCO_3]$
PARAMETERS	
Constants	: $KCO_2$ $KCa_{cb}$ $KAl_{ox}$ $KAl_{ex}$ $KH_{ex}$ $fr_{de}$ $r$
Soil properties	: $p_{rz}$ $\theta_{rz}$ $T_{rz}$ $CEC$ $\rho CO_2$

Table 6.4 Deposition levels of  $SO_x$ ,  $NO_x$  and  $NH_3$  (in  $mol_c ha^{-1} yr^{-1}$ ) limiting the different scenarios (cf Fig. 6.3)

Scenario	Level	$SO_x$	$NO_x$	$NH_x$	Total
1	European average	3000	1000	1000	5000
2	30% reduction	2100	700	700	3500
3	70% reduction	900	300	300	1500
4	Background level	300	100	100	500

The scenarios started with background levels for  $SO_x$ ,  $NO_x$  and  $NH_x$ , that increased to "European average" levels within 25 years and stayed there for another 25 years. The "European average" values were rough estimates based on average throughfall data from 51 sites in Europe (Ivens et al., 1989).

Within the next 25 years deposition levels were reduced by 0%, 30%, 70% and 90% for scenarios 1, 2, 3 and 4, respectively, and stayed there for another 25 years. The

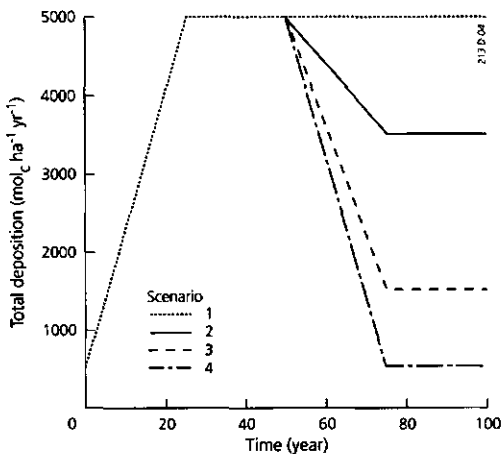


Figure 6.3 Total deposition levels for four scenarios (cf Table 6.4).

background levels were based on literature information for SO<sub>x</sub> and NO<sub>x</sub> (Galloway et al., 1982, 1984) and NH<sub>x</sub> (Asman, 1987).

The various reductions were related to political goals and critical loads for various receptors. The 30% reduction refers to the minimal reduction aimed at by most western European countries by the year 1993, a 70% reduction is the political goal in the Netherlands for the year 2015 based on a critical load of 1400 mol<sub>c</sub> ha<sup>-1</sup> yr<sup>-1</sup> for coniferous forests (De Vries, 1988; Section 4.2), and a 90% reduction might be the ultimate goal to protect the most sensitive surface waters (Hultberg, 1988). The aim of running simulations with these scenarios was to analyse the influence of various deposition reductions on the rate of recovery of different non-calcareous soils.

Simulations were also made for constant high ("European average") and low (background) deposition levels over 500 years on an initially calcareous soil, in order to illustrate the model's behaviour in the different buffer ranges. (see further). A sensitivity analysis of the model for varying inputs, initial conditions and parameters was mainly restricted to the calcareous soil.

### System inputs

The other system inputs, i.e. BC deposition, the net interaction fluxes and the precipitation excess were kept constant over time in all simulations, and their respective values are given in Table 6.5.

BC deposition varies strongly over Europe. It is generally high near the coast (upper value in Table 6.5), whereas it can be low inland (lower value in Table 6.5). The values were based on data from the Netherlands (KNMI/RIVM, 1985) and Scandinavia (Rosén, 1988; Mulder et al., 1988).

BC weathering varies with soil type (geological formation) and temperature. Estimates were based on chemical analyses of soil profiles (Fölster, 1985; De Vries and Breeuwsma, 1986), input-output budgets (van Breemen et al., 1986; Mulder et al., 1987, 1988) and model calculations (Sverdrup and Warfvinge, 1988a,b). Representative parent rock

Table 6.5 Values of model inputs used in the simulations

Variable	Unit	Reference value	Upper value	Lower value
BC <sub>id</sub>	mol <sub>c</sub> ha <sup>-1</sup> yr <sup>-1</sup>	400	800	200
BC <sub>we</sub>	mol <sub>c</sub> ha <sup>-1</sup> yr <sup>-1</sup>	250	500	125
BC <sub>gu</sub>	mol <sub>c</sub> ha <sup>-1</sup> yr <sup>-1</sup>	400	-	-
N <sub>gu</sub>	mol <sub>c</sub> ha <sup>-1</sup> yr <sup>-1</sup>	800	-	-
N <sub>im</sub>	mol <sub>c</sub> ha <sup>-1</sup> yr <sup>-1</sup>	0	-	-
PE	mm yr <sup>-1</sup>	300	600	150



materials (geological formations) related to this data are gneiss for the reference value, schists for the upper value and granites for the lower value (Sverdrup and Warfvinge, 1988a).

BC and N uptake varies with tree species and site quality. The data were derived by multiplying the average annual biomass increase of stems, branches and needles in central Europe by the BC and N content in the various compartments (De Vries et al., 1990), assuming whole-tree harvesting. N immobilization was assumed negligible in all simulations. Contrary to BC deposition and BC weathering, the model's sensitivity to BC uptake was not evaluated, because it is obvious from the sensitivity to the other BC inputs. An increase in  $BC_{gu}$  is equal to a decrease in  $BC_{fd}$  or  $BC_{we}$ . Similarly, an increase in  $N_{gu}$  is equal to a decrease in N deposition as simulated by the different scenarios.

The annual precipitation excess,  $PE$ , varies significantly over Europe, ranging from less than 100 mm in Mediterranean countries to more than 1000 mm in Scandinavia (Müller, 1982). As a basis for our simulations, 300 mm per year was considered as typical; the upper and lower values cover most of the variation in Europe.

## Model variables

Initial conditions of variables used in the simulations are given in Table 6.6.

Table 6.6 Values of initial conditions used in the simulations

Variable	Unit	Calcareous soil	Non-calcareous soil		
			Reference value	Upper value	Lower value
$ctCa_{cb}$	$mmol_c kg^{-1}$	100 <sup>1)</sup>	0	-	-
$ctAl_{ox}$	$mmol_c kg^{-1}$	75 <sup>2)</sup>	150 <sup>2)</sup>	-	-
$frBC_{ac}$	-	1.0	0.2	0.4	0.1

1)  $100 mmol_c kg^{-1}$  is equal to 0.5%

2) Refers to oxalate extractable Al contents. The value for the calcareous soil is an overestimate (cf Section 6.3)

The initial content of Ca carbonate in the calcareous soil was assumed to be low in order to illustrate the model's behaviour in all buffer ranges using the constant high acid input during 500 years (Ca carbonate and Al hydroxides are depleted). The value of  $ctAl_{ox}$  in the non-calcareous soils was derived from data for A and B horizons in acid sandy soils in the Dutch soil information system (Bregt et al., 1986). This value is so high, that the soil stayed in the aluminium buffer range for 100 year simulations with the various deposition scenarios (Al hydroxides are not depleted). The initial base saturation,  $frBC_{ac}$ , was set 100% in the calcareous soil and 20% in the non-calcareous soil (Table 6.6). The initial values of  $frH_{ac}$  and  $frAl_{ac}$ , as well as the initial concentrations of H, BC and Al were derived by combining

cation exchange equations with the charge balance equation. However, in some simulations the initial base saturation was determined by the net BC input (cf Eq. 6.17) using the values given in Table 6.5. Initial concentrations of  $\text{SO}_4$ ,  $\text{NO}_3$  and  $\text{NH}_4$  were determined by the initial values of  $\text{SO}_x$ ,  $\text{NO}_x$  and  $\text{NH}_x$  deposition, respectively (cf Annex C).

### Model parameters

Parameters in SMART are constants and soil properties that are assumed to be constant over the simulation period. The values used in the model are given in Table 6.7. Nitrification was assumed to be complete in all simulations ( $fr_{ni}=1$ ), whereas denitrification was assumed to be negligible ( $fr_{do}=0$ ). The stoichiometric ratio of Al to BC weathering was an average value for Ca-Mg silicates. Estimates of the constants  $K\text{Ca}_{cb}$ ,  $K\text{CO}_2$  and  $K\text{Al}_{ox}$  were derived from the literature (Robie and Waldbaum, 1968; May et al., 1979; Lindsay, 1979). The values for  $K\text{Al}_{ox}$  are representative for natural gibbsite (reference value), microcrystalline gibbsite (upper value) and synthetic gibbsite (lower value). The exchange constants were calculated from observed ion ratios at the adsorption complex and in soil water at 40 sites and 4 depths in acid forest soils (Kleijn and De Vries, 1987; Kleijn et al., 1989).

The values for  $K\text{Al}_{ox}$  are low, although values of a similar order of magnitude have been reported in the literature for sandy topsoils (Bache, 1974). Estimates of the physical soil properties  $\rho_{rz}$ ,  $\theta_{rz}$  and  $p\text{CO}_2$ , are indicative of well-drained sandy soils (Cosby et al., 1985b). The value of  $\theta_{rz}$  refers to the moisture content at field capacity. Actually, the yearly averaged moisture content might be much lower, but the model output was almost insensitive for this parameter. Data given for the CEC refer to pH values of 6.5, because the CEC of organic matter decreases with decreasing pH (Helling et al., 1964). The reference, upper and lower values for CEC are representative for a podzolic soil, an organic-rich loamy soil, and an extremely poor sandy soil, such as the dunes in the Netherlands (cf Section 6.3; De Vries et al., 1994a).

Table 6.7 Values of model parameters used in the simulations

Parameter	Unit	Reference	Upper	Lower
$fr_{ni}$	-	1.0	-	-
$fr_{do}$	-	0.0	-	-
$r$	-	2.0	-	-
$K\text{CO}_2$	$\text{mol}^2 \text{l}^{-2} \text{bar}^{-1}$	$10^{-7.8}$	-	-
$K\text{Ca}_{cb}$	$\text{mol}^3 \text{l}^{-3} \text{bar}^{-1}$	$10^{-5.83}$	-	-
$K\text{Al}_{ox}$	$\text{mol}^{-2} \text{l}^2$	$10^{9.77}$	$10^{9.35}$	$10^{8.11}$
$K\text{Al}_{ox}$	$\text{mol l}^{-1}$	1.0	10	0.1
$K\text{H}_{ox}$	$\text{mol}^{-1} \text{l}$	$15 \cdot 10^4$	$30 \cdot 10^4$	$7.5 \cdot 10^4$
$\rho_{rz}$	$\text{kg m}^{-3}$	1300	-	-
$\theta_{rz}$	$\text{m}^3 \text{m}^{-3}$	0.3	-	-
$p\text{CO}_2$	bar	0.02	0.04	0.01
CEC	$\text{mmol}_c \text{kg}^{-1}$	50	100	15

## MODEL BEHAVIOUR IN VARIOUS BUFFER RANGES

The behaviour of SMART in the various buffer ranges was evaluated by analysing the response of a calcareous soil to a constant high acid load ( $5000 \text{ mol}_c \text{ ha}^{-1} \text{ yr}^{-1}$ ) and a constant low acid load ( $500 \text{ mol}_c \text{ ha}^{-1} \text{ yr}^{-1}$ ) for a time period of 500 years. In this section we emphasize the results of a high acid load. First, results are given of the temporal response in soil pH, and the buffer mechanisms regulating this response are discussed. Secondly, the relationships between pH, base saturation and the A/BC ratio are discussed and results are given of the effect of parameter variation on the temporal response of these model outputs. Here, the A/BC ratio refers to the molar ratio of inorganic Al to the sum of Ca and Mg since the role of organic acids is not included in the model. However, effects on soil roots are mostly related to inorganic Al and not to total Al (Ulrich and Matzner, 1983; cf Section 4.2).

### Temporal response in soil pH

In Figure 6.4 the temporal pH trajectories are given for different values of the CEC. For roughly the first 50 years the soils stayed in the carbonate buffer range and the pH remained high. However, as soon as the carbonates were exhausted, there was a sudden drop in pH at high acid loads (Fig. 6.4A), which became even more pronounced with decreasing CEC. This is obvious, because the proton production in non-calcareous soils is initially mainly neutralized by exchange between H and BC, and the buffer capacity of the soil related to this mechanism decreases strongly with decreasing CEC.

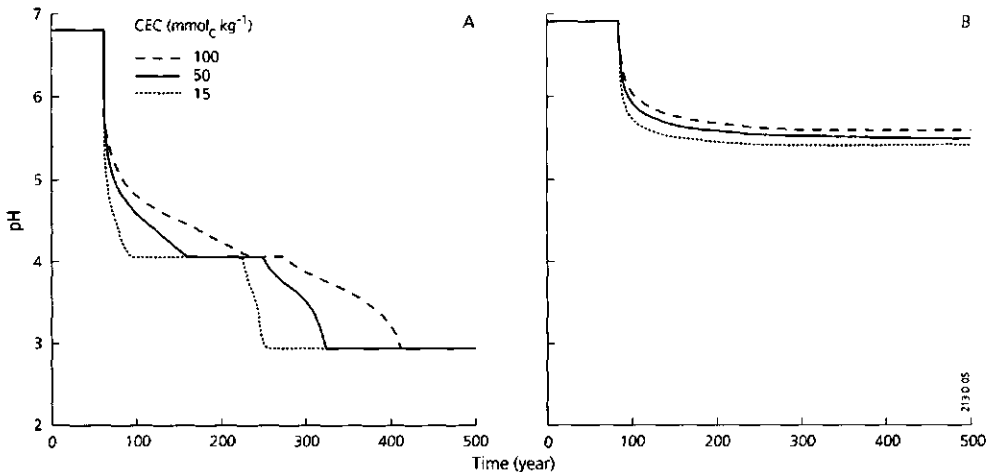


Figure 6.4 Temporal development of the pH of the calcareous soil in response to a constant high acid load (A) and a constant low acid load (B) (cf Table 6.4) for varying CEC values

The extremely sharp drop in pH for the lower *CEC* value resulted from the almost negligible exchange buffer capacity in this poor sandy soil. This caused an almost direct switch from the carbonate buffer range (pH ~ 6.8) to the aluminium buffer range (pH ~ 4.0), because BC weathering is far too low to neutralize this high acid input. Actually, this predicted sudden drop in pH has been found in dunes in the Netherlands at the boundary of calcareous and decalcified parent material (De Vries, unpublished pH data).

An increase in *CEC* caused a more gradual decrease in pH, especially in the pH range 5.0 to 4.0, which corresponds to the cation exchange buffer range defined by Ulrich (1981a, 1983). As long as the soil contains Al hydroxides, the pH remained above 4.0, but as soon as these minerals were depleted, the pH dropped further to values near 3.0. Again, this is illustrated most clearly for the poor sandy soil, where the pH dropped suddenly, after depletion of Al hydroxides. In the other soils, the change was more gradual, because of exchange between H and Al. The pH range between 4.0 and 3.0 coincides with the aluminium buffer range of Ulrich (1981a). However, Ulrich did not explicitly discuss the role of H/Al exchange in this pH range (see next section on buffer mechanisms).

At a low acid load (Fig. 6.4B) the soil pH finally dropped to about 5.5 and remained there in the so-called silicate weathering range (Ulrich 1981a, 1983). This final equilibrium pH can easily be explained by the fact that the external acid load ( $300 \text{ mol}_c \text{ ha}^{-1} \text{ yr}^{-1}$  because N is taken up by vegetation) is lower than the proton consumption by BC weathering ( $500 \text{ mol}_c \text{ ha}^{-1} \text{ yr}^{-1}$ , the upper value of  $BC_w$ ). Consequently, the steady-state soil pH was determined by the  $\text{CO}_2$  equilibrium. This evaluation of the behaviour of the model suggests that the concept of buffer ranges as introduced by Ulrich (1981a) and used in the old RAINS soil acidification model (Kauppi et al., 1986) is valid.

### Buffer mechanisms

Acid neutralization fluxes due to the various buffer mechanisms in non-calcareous soils, i.e. BC weathering, H adsorption and Al dissolution, are shown in Figure 6.5 as a function of pH and time, using the reference values as model inputs. BC weathering remained constant over the whole pH range (cf modelling approach). Al dissolution was negligible above pH 5.5 because Al, released by silicate weathering, precipitated as Al hydroxide (incongruent weathering). In this range the acid load was almost completely neutralized by exchange between H and BC at a rate that was even higher than  $5000 \text{ mol}_c \text{ ha}^{-1} \text{ yr}^{-1}$  (the external acid load) because of the internal H production by dissociation of  $\text{CO}_2$ .

Below pH 5.5, Al dissolution started to become an increasingly dominating buffer mechanism. This seems to contradict Ulrich's (1981a) hypothesis that the aluminium buffer range is between pH 4.2 and 3.0. However, above pH 4.2 Al dissolved by weathering, was almost completely adsorbed at the exchange complex. Consequently, one might argue that Al dissolution above pH 4.0 to 4.5 is only an internal redistribution of Al from hydroxides

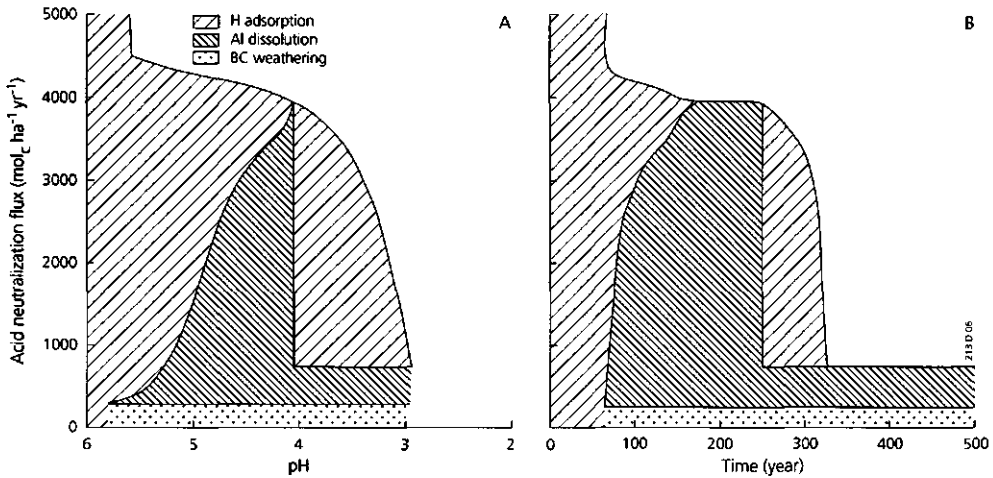


Figure 6.5 Acid neutralization fluxes of the calcareous soil as a function of pH (A) and time (B)

and silicates to the exchange complex (similar to the redistribution of Al from silicates to hydroxides above pH 5.0), whereas depletion of exchangeable BC is the ultimate buffer mechanism. When the Al hydroxides were depleted, the soil pH in the range between pH 4 and 3 was mainly buffered by H/Al exchange. This buffer mechanism was not described by Ulrich (1981a, 1983c), who limited the role of cation exchange to the pH range 5.0 to 4.2. He only refers to Al dissolution in the range between pH 4 and 3. Most likely, buffering in acid topsoils (below pH 4) will be regulated both by rate-limited Al dissolution from hydroxides and by H/Al exchange (cf Section 6.2; De Vries et al., 1994b).

The redistribution of Al in various buffer ranges (Fig. 6.6), illustrates the incongruent Al weathering above pH 5.0, Al redistribution from secondary precipitates to the exchange complex between pH 5.0 and 4.0 and Al desorption resulting from H/Al exchange below pH 4.0. As soon as Al hydroxides were depleted, H neutralization was completely due Al desorption (cf Fig. 6.5A and 6.6). The system was directly forced into a new equilibrium between H and Al on the exchange complex and in the soil solution. Mathematically, the equilibrium relationship between H and Al regulated by dissolution of  $\text{Al}(\text{OH})_3$  and by H/Al exchange is similar.

The role of cation exchange is also illustrated in Figure 6.7, which shows that H adsorption started near pH 5.5, whereas the increase in Al at the adsorption complex started near pH 5.0. In the Al buffer range the base saturation ( $frBC_{ac}$ ) decreased to almost zero (near pH 4.0), whereas the exchangeable H and Al fractions ( $frH_{ac}$  and  $frAl_{ac}$ ) were approximately 0.45 and 0.55, respectively. This is reasonably consistent with available data for acid forest soils although the base saturation in forest topsoils is generally higher (ca. 5-10%; cf Section 2.3). Underestimation of the base saturation is most likely due to the neglect of

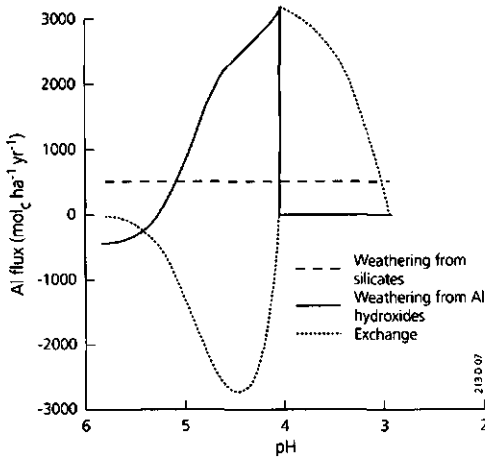


Figure 6.6 Al fluxes of the calcareous soil as a function of pH

nutrient cycling in SMART. The prediction of an almost negligible base saturation near pH 4.0 was nearly insensitive to the values of the exchange and solubility constants used. However, the exchange constants ( $KH_{ex}$  and  $KAl_{ex}$ ) and the Al solubility constant ( $KAl_{ox}$ ) did influence the final values of  $frH_{ac}$  and  $frAl_{ac}$  (cf Annex C).

### Relationships between base saturation, pH and aluminium-base cation ratio

As shown before, the response in soil pH between 7 and 4 depends strongly on the CEC (exchangeable BC content). The relationship between pH and base saturation in this pH range is influenced by the values of the solubility and exchange constants. Furthermore, since pH is strongly related to the Al concentration, these constants also affect the relationship between Al (and Al/BC ratio) and base saturation. This is illustrated in Figure 6.8 for varying  $KAl_{ex}$  (cf Eq. 6.24; BC is reference ion).

The predicted relationship between pH and base saturation (Fig. 6.8A) is consistent with empirical data given by Clark and Hill (1964) for various soils, especially podzols. An increase in  $KAl_{ex}$  yielded somewhat higher pH values at the same base saturation, but the effect is not dramatic. The effects of  $KH_{ex}$  and  $KAl_{ox}$  on pH (not shown here) were similar to that of  $KAl_{ex}$ , although the effect of  $KH_{ex}$  was more pronounced, especially at higher base saturations (above  $frBC_{ac} \sim 0.6$ ). The empirical relationship between effective CEC and pH, as found by Helling et al. (1964), suggests that H adsorption in soils rich in organic matter might even be much stronger at high pH values. It is likely that in these soils  $KH_{ex}$  decreases with a decreasing base saturation (increasing H saturation). Laboratory experiments at various pH levels (Section 3.2) also indicate a decrease in  $KH_{ex}$  with decreasing pH. The total removal of Al by H in the pH range below 4.0 (when Al hydroxides are depleted) is therefore questionable.

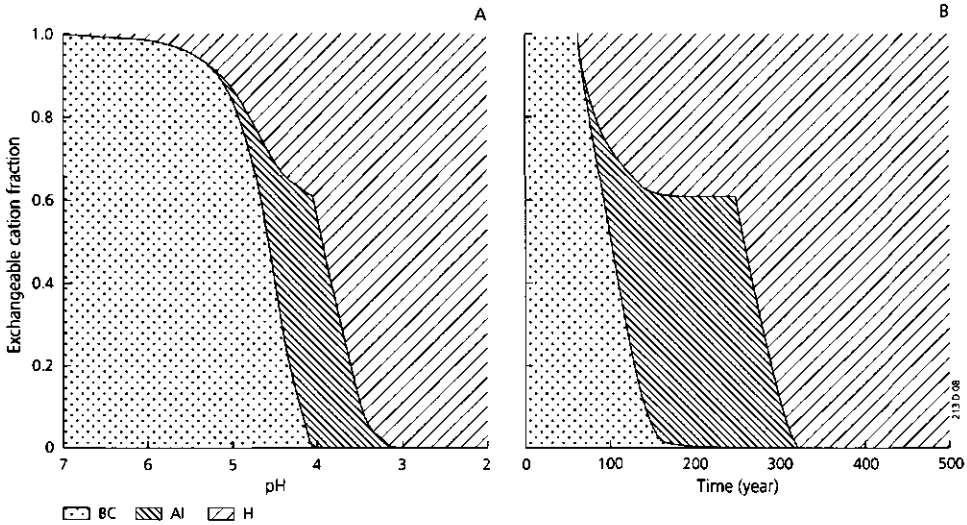


Figure 6.7 Exchangeable fractions of BC, Al and H of the calcareous soil as a function of pH (A) and time (B), using reference values as input data

The predicted relationship between Al/BC ratio and the base saturation (Fig. 6.8B) illustrates the preference of the adsorption complex for Al above BC. Unless the base saturation was depleted to about 30-40% ( $fr_{BC_{ac}} \sim 0.3-0.4$ ), Al did not come into solution. Higher values of  $KAl_{ex}$  caused an even more pronounced shape of the curve. The same was true for  $KH_{ex}$  and  $KAl_{ox}$ , although the effect of  $KAl_{ox}$  was small (not shown here).

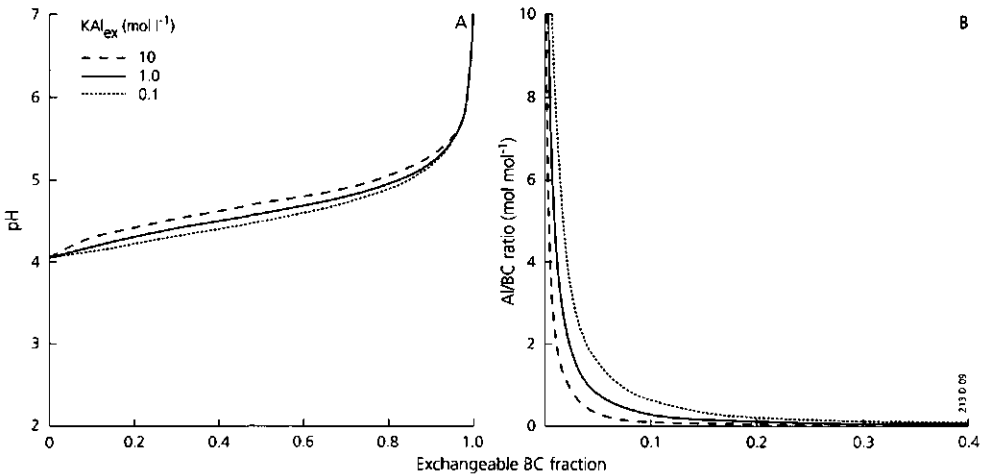


Figure 6.8 Relationships between the exchangeable BC fraction (base saturation) and pH (A) and Al/BC ratio (B) for varying  $KAl_{ex}$  values. Note that the values for  $ctAl_{ox} = 0$  are not displayed

Similar relationships were derived by Reuss (1983), using a model including Al dissolution from oxides and/or hydroxides and Al/BC exchange. Below a base saturation of 5-10% ( $fBC_{ac}=0.05$  to 0.10) the Al/BC ratio increased rapidly (cf Fig. 6.8B), whereas the pH was only slightly sensitive to changes in  $fBC_{ac}$  in this range (Fig. 6.8A). Consequently, the predicted relationship between Al/BC ratio and pH was also very pronounced. Near pH 4.0 a small change in pH causes a dramatic change in the Al/BC ratio. This pH value and the above-mentioned base saturation coincide with a critical Al/BC ratio of 1.0 (Ulrich and Matzner, 1983; Roelofs et al., 1985). However, the Al/BC ratio is a much more sensitive parameter than pH.

### Effects of parameter variation on the temporal development of the base saturation, aluminium-base cation ratio and pH

Contrary to the exchange constants, the CEC did not influence the relationship between pH or Al/BC ratio and base saturation. However, this soil property strongly influences the time development of these variables (Fig. 6.9). An increase in CEC leads to a longer time period for depleting the exchangeable base cations (Fig. 6.9A), thus causing a longer time lag before the Al/BC ratio starts to increase (Fig. 6.9B). The final Al/BC ratio was equal to the stoichiometric weathering ratio ( $r$ ), because BC deposition equalled BC uptake in the simulation.

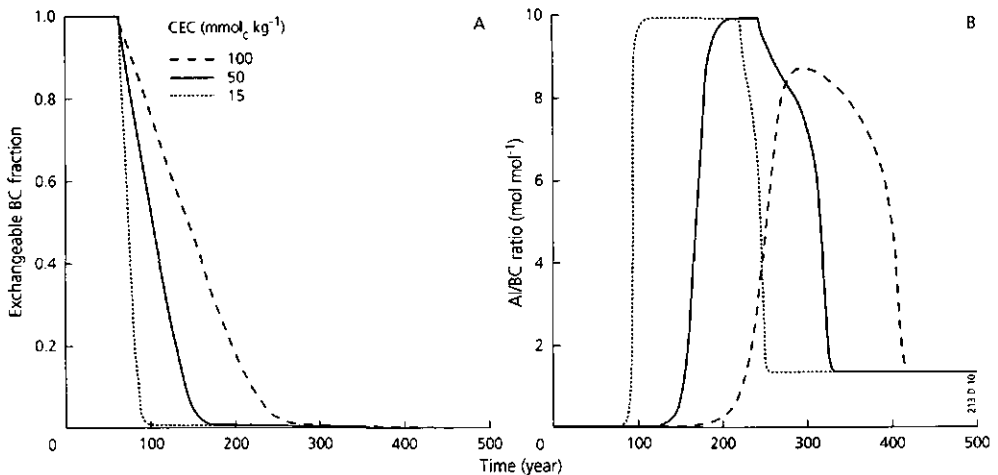


Figure 6.9 Temporal development of the exchangeable BC fraction (base saturation) (A) and Al/BC ratio (B) of the calcareous soils for different CEC values



The exchange constants also influence the temporal development of base saturation, pH and Al/BC ratio. An increase in either  $KAl_{ex}$  or  $KH_{ex}$  caused a faster depletion of exchangeable base cations and thus a shorter time period before the Al/BC ratio started to increase. This is illustrated in Figure 6.10 for  $KAl_{ex}$ .

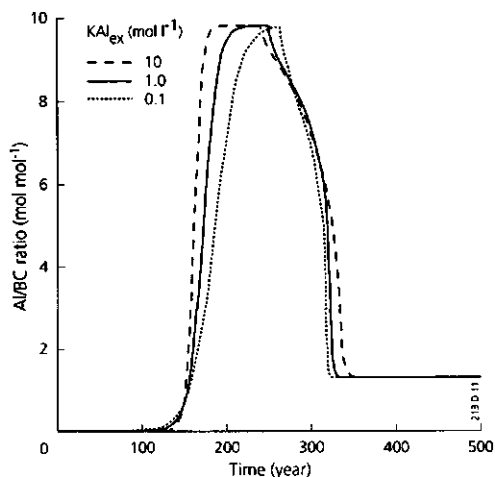


Figure 6.10 Temporal development of the Al/BC ratio of the calcareous soil for different  $KAl_{ex}$  values

The influence of total BC deposition and BC weathering on the temporal trajectories of pH, Al/BC ratio and base saturation is obvious. An increased input of BC, either by deposition or weathering, only slightly affected the trajectories of pH and base saturation, but it caused higher BC concentrations, leading to significantly lower Al/BC ratios in the Al buffer range (not shown here).

The influence of the precipitation excess,  $PE$ , is also very obvious; a lower  $PE$  caused higher concentrations of H (lower pH), Al and BC, whereas the Al/BC ratio remained unaffected. However, starting with an initially calcareous soil, a decrease in  $PE$  also caused an increase in the duration of carbonate weathering, thus causing a time lag in the decrease of pH and base saturation and the increase of the Al/BC ratio. This is illustrated for the pH in Figure 6.11. The influence of variations in  $pCO_2$  was similar to  $PE$  (not shown), because a decrease in  $pCO_2$  also increases the duration of carbonate weathering. However, at lower pH (below pH 4.5) the influence of variations in  $pCO_2$  was negligible.

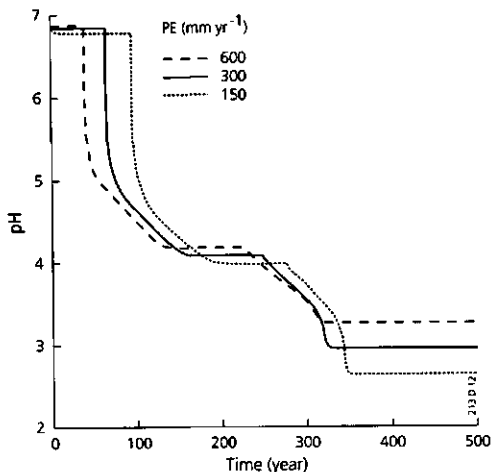


Figure 6.11 Temporal development of the pH of the calcareous soil for different precipitation excesses

## SCENARIO ANALYSIS

The temporal response of the Al/BC ratio and the base saturation of the non-calcareous soil to the four deposition scenarios (Fig. 6.12) showed a considerable time lag between the period of acid deposition increase (25 years) and Al/BC ratio increase. The time period before the Al/BC ratio became critical (above 1.0) was approximately 35 years (cf Fig. 6.12A). This coincides with a base saturation of approximately 5% and is consistent with the relationship between Al/BC ratio and base saturation given earlier (Fig. 6.8B).

The deposition reductions between the 50<sup>th</sup> and 75<sup>th</sup> year for scenarios 2, 3 and 4 almost directly influenced the predictions of the Al/BC ratio. This is conceivable, because a decreased input of S and N directly influences the concentrations of SO<sub>4</sub> and NO<sub>3</sub> and, in turn, this directly influences the Al concentration (charge balance), because Al dissolution is the dominant buffer mechanism in acid sandy soils. For some soils the time lag might be somewhat longer because of SO<sub>4</sub> desorption, but this process is not included in the model. Figure 6.12A shows that a deposition reduction of 30% still caused an increase in the Al/BC ratio. A reduction of at least 70% (up to 1000 mol<sub>c</sub> ha<sup>-1</sup> yr<sup>-1</sup>) was needed to arrive at a final Al/BC ratio of 1.0, but the time taken to achieve this ratio was more than 100 years (not shown in Fig. 6.12A). However, one should be aware that the nutrient cycle is not included in the model. The Al/BC ratio is completely dependent on geochemical interactions, because net BC uptake equalled BC deposition in these simulations (cf the reference values in Table 6.5).

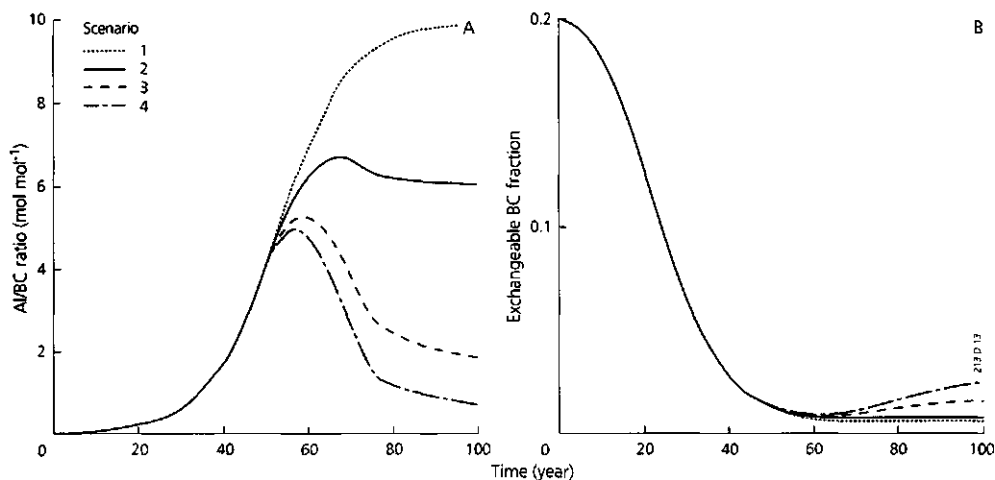


Figure 6.12 Temporal development of the Al/BC ratio (A) and exchangeable BC fraction (base saturation) (B) of the non-calcareous soil in response to four deposition scenarios (reference values were used for initial conditions and parameters)

Consequently, the predicted ratios will be most reliable for subsoils (e.g. below B-horizons). In the topsoil the Al/BC ratio will be more favourable because of a net input of base cations by deposition and mineralization. Nevertheless, a deposition level of 1000-1500 mol<sub>c</sub> ha<sup>-1</sup> yr<sup>-1</sup> is consistent with critical loads of 1400 to 1800 mol<sub>c</sub> ha<sup>-1</sup> yr<sup>-1</sup> that have been derived for Dutch forest soils in relation to a critical Al/BC ratio of 1.0 for the top 30 cm by using a steady-state soil acidification model including the biocycle (De Vries, 1988). However, in this model lower values were taken for N uptake and BC weathering.

The results of scenario 4 show that the decrease in the Al/BC ratio between 50 and 75 years was very fast, but the decrease of this ratio at background deposition levels after 75 years was very slow. It took hundreds of years to regain the initial ratio. This can easily be explained by the pronounced relationship between the Al/BC ratio and base saturation (Fig. 6.8B). A small increase in base saturation at low levels (Fig. 6.12B) caused a sharp decline in the Al/BC ratio, but this effect was much less pronounced at higher levels. Furthermore, the "recovery period" required to regain the original base saturation was always longer than the "acidification period". The relatively high net acid input (acid load minus N uptake minus BC weathering) during the "acidification period" caused a much faster depletion of exchangeable base cations than the addition of base cations during the "recovery period" with a very low net acid input. In other words, depletion of exchangeable bases resulting from Al/BC exchange induced by Al dissolution, is always faster than the addition of exchangeable bases resulting from BC/Al exchange, induced by BC weathering. This result has also been shown using the MAGIC model (Cosby et al., 1985c).

For a given scenario the temporal trajectory of the Al/BC ratio mainly depended on the initial amount of exchangeable base cations. This is illustrated for scenario 4 for varying CEC values (Fig. 6.13A). The time lag between the maximum acid load (after 25 years) and the maximum Al/BC ratio increased with increasing CEC, but the recovery time was also longer. This is shown most clearly by the difference between the reference CEC and the lower CEC value. In the latter case, changes in the acid load were followed almost immediately by changes in the Al/BC ratio, because the exchange buffer is nearly negligible. Variations in  $frBC_{ac}$  were comparable with CEC changes. Apart from initial conditions, the temporal Al/BC trajectory was also influenced by the exchange constants, because higher constants caused a faster depletion. However, this effect was relatively small (Fig. 6.13B), although it increased with increasing initial base saturation (cf Fig. 6.10).

Variations in precipitation excess and partial  $CO_2$  pressure had negligible effects on changes in base saturation and Al/BC ratio. However, a change in net BC input, either by deposition or by weathering, did influence both output variables. This is again illustrated for the Al/BC ratio for varying base cation weathering rates, using scenario 4 (Fig. 6.14). During the first 20 to 30 years the effect was small, because of the pronounced relationship between Al/BC ratio and base saturation. However, after 50 years the Al/BC ratio was significantly influenced. This was even more pronounced when a relationship between BC weathering and the initial base saturation was assumed (Fig. 6.14B). The initial base saturation was regulated by the initial concentration of BC, which depends on deposition, weathering and uptake, and the initial concentration of Al, which depends on the background deposition of  $SO_x$ ,  $NO_x$  and  $NH_x$  and BC weathering.

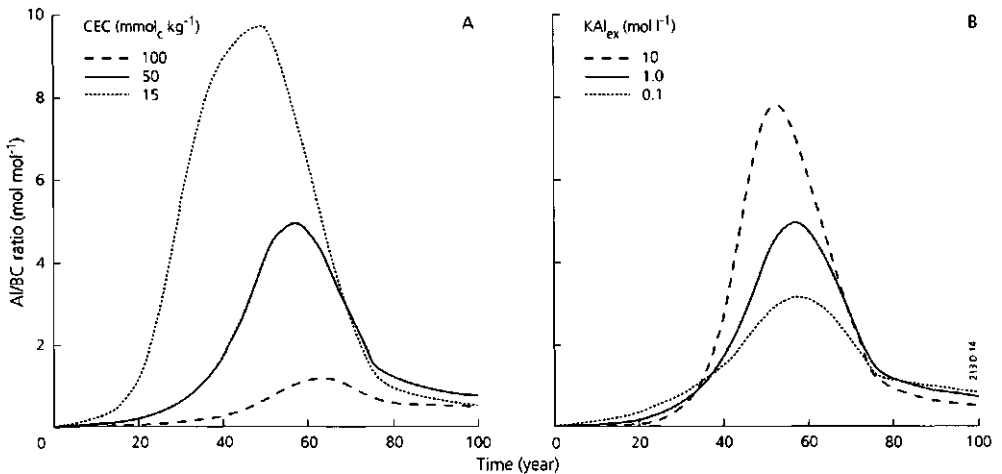


Figure 6.13 Temporal development of the Al/BC ratio of the non-calcareous soil in response to scenario 4 (90% reduction; cf Table 6.4 and Figure 6.3) for different CEC (A) and  $KAl_{ex}$  (B) values

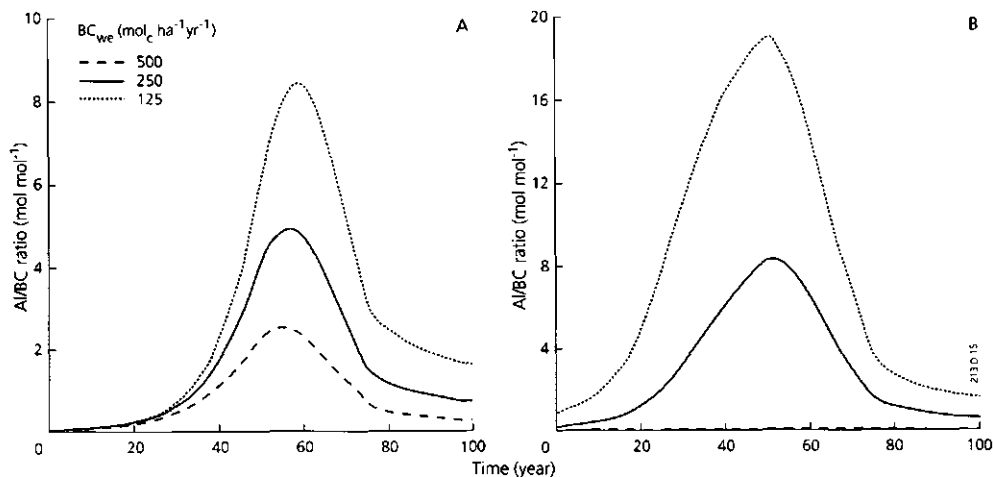


Figure 6.14 Temporal development of the Al/BC ratio of the non-calcareous soil in response to scenario 4 (90% reduction; cf Table 6.4 and Figure 6.3) for different base cation weathering rates using an initial base saturation of 20% (A) and an initial base saturation determined by the model (B)

Initial base saturation thus calculated varied between 80% and 5%. In the first case the Al/BC ratio hardly increased, because the base saturation was only depleted to 30%. In the last case the Al/BC ratio increased to a value near 20, because the exchangeable bases were nearly exhausted.

## CONCLUDING REMARKS

The question whether the long-term soil responses estimated by SMART are accurate projections of the real system cannot be answered satisfactorily, since historical observations of past soil chemistry are too scarce to be suitable for a rigorous model testing (cf Van Oene and De Vries, 1994). However, we can conclude that SMART - including processes that are thought to be most important in influencing soil responses to acidic deposition and using parameter values within ranges appropriate for natural soils - produces plausible results, which are reasonably consistent with Ulrich's concept of buffer ranges. However, in this concept the role of cation exchange is somewhat underestimated. This buffer mechanism does not only neutralize protons between pH 5.2 and 4.0, as suggested by Ulrich (1981a), but it plays a role in the entire pH range between 7 and 3.

The model results show that soil response depends mainly on its initial conditions. In calcareous soils, weathering is rapid and the pH remains high until the carbonates are exhausted. For a soil layer of 50 cm and a bulk density of  $1300 \text{ kg m}^{-3}$  one per cent of  $\text{CaCO}_3$  corresponds to a buffer capacity of  $1300 \text{ kmol}_c \text{ ha}^{-1}$ . This clearly shows that acidic inputs to these soils will not cause a problem in the near future, although this amount can

be exhausted in approximately 100 years because of the high internal production of protons by dissociation of  $\text{CO}_2$ .

The response of slightly acid soils largely depends on the initial amount of exchangeable base cations. Taking the same layer thickness and bulk density, an average exchangeable BC content of  $10 \text{ mmol}_c \text{ kg}^{-1}$  (based on reference values for the base saturation and CEC; cf Table 6.6 and 6.7) results in a buffer capacity of  $65 \text{ kmol}_c \text{ ha}^{-1}$ . At high acid loads, this amount can be exhausted in several decades, as shown by the various simulation results. A further decrease in pH depends on the amount of Al hydroxides, which in general are abundant. Again, taking the same soil thickness and bulk density, and assuming an average Al hydroxide content of  $150 \text{ mmol}_c \text{ kg}^{-1}$  (cf Table 6.6), the buffer capacity equals  $975 \text{ kmol}_c \text{ ha}^{-1}$ . This seems an almost infinite amount, as suggested in most of the literature. However, considering a layer thickness of 10 cm only and a high acid input typical for large parts of Western and Eastern Europe, this amount could be exhausted in several decades. This dramatic change in soil chemistry may have serious ecological consequences.

## 6.2 IMPACTS ON A CHARACTERISTIC FOREST SOIL IN THE NETHERLANDS

### ABSTRACT

*The long-term (60 yr) impact of a reducing atmospheric deposition scenario on the soil and soil solution chemistry of a representative acid forest soil in the Netherlands was evaluated using RESAM (Regional Soil Acidification Model), a process-oriented soil acidification model. The model simulates the major biogeochemical processes occurring in the forest canopy, humus layer and mineral horizons including canopy interactions, element cycling processes, nitrogen transformation processes, and geochemical weathering and exchange reactions. The deposition scenario used was based on expected policy measures in the Netherlands. At high inputs of S and N, model results showed (i) a dominant role of (N transformations by) mineralization, root uptake and nitrification and of Al mobilization in the uppermost soil layers on the proton budget, (ii) tracer behaviour of  $SO_4$  and retention of N, (iii) a strong relationship between leaching of Al and that of  $SO_4$  plus  $NO_3$  and (iv) a dominant role of Al hydroxide dissolution in Al mobilization which are all in agreement with field and/or laboratory measurements. At reduced deposition levels RESAM predicted (i) an inversion from net N retention to net N mobilization followed by net N retention again, (ii) a strong decrease in Al hydroxide dissolution and (iii) a relative fast de-acidification of the soil, reflected by an increase in pH and base saturation and a decrease in Al concentration. The reliability of these predictions is discussed in view of available data.*

### INTRODUCTION

Governments in Europe and North America are currently under increasing pressure to take remedial action against the acidification of the environment. However, decisions on policies regarding emission-reductions require insight in the effectiveness of abatement strategies in reducing long-term environmental effects. In this respect, models provide an important management tool to assist decision makers in their evaluation of strategies to control sulphur and nitrogen emissions. Consequently, the Dutch Priority Programme on Acidification initiated the development of a model system, i.e. the Dutch Acidification Systems (DAS) model which quantitatively predicts environmental impacts, for given geographical areas over a given time, for alternative emission scenarios (Olsthoorn et al., 1990).

In the overall framework, the REgional Soil Acidification Model RESAM forms an important linkage between atmospheric deposition and effects on terrestrial and aquatic ecosystems. This section gives a complete and extensive description of the RESAM model and its behaviour by analyzing the long-term (60 yr) impact of a reducing deposition scenario on a representative forest-soil combination in the Netherlands, i.e. a Cambic Podzol (Entic Haplorthod) covered with Douglas Fir. Results are limited to the soil and soil solution chemistry in the rootzone. In Section 7.2 (cf De Vries et al., 1994c) the application of RESAM to the Netherlands is described.

## THE RESAM MODEL

### Modelling approach

At present, various acidification models are available, ranging from a simple static lumped empirical model (e.g. Wright and Hendriksen, 1983) to a complex dynamic distributed process-oriented model (e.g. Chen et al., 1983). Most acidification models are process-oriented. Examples are 'the Birkeness model' (Christophersen et al., 1982), 'ILWAS' (Chen et al., 1983; Gherini et al., 1985), 'MAGIC' (Cosby et al., 1985a, b) and 'SMART' (De Vries et al., 1989b; Section 6.1). These so-called soil-oriented charge balance models (Reuss et al., 1986) are based on the anion mobility concept through the charge balance principle and incorporate common geochemical processes, such as cation exchange,  $\text{SO}_4$  adsorption and dissolution of Al from hydroxides. Apart from 'ILWAS', these models do not simulate the cycling of nutrients in the vegetation through biochemical processes such as uptake, litterfall and mineralization. However, incorporation of the nutrient cycle is of major importance in predicting the concentration of nutrients ( $\text{NH}_4$ ,  $\text{NO}_3$ , Ca, Mg and K) within the rootzone, especially in the upper soil layers. Since RESAM is linked with models describing the effect of acidification on terrestrial ecosystems (SOILVEG; Berdowski et al., 1991 and FORGRO; Mohren et al., 1991), these predictions are very important. Consequently, incorporating biochemical processes, as was done in ILWAS, was considered necessary. The reason for not adopting ILWAS itself is the focus of this model on short term interannual dynamics, whereas RESAM focuses on long-term impacts of acid deposition on soils.

A modelling approach is largely determined by the goals of the model application. In order to use RESAM both as a research tool and a management tool (cf Chapter 1), the model is characterized by: (i) a deterministic process-oriented approach with relative simple process descriptions and (ii) dynamic simulation with spatially (regionally) distributed data input. Stochastic aspects can, however, be included by using a Monte Carlo approach, while specifying the range in input data (e.g. Kros et al., 1993). Simplifications of process descriptions in RESAM refer especially to solute transport. It is assumed that: (i) all soil layers are homogeneous compartments of constant density, (ii) the element input mixes completely in all soil layers and (iii) the water flow is stationary on a yearly basis, which implies that the annual average water flux leaching from a soil layer equals the infiltration minus the transpiration. Furthermore, N fixation,  $\text{SO}_4$  reduction and  $\text{SO}_4$  precipitation and complexation reactions are not included and the various process descriptions for bio- and geochemical interactions are simplified to minimize input data. The temporal resolution of model input and output is one year as RESAM is developed to gain insight in the long-term chemical response of forest ecosystems to acid deposition. However, the time step of the model is five days to avoid numerical instability and to minimize numerical dispersion. The regional distribution of data related to atmospheric input, tree species and soil type is taken into account by using geographic information systems. The model is described in terms of



parameters that can be related to these data (e.g. soil survey information) with so-called pedotransfer functions.

### General model concept

Figure 6.15 shows the general concept and structure of the RESAM model. State variables depict the quantity of water or chemical constituent in each compartment at any given time. Rate variables depict the processes influencing state variables (including soil water chemistry). The acidification process is conceptualized in RESAM as a disturbance in the S and N cycle in forests, resulting from the deposition of  $\text{SO}_x$ ,  $\text{NO}_x$  and  $\text{NH}_x$ . This induces an

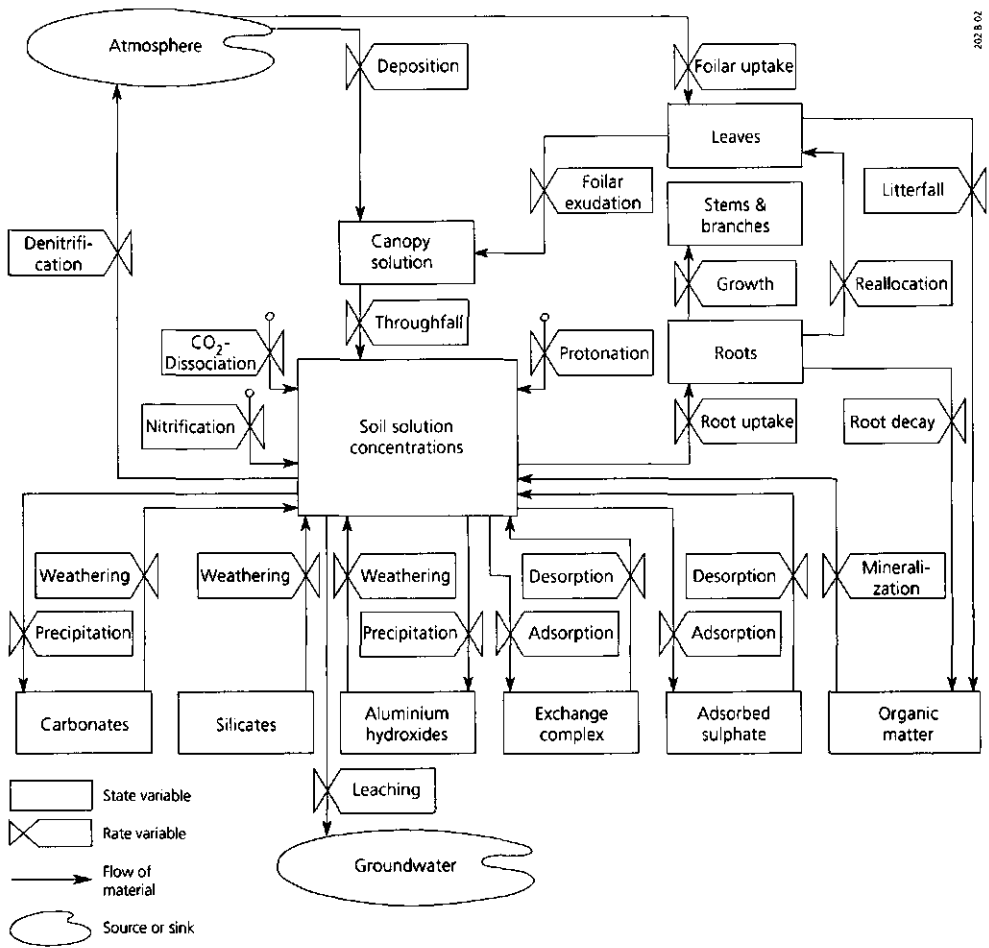


Figure 6.15 Relation diagram of the RESAM model

excess of strong acid anions ( $\text{SO}_4$  and  $\text{NO}_3$ ) over basic cations (Ca, Mg and K) associated with a strong proton production (Reuss and Johnson, 1986). Processes in the forest canopy affecting the element and proton input to the soil (throughfall) are filtering and uptake of gaseous air pollutants ( $\text{SO}_2$ ,  $\text{NO}_x$ ,  $\text{NH}_3$ ) and exudation of base cations (Ca, Mg and K) by exchange with  $\text{NH}_4$  and H. Retention of potential acid S and N compounds in biomass (vegetation and soil organic matter) is influenced by processes related to element cycling, i.e. litterfall, root decay, net mineralization and root uptake. The N cycle is further influenced by nitrification and denitrification. The proton load, resulting from atmospheric deposition and from the mentioned biochemical processes, is partly neutralized by mineral weathering, which is a slow buffer process, and by (relatively) fast buffer processes, such as protonation of organic anions (RCOO),  $\text{SO}_4$  adsorption, cation exchange and Al dissolution from hydroxides.

### Basic process formulations

RESAM consists of a set of mass balance equations, to describe input-output relationships for the various elements included, combined with equilibrium equations and rate-limited equations to describe the various processes in a forest ecosystem. An overview of the processes and process descriptions in RESAM in relation to the various elements considered is given in Table 6.8

Table 6.8 Overview of the elements and processes included in RESAM.  
(\*+ = ion included, \*- = ion not included)

Process	Description	H	Al	Ca	Mg	K	Na	$\text{NH}_4$	$\text{NO}_3$	$\text{SO}_4$	Cl	$\text{HCO}_3$	RCOO
Foliar uptake	Rate-limited	+	-	-	-	-	-	+	+	+	-	-	-
Foliar exudation	Rate-limited	+	-	+	+	+	-	-	-	-	-	-	-
Litterfall	Rate-limited	-	-	+	+	+	-	(+) <sup>1)</sup>	(+) <sup>1)</sup>	+	-	-	-
Root decay	Rate-limited	-	-	+	+	+	-	(+)	(+)	+	-	-	-
Mineralization	Rate-limited	+	-	+	+	+	-	+	-	+	-	-	+
Maintenance uptake	Rate-limited <sup>2)</sup>	+	-	+	+	+	-	+	+	+	-	-	-
Growth uptake	Rate-limited <sup>2)</sup>	+	-	+	+	+	-	+	+	+	-	-	-
Nitrification	Rate-limited	+	-	-	-	-	-	+	+	-	-	-	-
Denitrification	Rate-limited	+	-	-	-	-	-	-	+	-	-	-	-
Dissociation	Equilibrium	+	-	-	-	-	-	-	-	-	-	+	-
Protonation	Rate-limited	+	-	-	-	-	-	-	-	-	-	-	+
Carbonate weathering	Rate-limited	+	-	+	-	-	-	-	-	-	-	+	-
Silicate weathering	Rate-limited	+	+	+	+	+	+	-	-	-	-	-	-
Al hydroxide weathering	Rate-limited	+	+	-	-	-	-	-	-	-	-	-	-
Cation exchange	Equilibrium	+	+	+	+	+	+	+	-	-	-	-	-
Sulphate adsorption	Equilibrium	+	-	-	-	-	-	-	-	+	-	-	-

<sup>1)</sup> Input by litterfall and root decay is in the form of organic N.

<sup>2)</sup> Forcing function

The mass balance equations describe the input-output relationships for all cations and anions (except for  $\text{HCO}_3$  and H) in each soil layer  $l$  according to:

$$\frac{dX_{tot(l)}}{dt} = X_{in(l-1)} + X_{int(l)} - X_{out(l)} \quad (6.26)$$

where  $X_{tot}$  stands for the total amount of element X in a layer ( $\text{mol}_c \text{ ha}^{-1}$ ) and where the subscript *in* refers to the input from a previous layer, *int* to the interaction in a layer and *out* to the output from a layer ( $\text{mol}_c \text{ ha}^{-1} \text{ yr}^{-1}$ ). To simplify the presentation of various equations, the index  $l$  for soil layer is not used further in this section.

The soil compartment is confined by the mean lowest water table. The model contains a mass balance for Ca in carbonates, for Ca, Mg, K and Na in litter, primary minerals and at the adsorption complex, for Al in hydroxides and at the adsorption complex, for N in litter and for S in litter and at the adsorption complex. The concentration of  $\text{HCO}_3$  in each layer is calculated by assuming equilibrium with  $\text{CO}_2$  according to:

$$[\text{HCO}_3] = K\text{CO}_2 \cdot p\text{CO}_2 / [\text{H}] \quad (6.27)$$

The H and  $\text{HCO}_3$  concentration are also determined by the charge balance equation ( [ ] denotes the concentration in  $\text{mol}_c \text{ m}^{-3}$ ):

$$[\text{H}] + [\text{Al}] + [\text{Ca}] + [\text{Mg}] + [\text{K}] + [\text{Na}] + [\text{NH}_4] = [\text{NO}_3] + [\text{SO}_4] + [\text{Cl}] + [\text{HCO}_3] + [\text{RCOO}] \quad (6.28)$$

## Biochemical process formulations

### Canopy interactions

The solute input fluxes to the (organic) topsoil by throughfall are calculated in RESAM from the total deposition corrected for canopy interactions, i.e. foliar uptake and foliar exudation. Foliar uptake of  $\text{NH}_4$ ,  $\text{NO}_3$ ,  $\text{SO}_4$  ( $\text{mol}_c \text{ ha}^{-1} \text{ yr}^{-1}$ ) and H is described as a linear function of the total deposition of these elements:

$$X_{fu} = frX_{fu} \cdot X_{td} \quad (6.29)$$

where  $frX_{fu}$  is the foliar uptake fraction of element X (-) and where the subscript *fu* refers to foliar uptake and *td* to total deposition. The total deposition of free H,  $H_{td}$ , is calculated from the charge balance:

$$H_{td} = SO_{4,td} + NO_{3,td} + Cl_{td} - Ca_{td} - Mg_{td} - K_{td} - Na_{td} - NH_{4,td} \quad (6.30)$$

Foliar exudation of the cations Ca, Mg and K is assumed to be triggered by exchange with  $NH_4$  (Roelofs et al., 1985) and H (Ulrich and Matzner, 1983) according to:

$$Ca_{fe} + Mg_{fe} + K_{fe} = NH_{4,fu} + H_{fu} \quad (6.31)$$

where the subscript *fe* refers to foliar exudation. The foliar exudation flux of each individual cation,  $X_{fe}$ , is calculated as:

$$X_{fe} = frX_{fe} \cdot (Ca_{fe} + Mg_{fe} + K_{fe}) \quad (6.32)$$

where  $frX_{fe}$  is the foliar exudation fraction of Ca, Mg or K (-). The sum of  $frCa_{fe}$ ,  $frMg_{fe}$  and  $frK_{fe}$  equals 1.

#### *Litterfall and root decay*

In RESAM, litterfall and root decay are the input to the organic pools of N, Ca, Mg, K and S, i.e. litter and dead fine roots (root necro-mass). Input fluxes of N, Ca, Mg, K and S by litterfall,  $X_{lf}$ , and root decay,  $X_{rd}$  (both in  $mol_c ha^{-1} yr^{-1}$ ), are described similar, i.e.:

$$X_{lf} = (1 - frX_{re,lv}) \cdot k_{lf} \cdot Am_{lv} \cdot ctX_{lv} \quad (6.33)$$

$$X_{rd} = (1 - frX_{re,rt}) \cdot k_{rd} \cdot Am_{rt} \cdot ctX_{rt} \quad (6.34)$$

where  $k_{lf}$  and  $k_{rd}$  are the litterfall and root decay rate constants ( $yr^{-1}$ ),  $Am_{lv}$  and  $Am_{rt}$  are the amounts of leaves (or needles) and fine roots ( $kg ha^{-1}$ ),  $ctX_{lv}$  and  $ctX_{rt}$  are the contents of element X in leaves and fine roots ( $mol_c kg^{-1}$ ) and  $frX_{re,lv}$  and  $frX_{re,rt}$  are reallocation fractions for element X in leaves and fine roots respectively (-).

Root decay is limited to the dynamic turnover of fine roots. The distribution of this process with depth is determined by the distribution of fine roots. Reallocation of Ca, Mg, K and S in leaves and fine roots prior to litterfall or root death is considered negligible. However, reallocation of N from the older needles to younger needles litterfall cannot be neglected unless N contents are very high (Oterdoom et al., 1987). Consequently, the reallocation fractions are described as a function of the N contents according to:

$$fr_{re} = fr_{re,max} \cdot \left( \frac{ctN_{re,max} - ctN}{ctN_{re,max} - ctN_{re,min}} \right) \quad \text{for } ctN_{re,min} \leq ctN \leq ctN_{re,max} \quad (6.35)$$

where  $ctN_{re,max}$  is a maximum N content in leaves or fine roots ( $mol_c kg^{-1}$ ) above which reallocation is nihil and  $ctN_{re,min}$  is the minimum N content in leaves or fine roots ( $mol_c kg^{-1}$ ) below which reallocation is at its maximum. When  $ctN$  is less than  $ctN_{re,max}$ ,  $fr_{re} = fr_{re,max}$  and when  $ctN$  is more than  $ctN_{re,max}$ ,  $fr_{re} = 0$

High contents of N in leaves and fine roots in Dutch forests are caused by the high N deposition level. To account for this effect, the N content in leaves and fine roots is calculated as a function of the N deposition according to:

$$ctN = ctN_{min} + (ctN_{max} - ctN_{min}) \cdot \left( \frac{N_{td} - N_{td,min}}{N_{td,max} - N_{td,min}} \right) \quad \text{for } N_{td,min} < N_{td} < N_{td,max} \quad (6.36)$$

where  $ctN_{min}$  and  $ctN_{max}$  are the minimum and maximum N content in leaves or fine roots respectively ( $mol_c kg^{-1}$ ) and  $N_{td,min}$  and  $N_{td,max}$  are the minimum and maximum total deposition levels of N ( $mol_c ha^{-1} yr^{-1}$ ) between which the N content of leaves and fine roots is influenced. When  $N_{dt}$  is less than  $N_{dt,min}$ ,  $ctN = ctN_{min}$  and when  $N_{td}$  is more than  $N_{td,max}$ ,  $ctN = ctN_{max}$ . Equation (6.36), is included in RESAM with a certain delay period between deposition change and change in N content.

#### Mineralization

For the simulation of the decomposition of above ground organic matter (litter) a distinction is made between a rapidly decomposing pool of fresh litter (less than 1 year old) and a slowly decomposing pool of old litter (more than 1 year) (Janssen, 1984). The mineralization flux of N (during mineralization, N is released as  $NH_4$ ), Ca, Mg, K and  $SO_4$  ( $mol_c ha^{-1} yr^{-1}$ ) from fresh litter,  $X_{mi,fl}$  is described as:

$$X_{mi,fl} = (fr_{le} + fr_{mi} \cdot (1 - fr_{le})) \cdot X_{fl} \quad (6.37)$$

where  $fr_{mi}$  is a mineralization fraction (-) and  $fr_{le}$  is a leaching fraction (-). Leaching only refers to the release of cations from fresh litter just after litterfall, a process which is especially important for K. Actually, leaching is a process which differs from mineralization since organic matter is not decomposed. However, both processes have been lumped since both leaching and mineralization lead to a release of elements to the soil solution. Fresh litter which is not mineralized is transferred to the old litter (humus) pool. The mineralization flux of  $NH_4$ , Ca, Mg, K and  $SO_4$  from this litter pool,  $X_{mi,lt}$  is described by first order kinetics (Van Veen, 1977):

$$X_{mi,lt} = k_{mi,lt} \cdot Am_{lt} \cdot ctX_{lt} \quad (6.38)$$

where  $k_{mi,lt}$  is the mineralization rate constant from old litter ( $yr^{-1}$ ),  $Am_{lt}$  is the amount of old litter ( $kg ha^{-1}$ ) and  $ctX_{lt}$  is the content of element X in old litter ( $mol_c kg^{-1}$ ). At present,

mineralization of organic matter in the mineral soil layers is not considered in RESAM, except for the mineralization from root necro-mass, which is fed by root decay as described before. As with old litter, mineralization of root necromass,  $X_{mi,mr}$  is described as:

$$X_{mi,m} = k_{mi,m} \cdot Am_m \cdot ctX_m \quad (6.39)$$

where  $k_{mi,m}$  is the mineralization rate constant of root necro-mass ( $yr^{-1}$ ),  $Am_m$  is the amount of root necro-mass ( $kg\ ha^{-1}$ ) and  $ctX_m$  is the content of element X in root necro-mass ( $mol_c\ kg^{-1}$ ). The flux of organic anions,  $R_{COO_{mi}}$  produced during mineralization from both fresh and old litter and from root necro-mass ( $mol_c\ ha^{-1}\ yr^{-1}$ ) is calculated from charge balance considerations:

$$R_{COO_{mi}} = NH_{4,mi} + Ca_{mi} + Mg_{mi} + K_{mi} - SO_{4,mi} \quad (6.40)$$

Rate constants and fractions describing mineralization, are described in RESAM as maximum values, which are reduced for environmental factors such as ground water level and pH (cf De Vries et al., 1988). Maximum values for the mineralization fraction,  $f_{mi,max}$ , and mineralization rate constants,  $k_{mi,lt,max}$  and  $k_{mi,m,max}$ , are taken equal for all elements except for nitrogen, for which the values are reduced at low N contents (high C/N ratios) to account for immobilization by microbes according to (Janssen, 1983):

$$f_{N_{mi}} = 1 + \frac{1}{RDA_{mo}} \cdot \left( \frac{C/N_{mo} - C/N_s}{C/N_{mo}} \right) \quad \text{for } C/N_{mo} < C/N_s < (1+RDA_{mo}) \cdot C/N_{mo} \quad (6.41)$$

where  $f_{N_{mi}}$  is the reduction factor by which the mineralization fraction and rate constants are multiplied (-),  $C/N_{mo}$  is the C/N ratio of the micro-organisms decomposing the substrate (-),  $C/N_s$  is the C/N ratio of the substrate (fresh litter, old litter or dead roots) and  $RDA_{mo}$  is the dissimilation to assimilation ratio of the decomposing microbes (-). When  $C/N_s$  is less than  $C/N_{mo}$ ,  $f_{N_{mi}} = 1$  and when  $C/N_{mo}$  is more than  $(1+RDA_{mo}) \cdot C/N_{mo}$ ,  $f_{N_{mi}} = 0$ . Values for  $RDA_{mo}$  and  $C/N_{mo}$  are related to fungi because they are mainly responsible for mineralization of forest litter.

#### Root uptake

Total root uptake of  $NH_4$ ,  $NO_3$ , Ca, Mg, K and  $SO_4$  ( $mol_c\ ha^{-1}\ yr^{-1}$ ) is described in RESAM as a demand function, which consists of maintenance uptake, to resupply the needles/leaves and roots (steady-state situation), and net (growth) uptake in stems and branches according to:

$$X_{ru} = X_{lf} + X_{rd} + X_{le} + X_{gu} \quad (6.42)$$

where X stands for Ca, Mg, K or SO<sub>4</sub> and where the subscript *ru* refers to root uptake and *gu* to growth uptake. For SO<sub>4</sub> the foliar exudation is negative (uptake). RESAM has two options for growth uptake; i.e. a constant growth and a logistic growth according to:

$$X_{gu} = k_{gc} \cdot ctX_{st} \quad (6.43)$$

$$X_{gu} = k_{gt} \cdot \left( 1 - \frac{Am_{st}}{Am_{st,max}} \right) \cdot ctX_{st} \quad (6.44)$$

where  $k_{gc}$  and  $k_{gt}$  are a constant and a logistic growth rate constant ( $\text{kg ha}^{-1} \text{ yr}^{-1}$ ),  $Am_{st}$  and  $Am_{st,max}$  are the present and maximum amount of stemwood ( $\text{kg ha}^{-1}$ ) and  $ctX_{st}$  is the content of element X in stemwood ( $\text{mol}_c \text{ kg}^{-1}$ ). Growth uptake by branches is described as a fraction of the growth uptake by stems.

As with leaves and fine roots, the N content in stems and branches is calculated as a function of the N deposition according to Equation (6.37). This implies that, unlike Ca, Mg, K and S, there is not a steady-state situation with respect to N in these compartments. The total root uptake flux for N,  $N_{ru}$  is calculated as:

$$N_{ru} = N_{rl} + N_{rd} - N_{lv} + N_{gu} + Am_{lv} \cdot (ctN_{lv(t)} - ctN_{lv(t-1)}) + Am_{rt} \cdot (ctN_{rt(t)} - ctN_{rt(t-1)}) \quad (6.45)$$

The nutrient uptake from a given soil layer is derived by multiplying the total uptake flux with the ratio of water uptake from that layer to the total water uptake. Nutrient and water uptake are thus coupled in RESAM. RESAM includes the possibility for preferent uptake of NH<sub>4</sub> based on literature information (e.g. Gijsman, 1990) according to:

$$NH_{4,ru} = \frac{1}{1 + 1 / f_p NH_{4,ru}} \cdot N_{ru} \quad (6.46)$$

where  $f_p NH_{4,ru}$  is a preference factor for the uptake of NH<sub>4</sub> above NO<sub>3</sub>. When NH<sub>4,ru</sub> exceeds  $N_{ru}$  NH<sub>4</sub> uptake is set equal to N uptake. NO<sub>3</sub> uptake is calculated as the difference between total N uptake and NH<sub>4</sub> uptake.

#### Nitrogen transformations

Nitrification and denitrification in a given soil layer ( $\text{mol}_c \text{ ha}^{-1} \text{ yr}^{-1}$ ) are described in RESAM as first-order reactions according to:

$$NH_{4,ni} = - \theta \cdot f_c \cdot T \cdot k_{ni} \cdot [NH_4] \quad (6.47)$$

$$NO_{3,de} = - \theta \cdot f_c \cdot T \cdot k_{de} \cdot [NO_3] \quad (6.48)$$

where  $\theta$  is the volumetric moisture content ( $\text{m}^3 \text{m}^{-3}$ ),  $T$  the thickness (m) and  $k_{ni}$  and  $k_{de}$  are the nitrification and denitrification rate constants ( $\text{yr}^{-1}$ ) of the soil layer respectively and where  $f_c$  is a conversion factor ( $10^4 \text{m}^2 \text{ha}^{-1}$ ). As with mineralization, the maximum values for the nitrification and denitrification rate constant,  $k_{ni,max}$  and  $k_{de,max}$ , are adjusted by the mean ground water level. Values are reduced with a decreasing mean ground water level for nitrification since this process is restricted to aerobic conditions, whereas the opposite is true for denitrification. Both rate constants are also reduced with decreasing pH. A description of the reduction functions is given in De Vries et al. (1988). The maximum value of the nitrification rate constant is also reduced according to the presence of organic matter. Consequently, the nitrification rate is high in the humus layer whereas it reduces to zero in the subsoil. This is in accordance with field data (De Boer, 1989; Tietema and Verstraten, 1991; Tietema, 1992). Finally, in the humus layer the value of the nitrification rate constant is reduced with an increase in thickness of this layer. This is based on various literature sources (Lensi et al., 1986; Clays-Josserand et al., 1988; Tietema, et al., 1992) and can be explained by the fact that litter forms a barrier for  $\text{O}_2$  diffusion from the atmosphere, thus creating unfavourable anaerobic conditions for nitrifying bacteria (Lensi et al., 1986). The description is such that above a thickness of 5 cm, the product of  $T$  and  $k_{ni}$  (cf Eq. 6.47) does not increase any more.

## Geochemical process formulations

### *Rate-limited equations*

Protonation and weathering are described by rate-limited equations. Protonation, which refers to the association of organic anions with the hydrogen ion, is in fact an equilibrium process. At low pH, the equilibrium is forced to the right hand side. Since information on equilibrium constants was considered inadequate, protonation in each soil layer,  $\text{RCOO}_{pr}$  ( $\text{mol}_c \text{ha}^{-1} \text{yr}^{-1}$ ), is provisionally described in RESAM by a first-order reaction, according to:

$$\text{RCOO}_{pr} = -\theta \cdot f_c \cdot T \cdot k_{pr} \cdot [\text{RCOO}] \quad (6.49)$$

where  $k_{pr}$  is the protonation rate constant ( $\text{yr}^{-1}$ ), which is described as a maximum value,  $k_{pr,max}$ , that is reduced with an increase in pH (cf De Vries et al., 1988). The weathering (dissolution) flux of Al and base cations from carbonates, silicates (primary minerals) and aluminium hydroxides ( $\text{mol}_c \text{ha}^{-1} \text{yr}^{-1}$ ) is also described by first-order reactions according to:

$$\text{Ca}_{we,cb} = \rho \cdot f_c \cdot T \cdot k\text{Ca}_{we,cb} \cdot ct\text{Ca}_{cb} \cdot ([\text{Ca}_e] - [\text{Ca}]) \quad (6.50)$$

$$\text{X}_{we,pm} = \rho \cdot f_c \cdot T \cdot k\text{X}_{we,pm} \cdot ct\text{X}_{pm} \cdot [\text{H}]^\alpha \quad (6.51)$$

$$\text{Al}_{we,ox} = \rho \cdot f_c \cdot T \cdot k\text{Al}_{we,ox} \cdot ct\text{Al}_{ox} \cdot ([\text{Al}_e] - [\text{Al}]) \quad (6.52)$$



where  $kCa_{we,cb}$ ,  $kX_{we,pm}$  and  $kAl_{we,ox}$  are the weathering rate constants ( $m^3 mol_c^{-1} yr^{-1}$ ) of Ca from carbonates of base cations from primary minerals and of Al from hydroxides, respectively;  $ctCa_{cb}$ ,  $ctX_{pm}$  and  $ctAl_{ox}$  are the contents ( $mol_c kg^{-1}$ ) of Ca in carbonates, of base cations (Ca, Mg, K and Na) in primary minerals and of Al in hydroxides, respectively;  $\alpha$  is a dimensionless exponent;  $[Ca_e]$  and  $[Al]_e$  are the Ca and Al concentration ( $mol_c m^{-3}$ ) in equilibrium with Ca carbonate and Al hydroxide, respectively and  $[Ca]$ ,  $[H]$  and  $[Al]$  are the actual concentrations ( $mol_c m^{-3}$ ) of Ca, H and Al, respectively.

The rate-limited expression for carbonate weathering is based on the generally measured exponential decrease of calcium carbonate with time (Stuijzand, 1984). This can be interpreted as the result of increasingly incomplete contact of the percolating water with larger calcareous particles such as shell fragments, that remain when decalcification proceeds (Klijn, 1981). When the soil solution is supersaturated with respect to calcite, equilibrium is enforced (cf Eq. 6.54).

The kinetic expression for base cation weathering is based on laboratory experiments (Van Grinsven et al., 1988; Section 3.1). The influence of pH on the weathering rate (cf Eq. 6.51) is particularly important for Mg and K weathering in the very acid range (Van Grinsven et al., 1988). The production of Al from the congruent dissolution of silicate minerals is directly related to the production of base cations. Standard minerals are assumed as pools for K (microcline), Na (albite), Ca (anorthite) and Mg (chlorite). Stoichiometric equivalent ratios of Al to base cations in these minerals are 3 for K, 3 for Na, 3 for Ca and 0.6 for Mg (cf Section 5.2; Eq. 5.72).

The rate-limited expression for Al hydroxide weathering is based on the generally measured equilibrium with gibbsite in sandy subsoils, whereas undersaturation occurs in the topsoil (e.g. Driscoll et al., 1985; Mulder and Van Breemen, 1987). In the model,  $ctAl_{ox}$  is restricted to the amount of oxalate extractable Al, which includes amorphous hydroxides, since gibbsite (a crystalline phase) rarely occurs in acid sandy soils. However, soil solution analysis shows that the Al concentration in subsoils can be predicted successfully by assuming equilibrium with natural gibbsite (e.g. Mulder and Van Breemen, 1987). As with Ca carbonate, equilibrium is enforced with respect to Al hydroxide when the soil solution is supersaturated (cf Eq. 6.55). Regarding Al weathering, RESAM also contains the option of an Elovich-equation according to:

$$Al_{we,ox} = \rho \cdot f_c \cdot T \cdot kEL_1 \cdot \exp(kEL_2 \cdot ctAl_{ox}) \cdot ([Al]_e - [Al]) \quad (6.53)$$

where  $kEL_1$  ( $m^3 kg^{-1} yr^{-1}$ ) and  $kEL_2$  ( $kg mol_c^{-1}$ ) are so called Elovich constants. Use of this equation, which is also used for the description of P adsorption (e.g. Van Riemsdijk and De Haan, 1981), is based on laboratory experiments on acid neutralization by Al mobilization (Van Grinsven et al., 1992; Section 3.2).

### Equilibrium equations

Equilibrium equations in RESAM include the dissociation and association of  $\text{CO}_2$  (described according to Eq. 6.27), the calculation of Ca and Al in equilibrium with Ca carbonate (cf Eq. 6.50) and Al hydroxide (cf Eq. 6.52) and adsorption/desorption of cations and  $\text{SO}_4$ . The concentrations of Ca and Al in equilibrium with Ca carbonate and Al hydroxide, respectively, are calculated as (cf Section 6.1; Eq. 6.21 and 6.22):

$$[\text{Ca}_e] = K\text{Ca}_{cb} \cdot p\text{CO}_2 / [\text{HCO}_3]_e^2 \quad (6.54)$$

$$[\text{Al}_e] = K\text{Al}_{ox} \cdot [\text{H}]^3 \quad (6.55)$$

Cation exchange is described by Gaines-Thomas equations with Ca as a reference ion according to (cf Section 6.1; Eq. 6.23 and 6.24):

$$\frac{\text{fr}X_{ac}^2}{\text{frCa}_{ac}^{z_x}} = KX_{ex} \cdot \frac{(X)^2}{(\text{Ca})^{z_x}} \quad (6.56)$$

where  $z_x$  is the valence of cation X,  $KX_{ex}$  is the Gaines-Thomas selectivity constant for exchange of cation X against Ca ( $(\text{mol l}^{-1})^{z_x-2}$ ), (X) is the activity of cation X in the soil solution ( $\text{mol l}^{-1}$ ) and  $\text{fr}X_{ac}$  is the fraction of cation X on the adsorption complex (-). The activity of each cation is calculated by multiplying the concentration with an activity coefficient which is related to the ionic strength using the Debye-Hückel equation. The fraction of each cation on the adsorption complex is calculated by dividing the content of cation X on the adsorption complex by the cation exchange capacity (CEC). In order to solve the set of Gaines Thomas equations for six ions (H, Al, Mg, K, Na and  $\text{NH}_4$ ) with seven unknowns (the adsorbed fractions of the same ions plus Ca), an additional requirement is met:

$$\text{fr}H_{ac} + \text{frAl}_{ac} + \text{frCa}_{ac} + \text{frMg}_{ac} + \text{frK}_{ac} + \text{frNa}_{ac} + \text{frNH}_{4,ac} = 1 \quad (6.57)$$

$\text{SO}_4$  adsorption in each soil layer is described with a Langmuir equilibrium equation according to:

$$\text{ctSO}_{4,ac} = \frac{\text{SSC} \cdot K\text{SO}_{4,ad} \cdot [\text{SO}_4]}{1 + K\text{SO}_{4,ad} \cdot [\text{SO}_4]} \quad (6.58)$$

where  $\text{ctSO}_{4,ac}$  is the  $\text{SO}_4$  content at the adsorption complex ( $\text{mol}_c \text{kg}^{-1}$ ), SSC is the sulphate sorption capacity ( $\text{mol}_c \text{kg}^{-1}$ ) and  $K\text{SO}_{4,ad}$  is the equilibrium constant for  $\text{SO}_4$  adsorption ( $\text{m}^3 \text{mol}_c^{-1}$ ). The sorption flux is calculated from the difference between the

amount of element X (H, Al, Ca, Mg, K, Na, NH<sub>4</sub> and SO<sub>4</sub>) on the adsorption complex in the current and the preceding timestep.

## INPUT DATA

To run RESAM, data are needed with respect to system inputs (driving variables), the initial state of model variables and model parameters. The data used in this application do not refer to a specific site. Model inputs refer to a specific deposition scenario for the central, most forested, part of the Netherlands (Veluwe) whereas the model variables (and parameters) are average values for a Douglas Fir on a generic soil profile that is typical for a Cambic Podzol in the Netherlands.

### System inputs

The most important system inputs in RESAM are the atmospheric deposition fluxes of SO<sub>4</sub> (SO<sub>x</sub>), NO<sub>3</sub> (NO<sub>x</sub>), NH<sub>4</sub> (NH<sub>x</sub>), Ca, Mg, K, Na and Cl. Deposition fluxes of Al, HCO<sub>3</sub> and RCOO were assumed negligible. Total deposition data for SO<sub>4</sub>, NO<sub>3</sub> and NH<sub>4</sub>, which were used in the presented model calculations, are shown in Table 6.9.

Table 6.9 Deposition scenario for SO<sub>4</sub>, NO<sub>3</sub> and NH<sub>4</sub> used in the simulation

Year	Deposition (mol <sub>c</sub> ha <sup>-1</sup> yr <sup>-1</sup> )			
	SO <sub>4</sub>	NO <sub>3</sub>	NH <sub>4</sub>	SO <sub>4</sub> +NO <sub>3</sub> +NH <sub>4</sub>
1990	3170	1060	2920	7150
2000	2080	650	1490	4220
2010 <sup>1)</sup>	1220	350	760	2330

<sup>1)</sup> Between 2010 and 2050 these values were kept constant

Deposition data up to the year 2000 were based on calculations with the model TREND (Van Jaarsveld and Onderdelinden, 1993) for the Veluwe, using expected emissions in the Netherlands and the other European countries (Netherlands Environmental Policy Plan). For the period 2000 and 2050 no emission scenarios were available. Instead deposition targets were formulated for 2010, based on critical load calculations (De Vries and Kros, 1991), which remained constant after 2010. The effect of forests on scavenging dry deposition was included by multiplying the deposition values with a factor of 1.8 for SO<sub>4</sub>, 0.9 for NO<sub>3</sub> and 1.7 for NH<sub>4</sub> on the basis of a comparison between throughfall data and deposition estimates predicted by the TREND model (cf De Vries, 1991).

Values used for the deposition of base cations and Cl (Table 6.10) were kept constant during the 60 year simulation period (1990-2050). The potential acid load which can be derived by adding the loads for SO<sub>4</sub>, NO<sub>3</sub> and NH<sub>4</sub> and subtracting the base cation input

Table 6.10 Deposition data for base cations and chloride used in the simulation

Type of deposition	Deposition ( $\text{mol}_e \text{ ha}^{-1} \text{ yr}^{-1}$ )					
	Ca	Mg	K	Na	Cl	BC <sup>3)</sup>
Wet <sup>1)</sup>	240	180	37	740	860	337
Dry <sup>2)</sup>	480	360	73	1480	1720	673
Total	720	540	110	2220	2580	1010

1) Based on an interpolation of data from 22 weather stations in the Netherlands for the period 1978-1985 (KNMI/RIVM, 1985).

2) Derived by multiplying the bulk deposition values with a factor two on the basis of a comparison of Na in throughfall and bulk deposition at more than 20 sites with Douglas fir in the Netherlands (cf De Vries, 1991).

3) BC<sup>3)</sup> is Ca+Mg+K+Na-Cl

not accompanied by Cl (BC<sup>3)</sup> decreased from approximately  $6100 \text{ mol}_e \text{ ha}^{-1} \text{ yr}^{-1}$  in 1990 to  $1300 \text{ mol}_e \text{ ha}^{-1} \text{ yr}^{-1}$  in 2050 (cf Table 6.9 and 6.10).

Values used for the average annual infiltration of water (precipitation minus interception evaporation and soil evaporation) and of transpiration equalled  $475 \text{ mm yr}^{-1}$  and  $248 \text{ mm yr}^{-1}$ , respectively, causing a precipitation excess of  $227 \text{ mm yr}^{-1}$ . Data were based on calculations of the transpiration rate (and moisture content) per soil layer, that were made with the hydrological model SWATRE (Belmans et al., 1983), using a mean hydrological year for the period 1950-1980 with a total precipitation of  $780 \text{ mm yr}^{-1}$  (De Visser and De Vries, 1989).

### Model variables and model parameters

Model variables, that must be known at the beginning of the simulation, include the amount of elements in the various compartments of the forest soil ecosystem, i.e. leaves, roots, stems, branches, litter, primary minerals, amorphous Al hydroxides, the adsorption complex and the soil solution. Data related to the various tree compartments are given in Table 6.11. Biomass data of needles and fine roots, and elements contents in fine roots and stems were based on a literature survey (De Vries et al., 1990) whereas the element contents in needles were based on a field survey in 1987 in eight Douglas stands (Oterdoom et al., 1987). The biomass of stems was derived from a logistic growth function for Douglas Fir (La Bastide and Faber, 1972) using a tree age of 30 years (At this age, the amount of needles and fine roots can be assumed at this maximum). Net uptake in branches was neglected in this study, since removal of stemwood only is common forestry practice in the Netherlands. The initial litter amount,  $Am_{lr}$  was calculated by integrating the various mineralization equations (cf Eq. 6.37 and Eq. 6.38 with X is Carbon), using a stand age of 80 years. Initial element contents in litter were taken equal to needle contents except for K (0.08%).

Table 6.11 Data on biomass and element contents of leaves, fine roots and stems of the Douglas Fir used in the simulation (see text for data sources)

Compartment	Biomass (kg ha <sup>-1</sup> )	Element content (%)					
		N <sub>min</sub> <sup>1)</sup>	N <sub>max</sub>	Ca	Mg	K	S
Needles	10.850	1.0 (2.0)	3.5	0.33	0.10	0.43	0.20
Fine roots	4.700	0.4 (0.7)	1.0	0.21	0.02	0.05	0.05
Stems	200.340	0.08	0.2	0.07	0.01	0.04	0.01

<sup>1)</sup> Values in brackets are the minimum N contents above which reallocation occurs (cf Eq. 6.35)

Data used for the element amounts in primary minerals, (amorphous) Al hydroxides and the adsorption complex are given in Table 6.12. The initial sorbed SO<sub>4</sub> content was calculated from the equilibrium with the SO<sub>4</sub> concentration, using a sulphate sorption capacity (SSC) equal to 2% of the Al oxalate content (Johnson and Todd, 1983). The initial (i.e. 1990) ion concentrations in each soil layer were derived by running the model during 25 years (1965-1990) using historical emission-deposition data for the Veluwe area. Anion concentrations in 1965 were estimated from the annual atmospheric input at that time and the annual average water flux per layer. Cation concentrations in 1965 were derived by combining the charge balance equation (Eq. 6.28) with the various cation exchange equations (Eq. 6.56), using given initial exchangeable cation fractions (Table 6.12) and cation exchange constants (cf Table 6.14). During the initialization period (1965-1990), the cation contents in primary minerals and hydroxides were kept constant, while the sorbed SO<sub>4</sub> and cation contents were continuously updated.

An overview of the various overall parameters that were used is given in Table 6.13. Most data were derived indirectly from available literature. For example, foliar uptake and foliar exudation fractions were derived from throughfall and bulk deposition data of more than 20 Douglas stands as summarized in Erisman (1990) while using a derivation procedure described in Van der Maas and Pape (1991).

Table 6.12 Data on element contents in primary minerals, hydroxides and at the adsorption complex of the Cambic Podzol used in the simulation

Soil layer	Soil horizon	Depth (cm)	Density <sup>1)</sup> (kg m <sup>-3</sup> )	Total contents <sup>2)</sup> (mmol <sub>c</sub> kg <sup>-1</sup> )				ctAl <sub>ox</sub> <sup>3)</sup> (mmol <sub>c</sub> kg <sup>-1</sup> )	CEC <sup>1)</sup> (mmol <sub>c</sub> kg <sup>-1</sup> )	Exchangeable fractions <sup>1)</sup> (-)			
				Ca	Mg	K	Na			H	Al	BC <sup>5)</sup>	NH <sub>4</sub>
0	O	3.5-0 <sup>4)</sup>	140					275	0.30	0.08	0.54	0.08	
1	Ah	0-10	1345	35	40	230	155	95	42	0.33	0.50	0.12	0.05
2	Ah	10-20	1345	35	40	230	155	95	42	0.33	0.50	0.12	0.05
3	Bhs	20-40	1460	25	45	225	150	185	18	0.10	0.77	0.08	0.05
4	BC	40-60	1535	30	45	240	140	175	18	0.05	0.77	0.08	0.10

<sup>1)</sup> Derived from a field survey (Kleijn et al., 1989). The CEC was measured in an unbuffered solution of silverthiureum. In a buffered solution, both the CEC and exchangeable H content would be higher

<sup>2)</sup> Derived from laboratory analyses

<sup>3)</sup> Derived from a soil information system (Bregt et al., 1986)

<sup>4)</sup> This thickness was calculated at the beginning of the simulation period in 1990

<sup>5)</sup> BC is the sum of Ca, Mg, K and Na

Table 6.13 Values used for soil-layer independent model parameters used in the simulation

Process	Parameter	Unit	Value	Derivation
Foliar uptake	$f_{rNH_4,lu}$ <sup>1)</sup>	-	0.30	Via Erisman (1990)
	$f_{rNO_3,lu}$	-	0.05	Via Erisman (1990)
	$f_{rSO_4,lu}$	-	0.10	Via Erisman (1990)
Foliar exudation	$f_{rCa_{le}}$	-	0.24	Via Erisman (1990)
	$f_{rMg_{le}}$	-	0.13	Via Erisman (1990)
	$f_{rK_{le}}$	-	0.63	Via Erisman (1990)
Litterfall	$k_{fl}$	yr <sup>-1</sup>	0.28	De Vries et al. (1990)
Rootdecay	$k_{rd}$	yr <sup>-1</sup>	1.40	De Vries et al. (1990)
Reallocation	$f_{r_{re,max}}$	-	0.36	Berdowski et al. (1991)
Mineralization	$f_{r_{mi,fl,max}}$	-	0.40	De Vries et al. (1990)
	$k_{mi,fl,max}$	yr <sup>-1</sup>	0.05	De Vries et al. (1990)
	$RDA_{mo}$	-	1.5	Janssen (1983)
	$C/N_{mo}$	-	15	Janssen (1983)
Root uptake	$f_{pNH_4,ru}$	-	1.5	Via Gijsman (1990)
Nitrification	$k_{ni,max}$	yr <sup>-1</sup>	40	Calibration
Denitrification	$k_{de,max}$	yr <sup>-1</sup>	10	Via Reddy et al. (1982)
Protonation	$k_{pr,max}$	yr <sup>-1</sup>	40	Calibration
Al dissolution	$KAl_{ox}$	mol <sup>-2</sup> l <sup>2</sup>	10 <sup>-8</sup>	Via Kleijn et al. (1989)
SO <sub>4</sub> dissolution	$KSO_{4,ad}$	mol <sup>-1</sup> l	5.10 <sup>-4</sup>	Via Foster et al. (1986)

1) In this study, the foliar uptake fractions for H and NH<sub>4</sub> were taken equal. Both ions were assumed to have equal preference for exchange with base cations in the forest canopy. This implies that a decrease in NH<sub>4</sub> deposition, which is compensated by an increase in H deposition (cf Eq. 6.30) does not influence the foliar exudation flux of base cations. This flux is mainly triggered by a decrease or increase in SO<sub>4</sub> or NO<sub>3</sub> deposition.

Maximum values for the nitrification and protonation rate constants were derived by calibration of model results on measured NH<sub>4</sub>/NO<sub>3</sub> ratios and RCOO concentrations as given in Van Breemen and Verstraten (1991). An overview of soil parameters used for the various soil layers is given in Table 6.14.

Table 6.14 Elovich constants for Al dissolution, base cation weathering rate constants and Gaines Thomas exchange constants used in the simulation

Soil horizon	$kEL_1$ <sup>1)</sup> (10 <sup>-7</sup> m <sup>3</sup> kg <sup>-1</sup> yr <sup>-1</sup> )	$kEL_2$ <sup>1)</sup> (10 <sup>-2</sup> kg mol <sub>c</sub> <sup>-1</sup> )	Weathering rate constants (10 <sup>-5</sup> yr <sup>-1</sup> ) <sup>1)</sup>				Exchange constants <sup>2)</sup> (mol l <sup>-1</sup> ) <sup>2</sup> x <sup>-2</sup>					
			Ca	Mg	K	Na	H	Al	Mg	K	Na	NH <sub>4</sub>
Ah	5.7	9.3	25	11	2.3	2.9	1870	0.62	0.35	0.21	0.77	1.05
Bh	6.4	6.3	9.1	1.8	5.3	8.5	7830	1.77	0.30	1.31	3.35	6.53
BC	42	4.4	2.9	0.16	3.1	5.9	11470	1.91	0.33	6.14	5.00	30.7

1) Derived from laboratory (batch) experiments that were conducted during one year for two Cambic Podzols (cf Section 3.3; De Vries et al, 1994g). Base cation weathering rate constants thus derived were divided by 50 to scale results to field weathering rates, that were estimated by the depletion of base cations in these two soil profiles (cf Section 2.2; De Vries and Breeuwsma, 1986). In this model application we assume a negligible pH influence on the weathering rate ( $\alpha=0$ ; cf Eq. 6.51)

2) Derived from the simultaneous measurement of the cations H, Al, Ca, Mg, K, Na and NH<sub>4</sub> on the adsorption complex and in the soil solution of two Carbic Podzols at five locations and at four soil depths (Kleijn et al., 1989). Results show a very high affinity of protons compared to the other monovalent ions, i.e. K, Na and NH<sub>4</sub>.

## RESULTS

### Element fluxes in the forest ecosystem

Except for base cations, the predicted fluxes of major ions in the forest ecosystem strongly differed at the beginning and the end of the simulation period (Table 6.15). Fluxes of nutrients ( $\text{SO}_4$ ,  $\text{NO}_3$ ,  $\text{NH}_4$ , Ca, Mg and K) were almost completely determined by the input from the atmosphere and the nutrient cycle (mineralization and uptake) including effects of canopy interactions. The latter process was especially important for  $\text{NH}_4$  and the base cations (Ca, Mg and K; lumped in Table 6.15). In case of  $\text{NO}_3$  and  $\text{NH}_4$ , the nitrification process also played a dominant role, whereas denitrification was estimated to be negligible in this well-drained acid forest soil. Unlike nutrients, the (leaching) flux of Al was almost completely determined by weathering, both from silicates and hydroxides.

The flux of organic anions (not given in Table 6.15) was completely determined by mineralization and protonation, which nearly equalled each other within the soil profile, causing a nearly negligible leaching flux from the rootzone ( $30 \text{ mol}_c \text{ ha}^{-1} \text{ yr}^{-1}$ ; cf Table 6.16) both at the beginning and the end of the simulation period.

Table 6.15 Element fluxes of  $\text{SO}_4$ ,  $\text{NO}_3$ ,  $\text{NH}_4$ ,  $\text{BC}^+$ , Al and H induced by various processes in the forest canopy and the forest soil (rootzone) at the beginning and end of the simulation period<sup>1)</sup>.

Process	Element flux ( $\text{mol}_c \text{ ha}^{-1} \text{ yr}^{-1}$ )											
	$\text{SO}_4$		$\text{NO}_3$		$\text{NH}_4$		$\text{BC}^{+2)}$		Al		H	
	1990	2050	1990	2050	1990	2050	1990	2050	1990	2050	1990	2050
Deposition	3170	1220	1060	350	2920	760	1010	1010			300	-200 <sup>3)</sup>
Foliar interaction <sup>4)</sup>	-260	-100	-40	-10	-880	-230	1000	240			-420	-120
Mineralization	580	580			4480	2870	1960	1970			-5830 <sup>5)</sup>	-4230 <sup>5)</sup>
Nitrification			3290	1520	-3290	-1520					6580	3040
Denitrification			0	0							0	0
Root uptake	-370	-540	-1900	-1140	-2850	-1710	-3390	-2630			3790	2660
Weathering							190	190	4730	780	-4920	-970
Sorption <sup>6)</sup>	190	0			10	10	-220	-140	-330	70	730	60
Storage <sup>7)</sup>	40	0	30	0	10	0	0	0	50	0	10	0
Leaching	3350	1160	2440	720	400	180	550	640	4450	850	420	240

1) The sign of the fluxes in this Table are related to the ion amount in the dissolved phase, i.e. '+' when it increases and '-' when it decreases)

2)  $\text{BC}^+ = \text{Ca} + \text{Mg} + \text{K} + \text{Na} - \text{Cl}$

3) This negative proton flux, which is calculated as:  $\text{H} = \text{SO}_4 + \text{NO}_3 - \text{NH}_4 - \text{BC}^+$ , does not occur as it is counteracted by  $\text{HCO}_3$  (not given in Table 6.15)

4) A positive value implies foliar exudation and a negative value foliar uptake

5) This value refers to the proton flux induced by the sum of mineralization and protonation of organic anions. Organic anions are assumed to compensate the (excess of) cations over anions mobilized during mineralization (cf Eq. 6.40) but the protonation of these anions (cf Eq. 6.49) causes proton consumption

6) A positive value implies desorption and a negative value adsorption

7) A positive value implies a decrease in element storage whereas a negative value implies the opposite

Due to the large emission of  $\text{NH}_3$ , which buffers protons in the atmosphere, the direct input of protons via throughfall was nearly negligible. Proton production was mainly induced by nitrification of  $\text{NH}_4$ , entering the soil solution via throughfall and mineralization, and by root uptake, since the uptake of cations ( $\text{NH}_4$ , Ca, Mg and K) was much larger than that of anions ( $\text{NO}_3$  and  $\text{SO}_4$ ). Proton consumption was mainly regulated by protonation of organic anions and weathering (dissolution) of Al. Since protonation of organic anions nearly equalled the amount produced during mineralization (see above), the net effect of mineralization was the consumption of protons caused by the release of base cations and  $\text{NH}_4$  (cf Table 6.15). In summary, the long-term effect of the deposition scenario on the proton budget was mainly governed by changes in the nutrient cycle (mineralization and root uptake) and in the occurrence of nitrification and Al dissolution.

Table 6.16 Leaching fluxes of major ions from the various layers of the forest soils at the beginning and end of the simulation period.

Soil layer	Soil depth (cm)	Leaching flux ( $\text{mol}_c \text{ ha}^{-1} \text{ yr}^{-1}$ )									
		$\text{SO}_4 + \text{NO}_3 - \text{NH}_4$		RCCO		BC <sup>*</sup>		Al		H	
		1990	2050	1990	2050	1990	2050	1990	2050	1990	2050
0 <sup>1)</sup>	3.5-0	2080	680	2440	1740	2410	1890	0	0	2190	590
1	0-10	3880	1310	750	680	1410	1220	1750	220	1410	490
2	10-20	5020	1740	230	240	1010	950	3110	450	1070	530
3	20-40	5410	1790	80	80	710	730	4320	870	460	270
4	40-60	5390	1700	30	30	550	640	4450	850	420	240

<sup>1)</sup> Layer 0 is the humus layer above the mineral soil

A comparison of inputs by deposition and outputs by leaching from the root zone during the simulation period (Fig. 6.16) showed that (i)  $\text{SO}_4$  mostly behaved as a tracer (input and output were approximately similar) except for the period between 1995 and 2015 when significant  $\text{SO}_4$  mobilization occurred, (ii) initial net N retention (about 30% in 1990,  $1100 \text{ mol}_c \text{ ha}^{-1} \text{ yr}^{-1}$ ) changed to net N mobilization (between 2000 and 2030) followed by net N retention again (about 20% in 2050;  $210 \text{ mol}_c \text{ ha}^{-1} \text{ yr}^{-1}$ ) and (iii) BC retention first increased up to 2015, followed by a decrease after 2015.

$\text{SO}_4$  mobilization up to 2015 was due to the occurrence of  $\text{SO}_4$  desorption, induced by a decrease in  $\text{SO}_4$  concentration in response to reduced  $\text{SO}_4$  inputs. N mobilization after 2000 was due to the occurrence of net N mineralization, (N mineralization in excess of N input by litterfall and root decay) induced by decreasing N contents in leaves and fine roots in response to reduced N inputs (cf Eq. 6.37). Net mineralization, causing a decrease in accumulated N in the humus layer, occurred upto the end of the simulation period. The change to net N retention again was due to the occurrence of N uptake by forest growth ( $320 \text{ mol}_c \text{ ha}^{-1} \text{ yr}^{-1}$  at the end of the simulation period which exceeds the net retention of  $210 \text{ mol}_c \text{ ha}^{-1} \text{ yr}^{-1}$ ). Finally, the increase in BC retention up to 2015 was due to an increase in BC adsorption, mainly in exchange with H, in response to the large decrease in H concentration (pH increase) in that period, especially in the upper soil layers (see further).



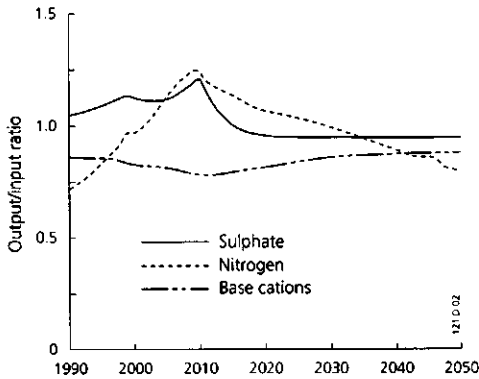


Figure 6.16 Changes in the output/input ratios of S, N and BC for the forest soil during the simulation period. (Output equals leaching from the rootzone, whereas input equals deposition on the forest canopy).

The importance of the various processes with soil depth can be derived from the leaching fluxes of major ions from the various soil layers (Table 6.16). Here we lumped the fluxes of  $\text{SO}_4$ ,  $\text{NO}_3$  and  $\text{NH}_4$ , which mainly reflect anthropogenic soil acidification, whereas we included  $\text{RCOO}$  fluxes, which mainly reflect natural soil acidification, because of its importance in upper soil layers. For all major ions, the largest changes in element fluxes with depth took place in the first two mineral layers, i.e. the Ah horizon with a thickness of 20 cm (cf Table 6.12). The processes which mainly governed these changes were nitrification for  $\text{SO}_4 + \text{NO}_3 - \text{NH}_4$ , protonation for  $\text{RCOO}$ , root uptake for  $\text{BC}^+$  and weathering for Al. Regarding the Al and H flux, a rather large change also took place in the third layer induced by Al weathering from the Bhs horizon (cf the oxalate extractable Al content of this layer in Table 6.12). Below the third layer (at 40 cm depth) changes were minimal (Table 6.16).

Compared to 1990, the absolute flux of organic anions in 2050 decreased in the upper layers but the relative importance compared to inorganic anions ( $\text{SO}_4 + \text{NO}_3$ ) increased significantly, especially in the humus layer. In 2050, the predicted flux of organic anions in the first mineral layer was even larger than that for Al. Table 6.16 also shows that the large decrease in atmospheric input of S and N compounds, reflected by the decrease in  $\text{SO}_4 + \text{NO}_3 - \text{NH}_4$  flux, mainly affected the flux of Al and H, whereas the flux of base cations remained almost unaffected, except for the uppermost soil layers. The BC flux in these layers was strongly influenced by the BC input via throughfall, which decreased in time because of a decrease in acid input, which is assumed to cause foliar exudation of base cations in RESAM. The strong relationship between  $\text{SO}_4 + \text{NO}_3 - \text{NH}_4$  leaching and Al leaching was especially clear at greater soil depth at the beginning of the simulation period, i.e. at high acid loads. At that time the ratio of both leaching fluxes from the rootzone approached a 1:1 relationship (cf Fig. 6.17).

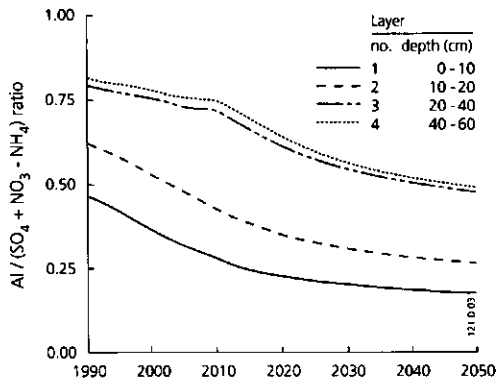


Figure 6.17 Changes in the  $Al/(SO_4 + NO_3 - NH_4)$  ratio in the four mineral layers of the forest soil during the simulation period

At decreased acid input, the relative contribution of base cations was much larger, whereas in the upper soil layers both base cation and proton concentrations were larger, because of nutrient cycling and limited Al dissolution, respectively.

### Changes in soil solid phase chemistry

Changes in the soil solid phase were mainly characterized by mobilization of Al from Al hydroxides and to a lesser extent by an increase in base cations on the exchange complex. A comparison of Al mobilization from silicates, hydroxides and the exchange complex at the beginning and end of the simulation (Table 6.17) showed that Al hydroxide dissolution was the dominant source of Al in 1990, at high acid loads, whereas silicate weathering was the major source in 2050, at relatively low acid loads. Furthermore, Al was adsorbed at the

Table 6.17 Fluxes of aluminium from silicates, hydroxides and the adsorption complex in the four mineral soil layers of the forest ecosystem at the beginning and end of the simulation period.

Soil layer	Soil depth (cm)	Al mobilization flux ( $mol_c \text{ ha}^{-1} \text{ yr}^{-1}$ )							
		Silicate weathering		Hydroxide dissolution <sup>1)</sup>		Exchange mobilization		Total	
		1990	2050	1990	2050	1990	2050	1990	2050
1	0-10	70	70	1910	120	-240	20	1740	210
2	10-20	70	70	1390	140	-100	20	1360	230
3	20-40	230	230	950	170	10	20	1190	420
4	40-60	140	140	-20	-160	-10	10	110	-10
Total	0-60	510	510	4230	270	-340	70	4400	850

<sup>1)</sup> Stands for the charge in oxalate extractable Al, which also includes the dissolution of Al from organic pools

beginning of the simulation period, mainly against protons (during the initialization period there was not yet an equilibrium obtained), whereas the opposite occurred at the end of the simulation period. Predicted Al weathering from silicates did not change during the simulation since this process was related to BC weathering which was assumed to be independent of the pH in this study. In 1990, there was a small difference between total Al mobilization ( $4400 \text{ mol}_c \text{ ha}^{-1} \text{ yr}^{-1}$ ) and Al leaching from the soil profile ( $4450 \text{ mol}_c \text{ ha}^{-1} \text{ yr}^{-1}$ ) due to a decrease in Al storage ( $50 \text{ mol}_c \text{ ha}^{-1} \text{ yr}^{-1}$ ; cf Table 6.15), whereas Al mobilization and Al leaching were similar in 2050 ( $850 \text{ mol}_c \text{ ha}^{-1} \text{ yr}^{-1}$ ) since the change in Al storage was negligible at that time (cf Table 6.15).

During the entire simulation period, Al hydroxide dissolution was restricted to the first three mineral layers (up to a depth of 40 cm; cf Table 6.17). Some precipitation of hydroxides occurred in the lowest soil layer, where Al was predicted to be in equilibrium with Al hydroxide. Al hydroxide dissolution decreased strongly with time and was rather evenly distributed in the first two soil layers (Ah horizon) during the entire simulation period (cf Fig. 6.18A). In the third layer the Al dissolution rate was (much) lower at the beginning of the simulation period as compared to the first two layers, whereas values were nearly equal at the end. Complete Al depletion did not occur in any of the layers at such a reducing deposition scenario (Fig. 6.18A). In 2050

Al hydroxide dissolution even approached zero since the net acid input was completely neutralized by silicate weathering. However, at present deposition rates, total depletion of the first soil layer would almost be possible during a 60 year period. The first mineral layer contained an initial Al hydroxide amount of approximately  $128 \text{ kmol}_c \text{ ha}^{-1}$  (cf Table 6.11) which is depleted in approximately 67 years at a hydroxide dissolution rate of  $1.91 \text{ kmol}_c \text{ ha}^{-1} \text{ yr}^{-1}$  (cf Table 6.16). Similar predictions at present deposition rates were made by Mulder et al. (1989).

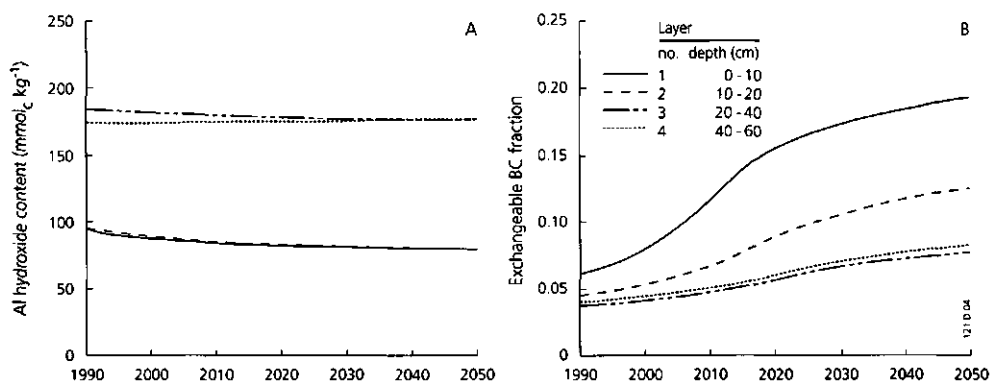


Figure 6.18 Changes in the Al hydroxide content (A) and the exchangeable base cation fraction (B) in the four mineral layers of the forest soil during the simulation period

Changes in exchangeable cation contents during the simulation period were mainly limited to the humus layer and the first two mineral layers, i.e. the Ah horizon (Table 6.18). Major changes were a decrease in the exchangeable H fraction and an increase in the exchangeable BC fraction (base saturation) in the humus layer and the first mineral layer, indicating that exchange of BC against H was the dominating mechanism in these layers. In the other mineral layers, exchange of BC against Al appeared to more important (cf Table 6.18). The largest changes in base saturation with time depended upon the soil layer, but it mostly occurred somewhere between 2010 and 2030 (cf Fig. 6.18B).

*Table 6.18 Exchangeable fractions of H, Al, BC and NH<sub>4</sub> in the various soil layers of the forest soil at the beginning and end of the simulation period*

Soil layer	Soil depth (cm)	Exchangeable fraction (-)							
		H		Al		BC		NH <sub>4</sub>	
		1990	2050	1990	2050	1990	2050	1990	2050
0	3.5-0	0.19	0.06	0.06	0.05	0.66	0.84	0.09	0.05
1	0-10	0.33	0.23	0.60	0.57	0.06	0.19	0.01	0.01
2	10-20	0.25	0.22	0.71	0.65	0.04	0.13	0.00	0.00
3	20-40	0.19	0.18	0.76	0.74	0.04	0.08	0.01	0.00
4	40-60	0.22	0.20	0.73	0.70	0.04	0.09	0.01	0.01

### Changes in soil solution chemistry

Concentrations of SO<sub>4</sub>, NO<sub>3</sub> and NH<sub>4</sub> decreased strongly in all soil layers between 1990 and 2010 in response to the decrease in atmospheric deposition in that period (cf Fig. 6.19 and Table 6.9). After 2010, when deposition levels remained constant, the SO<sub>4</sub> concentration stabilized quickly, especially in the topsoil (Fig. 6.19A), but concentrations of NO<sub>3</sub> and NH<sub>4</sub> continued to decrease (Fig. 6.19B,C). Unlike SO<sub>4</sub>, concentrations of NO<sub>3</sub> and NH<sub>4</sub> are strongly influenced by N cycling which responded to the decreased N deposition by a decrease in the N content in needles and fine roots. This in turn caused a decrease in the N content of the humus layer thus mobilizing N from this layer (cf Section on element fluxes). Actually, the reduction in SO<sub>4</sub> concentration in deeper soil layers also continued up to 2025 (Fig. 6.19A) due to SO<sub>4</sub> desorption. Between 1990 and 2025 the adsorbed amount of SO<sub>4</sub> in the rootzone decreased from 15.2 to 8.8 kmol<sub>c</sub> ha<sup>-1</sup>, i.e. an average desorption flux of approximately 180 mol<sub>c</sub> ha<sup>-1</sup> yr<sup>-1</sup>. The predicted increase in SO<sub>4</sub> concentration with soil depth mainly reflects the effect of water uptake. Regarding NO<sub>3</sub>, the major process causing an increase with depth was nitrification, which in turn reduced the NH<sub>4</sub> concentration with depth (cf Fig. 6.19C).

Aluminium, base cations and protons all responded differently to a change in acid deposition (Fig. 6.20). The Al concentrations showed the same trend as the concentrations of SO<sub>4</sub> and NO<sub>3</sub> since Al mobilization was predicted to be the major buffer mechanism in this acid sandy forest soil (Fig. 6.20A). As with SO<sub>4</sub> and NO<sub>3</sub>, Al increased with depth due

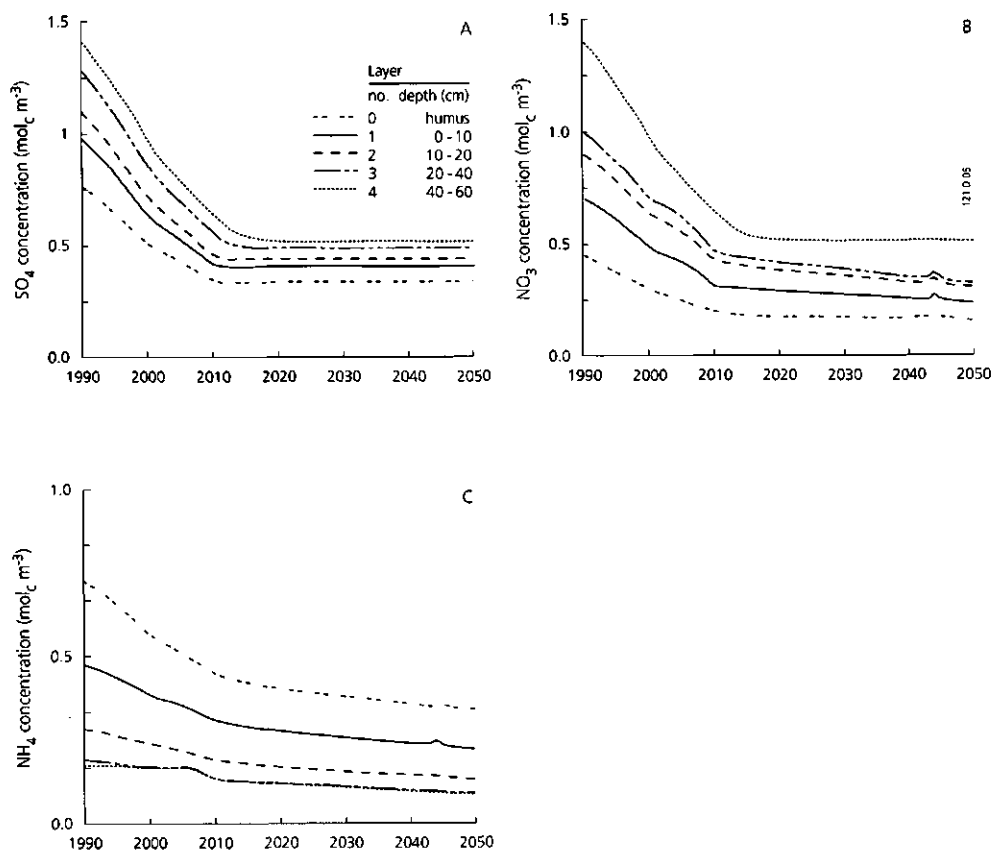


Figure 6.19 Changes in the concentrations of  $SO_4$  (A),  $NO_3$  (B) and  $NH_4$  (C) in the various layers of the forest soil during the simulation period.

to water uptake and Al mobilization with depth, whereas BC concentrations decreased with depth due to root uptake (cf Table 6.16). Even though BC deposition remained constant, the concentration of base cations and especially that of Ca, showed an initial reduction up to 2015 (Fig. 6.20B) due to adsorption of BC (especially Ca), in exchange with H induced by a large pH increase in that period (cf Section on element fluxes and Fig. 6.20D). Between 1990 and 2015 the total Ca adsorption flux in the rootzone increased from 140 to 280  $mol_c ha^{-1} yr^{-1}$ . After 2015 Ca adsorption decreased, thus causing an increase in Ca concentration. In 2050 the Ca (BC) concentration was not yet in equilibrium with the adsorbed Ca (BC) content (the base saturation). The Ca adsorption flux at that time was still 90  $mol_c ha^{-1} yr^{-1}$ , whereas the total BC adsorption flux equalled 120  $mol_c ha^{-1} yr^{-1}$ .

The molar Al/Ca ratio, which is an important indicator for the adverse effects of soil acidification on roots showed a similar trend as the Al concentration in the first two mineral

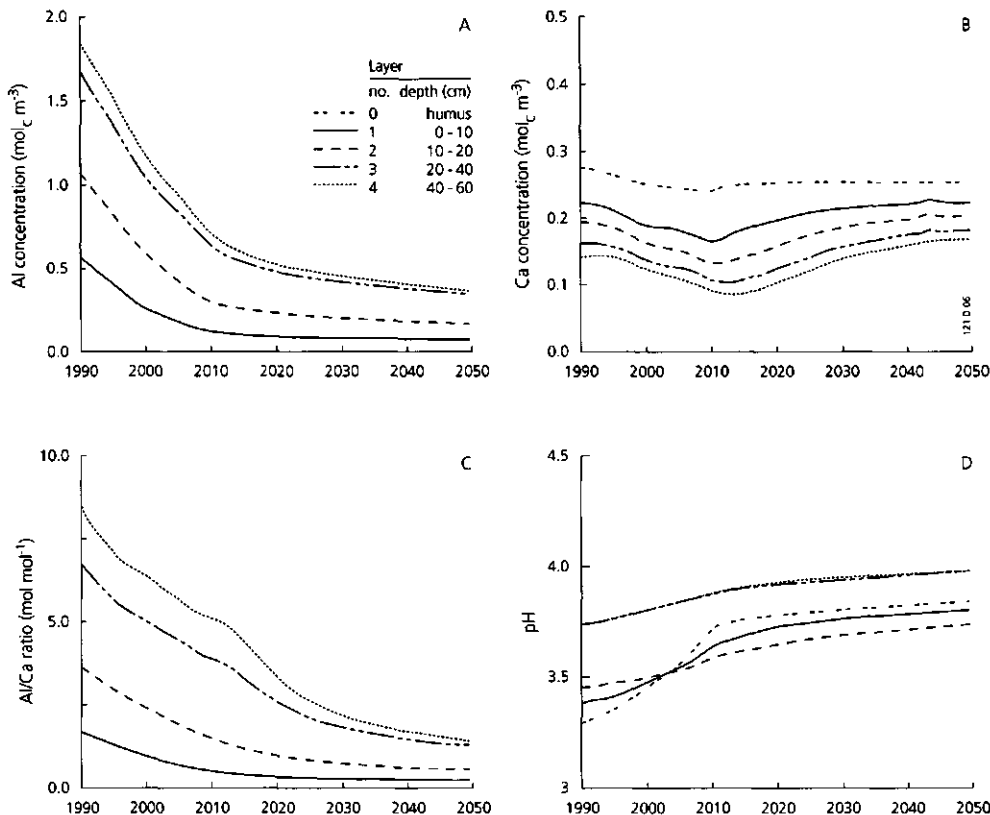


Figure 6.20 Changes in the Al concentration (A), Ca concentration (B), molar Al/Ca ratio (C) and pH (D) in the various layers of the forest/soil during the simulation period

soil layers (Ah horizon), i.e. a large reduction up to 2010, followed by a small reduction afterwards (Fig. 6.20C). In these layers, the simulated molar Al/Ca ratio decreased below a value of 1.0 which is considered to be critical (De Vries, 1991). Considering that (i) the Al concentration in the topsoil also decreased below a concentration of  $0.2 \text{ mol}_c \text{ m}^{-3}$  (cf Fig. 6.20A) which is considered critical and (ii) Al hydroxide depletion hardly occurred in 2050, one can conclude that the deposition level at that time is close to a critical acid load (cf De Vries and Kros, 1991). However, in the subsoil (between 40 and 60 cm depth) the Al/Ca ratio and Al concentration remained above the critical values. The reduction in Al/Ca ratio accelerated between 2015 and 2025, mainly caused by the increase in Ca concentration during that period. The effect of an increase in Ca concentration on the Al/Ca ratio was most pronounced at greater soil depth because of the low Ca concentrations in the deeper soil layers (cf Fig. 6.20A,B and C).

The pH, which reflects the result of all acid producing and acid consuming processes, increased in all soil layers during the entire simulation period (Fig. 6.20D). The largest increase occurred in the humus layer (layer 0), and to a lesser extent in the first mineral layer (layer 1), between 1990 and 2010. After 2010, the pH in these soil layers was even higher than in the second soil layer (cf Fig. 6.20D). This phenomenon was mainly caused by the relative increase in the internal acid consumption with time, induced by the large protonation flux at shallow soil depth up to 10 cm. At low deposition levels this appeared to overwhelm the acid consumption flux due to Al mobilization in deeper soil layers.

## DISCUSSION AND CONCLUSIONS

### Evaluation of model results for 1990

Major features of the model predictions in 1990, i.e. when the (acid) forest soil received large inputs of S and N were a:

- (i) significant interaction between  $\text{NH}_4$  and base cations in the forest canopy;
- (ii) large role of N transformations by mineralization, root uptake and nitrification and of Al mobilization in the proton budget;
- (iii) dominant of change in element fluxes in the upmost soil layers;
- (iv) difference in the behaviour of  $\text{SO}_4$  (conservative) as compared to N (retention);
- (v) strong relationship between Al leaching and leaching of the sum of  $\text{SO}_4$  and  $\text{NO}_3$  from the rootzone;
- (vi) dominant role of Al hydroxide dissolution in Al mobilization and the risk of complete Al depletion in the topsoil of Dutch forests at present deposition levels.

Considering the data for two Douglas fir sites in the central part of the Netherlands with nearly similar  $\text{NH}_4$  inputs (approximately  $2700 \text{ mol}_c \text{ ha}^{-1} \text{ yr}^{-1}$ ), the simulated large interaction between  $\text{NH}_4$  and base cations in the forest canopy (i) is likely to be overestimated by at least 50% (Mohren, 1991), although the canopy interactions remain significant at high  $\text{NH}_4$  inputs. The predicted importance of N transformation processes and Al mobilization on the proton budget (ii) and the dominance of these processes (especially N transformations) in the upmost soil layers (iii) is in agreement with measured input-output budgets between 1980 and 1990 at 18 sites (Section 2.3; De Vries et al., 1994b) and with results from N transformation studies at 5 sites (Tietema, 1992) in Dutch forest stands. The leaching of  $\text{NH}_4$  and  $\text{NO}_3$ , which is mainly determined by mineralization, nitrification and uptake of  $\text{NH}_4$  in the humus layer and the upmost soil layer (Tietema and Verstraten, 1991), is indeed the major determinant of net proton production which is mainly counteracted by Al mobilization in Dutch forest soils (Van Breemen et al., 1988).

The predicted behaviour of  $\text{SO}_4$  and N (iv) and the relationship between Al leaching and the leaching of  $\text{SO}_4$  plus  $\text{NO}_3$  (v) at the beginning of the simulation period (1990) is also in good agreement with results of the input-output studies mentioned above (Table 6.19).

Table 6.19 Simulated and measured input-output budgets for major ions in Dutch forest soils (Measured data are averages for 17 forest stands based on Heij et al., 1991).

	Element flux ( $\text{kmol}_c \text{ ha}^{-1} \text{ yr}^{-1}$ )							
	$\text{SO}_4$		$\text{NO}_3 + \text{NH}_4$		$\text{SO}_4 + \text{NO}_3 - \text{NH}_4$		Al	
	in	out	in	out	in	out	in	out
Simulated	3.17	3.35	3.98	2.88	1.31	5.39	0	4.45
Measured	2.95	3.05	4.35	2.96	0.38	5.35	0	4.51 <sup>1)</sup>

<sup>1)</sup> Results from two sites containing calcium carbonate in the subsoil were not used in calculating an average value

$\text{SO}_4$  indeed appears to behave conservative (simulated and measured average output/input ratios are 1.05 and 1.04 respectively) whereas an average of about 30% of N is still retained in the soil (simulated and average measured output/input ratios are 0.72 and 0.68 respectively). Furthermore, the similarity between the simulated and measured ratio of Al leaching as compared to leaching of  $\text{SO}_4 + \text{NO}_3 - \text{NH}_4$  is striking i.e. 0.83 and 0.84 respectively (cf Table 6.19). However, the reasonable agreement between simulated and measured N retention is questionable. The average measured output value was strongly influenced by large estimated output fluxes from seven Douglas fir stands which were derived by multiplying modelled annual drainage fluxes, corrected by equating Cl input to Cl output, with the solute concentrations in early spring. Excluding these sites, i.e. limiting to ten intensively monitored sites only, gives an average N retention of 50% ( $1.94 \text{ kmol}_c \text{ ha}^{-1} \text{ yr}^{-1}$ ). De Vries and Jansen (1994) even estimated a median N retention of 80% ( $3.33 \text{ kmol}_c \text{ ha}^{-1} \text{ yr}^{-1}$ ) for 150 forest stands, using the method to calculate leaching fluxes as described above (cf Section 2.3; Table 2.17). Most likely, RESAM underestimated N retention by immobilization in the humus layer. Data on N accumulation in the humus layer of an intensively monitored oak-birch woodland between 1960 and 1985 was estimated at  $1.2$  to  $2.0 \text{ kmol}_c \text{ ha}^{-1} \text{ yr}^{-1}$  (Van Breemen et al., 1988) whereas RESAM predicted an N immobilization rate of  $0.4 \text{ kmol}_c \text{ ha}^{-1} \text{ yr}^{-1}$  in 1990. The remaining difference between N input and N output was uptake of  $0.7 \text{ kmol}_c \text{ ha}^{-1} \text{ yr}^{-1}$  (cf Table 6.19). Furthermore, N immobilization in the mineral soil may play a role and this process is not included in RESAM.

The important role of Al hydroxide dissolution (vi) agrees with results from laboratory experiments (Chapter 3; Mulder et al., 1989), which show that mobilization of pyrophosphate or oxalate-extractable Al is the dominant buffermechanism of non-calcareous sandy soils at high acid inputs. Actually, the pool of readily available Al includes both organic and inorganic secondary Al compounds (cf Section 3.1; De Vries, 1994a).

### Evaluation of future model predictions

Major features of model predictions at reducing deposition levels were:

- (i) the inversion from net N retention (in 1990) to net N mobilization (between 2000



- and 2030) followed by net N retention again;
- (ii) the strong decrease in Al hydroxide dissolution;
  - (iii) the reversibility of soil acidification, reflected by the relatively fast/decrease in Al concentration and the increase in pH and base saturation.

It is difficult to indicate the reliability of the RESAM predictions because of a lack of long-term series of observations to calibrate the model. In RESAM several assumptions and simplifications are made with respect to the model structure either because of insufficient knowledge or to limit data requirements. Essential processes in acidifying systems, which are adequately known include (Jenkins et al., 1989); (i) the dynamics of organic matter including the behaviour of dissolved organic matter (DOC); (ii) the dynamics of solid phase Al and Al complexation by organic anions; (iii) N transformations in the soil, i.e. mineralization, nitrification and denitrification, and (iv) the dynamics of forest growth in relation to the acidification status of the soil. This lack of knowledge is reflected in RESAM by (cf modelling approach): (i) neglecting the role of DOC, (ii) neglecting the formation of complexes between Al and organic anions, (iii) a simple description of N transformation processes, and (iv) the assumption of a steady-state situation for the biomass of needles and fine roots and the simple direct relationship between N deposition and N contents in needles and fine roots. Uncertainties in Al and N dynamics may seriously affect the quality of the model predictions (De Vries and Kros, 1989). Furthermore, the annual (input) time step of the model may affect the long-term predictions. However, a comparison of model predictions with the RESAM model presented here, and a more detailed version including inter annual dynamics showed that this has only a minor effect (Kros et al., unpublished).

Nonwithstanding these shortcomings, the behaviour of the RESAM model seems reliable considering the consistence between predicted and measured behaviour of ions at elevated acid inputs presented in this study. Furthermore, measurements indeed show that at reduced inputs net N removal may occur (Roelofs, Catholic University Nijmegen, pers. comm. on the effects of removing atmospheric inputs by a roof on the forest), Al mobilization does reduce considerably (Mulder et al., 1988) and soil acidification is reversible (Hauhs and Wright, 1989). As with the model predictions, measurements also show that the pH of the humus layer is lower than the mineral topsoil in forest soils receiving high acid inputs (De Vries and Leeters, 1994) whereas the opposite is generally true at low acid inputs (Tamminen and Starr, 1990). Finally, the agreement in model predictions and data about the average decrease in pH of the mineral topsoil of Dutch forest soils in the past (Table 6.20) implies that the predicted increase in pH is plausible.

Although the general model behaviour seems feasible, the accuracy of the predicted soil response in time is influenced by uncertainties in data and model structure. The influence of uncertainty and/or spatial variability in data on the RESAM predictions was investigated by Kros et al. (1993) for the same forest-soil combination, i.e. a douglas fir on a Haplic Podzol. Results of 200 Monte Carlo simulation runs, in which the uncertainty/variability of input data was accounted for, showed that (i) uncertainties in rate and/or equilibrium

*Table 6.20 Measured and simulated pH changes in the mineral topsoil (0-10 cm) of Dutch forest soils during periods of 25 to 30 years*

	pH change in a 25-30 year period	
	past	future
Measured	-0.35 <sup>1)</sup>	-
Simulated	-0.32 <sup>2)</sup>	+0.35

<sup>1)</sup> Average decrease in pH in fourteen forest soils (from 3.60 to 3.25) during the period 1953 to 1984 (DLO Winand Staring Centre, unpublished data)

<sup>2)</sup> Simulated decrease in pH during the initialization period (1965-1990)

constants influencing Al hydroxide dissolution and nitrification strongly influenced the model predictions and (ii) a simulation run with average data gave nearly similar trends in soil solution chemistry than the mean of the 200 simulation runs. Using average data, RESAM thus seems to reproduce the mean response of a forest soil, assuming that the model structure is correct.

## 6.3 IMPACTS ON TWO CHARACTERISTIC DUNE SOILS IN THE NETHERLANDS

### ABSTRACT

The long-term impact of present levels of acid deposition on sandy soils in dune areas was simulated for calcareous and non-calcareous (coastal) dune ecosystems in the Netherlands for a 100 year period. Simulations were made with a process-oriented Regional Soil Acidification Model (RESAM). The model uses mechanistic descriptions for processes in the vegetation canopy, humus layer and mineral soil horizons which significantly influence the soil chemistry (amounts in minerals and at the adsorption complex) and the soil solution chemistry (ionic concentrations). Simulations indicated that the impact of atmospheric deposition on a calcareous dune soil becomes very important when the calcium carbonate content has fallen below 0.3%. In these soils, the pH in the topsoil (first 10 cm) will decline from about 6.5 to 3.0 over several decades, and acid deposition will become the dominating acidifying mechanism (more than 95%). This is because the weathering rate of silicates is very low and the buffering capacity of the exchange complex and of amorphous Al hydroxides is almost negligible in dune soils. Under natural conditions the pH will not fall below 4. Simulations for a non-calcareous dune soil indicated that present deposition levels cause a depletion of amorphous Al hydroxides, which leads to a pH decline from about 3.5-4.5 to 3.0-3.5 over a depth of more than 50 cm during the simulation period. Evidence is given that this will lead to a decrease in plant species. Finally, various management practices, designed to minimize the effects of acidification are discussed.

### INTRODUCTION

The effects of increased atmospheric deposition of  $\text{SO}_x$ ,  $\text{NO}_x$  and  $\text{NH}_x$  on forests and heathlands have received much attention in the Netherlands during the last decade (Heij and Schneider, 1991). However, the impact of acid deposition on soils and vegetation types in coastal dunes has received little attention. Research has mainly been focused on the natural decalcification of soils (Klijn, 1981; Rozema et al., 1985). Grootjans et al. (1988), investigated dune slacks in relation to ground water quality and acidification. However, attention to the effects of increased soil acidification and nitrogen enrichment due to atmospheric inputs on dry coastal dunes is also highly relevant. During the last decades dry dune ecosystems in the Netherlands show (i) a decrease in rare species and in lichen cover, (ii) an increase of nitrophilous species and of graminoid components (*Carex arenaria*, *Ammophila arenaria*, *Molinia caerulea*, *Calamagrostis epigeios* and *Deschampsia flexuosa*) in formerly oligotrophic communities (heather - and lichens vegetation) and (iii) an accelerated spread of shrubs and moss cover (Vertegaal et al., 1989; Ketner-Oostra, 1993). Another sign of unnatural conditions is the rapid spread of the moss species *Campylopus introflexus* (Van der Meulen et al., 1987).

Several studies based on repeated vegetation mapping and comparisons of releves in the Dutch dry dunes point to a higher nutrient status (Van Dorp et al, 1985; Van der Maarel et al, 1985). Westhoff (1989) also mentions a decrease of superficially rooting annuals due to base cation leaching of upper soil layers that may be caused by acid precipitation. The

vegetation changes do indeed coincide with changes in emissions of  $\text{NH}_3$ ,  $\text{NO}_x$  and  $\text{SO}_2$  in the last decades. Comparison of data on atmospheric deposition from different periods by Leeftang (1938), Vermeulen (1977), Stuyfzand (1984) and Houdijk (1993) showed (i) a continuous increase in  $\text{NH}_4$  deposition since 1935, (ii) an increase in both  $\text{SO}_4$  and  $\text{NO}_3$  deposition from 1935 to 1975 and (iii) a decrease in  $\text{SO}_4$  deposition after 1975 whereas the  $\text{NO}_3$  deposition remains constant.

The changes in dune vegetation described above cannot unambiguously be ascribed to atmospheric deposition alone, because natural soil development and vegetation succession also play a role. Since the beginning of the 20<sup>th</sup> century the disappearance of extensive grazing of the dunes and an almost entire fixation of dunes caused a convergence of soil forming processes and plant succession in large areas. Soil acidification, change in nutrient levels and shifts in vegetation are 'natural trends' in such a stabilized landscape (Klijn, 1981; Westhoff, 1989; De Raeye, 1989). Formerly important differences in soils, expressed by differences in organic matter, pH of the top soil and nutrients, seem to be levelled out by convergent soil and vegetation developments. These changes could partly explain the floristic changes. A number of declining species, especially those belonging to the *Viola caninae*, are correlated to areas that were extensively grazed in the past. However, atmospheric deposition will add to these developments, by both a stronger acidification and nitrogen enrichment. The character, rate and scale of the vegetation changes even point to atmospheric deposition as the dominant factor in some cases.

Insight in the long-term impact of acid deposition on dunes is important in view of their great ecological value. Internationally the Dutch coastal dunes are regarded as unspoilt and relatively rich in plant species (Bakker et al., 1981). They form only 1% of the land area of The Netherlands but contain 66% of species in the Dutch flora, of which 15% is not found outside the dune area. Syntaxonically, coastal dunes harbour about one quarter of the plant associations described for the country (Westhoff and Den Held, 1969). Two thirds of the plant associations found in the coastal dunes are confined to this landscape.

In this section, the long-term acidifying impact of atmospheric deposition on representative Dutch dune soils and related plant cover is studied by simulating the effect of the present acid deposition during a 100 year period. Estimates are given of changes in (i) natural and man-induced acidification and (ii) soil and soil solution chemistry going from calcareous to non-calcareous soils. Model predictions are focused on soil acidification, i.e. changes in the pH and in the chemistry of Al and base cations. Results are discussed in relation to the possible adverse effects on the dune ecosystem. Furthermore, management practices that might avoid these effects are evaluated.

## STUDY AREA

### Dutch coastal dunes

Coastal dunes in the Netherlands are geologically young. The so-called 'Younger Dunes' have developed since approximately AD 900. Most areas date from AD 1300 onwards and witnessed frequent sand blowing until 1850 (Jelgersma et al., 1970; Klijn, 1981, 1990). Compared to other regions, soil development is relatively uninfluenced by man. A unique aspect of Dutch coastal dunes is the presence of two mineralogically distinct dune regions with strikingly different soils and ecosystems (Eisma, 1968; Depuydt, 1972; Rozema et al., 1985). The dunes north of Bergen (Fig. 6.21), the Wadden district, consist of sand with very low contents of calcium-carbonate (< 2%), usually lower than 0.5%. Furthermore, the content of silicate minerals, mainly feldspars, is also very low (generally between 6 and 8%). In contrast, the area south of Bergen, the Dune district, has relatively high carbonate contents (usually between 2 and 10%). The content of feldspars is higher too and varies generally between 13 and 17% (Eisma, 1968). The boundary between these areas is rather sharp (Rozema et al., 1985).

### Selection of ecosystems

In the Wadden district, soil formation involved rapid decalcification and (micro-) podzolization. Natural succession has led to heather and lichens or grassland of low productivity on rather acid soils. In the Dune district several more productive dune grass communities, shrubs or even forests have developed on soil profiles which show decalcification to shallow depth (Van Oosten, 1986; Westhoff, 1989).

Simulations were carried out on two representative dune ecosystems in the Dune- and Wadden districts. For practical reasons the ecosystems selected do not refer to a specific site. Instead, average values for typical soil profiles and vegetation types were taken from literature. For the Dune district, this vegetation is a combination of *Rubus caesius* L., *Salix repens* L., *Gramineae* and *mosses* and for the Wadden district it is a combination of *Calluna vulgaris* L., *Corynephorus canescens* L., *lichens* and *mosses* (Plant nomenclature according to Van der Meijden and Vanhecke, 1986). Characteristic soil types are a calcareous Arenosol (FAO, 1981) or a humus poor Calcimagnesian soil (Duchaufour, 1977) in the Dune district and a non-calcareous Arenosol (FAO, 1981) or a slightly developed sandy soil (Duchaufour, 1977) in the Wadden district. To compare the influence of mineralogical composition unambiguously, the horizon designations and horizon thicknesses were kept the same for both soils. Both profiles lie well above ground water (> 2 m), excluding capillary influences. Furthermore, data on atmospheric deposition, precipitation and evapotranspiration were assumed to be similar. Both locations were assumed to be situated close to the sea (less than one km) to include the sea spray effect.

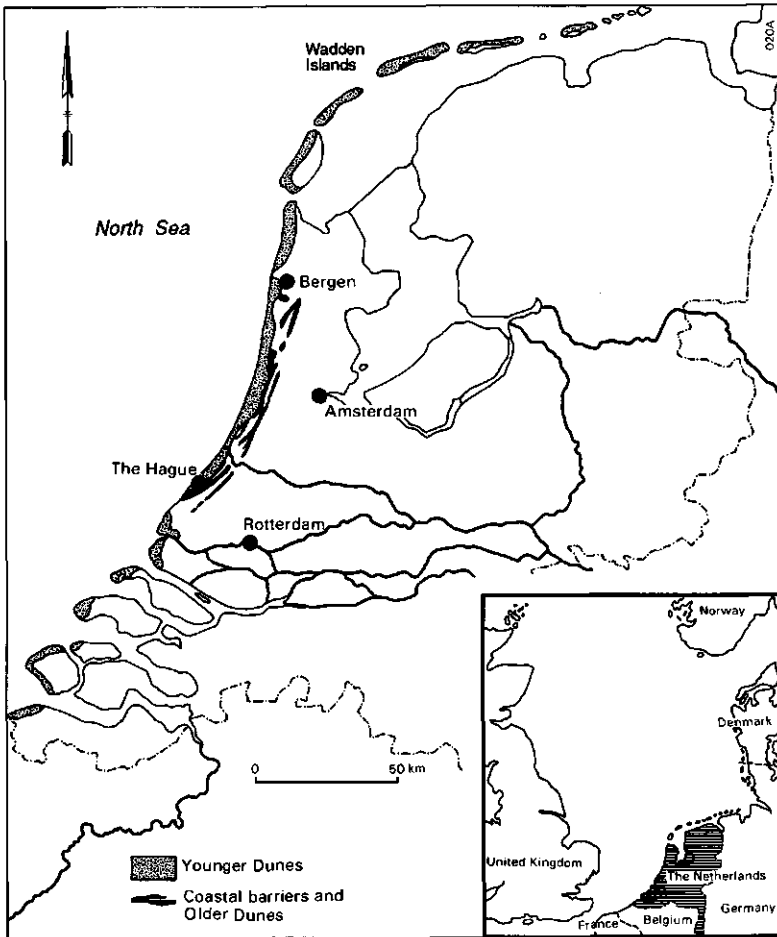


Figure 6.21 The coastal dune area of The Netherlands

## METHODS AND DATA

### The model RESAM

To gain insight in the long-term effect of acid deposition on dune soils, a process-oriented Regional Soil Acidification Model (RESAM) was used (Section 6.2; De Vries et al., 1994b). RESAM describes the changes in soil chemistry in both the solid phase (minerals and adsorption complex) and liquid phase caused by natural and man-induced processes. The model enables us to predict long-term changes under defined boundary conditions for a given soil profile. RESAM includes the major ions in dune soils i.e. the macro nutrients  $\text{NH}_4$ ,  $\text{NO}_3$ ,  $\text{SO}_4$ , Ca, Mg and K plus H, Al, Na, Cl,  $\text{HCO}_3$  and organic anions ( $\text{RCOO}$ ). The

model input includes atmospheric deposition, precipitation and evapotranspiration. The vertical heterogeneity is taken into account by differentiating between soil horizons. The temporal resolution of model input and output is one year since the model is intended to give insight into the long-term soil chemical response of forest ecosystems to acid deposition.

RESAM consists of a set of mass balance equations, rate limited equations and equilibrium equations. The mass balance equations describe the input-output relationships in each horizon for all cations and anions. Rate-limited and equilibrium equations describe those processes in the canopy, humus layer and mineral soil horizons which significantly influence the concentration of major ions in the soil solution. A list of the various process formulations including the compounds involved in each process is given in Table 6.21. Canopy interactions, nutrient cycling processes, N-transformations and weathering are considered as rate-limited processes. Adsorption and desorption of cations and  $\text{SO}_4$  are considered to be described well by chemical equilibria.

The geochemical interactions, especially weathering and cation exchange, are the main determinants of long-term soil changes, because they are the major buffer mechanisms counteracting acid production in the soil. More information on the various buffer

Table 6.21 Processes and process formulations included in RESAM

Processes	Compounds involved	Process formulation
Leaf uptake Leaf exudation	$\text{NH}_3, \text{NO}_x, \text{SO}_2$ $\text{Ca}, \text{Mg}, \text{K}$	linear function of dry deposition
Litterfall	$\text{N}, \text{Ca}, \text{Mg}, \text{K}, \text{S}$	first-order reaction
Root decay	$\text{N}, \text{Ca}, \text{Mg}, \text{K}, \text{S}$	first-order reaction
Mineralization	$\text{N}, \text{Ca}, \text{Mg}, \text{K}, \text{S}$	first-order reaction
Root uptake	$\text{N}, \text{Ca}, \text{Mg}, \text{K}, \text{S}$	fixed <sup>1)</sup>
Nitrification	$\text{NH}_4, \text{NO}_3$	first-order reaction <sup>2)</sup>
Denitrification	$\text{NO}_3$	first-order reaction
Dissociation of $\text{CO}_2$	$\text{HCO}_3$	$\text{CO}_2$ equilibrium equation
Protonation of $\text{RCOO}$	$\text{RCOO}$	first-order reaction
Weathering of carbonates	$\text{HCO}_3$	first-order reaction
Weathering of silicates	$\text{Al}, \text{Ca}, \text{Mg}, \text{K}, \text{Na}$	first-order reaction
Weathering/precipitation of Al hydroxides	Al	first-order reaction <sup>3)</sup>
Cation exchange	$\text{H}, \text{Al}^{3+}, \text{Ca}, \text{Mg}, \text{K}, \text{Na}, \text{NH}_4$	Gaines-Thomas equations
Adsorption/desorption of sulphate	$\text{SO}_4^{2-}$	Langmuir equation

1) Fixed uptake based on a given net uptake and a steady state recycling of elements in leaves and roots, allocated per soil layer by the wateruptake pattern.

2) Limited to the rootzone (up to 1 meter).

3) Al weathering is also described by an elovich equation but that option was not used in this study.

mechanisms and buffer ranges is given in Section 6.1. The major acid neutralizing reactions in calcareous and non-calcareous sandy dune soils are dissolution of Ca carbonates and Al hydroxides, respectively, since silicate weathering is very low and the role of cation exchange is also limited by the low cation exchange capacity (CEC). As with most rate-limited processes in RESAM, weathering fluxes of Ca carbonate and Al hydroxide are described by first-order reactions (cf Section 6.2; Eq. 6.50 and 6.52).

In this study mineralization was assumed to equal the sum of litterfall, and root decay, and nutrient uptake from the soil was taken equal to the mineralization rate. This assumption of steady state nutrient cycling is fairly theoretical since vegetation type and performance will change during natural succession. It implies that the long-term impact of present N deposition on increased N availability is not simulated (steady-state N pool in the soil). However, the neglect of changes in the N pool on predictions of the long-term changes of the acid-base status of the considered dune soils is likely to be small (cf Discussion).

### Input data

Inputs to the model include system inputs, initial state of variables and parameters. Values for the major system inputs, i.e. the total atmospheric deposition of  $\text{NH}_4^+$ ,  $\text{NO}_3^-$ ,  $\text{SO}_4^{2-}$ , Cl and the base cations Ca, Mg, K and Na (Table 6.22) were kept constant during the simulation

Table 6.22 Wet, dry and total deposition values used during the 100 year simulation period

	Deposition ( $\text{kmol}_e \text{ ha}^{-1} \text{ yr}^{-1}$ )								
	H	Ca	Mg	K	Na	$\text{NH}_4$	$\text{NO}_3$	$\text{SO}_4$	Cl
Wet	0.3	0.5 <sup>1)</sup>	1.0 <sup>1)</sup>	0.15 <sup>1)</sup>	4.0 <sup>2)</sup>	0.5 <sup>3)</sup>	0.4 <sup>3)</sup>	1.05 <sup>3)</sup>	5.0 <sup>2)</sup>
Dry	0.7	1.0	2.0	0.30	8.0	0.5	0.4	2.10	10.0
Total <sup>4)</sup>	1.0	1.5	3.0	0.45	12.0	1.0	0.8	3.15	15.0

<sup>1)</sup> Based on the KNMI/RIVM measuring network (KNMI/RIVM, 1985). For Na, Mg and K, nearly the same values are derived when assuming that the input comes only from sea salt, i.e. by multiplying the Cl inputs with the Na/Cl, Mg/Cl and K/Cl ratios in sea salt (0.86, 0.2 and 0.02 respectively; cf. Cl deposition).

<sup>2)</sup> Derived from Leeftang (1938), Vermeulen (1977) and Kooistra (1971).

<sup>3)</sup> Based on Stuyfzand (1984) and Houdijk (1993b).

<sup>4)</sup> Total deposition was assumed three times as high as wet deposition for Ca, Mg, K, Na, Cl and  $\text{SO}_4$  ('seaspray') and twice as high as wet deposition for  $\text{NH}_4$  and  $\text{NO}_3$ . This is based on data from Houdijk (1993) who found a throughfall/bulk deposition ratio of 6 for base cations, Cl and  $\text{SO}_4$  and of 4 for  $\text{NH}_4$  and  $\text{NO}_3$  below coniferous forest at two locations near the coast (Terschelling and Schoorl). We halved these values based on data from Stuyfzand (1984), from a lysimeter study in calcareous dunes near Castricum. For the relative inert elements Cl and  $\text{SO}_4$  he found a ratio of 5 between the leaching from the soil system and bulk (open field) deposition for a coniferous forest and of 2.5 for a dune vegetation. This suggests that coniferous forests are twice as efficient in filtering dry deposition as short vegetations. Similarly in inland sites throughfall/bulk deposition ratios for  $\text{SO}_4$  are approximately 5 for coniferous forests (Kleijn et al., 1989), and 2.5 for short vegetations such as grasslands (Heil et al., 1988).



period (1987-2087). The deposition of Al, HCO<sub>3</sub> and RCOO was assumed negligible. The potential acid load, which can be calculated from the sum of SO<sub>4</sub>, NO<sub>3</sub> and NH<sub>4</sub> deposition (4.95 kmol<sub>c</sub> ha<sup>-1</sup> yr<sup>-1</sup>) minus the base cation deposition not associated with chloride (1.95 kmol<sub>c</sub> ha<sup>-1</sup> yr<sup>-1</sup>), equalled 3.0 kmol<sub>c</sub> ha<sup>-1</sup> yr<sup>-1</sup>. This value can also be derived from the load of free H (1.0 kmol<sub>c</sub> ha<sup>-1</sup> yr<sup>-1</sup>) plus twice the NH<sub>4</sub> load (2.0 kmol<sub>c</sub> ha<sup>-1</sup> yr<sup>-1</sup>; cf Table 6.22). The relative large difference between the potential acid load and the sum of SO<sub>4</sub>, NO<sub>3</sub> and NH<sub>4</sub> deposition is due to the large contribution of SO<sub>4</sub> from seasalts. From the SO<sub>4</sub>/Cl ratio in seasalt (0.1) the contribution of seasalt to SO<sub>4</sub> deposition is estimated to be 1.5 kmol<sub>c</sub> ha<sup>-1</sup> yr<sup>-1</sup>.

For both dune ecosystems the average annual infiltration was set at 600 mm yr<sup>-1</sup>, based on an average precipitation of 725 mm yr<sup>-1</sup> (Bakker, 1981) and a combined interception plus soil evaporation of 125 mm yr<sup>-1</sup> (De Vries, 1991). Total evapotranspiration was set at 375 mm yr<sup>-1</sup> (cf Bakker, 1990). Total transpiration (water uptake) was thus taken at 250 mm yr<sup>-1</sup> and the precipitation surplus equalled 350 mm yr<sup>-1</sup>; a value that was also found by Stuyfzand (1984). The water uptake per soil layer was assumed proportional to the root distribution (see further).

Model variables include the element amounts in the various compartments of the dune ecosystem i.e. shoots, (fine) roots, the soil solid phase, i.e. carbonates, silicates (primary minerals), hydroxides and adsorption complex and the soil solution. Data related to the vegetation are given in Table 6.23, whereas the soil data (including the fine root distribution) are given in Table 6.24 and 6.25. Except for the carbonate content all basic soil characteristics, i.e. bulk density, cation exchange capacity (CEC) and Al hydroxide content, were taken equal for both dune soils (Table 6.24).

Table 6.23 Biomass and element contents of shoots and fine roots of used in the simulations for the calcareous and non-calcareous dune ecosystem

Dune ecosystem	Compartment	Biomass (kg ha <sup>-1</sup> )	Elements contents (%)				
			N	Ca	Mg	K	S
Calcareous	shoots	3000 <sup>1)</sup>	1.4 <sup>4)</sup>	1.7 <sup>5)</sup>	0.45	1.0 <sup>5)</sup>	0.2
	fine roots	4000 <sup>2)</sup>	1.2	0.8	0.10	0.35	0.1
Non-calcareous	shoots	750 <sup>3)</sup>	1.4 <sup>4)</sup>	0.6 <sup>5)</sup>	0.15	0.25 <sup>6)</sup>	0.2
	fine roots	1000 <sup>3)</sup>	1.2	0.2	0.05	1.0	0.1

<sup>1)</sup> Based on Klinkhamer and De Jong (1985), Bobbink et al. (1988) and Van der Hagen (1986)

<sup>2)</sup> Based on Tinhout and Werger (1988) and Berendse (1988) for dry *Calluna* heathlands since data for dune vegetation were scarce

<sup>3)</sup> Based on Whittaker and Likens (1975) for low vegetation in a harsh environment (conditioned by an extremely low mineral status and often drought stress).

<sup>4)</sup> Based on Bobbink et al. (1988) and Van der Hagen (1986)

<sup>5)</sup> Based on Pruyt (1984)

<sup>6)</sup> Derived from data for dry *Calluna* heathlands (Heil and Diamond, 1983)

Table 6.24 Root distribution data and basic soil characteristics used in the simulation of both dune ecosystems

Soil layer	Horizon	Thickness (cm)	Root <sup>1)</sup> distribution (%)	Bulk <sup>2)</sup> density (kg m <sup>3</sup> )	CEC <sup>2)</sup> (mmol <sub>c</sub> kg <sup>-1</sup> )	Carbonate <sup>4)</sup> content (mmol <sub>c</sub> kg <sup>-1</sup> )	Al hydroxide <sup>5)</sup> content (mmol <sub>c</sub> kg <sup>-1</sup> )
0	0	2	15	150	1200	100	0
1	Ah	8	60	1450	30	360	8
2	AC	15	25	1540	10	720	10
3	C	37	0	1540	5	800	12

<sup>1)</sup> Based on Tinhout and Werger (1988) and Berendse (1988)

<sup>2)</sup> Derived from transfer functions with the organic matter content (Hoekstra and Poelman, 1982)

<sup>3)</sup> Derived from transfer functions with the organic matter content (Breeuwsma et al., 1986). Values for the CEC refer to a determination at pH 6.5. In non-calcareous soils, the CEC measured at the actual pH is lower due to non-exchangeable H adsorption.

<sup>4)</sup> Derived from the Netherlands Soil Information System (Bregt et al., 1986). Relates only to the calcareous soil (1% CaCO<sub>3</sub> = 200 mmol<sub>c</sub> kg<sup>-1</sup>).

<sup>5)</sup> Derived from the Netherlands Soil information System (Bregt et al., 1986). Values refer to the content of oxalate extractable Al. Note that the Al hydroxide content of dune soils is extremely low (about ten times as low) compared to other sandy soils such as podzols (De Vries et al., 1989a).

Data for the initial total cation amounts (in silicates) and the exchangeable cation fractions in both dune soils (Table 6.25) were kept equal for all mineral soil horizons, except for total cation amounts in the Ah horizon which are approximately 20% lower in both soils. Initial concentrations of the anions were calculated from the annual input from the atmosphere and the annual average water flux per layer. Initial concentrations of the cations were derived by combining exchange (Gaines-Thomas) equations with a charge balance equation, using given exchange constants and the initial cation amounts on the adsorption complex.

Table 6.25 Total cation amounts and exchangeable cation fractions used in the simulations for the calcareous and non-calcareous dune ecosystems

Cation	Exchangeable cation fraction (-) <sup>1)</sup>		Total cation amount (mmol <sub>c</sub> kg <sup>-1</sup> )	
	calcareous	non-calcareous	calcareous	non-calcareous
H	-	0.55		
NH <sub>4</sub>	-	0.05		
Al	-	0.20	1350 <sup>2)</sup>	450 <sup>2)</sup>
Ca	0.91	0.11	30 <sup>3)</sup>	10 <sup>4)</sup>
Mg	0.06	0.06	45 <sup>3)</sup>	15 <sup>4)</sup>
K	0.01	0.01	210 <sup>3)</sup>	70 <sup>4)</sup>
Na	0.02	0.02	150 <sup>3)</sup>	50 <sup>4)</sup>

<sup>1)</sup> Based on Pruyt (1984) and Van Oosten (1986). Values are related to a CEC determined at pH 6.5

<sup>2)</sup> Based on Eisma (1968)

<sup>3)</sup> Derived from a total analysis of a soil profile. Data indicate the dominance of potassium and sodium feldspars (KAlSi<sub>3</sub>O<sub>8</sub> and NaAlSi<sub>3</sub>O<sub>8</sub>) in dune soils

<sup>4)</sup> Derived by assuming a similar stoichiometry between Al, Ca, Mg, K and Na in both dune soils. Values thus derived for non-calcareous dune sand are low compared to those in pleistocene sandy soils at inland sites

A list of the various rate constants used, together with their derivation, is given in Table 6.26. Equilibrium constants for dissolution of Ca carbonate and Al hydroxide and for the dissociation of CO<sub>2</sub> were taken from Lindsay (1979). Cation exchange constants (Table 6.27) were calculated from data on ion ratios, at the adsorption complex and in soil water, at 40 sites and 4 depths in acid sandy forest soils (Kleijn et al., 1989).

Table 6.26 Rate constants used in the simulations

Rate constant	Unit	Value	Derivation after
Shoot turnover	yr <sup>-1</sup>	0.7	Berendse (1988)
Root turnover	yr <sup>-1</sup>	1.5	Tinhout and Werger (1988)
Nitrification	yr <sup>-1</sup>	100 <sup>1)</sup>	De Vries (1991)
Denitrification	yr <sup>-1</sup>	5 <sup>1)</sup>	De Vries (1991)
Carbonate weathering	mol <sub>c</sub> m <sup>3</sup> yr <sup>-1</sup>	10 <sup>-4</sup>	Stuyfzand (1984)
Ca+Mg weathering	yr <sup>-1</sup>	5.10 <sup>-4 2)</sup>	De Vries and Breeuwsma (1986)
Na+K weathering	yr <sup>-1</sup>	10 <sup>-4 2)</sup>	De Vries and Breeuwsma (1986)
Al hydroxide weathering	mol <sub>c</sub> m <sup>3</sup> yr <sup>-1</sup>	0.2 <sup>1)</sup>	De Vries (1991)

<sup>1)</sup> Derived from a model calibration on the soil solution composition of forest soils (De Vries, 1991)

<sup>2)</sup> Derived by assuming the weathering rates given in De Vries and Breeuwsma (1986) for non-calcareous sandy soils to be proportional to their total base cation contents

Table 6.27 Gaines Thomas exchange constants used in the simulations

Soil horizon	Gaines Thomas constants relative to Ca (mol l <sup>-1</sup> ) <sup>z<sub>x</sub></sup>					
	H	Al	Mg	K	Na	NH <sub>4</sub>
Ah	31000	0.84	0.28	0.18	0.18	2
AC	48000	0.84	0.24	0.82	0.31	15
C	48000	0.34	0.15	2.04	1.34	80

z<sub>x</sub> is the valency of ion x competing with Ca

## MODELPREDICTIONS

### The calcareous dune ecosystem

Changes in the soil solid phase and soil solution chemistry of the calcareous ecosystem were characterized mainly by the decalcification of the Ah horizon, i.e. the first mineral layer. Decalcification was associated with a decrease in Ca and HCO<sub>3</sub> leaching, and a decrease in pH (and base saturation), followed by enhanced Al and NH<sub>4</sub> leaching at low pH levels (Table 6.28). The results presented are therefore restricted to changes in (i) the decalcification rate (related to Ca and HCO<sub>3</sub> fluxes), (ii) the contribution of natural and man-induced acidification (related to HCO<sub>3</sub> and seasalt corrected SO<sub>4</sub> and NO<sub>3</sub> fluxes, denoted as SO<sub>4</sub> and NO<sub>3</sub>), (iii) the pH in the Ah horizon (related to H flux) and (iv) the concentrations and adsorbed amounts in the Ah horizon (related to cation fluxes).

Table 6.28 Leaching fluxes of H, Al, Ca, NH<sub>4</sub>, SO<sub>4</sub>, NO<sub>3</sub> and HCO<sub>3</sub> through the various soil layers of the calcareous dune soil at the beginning and the end of the simulation period

Soil horizon	Simulation period	Leaching fluxes (kmol <sub>c</sub> ha <sup>-1</sup> yr <sup>-1</sup> )								
		H	Al	Ca	NH <sub>4</sub>	SO <sub>4</sub>	SO <sub>4</sub> <sup>-</sup>	NO <sub>3</sub>	NO <sub>3</sub> <sup>-</sup>	HCO <sub>3</sub>
Ah	Begin (1987)	0.00	0.00	16.66	0.25	3.18	1.68	1.97	1.52	10.34
	End (2087)	3.52	0.22	2.02	0.57	3.18	1.68	1.72	1.27	0.00
AC	Begin (1987)	0.00	0.00	17.15	0.04	3.15	1.68	1.57	1.12	12.07
	End (2087)	0.00	0.00	15.02	0.10	3.15	1.65	1.58	1.13	10.03
C	Begin (1987)	0.00	0.00	15.62	0.04	3.15	1.65	1.11	0.66	12.74
	End (2087)	0.00	0.00	15.60	0.10	3.15	1.65	1.12	0.67	12.75

\* denote seasalt corrected fluxes

### Decalcification rates

Decalcification rates were nearly equal to Ca leaching fluxes. At the beginning of the simulation period nearly all Ca was mobilized in the Ah horizon whereas the AC horizon (the second mineral layer) is the dominant Ca source at the end of the simulation period (Table 6.28). Carbonate dissolution decreased with time in the Ah horizon whereas it increased in the AC horizon. This was due to the decreasing carbonate amount in the Ah horizon, leading to an almost complete exhaustion within 50 years. In the C horizon (the third mineral layer) some precipitation of carbonate occurred (Fig. 6.22).

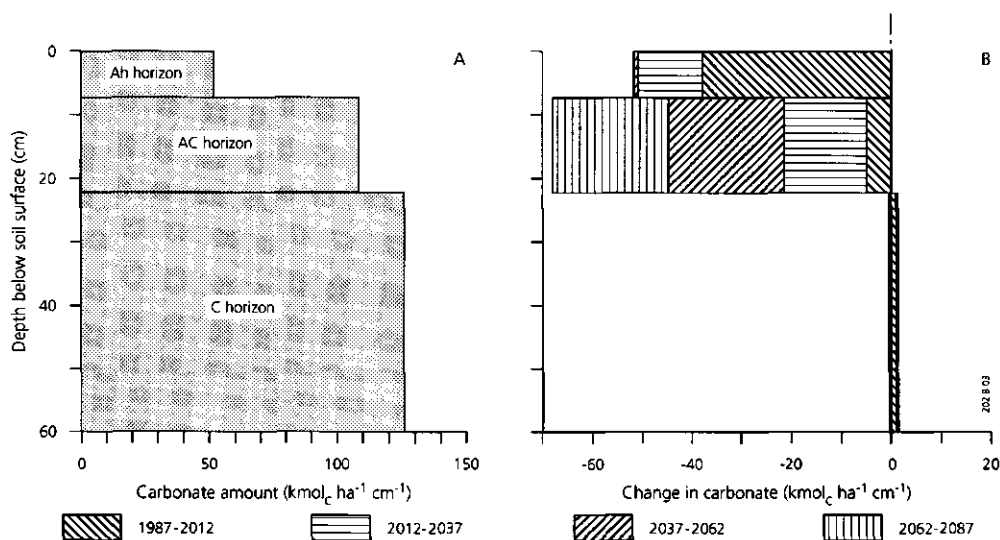


Figure 6.22 The initial amount of Ca-carbonate in the three mineral layers of the calcareous dune soil (A) and the changes in that amount over the simulation period during intervals of 25 years (B)

The Ca leaching rate from the C horizon remained nearly constant and equalled  $15.6 \text{ kmol}_c \text{ ha}^{-1} \text{ yr}^{-1}$ . Part of this flux was due to deposition ( $1.5 \text{ kmol}_c \text{ ha}^{-1} \text{ yr}^{-1}$ ) and silicate weathering ( $0.3 \text{ kmol}_c \text{ ha}^{-1} \text{ yr}^{-1}$ ) but the dominant source was carbonate dissolution ( $13.8 \text{ kmol}_c \text{ ha}^{-1} \text{ yr}^{-1}$ ). Ca leaching was mainly due to natural  $\text{HCO}_3$  production caused by dissociation of  $\text{CO}_2$  (Table 6.28).

#### *Natural and man-induced soil acidification*

The contribution of natural acid production ( $\text{CO}_2$  dissociation) and acid deposition on the rate of carbonate removal can be estimated by comparing  $\text{HCO}_3$  and seasalt corrected  $\text{SO}_4$  and  $\text{NO}_3$  fluxes in drainage water (Stuyfzand, 1984; Rozema et al., 1985). As with Ca, the leaching fluxes of these ions in the subsoil remained nearly constant (cf Table 6.28).  $\text{SO}_4$  leaching equalled  $\text{SO}_4$  deposition while  $\text{NO}_3$  leaching equalled the sum of  $\text{NH}_4$  and  $\text{NO}_3$  deposition ( $1.8 \text{ kmol}_c \text{ ha}^{-1} \text{ yr}^{-1}$ ) corrected for denitrification ( $0.65 \text{ kmol}_c \text{ ha}^{-1} \text{ yr}^{-1}$ ) and for  $\text{NH}_4$  leaching ( $0.04 \text{ mol}_c \text{ ha}^{-1} \text{ yr}^{-1}$ ).

Assuming that base cation deposition associated with  $\text{SO}_4$  and  $\text{NO}_3$  ( $1.95 \text{ kmol}_c \text{ ha}^{-1} \text{ yr}^{-1}$ ), can be separated into  $1.5 \text{ kmol}_c \text{ ha}^{-1} \text{ yr}^{-1}$  associated with  $\text{SO}_4$ , and  $0.45 \text{ kmol}_c \text{ ha}^{-1} \text{ yr}^{-1}$  associated with  $\text{NO}_3$  (see input data), the sea salt-corrected  $\text{SO}_4$  and  $\text{NO}_3$  fluxes, denoted as  $\text{SO}_4$  and  $\text{NO}_3$ , below the root zone were  $1.65$  and  $0.66 \text{ kmol}_c \text{ ha}^{-1} \text{ yr}^{-1}$  respectively (see Table 6.28). Using these data, the relative contribution of  $\text{HCO}_3$ ,  $\text{SO}_4$  and  $\text{NO}_3$  equalled 85%, 11% and 4% respectively. This is consistent with data given by Stuyfzand (1984) for a lysimeter study below a calcareous dune vegetation, i.e. 82%, 13% and 5% respectively.

The contribution of acid deposition to the decalcification in the whole soil profile was low, but it was very significant in the Ah horizon when the carbonate content was nearly depleted. This is shown in Figure 6.23. The contribution of  $\text{SO}_4$  and  $\text{NO}_3$  increased suddenly between 2010 and 2025 (Fig. 6.23A) when the carbonate content decreased from about 0.6 to 0.1% (Fig. 6.23B). In this period the decreasing rate of buffering by carbonates caused a significant decline in pH from about 6.7 to 5.0 (cf Fig. 6.24A) which in turn caused a strong inhibition of the proton production by dissociation of  $\text{CO}_2$ . In non-polluted situations soil acidification would decrease accordingly, but in polluted areas the constant input of strong acids causes an ongoing depletion of cations and decrease of pH in topsoils.

#### *pH*

The decalcification of the Ah horizon caused a strong pH decline (Figure 6.24) which is also reflected by the increased H flux in this horizon (cf Table 6.28). The sharp pH decline from about 6.5 to 3.0 over a period of 30 years (2015-2045) at constant deposition rates (Fig. 6.24) is due to the low CEC and Al hydroxide content.

The low exchange buffer capacity causes a fast switch from the carbonate buffer range (pH > 6.5) to the aluminium buffer range (pH < 4.5). The low aluminium buffer capacity in turn causes a fast switch to a buffer range where weathering by silicates is the only neutralizing

mechanism. Simulation results indicate a rather abrupt pH decline occurring at a carbonate content near 0.3% (Fig. 6.24B).

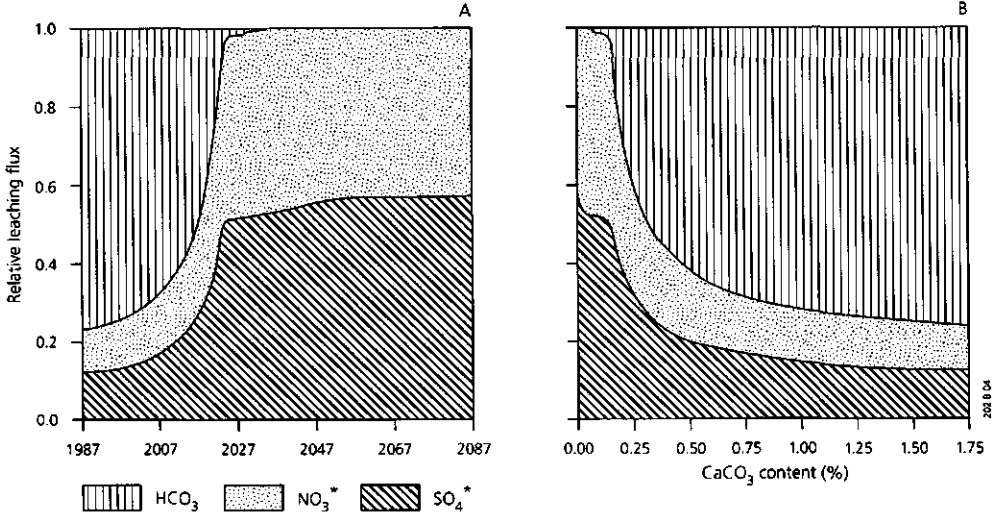


Figure 6.23 The relative contribution of HCO<sub>3</sub><sup>-</sup>, SO<sub>4</sub><sup>-</sup> and NO<sub>3</sub><sup>-</sup> in the acidification of the Ah horizon of the calcareous dune soil as a function of time (A) and as a function of the carbonate content (B)

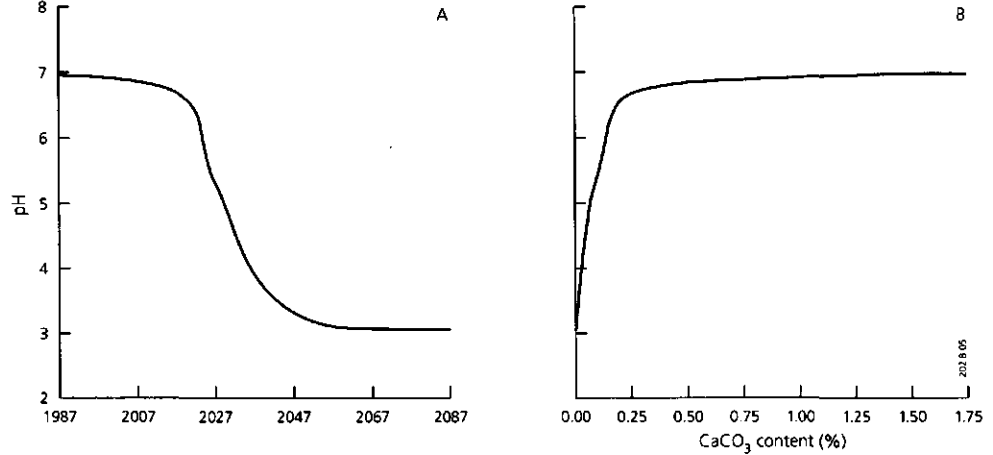


Figure 6.24 The pH in the Ah horizon of the calcareous dune soil as a function of time (A) and carbonate content (B)

For background deposition rates, the time period to deplete the carbonate content was much longer and the pH stayed at a higher level, especially in the AC and C horizon. A simulation with background data for the deposition of  $\text{SO}_4$ ,  $\text{NO}_3$  and  $\text{NH}_4$ , such that the potential acid load equalled  $0.5 \text{ kmol}_e \text{ ha}^{-1}$ , revealed that the pH in the Ah horizon still falls to about pH 4 within 70 years (not shown). This is due to a relatively large proton production in the Ah horizon caused by (i) N transformations (proton production in the topsoil by mineralization and nitrification is only partly counteracted by  $\text{NO}_3$  uptake) and (ii) organic acid dissociation (which deprotonate in the Ah horizon while protonation occurs in the subsoil). In the AC and C horizon, the difference between the impact of present and background deposition on the final soil pH was much higher. In this horizon, the soil pH after decalcification stayed close to 5 at background levels (cf Section 6.1). This illustrates the importance of acid deposition in the acidification of calcareous soils at low carbonate contents.

*Concentration and adsorbed amounts of cations*

In addition to a decline in Ca concentration and pH, acidification of the Ah horizon also caused an increase in dissolved Al and  $\text{NH}_4$  as illustrated by the increased Al and  $\text{NH}_4$  fluxes in this horizon (Table 6.28). The temporal response of the cation composition of the Ah horizon in both the soil solution and at the adsorption complex is illustrated in Figure 6.25.

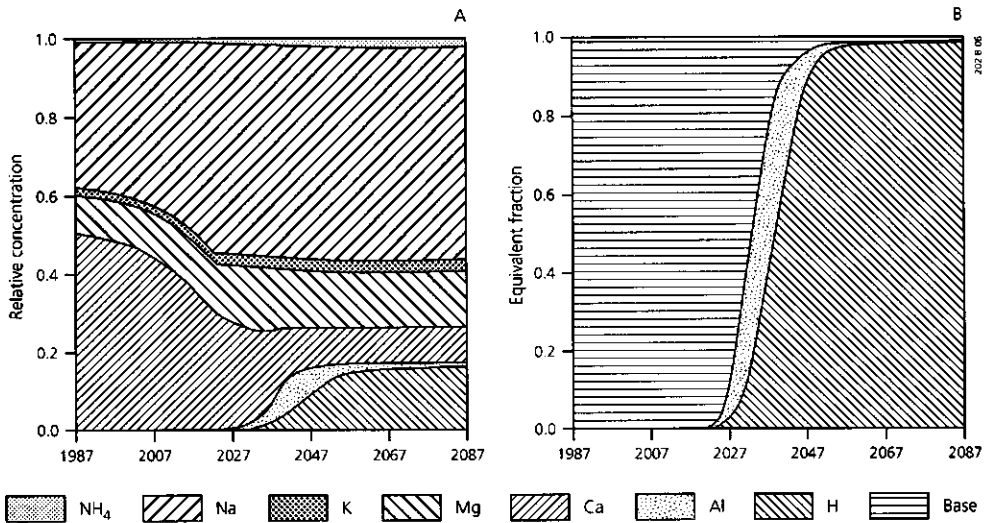


Figure 6.25 The temporal response in equivalent fractions of H, Al, base cations and  $\text{NH}_4$  in the soil solution (A) and solid phase (B) of the Ah horizon of the calcareous dune soil

The soil solution was initially dominated by Ca and Na (Fig. 6.25A) while Ca was the dominant adsorbed cation (Fig. 6.25B; the bases are not distinguished since Ca is the dominant base cation). H, Al and  $\text{NH}_4$  played a negligible role. During the simulation period dissolved Ca decreased but this hardly influenced the adsorbed Ca amount until 2025. By that time dissolved H and Al became significant as reflected by a sharp change from nearly complete Ca to H saturation between 2025 and 2050. Levels of dissolved and adsorbed Al remained low however, because of the low dissolution rate of Al hydroxides. This in turn was caused by the low Al hydroxide content, which moreover was almost completely exhausted within 25 years. Al depletion was reflected by the nearly negligible levels of dissolved Al (Fig. 6.25A) and adsorbed Al (Fig. 6.25B) after 2050. Even between 2025 and 2050, dissolved Al concentration was always lower than dissolved Ca. The molar Al/Ca ratio thus never exceeded 1.0, a value that is considered critical for effects on the root system of various trees (De Vries, 1991).

Simulated  $\text{NH}_4$  concentrations showed a small increase between 2025 and 2050. This was due to a decrease in the nitrification rate which is modeled as a function of pH. In heather communities a change from  $\text{NO}_3$  domination ( $\text{NH}_4/\text{NO}_3$  ratio < 1) to  $\text{NH}_4$  domination ( $\text{NH}_4/\text{NO}_3$  ratio > 1) has even been observed over a pH range between 6 and 4, causing inhibition of cation uptake (Houdijk, 1993b). However, here the system remained  $\text{NO}_3$  dominated (see Table 6.28).

### **The non-calcareous dune ecosystem**

Changes in the soil and soil solution chemistry of the non-calcareous system were dominated by the depletion of Al hydroxides in the soil profile. This was associated with a decrease in Al and an increase in H concentration (Table 6.29). In similar manner to the calcareous system, the results are restricted to changes in: (i) the rates of Al hydroxide removal (related to Al leaching flux), (ii) the contribution of natural and man-induced acidification (related to  $\text{RCOO}$ ,  $\text{SO}_4$  and  $\text{NO}_3$  leaching fluxes) and (iii) the pH in the mineral soil (related to H leaching flux). Rates of Al hydroxide removal were nearly equal to Al leaching fluxes from the various soil layers. Figure 6.26 and Table 6.29 show that Al mobilization was restricted to the Ah and AC horizon at the beginning of the simulation period and to the C horizon at the end. In the first two horizons Al hydroxide was nearly depleted within 25 years while the C horizon was also nearly depleted at the end of the simulation period.

At the end the Al concentration in that horizon was not in equilibrium with Al hydroxide as illustrated by the decrease in Al leaching flux from the C horizon from 2.26 to 1.12  $\text{kmol}_c \text{ ha}^{-1} \text{ yr}^{-1}$  (Table 6.29). At greater depth (1 m) the Al leaching flux remained at 2.26  $\text{kmol}_c \text{ ha}^{-1} \text{ yr}^{-1}$ . Part of the Al leaching flux was due to silicate weathering (0.62  $\text{kmol}_c \text{ ha}^{-1} \text{ yr}^{-1}$ ) but the dominant source was Al hydroxide dissolution (1.64  $\text{kmol}_c \text{ ha}^{-1} \text{ yr}^{-1}$ ). Results for the



**Table 6.29** Leaching fluxes of H, Al, Ca, SO<sub>4</sub>, NO<sub>3</sub> and RCOO through the various mineral soil layers of the non-calcareous dune soil at the beginning and the end of the simulation period

Soil horizon	Simulation period		Leaching fluxes (kmol <sub>c</sub> ha <sup>-1</sup> yr <sup>-1</sup> )							
			H	Al	Ca	SO <sub>4</sub>	SO <sub>4</sub>	NO <sub>3</sub>	NO <sub>3</sub>	RCOO
Ah	Begin	(1987)	1.87	0.97	1.55	3.15	1.65	1.60	1.15	0.45
	End	(2087)	2.73	0.06	1.55	3.15	1.65	1.57	1.12	0.45
AC	Begin	(1987)	0.85	2.02	1.53	3.15	1.65	1.68	1.23	0.21
	End	(2087)	2.55	0.21	1.52	3.15	1.65	1.62	1.17	0.21
C	Begin	(1987)	0.18	2.26	1.58	3.15	1.65	1.60	1.15	0.03
	End	(2087)	1.25	1.12	1.58	3.15	1.65	1.62	1.17	0.03

\* denote seasalt corrected fluxes

Al and Ca fluxes in the Ah, AC and C horizon (Table 6.29) showed a decline in (molar) Al/Ca ratios from 0.41, 0.88 and 0.95: 1 respectively in 1987 to 0.03, 0.09 and 0.47: 1 in 2087.

The contribution of natural - and man-induced sources to total soil acidification can be obtained by comparing leaching fluxes of RCOO (natural) and of Cl-corrected SO<sub>4</sub> and NO<sub>3</sub> (man-induced) leaching (Section 2.1 and 2.2). Leaching fluxes of these ions in the C horizon were 0.03, 1.65 and 1.17 kmol<sub>c</sub> ha<sup>-1</sup> yr<sup>-1</sup> respectively (cf Table 6.29). Using these data, the relative contribution of RCOO, SO<sub>4</sub> and NO<sub>3</sub> equalled 1%, 58% and 41% respectively.

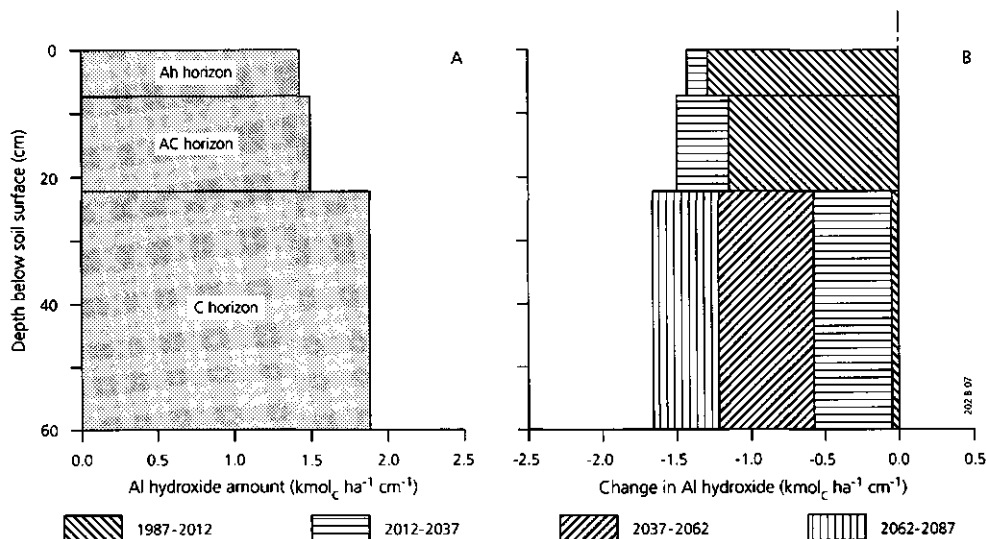


**Figure 6.26** The initial amount of Al hydroxide in the three mineral layers of the non-calcareous dune soil (A) and the changes in that amount over the simulation period during intervals of 25 years (B)

The depletion of Al hydroxides in the various soil layers was associated with a strong pH decline (Fig. 6.27), which is reflected by the increased H fluxes in the mineral soil layers (cf Table 6.29). The pH in all layers decreased to a level close to 3.0. Major changes occurred in the C horizon. Here the pH originally was in equilibrium with Al hydroxide (gibbsite) at a level above 4.0. As with the calcareous system, the very low final pH after depletion of Al hydroxides might be exaggerated since Fe buffering, which may be relevant at pH levels below 3.5 (cf Section 3.1), is not included in the model.

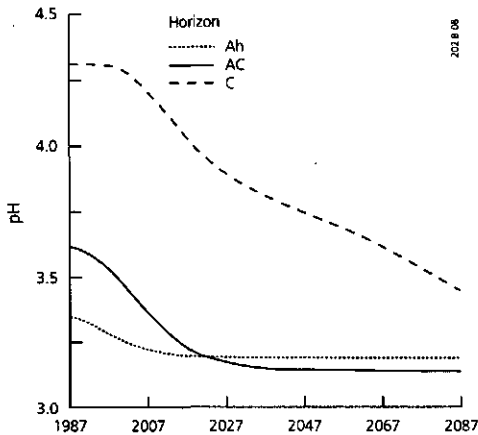


Figure 6.27 The temporal response in pH of the three mineral soil layers of the non-calcareous dune soil

## DISCUSSION AND CONCLUSIONS

### Evaluation of major model results

Major features of the model predictions were a:

- (i) large difference in the acidification rate of calcareous soils (decalcification rate) and non-calcareous soils (cation removal rate)
- (ii) large difference in the contribution of natural soil acidification, going from calcareous to non-calcareous dune soils, i.e. from 85%, to 1% respectively,
- (iii) abrupt decrease in pH near a carbonate content of 0.3% and
- (iv) short time period to deplete Al hydroxides in non-calcareous dune soils.

The predicted large decalcification rate (i), i.e.  $13.8 \text{ kmol}_c \text{ ha}^{-1} \text{ yr}^{-1}$  (see model predictions) is consistent with literature data on current carbonate removal rates from various soils and watercatchments, which range between 5 and  $20 \text{ kmol}_c \text{ ha}^{-1} \text{ yr}^{-1}$  (Van Breemen and Protz, 1988). Most values vary between 8 and  $13 \text{ kmol}_c \text{ ha}^{-1} \text{ yr}^{-1}$  (e.g. Minderman and Leeflang,

1968; Stuyfzand, 1984). The validity of the predicted carbonate removal rate can also be checked by comparing simulated and measured Ca and  $\text{HCO}_3$  concentrations in the subsoil. The simulated Ca and  $\text{HCO}_3$  concentration in the C horizons equalled 4.45 and 3.64  $\text{mol}_c \text{ m}^{-3}$ . (This can also be calculated by dividing the Ca and  $\text{HCO}_3$  leaching fluxes given in Table 6.28 by the water drainage flux of 350  $\text{mm yr}^{-1}$ ). This is consistent with data given by Van Breemen and Protz (1988) and Bakker (1981). Van Breemen and Protz (1988), who calculated Ca concentrations by dividing Ca removal rates by water drainage rates, give a range between 1.5 and 8.5  $\text{mol}_c \text{ m}^{-3}$ , with most data between 2 and 5  $\text{mol}_c \text{ m}^{-3}$ . A very similar range has been given by Bakker (1981) for measured  $\text{HCO}_3$  concentrations in Dutch coastal dunes, i.e. 1.8-7.7  $\text{mol}_c \text{ m}^{-3}$  with most data between 2.5 and 4.5  $\text{mol}_c \text{ m}^{-3}$ . The range between 2 and 5  $\text{mol}_c \text{ m}^{-3}$  can be expected for soil solutions in equilibrium with calcite at  $\text{CO}_2$  pressures between 5 and 40 mbar (Section 2.2; Table 2.3). This is a commonly encountered range in the soil atmosphere (Van Breemen and Protz, 1988). For the simulation a constant  $\text{CO}_2$  pressure of 20 mbar was used.

The predicted large contribution (85%) of natural soil acidification in calcareous soils (ii) is consistent with data of Stuyfzand (1984) for a calcareous dune vegetation (82%) and data of Van Dam et al. (1990) for a chalk grassland (88%). However, the predicted contribution of natural acidification of 1% for the non-calcareous soil (a rate of 0.03  $\text{kmol}_c \text{ ha}^{-1} \text{ yr}^{-1}$ ) is low compared to data given in Section 2.2 (De Vries and Breeuwsma, 1986) for non-calcareous sandy forest soils in The Netherlands (about 0.5  $\text{kmol}_c \text{ ha}^{-1} \text{ yr}^{-1}$ ). This might be due to an underestimation of the leaching flux of  $\text{RCOO}$  in the non-calcareous dune soil. Furthermore, some  $\text{NO}_3$  and  $\text{SO}_4$  leaching also occurs at background deposition levels. In any event, the contribution of natural acidification tends to become very low in non-calcareous dune soils and is likely to be less than 10%.

The predicted abrupt decline in pH at a carbonate content of 0.3% (iii) is consistent with literature data about the relationship between pH and carbonate content (Boerboom, 1963 and Rozema et al., 1985). This behaviour can be explained by the extremely low exchange capacity of dune soils, which mainly buffers the soil in the range between 4.5 and 6.5.

The predicted time period to deplete Al hydroxides of non-calcareous dune soils (iv; less than 25 years for the Ah horizon) is much lower than predictions for a similar horizon in acid forest soils (nearly 100 years; De Vries and Kros, 1989), even though the dissolution rate of Al hydroxides was relatively low compared to forest soils, due to a relatively atmospheric input of S and N. This is caused by the very low Al hydroxide content of dune soils. Unless acid inputs are decreasing, depletion of Al hydroxides, accompanied by pH decrease, is therefore a real danger for non-calcareous dune soils in the Netherlands.

The model simulations anyhow showed that present loads of acidity on Dutch coastal dunes are above critical loads as they ultimately cause a depletion of Al hydroxides, associated with a decline in pH and possibly a reduced P availability. Critical loads of potential acidity can be derived by summation of the net input of base cations (sea salt-

corrected deposition plus weathering minus net uptake), net N uptake and a critical leaching rate of acidity (H + Al). Critical loads, thus derived for forests on pleistocene deposits vary between 1.1 and 1.7 kmol<sub>c</sub> ha<sup>-1</sup> yr<sup>-1</sup> (De Vries and Heij, 1991). For both inland and dune heath communities it is difficult to define a critical H and/or Al concentration. However, to avoid Al depletion from hydroxides, the critical Al leaching rate should be less or equal to the Al weathering rate from primary minerals (silicates). Weathering of both base cations and Al from primary minerals is likely to be lower in non-calcareous dune sand than in Pleistocene deposits, since the total cation amounts in primary minerals are lower in dunes (cf Table 6.25). Consequently, the critical load of potential acidity is likely to be equal or lower than for inland sites (about 1.0-1.5 kmol<sub>c</sub> ha<sup>-1</sup> yr<sup>-1</sup>). This is much lower than the present load of 3.0 kmol<sub>c</sub> ha<sup>-1</sup> yr<sup>-1</sup> (cf Table 6.22).

### Uncertainties in model predictions

Even though RESAM predicts important features of soil acidification found in the field, the question about the reliability of the long-term soil responses predicted by RESAM cannot be answered satisfactorily. This is because historical observations of soil chemistry changes in slightly calcareous and non-calcareous dune soils are not available. Future research will therefore focus on a validation of these model predictions by intermittent monitoring of soil and soil solution at various sites in calcareous and non-calcareous dunes.

Uncertainties in the predictions of the RESAM model are mainly due to model assumptions and to the uncertainty of input data. A very important modeling assumption is the neglect of N immobilization in this study. The effect of this assumption is likely to be small since the potential for N immobilization is low because of the very low content of organic matter. The total pool of organic matter in both dune soils is approximately 70 t ha<sup>-1</sup>. Assuming a fixed pool of organic matter and an increase of the N content in organic matter of 0.5% during the simulation period implies an increase of 350 kg ha<sup>-1</sup> or 25 kmol<sub>c</sub> ha<sup>-1</sup>. Compared to an acid input of 300 kmol<sub>c</sub> ha<sup>-1</sup> during this period (cf Table 6.22) this is relatively low.

Regarding the input data, the uncertainty in the initial contents of carbonates and Al hydroxides in calcareous and non-calcareous dune soils, respectively, is likely to be very important, since dissolution of carbonates and Al hydroxides are the most important acid neutralizing processes in these soils. Regarding non-calcareous soils, results from a sensitive analysis (De Vries and Kros, 1989) and from an uncertainty analysis (Kros et al., 1993) for an acid forest soil showed that the parameters determining Al hydroxide dissolution and nitrification were generally most sensitive and uncertain. Together with the uncertainty in the deposition of SO<sub>x</sub>, NO<sub>x</sub> and NH<sub>x</sub>, these parameters contributed most to the uncertainty of the considered model output. However, despite such uncertainties, the predicted trends for acid soils remained similar (Kros et al., 1993). The same conclusion is warranted for slightly calcareous and non-calcareous dune soils.

## Potential dune vegetation response

Insight in the response of natural dune vegetation to soil acidification is limited since (i) effects of acidification and eutrophication cannot be clearly distinguished from each other  $\text{NO}_x$  and  $\text{NH}_3$  play a role in both processes. Moreover a change in pH affects the availability of other nutrients like P, and the form in which N occurs; (ii) direct effects of atmospheric pollution on aboveground parts of the vegetation cannot clearly be distinguished from indirect effects; and (iii) changes in plant numbers or even disappearance of species can seldomly be attributed to these environmental effects alone. Other factors can also be involved, such as a lower grazing intensity (cattle and/or rabbits) or an increasing stabilization of dunes with a vegetation cover that responds to these changes as well.

Negative effects of soil acidification on plants may include: (i) direct injury by H ions; (ii) reduced availability of nutrients such as Ca, Mg and  $\text{H}_2\text{PO}_4$ ; (iii) increased solubility of toxic ions such as Al, Fe and Mn; (iv) impaired microbial soil activity leading to a disturbed N cycling and (v) increase in soil pathogens and increased sensitivity for diseases and/or frost damage (Grime et al., 1988). Later investigations stressed the importance of a disturbed ionic balance in soil moisture, such an increased Al/Ca,  $\text{NH}_4/\text{K}$ ,  $\text{NH}_4/\text{Mg}$  and  $\text{NH}_4/\text{NO}_3$  ratios, by impairing cation uptake (Houdijk, 1993b).

The ecological consequences of the predicted changes in pH and Al chemistry are not yet clear, although they might be significant. The predicted strong decrease in pH may cause direct injury to plant roots by H ions. However, the associated decrease in Al concentration (and Al/Ca ratio) might lead to a decrease in Al toxicity effects. Whether negative effects of high Al/Ca and  $\text{NH}_4/\text{NO}_3$  (or  $\text{NH}_4/\text{K}$  and  $\text{NH}_4/\text{Mg}$ ) ratios do occur in dune ecosystems is also not yet clear. Relative low levels of acid and  $\text{NH}_4$  deposition and high levels of base cation (especially Mg) deposition from sea-spray cause lower ratios in dunes than in inland sites such as heathlands on Pleistocene sands. Simulated molar Al/Ca and  $\text{NH}_4/\text{NO}_3$  ratios mostly remained below 1.0, i.e. below critical values for several plant species in dry heath communities (Houdijk, 1993b). So, it is more likely that direct toxic effects of increased Al and H concentrations, do occur in the low pH range.

A qualitative assessment of dune vegetation responses to acidification can be derived from results about changes in plant composition and distribution in Dutch dunes, as compiled by Vertegaal et al. (1989), combined with data on pH ranges for these plant species (Grime et al., 1988; Runhaar et al., 1987). Such a comparison strongly suggests that soil acidification has negative effects on the majority of species typical of dry dunes for which a decrease has been reported, especially when the soil pH becomes lower than 4.0. Many declining species, of which a total number of 23 relates to dry dune habitats, belong to the *Galio Koelerion* and *Violion caninae* (Vertegaal et al., 1989). The species decline in the *Violion caninae* is in accordance with results given by Van Dam et al. (1986), who found a

correlation between the decline of related plant species of coastal and inland dunes, dry heathland and forests in The Netherlands and  $\text{SO}_2$  concentration levels.

In addition to soil acidification, eutrophication will also affect plants. Compared to inland sites, such as forests and heathlands on pleistocene sands, Dutch coastal dunes are subject to much lower levels of N deposition, especially of  $\text{NH}_4$ . However, present N loads ( $1.8 \text{ kmol}_e \text{ ha}^{-1} \text{ yr}^{-1}$ ; cf Table 6.22) will certainly affect the dune vegetation, considering the fact that critical N loads on heathlands, to avoid a shift towards nitrophilous grass species, equal about  $0.7\text{-}1.1 \text{ kmol}_e \text{ ha}^{-1} \text{ yr}^{-1}$  (Van Dobben, 1991). For example, the decrease *Calluna vulgaris* and *Nardus stricta* in Dutch dunes as reported by Vertegaal et al. (1989), species that are well adapted to acidic soils, can be related primarily to high N deposition levels (Berendse and Aerts, 1984).

### Implications for dune management

Dune management strategies to mitigate adverse effects of acid atmospheric deposition can be divided in small scale and large scale measures (Vertegaal et al., 1991). Small scale measures such as cutting of shrubs and trees, mowing and sod cutting contribute to the removal of nitrogen. Such measures have thus far been practised mostly in moist or wet dune slacks and rarely in dry dunes. However, removal of biomass can lead to a greater output of cations than of anions, implying an increase in soil acidification. On the other hand, a decrease of shrubs or taller vegetation leads to less effective filtering processes of atmospheric components and therefore to lower loads of acid deposition (Stuyfzand, 1984; Houdijk, 1993b). Excavation of dunes in order to remove both nutrients from organic horizons and decalcified soil layers can be more effective measure to restart vegetation succession on parent material, but this measure is rather expensive.

Large scale measures, using natural landscape dynamics common in dune areas, are extensive grazing, local sand blowing and coastal management aimed at the formation of new outer dunes. Removal of nutrients by extensive grazing by cattle, that was widespread in dunes until the beginning of this century (Bakker et al., 1981), cannot cope with the present high inputs from the atmosphere (Bakker, 1989). However, it adds to the micro and mesovariation in space and time, e.g. by redistribution of nutrients over the area and by the effects of trampling. Trampling can also trigger geomorphological and pedological rejuvenation such as sand blowing or sand transport by surface runoff on slopes (Jungerius and Van der Meulen, 1988). Re-introduction of sand blowing on a much larger scale was promoted by Bakker et al. (1981) to start renewed soil and vegetation development. It will decrease the acidification rate by the input of calcareous sand. These dynamics would be consistent with natural landscape history as described by Klijn (1981). The same conclusion is valid for the use of other mechanisms in areas where coastal accretion could allow the formation of new dunes on beach plains. The return to these types of geomorphological rejuvenation in dry dunes is a necessary and often unexpensive measure

to restore boundary conditions for the existence of a full spectrum of pioneer stages, intermediate stages to end stages in soil and vegetation development. As such they form a long term investment of which positive effects can be expected albeit with some delay. Small scale measures, aimed at the conservation of highly endangered species or communities, could be an intermediate remedy and are very useful in testing hypotheses and for monitoring purposes.

# Chapter 7

## REGIONAL VARIABILITY IN LONG-TERM IMPACTS OF ACID DEPOSITION ON SOILS

### 7.1 IMPACTS ON FOREST SOILS IN EUROPE

- INTRODUCTION
- METHODS AND DATA
- MODEL PREDICTIONS
- UNCERTAINTIES
- DISCUSSION AND CONCLUSIONS

### 7.2 IMPACTS ON FOREST SOILS IN THE NETHERLANDS

- INTRODUCTION
- METHODS AND DATA
- COMPARISON OF MODEL RESULTS AND FIELD DATA
- MODEL PREDICTIONS
- DISCUSSION AND CONCLUSIONS



Section 7.1 is a slightly revised version of:

W. de Vries, M. Posch, G.J. Reinds and J. Kämäri, 1994. *Simulation of soil response to acid deposition scenarios in Europe*. *Water Air and Soil Pollution* 78 (in press).

Section 7.2 is a slightly revised version of:

W. de Vries, J. Kros and C. van der Salm, 1994. *The long-term impact of three emission-deposition scenarios on Dutch forest soils*. *Water Air and Soil Pollution* 75: 1-35.

## 7.1 IMPACTS ON FOREST SOILS IN EUROPE

### ABSTRACT

*The chemical response of European forest soils to three emission-deposition scenarios for the years 1960-2050, i.e. official energy pathways (OEP), current reduction plans (CRP) and maximum feasible reductions (MFR), was evaluated with the SMART model (Simulation Model for Acidification's Regional Trends). Calculations were made for coniferous and deciduous forests on 80 soil types occurring on the FAO soil map of Europe, using a gridnet of 1.0° longitude x 0.5° latitude. Results indicated that the area with N saturated soils, i.e. soils with elevated  $\text{NO}_3$  concentrations ( $> 0.02 \text{ mol}_c \text{ m}^{-3}$ ), will increase in the future for all scenarios, even for the MFR scenario. The area with acidified soils, with a high Al concentration ( $> 0.2 \text{ mol}_c \text{ m}^{-3}$ ) and Al/BC ratio ( $> 1 \text{ mol mol}^{-1}$ ) and a low pH ( $< 4$ ) and base saturation ( $< 5\%$ ), was predicted to increase for the OEP scenario and to decrease for the MFR scenario. The CRP scenario resulted in a continuous increase in the forested area with an Al/BC ratio above critical values. A small decrease was predicted in the area exceeding a critical Al concentration up to the year 2000 followed by a slight increase after 2000. Areas with very high  $\text{NO}_3$  and Al concentrations mainly occurred in western, central and eastern Europe. Uncertainties in the initial values of C/N ratios and base saturation, and in the description of N dynamics in the SMART model had the largest impact on the temporal development of forested areas exceeding critical chemical values. Despite uncertainties involved, the predicted general trends seem reliable.*

### INTRODUCTION

Detrimental impacts of the deposition of sulfur ( $\text{SO}_x$ ) and nitrogen ( $\text{NO}_x$ ,  $\text{NH}_x$ ) on forest ecosystems, being a subject of wide public and political discussion in Central Europe since the beginning of the eighties, are mainly due to soil-mediated effects on the roots (Roberts et al., 1989). Important effects are inhibition of the uptake of divalent base cations (BC) by trees due to mobilization of Al (Ulrich and Matzner, 1983) and accumulation of  $\text{NH}_4$  (Roelofs et al., 1985). Furthermore, elevated N deposition may cause changes in the composition of the ground flora. In this context, critical values for the concentration of Al and  $\text{NO}_3$  and for the Al/Ca ratio have been derived (cf Table 7.1). These values were used to calculate and map so-called critical loads for S, N and total acidity for forest ecosystems in Europe using the steady-state START model (Section 5.1; De Vries et al., 1994e). In START, N immobilization and cation exchange is ignored. However, the response of soil conditions to acid deposition is strongly influenced by these processes. For example, in well-buffered soils, with a large pool of exchangeable base cations, it may take decades or even centuries before measurable changes in the Al/BC ratio occur, even with high atmospheric deposition, whereas it may take less than a decade in very sensitive soils (Section 6.1; De Vries et al., 1989b). Using a dynamic soil acidification model, areas can be mapped where critical chemical values defined for forest soils (e.g. Al/BC ratio, pH, Al and  $\text{NO}_3$  concentration) are exceeded in the course of time.

In this section the application of the dynamic model SMART (Simulation Model for Acidification's Regional Trends) to European forest soils is described, to elucidate the temporal and geographical pattern of nitrogen saturation and soil acidification for alternative emission scenarios. For given scenarios of S, N and BC deposition, the simulated temporal development of the nitrogen and acidification status of the soil, as expressed by the  $\text{NO}_3$  concentration and C/N ratio (nitrogen status) and the Al concentration, Al/BC ratio, pH and base saturation (acidification status) is presented. Special emphasis is given to the derivation of soil data for such a large-scale application using transfer functions with available basic soil survey information. Results are presented in tables and graphs, showing the temporal development of the forested area in Europe where critical values (Table 7.1) are exceeded, and on maps showing the geographical pattern of N saturation and soil acidification. Uncertainties in the predictions are also discussed extensively.

Table 7.1 Critical chemical values used for various parameters describing the nitrogen and acidification status of the soil

Criteria	Unit	Critical values <sup>1)</sup>	Effect above/below critical values
$\text{NO}_3$ concentration	$(\text{mol}_c \text{ m}^{-3})$	0.1	Vegetation changes
C/N ratio	$(\text{g g}^{-1})$	40 <sup>2)</sup>	$\text{NO}_3$ leaching
Al concentration	$(\text{mol}_c \text{ m}^{-3})$	0.2 <sup>3)</sup>	Damage to root system
Al/BC ratio	$(\text{mol mol}^{-1})$	1.0 <sup>4)</sup>	Inhibition of BC uptake

1) More information on the background of these values is given in De Vries (1991)

2) For calcareous soils a value of 20 was used

3) This Al concentration is generally related to a pH value near 4.0

4) This Al/BC ratio is generally related to a base saturation near 5%

## METHODS AND DATA

### The SMART model

#### Model structure

The SMART model consists of a set of mass balance equations, describing the soil input-output relationships, and a set of equations describing the rate-limited and equilibrium soil processes (Table 7.2). All major ions have been included, except for Na, K and Cl which were assumed to balance each other in the soil solution. Compared to an earlier version (De Vries et al., 1989b; Section 6.1), the model has been extended by describing N immobilization (formerly a model input) and by including denitrification.

SMART was constructed by using a process-aggregated approach, to minimize the input data requirements for applications on a regional scale. This implied the following simplifying assumptions:

**Table 7.2** The processes and process descriptions included in the (extended) SMART model

Process	Element	Process description
<i>Rate-limited reactions:</i>		
Growth uptake	BC <sup>1)</sup> , NH <sub>4</sub> , NO <sub>3</sub>	Constant growth
N immobilization <sup>2)</sup>	NH <sub>4</sub> , NO <sub>3</sub>	Proportional to N deposition
Nitrification	NH <sub>4</sub> , NO <sub>3</sub>	Proportional to net NH <sub>4</sub> input
Denitrification <sup>2)</sup>	NO <sub>3</sub>	Proportional to net NO <sub>3</sub> input
Silicate weathering	Al, BC	Zero order reaction
<i>Equilibrium reactions:</i>		
Dissociation/association	HCO <sub>3</sub>	CO <sub>2</sub> equilibrium equation
Carbonate weathering	BC	Carbonate equilibrium equation
Al hydroxide weathering	Al	Gibbsite equilibrium equation
Cation exchange	H <sup>3)</sup> , Al, BC	Gaines Thomas equations

<sup>1)</sup> BC stands for divalent base cations

<sup>2)</sup> An extension compared to SMART described by De Vries et al. (1989b; Section 6.1)

<sup>3)</sup> Implicitly, H is affected by all processes. This is accounted for by the charge balance principle

i. The various ecosystem processes have been limited to a few key processes:

The soil solution chemistry in SMART depends solely on the net element input from the atmosphere (deposition minus net uptake minus net immobilization) and the geochemical interaction in the soil (CO<sub>2</sub> equilibria, weathering of carbonates, silicates and/or Al hydroxides and cation exchange). Processes that are not taken into account, are: (i) canopy interactions, (ii) nutrient cycling processes, (iii) N fixation and NH<sub>4</sub> adsorption, (iv) uptake, immobilization and reduction of SO<sub>4</sub>, (v) formation and protonation of organic anions, (RCOO) and (vi) complexation of Al with anions such as OH, SO<sub>4</sub> and RCOO.

ii. The included processes have been represented by simplified conceptualizations:

Soil interactions are either described by simple rate-limited (zero-order) reactions (e.g. uptake and silicate weathering) or by equilibrium reactions (e.g. carbonate and Al hydroxide weathering and cation exchange). Influence of environmental factors such as pH on rate-limited reactions and rate-limitation of weathering and exchange reactions are ignored. Solute transport is described by assuming complete mixing of the element input within one homogeneous soil compartment with a constant density and a fixed depth (at least the rooting zone). Since SMART is a single layer soil model, neglecting vertical heterogeneity, it predicts the concentration of the soil water leaving the rootzone. The annual water flux percolating from this layer is taken equal to the annual precipitation excess that is assumed constant during the model runs (steady-state hydrology). The time step of the model is one year, so seasonal variations are not considered. Justifications for the various assumptions and simplifications have been given in Section 6.1 (De Vries et al., 1989b).

### Process descriptions

An overview of the basic process descriptions used in the (extended) SMART model to predict the soil solution chemistry of non-calcareous soils is given in Table 7.3. An explanation of the symbols used is given in Table 7.4.

Table 7.3 Process descriptions used in the (extended) SMART model to predict the soil solution chemistry of non-calcareous soils

Mass balance equations:

$$\frac{d}{dt} (\theta_{rz} \cdot f_c \cdot T_{rz} \cdot [\text{SO}_4]) = \text{SO}_{4,td} - PE \cdot [\text{SO}_4] \quad (7.1)$$

$$\frac{d}{dt} (\theta_{rz} \cdot f_c \cdot T_{rz} \cdot [\text{NO}_3]) = N_{td} - N_{gu} - N_{de} - N_{im} - PE \cdot [\text{NO}_3] \quad (7.2)$$

$$\frac{d}{dt} (\theta_{rz} \cdot f_c \cdot T_{rz} \cdot [\text{BC}] + \rho_{rz} \cdot f_c \cdot T_{rz} \cdot CEC \cdot frBC_{ac}) = (\text{BC}_{td} + \text{BC}_{we} - \text{BC}_{gu}) - PE \cdot [\text{BC}] \quad (7.3)$$

Equilibrium and charge balance equations:

$$[\text{HCO}_3] = K\text{CO}_2 \cdot p\text{CO}_2 / [\text{H}] \quad (7.4)$$

$$[\text{Al}] = K\text{Al}_{ox} \cdot [\text{H}]^3 \quad (7.5)$$

$$[\text{H}] = [\text{SO}_4] + [\text{NO}_3] + [\text{HCO}_3] - [\text{BC}] - [\text{Al}] \quad (7.6)$$

Cation exchange equations:

$$fr\text{H}_{ac}^2 / fr\text{BC}_{ac} = K\text{H}_{ex} \cdot [\text{H}]^2 / [\text{BC}] \quad (7.7)$$

$$fr\text{Al}_{ac}^2 / fr\text{BC}_{ac}^3 = K\text{Al}_{ex} \cdot [\text{Al}]^2 / [\text{BC}]^3 \quad (7.8)$$

$$fr\text{H}_{ac} + fr\text{BC}_{ac} + fr\text{Al}_{ac} = 1 \quad (7.9)$$

N transformations:

$$N_{de} = fr_{de} \cdot (N_{td} - N_{gu} - N_{im}) \quad (7.10)$$

$$N_{im} = (N_{td} - N_{gu} - N_{de,min}) \cdot \left( \frac{C/N_{om} - C/N_{min}}{C/N_{cr} - C/N_{min}} \right) \quad \text{for } C/N_{cr} > C/N_{om} > C/N_{min} \quad (7.11)$$

Concentrations of  $\text{SO}_4$  and  $\text{NO}_3$  are fully determined by a mass balance equation (cf Eq. 7.1 and 7.2). For  $\text{SO}_4$  the net input to the soil equals the  $\text{SO}_x$  deposition and for  $\text{NO}_3$  it equals the sum of  $\text{NO}_x$  and  $\text{NH}_x$  deposition minus uptake, immobilization and denitrification of N.  $\text{NH}_4$  was neglected in this study, by assuming complete nitrification within the root zone. This assumption is based on the observation that leaching of  $\text{NH}_4$  from the rootzone is rare except in areas with a very high  $\text{NH}_4$  deposition, such as the Netherlands (Schulze et al., 1989; Kleijn et al., 1989). Low  $\text{NH}_4$  leaching rates may also

be due to preferential uptake of  $\text{NH}_4$  over  $\text{NO}_3$  which has the same ultimate effect on the soil solution at given N uptake rates. The concentration of base cations in non-calcareous soils is determined by both the net input (deposition plus weathering minus uptake) and a change in the adsorbed amount of base cations (Eq. 7.3). This change is determined by cation exchange equilibrium reactions (Eqs. 7.7, 7.8 and 7.9). The concentrations of  $\text{HCO}_3$  and Al are determined by an equilibrium with H (cf Eqs. 7.4 and 7.5). The H concentration is determined by charge balance (Eq. 7.6) since the model structure of SMART is based on the anion mobility concept (Reuss and Johnson, 1986). The pH is thus influenced by all rate-limited and equilibrium processes causing proton production or consumption.

N transformations, i.e. nitrification, denitrification and N immobilization, are described in the extended SMART model by rate-limited equations. SMART does contain a rate-limited description for nitrification (cf Table 7.2; De Vries et al., 1989b) but in this study nitrification was assumed to be complete (see before). Denitrification is described as a fraction of the net input to the soil (Eq. 7.10). The description of N immobilization is based on the assumption that the amount of organic matter (carbon) is in steady-state. Consequently, immobilization of base cations is not considered. N immobilization is described in SMART by an increase in N content in organic matter. When the C/N ratio

Table 7.4 List of symbols used in the process descriptions in SMART

Symbol	Explanation	Unit
[X]	concentration of ion X ( $\text{SO}_4$ , $\text{NO}_3$ , BC, $\text{HCO}_3$ , Al and H) in soil water	$\text{mol}_c \text{ m}^{-3}$
$frX_{ac}$	fraction of ion X (BC, Al, H) on the adsorption complex	-
CEC	cation exchange capacity	$\text{mol}_c \text{ kg}^{-1}$
$p\text{CO}_2$	partial $\text{CO}_2$ pressure in the soil	bar
$\theta_{rz}$	volumetric moisture content of the soil in the rootzone	$\text{m}^3 \text{ m}^{-3}$
$\rho_{rz}$	bulk density of the soil in the rootzone	$\text{kg m}^{-3}$
$\rho_{im}$	bulk density of the soil in the zone where N immobilization occurs	$\text{kg m}^{-3}$
$T_{rz}$	thickness of the rootzone	m
$T_{im}$	thickness of the zone where N mobilization occurs	m
dt	time step	yr
PE	precipitation excess	$\text{m}^3 \text{ ha}^{-1} \text{ yr}^{-1}$
$X_{td}$	total deposition of ion X ( $\text{SO}_4$ , $\text{NH}_4$ + $\text{NO}_3$ , BC)	$\text{mol}_c \text{ ha}^{-1} \text{ yr}^{-1}$
$X_{gu}$	growth uptake flux of element X ( $\text{NO}_3$ , BC)	$\text{mol}_c \text{ ha}^{-1} \text{ yr}^{-1}$
$N_{im}$	N immobilization flux	$\text{mol}_c \text{ ha}^{-1} \text{ yr}^{-1}$
$N_{de}$	denitrification flux	$\text{mol}_c \text{ ha}^{-1} \text{ yr}^{-1}$
$N_{la,min}$	Minimum N leaching flux	$\text{mol}_c \text{ ha}^{-1} \text{ yr}^{-1}$
$\text{BC}_{we}$	base cation weathering flux	$\text{mol}_c \text{ ha}^{-1} \text{ yr}^{-1}$
$ctC_{im}$	organic carbon content in the zone where N immobilization occurs	$\text{mol}_c \text{ kg}^{-1}$
$AmN_{im}$	Amount of nitrogen in the zone where N immobilization occurs	$\text{mol}_c \text{ ha}^{-1}$
$\text{C/N}_{om}$	C/N ratio of the soil	$\text{g g}^{-1}$
$\text{C/N}_{cr}$	critical C/N ratio of the soil	$\text{g g}^{-1}$
$\text{C/N}_{min}$	minimum C/N ratio of the soil	$\text{g g}^{-1}$
$fr_{de}$	denitrification fraction	-
$K\text{CO}_2$	Equilibrium constant for $\text{CO}_2$ dissociation	$\text{mol}^2 \text{ l}^{-2} \text{ bar}^{-1}$
$K\text{Al}_{ox}$	Equilibrium constant for Al hydroxide dissolution	$\text{mol}^2 \text{ l}^2$
$K\text{H}_{ex}$	selectivity constant for H/BC exchange	$\text{mol l}^{-1}$
$K\text{Al}_{ex}$	selectivity constant for Al/BC exchange	$\text{mol}^{-1} \text{ l}$

of the soil varies between a critical and a minimum value, the immobilization rate is assumed to decrease according to Eq. (7.11). At the minimum C/N ratio, N immobilization equals zero. Above the critical value all excess nitrogen ( $N_{td} - N_{gu} - N_{le,min}$ ) is assumed to immobilize. The minimum N leaching rate ( $N_{le,min}$ ) is calculated by multiplying the precipitation excess by a natural background  $NO_3$  concentration in drainage water of  $0.02 \text{ mol}_e \text{ m}^{-3}$  (Rosén, 1990). During the simulation, the C content is fixed whereas the N content is continually updated, by adding the amount of N immobilized during each step to the available N amount in the mineral topsoil. The C/N ratio is in turn updated by dividing the fixed C pool by the variable N pool according to:

$$C/N = \frac{\rho_{im} \cdot f_c \cdot T_{im} \cdot cC_{im}}{AmN_{im}} \quad (7.12)$$

Since N immobilization mainly occurs in the humus layer and the upper mineral soil (Tietema, 1992), the thickness of the zone where N immobilization ( $T_{im}$ ) occurs is taken at 20 cm.

The dissolved and adsorbed concentrations are calculated by simultaneously solving the equations in Table 7.3, leading to nine equations with nine unknowns, i.e. six concentrations ([H], [Al], [BC], [SO<sub>4</sub>], [NO<sub>3</sub>], [HCO<sub>3</sub>]) and three exchangeable fractions ( $frH_{ac}$ ,  $frBC_{ac}$ ,  $frAl_{ac}$ ). The numerical solution procedure is given in Posch et al. (1993b).

### Application methodology

Runs with SMART were restricted by defining a grid net of  $1.0^\circ$  longitude versus  $0.5^\circ$  latitude in which deposition fluxes were assumed to be constant (deposition areas). A higher resolution was not considered worthwhile in view of the uncertainty in the calculated atmospheric deposition fluxes. Within each gridcell calculations were made for all major combinations of tree species and soil types. A distinction was made between coniferous and deciduous trees to account for differences in dry deposition, transpiration and growth uptake. The spatial variability of the soil was taken into account by distinguishing 80 different soil types according to the FAO-UNESCO Soil Map of the World (Section 5.1; De Vries et al., 1994e). The areal distribution of soils and forests was assessed by estimating the fraction of each mapping unit (soil type, texture class and slope class) and forest type within each gridcell using the FAO-UNESCO soil map and aeronautic maps, respectively. The distribution of forest/soil combinations within a gridcell was estimated by assuming that forests are not evenly distributed over all soil types, but instead, they are located mainly on areas with steep slopes and poor soils (with low weathering rates and coarse textures; Section 5.1). According to this procedure most forests are located on Podzols and Podzoluvisols (especially in the Nordic countries), and to a lesser extent on Cambisols and Luvisols (Table 7.5).

**Table 7.5** Dominant forest soil types as a percentage of the coniferous, deciduous and total forest area in Europe

Soil type (FAO, 1981)	Forested area (%)		
	coniferous	deciduous	total
Orthic Podzol	41.5	20.3	33.8
Eutric Podzoluvisol	11.1	15.3	12.6
Dystric Cambisol	7.4	13.0	9.4
Eutric Cambisol	5.0	8.7	6.4
Gleyic Luvisol	4.8	5.2	4.9
Orthic Luvisol	3.5	3.9	3.6
Dystric Histosol	4.2	2.4	3.5
Dystric Podzoluvisol	2.5	4.5	3.3
Calcic Cambisol	2.9	2.5	2.7
Rendzina	1.9	3.5	2.5
Leptic Podzol	2.5	1.6	2.2
Chromic Luvisol	0.9	2.2	1.4
Gleyic Podzol	0.9	1.6	1.2
Lithosol-Ranker	1.2	1.0	1.1
Humic Cambisol	1.2	0.8	1.1
	$\Sigma=91.5$	$\Sigma=86.5$	$\Sigma=89.7$

### Emission-deposition scenarios

The temporal trends of chemical soil parameters predicted by SMART is driven by emission-deposition scenarios for  $\text{SO}_2$ ,  $\text{NO}_x$ ,  $\text{NH}_3$  and base cations. Emission-deposition estimates for the European countries were taken from Alcamo et al. (1990) and Lövblad et al. (1992). The consequences for the acidification status of the European forest soils were evaluated for (i) the "Official Energy Pathways" scenario (OEP), based on governments projections for future energy use; (ii) the "Current Reduction Plans" scenario (CRP) which takes into account likely reductions of emission due to proposed abatement measures, and (iii) the "Maximum Feasible Reductions" scenario (MFR), which assesses the impacts of a radical, but technologically by feasible, decrease in emissions (mostly  $\text{SO}_2$ ). The resulting total emissions for Europe in the period 1960-2050 for  $\text{SO}_2$ ,  $\text{NO}_x$  and  $\text{NH}_3$  are shown in Figure 7.1.

Average deposition values for  $\text{SO}_x$ ,  $\text{NO}_x$  and  $\text{NH}_x$  on each gridcell were obtained by multiplying the countries' emissions by so-called source-receptor matrices from the RAINS model (Alcamo et al., 1990), that were derived from the EMEP model, developed under the auspices of the UN-ECE (Iversen et al., 1989). The effect of forest filtering on the deposition was included by multiplying the average deposition of  $\text{SO}_x$ ,  $\text{NO}_x$  and  $\text{NH}_x$  on each gridcell by filtering factors for both coniferous and deciduous forests, using data based on Ivens et al. (1989). In densely forested areas, e.g. in parts of Scandinavia, the filtering factors were corrected downwards, since we assumed that the total deposition on forests and open land in each grid was correct (conservation of mass) and that the



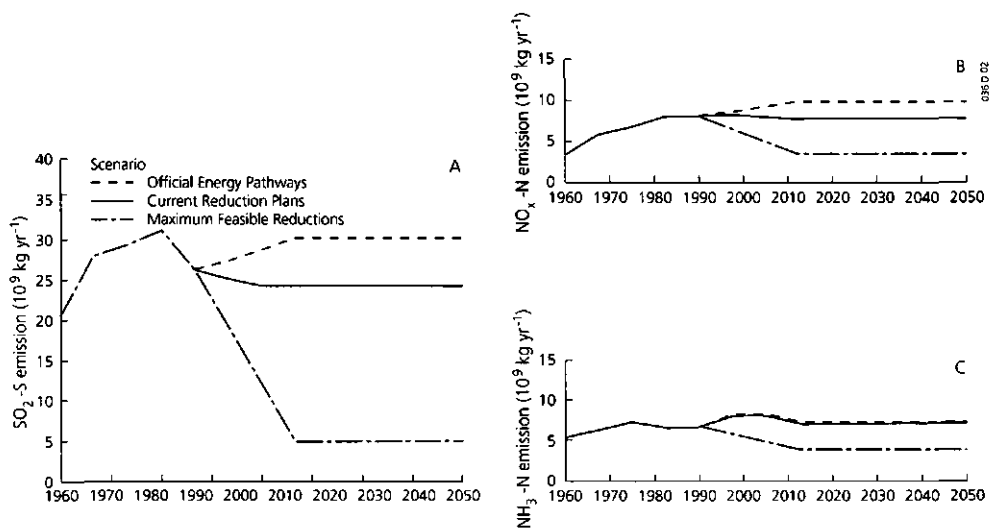


Figure 7.1 Trends in total emissions of  $\text{SO}_2$ ,  $\text{NO}_x$  and  $\text{NH}_3$  in Europe for the three scenarios used in this study

total deposition on open land was at least as high as the modeled wet deposition for the grid (cf Section 5.1).

The bulk deposition of base cations (sea salt-corrected) was derived from measurements at 65 EMEP stations in Europe (Pedersen et al., 1990). Grid values over Europe were obtained by interpolating between the five nearest stations. Dry deposition data were derived by multiplying the wet (bulk) deposition with a dry deposition factor, which was both grid and tree species dependent (cf Section 5.1). No estimates for future base cation deposition were available and therefore it was assumed constant throughout the whole modeling period (1960-2050). Depending on the scenario, this may cause an underestimation (OEP scenario) or overestimation (MFR scenario) of the future base cation deposition since part of it originates from fuel combustion (Alcamo et al., 1990).

## Input data

Input data for SMART include system inputs and soil data. System inputs (and outputs), i.e. deposition, precipitation, evapotranspiration and growth uptake, were derived as a function of location (gridcell) and of forest type, as given in Section 5.1 (De Vries et al., 1994e). Soil data were derived as a function of soil type irrespective of the location. Most soil data were related to readily available soil (and land) characteristics, such as texture and organic matter, using so-called transfer functions (Figure 7.2). A subdivision was made between characteristics that have a continuous range of values (e.g. % clay)

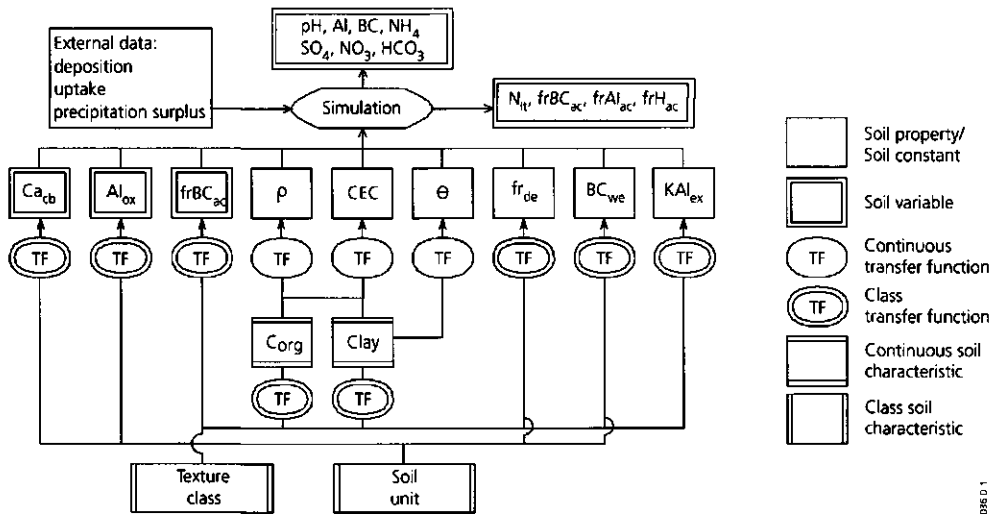


Figure 7.2 Schematic diagram illustrating the use of soil survey information in simulating the soil (solution) chemistry with SMART (see Table 7.4 for an explanation of symbols used).

and characteristics that are defined by a specified range of values within a class (e.g. texture class) or by a symbol (e.g. soil type). Similarly, transfer functions relating soil properties to soil (and land) characteristics, were divided into continuous and class transfer functions (cf Bouma et al., 1986). Detailed information on the transfer functions used is given below.

#### Soil variables

Soil variables in SMART that have to be initialized are the C/N ratio, the carbonate and Al hydroxide content of the mineral soil, the fraction of BC, Al and H at the adsorption complex and the element concentrations in the soil solution. The initial C/N ratio was calculated as a function of the N deposition by linear interpolation between a minimum and maximum C/N ratio in organic matter.

Minimum and maximum values used for the C/N ratio in non-calcareous soils and for the N deposition corresponding to these values (Table 7.6) were based on data for C/N ratios and N deposition levels (i) for Dutch forests in 1940 (De Vries and Van Vliet, 1945) and in 1990 (De Vries and Leeters, 1994) and (ii) along a gradient from relatively unpolluted areas in Scandinavia (Mälkönen et al., 1990; Rosén, pers. comm.) to highly polluted areas in the Netherlands (Kleijn et al., 1989). Maximum and minimum C/N ratios used for calcareous soils were derived from Kuylenstierna and Chadwick (1992).

**Table 7.6** Minimum and maximum C/N ratios and corresponding N deposition values used in the calculation of the initial C/N ratio

Soil type	C/N ratio (g g <sup>-1</sup> )		N deposition (mol <sub>c</sub> ha <sup>-1</sup> yr <sup>-1</sup> )	
	minimum	maximum	minimum	maximum
Calcareous	10	20	700	3500
Non-calcareous <sup>1)</sup>	15	50	700	3500

<sup>1)</sup> Values are based on light textured (sandy) soils. For clay soils similar values were assumed

The minimum C/N ratios correspond to the situation where N immobilization is negligible but the maximum values do not necessarily equal the critical C/N ratios (values above which all N is assumed to immobilize; cf Eq. 7.3). For calcareous soils this value was set at 20 (which is the maximum C/N ratio in these soils) but for non-calcareous soils a value of 40 was used (less than the maximum value of 50). Note that critical C/N ratios reported in literature refer to the situation that net N mineralization starts to occur, whereas the use of this ratio in SMART refers to a situation where the external N input ceases to be completely immobilized. The critical value for total N immobilization is likely to be somewhat higher than literature data, which are generally close to 25 (Ågren and Bosatta, 1988; Tietema, 1992), although values near 40 have been reported as well (Berg and Staaf, 1981).

Data for the carbonate and Al hydroxide content were based on information in the FAO soil map of Europe (FAO, 1981). The initial base saturation of soils was calculated as the maximum of (i) a relation with the texture class of soils (Table 7.7) and (ii) an equilibrium with deposition levels of SO<sub>x</sub>, NO<sub>x</sub>, NH<sub>x</sub> and BC in 1960. As a result, the

**Table 7.7** Soil parameters used for European forest soils as a function of texture class

Texture classes <sup>1)</sup>	Clay content (%)	Base saturation (%) <sup>2)</sup>	Denitrification fraction (-)	Al exchange constant <sup>4)</sup>
1 (sand)	5	5	0.1 <sup>3)</sup>	1
1/2 (sand+clay)	10	10	0.1 <sup>3)</sup>	10
1/3 (sand+clay)	15	10	0.3	10
2 (clay)	25	15	0.7	100
2/3 (clay)	40	40	0.7	1000
3 (heavy clay)	50	50	0.7	1000
- (peat)	0	70 (10)	0.8	1

<sup>1)</sup> Meaning texture classes: 1 = coarse: clay content less than 18%, 2 = medium: clay content between 18 and 35% and 3 = fine: clay content above 35%. When two texture classes occur within one mapping unit, this is indicated as 1/2, 2/3 or 1/3

<sup>2)</sup> Data based on FAO (1981) and Gardiner (1987). For histosols (peat soils) the initial base saturation was put equal to 70% for the Eutric Histosol, and to 10% for the Dystric Histosol (codes Oe and Od on the FAO soil map)

<sup>3)</sup> For soils with gleyic features a value of 0.5 was used. Based on Breeuwsma et al. (1991)

<sup>4)</sup> Based on data by Coulter and Talibudeen (1968) and Bache (1974). Values for peat soils were taken equal to sand

initial base saturation was never lower than the value in equilibrium with the acid load of 1960. Otherwise, the base saturation would increase even though the acid deposition level increases. Especially in southern European countries and in Scandinavia, where the acid deposition is relatively low and/or the base cation input is high, the base saturation in equilibrium with the present load can be higher than the value assigned according to Table 7.7. The Al and H saturation was calculated by the SMART model as outlined by De Vries et al. (1989b) (cf Annex C).

When the base saturation was in equilibrium with deposition levels in 1960, the initial ion concentrations in soil water were calculated from the 1960 atmospheric net input and the precipitation excess ( $SO_4$ ,  $NO_3$  and BC; cf Eqs. 7.1 to 7.3 in Table 7.3 with  $\theta_{rz}$  and  $\rho_{rz} = 0$ ) and from equilibrium and charge balance equations ( $HCO_3$ , Al and H; cf Eqs. 7.4 to 7.6 in Table 7.3). Otherwise, the concentrations of BC, Al, H and  $HCO_3$  were derived by simultaneously solving the Eqs. (7.4) to (7.6) with the exchange equations for [H], [Al] and [BC] (cf Eqs. 7.7 to 7.9 in Table 7.3).

**Soil properties**

Physical and chemical soil properties, such as the bulk density ( $\rho$ ), volumetric moisture content ( $\theta$ ), organic carbon content ( $ctC$ ) and cation exchange capacity ( $CEC$ ), were derived directly from available data ( $ctC$ ) and by continuous transfer functions with the content of organic carbon and clay, as given in Table 7.8. The clay content was related to the texture class as shown in Table 7.7. The organic carbon content of the various soil types was derived from FAO (1981) and Gardiner (1987). Value ranged between 0.1% for Arenosols (Qc) to 50% for peat soils (Od). The bulk density thus varied between 150 and 1600  $kg\ m^{-3}$  whereas the CEC ranged between 25 and 1350  $mmol_c\ kg^{-1}$  (cf Table 7.8).

**Soil constants**

Soil constants in the SMART model are the denitrification fraction,  $fr_{de}$ , the base cation weathering rate,  $BC_{we}$ , cation exchange constants,  $KH_{ex}$  and  $KAl_{ex}$ , and equilibrium constants for the dissociation of  $CO_2$ ,  $KCO_2$ , and the dissolution of carbonate,  $KCa_{cb}$ , and Al hydroxide,  $KAl_{ox}$ .

*Table 7.8 Transfer functions between soil properties and soil characteristics*

Soil property	Transfer function	Condition	Reference
$\rho$ ( $kg\ m^{-3}$ ) <sup>1)</sup>	$1000 / (0.625 + 0.05 \cdot ctC + 0.0015 \cdot clay)$	$ctC \leq 5\%$	Hoekstra and Poelman (1982)
$\theta$ ( $m^3\ m^{-3}$ ) <sup>2)</sup>	$725 - 337 \cdot \log ctC$	$ctC \geq 15\%$	Van Wallenburg (1988)
	$0.04 + 0.0077 \cdot clay$	$clay \leq 30\%$	Brady (1972)
$CEC$ <sup>3)</sup> ( $mmol_c\ kg^{-1}$ )	0.27	$clay \geq 30\%$	
	$5 \cdot clay + 27.25 \cdot ctC$		Helling et al. (1964); Breeuwsma et al. (1986)

1) For  $5\% < ctC < 15\%$ ,  $\rho$  is interpolated linearly  
 2) Refers to the situation at field capacity  
 3) Refers to a value measured at pH 6.5

Denitrification fractions and Al exchange were related to soil type and texture class as given in Table 7.7. For  $KH_{ox}$  a value of 1.5 was used, independent of soil type. Values for  $KCO_2$  and  $KCa_{cb}$  were taken from the literature (cf De Vries et al., 1989b; Section 6.1). For  $KAl_{ox}$  a value of  $10^8 \text{ mol}^{-2} \text{ l}^2$  was used on the basis of soil solution data in the subsoil of 150 Dutch forest stands (De Vries and Leeters, 1994), except for peat soils where  $KAl_{ox}$  was set equal to  $10^6 \text{ mol}^{-2} \text{ l}^2$  on the basis of data in Wood (1989).

Weathering rates were derived by using a class transfer function with the dominant parent material and texture class of the dominant soil unit(s) (Table 7.9), based on results of a weathering rate model (Sverdrup and Warfvinge, 1988a,b). Values refer to the rootzone for which a standard depth of 0.5 m was assumed. The assumed dominant parent material class (cf Table 7.9) for each soil type on the FAO soil map of Europe below forests has been given in De Vries (1991). The weathering rates thus assigned to each soil type were corrected for the effect of temperature according to a procedure described in Section 5.1 (De Vries et al., 1994e). The temperature correction procedure implied that the weathering rates given in Table 7.9 are average values, which decrease and increase with a lower and higher temperature within the range of occurrence of each soil type.

Table 7.9 Weathering rates in a soil depth of 50 cm used for the various combinations of parent material class and texture class (indicated by 1, 1/2 etc.; see Table 7.7)

Parent material class	Weathering rate ( $\text{mol}_c \text{ ha}^{-1} \text{ yr}^{-1}$ )					
	1	1/2	1/3	2	2/3	3
Acidic <sup>1)</sup>	125	375	-	875	875	-
Intermediate <sup>2)</sup>	375	625	875	875	1125	1375
Basic <sup>3)</sup>	375	625	-	1125	1375	-

- <sup>1)</sup> acidic : Sand (stone), gravel, granite, quartzine, gneiss (schist, shale, greywacke, glacial till). Schist, shale, greywacke and glacial till are put between brackets. A soil type containing these parent materials can be converted to the acidic or intermediate parent material class, depending on the other parent materials available
- <sup>2)</sup> Intermediate : Gronodiorite, loess, fluvial and marine sediments (schist, shale, greywacke, glacial till)
- <sup>3)</sup> Basic : Gabbro, basalt, dolomite, volcanic deposits

## MODEL PREDICTIONS

### Trends in nitrogen saturation

#### *Relationship between parameters indicating N saturation.*

The term 'N saturation' is still a subject of debate. Different definitions are used, based on different stages in the continuum between N limitation and N excess (e.g. Nilsson, 1986; Ågren and Bosatta, 1988; Aber et al., 1989). The definition of an N saturated

ecosystem that is used in this study is "an ecosystem in which availability of inorganic N is in excess of total plant and microbial nutritional demand" (Aber et al., 1989). Using this definition, soils are N saturated when atmospheric N inputs are no longer immobilized completely and  $\text{NO}_3$  leaching increases above a natural background value.

In the SMART model, N immobilization is assumed to be incomplete when the C/N ratio becomes less than 40. This is associated with a  $\text{NO}_3$  concentration in soil water draining from the rootzone above a natural value of  $0.02 \text{ mol}_c \text{ m}^{-3}$  (cf Eq. 7.11). Below a critical C/N ratio of 40 the relationship between the predicted  $\text{NO}_3$  concentration and the predicted C/N ratio with SMART appeared to be very weak (Fig. 7.3A). Use of a critical C/N ratio of 25, (Ågren and Bosatta, 1988; Tietema, 1992), caused a much more pronounced relationship between  $\text{NO}_3$  concentration and C/N ratio in accordance with data given by Kriebitzsch (1978). However, data given by Driscoll et al. (1989) suggest a much weaker relationship. Furthermore,  $\text{NO}_3$  concentrations below the rootzone of 150 Dutch forest stands, measured in early spring 1990 (De Vries and Leeters, 1994), were also weakly correlated with the C/N ratio of the mineral topsoil (Fig. 7.3B). These data confirm the pattern of Fig. 7.3A with a critical C/N ratio of 40. The generally higher measured  $\text{NO}_3$  concentrations in the Netherlands compared to SMART predictions (cf Fig. 7.3A and 7.3B) are most likely due to high N deposition in the Netherlands as compared to the rest of Europe.

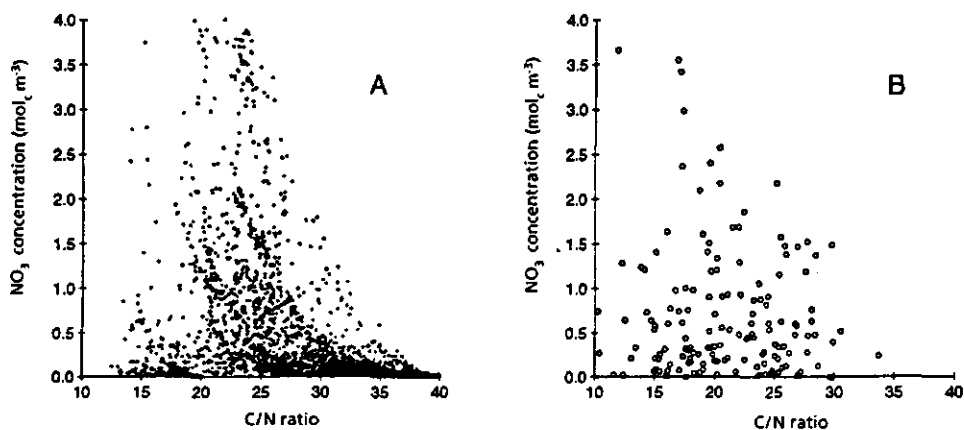


Figure 7.3 Relationship between the  $\text{NO}_3$  concentration and C/N ratio based on SMART predictions in the year 2000 with the CRP scenario using a critical C/N ratio of 40 (A) and measurements in 150 Dutch forest soils in 1990 (B).

#### Trends in parameters indicating N saturation.

The predicted forested area with a C/N ratio below 40 (or a  $\text{NO}_3$  concentration above  $0.02 \text{ mol}_c \text{ m}^{-3}$ ) increased continuously between 1960 and 1985 from 23.3% to 35.8% (Fig. 7.4A). After 1985, the increase continued for all scenarios but at a lower rate, especially for the maximum feasible reductions (MFR) scenario. The Official Energy

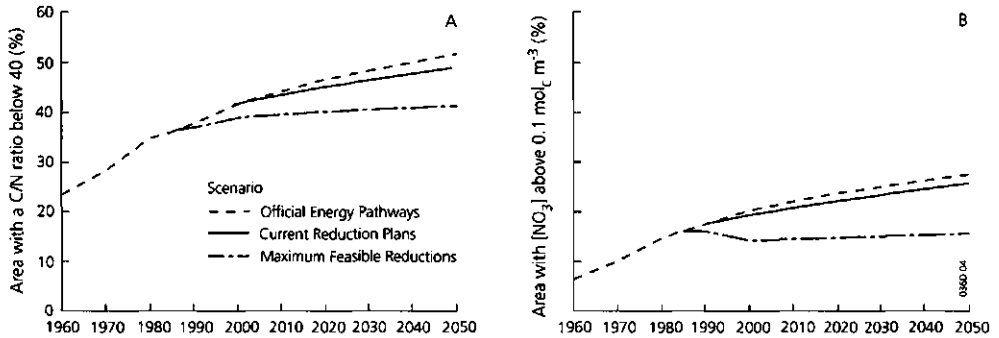


Figure 7.4 Temporal development of the forested area in Europe (%) with a C/N ratio below 40 (A) and a  $NO_3$  concentration above  $0.1 \text{ mol}_c \text{ m}^{-3}$  (B) in response to three scenarios.

Pathway (OEP) and Current Reduction Plans (CRP) scenarios did not differ significantly in their effects on N saturation. In 2050 the predicted forested area with a C/N ratio below 40 equalled 51.6% for the OEP scenario and 49.2% for the CRP scenario compared to a value of 41.3% for the MFR scenario.

The calculated forested area with a  $NO_3$  concentration above  $0.1 \text{ mol}_c \text{ m}^{-3}$  (cf Table 7.1) increased from 6.2% to 16.0% between 1960 and 1985 (Fig. 7.4B). A small reduction between 1985 and 2000 was found for the MFR scenario (due to deposition reductions) followed by a small gradual increase after 2010. For both the OEP and CRP scenarios the area still increased after 1985 to more than 25% in 2050. The  $NO_3$  concentrations at that time were by far not yet at steady-state with N deposition levels. Calculations with the START model (a steady-state version of SMART excluding dynamic N immobilization and cation exchange) showed that the forested area in Europe exceeding a  $NO_3$  concentration of  $0.1 \text{ mol}_c \text{ m}^{-3}$  was as high as 50% in an equilibrium situation when using 1985 deposition values (Section 5.1). Note that the total N emission for the CRP scenario remains almost the same during the entire simulation period (cf Figure 7.2) which means that the N deposition in 2050 was nearly equal to that in 1985.

## Trends in soil acidification

### Relationship between parameters indicating soil acidification.

The various parameters indicating soil acidification, i.e. base saturation, pH, Al concentration and Al/BC ratio are closely related to each other. The relationship between pH and Al concentration is fully determined in SMART by an Al hydroxide equilibrium (Eq. 7.8). Relationships between the simulated base saturation and the simulated Al parameters showed that (i) the Al concentration stayed below the critical value of  $0.2 \text{ mol}_c \text{ m}^{-3}$  as long as the base saturation remained above 30 to 40%, and (ii)

the critical Al/BC ratio of 1.0 was exceeded only at very low base saturations, i.e. near or below 5% (cf Section 6.1; De Vries et al., 1989b).

At low base saturation, however, a large variation in Al concentration and Al/BC ratio was predicted, which is also found in the field (e.g. Cronan et al., 1989; Kleijn et al., 1989). In both cases this variation is largely explained by the variation in  $\text{SO}_4$  and  $\text{NO}_3$  concentration (Fig. 7.5A). However, low Al concentrations do occur at high  $\text{SO}_4$  and  $\text{NO}_3$  concentrations, especially in soils with an extremely low solubility of Al (mainly peat soils) and in soils with a very strong preference for Al on the adsorption complex (mainly clay soils in areas with a high input of base cations from the atmosphere, i.e. predominantly in the southern part of Europe; cf Section 5.1). The variation in  $\text{SO}_4$  and  $\text{NO}_3$  concentration also influenced the predicted pH in these soils with a low base saturation, especially in the concentration range below  $1 \text{ mol}_c \text{ m}^{-3}$  (Fig. 7.5B). A similar relationship between pH and  $\text{NO}_3$  concentration was observed by Bergkvist and Folkesson (1992) in the field.

#### *Trends in parameters indicating soil acidification.*

Trends in the forested area exceeding critical values for the various acidification parameters (Table 7.10) illustrate the relationship between the Al concentration, Al/BC ratio, base saturation and pH. Except for the Al/BC ratio, the forested area exceeding the different critical values (cf Table 7.1) was quite comparable. As reported before (Section 5.1; De Vries et al., 1994e), the critical value for Al appeared to be more stringent than the critical Al/BC ratio. The area exceeding a critical Al/BC ratio and a critical base saturation increased continually, whereas the temporal development for pH was similar to the Al concentration, i.e. a small decrease between 1985 and 2000 followed by a gradual increase.

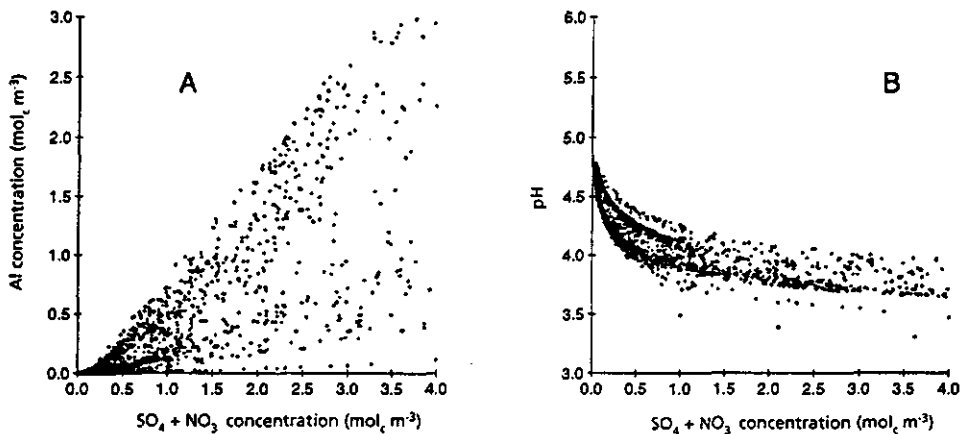


Figure 7.5 Relationship between the predicted  $\text{SO}_4$  and  $\text{NO}_3$  concentration and the Al concentration (A) and pH (B) for soils with a base saturation below 10%. The relationship is based on predictions in the year 2000 with the CRP scenario.



**Table 7.10** The predicted forested area with an Al concentration, Al/BC ratio, pH and base saturation above critical values (cf Table 7.1) from 1960 to 2030 using the CRP scenario

Year	Forested area exceeding critical values (%)			
	[Al] > 0.2 mol <sub>c</sub> m <sup>-3</sup>	Al/BC > 1	pH < 4	Base saturation < 5%
1960	19	2	16	14
1985	23	5	21	16
1990	23	6	20	16
2000	22	6	19	18
2010	23	7	20	19
2050	25	10	22	23

The predicted change in the forested area exceeding a critical value between 1960 and 2050 was nearly equal for all parameters, i.e. between 6 and 9%. This is much smaller than the predicted change in nitrogen saturated areas. In relative terms, the increase was largest for the Al/BC ratio, i.e. nearly a fivefold increase between 1960 and 2050.

Impacts of the different scenarios on the Al concentration and Al/BC ratio are illustrated in Figure 7.6. Predictions for the area exceeding a critical Al concentration after 1985 showed a steady increase for the OEP scenario, a small reduction between 1985 and 2000 followed by a slight increase for the CRP scenario and a marked decrease, especially between 1985 and 2000, for the MFR scenario (Fig. 7.6A). The response of the Al/BC ratio was similar except for the CRP scenario. Unlike Al, the area exceeding a critical Al/BC ratio increased after 1985 for this scenario (Fig. 7.6B). Apparently, the decrease in BC concentration, induced by a decrease in base saturation change in response to ongoing acid deposition, compensated the decrease in Al concentration. As with NO<sub>3</sub>, the concentrations in 2050 were not yet at steady-state with respect to the deposition level at that time. Even when using the OEP scenario, with higher total S and N emissions in 2050 compared to 1985 (cf Fig. 7.2), the predicted areas with an Al

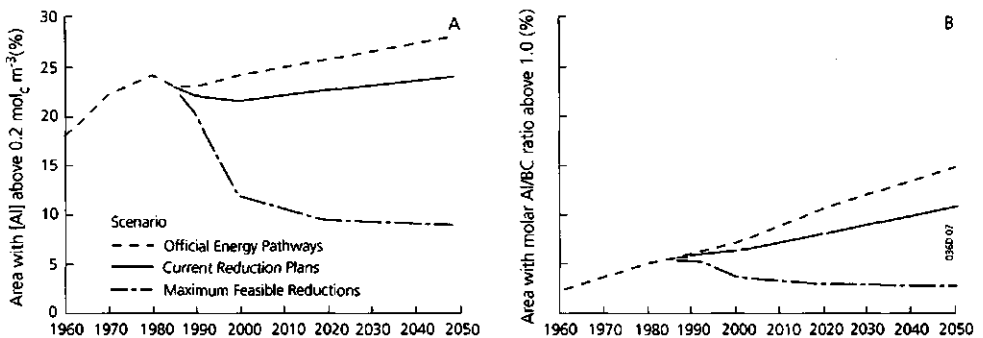


**Figure 7.6** Temporal development of the forested area in Europe (%) with an Al concentration above 0.2 mol<sub>c</sub> m<sup>-3</sup> (A) and an Al/BC ratio above 1.0 (B) in response to three scenarios

concentration and Al/BC ratio exceeding critical values in 2050 were 'only' about 28% and 14% respectively in 2050. Calculations with the steady-state model START showed that these areas would increase up to 43% and 30% respectively at constant 1985 atmospheric deposition (Section 5.1).

### **Geographical patterns of nitrogen saturation and soil acidification**

The predicted geographical patterns of N-saturated and (strongly) acidified forest soils changed with time. However, throughout the simulation period most of these soils were concentrated in the central, western and eastern European countries, i.e. Denmark, the Netherlands, Belgium, Luxembourg, Germany, Poland, Czechoslovakia, Romania and large parts of the former Soviet Union. The situation for the year 2000 using the CRP scenario is illustrated with maps for the predicted median  $\text{NO}_3$  concentration (Fig. 7.7A), Al concentration (Fig. 7.7B), pH (Fig. 7.7C) and base saturation (Fig. 7.7D). The medians were calculated by weighting the results with the area of each forest soil combination in a grid.

The regions with high  $\text{NO}_3$  concentrations ( $> 0.1 \text{ mol}_c \text{ m}^{-3}$ ) coincided largely with those with high Al concentrations ( $> 0.2 \text{ mol}_c \text{ m}^{-3}$ ; cf Fig. 7.7A and 7.7B). Very high Al concentrations, exceeding  $3.0 \text{ mol}_c \text{ m}^{-3}$ , were mainly limited to the central European countries, i.e. Germany, Poland and former Czechoslovakia, whereas high  $\text{NO}_3$  concentrations also were predicted in the Netherlands, Belgium and Luxembourg and in large parts of the former Soviet Union (cf Fig. 7.7A and 7.7B). The very high Al and  $\text{NO}_3$  concentrations in Poland and the former Soviet Union are probably overestimated, caused by an underestimation of the precipitation excess in these countries (cf Section 5.1; De Vries et al., 1994e). Comparison of the maps for the Al concentration pH and base saturation shows that low values for pH ( $< 4.5$ ) and base saturation ( $< 5\%$ ) in combination with low Al concentrations ( $< 0.2 \text{ mol}_c \text{ m}^{-3}$ ) were predicted for the (podzolic) soils in Scotland and in the southern part of Sweden and Norway (cf Fig. 7.7B, 7.7C and 7.7D). The low pH and base saturation in these areas is induced by the poor parent material (low weathering rates), whereas the low Al concentration is partly due to the relatively low input of  $\text{SO}_4$  and  $\text{NO}_3$  (cf Fig. 7.6A) and partly because of the high precipitation excess (strong dilution), especially in Scotland and in the coastal region of Norway.

Predictions of the forested area with a  $\text{NO}_3$  concentration above  $0.1 \text{ mol}_c \text{ m}^{-3}$  and an Al concentration above  $0.2 \text{ mol}_c \text{ m}^{-3}$  in a steady-state situation (calculated with the steady-state START model using 1985 deposition data; Section 5.1) also included large areas in the southern part of Sweden, Norway and Finland. Since these Nordic countries are densely forested, this explains the large increase in the forested area in Europe above critical values for  $\text{NO}_3$  and Al, going from the non-steady-state (SMART) predictions to the steady-state (START) predictions.

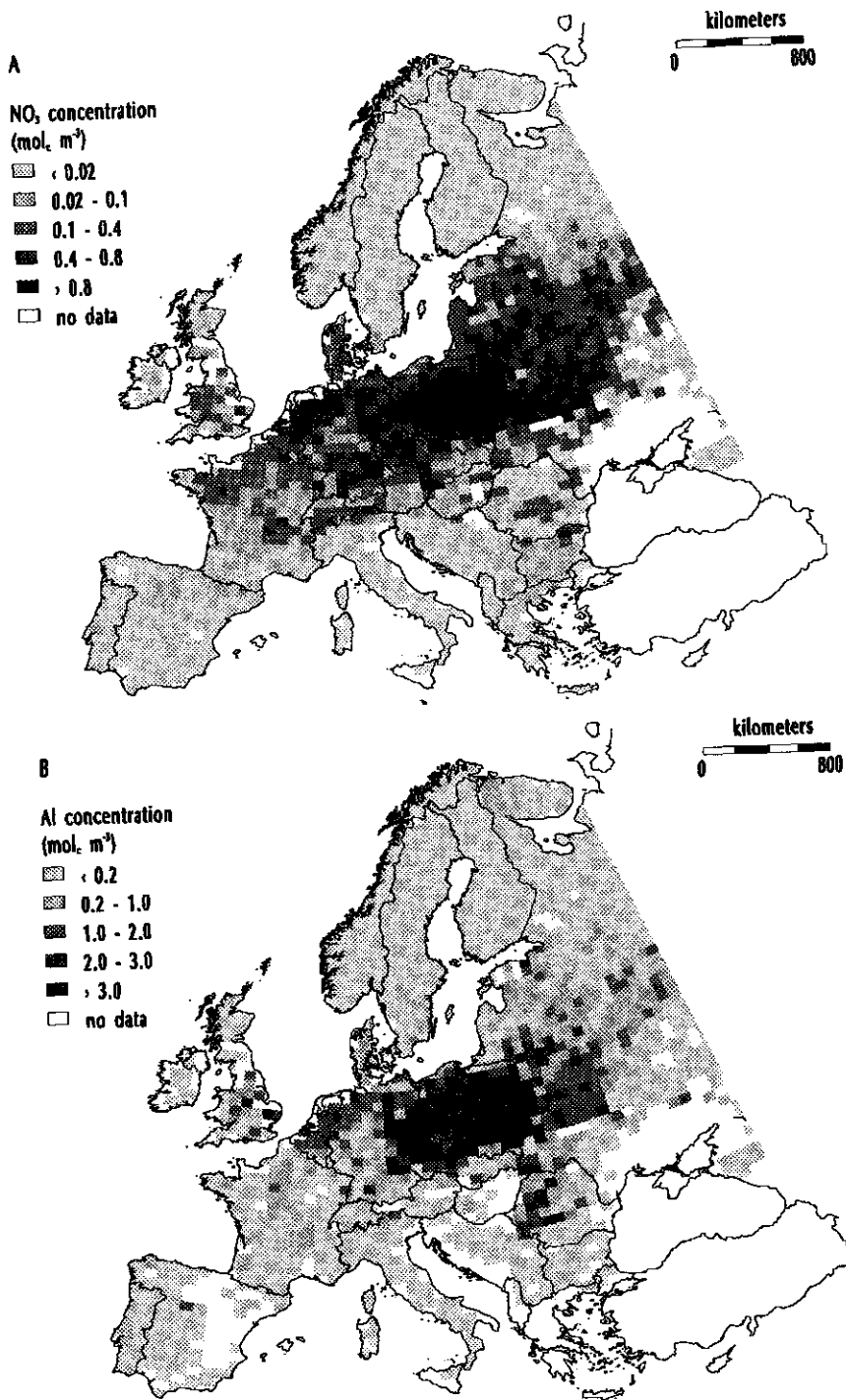


Figure 7.7 Maps of the predicted median NO<sub>3</sub> concentration (A) and Al concentration (B) for the year 2000 using the CRP scenario

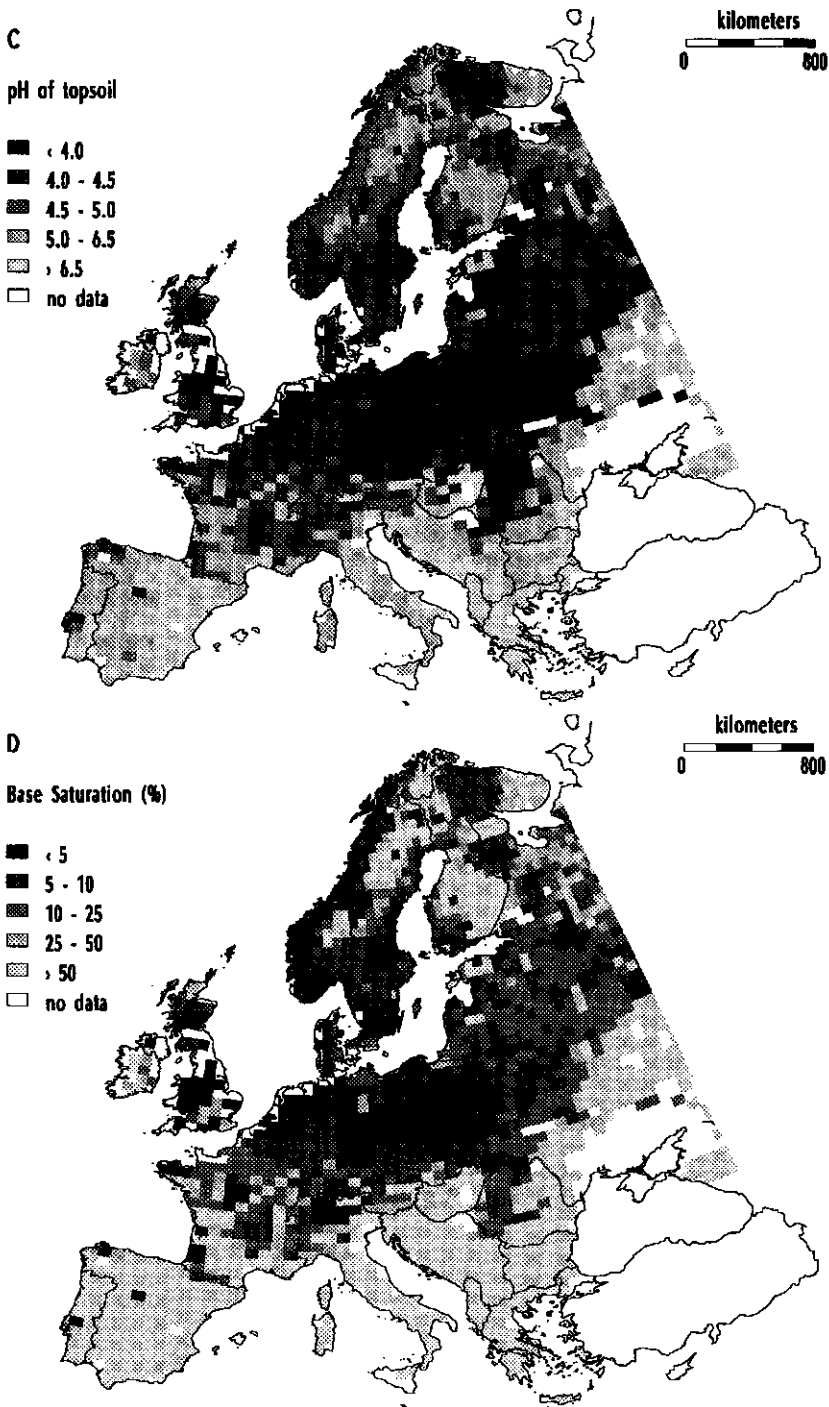


Figure 7.7 continued. Maps of the predicted median pH (C) and base saturation (D) for the year 2000 using the CRP scenario

However, during the simulation period up to 2050 the N saturated and acidified areas in the Nordic countries hardly increased. The predicted time period to reach steady state was several hundreds and sometimes even thousands of years in areas with a large N immobilization potential and relatively low N inputs.

## UNCERTAINTIES

Uncertainties in the predictions of the forested area exceeding critical chemical values are determined by uncertainties in critical chemical values, model structure and input data. Here, we mainly limit the discussion to effects on the predicted area exceeding critical values for the  $\text{NO}_3$  and Al concentration and the molar Al/BC ratio, using the (most likely) CRP scenario.

### Critical chemical values

The effect of uncertainties in the criteria used is illustrated in Figure 7.8. The uncertainty in critical C/N ratio used is partly related to the definition of N saturation. The definition given by Aber et al. (1989), used in this study, implies that N saturation of non-calcareous soils is predicted by the SMART model at a C/N ratio below 40. The other extreme is the definition by Ågren and Bosatta (1988), who argue that true saturation occurs when N outputs from the system equal N inputs to the systems, which implies that net N immobilization is zero. Complete saturation is predicted in SMART at a C/N ratio of 15 in non-calcareous soils. Furthermore, using the definition of Aber et al. (1989) there is uncertainty in the C/N ratio where N immobilization is no longer complete (e.g. 25 instead of 40; see before). Differences in the predicted area exceeding critical C/N ratios of 40, 25 and 16 (since a critical C/N ratio of 15 is never reached (cf Eq. 7.10) we used a value of 16) appeared to be large and increased with time (Fig. 7.8A). In 1960, the forested area where critical values were exceeded was about 23%, 10% and 3% for C/N ratios of 40, 25 and 16 respectively whereas it increased to 49%, 32% and 5% in 2050.

The uncertainty in the (critical)  $\text{NO}_3$  concentrations above which vegetation changes will occur is quite large (Warfvinge et al., 1992a). The abundance of lichens may decrease at  $\text{NO}_3$  concentrations exceeding a value as low as  $0.02 \text{ mol}_c \text{ m}^{-3}$  (Rosén, 1990) but values above  $0.1 \text{ mol}_c \text{ m}^{-3}$  are also given, related to changes from grasses to herbs in forests (Warfvinge et al., 1992a). The uncertainty in critical  $\text{NO}_3$  concentrations largely affected the predicted forested area at risk (Fig. 7.8B). In 1960, the forested area with  $\text{NO}_3$  concentrations above of  $0.02$ ,  $0.1$  and  $0.2 \text{ mol}_c \text{ m}^{-3}$  was calculated at 13%, 6% and 4% respectively, whereas it increased to 40%, 26% and 19% in 2050.

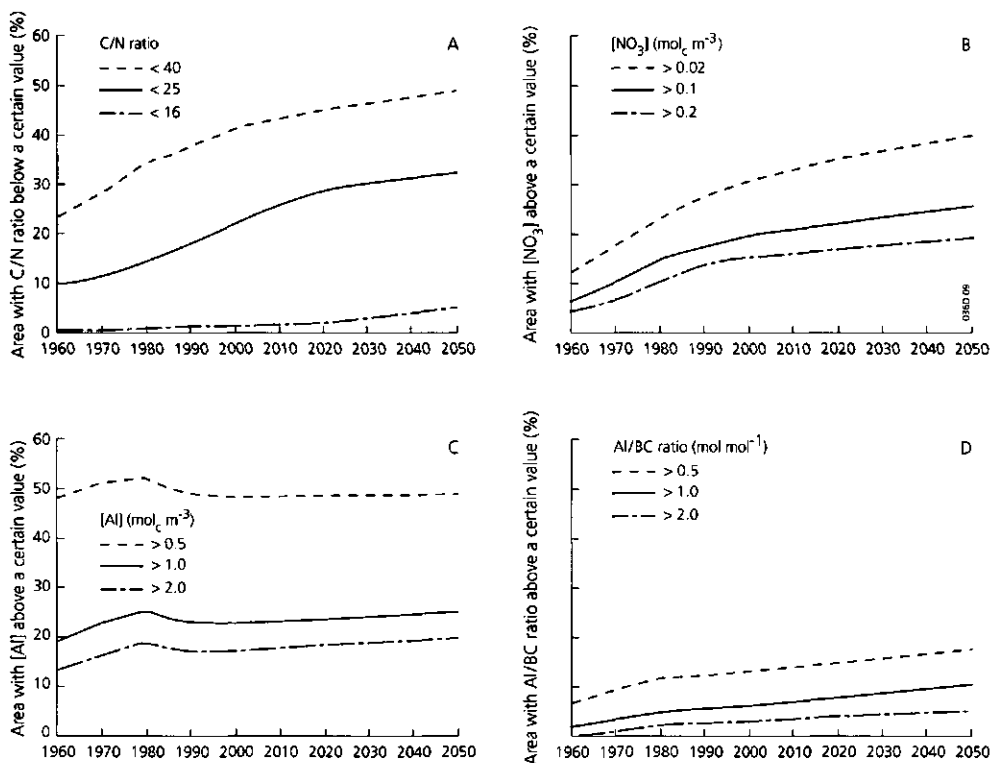


Figure 7.8 Temporal development of the forested area in Europe (%) exceeding different critical values for the C/N ratio (A), NO<sub>3</sub> concentration (B), Al concentration (C) and Al/BC ratio (D) using the CRP scenario.

A critical Al concentration of 0.2 mol<sub>c</sub> m<sup>-3</sup> and a critical molar Al/BC ratio of 1.0 was used in relation to the occurrence of root damage (cf Table 7.1). However, much higher values have been reported in literature to mark the onset of Al toxicity (e.g. Al concentrations up to 1.0 mol<sub>c</sub> m<sup>-3</sup>; Keltjens and Van Loenen, 1989). On the other hand one may want to avoid any increase in Al concentration to avoid a strong depletion of exchangeable base cations (cf Section 5.1). Differences in critical Al concentrations and Al/BC ratios used had a large effect on the predicted area where these values were exceeded (Fig. 7.8C and 7.8D). Especially the use of a nearly negligible Al concentration (since an Al concentration of 0.0 mol<sub>c</sub> m<sup>-3</sup> is never predicted in SMART, except for calcareous soils, a value of 0.01 mol<sub>c</sub> m<sup>-3</sup> was used) increased the area tremendously. Values were nearly equal at the beginning and the end of the simulation period, i.e. 48% in 1960 and 47% in 2050. In a steady-state situation an exceedance of 71% was predicted using 1985 deposition levels (Section 5.1). Differences in the predicted area exceeding critical Al concentrations were almost constant in time (Fig. 7.8C) whereas they slightly increased with time for the Al/BC ratios (Fig. 7.8D).

## Model structure

### *Neglection of nutrient cycling*

Uncertainties in model predictions caused by the various simplifying assumptions in the SMART model are numerous and difficult to quantify. The most important assumption in SMART is the assumed homogeneity within the rootzone, thus neglecting effects of canopy interactions and nutrient cycling. Those processes will hardly affect solute concentrations at the bottom of the rootzone, but at shallow soil depth such effects may be substantial. At shallow depth Al concentrations are generally lower (less Al mobilization and higher water flux) whereas BC concentrations are generally higher (less BC uptake). For example, using the steady-state START model, the forested area in Europe exceeding a critical Al concentration of  $0.02 \text{ mol}_c \text{ m}^{-3}$  at a depth of 25 cm was estimated to be 25%, compared to 43% at the bottom of the rootzone, using 1985 deposition levels (Section 5.1)

### *Description of N dynamics*

N dynamics is described very simply in SMART by linking net immobilization of atmospheric N input to the C/N ratio (Eq. 7.10), while the carbon pool in the soil is fixed. This is a rather hypothetical description based on the fact that the C/N ratio of organic matter is an important parameter for the potential N accumulation in a soil profile and a practical parameter in relation to mapping (Kuylenstierna and Chadwick, 1992). It only gives a rough estimate of the time period before the soil system is (completely) N saturated. For example, a soil with a C content of 2% and a C/N ratio of 50 in a topsoil of 20 cm with a bulk density of  $1500 \text{ kg m}^{-3}$  contains  $1200 \text{ kg ha}^{-1}$  N in this layer. A decrease in C/N ratio to 40, where N immobilization is no longer complete, implies an increase up to  $1500 \text{ kg ha}^{-1}$  N. Excess N inputs (deposition minus uptake minus a minimum leaching rate, cf Eq. 7.10) vary mostly between 3 and  $30 \text{ kg ha}^{-1} \text{ yr}^{-1}$  (cf Section 5.1) causing a time period of 10 to 100 years before N saturation occurs. A further decrease to a C/N ratio of 15, where the soil system is fully saturated, implies an increase up to  $4000 \text{ kg ha}^{-1}$  N. Even with complete N immobilization this takes more than 100 years in most of Europe. The predicted time period to reach N saturation with SMART was influenced by the organic C content (carbon pool) of the soil, that varied mostly between 1 and 5%, the initial C/N ratio, that varied between 50 and 15, and the thickness of the soil layer (including the humus layer) in which N immobilization is assumed to occur. In this study, we took the upper 20 cm of the soil, with a carbon pool that generally varies between 30 and  $150 \text{ t ha}^{-1}$ . This is based on Tietema (1992) who observed that N mineralization/immobilization mainly occurs in the humus layer and the mineral topsoil. An increase in the thickness of the 'active' soil layer increases the time before N saturation occurs and vice versa.

The simple description of N immobilization in SMART, neglecting effects of nutrient cycling, certainly affects the prediction of N saturation. Literature information suggests that N dynamics in a forest soil is strongly determined by the interaction with vegetation.

In an N deficient system, additional N input is efficiently used by an increased production in stem and leaf (needle) biomass (Aber et al., 1989). This in turn increases the litterfall and through that the amount of organic matter (C pool) in the humus layer. Owing to this effect the N pool may increase whereas the C/N hardly changes (Billet et al., 1990a; Mälkönen et al., 1990). At continuing elevated N inputs, N cycling will further increase due to elevated N contents in foliage (Lang et al., 1982) and reduced N translocation from old to new tissue (Oterdoom et al., 1987). This will cause a decrease in the C/N ratio of litter, thus stimulating N mineralization and N availability. This in turn may cause elevated N leaching, especially when the limitation of essential resources other than N, such as light, water and nutrient availability, inhibit a further increase in root uptake (Aber et al., 1991; Gundersen, 1991; 1992). There are dynamic integrated soil-vegetation models such as VEGIE (Aber et al., 1991) and SOILVEG (Berdowski et al., 1991), which include (several of) these aspects, but the parameters and the initial conditions of variables needed are not available on a European scale (cf Gundersen, 1992). Furthermore, results of SMART are at least consistent with integrated soil-vegetation models, which also show that N inputs and soil type are decisive for the development of N saturation, and time periods to reach N saturation predicted with SMART are in a similar order of magnitude as given by these models (Ågren and Bosatta, 1988; Aber et al., 1991).

Another uncertainty in the description of N immobilization is the important role of the C/N ratio. Because of the weak relationship between  $\text{NO}_3$  concentration and C/N ratio, it has been suggested that the C/N ratio hardly controls N immobilization (Driscoll et al., 1989). However, SMART reproduces this weak relationship while using the C/N ratio as the key parameter in describing N dynamics. Because the N immobilization flux is calculated as a C/N determined fraction of the excess N input (cf Eq. 7.10), the  $\text{NO}_3$  leaching flux, which is determined by excess N input and N immobilization, is also calculated as a C/N determined fraction of the excess N input. This implies that even at C/N ratios close to 40 the  $\text{NO}_3$  leaching flux, and through that the  $\text{NO}_3$  concentration, can be high if the atmospheric N input is high. Similarly, the  $\text{NO}_3$  concentration can be low at a low C/N ratio because of a low N input.

Other uncertainties related to N dynamics (cf the description of the model structure) result from (i) neglecting N fixation which is important for trees such as red alder (Van Miegroet and Cole, 1984), (ii) neglecting  $\text{NH}_4$  fixation which may play a role in clay soils, (iii) assuming that nitrification is complete, while it is likely to be inhibited at high C/N ratios (Gundersen and Rasmussen, 1990), (iv) the description of denitrification (in SMART denitrification is calculated after N immobilization has taken place. Reversing this order causes an increase in denitrification rate and thus a longer period before N saturation occurs) and (v) neglecting the interaction between net N uptake and a change in soil conditions. The latter aspect also refers to the uptake of base cations, which may reduce at elevated Al concentrations. However, considering the uncertainty in present uptake estimates this aspect is likely to be unimportant.



### *Other simplifying assumptions*

Other assumptions in the SMART model such as (i) disregarding  $\text{SO}_4$  interactions, (ii) neglect of complexation of Al with inorganic and organic anions and (iii) a very simple hydrology are likely to be less significant. First, most European forest soils are  $\text{SO}_4$ -saturated (Berdén et al., 1987). Second, complexation of Al with inorganic anions such as  $\text{SO}_4$  and OH only causes a small increase in the total inorganic Al concentration in the soil solution. A comparison between results of SMART and the MAGIC model, which includes complexation reactions (Cosby et al., 1985a,b), for three catchments in Norway, Sweden and Finland also showed minor differences (Wright et al., 1991). Disregarding organic acid as a source of acidity is not likely to have a significant effect on the concentration of inorganic Al since it mainly causes formation of non-toxic organically complexed Al. Third, ignoring surface runoff and preferential flow likely has a small effect since both water and ions are removed from the soil in situations where this occurs.

### **Input data**

A discussion of the uncertainties in model predictions caused by uncertain input data is limited here to the uncertainty and spatial variability of the most important input data, i.e. the initial conditions of the C/N ratio and the base saturation (exchangeable BC amount). The impact of uncertainties in system inputs/outputs, i.e. precipitation excess and growth uptake, and in soil constants, i.e. base cation weathering rate, the Al hydroxide dissolution constant ( $K\text{Al}_{\text{ox}}$ ) and denitrification fraction, is likely to be small. An uncertainty analysis with the steady-state START model, showed that the area exceeding critical Al concentrations and Al/BC ratios at steady state (45% using reference input data) changed (i) by  $\pm 6\%$  in response to a 50% change in precipitation excess and base cation weathering, (ii) by  $\pm 4\%$  in response to a change in  $K\text{Al}_{\text{ox}}$  by a factor of  $\pm 10$  and (iii) by only  $\pm 1\%$  in response to a 50% change in growth uptake. The low impact of growth rate was due to the counteracting effect of N and BC uptake on the acidity balance of the soil (Section 5.1).

The estimated initial C/N ratios in the forest topsoil are very uncertain since this variable does not only depend on bedrock characteristics and N deposition level (cf Table 7.6) but also on soil type, climate and vegetation type. Insight in the maximum impact of an uncertain C/N ratio is given in Fig. 7.9. Predictions of the area with a  $\text{NO}_3$  concentration above  $0.1 \text{ mol}_c \text{ m}^{-3}$  varied strongly when the initial C/N ratio was varied between its minimum and maximum value (Fig. 7.9A). Especially, when the minimum C/N ratio of 15 was used (implying that all non-calcareous soils were already complete N saturated in 1960 which is an unrealistic assumption), the effect was large. In this case the predicted area directly followed the trend in N deposition over time. Using the maximum C/N ratio of 50, there was a considerable difference with the reference run in 1960 (no forests exceeding a  $\text{NO}_3$  concentration of  $0.1 \text{ mol}_c \text{ m}^{-3}$  as compared to 6% exceedance; cf Fig.

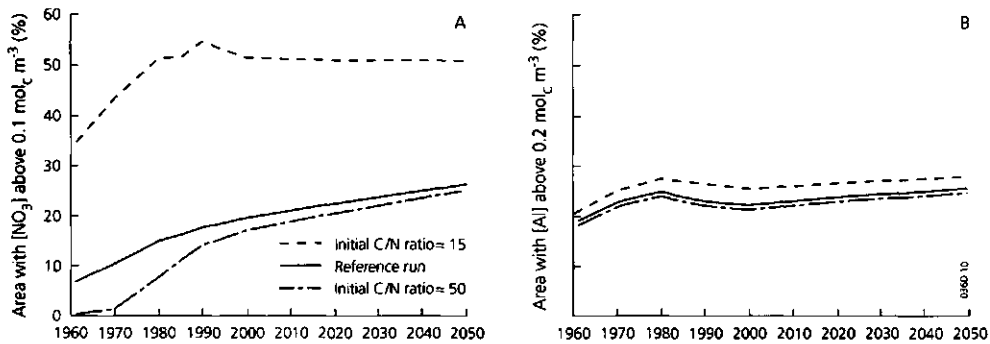


Figure 7.9 Influence of the initial C/N ratio on the forested area in Europe (%) with a  $\text{NO}_3$  concentration above  $0.1 \text{ mol}_c \text{ m}^{-3}$  (A) and an Al concentration above  $0.2 \text{ mol}_c \text{ m}^{-3}$  (B) using the CRP scenario.

7.9A), that increased up to 1970 but decreased strongly between 1970 and 1990 and in 2050 the difference was very small. In view of these results the statement by Kuylenstierna and Chadwick (1992) that "the error introduced by not incorporating dynamic aspects of C/N change" may be smaller than "the error in extrapolating available C/N ratios to a wider area" is questionable. Dynamic aspects may cause a considerable change in C/N ratios in the near future. Effects of varying initial C/N ratios on the Al concentration were much smaller, especially between the reference run and the model run where all initial C/N ratios were set at 50 (Fig. 7.9B). This is due to the large impact of  $\text{SO}_4$  on the Al concentration. Consequently, the differences between both model runs also remained quite constant with time.

The critical C/N ratio also had a large influence on the area where the critical  $\text{NO}_3$  concentration was exceeded (cf Fig. 7.10A). The difference remained quite constant,

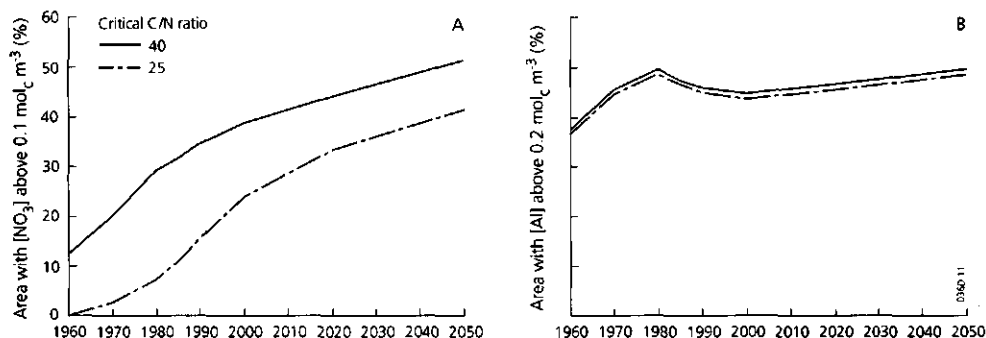


Figure 7.10 Influence of the critical C/N ratio on the temporal development of the forested area in Europe (%) with a  $\text{NO}_3$  concentration above  $0.1 \text{ mol}_c \text{ m}^{-3}$  (A) and an Al concentration above  $0.2 \text{ mol}_c \text{ m}^{-3}$  (B) using the CRP scenario.

approximately 6%, during the simulation period whereas the effect was small on the area where the critical Al concentration was exceeded (cf Fig. 7.10B).

Effects of the initial base saturation on the forested area exceeding a critical Al concentration (Fig. 7.11A) and Al/BC ratio (Fig. 7.11B) were significant. In all model simulations we used an initial base saturation that was the maximum of a relation with soil type and an equilibrium with the acid deposition level in 1960. Assuming that base saturation was everywhere at steady-state with acid inputs in 1960, strongly increased the area exceeding critical values for Al and especially for the Al/BC ratio as compared to the reference run. As with the use of a C/N ratio of 15, the trends in time directly followed the change in acid inputs with time. When the initial base saturation was related to soil type only, the difference with the reference run was much less, especially for the Al/BC ratio (cf Fig. 7.11A and 7.11B).

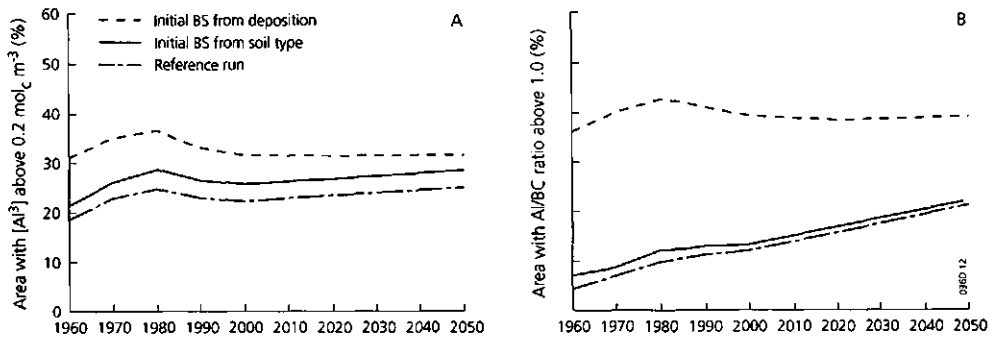


Figure 7.11 Influence of the initial base saturation on the forested area in Europe (%) with an Al concentration above  $0.2 \text{ mol}_c \text{ m}^{-3}$  (A) and an Al/BC ratio above  $1.0 \text{ mol}_c \text{ mol}^{-1}$  (B) using the CRP scenario

## DISCUSSION AND CONCLUSIONS

In this study we predict that the acidity and N-status of European forest soils do not improve when current reduction plans are being implemented. The forested area exceeding critical values for the  $\text{NO}_3$  concentration and Al/BC ratio is likely to increase, whereas the forested area where critical values for the Al concentration are exceeded is likely to decrease slightly up to the year 2000 followed by a slow but gradual increase after 2000. Soil acidification is expected to decrease quite drastically following maximum feasible emission reductions (MFR scenario). The problem of N saturation appears to be more persistent and likely increases in the future, even for the MFR scenario. N-saturated and acidified forest soils were concentrated in central, western and eastern European countries during the entire simulation period for all scenarios. Very high Al concentrations mainly occurred in central Europe (Germany, Poland and former

Czechoslovakia) whereas high  $\text{NO}_3$  concentrations also showed up in the Netherlands, Belgium, Luxembourg and large parts of the former Soviet Union.

The question about the accuracy of the long-term soil responses estimated by the SMART model cannot be answered satisfactorily. The model was verified by comparing simulations with historical observations of changes in (i) soil chemistry between 1949 and 1984 for five sites in Sweden (Van Oene and De Vries, 1994) and (ii) soil solution chemistry between 1974 and 1989 in a continuously monitored spruce site in Solling, Germany (Van der Salm et al., 1994). However, these data were too few for a rigorous testing of the model. Furthermore, the time period of the data set on soil solution chemistry in Solling (15 years) was still far to short to test the hypothesis that the system approaches N saturation at lower C/N ratios. During the 15 year period the C/N ratio hardly changed, and changes in  $\text{NO}_3$  concentration were mainly due to hydrologic differences (Van der Salm et al., 1994). However, the reasonable comparison between simulated and measured changes in (i) base cation amounts in the rootzone of the Swedish sites (Van Oene and De Vries, 1994) and (ii) soil solution chemistry in the Solling site (Van der Salm et al., 1994) and the consistency between predicted and measured relationships between parameters indicating N saturation and soil acidification, presented in this study, show that SMART produces plausible results.

Plausibility of the results is an important feature of the SMART model. Especially the N part of the model is weak and real N dynamics are far more complicated. Still, the description used will give insight in the temporal change in N status, i.e. a faster change in soils with a large excess input of N (deposition minus uptake minus a minimum leaching rate) and a limited potential N pool. Furthermore, the acidity status (Al concentration, Al/Ca ratio) is not strongly influenced by the  $\text{NO}_3$  concentration since  $\text{SO}_4$  appears to have a more dominant influence. Finally, the general trends described above were predicted irrespective of the uncertainties involved in the critical values and input data used. This also holds for the uncertainty induced by the definition of N saturation, that causes uncertainty in a critical C/N ratio. These uncertainties (sometimes strongly) affected the predicted area where critical values are exceeded in a given year but not so much the trends in time. Even though SMART has not been (and cannot be) strictly verified for its ultimate use of long-term predictions, it can be used as a tool to obtain a conceptual understanding of long-term soil responses and to make general predictions (will the acidity and N-status of forests improve or not) for policy-makers.

Improvements of the predictions will be possible by collecting more data on important soil properties and soil variables such as CEC, base saturation and C/N ratio. The uncertainty in these variables is likely to be large due to (i) the uncertainty in soil type, depicted on the soil map of Europe with a scale 1 : 5 000 000 and (ii) the spatial variability within each soil type. Soil data used in this study were based only on one selected profile for each soil type. At present an extensive database on the actual nitrogen and acidity status of European forest soils is under development at the DLO

Winand Staring Centre, based on data provided by various countries. This database will enable us to account for the spatial variability between and within soil types. Furthermore, there are ongoing activities to improve the quality of a soil map of Europe (at a scale of 1 : 1 000 000). Use of such an improved map, combined with information on the frequency distribution of important soil data, should improve the quality of soil chemistry predictions.

## 7.2 IMPACTS ON FOREST SOILS IN THE NETHERLANDS

### ABSTRACT

*The long-term impact of three deposition scenarios on Dutch forest soils was evaluated using the model RESAM (Regional Soil Acidification Model), which is part of the overall DAS (Dutch Acidification Simulation) model. RESAM was applied to seven tree species and fourteen non-calcareous sandy soils covering about 65% of the Dutch forest area. Deposition scenarios for  $SO_x$ ,  $NO_x$  and  $NH_x$  were generated for twenty deposition areas by the air transport model of DAS for the period 1965 to 2050. Data related to tree species and soil types were derived from literature surveys, field research, laboratory experiments and model calibration. Results discussed here are restricted to important model outputs indicating N accumulation or soil acidification. A comparison of model results for 1990 with measurements in 150 forest stands during this year showed that the agreement was good for the N content, base saturation, pH and  $SO_4$  concentration, reasonable for the  $NO_3$  concentration, Al/Ca ratio and Al concentration in the topsoil and unfavourable for the  $NH_4/K$  ratio and Al concentration in the subsoil. Future trends in soil solution parameters in response to the three scenarios, showed that deposition reductions generally lead to a fast increase in pH and a fast decrease in Al and  $SO_4$  concentration and Al/Ca ratio. However, for the  $NO_3$  concentration and  $NH_4/K$  ratio there was a clear time lag between deposition reduction, and concentration reduction, which is mainly due to N mobilization from the humus layer. A decrease in average deposition level to  $1400 \text{ mol}_e \text{ ha}^{-1} \text{ yr}^{-1}$  appeared to be sufficient to avoid substantial exceedance of critical values for Al and  $NO_3$  concentration and Al/Ca ratio.*

### INTRODUCTION

To gain insight in the long-term effect of acid deposition on Dutch forest soils, a process-oriented Regional Soil Acidification Model (RESAM) has been developed (Section 6.2; De Vries, 1991; De Vries et al., 1994b). RESAM describes changes in soil chemistry, both in the solid phase (minerals and adsorption complex) and liquid phase, due to natural and man-induced processes. The model includes the major elements in forest soils i.e. H, Al, Ca, Mg, K, Na,  $NH_4$ ,  $NO_3$ ,  $SO_4$ , Cl,  $HCO_3$  and RCOO. The temporal resolution of model input and output is one year, as the model is intended to give insight into the long-term soil chemical response of forest ecosystems to acid deposition. RESAM enables us to predict long-term changes under defined boundary conditions for a given soil profile. For its regional application, RESAM is linked as a submodel in the integrated Dutch Acidification Simulation (DAS) model. DAS was developed to evaluate the effectiveness of abatement strategies by analysing environmental impacts of different emission-deposition scenarios (Olsthoorn et al., 1990).

DAS has a modular construction: each aspect of the problem is represented by a separate compartment. The ultimate aim is to evaluate protection strategies, based on a quantitative description of the linkages between emissions, atmospheric deposition, soil

acidification and effects on terrestrial and aquatic ecosystems, agricultural production and materials. A schematic diagram of the model compartments and submodels illustrating the model use is given in Figure 7.12. Similar model systems, although less comprehensive, have been developed for Denmark (Petersen, 1984), Finland (Johansson et al., 1989) and for Europe as a whole (Alcamo et al., 1990).

In this section long-term impacts of three emission-deposition scenarios on Dutch forests soils are described for a period of 60 years (1990-2050), based on predictions with RESAM. Emphasis is given on the application methodology and data acquisition strategy used for such a large scale application. The model output is described in terms of major parameters regarding the chemistry of (i) the soil solid phase, i.e. the N content of the humus layer, the content of H, Al and base cations (Ca+Mg+K+Na) on the adsorption complex and the content of secondary (oxalate-extractable) Al compounds, and (ii) the soil solution chemistry, i.e. the concentration of H (pH), Al, Ca, K,  $\text{NH}_4$ ,  $\text{NO}_3$  and  $\text{SO}_4$ . For 1990, results are compared with field data. Regarding the soil solution, special emphasis is given to the impact of the scenarios on the pH, Al concentration, Al/Ca ratio and  $\text{NH}_4/\text{K}$  ratio in the topsoil (top 20 to 30 cm) and the pH, Al and  $\text{NO}_3$  concentration in the subsoil (bottom of the rooting zone). The parameters in the topsoil are important indicators of forest stress for which critical concentration levels have been defined (De Vries, 1991; cf Table 7.1). The parameters in the subsoil are important indicators of potential ground water pollution.

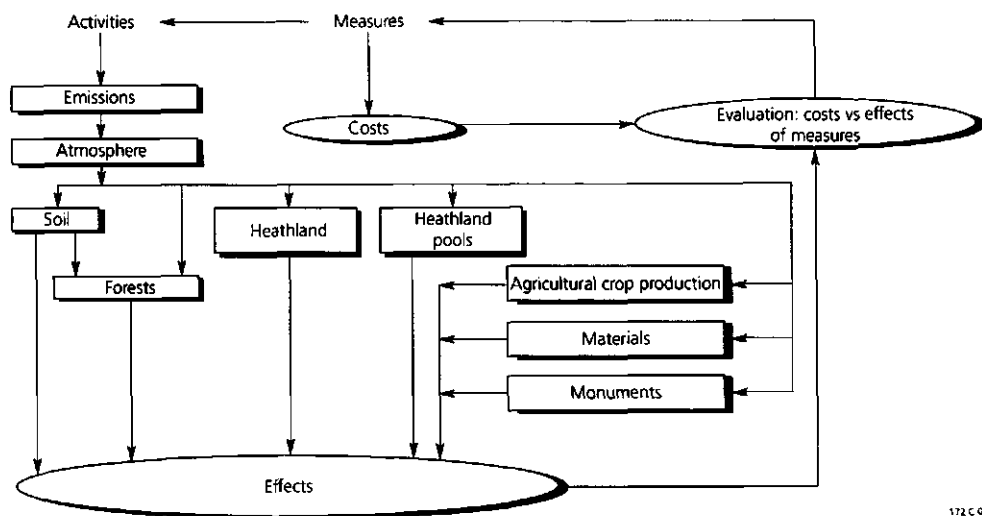


Figure 7.12 Schematic diagram of the DAS model

## METHODS AND DATA

### The model RESAM

RESAM can be used both as a research tool (to get insight in system behaviour) and a management tool (to help decision makers in designing environmental policies). To serve both needs the model is characterized by a process-oriented approach with relatively simple process descriptions to minimize input data. RESAM describes all processes in the vegetation canopy, humus layer and mineral soil horizons which significantly influence the concentration of major ions in the soil solution. The model consists of a set of mass balance equations, kinetic equations and equilibrium equations. The mass balance equations describe the input-output relationship in each horizon for all cations and anions, except for H and  $\text{HCO}_3^-$ . The concentration of  $\text{HCO}_3^-$  is determined by the  $\text{CO}_2$  equilibrium equation, whereas the H concentration (pH) is determined by the concentration of all other ions using the charge-balance principle. Canopy interactions, nutrient cycling processes, N transformations and weathering processes are described by kinetic equations whereas equilibrium equations are used to describe adsorption and desorption of cations and  $\text{SO}_4$ .

An overview of the various process formulations, including the compounds involved in each process, is given in Table 7.11.

Table 7.11 Processes and process formulations included in RESAM

Process	Constituents involved	Process formulation
Dry deposition	Ca, Mg, K, Na, Cl	Linear function of wet deposition
Foliar uptake	$\text{NH}_3$ , $\text{NO}_x$ , $\text{SO}_2$	Linear function of dry deposition
Foliar exudation	Ca, Mg, K	Linear function of H and $\text{NH}_4$ uptake
Litterfall	N, Ca, Mg, K, S	First-order reaction
Root decay	N, Ca, Mg, K, S	First-order reaction
Mineralization	N, Ca, Mg, K, S	First-order reaction
Root uptake	N, Ca, Mg, K, S	Fixed <sup>1)</sup>
Nitrification	$\text{NH}_4$ , $\text{NO}_3$	First-order reaction
Denitrification	$\text{NO}_3$	First-order reaction
Dissociation of $\text{CO}_2$	$\text{HCO}_3^-$	$\text{CO}_2$ equilibrium equation
Protonation of $\text{RCOO}^-$	$\text{RCOO}^-$	First-order reaction
Weathering of carbonates	Ca	First-order reaction
Weathering of silicates	Al, Ca, Mg, K, Na	First-order reaction
Weathering/precipitation of Al hydroxides	Al	Elovich equation <sup>2)</sup>
Cation exchange	H, Al, Ca, Mg, K, Na, $\text{NH}_4$	Gaines-Thomas equations
Adsorption/desorption of sulphate	$\text{SO}_4$	Langmuir equation

<sup>1)</sup> Fixed uptake based on a given net uptake in stems and branches and a steady state recycling of elements in leaves and roots, allocated per soil layer by the water uptake pattern. Net uptake is calculated by multiplying the annual growth of stems and branches with the element contents

<sup>2)</sup> Al weathering is also described by a first-order reaction but that option was not used in this study



A description of the various formulations is given in Section 6.2 (De Vries et al., 1994b). Kinetic processes are described by first-order reactions (flux is linearly related to the available amount) or by linear relationships with fluxes induced by other processes. The only exception is the dissolution of Al from hydroxides where a so called Elovich equation (cf Section 6.2; Eq. 6.33) was used on the basis of laboratory experiments (Chapter 3).

### Application methodology

To limit both the data acquisition and computation time, runs with RESAM were restricted by defining 20 areas in which the deposition was assumed to be constant (deposition areas; cf Fig. 7.13), 7 major tree species and 14 non-calcareous sandy soils, based on a recent 1 : 250 000 soil map of the Netherlands (Steur et al., 1986). In this study, the soil profile was confined to the rooting zone.

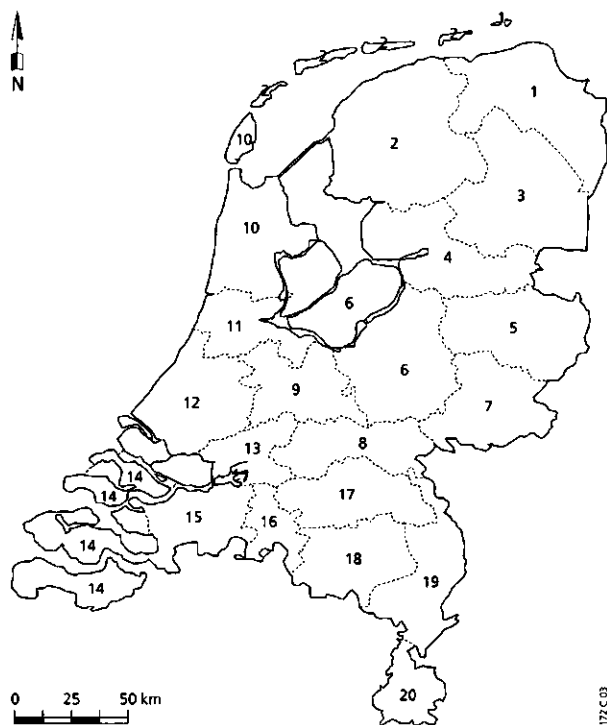


Figure 7.13 Delineation of the 20 deposition areas considered in the application of the model RESAM

The vertical heterogeneity was taken into account by differentiating between soil layers (horizons). The total area of the forest/soil combinations considered in the model application (Table 7.12) comprises 64% of the total forest area in the Netherlands, of which more than 50% is covered by Scots pine. The remaining 35% comprises other tree species, such as poplar and birch (approximately 20%) and other soil types, such as calcareous soils, clay soils, loess soils and peat soils (approximately 15%).

Table 7.12 Area of the forest/soil combinations considered in the model application in percent of the total forest area in the Netherlands (321 500 ha)<sup>1)</sup>

Soil type <sup>2)</sup> (FAO, 1988)	Area (%)							
	Scots pine	Black pine	Douglas fir	Norway spruce	Japanese larch	Oak	Beech	Total
Cambic Podzol	4.96	0.32	1.15	0.40	0.88	1.87	0.80	10.38
Gleyic Podzol	6.18	0.96	0.81	0.91	1.05	2.67	0.30	12.88
Carbic Podzol	10.52	1.37	1.43	0.87	1.33	2.78	0.53	18.83
Fimic Anthrosol	2.15	0.17	0.35	0.28	0.31	2.12	0.30	5.68
Umbric Gleysol	0.91	0.09	0.11	0.15	0.18	1.23	0.14	2.81
Haplic Arenosol <sup>3)</sup>	9.62	1.14	0.73	0.21	0.31	1.54	0.21	13.76
	$\Sigma=34.34$	$\Sigma=4.05$	$\Sigma=4.58$	$\Sigma=2.82$	$\Sigma=4.06$	$\Sigma=12.21$	$\Sigma=2.28$	$\Sigma=64.34$

<sup>1)</sup> Information on the areal distribution of tree species and soil types in each deposition area was derived by overlaying a forest database with tree species information (CBS, 1985) and a soil database with soil type information in a 500 m x 500 m grid. The latter database was derived by transforming the digitized 1 : 250 000 soil polygon map of the Netherlands (Steur et al., 1986).

<sup>2)</sup> The soil types include both coarse and fine sandy soils, which were distinguished in the model application in view of differences in hydrology, uptake and weathering rates.

<sup>3)</sup> Including Gleyic Arenosol.

Information on the forest coverage in the most densely forested deposition areas is given in Table 7.13. Total coverage of the same tree species in the deposition areas 4, 7, 8, 9, 15, 16, 17, 19 en 20 (cf Fig. 7.13) varies between 3 and 5%. In the coastal regions (deposition areas 1, 2, 10, 11, 12, 13 and 14) it is generally less than 1%.

Soil and vegetation data were related to each tree species and soil type (and the combination of both) irrespective of the deposition area, using pedotransfer functions. The spatial distribution of these data was taken into account by using geographic

Table 7.13 Forests coverage in the most densely forested deposition areas, in percent of the total forest area in the Netherlands (321 000 ha)

Deposition area	Forest coverage (%)							
	Scots pine	Black pine	Douglas fir	Norway spruce	Japanese larch	Oak	Beech	Total
3	1.70	0.20	0.53	1.09	1.50	1.97	0.21	7.20
5	2.89	0.08	0.32	0.36	0.38	1.29	0.13	5.45
6	10.56	0.43	1.74	0.42	1.04	2.42	1.00	17.61
18	4.66	0.93	0.39	0.29	0.33	0.97	0.05	7.62

information systems on tree species and soil type (cf Table 7.12). In this way available forest and soil survey information was linked to RESAM and consequently, the model could be used to identify areas vulnerable to acidification. Model simulations were made for each unique combination of deposition area (20), tree species (7) and soil type (14), rather than running simulations at the scale for which information on tree species and soil type was available (500 m x 500 m grids). Since not all combinations did occur in the deposition areas, the total number of model runs for each scenario was equal to 1314 instead of the theoretical maximum of 1960. By restricting runs to forest/soil combinations of at least 25 ha, this number was further reduced to 550 while the aerial reduction was only 2%. A selection program called GENINP was developed to apply RESAM on a regional scale (Kok and Bultman, 1990). This program generates input files for all relevant forest/soil combination in all deposition areas from the various files containing data that depend on the deposition area, tree species and soil type.

### **Emission-deposition scenarios**

Deposition scenarios for  $\text{SO}_x$ ,  $\text{NO}_x$  and  $\text{NH}_x$  for the period 1950-2050 were generated by source-receptor matrices in the model DAS, based on the deposition model TREND (De Leeuw and Van Jaarsveld, 1992). Deposition calculations were based on (cf Tiktak et al., 1991): (i) historical emission data (1950-1990) given in Thomas et al. (1988) and Asman (1990); (ii) expected emissions in the near future (1990-2000) in view of the measures and emission targets described in the Netherlands Acidification Abatement Plan and the National Environmental Policy Plan Plus (NEPP+) and (iii) deposition targets (2000-2050) since no emission policy has been developed for the period after 2000. For this period three scenarios were used (the scenarios were identical up to 2000) based on deposition targets that were formulated for the years 2010 and 2050 as given in Table 7.14.

Trends in the average deposition of potential acidity in the Netherlands (cf Fig. 7.14) showed a peak in 1965 due to large  $\text{SO}_2$  emissions which declined afterwards. Contrary, emissions for  $\text{NO}_x$  and  $\text{NH}_3$  increased up to 1980 and stayed quite constant up to 1990. The strong reduction between 1990 and 2000 was based on an expected reduction of 80% for  $\text{SO}_x$ , 50% for  $\text{NO}_x$  and 70% for  $\text{NH}_x$  as compared to 1980 (cf De Vries, 1993; Section 4.2).

Deposition levels of potential acidity on forests, calculated by the TREND model, are relatively low in the northern and western part of the Netherlands (Fig. 7.15). In the central and southern part there is a strong relationship between acid deposition and N deposition that mainly stems from  $\text{NH}_3$  emissions in areas with intensive animal husbandry.

Table 7.14 Average values used for the potential acid deposition in 2010 and 2050 for three scenarios. Official deposition targets are underlined

Receptor	Potential acid deposition ( $\text{mol}_e \text{ ha}^{-1} \text{ yr}^{-1}$ ) <sup>1)</sup>					
	scenario 1		scenario 2		scenario 3	
	2010	2050	2010	2050	2010	2050
The Netherlands	<u>2240</u> <sup>2)</sup>	<u>2240</u>	<u>1400</u> <sup>3)</sup>	1230	1230	<u>700</u> <sup>4)</sup>
Forest in the Netherlands <sup>5)</sup>	2550	2550	1600	<u>1400</u>	<u>1400</u>	800

- 1) Potential acid deposition in the Netherlands is defined as the sum of  $\text{SO}_x$ ,  $\text{NO}_x$  and  $\text{NH}_x$  deposition minus seasalt corrected bulk deposition of base cations
- 2) The official target was  $2400 \text{ mol}_e \text{ ha}^{-1} \text{ yr}^{-1}$  (cf De Vries, 1993) but on the basis of the measures described in NEPP+ a somewhat lower value was calculated
- 3) A critical acid load related to root damage caused by Al toxicity (cf Section 4.2; De Vries, 1993)
- 4) A critical acid load that prevents nearly all possible negative effects including ground water pollution (cf Section 4.2; De Vries, 1993).
- 5) Increased deposition on forests, due to filtering of gaseous air pollutants, was accounted for by multiplying the average dry deposition by empirically derived correction factors, specific for each compound and deposition area (Erismann, 1991). The average increase in dry deposition thus calculated was about 20%, i.e. an average increase in total deposition of 14%.

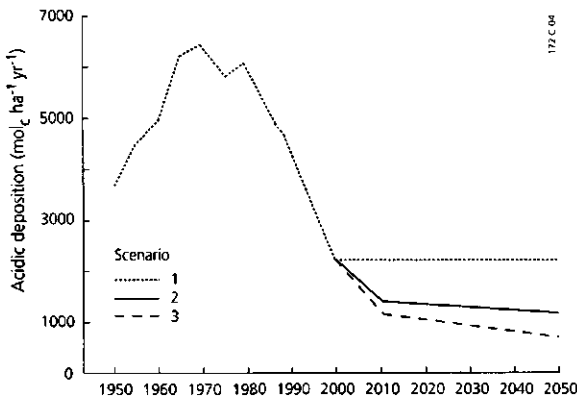


Figure 7.14 Trends in the deposition of total acidity in the Netherlands for three scenarios

Data on the bulk deposition of base cations (Ca, Mg, K and Na) and Cl for each deposition area were interpolated from 22 weather stations in the Netherlands for the period 1978-1985 (KNMI/RIVM, 1985). These values were kept constant during the simulation period. The variation in base cation deposition levels in the four most densely forested deposition areas (Table 7.15) was quite small except for Na deposition, which is influenced by differences in seaspray. Dry deposition of base cations was estimated by multiplying bulk deposition data with tree species dependent dry deposition factors. Factors used were 1.5 for pine forests (Scots pine, black pine), 2.0 for spruce forests

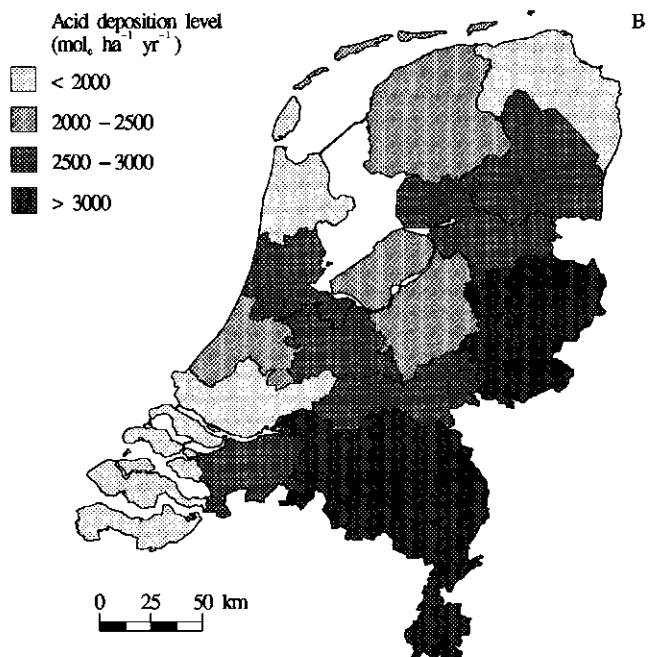
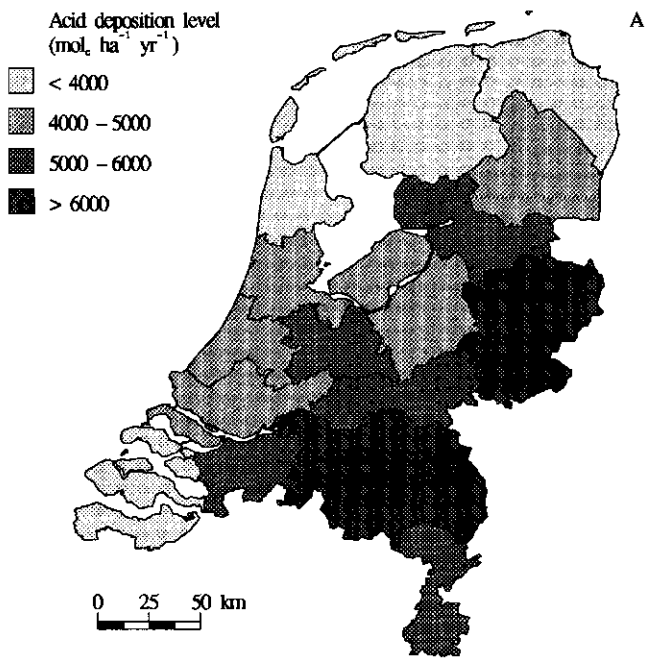


Figure 7.15 Geographic distribution of the total acid deposition in the Netherlands in 1990 (A) and 2000 (B)

**Table 7.15** Average bulk deposition levels for base cations in the most densely forested deposition areas

Deposition area	Deposition level (mol <sub>c</sub> ha <sup>-1</sup> yr <sup>-1</sup> )			
	Ca	Mg	K	Na
3	190	170	35	690
5	195	125	30	480
6	240	180	35	740
18	220	120	30	440

and 1.0 for deciduous forests (oak, beech and the needle shedding Japanese larch). Data were derived from a comparison of Na in throughfall and bulk deposition at 42 forest sites in the Netherlands (cf De Vries, 1991).

## Input data

### *Data related to tree species*

For each of the tree species considered, data were gathered on: (i) canopy interaction factors, (ii) nutrient cycling parameters and (iii) mineralization rate constants for fresh litter, old litter and root necromass. Canopy interaction factors, i.e. foliar uptake and foliar exudation fractions (Table 7.16) were based on data from 42 forested sites in the Netherlands where both throughfall and bulk deposition were measured (cf Section 5.2; Table 5.15).

Data for the parameters influencing nutrient cycling (Table 7.16) were based on a literature survey (De Vries et al., 1990). Data for the element contents in leaves, differed from those used in the MACAL application, which were derived from a field survey in 1990 in 150 stands.

The N content in leaves and fine roots was calculated as a linear function of the N deposition in a deposition range between 1500 (minimum N content) and 7000 mol ha<sup>-1</sup> yr<sup>-1</sup> (maximum N content). Furthermore, reallocation of N from the older needles and fine roots to younger needles and fine roots was included. The reallocation fraction was assumed to decrease linearly from a maximum value of 0.36 to 0.0 with an increasing N content (De Vries, 1991). Values for the absolute minimum and maximum N contents in leaves and fine roots and for those related to reallocation are given in Table 7.17. As with leaves and fine roots, the N content in stems was assumed to vary with N deposition between a minimum value (0.05-0.15% depending upon tree species) and a maximum value (0.15-0.25% depending upon tree species; cf De Vries, 1991). Data used for contents of Ca, Mg and K in stems are given in Table 5.18 (Section 5.2).

Table 7.16 Average values used for the biomass, turnover constants and the Ca, Mg, K and S content in leaves (needles) and fine roots of the considered tree species<sup>1)</sup>

Tree species	Biomass (kg ha <sup>-1</sup> )		Turnover constants (yr <sup>-1</sup> )		Content in leaves (%)			Content in fine roots (%)		
	leaves	fine roots	leaves	fine roots	Ca	Mg	K	Ca	Mg	K
Scots pine	5500	5000	0.55	1.4	0.35	0.08	0.51	0.13	0.05	0.15
Black pine	7250	5000	0.35	1.4	0.52	0.11	0.55	0.06	0.04	0.13
Douglas fir	10850	4700	0.28	1.4	0.33	0.10	0.43	0.21	0.02	0.05
Norway spruce	16600	5650	0.20	1.4	0.38	0.06	0.68	0.27	0.07	0.34
Japanese larch	4350	5200	1.0	1.4	0.48	0.15	1.11	0.27	0.07	0.34
Oak	3300	5500	1.0	1.4	0.94	0.18	0.94	0.27	0.09	0.35
Beech	2850	6500	1.0	1.4	0.41	0.08	0.88	0.12	0.03	0.16

<sup>1)</sup> Owing to limited data, the S content was set to 0.2% for leaves and to 0.05% for fine roots for all tree species (cf De Vries et al., 1990)

Table 7.17 Average values used for the minimum and maximum N content in leaves (needles) and fine roots of the considered tree species

Tree species	N content in leaves (%)		N content in fine roots (%)	
	min. <sup>1)</sup>	max.	min. <sup>1)</sup>	max.
Scots pine	1.0 (2.0)	3.5	0.4 (0.7)	1.0
Black pine	1.0 (2.0)	2.5	0.4 (0.7)	1.0
Douglas fir	1.0 (2.0)	3.5	0.4 (0.7)	1.0
Norway spruce	1.5 (2.5)	3.5	0.5 (1.0)	1.5
Deciduous trees <sup>2)</sup>	1.5 (2.5)	3.5	0.5 (1.0)	1.5

<sup>1)</sup> Values between brackets are the minimum N contents below which maximum reallocation occurs. Maximum N contents where reallocation is negligible were set equal to the absolute maximum values

<sup>2)</sup> Oak, beech and Japanese larch

Maximum values used for the mineralization rate constants were 0.4 yr<sup>-1</sup> for fresh litter, 0.05 yr<sup>-1</sup> for old litter and 0.17 yr<sup>-1</sup> for root necromass based on a literature survey (De Vries et al., 1990). Values were reduced as a function of ground water level and pH (De Vries et al., 1988).

#### Data related to soil type

For each soil horizon in each of the considered soil types considered, data were gathered on soil variables, soil properties and soil constants, i.e. rate and equilibrium constants influencing the rate of the modelled soil processes. The rooting zone of the considered soil types varied between 60 and 80 cm. An overview of the designation and thickness of the horizons in the fourteen soil profiles considered has been given in De Visser and De Vries (1989).

Initial cation contents on the adsorption complex were based on available data for about 220 soil samples, sampled in the period between 1970 and 1990 (e.g. Kleijn et al.,

1989). Generally, base saturation was less than 10%, whereas Al saturation was more than 60%. The relative occupation of K, Na and  $\text{NH}_4$  on the adsorption complex was very low. Average values used for element amounts in Al hydroxides and in primary minerals (Table 7.18) were derived from a soil information system (Bregt et al., 1986; Al hydroxide contents) and from laboratory analyses on several sandy soils (total contents of Ca, Mg, K and Na). Total contents of K + Na were much higher than those of Ca + Mg (Table 7.18). These data agree well with the fact that K and Na feldspars are the dominant primary minerals in Dutch sandy soils.

Table 7.18 Average values used for Al hydroxide - and total base cation contents in A, B and C horizons of the considered soil types<sup>1)</sup>

Soil type (FAO, 1988)	$\text{Al}_{\text{ox}}$ (mmol <sub>c</sub> kg <sup>-1</sup> )			Ca + Mg (mmol <sub>c</sub> kg <sup>-1</sup> )			K + Na (mmol <sub>c</sub> kg <sup>-1</sup> )		
	A	B	C	A	B	C	A	B	C
Cambic Podzol	95	185	90	75	70	80	385	375	400
Gleyic Podzol	160	220	95	40	55	90	160	295	365
Carbic Podzol	150	350	115	45	65	105	265	55	370
Fimic Anthrosol	95	275	140	100	105	110	540	480	410
Umbric Gleysol	90		30	115		130	400		470
Haplic Arenosol <sup>1)</sup>	55		65	135		75	910		400

<sup>1)</sup> The same data were used for both fine and coarse sandy soils

<sup>2)</sup> Including Gleyic Arenosol

Data on the bulk density ( $\rho$ ), cation exchange capacity (CEC) and sulphate sorption capacity (SSC) were all derived by relationships with basic soil data (pedotransfer functions) as given in Table 7.19. Overall soil constants, that were used independent of soil type and soil layer, are given in Table 7.20.

Table 7.19 Transfer functions between soil properties and basic soil data

Soil properties	Transfer functions	Reference
$\rho$ (kg m <sup>3</sup> )	$1000 / (a_0 + a_1 \cdot ctC)^{1)}$	Hoekstra and Poelman (1982)
CEC (mmol <sub>c</sub> kg <sup>-1</sup> ) <sup>2)</sup>	$15.2 \cdot ctC$	Kleijn et al. (1989)
SSC (mmol <sub>c</sub> kg <sup>-1</sup> )	$0.02 \cdot ctAl_{\text{ox}}^{3)}$	Johnson and Todd (1983)

<sup>1)</sup> Data for  $a_0$  and  $a_1$  in acid sandy soils generally ranged between 0.6 and 0.65 and between 0.04 and 0.06 respectively, depending upon soil type and soil horizon.

The organic carbon content (%) of the various soil types and soil horizons was derived from the Dutch soil information system (Bregt et al., 1986)

<sup>2)</sup> Refers to the value at the actual pH in the field

<sup>3)</sup> Oxalate-extractable Al in mmol<sub>c</sub> kg<sup>-1</sup>

Dissolution rate constants for Al hydroxides (cf Eq. 6.53; Section 6.2) were obtained from one-year batch experiments on nearly all soil types and soil horizons included in the regional application (Section 3.3; De Vries et al., 1994g). Values varied mostly between  $10^{-4}$  and  $10^{-8}$  m<sup>3</sup> kg<sup>-1</sup> yr<sup>-1</sup> for  $\text{KEI}_1$  and between 5 and 13 for the product of  $\text{KEI}_2$  and  $ctAl_{\text{ox}}$  (cf Section 3.3). Weathering rate constants were also based on one-year batch experiments. Results were scaled to field conditions by division with a factor 50,



Table 7.20 Overall soil constant used in the simulation

Soil constant	Unit	Value	Derivation
Nitrification rate constant <sup>1)</sup>	yr <sup>-1</sup>	40	Calibration <sup>2)</sup>
Denitrification rate constant <sup>1)</sup>	yr <sup>-1</sup>	10	Via Reddy et al. (1982)
Protonation rate constant <sup>1)</sup>	yr <sup>-1</sup>	40	Calibration <sup>2)</sup>
Equilibrium constant for Al hydroxides dissolution	mol <sup>-2</sup> l <sup>2</sup>	10 <sup>8.0</sup>	Via De Vries and Leeters (1994) <sup>3)</sup>
SO <sub>4</sub> adsorption constant	m <sup>3</sup> mol <sub>c</sub> <sup>-1</sup>	1.0	Singh and Johnson (1986); Foster et al. (1986)

1) Maximum values that were reduced as a function of the organic matter content, ground water level and/or pH (cf De Vries et al., 1988)

2) Calibration on data with respect to nitrification rates (Tietema and Verstraten, 1991; Tietema et al., 1990) and NH<sub>4</sub>/NO<sub>3</sub> ratios and RCOO concentrations in the various layers of forest soils (Van Breemen and Verstraten, 1991; Heij et al., 1991)

3) Based on the soil solution composition below the rooting zone of 150 forest stands

based on field weathering rates estimated by the depletion of base cations in the soil profile and budget studies (De Vries and Breeuwsma, 1986; Van Breemen et al., 1986). Values generally ranged between 5.10<sup>-6</sup> and 5.10<sup>-4</sup> yr<sup>-1</sup> for K and Na and between 2.10<sup>-5</sup> and 5.10<sup>-4</sup> yr<sup>-1</sup> for Ca and Mg. Weathering rates calculated for the total soil profile were equal to those given in Table 5.17 (Section 5.2).

Cation exchange constants were derived from the simultaneous measurement of the cations H, Al, Ca, Mg, K, Na and NH<sub>4</sub> on the adsorption complex and in the soil solution of the most important soil types, i.e. all Podzols and the Haplic Arenosol (Kleijn et al., 1989). Average values thus derived for podzolic soils (Table 7.21) show the high affinity of the adsorption complex for protons compared to all other monovalent cations.

Table 7.21 Average cation exchange constants used for A, B and C horizons of the considered podzolic soils

Soil horizon	Exchange constants related to Ca (mol l <sup>-1</sup> )z <sub>x</sub> <sup>-2</sup>					
	H	Al	Mg	K	Na	NH <sub>4</sub>
A	39500	2.2	0.28	0.30	0.69	170
B	126000	16.0	0.36	1.8	2.7	5940
C	39000	4.4	0.85	8.1	4.0	5430

z<sub>x</sub> is the valence of ion X competing with Ca

#### Data related to tree species and soil type

For all considered combinations of tree species and soil type, hydrologic data and stem growth data were collected. Annual average waterfluxes and soil moisture data were calculated with the hydrological model SWATRE (Belmans et al., 1983) for an average hydrological year in the period 1950 to 1980 with a total precipitation of 780 mm yr<sup>-1</sup> (De Visser and De Vries, 1989). Infiltration of water was calculated by subtracting interception evaporation and soil evaporation from the precipitation. Water fluxes in each

layer were derived by subtracting the transpiration flux in each layer from the infiltration rate. Information on the waterflux per layer has been given in De Visser and De Vries (1989). The resulting precipitation excess (water flux leaving the root zone) thus calculated showed a decrease in the direction deciduous forests (oak, beech and the needle shedding Japanese larch) > pine forests (Scots pine and black pine) > spruce forests (Douglas fir and Norway spruce) (Table 7.22).

Table 7.22 Annual average precipitation excesses used for pine, spruce and deciduous forests on the considered soil types<sup>1)</sup>

Soil type (FAO, 1988)	Precipitation excess (mm yr <sup>-1</sup> )		
	Pine	Spruce	Deciduous
Cambic Podzol	225	169	278
Gleyic Podzol	165	100	221
Carbic Podzol	208	146	264
Fimic Anthrosol	212	151	267
Umbric Gleysol	133	97	221
Gleyic Arenosol	221	200	
Haplic Arenosol	208	146	264

<sup>1)</sup> The precipitation excesses refer to fine sandy variants. In coarse sandy soils, precipitation excesses were taken 60 mm yr<sup>-1</sup> higher

Annual tree growth was kept constant during the simulation period. Values were based on the average annual stem growth rate during the lifetime of a tree. The uptake in branches was neglected since tree harvesting in the Netherlands is restricted to stemwood removal only. RESAM also includes an option to simulate tree growth as a function of time using a logistic function. However, this option was not considered feasible for a regional application because it requires information on the initial stem mass on a regional scale. Growth rates of stems were derived by defining suitability classes (good, medium or low) for each tree/combination, which in turn were related to an average growth rate (Table 7.23). Growth rates were based on a literature survey (De Vries et al., 1990).

Table 7.23 Average growth rates used for the considered forest/soil combinations

Soil type (FAO, 1988)	Growth rate (m <sup>3</sup> ha <sup>-1</sup> yr <sup>-1</sup> ) <sup>1)</sup>						
	Scots pine	Black pine	Douglas fir	Norway spruce	Japanese larch	Oak	Beech
Cambic Podzol	7.1	10.0	14.7	8.9	10.9	6.0	6.0
Gleyic Podzol	7.1	10.0	11.1	8.9	10.9	6.0	6.0
Carbic Podzol	5.5	7.4	6.6	5.0	5.7	4.0	4.0
Fimic Anthrosol	7.1	10.0	14.7	13.6	14.0	8.0	8.0
Umbric Gleysol	7.1	10.0	11.1	13.6	14.0	8.0	6.0
Haplic Arenosol <sup>2)</sup>	3.1	5.0	6.6	5.0	5.7	4.0	4.0

<sup>1)</sup> The growth rates refer to fine sandy variants. In most cases growth rates on coarse sandy variants were assumed to be similar

<sup>2)</sup> Including Gleyic Arenosol

### *Data derived by model initialization*

Initial (i.e. 1990) element concentrations in the soil layers of the considered forest/soil combinations in all deposition areas were derived by running the model during 25 years (1965-1990) using historical emission-deposition data. Anion concentrations in 1965 were estimated from the annual atmospheric input at that time and the annual average water flux per layer. Cation concentrations in 1965 were derived by combining the charge balance equation with the various cation exchange equations, using the given amounts of adsorbed cations and cation exchange constants in the soil database. The adsorbed amounts of  $\text{SO}_4$  and cations were continuously updated during the initialization period (1965-1990) but the cation amounts in primary minerals and in hydroxides were kept constant. Initial humus amounts were simulated by assuming that all forests stands were planted in the beginning early part of the 20<sup>th</sup> century, succeeding heathlands, without any humus layer. Element contents in litter in 1965 were taken equal to needle contents and were continuously updated during the initialization period.

## COMPARISON OF MODEL RESULTS AND FIELD DATA

### **Limitations of the comparison**

To gain insight in the reliability of the model predictions from 1990 onwards, a comparison was made between results of the 550 model simulations on the soil solid phase and soil solution chemistry in 1990 with measurements in 150 forest stands during the period March to May in the same year (cf Section 2.3; De Vries et al., 1994h). The tree species and soil types included in the field survey were similar to those included in the simulations. However, one should be aware of the following differences:

- 1 The distribution of tree species differed between the field survey and the simulation runs. For the comparison, the model results were not weighted with the area of the considered forest/soil combinations. This was done since weighting with the area caused a much larger bias (cf Table 7.24). The higher occurrence of Douglas fir and Norway spruce in the model results compared to the field data (cf Table 7.26) will tend towards higher estimated concentrations since these tree species have a relatively high filtering capacity and evapotranspiration compared to the other coniferous tree species. The distribution of soil types also differed between the field survey and the model simulations with a clear bias to poorly drained soil types, such as Umbric Gleysols, in the field survey.
- 2 RESAM predicted water flux weighted annual average concentrations, whereas the field data were single measurements in early spring. Comparison of those concentrations in intensively monitored plots (Section 2.3) showed reasonable agreement. Furthermore, the concentrations in the field were influenced

Table 7.24 Distribution of tree species in the field survey (n=150) and model simulations (n=550)

Tree species	Field survey distribution (%)	Model comparison distribution <sup>1)</sup> (%)	Model prediction distribution <sup>2)</sup> (%)
Scots Pine	30	20.6	53.3
Black Pine	10	9.7	6.3
Douglas Fir	10	12.6	7.1
Norway Spruce	10	12.6	4.4
Japanese Larch	10	12.7	6.3
Oak	20	23.8	19.0
Beech	10	8.2	3.6

1) Excludes information about the area of the forest soil combinations, i.e. each result is considered of equal importance: used for comparison of model results and field data

2) Includes information about the area of the forest soil combinations: used for model predictions only

by the actual water fluxes in each stand for the year 1990, whereas RESAM used water fluxes based on 30 year averaged meteorologic data (differences in temporal scale).

- RESAM predictions for the topsoil were an average of two soil layers with a total depth varying between 20 and 30 cm, whereas the topsoil in the field data set referred to a layer of 0 to 30 cm. For the subsoil, RESAM predictions related to the bottom of the rooting zone, varying between 50 and 80 cm, whereas the field data referred to a layer of 60-100 cm (differences in vertical scale).
- RESAM used average data for the deposition on each deposition area and for all soil and tree parameters, whereas the field data were influenced by the actual circumstances at each site (differences in spatial scale). It can thus be expected that the range in predicted element concentrations is smaller than the range of the field data (cf Fig. 7.18 and 7.19).

The agreement between field data and model results, that was investigated by comparing inverse cumulative frequency distributions of the various chemical parameters is discussed below. The frequency is given as the forested area (%) with soils above a certain element concentration (in mol<sub>c</sub> m<sup>-3</sup>) or element ratio (in mol mol<sup>-1</sup>).

### Comparison of frequency distributions

The agreement between model results and field data on soil parameters, i.e. N contents (Fig. 7.16A) and N amounts (Fig. 7.16B) in the humus layer and Al saturation (Fig. 7.16C) and base saturation (Fig. 7.16D) in the mineral topsoil, appeared to be good (median difference < 10%), except for the base saturation which was clearly underestimated (median difference of 35%). However, the relative large base saturation

values in the field data set were mainly related to (i) poorly drained soils, where Ca input via seepage of ground water may play a role; a process that is not included in the RESAM application and (ii) soils below oak stands, which nearly all bordering agricultural land within 50 m. These stands gain extra dry deposition inputs of Ca caused by fertilization and liming (Draayers et al., 1992) and this aspect was not included in the model application. Further reasons for the differences are given before.

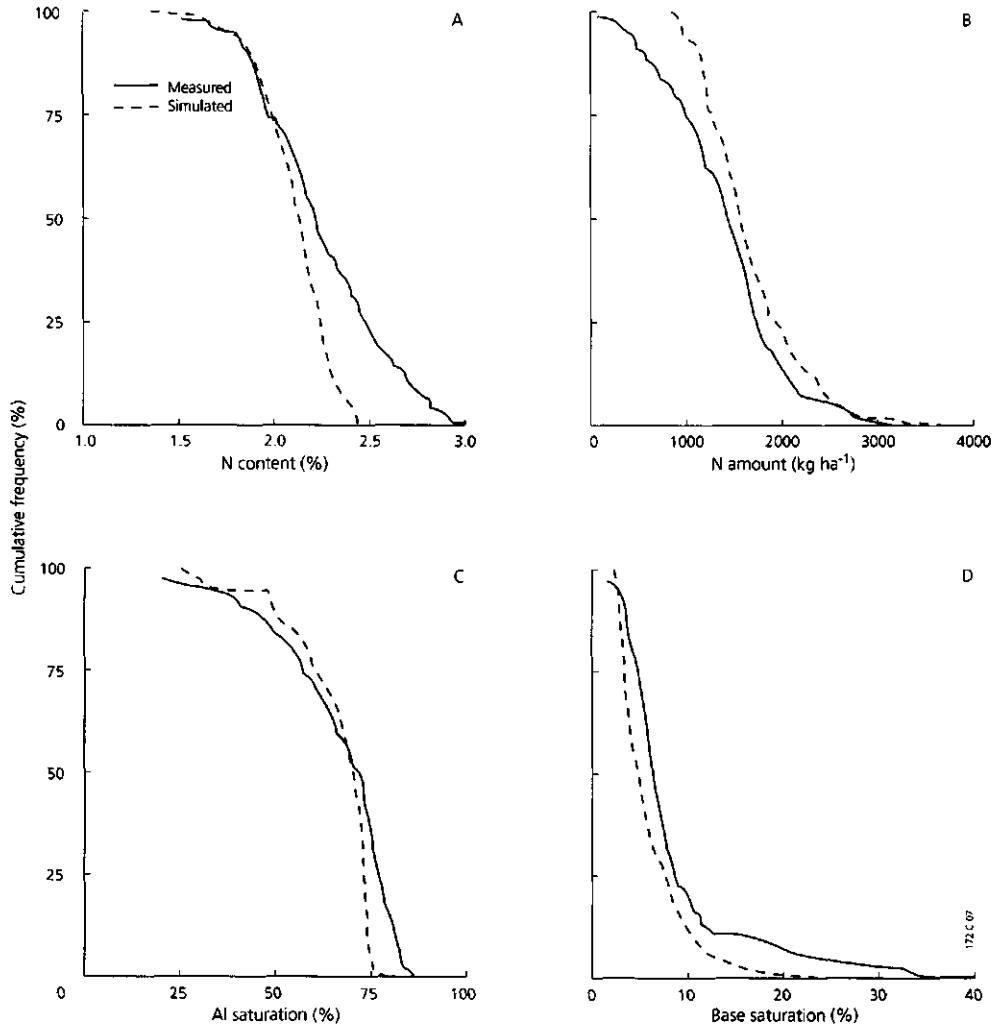


Figure 7.16 Frequency distributions of field data and model results of the N content (A) and N amount (B) in the humus layer and of the Al saturation (C) and base saturation (D) in the mineral topsoil

The agreement between field data and model results on soil solution parameters in the topsoil was good for the pH (Fig. 7.17A). The Al concentration was, however, underestimated (Fig. 7.17B), whereas the Al/Ca ratio (Fig. 7.17C) and the  $\text{NH}_4/\text{K}$  ratio (Fig. 7.17D) were overestimated. Median relative differences between model results and data ranged between 30% (Al/Ca ratio) and 60% ( $\text{NH}_4/\text{K}$  ratio).

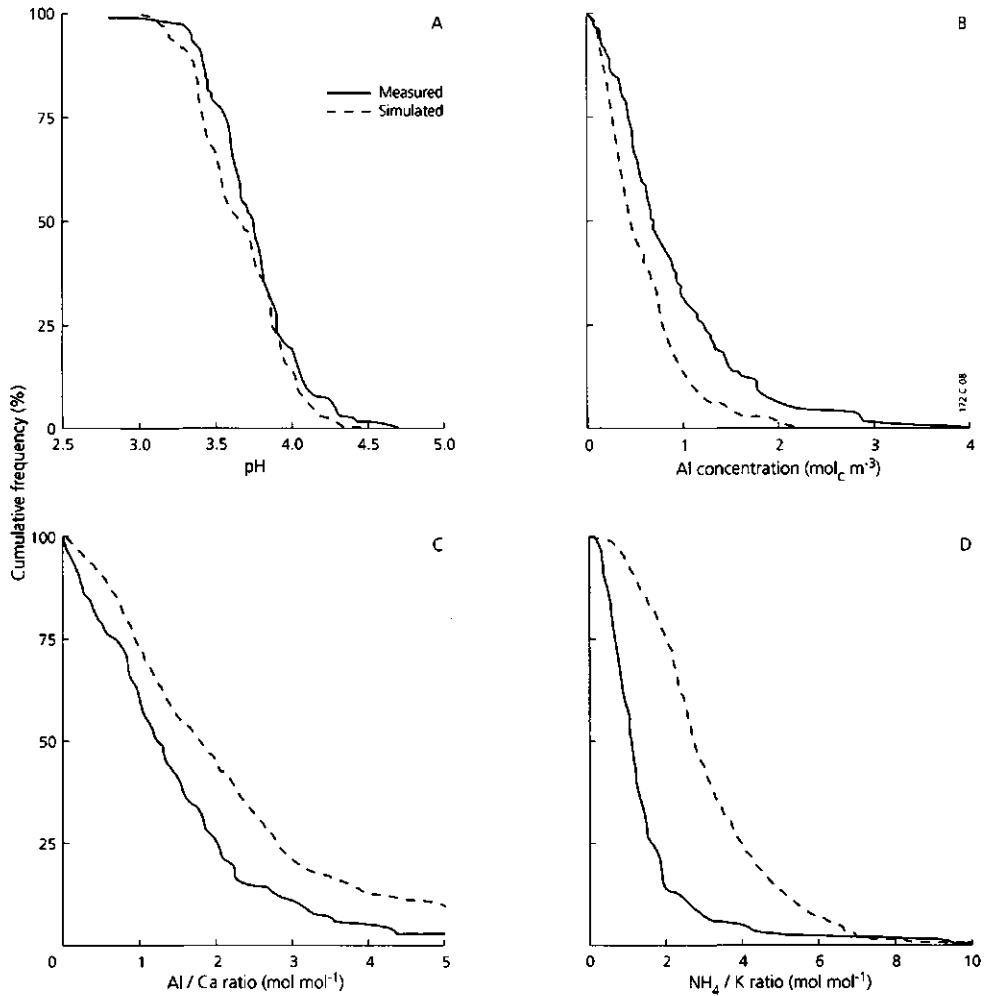


Figure 7.17 Frequency distributions of field data and model results of the pH (A), Al concentration (B), molar Al/Ca ratio (C) and molar  $\text{NH}_4/\text{K}$  ratio (D) in the mineral topsoil

In the subsoil the agreement between field data and model results was good for pH (Fig. 7.18A) and  $\text{SO}_4$  concentration (Fig. 7.18D), but the Al concentration (Fig. 7.18B) and  $\text{NO}_3$  concentration (Fig. 7.18C) where both overestimated. The comparison between model results and field data in the subsoil for the  $\text{SO}_4$  concentration was added to gain insight in the relative contribution of  $\text{NO}_3$  and  $\text{SO}_4$  in soil acidification as predicted by RESAM and measured in the field. Median (50 percentile) values for the concentrations of these elements were approximately 0.5 and 1.1  $\text{mol}_c \text{m}^{-3}$  for the field data and 0.7

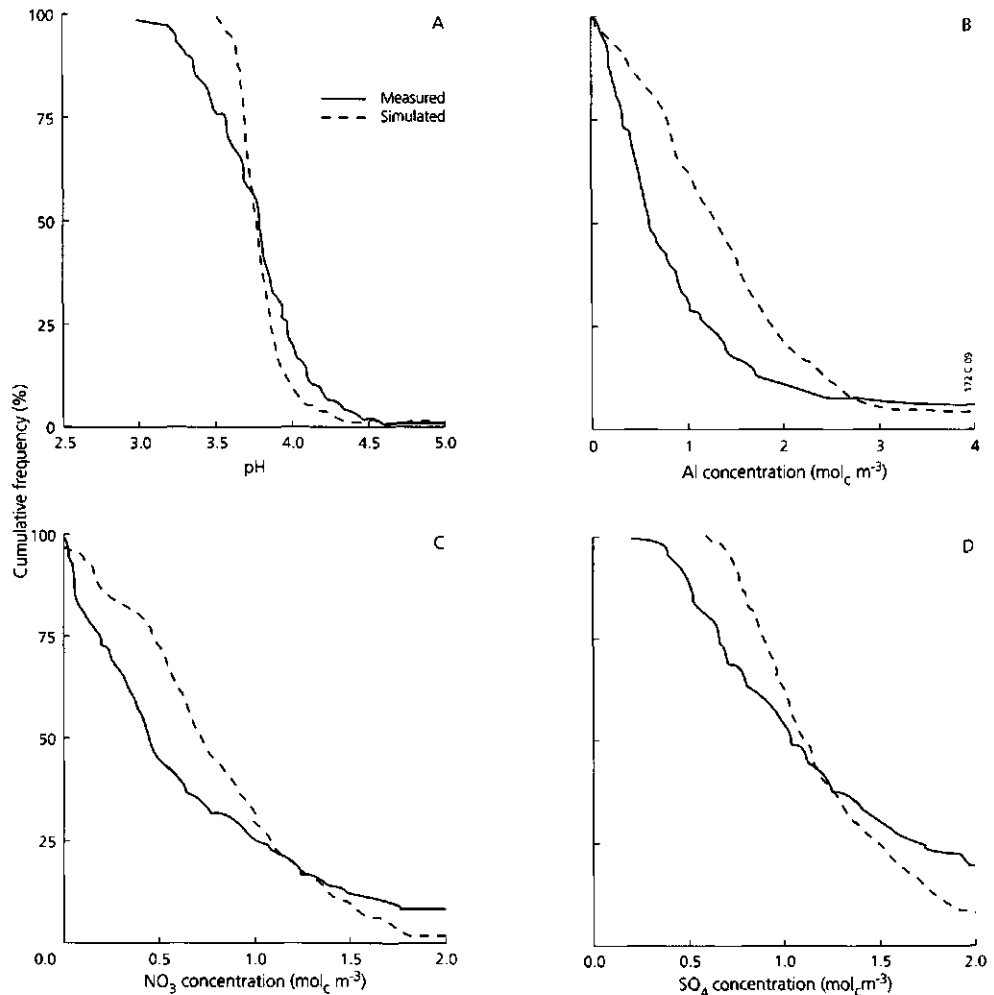


Figure 7.18 Frequency distributions of field data and model results of the pH (A), Al concentration (B),  $\text{NO}_3$  concentration (C) and  $\text{SO}_4$  concentration (D) in the mineral subsoil

and  $1.1 \text{ mol}_c \text{ m}^{-3}$  for the model predictions, respectively (Fig. 7.18C and 7.18D). RESAM thus overpredicted the contribution of N to soil acidification by about 40%.

The large differences between the predicted and measured Al concentrations in the subsoil (median values equal approximately  $1.2$  and  $0.6 \text{ mol}_c \text{ m}^{-3}$  respectively; cf Fig. 7.18B) were mainly due to an underestimation in base cation concentration. The relative poor agreements for the Al/Ca and  $\text{NH}_4/\text{K}$  ratios in the topsoil were also mainly due to an underestimation of the Ca and K concentration. In the subsoil, the underestimations of the Ca and K concentration were even more pronounced. Base cation budgets showed that this difference was most likely due to (i) measured concentrations below deciduous trees, that were much larger than flux-weighted annual average concentrations (cf Section 2.3), and (ii) an underestimation of the atmospheric input (dry deposition) of Ca and K, since uncertainties in the input by deposition have a much larger influence on the model results than uncertainties in the weathering and net uptake estimates (cf Table 7.25 for Ca). After correcting the base precipitation excess, by equating Cl input to Cl output (cf Section 2.3; Table 2.12), large underpredictions still occurred for oak, that nearly always bordered agricultural land, where base cation input can be much larger (see before), and for Douglas fir and Norway spruce with a large canopy coverage. The large differences for oak may also be due to input of Ca by ground water since most oak stands were located on poorly drained soil types. Finally, the discrepancy between model results and field data may partly be caused by the long-term effect of liming and fertilization at the time of planting.

The overestimation of the  $\text{NH}_4/\text{K}$  ratio in the topsoil was also partly due to a (small) underestimation of the nitrification rate ( $\text{NH}_4/\text{NO}_3$  ratios were lower in the field situation) and the N immobilization rate (the  $\text{NH}_4 + \text{NO}_3$  concentration is overpredicted both in the

Table 7.25 Average Ca leaching fluxes for the tree species considered, as predicted with RESAM and estimated from concentration measurements in the field

Tree species	Deposition ( $\text{mol}_c \text{ ha}^{-1} \text{ yr}^{-1}$ )	Weathering ( $\text{mol}_c \text{ ha}^{-1} \text{ yr}^{-1}$ )	Net uptake ( $\text{mol}_c \text{ ha}^{-1} \text{ yr}^{-1}$ )	Leaching ( $\text{mol}_c \text{ ha}^{-1} \text{ yr}^{-1}$ )	
				Predicted <sup>1)</sup>	Estimated <sup>2)</sup>
Scots pine	665	90	145	610	905 (935)
Black pine	700	75	130	645	880 (730)
Douglas fir	720	85	205	600	1170 (1250)
Norway spruce	785	85	295	575	1220 (1390)
Japanese larch	480	85	170	395	1375 (600)
Oak	540	90	175	455	1875 (970)
Beech	485	85	195	375	1065 (615)

<sup>1)</sup> These fluxes were calculated for a steady-state situation. Leaching thus equalled the input by deposition and weathering minus net uptake by forest growth

<sup>2)</sup> These fluxes were calculated by multiplying the annual precipitation excess for the stands with the measured Ca concentration in early spring. Values between brackets were derived by using a precipitation excess based on a fitted Cl balance for each tree species (De Vries and Jansen, 1994)



topsoil and in the subsoil; see also Fig. 7.18C and note that the  $\text{NH}_4$  concentration is very small in the subsoil). In RESAM, N mineralization and N immobilization is limited to the humus layer and this may have affected the predictions.

## MODEL PREDICTIONS

### Overall trends

#### Soil parameters

Future trends in soil chemistry, as predicted by RESAM in response to the three scenarios, are presented in Fig. 7.19 by the median value of all results, i.e. including all deposition areas, tree species and soil types. Median N contents (Fig. 7.19A) and N

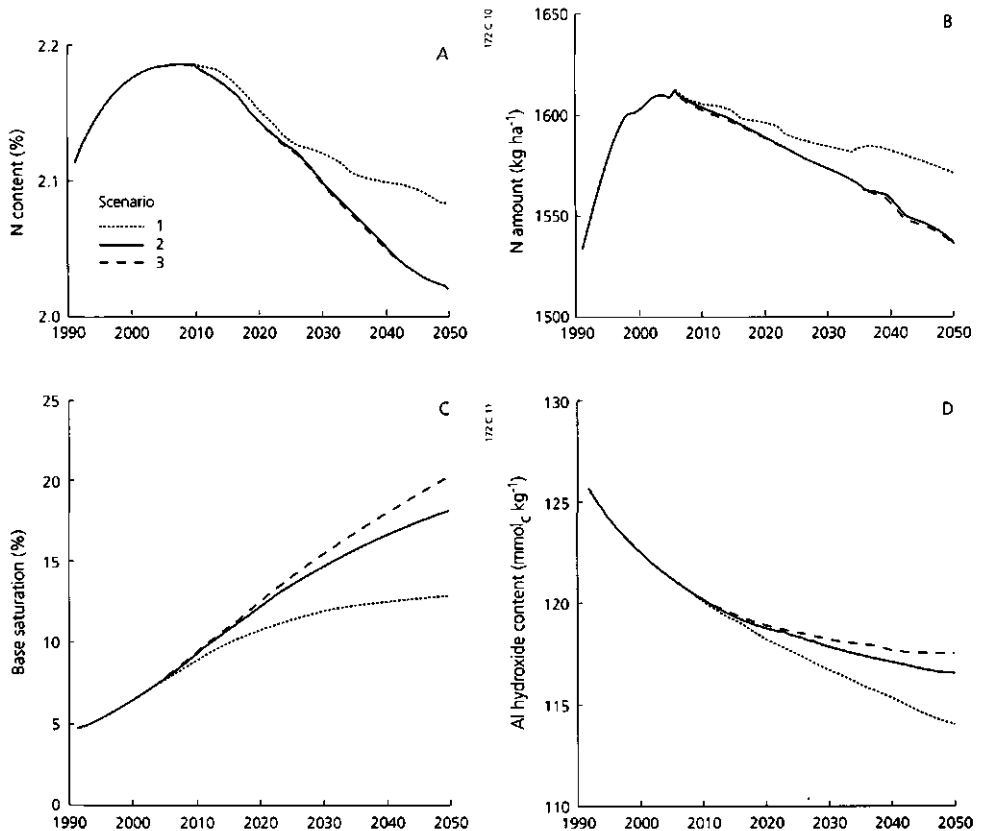


Figure 7.19 Future trends in the median N content (A) and N amount (B) in the humus layer and in the median base saturation (C) and Al hydroxide content (D) in the mineral topsoil for three deposition scenarios

amounts (Fig. 7.19B) in the humus layer increased up to 2010 followed by a steady decrease up to 2050, especially for *scenarios 2 and 3*. The difference between these scenarios was hardly discernible. Apparently, the N content in the humus layer was not yet in equilibrium with the N deposition in 1990. Between 1990 and 2000 there was no difference in trends for the three scenarios because the deposition values were similar (Fig. 7.14). N mobilization from the humus layer after 2010 was mainly due to a changing N content and not to a decrease in litter amount (cf Fig. 7.19A and 7.19B). The carbon mineralization rate was hardly affected by the small increase in pH in the humus layer.

The most important buffer mechanisms in the mineral soil are cation exchange and Al mobilization. Median base saturations predicted in the mineral topsoil (Fig. 7.19C) steadily increased with time, with clear differences between the three scenarios. However, in 2050 the base saturation generally stayed below 30%, even for *scenario 3*, although a steady-state situation was not yet reached at that time. This relatively low value was caused by Al weathering from silicates, a process that was still predicted to occur, even at a deposition level below  $1000 \text{ mol}_c \text{ ha}^{-1} \text{ yr}^{-1}$ , and by a relatively high affinity of Al for the adsorption complex. Median Al hydroxide contents in the mineral topsoil (Figure 7.19D) steadily decreased between 1990 and 2050 for *scenario 1*. The effect was much less pronounced for *scenario 2*, whereas Al hydroxide depletion nearly stopped after 2030 in *scenario 3*. The average deposition level on forests at that time was close to  $1400 \text{ mol}_c \text{ ha}^{-1} \text{ yr}^{-1}$  which indeed is the average critical acid load derived for this effect (Section 4.2; De Vries, 1993). Complete depletion of Al hydroxides, as predicted by De Vries and Kros (1989) for a 100 yr simulation with present deposition levels, was not found for any forest/soil combination in any of the scenarios. However, the average deposition targets of the three scenarios (cf Table 7.14) were remarkably lower than the deposition levels used by De Vries and Kros (1989) ( $6000 \text{ mol}_c \text{ ha}^{-1} \text{ yr}^{-1}$ ).

#### *Soil solution parameters*

Median values of the pH in the topsoil (Fig. 7.20A) and subsoil (Fig. 7.20B) showed a significant increase with time, especially in the topsoil for *scenario 2 and 3*. In response to the large deposition reduction between 1990 and 2000, a large reduction in H concentration was predicted. However, the (logarithmic) pH increased most strongly after 2000. The predicted pH increase in the topsoil was larger than in the subsoil (bottom of the rooting zone). In 2050 the ultimate median pH value in the topsoil was even higher than in the subsoil for all scenarios (cf Fig. 7.20A and 7.20B). Furthermore, the difference between *scenario 2 and 3* was much smaller than between *scenario 1 and 2*. This is consistent with the difference in average deposition values in 2050, i.e. 2240, 1230 and  $700 \text{ mol}_c \text{ ha}^{-1} \text{ yr}^{-1}$  respectively (cf Table 7.14).

Median predicted Al concentrations (Fig. 7.20C) and Al/Ca ratios (Fig. 7.20D) in the topsoil decreased considerably in response to the large deposition reduction between

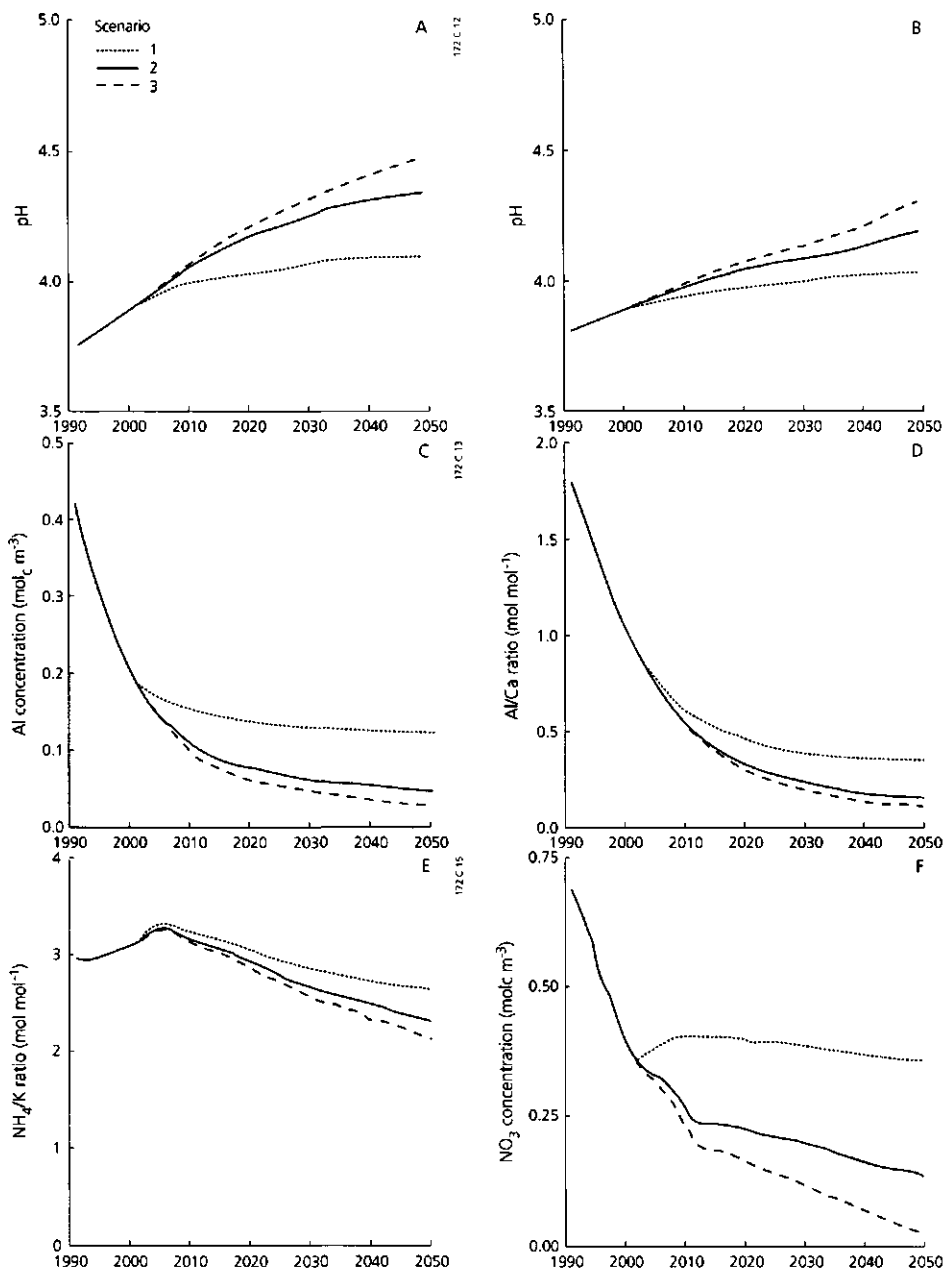


**Figure 7.20** Future trends in median values of the pH in the topsoil (A) and subsoil (B), the Al concentration (C), molar Al/Ca ratio (D) and the molar  $\text{NH}_4^+/\text{K}$  ratio in the topsoil (E) and  $\text{NO}_3^-$  concentration in the subsoil (F) for three deposition scenarios

1990 and 2000. Both values dropped below a critical value of  $0.2 \text{ mol}_c \text{ m}^{-3}$  and  $1.0 \text{ mol mol}^{-1}$  (cf Section 4.2; De Vries, 1993) respectively before the year 2000. Between 2000 and 2050 there was a small further decrease in Al concentration and Al/Ca ratio for *scenario 1* even though the deposition level remained the same. For the *scenarios 2* and *3* there was still a substantial decrease in median values especially up to 2030.

Trends in the predicted median  $\text{NH}_4/\text{K}$  ratio in the topsoil (Fig. 7.20E) and  $\text{NO}_3$  concentration in the subsoil (Fig. 7.20F) showed that these 'N related' parameters behave markedly different than the 'Al related' parameters (cf Fig. 7.20C, 7.20D). This holds especially for the  $\text{NH}_4/\text{K}$  ratio, which increased to 2000-2010 before the ratio dropped between 2000-2010 and 2050 for all scenarios. The initial increase was due to a relative small decrease in  $\text{NH}_4$  concentration and a relative large decrease in K concentration. The small decrease in  $\text{NH}_4$  was due to N mineralization from the humus layer, resulting from a decrease in the N content in litterfall (needles) in response to decreased N deposition. The relative large decrease of K was due to decreased  $\text{NH}_4$  inputs: the K concentration in the topsoil is mainly determined by foliar exudation, a process modelled in RESAM as a function of  $\text{NH}_4$  uptake, which in turn is described as a function of  $\text{NH}_4$  deposition (cf Table 7.11). Consequently, the predicted impact of the deposition scenario on the  $\text{NH}_4/\text{K}$  ratio was also relatively small (cf Fig. 7.20E).

Contrary to the  $\text{NH}_4/\text{K}$  ratio, the predicted  $\text{NO}_3$  concentration in the subsoil decreased between 1990 and 2000 but not as considerable as the Al concentration and Al/Ca ratio (Fig. 7.20F). This is due to the above mentioned N mobilization from the humus layer, which causes a time lag between the decrease in N deposition and the decrease in  $\text{NO}_3$  concentration. The median  $\text{NO}_3$  concentration in the subsoil was below a critical value of  $0.8 \text{ mol}_c \text{ m}^{-3}$  (EC-standard) in 1990, and it dropped below  $0.4 \text{ mol}_c \text{ m}^{-3}$  (target value) between 2000 and 2010 for *scenario 2* and *3* (cf Fig. 7.20F). For *scenario 1* the  $\text{NO}_3$  concentration remained just above the target value up to 2050. The small increase in  $\text{NO}_3$  concentration after 2000 in *scenario 1* (constant deposition at that time; cf Fig. 7.14) is likely to be a model artefact, i.e. an overestimation of the N mobilization from the humus layer in response to the deposition reduction before 2000.

In Figure 7.21 results on several soil solution parameters are given by the area exceeding a critical value as a function of time. The percentage of forest soils exceeding a critical Al concentration of  $0.2 \text{ mol}_c \text{ m}^{-3}$  (Fig. 7.21A) and a critical Al/Ca ratio  $1.0 \text{ mol mol}^{-1}$  respectively in the mineral topsoil (Fig. 7.21B) decreased considerably, especially for *scenario 2* and *3*. The area exceeding critical values in 1990 was approximately 80% for the Al concentration and 70% for the Al/Ca ratio, respectively. In the year 2050 this area remained approximately 30% and 10% for the Al concentration and Al/Ca ratio, respectively for *scenario 1*, whereas this area was negligible for *scenario 2*. A deposition level of  $1400 \text{ mol}_c \text{ ha}^{-1} \text{ yr}^{-1}$  (the assumed average critical acid load) on forests (*scenario 2*) was enough to avoid exceedances in Al concentration or Al/Ca ratio in forest topsoils. This might seem remarkable since this critical acid load is based on average data

regarding tree species and soil type (Section 4.2). One would thus expect about 50% exceedance at this level. However, in deriving this value a one-layer steady-state model was used. The critical acid load was related to the bottom of the rooting zone, to avoid exceedances of a critical Al concentration or Al/Ca ratio up to this depth. Critical acid loads related to a depth of 30 cm, derived by a multi-layer steady-state model (Section 5.2; De Vries et al., 1994d), were higher.

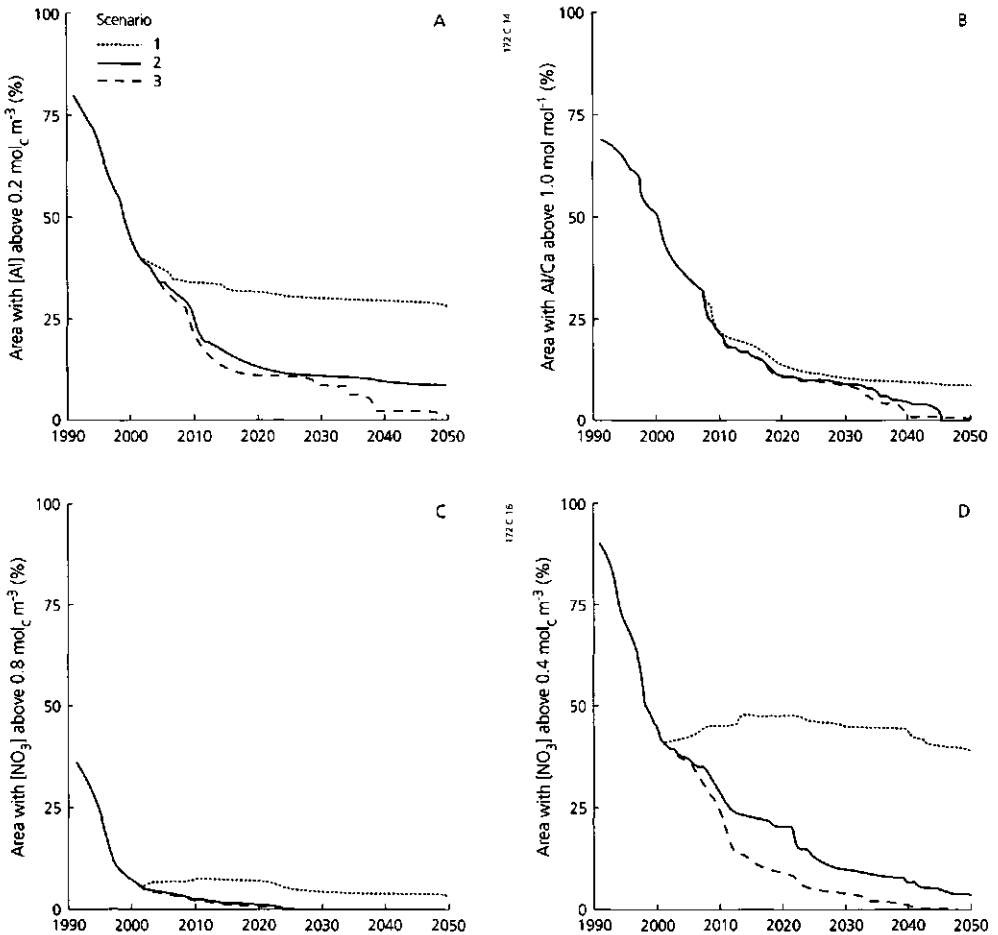


Figure 7.21 Percentage of forest soils with an Al concentration above 0.2 mol<sub>c</sub> m<sup>-3</sup> (A) and a molar Al/Ca ratio above 1.0 (B) in the topsoil and a NO<sub>3</sub> concentration above 0.8 mol<sub>c</sub> m<sup>-3</sup> (EC-standard) (C) and above 0.4 mol<sub>c</sub> m<sup>-3</sup> (target value) (D) in the subsoil for three deposition scenarios

Predicted areas exceeding the EC standard and the target value for  $\text{NO}_3$  in the subsoil (cf Fig. 7.21C,D) decreased from approximately 35% and 90%, respectively in 1990 to nearly zero in 2050 for the *scenarios 2 and 3*. For *scenario 1* the area exceeding the target value for  $\text{NO}_3$  was also negligible in 2050, whereas this area still remained approximately 40% for the area exceeding the EC standard for  $\text{NO}_3$  (cf Fig. 7.21C,D). Trends in the area exceeding a critical  $\text{NH}_4/\text{K}$  ratio of 5 are not given since the predicted area exceeding this value was only 15% in 1990 but the actual exceedance in the field was almost negligible at that time (cf Fig. 7.17D).

## Trends for different tree species, soil types and deposition areas

### Tree species

The tree species influences the soil solution chemistry by differences in (i) the nutrient input, induced by differences in forest filtering, (ii) the waterflux, induced by evapotranspiration differences and (iii) the nutrient cycle, induced by differences in litter-fall and root decay. This is illustrated in Table 7.26 for the pH, Al concentration and base saturation.

Mostly, pH and base saturation increased and the Al concentration decreased in the order: Norway spruce and douglas fir > black pine and Scots pine > Japanese larch, oak and beech. The effect was most pronounced for the Al concentration. This can mainly be explained by a decrease in evapotranspiration for these tree species in that order. This implies that the solution chemistry below douglas fir, which has been the tree with major research concern within the Dutch Priority Programme on Acidification (Heij et al., 1991), is certainly not representative for Dutch forests. The solution chemistry below Scots pine appeared to be most comparable to the overall results (cf Fig. 7.17B and Table 7.26). The differences between the tree species were in agreement with the field data, although differences appeared to be larger in the field. Most likely, this is due to differences in the forest filtering of N and S compounds between the various tree species which were not included in our model application. The influence of tree species

Table 7.26 Effect of tree species on the predicted median pH, Al concentration and base saturation (BS) in the mineral topsoil for 1990, 2010 and 2050 in response to scenario 2

Tree species	pH			Al ( $\text{mol}_e \text{ m}^{-3}$ )			BS (%)		
	1990	2010	2050	1990	2010	2050	1990	2010	2050
Scots pine	3.7	4.0	4.3	0.49	0.12	0.05	3.9	8.7	18.8
Black pine	3.8	4.1	4.3	0.54	0.17	0.07	6.1	13.7	22.8
Douglas fir	3.7	4.0	4.2	0.80	0.23	0.08	4.1	8.5	17.9
Norway spruce	3.7	4.0	4.2	0.77	0.24	0.10	3.7	7.7	15.3
Japanese larch	3.9	4.2	4.4	0.31	0.09	0.04	4.6	9.7	18.4
Oak	3.9	4.2	4.4	0.30	0.09	0.04	5.6	11.6	20.7
Beech	3.7	4.0	4.4	0.36	0.08	0.04	3.3	6.3	12.7

on pH stayed constant with time, it increased for base saturation whereas it decreased in time for the Al concentration (cf Table 7.26).

### Soil type

The effect of soil type on soil and soil solution chemistry was generally less important than that of tree species since soil types included were all non-calcareous sandy soils with a low base saturation, thus being sensitive to acidification. However, a clear difference was found between well-drained and poorly-drained soils (Table 7.27). Especially in future predictions (2010 and 2050) the occurrence of denitrification caused a high pH and base saturation and a low Al concentration in wet Gleyic Arenosols soils compared to the well-drained podzolic soils. Note however that poorly drained soils only cover a very small part of Dutch forests. Consequently, the overall effect of soil type on the soil solution chemistry was quite small.

Table 7.27 Effect of soil type on the predicted median pH, Al concentration and base saturation (BS) in the mineral topsoil for 1990, 2010 and 2050 in response to scenario 2

Soil type (FAO, 1988)	pH			Al (mol <sub>c</sub> m <sup>-3</sup> )			BS (%)		
	1990	2010	2050	1990	2010	2050	1990	2010	2050
Cambic Podzol <sup>1)</sup>	3.6	3.9	4.2	0.33	0.10	0.05	7.7	14.0	23.8
Carbic Podzol <sup>2)</sup>	3.9	4.1	4.3	0.47	0.12	0.06	3.5	6.6	11.3
Gleyic Arenosol <sup>3)</sup>	3.8	4.5	5.0	0.33	0.02	0.01	7.8	19.7	46.4

<sup>1)</sup> Well-drained relative rich soil

<sup>2)</sup> Well-drained relative poor soil

<sup>3)</sup> Poorly-drained soil

### Deposition area

The soil solid phase and soil solution chemistry predictions varied for the different deposition areas in response to different acid loads. Results for the pH, Al concentration and base saturation in the most densely forested (> 5%) deposition areas (Table 7.28) generally showed small pH differences, but higher Al concentrations and lower base saturations in the deposition areas with relatively high acid loads (areas 5 and 18) compared to deposition areas with relatively low acid loads (areas 3 and 6; cf Fig. 7.14 and 7.16). As with tree species, differences in pH remained quite constant, base saturation mostly increased in time whereas the opposite was found for the Al concentration (Table 7.28).

The deposition area appeared to have a smaller influence on the soil solution chemistry than the tree species (cf Table 7.26 and Table 7.28). This also explains why the difference between deposition area 3 and 5 was much smaller than we expected from the difference in average deposition values between these areas. Deposition area 3 contains a relative large number of Norway spruce stands (cf Table 7.13), for which relatively high Al concentrations and low pH and base saturations were predicted. The influence of tree species thus overshadowed the influence of deposition areas. This is

*Table 7.28 Effect of deposition area on the predicted median pH, Al concentration and base saturation (BS) in the mineral topsoil for 1990, 2010 and 2050 in response to scenario 2*

Deposition area	pH			Al (mol <sub>c</sub> m <sup>-3</sup> )			BS (%)		
	1990	2010	2050	1990	2010	2050	1990	2010	2050
3	3.8	4.1	4.4	0.48	0.13	0.05	3.8	6.9	13.2
5	3.8	4.0	4.3	0.39	0.12	0.07	3.1	6.5	10.0
6	3.8	4.1	4.5	0.30	0.07	0.04	4.9	9.6	18.6
18	3.5	3.9	4.2	0.56	0.14	0.06	3.2	7.2	12.9

illustrated in Figure 7.22, which shows the spatial variability in the area of forest soils exceeding a critical Al concentration of 0.2 mol<sub>c</sub> m<sup>-3</sup> in the topsoil in 1990 and 2000. The relationship between this result and the spatial variability in the deposition of potential acidity (cf Fig. 7.15) is obscured by the spatial distribution of tree species over the Netherlands.

## DISCUSSION AND CONCLUSIONS

Future predictions of the various soil and soil solution parameters with RESAM seem to be reliable in view of the reasonable to good agreement between most model results and field data. The Al/Ca and NH<sub>4</sub>/K ratio in the topsoil and the Al concentration in the subsoil were clearly overestimated, but this is most likely due to an underestimation of atmospheric deposition of base cations and possibly to the long-term effect of liming at various field sites. However, it remains difficult to indicate the reliability of long-term predictions on a national scale because of a lack of long-term series of observations to calibrate the model. Uncertainties induced by the model structure and the data do influence the reliability of the presented model predictions.

In RESAM several assumptions and simplifications are made with respect to the model structure, either because of insufficient knowledge or to limit data requirements. Essential processes in acidifying systems, which are imperfectly known include (Jenkins et al., 1989); (i) the dynamics of organic matter including the behaviour of dissolved organic matter (DOC); (ii) the dynamics of solid phase Al and Al complexation by organic anions; (iii) N transformations in the soil, i.e. mineralization, nitrification and denitrification, and (iv) the dynamics of forest growth in relation to the acidification status of the soil. This lack of knowledge is reflected in RESAM by (i) neglect of the role of DOC, and (ii) the formation of complexes between Al and organic anions, (iii) a simple description of N transformation processes, and (iv) the assumption of a steady-state situation in the various tree compartments except for stem growth.

Uncertainties in Al and N dynamics may seriously affect the quality of the model predictions (De Vries and Kros, 1989; Kros et al., 1993). Furthermore, the annual (input)



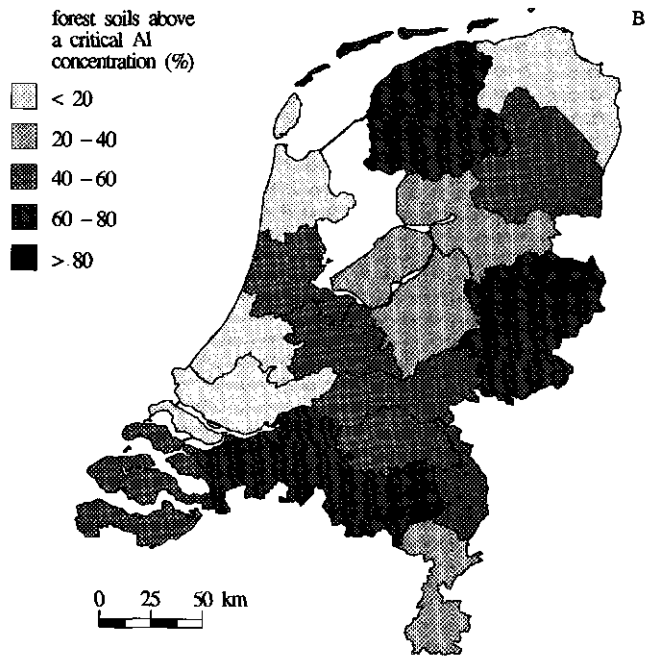
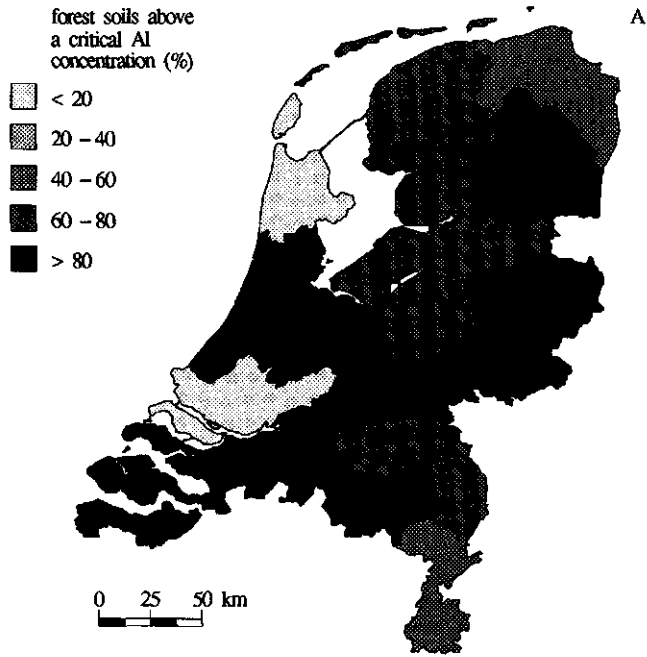


Figure 7.22 Geographic distribution of the area (% of total forested area) exceeding a critical Al concentration of  $0.2 \text{ mol}_c \text{ m}^{-3}$  in 1990 (A) and 2000 (B)

time step of the model may affect the long-term predictions but this effect is likely to be small (Kros et al., 1994). Although the model structure is possibly an important source of uncertainty, it is very difficult or even impossible to quantify.

The spatial variability and the uncertainty in the initial conditions of model variables and model parameters implies that the range in field data for chemical soil and soil solution parameters will be larger than in the model predictions. Regarding soil variables and soil properties, the uncertainty in the soil type depicted on the soil map may cause deviations. However, the aspect of spatial variability is particularly important. In this model application, average data were used for each tree species and soil type. Results of an uncertainty analysis showed that a simulation run using average data gave nearly similar trends in soil solution chemistry as the mean of 200 simulation runs in which the variability of input data was included (Kros et al., 1990; 1993). In this study, RESAM thus reproduced the mean behaviour of each forest/soil combination but not the extremes. The importance of including spatial variability in soil data was illustrated by De Vries et al. (1993) who predicted the effects of similar deposition scenarios up to 2050 on the Al hydroxide content of Dutch forest soils, using a much simpler model than RESAM. The model was applied on a national scale using a finer resolution for the deposition inputs, i.e. a 10 km x 10 km grid. Furthermore, the variation in Al hydroxide content in each soil type was included in the calculations by using ten percentile values (5, 15, ..., 95 percentile) instead of one average value. It was assumed that each percentile represented 10 percent of the area of the soil occurring in each grid. As with the RESAM predictions, results showed that the average depletion of Al hydroxides up to 2050 was low (8 to 12% depending on the scenario) but a depletion up to 50% and more was predicted for sensitive soils in areas with intensive animal husbandry.

Despite the uncertainties involved it can be concluded that RESAM produces plausible average results and it is a useful tool to help policy makers in choosing an optimal emission abatement scenario. Major conclusions that can be drawn from this study are:

- deposition reductions lead to a fast improvement of the soil solution chemistry i.e. an increase in pH and a decrease in Al and  $\text{NO}_3$  concentration and Al/Ca and  $\text{NH}_4/\text{K}$  ratio. Effects on the solid phase chemistry such as the N content in the humus layer and the base saturation appear to be lower.
- deposition reductions according to scenario 1 (up to  $2240 \text{ mol}_c \text{ ha}^{-1} \text{ yr}^{-1}$ ) are not sufficient, to reduce the effects of N and Al to an insignificant level, whereas reductions according to scenario 3 (up to  $700 \text{ mol}_c \text{ ha}^{-1} \text{ yr}^{-1}$ ) are overdone. Using the area above a critical level as a means to evaluate the deposition scenarios, reductions up to  $1400 \text{ mol}_c \text{ ha}^{-1} \text{ yr}^{-1}$  as an average for Dutch forest areas (scenario 2) appear to be enough to avoid substantial (< 10%) exceedance of a critical Al concentration ( $0.2 \text{ mol}_c \text{ m}^{-3}$ ) and molar Al/Ca ratio (1.0) in the topsoil and a critical  $\text{NO}_3$  concentration ( $0.4 \text{ mol}_c \text{ m}^{-3}$ ) in the subsoil. Reductions up to this level are also enough to avoid depletion of Al hydroxides.

- differences in (the median) soil solution chemistry between the various deposition areas in 1990 are relatively small compared to differences between tree species. The influence of tree species and deposition areas decreases in future predictions due to deposition reductions.

# **Chapter 8**

## **GENERAL DISCUSSION AND CONCLUSIONS**

## 8 GENERAL DISCUSSION AND CONCLUSIONS

This thesis deal with various research questions regarding the impact of acid atmospheric deposition on soils. Answers to most of these questions have a clear impact on policy measures regarding emission reductions for  $\text{SO}_2$ ,  $\text{NO}_x$  and  $\text{NH}_3$ . Answers to these questions, are summarized and evaluated in view of their reliability.

- (i) *What is the relative contribution of natural soil forming processes, land use and acid deposition to the acidification of soils in the Netherlands ?*

Acid atmospheric deposition is the dominant source of acidification in non-calcareous non-agricultural (sandy) soils in the Netherlands, whereas natural soil forming processes and land use are major sources of acidification in calcareous soils and agricultural soils, respectively. These conclusions can be derived from the data presented in Section 2.1 and Section 2.2.

The perspective of Krug and Frink (1983) and Krug (1991) that acid deposition is a minor contributor to soil acidification is largely due to an erroneous definition of soil acidification. This process should not be defined as an increase in exchangeable and dissolved acidity (decrease in base saturation and in pH) since acid inputs to the soil are only partially reflected by these 'intensity factors'. The rate in which exchangeable or soluble acidity increases for a given acid inputs reflects the sensitivity of a soil to acidification (De Vries et al., 1989a). A quantitative comparison of the contribution of different sources of acidification can only be based on 'capacity factors'. Consequently, the definition of soil acidification introduced by Van Breemen et al. (1983) was used in Section 2.1 and Section 2.2, i.e. a decrease in the acid neutralizing capacity (ANC) of the soil solid phase, where ANC is defined as the sum of the weatherable and exchangeable cations (basic components) in the soil. According to this definition, the rate of soil acidification can be derived from the removal rate of cations by uptake (biomass removal) and leaching from the soil. In case of cation leaching, the accompanying anion gives information about the cause of acidification. Natural soil acidification, resulting from dissociation of  $\text{CO}_2$  and organic acids, is reflected by  $\text{HCO}_3^-$  and/or  $\text{RCOO}^-$  leaching, whereas anthropogenic soil acidification, caused by enhanced deposition of  $\text{SO}_x$ ,  $\text{NO}_y$  and  $\text{NH}_x$  is reflected by leaching of  $\text{SO}_4$  and  $\text{NO}_3$  (cf Section 2.1).

- (ii) *What are the current impacts of atmospheric S and N deposition on the solution chemistry of Dutch forest soils ?*

Elevated atmospheric deposition of N and S compounds is mainly reflected by elevated concentrations of  $\text{SO}_4$ ,  $\text{NO}_3$  and Al in Dutch acid sandy forest soils.  $\text{SO}_4$  behaves

conservatively, whereas N is still retained. The acid input is mainly neutralized by Al dissolution. BC release by weathering and cation exchange only plays a minor role in buffering acid inputs. These major conclusions can be derived from results of input-output budgets of major ions in 165 forest stands on non-calcareous sandy forest soils in the Netherlands (Section 2.3).

The fate of N in Dutch forest soils is not unequivocal from the results of the various field studies. Input-output budgets of 147 survey sites, in which the soil solution composition was measured only once in early spring 1990, indicated a large N retention (a median retention of 80% of the N input). Input-output budgets of ten intensively (biweekly or monthly) monitored sites gave a similar result. Except for one site where N leaching exceeded N deposition, annual N retention varied between 31 and 100% of the N input, with an average of 63%. Input-output budgets of eight extensively (four times in one year) monitored sites, however, indicated that complete N saturation (N leaching equals or exceeds N deposition) occurs at an atmospheric N input above  $4 \text{ kmol}_e \text{ ha}^{-1} \text{ yr}^{-1}$ . Leaching estimates from the extensively monitored sites are, however, quite unreliable, since they were derived by multiplying an estimated, Cl-corrected, annual precipitation excess with a single concentration measurement in spring (cf Section 2.3). The same holds for the 147 survey sites. However, in the latter case median values for the N retention in soils below different tree species may still be rather accurate. The large number of sites most likely causes an averaging of the errors in input-output budgets for individual sites. This is supported by the calculated median  $\text{SO}_4$  leaching below each tree species, which equalled median  $\text{SO}_4$  deposition. This is in accordance with results from the (intensively) monitored sites, which also indicate conservative behaviour of  $\text{SO}_4$ . Summarizing, it is most likely that N is still largely retained in Dutch forest soils.

Whether Dutch forests are approaching complete N saturation (defined as a situation where N outputs from the system equal N inputs to the system) strongly depends on the (dis)equilibrium between N input to the humus layer by litterfall and the N output from this layer by mineralisation, respectively. N immobilization in this layer is likely to be the most important cause of N retention. Immobilization may be due to an increase in the pool of organic matter and in the N content in organic matter. The organic matter pool in the humus layer of Dutch forests generally varies between 20 and 100  $\text{ton ha}^{-1}$ , whereas the N content in organic matter generally ranges between 1.8% and 2.8% (De Vries and Leeters, 1994). Assuming a steady-state pool of organic matter, the maximum increase in the pool of organic N would equal  $1000 \text{ kg ha}^{-1}$  (an increase in N content from 1.8% to 2.8% in an organic matter pool of  $100 \text{ ton ha}^{-1}$ ). Even though the median increase in this pool will be much lower, it still may cause an appreciable retention of N during some decades, especially when one considers that organic matter still accumulates in many humus layers of Dutch forests (Van den Burg and Schoenfeld, 1988; cf Section 4.1). Furthermore, N may be retained in the organic pool in the mineral soil. The potential increase in this pool is even much larger than in the humus layer (De Vries and Leeters, 1994) the biological activity is much less, except for the top 10 cm

(Tietema, 1992). Even at the high N inputs encountered in the Netherlands, complete N saturation may thus still await some time. However, unless N inputs are decreased, it is clear that the forest area approaching N saturation will strongly increase in the coming decades.

*(iii) What is the role of various buffer mechanisms in neutralizing the acid input to Dutch forest soils ?*

Neutralization of acid inputs in acid soils is mostly dominated by the rate-limited dissolution of inorganic (mainly amorphous) secondary Al compounds. The Al release rate can be described reasonably well as a function of the secondary Al pool and the degree of undersaturation with respect to gibbsite. This major conclusion can be derived from laboratory experiments on a large number of soil samples from acid sandy forest soils (Chapter 3).

The interpretation of secondary Al compounds responsible for Al release strongly depends on the selectivity of the extractants used. Based on the decrease in pyrophosphate-extractable Al in short-term batch experiments, Mulder et al. (1989) concluded that organic Al complexes dominate Al release in the E, B and C horizons of acid sandy soils. However, Na pyrophosphate overestimates the pool of organically complexed Al in most B and C horizons. Pyrophosphate-extractable Al in these horizons usually exceeds the maximum complexing capacity of organic carbon (cf Section 3.1 and 3.3). In the upper Ah and E horizons, this is not the case. Organic Al complexes may thus govern overall Al behaviour in the upper Ah and E soil horizons, but acid neutralization by Al release is limited in these horizons (cf Section 3.3). Results of one-year batch experiments at different Al concentration levels, however, contradict the hypothesis that an equilibrium reaction between H and organic Al is the dominating process in the Bh horizon (Section 3.2). At high Al concentrations ( $\geq 5.0 \text{ mol}_c \text{ m}^{-3}$ ) an increase in the pool of lanthanum chloride-extractable Al (organic Al complexes) was observed, whereas the pool of oxalate-extractable Al (mainly inorganic Al compounds) still decreased. This result illustrates that release of Al from secondary Al minerals can continue as long as mineral saturation is not yet attained, while the exchange of H against complexed Al is completely limited or even reversed.

In the BCs and C horizons, a dominant role of organic Al compounds is absolutely unlikely. In these horizons secondary Al silicates may play an important role. This can be derived from (i) the molar Al/Si release ratio (cf Section 3.3) and (ii) the strong effect of an increase in Al concentration level on both Al and Si release (cf Section 3.2). In the field situation, release of Al from secondary Al silicates may be the dominating mechanism in Arenosols and Gleysols (Soil profiles with an Ah and C horizon). In podzolic soils, however, Al mobilization mainly occurs in the upper A and B horizons. Long-term overall release of Al in such soil profiles is most likely dominated by rate-

limited dissolution of non-silicate pools of Al, even though complexation reactions may initially be (very) important as well.

*(iv) What are average critical loads for N and acidity on sensitive terrestrial and aquatic ecosystems in the Netherlands ?*

Critical acid loads aiming to prevent adverse effects on forests are higher ( $1100-1700 \text{ mol}_c \text{ ha}^{-1} \text{ yr}^{-1}$ ) than critical acid loads for sensitive shallow ground waters and surface waters ( $300-500 \text{ mol}_c \text{ ha}^{-1} \text{ yr}^{-1}$ ). Inversely critical N loads aiming to prevent  $\text{NO}_3$  pollution in shallow ground water are higher ( $1500-3600 \text{ mol}_c \text{ ha}^{-1} \text{ yr}^{-1}$ ) than critical N loads for forests ( $800-3000 \text{ mol}_c \text{ ha}^{-1} \text{ yr}^{-1}$ ). Critical N loads are much lower ( $500-1400 \text{ mol}_c \text{ ha}^{-1} \text{ yr}^{-1}$ ) when the criterion is to prevent changes of the vegetation in forests, heathlands and surface waters. These conclusions can be drawn from empirical data and model results presented in Chapter 4.

The critical load values derived from simple steady-state models are subject to substantial uncertainty, due to uncertainties in critical chemical values, model assumptions and input data (cf Chapters 4 and 5). This holds specifically for critical loads which aim to prevent adverse effects on forests. Critical N loads related to vegetation changes in forests, heathlands and surface waters, and critical acid loads related to fish decline in surface waters are supported by empirical data, which are in the same order of magnitude as model results. However, for forests, such empirical data hardly exist. This also implies that an exceedance of critical loads is much better correlated with the occurrence of vegetation changes (e.g. Bobbink et al., 1992) and damage to fish populations (e.g. Henriksen and Hesthagen, 1993) than with damage to forests, even though there are clear indications for such a relationship in Norway spruce forests in Germany (North east Bavaria; Lenz and Schall, 1991) and Norway (Nelleman and Frogner, 1994).

It is difficult to derive a critical load for forests because forest vitality is also influenced by natural stress factors, such as drought, frost and diseases. Development of multi-stress models in which such effects are included is therefore very important. A simple steady-state mass balance model might be too simplified for the assessment of critical loads for forests. Critical acid loads for a Norway spruce stand at Solling, Germany, derived with this model and with several integrated soil chemistry-forest effect models, however, appeared to be comparable (De Vries et al., 1994i). However, further use of such models to support the critical loads concept is, needed. Considering the various stresses on forests and the possibility of adaptation, one has to be aware that critical loads for forests mainly have a signal function. When atmospheric inputs exceed critical loads, it does not necessarily cause visible effects, or even the dieback, of forests. However, an exceedance of critical loads does affect the long-term sustainability of



forests. This risk increases when the rate at which present loads exceed critical loads is higher and the duration is longer.

(v) *What is the regional variability in the amounts by which present loads exceed critical loads on forests in the Netherlands and in Europe ?*

Current atmospheric N and S loads exceed critical N and S loads on roughly half of the forested area in Europe. The rate at which critical S loads are exceeded is extremely high (up to 12000 mol<sub>c</sub> ha<sup>-1</sup> yr<sup>-1</sup>) in former Czechoslovakia, Poland and Germany. Current N loads largely exceed critical N loads (up to 3500 mol<sub>c</sub> ha<sup>-1</sup> yr<sup>-1</sup>) in Germany, Belgium and the Netherlands. In the Netherlands, present loads of N and S always exceed critical loads for forests on non-calcareous sandy soils. The largest exceedances occur in areas with intensive animal husbandry, where emission reductions of more than 80% are needed to meet the critical loads. These major conclusions can be drawn from the results of calculations with the models START and MACAL, presented in Chapter 5.

The uncertainty in critical acid loads is predominantly influenced by uncertainties in critical values for the Al concentration and Al/Ca, or Al/BC, ratio in soil solution, and the soil layer for which these criteria are applied. However, the uncertainty is relatively small when one also aims to avoid depletion of secondary Al compounds in the soil. That criterion appears to be very stringent. Unlike a critical Al concentration or a critical Al/BC ratio, the Al depletion criterion is not related to direct toxic effects on roots. Therefore it was not used in calculating critical acid loads for forests in Europe. However, considering the necessity of having long-term sustainable forest ecosystems, the criterion is very important. Depletion of secondary Al compounds causes a further lowering of the pH and, possibly, a further decrease in the availability of P and enhanced mineralization of organic matter.

A more fundamental problem with calculated critical loads is that they are liable to change in a long-term perspective. The input data for the most simple steady-state model, i.e. deposition, weathering and uptake of base cations, nitrogen uptake, denitrification and the precipitation excess, may all change. Estimates for these input data were average values during the rotation period of a forest. However, in the long-term there may be a change in (i) BC deposition, e.g. by paving dust roads or closing limestone quarries, (ii) BC weathering, e.g. due to an increase in global temperature, (iii) uptake of BC and N, e.g. by changes in forest management such as fertilization or a different harvesting regime, (iv) denitrification, e.g. because of changes in the soil moisture regime by lowering ground water tables and (v) the precipitation excess, e.g. due to a global change in precipitation and radiation. So, other environmental problems, such as global climate change and dessication, may affect critical loads. However, considering the uncertainty in input data, these effects are comparably small.

(vi) *What is the long-term impact of current atmospheric deposition levels on soils and how does the soil react on deposition changes ?*

Long-term continuation of current acid atmospheric deposition causes a depletion of the pool of secondary Al compounds in non-calcareous forest soils and dune soils in the Netherlands within several decades. Even in slightly calcareous dune soils, this effect may occur due to fast decalcification and a fast depletion of the small pool of exchangeable base cations. Reduction of the atmospheric deposition levels lead to a fast improvement of the soil solution quality (decrease in concentrations of  $\text{SO}_4$ ,  $\text{NO}_3$  and Al and increase in pH) in acid sandy soils. However, recharging the adsorption complex with base cations takes a very long time. These are the major conclusions from results of simulations with the models SMART and RESAM, presented in Chapter 6.

Even though a validation of model outputs on measured data is not presented in this thesis (cf Van Oene and De Vries, 1994; Van der Salm et al., 1994), the good agreement between measured and simulated soil interactions or ion behaviour implies that SMART and RESAM do produce plausible results. Examples are the simulated relationship between (i) Al concentration and base saturation; cf Section 6.1, (ii) leaching of Al and that of  $\text{SO}_4$  plus  $\text{NO}_3$ ; cf Section 6.2 and (iii) pH and carbonate content; cf Section 6.3), which all agree with field measurements.

That acidification is reversible, is further supported by field data from surface waters in North America and Europe. For example,  $\text{SO}_4$  concentrations in lakes near a large copper-nickel smelter complex at Sudbury, Ontario, Canada decreased by 20-60% between 1973 and 1985 in response to a 60% reduction in  $\text{SO}_2$  emissions. The decrease in  $\text{SO}_4$  concentration was partly (about 60%) compensated by a decrease in BC concentration and partly by a decrease in Al and H concentration (an increase in alkalinity and in pH level; Dillon et al., 1986). Similar trends, although less distinct, were observed in a survey of 200 lakes within a radius of 120 km of the  $\text{SO}_2$  point source at Sudbury (Keller et al., 1986). Monitoring of several rivers in the northeastern U.S. (Smith and Alexander, 1986) and in the eastern U.S. and Canada (Thompson, 1987) between 1967 and 1983 also indicate a close correlation between reduced  $\text{SO}_2$  emissions, a decline in  $\text{SO}_4$  concentrations and an increased alkalinity in these rivers. The recent decline in  $\text{SO}_2$  emissions, and parallel decline in  $\text{SO}_x$  deposition, has also reversed acidification trends in several lakes in south-western Scotland (Battarbee et al., 1988).

The reversibility of acidification of soils and waters is also supported by field experiments. The most illustrious example is the RAIN-project (Reversing Acidification in Norway), where a 860 m<sup>2</sup> head water catchment has been covered by a transparent roof to exclude ambient acid precipitation and where rain with natural levels of seawater salts is sprayed out underneath the roof (Wright et al., 1986; 1988). After 2.5 years, concentrations of  $\text{SO}_4$ ,  $\text{NO}_3$  and  $\text{NH}_4$  in runoff were lowered by more than 50%, compensated by a decrease in BC concentrations (45%) and an increase in alkalinity

(55%; Wright et al., 1988). Similar results were observed for ion concentrations in the soil solution underneath roofed sites in the Netherlands, Denmark and Sweden (Roelofs, Catholic University, Nijmegen, pers. comm.).

The examples of fast de-acidification given above, which are in accordance with the model simulations presented in Chapter 6, hold for acidified systems with a negligible  $\text{SO}_4$  interaction and a low base saturation. Soils or catchments that retain significant amounts of  $\text{SO}_4$  may continue to acidify at reduced acid ( $\text{SO}_4$ ) deposition levels, unless  $\text{SO}_4$  inputs are lower than  $\text{SO}_4$  outputs. Long-term monitoring data of a Norway spruce stand in Solling, for example, showed a large increase in concentration levels of  $\text{SO}_4$  and concurrent Al between 1973 and 1980, in response to a slight decrease in  $\text{SO}_4$  deposition. This was mainly due to a decrease in  $\text{SO}_4$  adsorption since the soil approached  $\text{SO}_4$  saturation, with  $\text{SO}_4$  inputs being equal to  $\text{SO}_4$  outputs, in that period (Khanna et al., 1987). A decrease in acid deposition may also not reverse the acidification of soils and catchments with a high base saturation. In such systems base saturation, and concurrently base cation concentrations and pH, will still decrease at reduced acid inputs, unless the acid input is lower than the output of acidity. Such a situation was observed in Plastic Lake, southern Ontario, Canada. There, base cation concentrations, alkalinity and pH decreased over the period 1979-1985, even though acid deposition decreased in the same period (Dillon et al., 1987).

Summarizing, rapid reversibility of acidification is typical for sensitive systems, such as the non-calcareous sandy forest soils in the Netherlands. In these soils, enhanced acid deposition directly gives rise to elevated Al concentrations, whereas the reverse is true at reduced acid inputs. However, in strongly buffered systems such a prompt response can not be expected, neither at elevated nor at reduced acid inputs (cf Reuss et al., 1987).

*(vii) What is the regional variability in long-term impacts of deposition scenarios on forest soils in the Netherlands and in Europe ?*

The acidity and N status of European forest soils will not improve when current reduction plans for  $\text{SO}_2$  and  $\text{NO}_x$  emission would be implemented. The forested area where critical values for the  $\text{NO}_3$  and Al concentration and the Al/BC ratio in soil solution are exceeded will either increase ( $\text{NO}_3$  concentration and Al/BC ratio) or stay relatively constant (Al concentration). Soil acidification in Europe will only decrease drastically in response to maximum feasible emission reductions, even though N will still accumulate in forest soils. In the Netherlands, expected emission reductions will cause a fast decrease in the concentrations of  $\text{SO}_4$ ,  $\text{NO}_3$ , Al and H (increase in pH) in acid sandy soils. N mobilization from the humus layer, however, causes a clear time lag between reduction in N deposition and reduction in  $\text{NO}_3$  concentration. These are the major conclusions from the results of model applications to Europe (SMART) and the

Netherlands (RESAM) presented in Chapter 7.

The reason for the different response of European and Dutch forest soils to deposition reductions is partly because of differences in the rate of reduction. In Europe, for example, current reduction plans hardly include reductions in N emission, whereas S emission is only reduced by 25%, whereas expected reductions for N and S emission in the Netherlands are approximately 50% (cf Section 7.1 and 7.2). Another reason, is that the RESAM model was only applied to non-calcareous sandy forest soils in the Netherlands, with a fast response to reduced acid inputs (see before). The SMART model, however, was applied to all major soil types in Europe, including soils with a high base saturation and a high potential for N immobilization. In many of these soils, base saturation still decreases and N still accumulates, even at reduced N and S inputs, which is reflected by a continuous increase in the area exceeding critical  $\text{NO}_3$  concentrations and Al/BC ratios.

There are large uncertainties in the large scale model predictions, due to uncertainties in input data and model structure. However, it is likely that the trends in time are reliable (cf Section 7.1 and 7.2). Furthermore, the reliability of large scale predictions of soil and soil solution chemistry with RESAM is supported by the reasonable comparison between model results for 1990 and measurements in 150 forest stands during the same year. For Europe, such a large scale comparison has not yet been made.

Summarizing, acid deposition is the dominant cause for the acidification of acid sandy soils in the Netherlands, which is manifested by elevated Al concentrations, due to dissolution of secondary Al compounds. The secondary Al pool in the topsoil can be completely depleted in several decades unless present acid inputs are reduced. In acid sandy soils, soil acidification will reverse rapidly at the expected emission reductions up to the year 2000, but further reductions are needed to avoid depletion of the pool of secondary Al compounds. In Europe, current emission reduction plans are inadequate to reverse the ongoing trend of soil acidification.

## SUMMARY

### *Research aims*

Enhanced acidification of soil, ground water and surface water by elevated deposition of S and N compounds is one of the most important large-scale environmental problems today. This thesis deals with the quantification of:

- (i) natural and man-induced sources of acidification in agricultural soils and forest soils in the Netherlands;
- (ii) current impacts of atmospheric S and N deposition on the solution chemistry of acid sandy forest soils in the Netherlands;
- (iii) various buffer mechanisms (i.e. mineral weathering, cation exchange and Al dissolution) in acid sandy soils in the Netherlands;
- (iv) average critical deposition levels (loads) for N and acidity (N and S) for forests, heathlands, ground water and surface water in the Netherlands;
- (v) regional variability in critical loads for N, S and acidity and the degree by which these loads are exceeded on forests in the Netherlands and in Europe;
- (vi) long-term impacts of acidic deposition on some characteristic non-agricultural soils;
- (vii) regional variability in long-term impacts of acidic deposition on forest soils in the Netherlands and in Europe.

Quantification was performed on the basis of interpretation of literature information, combined with field research (i and ii), laboratory research (iii), and model research (iv, v, vi and vii). In order to derive critical loads, steady-state soil models were developed, i.e. a one-layer model (START) for application on a European scale and a multi-layer model (MACAL) for application on a national scale. Similarly, two dynamic soil models were developed to assess the long-term soil response to acidic deposition, i.e. a one-layer model (SMART) for application in Europe and a multi-layer model (RESAM) for application in the Netherlands. The reasons for developing various models were the different research aims (critical loads vs long-term impacts of scenarios) and the decrease in availability of data with an increase in the area of application (Netherlands vs Europe; Chapter 1).

### *Natural and man-induced sources of acidification*

A theoretical overview of the relationship between the cycling of C, N, S and base cations in an ecosystem and the production and consumption of protons (H) is given in Section 2.1. This was done to provide a theoretical concept to (i) quantify the various causes of soil acidification and (ii) describe the various processes in a model. Three major causes of soil acidification were distinguished, i.e. natural acidification, land use and acidic deposition, which is mainly manifested by (i) leaching of  $\text{HCO}_3^-$  and organic anions ( $\text{RCOO}^-$ ), (ii) net uptake of base cations and (iii) leaching of  $\text{SO}_4$  and  $\text{NO}_3^-$ , respectively (Section 2.1).

A comparison between literature data on present (enhanced) soil acidification rates, and results on historical (natural) acidification rates, obtained by the analyses of total cation contents in a complete soil profile, showed that natural soil acidification plays a prominent

role in calcareous soils, whereas land use is an important cause for the acidification in non-calcareous agricultural soils. Consequently, the contribution of acidic deposition to soil acidification is of minor importance in calcareous soils ( $\leq 20\%$ ), intermediate in non-calcareous agricultural soils ( $\leq 50\%$ ) and dominant in non-calcareous forest soils in the Netherlands ( $\geq 80\%$ ) (Section 2.2).

#### *Current impacts of atmospheric S and N deposition on acid sandy forest soils*

Available soil chemistry data on 18 forested sites, monitored between 1979 and 1990, combined with results of a one-time survey of 150 forest stands in 1990, showed that  $\text{SO}_4$  deposition equals drainage output, whereas an appreciable part of the N deposition is still retained in Dutch forests soils (Section 2.3). Concentrations of  $\text{SO}_4$  and  $\text{NO}_3$  were largely correlated with that of Al. This implies that the acidity associated with  $\text{SO}_4$  and  $\text{NO}_3$  leaching is mainly buffered by Al dissolution. Concentrations of  $\text{SO}_4$ ,  $\text{NO}_3$  and Al in the soil solution were strongly related to tree species and tree height, through effects of canopy structure on the atmospheric input by dry deposition. Concentrations decreased in the order: fir and spruce trees (Douglas fir and Norway spruce) > pine trees (Scots pine and black pine) > deciduous trees (Japanese larch, oak and beech). Al concentrations and Al/Ca ratios generally exceeded values that are supposed to cause effects on fine roots (Section 2.3).

#### *Buffer mechanisms in acid sandy soils*

One-week column experiments and one-year batch experiments confirmed that Al dissolution is the dominant buffer mechanism in (Dutch) acid sandy soils (Chapter 3). During the experiment, the pH was kept constant by continuous (column experiment) or intermittent (batch experiment) titration. Total cation concentrations were also kept constant, since the H concentration in the titration solution was equal to the total cation concentration (including H) added initially to the batch solution. This was done to study weathering rates at (nearly) controlled pH and Al concentration. Batch experiments performed with four major soil horizons at pH 3.0, i.e. an (A+B)<sub>p</sub>, Bh, BCs and C horizon of podzolic soils, showed that fast dissolution of Al was mainly due to a decrease of the pool of inorganic (mainly amorphous) secondary Al compounds, which mainly consists. Secondary alumino-silicates were specifically important in the BCs and C horizon (Section 3.1), whereas non-silicate pools of Al (e.g. Al (hydr)oxides) dominated Al release in the (A+B)<sub>p</sub> and Bh horizon.

Results of batch and column experiments with the same soil horizons at five pH levels and five Al concentration levels, respectively, showed that the dissolution rate of Al can be described well as a function of the pool of secondary Al compounds and the degree of undersaturation with respect to gibbsite. Al dissolution rates decreased exponentially with a depletion of secondary Al compounds and increased proportionally with a power of the H concentration. Weathering rates of Si, Fe and BC (base cations) also increased with a power of the H concentration. The average power value (pH effect) decreased according to  $\text{Fe} > \text{Si} > \text{Al} > \text{Mg} > \text{Ca} \approx \text{K} \approx \text{Na}$  (Section 3.2).

Results of one-year batch experiments at several pH values for samples from a large number of soil types (Cambic, Carbic and Gleyic Podzols, Fimic Anthrosols, Umbric Gleysols and Haplic Arenosols) and soil horizons (Ah, Aan, (A+B)p, (A+C)p, E, Bhs, Bh, BCs, C and D horizons) confirmed that acid neutralization is mainly due to Al release from secondary Al compounds. Exceptions were six Aan horizons, an Ah horizon with an extremely large organic matter content and two C horizons with shell fragments (dune soils), in which BC release played a dominant role. Al release during one-year experiments at pH 3.0 increased from 20% of the secondary Al pool in Ah horizons to ca 90% in C horizons. This increase in relative Al depletion was correlated with a decrease of the fraction of organically bound Al in the secondary Al pool (Section 3.3).

#### *Critical loads for N and acidity*

Average critical loads for N and total acidity (N and S) for terrestrial and aquatic ecosystems were derived from empirical data and from results of simple mass balance models for N and acidity (Chapter 4). Critical N loads depended on the ecosystem involved and on the protection aim. Primary protection aims were to prevent (i) vegetation changes in forests, heathlands and oligotrophic surface waters, (ii) frost damage and fungal diseases in forests, (iii) nutrient imbalances in forests and (iv) elevated NO<sub>3</sub> leaching in forests and heathlands, causing the violation of target values for the NO<sub>3</sub> concentration in ground water. Empirical data and model results showed that vegetation changes can be expected at N inputs above 500-1400 mol<sub>c</sub> ha<sup>-1</sup> yr<sup>-1</sup>, nutrient imbalances above 800-1250 mol<sub>c</sub> ha<sup>-1</sup> yr<sup>-1</sup> (this relates only to NH<sub>3</sub>) and frost damage above 1500-3000 mol<sub>c</sub> ha<sup>-1</sup> yr<sup>-1</sup>. NO<sub>3</sub> concentrations in ground water above the EC target value of 50 mg l<sup>-1</sup> can be expected at atmospheric N inputs above 1500-3600 mol<sub>c</sub> ha<sup>-1</sup> yr<sup>-1</sup> (Section 4.1).

Critical acid loads were mainly derived by a simple model, such that unfavourably high Al concentrations in soil solution, ground water and surface water are avoided (Section 4.2). Critical Al concentrations were based on toxic effects on roots and soil organisms (soil solution), drinking water standards (ground water) and toxic effects on fish (surface water). In case of soil acidification the critical Al concentration was the minimum of (i) an Al concentration of 0.2 mol<sub>c</sub> m<sup>-3</sup>, (ii) an Al concentration determined by a critical molar Al/Ca ratio of 1.0 and (iii) an Al concentration, which avoids depletion of secondary Al compounds. Model results showed lower critical acid loads for surface waters and shallow ground waters (300-500 mol<sub>c</sub> ha<sup>-1</sup> yr<sup>-1</sup>) than for forests and deep ground waters (1100-1700 mol<sub>c</sub> ha<sup>-1</sup> yr<sup>-1</sup>). Critical acid loads were generally lower than critical loads for N (Section 4.2).

#### *Regional variability in critical loads*

The regional variability in critical loads for N, S and acidity (N and S) on forest soils and the degree by which these loads are exceeded in Europe and in the Netherlands, were assessed with the steady-state soil models START and MACAL, respectively (Chapter 5). Calculations with the one-layer START model were made for combinations of coniferous and deciduous forests on 80 soil types, occurring on the FAO soil map of Europe, using gridcells of 1.0° longitude x 0.5° latitude (Section 5.1). Results showed that atmospheric

inputs are much larger than critical loads for forests in central and western Europe. Atmospheric N and S loads were calculated to exceed critical N and S loads on roughly half of the forested area in Europe. The rate by which critical loads are exceeded was, however, calculated to be much larger for S (up to  $12000 \text{ mol}_e \text{ ha}^{-1} \text{ yr}^{-1}$  in former Czechoslovakia, Poland and Germany) than for N (up to  $3500 \text{ mol}_e \text{ ha}^{-1} \text{ yr}^{-1}$  in the Netherlands, Belgium and Germany). Furthermore, the critical N loads calculated relate to the risk of vegetation changes in forests. Critical N loads became much larger and areas in which these loads are exceeded thus became smaller (up to 29%) when the risk of forest vitality decrease was considered, due to the acidifying effect of N deposition. The uncertainty in N immobilization rate, and to a lesser extent in N uptake and denitrification strongly contributed to the uncertainty in the area where critical N loads are exceeded. Sensitivity analysis showed that this area ranged between 23% and 62% of the forested area in Europe. The forested area where acid inputs exceed critical acid loads was estimated at 45%. Sensitivity analysis showed that the forested area where critical acid loads are exceeded is much more influenced by the uncertainty in the critical values for the Al concentration and Al/BC (base cation) ratio in the soil solution, and the soil depth at which these criteria are applied (a range between 16% and 71%) than by the uncertainty in model inputs (a range between 38% and 57%). However, despite the estimated uncertainty in the area where critical loads are exceeded, current atmospheric inputs of N and S in western and central Europe clearly exceed critical loads in large areas (Section 5.1).

Calculations with the multi-layer MACAL model were made for combinations of 12 tree species and 23 aggregated soil types, occurring on the 1 : 250 000 soil map of the Netherlands, using gridcells of 10 km x 10 km (Section 5.2). Results showed that critical loads for N, S and acidity on Dutch forests are strongly exceeded on sandy soils in the central, eastern and southern part of the Netherlands, especially in areas with intensive animal husbandry. Critical acid loads increased in the order sand < peat < loess < clay, which was mainly due to an increase in denitrification (especially in peat soils) and base cation weathering (especially in clay soils). Median values for the percentages by which atmospheric inputs need to be reduced in order to meet the critical loads on non-calcareous soils, were 79% for N, 62% for S and 76% for total acidity. At these reductions, critical chemical values for Al are not exceeded in the whole rootzone. Critical acid loads calculated with MACAL increased strongly when critical chemical values for the Al concentration ( $0.2 \text{ mol}_e \text{ m}^{-3}$ ) and molar Al/Ca ratio (1.0) were applied at shallow soil depths. However, this did not hold for the criterion that depletion of secondary Al compounds should be avoided. Hence, the overall effect of soil depth appeared to be limited. Especially for non-calcareous sandy soils (85% of Dutch forest soils), the difference between critical acid loads related to 30 cm soil depth, where most fine roots occur, and the bottom of the rootzone was small. An evaluation of the various uncertainties showed that critical acid loads are: (i) greatly affected by uncertainties in critical values for the Al concentration and Al/Ca ratio, but the effects are relatively small when considering the necessity to avoid Al depletion (that criterion appeared to be very stringent), (ii) very uncertain for clay and peat soils due to great uncertainties associated with the model assumptions (however, these



soils only cover a small part of the forested area of the Netherlands; < 7.5%) and (iii) hardly affected by uncertain model inputs. It was concluded that, despite uncertainties, significant emission reductions are needed to meet critical acid loads for Dutch forest soils (Section 5.2).

#### *Long-term impacts of acid deposition*

Long-term impacts of present acid atmospheric deposition and soil responses to deposition scenarios on some characteristic non-agricultural soils were assessed with the dynamic models SMART and RESAM (Chapter 6). The long-term soil response to acid deposition in different buffer ranges between pH 7 and pH 3 was evaluated with the one-layer SMART model (Section 6.1). A simulation of the response of an initially calcareous soil of 50 cm depth to a constant high acid load ( $5000 \text{ mol}_e \text{ ha}^{-1} \text{ yr}^{-1}$ ) over 500 yr indicated that the pH remains high (near 7) until the carbonates are exhausted. A time lag of about 100 yr for each percent of  $\text{CaCO}_3$  was calculated before the pH starts to drop. In non-calcareous soils, the response in the range between pH 7 and 4 mainly depended on the initial amount of exchangeable base cations. A decrease in base saturation caused a strong increase in the Al/BC ratio near pH 4. Soil pH further decreased to values near 3 when the pool of secondary Al compounds was exhausted. The analyses indicated that such a pH drop could occur in acid soils within several decades. Model results about the impact of various deposition scenarios on non-calcareous soils over 100 years indicated that the time lag between reductions in deposition and a decrease in the Al/BC ratio is short (Section 6.1).

The reversibility of soil acidification was investigated in more detail by evaluating the long-term (60 yr) impact of a reducing atmospheric deposition scenario on the soil and soil solution chemistry of a representative acid forest soil in the Netherlands (Douglas fir on a Cambic Podzol) with the multi-layer RESAM model (Section 6.2). At high inputs of S and N, model results indicated (i) a significant interaction between  $\text{NH}_4$  and base cations in the forest canopy, (ii) an important role of N transformations (mineralization, root uptake and nitrification) and of Al mobilization in the proton budget, especially in the uppermost soil layers, (iii) conservative behaviour of  $\text{SO}_4$  and retention of N, (iv) a strong relationship between Al leaching and leaching of the sum of  $\text{SO}_4$  and  $\text{NO}_3$  from the rootzone and (v) a dominant role of secondary Al compounds in Al mobilization and the risk of complete Al depletion in the topsoil of Dutch forests at present deposition levels. These results are all in agreement with field and/or laboratory measurements. At reduced deposition levels RESAM predicted (i) an inversion from net N retention to net N mobilization followed by net N retention again, (ii) a strong decrease in dissolution of secondary Al compounds and (iii) a relative fast de-acidification of the soil, reflected by an increase in pH and base saturation and a decrease in Al concentration (Section 6.2).

The RESAM model was also used to simulate the long-term (100 yr) impact of present levels of acid deposition on a calcareous and a non-calcareous sandy soil, representative for the coastal dune areas of the Netherlands (Section 6.3). Simulations indicated that the impact of atmospheric deposition on a calcareous dune soil becomes very important when

the  $\text{CaCO}_3$  content has fallen below 0.3%. At these carbonate contents, the pH in the topsoil (first 10 cm) was predicted to decline from about 6.5 to 3.0 within a few decades. This rapid decrease in pH is due to the low weathering rate of silicates and the almost negligible buffering by cation exchange and by dissolution of secondary Al compounds in dune soils. The contribution of acid deposition to soil acidification was predicted to increase from less than 15% in a calcareous soil to more than 95% in a non-calcareous soil. Simulations for a non-calcareous dune soil indicated that present deposition levels cause a depletion of secondary Al compounds over a depth of more than 50 cm during the simulation period, which leads to a pH decline from about 3.5 - 4.5 to 3.0 - 3.5. Evidence is given that this may lead to a decrease in plant species (Section 6.3).

#### *Regional variability in long-term impacts*

The regional variability in chemical responses of forest soils in Europe and the Netherlands to various deposition scenarios was also investigated with the SMART and RESAM model, respectively (Chapter 7). The long-term impact of acid deposition on European soils was investigated for three emission-deposition scenarios for the years 1960-2050, i.e. Official Energy Pathways (OEP), Current Reduction Plans (CRP) and Maximum Feasible Reductions (MFR) (Section 7.1). As with the START model, calculations were made for coniferous and deciduous forests on 80 soil types, using gridcells of  $1.0^\circ$  longitude  $\times$   $0.5^\circ$  latitude. Results indicated that the acidity and N-status of European forest soils do not improve when current reduction plans would be implemented. The forested area where critical values for the  $\text{NO}_3$  and Al concentration and Al/BC ratio are exceeded was predicted to stay relatively constant (Al) or to increase ( $\text{NO}_3$ , Al/BC). Soil acidification decreased quite drastically following maximum feasible emission reduction (MFR scenario). The problem of N saturation (defined as a situation in which availability of inorganic N is in excess of total plant and microbial nutritional demand), appeared to be more persistent and even increased in response to the MFR scenario. N-saturated and acidified forest soils were concentrated in central, western and eastern European countries during the entire simulation period for all scenarios. Very high Al concentrations mainly occurred in central Europe (Germany, Poland and former Czechoslovakia) whereas high  $\text{NO}_3$  concentrations also showed up in the Netherlands, Belgium, Luxembourg and large parts of the former Soviet Union. Uncertainties in the initial values of C/N ratios and base saturation had a large impact on the area exceeding critical values for the concentrations of  $\text{NO}_3$  and Al and the Al/BC ratio but not so much on the trends in time (Section 7.1).

The long-term impact of acid deposition on Dutch forest soils was also evaluated for three deposition scenarios for the years 1965-2050 (Section 7.2). Calculations with the RESAM model were made for combinations of seven major tree species and fourteen non-calcareous sandy soils in 20 deposition areas. The forest-soil combinations cover about 65% of the Dutch forested area. Three deposition scenarios for  $\text{SO}_x$ ,  $\text{NO}_x$  and  $\text{NH}_x$  were generated with an air transport model using (i) historic emission data (1965-1990), (ii) expected emission reductions based on several environmental policy plans (1990-2000) and (iii) deposition targets for the years 2010 and 2050 (2000-2050). Up to 2000 all

scenarios were similar. A comparison of model results for 1990 with measurements in 150 forest stands in the same year showed that the agreement was good for the N content, base saturation, pH and  $\text{SO}_4$  concentration, reasonable for the  $\text{NO}_3$  concentration, Al/Ca ratio and Al concentration in the topsoil and poor for the  $\text{NH}_4/\text{K}$  ratio and Al concentration in the subsoil. At high deposition levels (1990), soil solution chemistry was more strongly influenced by tree species, than by deposition area. Soil solution parameters responded quickly to the change in atmospheric deposition in the three scenarios. The deposition reductions generally lead to a fast increase in pH and a fast decrease in Al and  $\text{SO}_4$  concentration and Al/Ca ratio. However, there was a clear time lag between reduction in N deposition and reduction in  $\text{NO}_3$  concentration and  $\text{NH}_4/\text{K}$  ratio in the soil solution, which was mainly due to N mobilization from the humus layer. Effects on the solid phase chemistry, such as the N content (in the humus layer) and the base saturation, appeared to be less. Deposition reductions up to an average of  $1400 \text{ mol}_e \text{ ha}^{-1} \text{ yr}^{-1}$  (scenario 2) appeared to avoid substantial (> 10%) exceedances of a critical Al concentration ( $0.2 \text{ mol}_e \text{ m}^{-3}$ ) and molar Al/Ca ratio (1.0) in the topsoil and a critical  $\text{NO}_3$  concentration ( $0.4 \text{ mol}_e \text{ m}^{-3}$ ) in the subsoil. Such reductions would also avoid depletion of secondary Al compounds (Section 7.2).

### *Conclusions*

Major conclusions of this thesis (Section 8) are: (i) Elevated atmospheric deposition of S and N is the dominant cause of the acidification ( $\geq 80\%$ ) of acid sandy forest soils in the Netherlands, (ii) man-induced soil acidification is mainly manifested by enhanced mobilization and leaching of Al, equivalent to the leaching of  $\text{SO}_4$  and  $\text{NO}_3$ , (iii) Al mobilization is mainly due to dissolution of secondary inorganic Al compounds, (iv) critical loads for N and acidity are much lower than present atmospheric inputs in the Netherlands, (v) uncertainties in critical Al concentrations and Al/Ca ratios cause a large uncertainty in critical acid loads, but the uncertainty is far less when zero depletion of secondary Al compounds is used as a criterion, (vi) the pool of secondary Al compounds can be depleted in several decades at current atmospheric deposition levels in the Netherlands, especially in non-calcareous dune soils and (vii) current emission reduction plans will not improve the acidity status of European forest soils, whereas it will strongly improve soil solution quality (in terms of pH,  $\text{SO}_4$ ,  $\text{NO}_3$  and Al concentration) in Dutch forest soils.

## SAMENVATTING

### *Onderzoeksdoeleinden*

De verzuring van bodem, grondwater en oppervlaktewater door de verhoogde depositie van zwavel(S)- en stikstof(N)-verbindingen is momenteel een zeer belangrijk grootschalig milieuprobleem. Doel van dit proefschrift is een kwantificering te geven van de:

- (i) natuurlijke en door de mens veroorzaakte (antropogene) verzuring van landbouwgronden en bosgronden in Nederland;
- (ii) effecten van atmosferische depositie van S- en N-verbindingen op de chemische samenstelling van bodemvocht in kalkloze zure zandgronden onder bos in Nederland;
- (iii) verschillende buffermechanismen, zoals mineraalverwerking, kationenuitwisseling en mobilisatie van aluminium (Al), in zure zandgronden in Nederland;
- (iv) gemiddelde kritische depositieniveaus voor N en het totaal aan zuur (N en S) voor bos, heide, grondwater en oppervlaktewater in Nederland;
- (v) regionale variatie in kritische depositieniveaus voor N, S en het totaal aan zuur en de mate waarin die worden overschreden door de huidige depositieniveaus op bossen in Nederland en in Europa;
- (vi) lange-termijneffecten van zure atmosferische depositie op een aantal karakteristieke niet-landbouwgronden;
- (vii) regionale variatie in lange-termijneffecten van zure atmosferische depositie op bosgronden in Nederland en in Europa.

De kwantificering is gebaseerd op interpretatie van bestaande literatuurgegevens, aangevuld met veldonderzoek (onderzoeksdoeleinden i en ii), laboratoriumonderzoek (onderzoeksdoel iii) en modelonderzoek (onderzoeksdoeleinden iv, v, vi en vii). Voor het afleiden van kritische depositieniveaus zijn statische bodemmodellen ontwikkeld. Daarbij is onderscheid gemaakt in een één-laagmodel (START) voor toepassing op Europese schaal en een meer-lagenmodel (MACAL) voor toepassing op nationale schaal. Om lange-termijneffecten van zure depositie vast te stellen zijn twee dynamische bodemmodellen ontwikkeld. Ook hier is onderscheid gemaakt in een één-laagmodel (SMART) voor toepassing in Europa en een meer-lagen model (RESAM) voor toepassing in Nederland. De redenen voor het ontwikkelen van verschillende modellen waren de verschillende onderzoeksdoeleinden (kritische depositieniveaus versus lange-termijneffecten van depositiescenario's) en de afnemende beschikbaarheid van data, gaande van Nederland naar Europa (Hoofdstuk 1).

### *Natuurlijke en antropogene bodemverzuring*

In paragraaf 2.1 staat een overzicht van de relatie tussen de kringloop van koolstof (C), N, S en basische kationen in een ecosysteem enerzijds en de productie en consumptie van protonen (H-ionen) anderzijds. Doel hiervan is het geven van een theoretisch concept om (i) de verschillende oorzaken van bodemverzuring te kwantificeren en (ii) de verschillende processen in het ecosysteem in een model te beschrijven. De drie belangrijkste oorzaken

van bodemverzuring zijn natuurlijke verzuring, bodemgebruik en zure depositie. Kwantificering hiervan in bosgronden is mogelijk op basis van de uitspoeling van bicarbonaat en organische anionen (natuurlijke verzuring), de netto-opname van basische kationen (bodemgebruik) en in- en uitvoer balansen van sulfaat ( $\text{SO}_4$ ), nitraat ( $\text{NO}_3$ ) en ammonium ( $\text{NH}_4$ ; zure depositie).

Gegevens over historische (natuurlijke) snelheden van bodemverzuring zijn verkregen voor kalkrijke en kalkloze gronden in Nederland op basis van een analyse van totaalgehalten aan kationen in een aantal bodemprofielen. Deze zijn vergeleken met literatuurgegevens over de huidige (verhoogde) snelheden van bodemverzuring. Hieruit bleek dat natuurlijke bodemverzuring een dominante rol speelt in kalkrijke gronden, terwijl bodemgebruik een belangrijke oorzaak is van verzuring in kalkloze landbouwgronden. De bijdrage van zure depositie aan bodemverzuring is dus gering in kalkrijke gronden ( $\leq 20\%$ ), relatief belangrijk in kalkloze landbouwgronden ( $\leq 50\%$ ) en dominant ( $\geq 80\%$ ) in kalkloze bosgronden in Nederland (paragraaf 2.2).

#### *Effecten van zure depositie op zure zandgronden onder bos*

In paragraaf 2.3 staat een overzicht van gemeten effecten van zure atmosferische depositie op concentraties en fluxen van  $\text{SO}_4$ ,  $\text{NO}_3$ , Al, BC (basische kationen, te weten Ca+Mg+K+Na) en H in kalkloze zandgronden onder bossen in Nederland. De resultaten zijn gebaseerd op (i) tijdreeksen van één tot zeven jaar over de chemische bodemvochtsamenstelling in 18 bosopstanden (onderzoek dat is uitgevoerd tussen 1979 en 1990), en (ii) een éénmalige bepaling van de chemische bodemvochtsamenstelling in 150 bosopstanden in 1990. Hieruit bleek dat de uitspoeling van  $\text{SO}_4$  in het algemeen gelijk is aan de  $\text{SO}_4$ -depositie, terwijl de N-uitspoeling (voornamelijk in de vorm van  $\text{NO}_3$ ) aanmerkelijk lager is dan de N-depositie. De concentraties en fluxen van  $\text{SO}_4$  en  $\text{NO}_3$  kwamen sterk overeen met die van Al. Dit betekent dat de zuurproductie, die samenhangt met uitspoeling van  $\text{SO}_4$  en  $\text{NO}_3$ , voornamelijk wordt gebufferd door het vrijkomen (door vertering of kationenomwisseling) van Al uit de bodem. De concentraties aan  $\text{SO}_4$ ,  $\text{NO}_3$  en Al in het bodemvocht in de 150 bosopstanden bleken in hoge mate te worden bepaald door de boomsoort en de boomhoogte. Beide hebben invloed op de droge depositie van S- en N-verbindingen. De concentraties namen af in de richting: sparrebomen (douglas en fijnspar) > dennebomen (grove den, Corsicaanse den en Oostenrijkse den) > loofbomen (de naalden verliezende Japanse lariks, eik en beuk). De Al-concentraties en Al/Ca-verhoudingen in het bodemvocht bevonden zich veelal boven kritisch geachte waarden voor de fijne wortels (paragraaf 2.3).

#### *Buffermechanismen in zure zandgronden*

De belangrijkste geochemische bufferprocessen in zure zandgronden zijn gekwantificeerd op basis van "schudexperimenten" van een jaar en "kolomexperimenten" van een week. De pH, Al-concentratie en temperatuur zijn gedurende de experimenten vrijwel constant gehouden (Hoofdstuk 3). Uit schudexperimenten bij pH 3,0 met monsters van vier belangrijke bodemhorizonten, te weten (A+B)p-, Bh-, BCs- en C-horizonten, bleek dat het

vrijkomen van Al uit secundaire Al-verbindingen het dominante buffermechanisme is in zure zandgronden (paragraaf 3.1). In de BCs- en C-horizonten bleken vooral secundaire aluminiumsilicaten een belangrijke rol te spelen. In de (A+B)p- en de Bh-horizonten was het vrijkomen van Al uit (hydr)oxiden belangrijker, hoewel omwisseling van H tegen organisch gecomplexeerd Al hier ook een belangrijke bijdrage aan de buffering leverde. De kwantificering van de verschillende bronnen is echter nogal onzeker, vanwege de geringe specificiteit van de extractiemethoden voor de verschillende secundaire Al-verbindingen (paragraaf 3.1).

Schud- en kolomexperimenten met dezelfde vier bodemhorizonten bij vijf verschillende pH- en Al-concentratieniveaus toonden aan, dat verweringsnelheden van silicium (Si), ijzer (Fe) en basische kationen (BC) toenemen met een macht van de protonactiviteit en afnemen met een macht van de Al activiteit. De waarde voor de macht of exponent was groter voor de protonactiviteit dan voor de Al-activiteit (het pH-effect was groter dan het effect van Al-concentratie). De invloed van pH op de oplosbaarheid van Al kon goed worden beschreven als functie van het gehalte aan secundaire Al-verbindingen en de mate van onderverzadiging ten opzichte van gibbsiet. Oplosnelheden van Al namen exponentieel af met het gehalte aan secundaire Al-verbindingen en namen evenredig toe met de mate van onderverzadiging ten opzichte van gibbsiet. Het effect van de Al-concentratie kon echter niet goed worden verklaard met dit model (paragraaf 3.2).

De resultaten van schudexperimenten bij verschillende pH niveaus in monsters van een groot aantal bodemtypen (holt-, haar- en veldpodzolgronden, enkele- en bekeerdgronden, duinvaag- en vlakvaaggronden) en bodemhorizonten (Ah-, Aan-, (A+B)p-, (A+C)p-, E-, Bhs-, BCs-, C- en D-horizonten) bevestigen dat zuurneutralisatie in kalkloze zandgronden voornamelijk plaatsvindt door het oplossen van Al uit secundaire Al-verbindingen (paragraaf 3.3). Uitzonderingen hierop waren zes Aan-horizonten, een Ah-horizont met een extreem hoog gehalte aan organische stof en twee C-horizonten uit duinvaaggronden met schelffragmenten. In deze horizonten speelde het vrijkomen van basische kationen door kationuitwisseling (vooral in Aan- en Ah-horizonten) en vertering (vooral in C-horizonten) een dominante rol. De uitputting van de voorraad aan secundaire Al-verbindingen door Al-mobilisatie in schudexperimenten van een jaar bij een pH van 3,0 nam toe van ca. 20% in Ah-horizonten tot ca. 90% in C-horizonten. Deze toename in relatieve Al-uitputting was gecorreleerd met een afname van de fractie aan organisch gecomplexeerd Al in de secundaire Al-verbindingen (paragraaf 3.3).

#### *Kritische depositieniveaus voor stikstof en het totaal aan zuur*

De gemiddelde kritische depositieniveaus voor N en het totaal aan zuur (N en S) voor terrestrische en aquatische ecosystemen zijn afgeleid uit empirische gegevens en uit resultaten van statische massabalansmodellen (Hoofdstuk 4). Kritische N-depositieniveaus varieerden afhankelijk van het beschouwde ecosysteem en het gewenste beschermingsniveau. De beschermingsniveaus zijn gerelateerd aan het voorkómen (vermijden) van (i) vegetatieveranderingen in bossen, heide en oligotrofe oppervlaktewateren, (ii) vorstschade

en schimmelziekten in bossen, (iii) verstoringen in de nutriëntenbalans (onbalans in nutriëntenniveaus) in bossen en (iv) een verhoogde  $\text{NO}_3$ -uitspoeling onder bossen en heide, waarbij streefwaarden voor de  $\text{NO}_3$ -concentratie in het grondwater worden overschreden. Empirische gegevens en modelresultaten toonden aan dat vegetatieveranderingen te verwachten zijn bij een N-depositie boven  $500\text{-}1400 \text{ mol}_e \text{ ha}^{-1} \text{ jr}^{-1}$ , onbalans in nutriëntenniveaus boven  $800\text{-}1250 \text{ mol}_e \text{ ha}^{-1} \text{ jr}^{-1}$  (dit geldt alleen voor  $\text{NH}_3$ ), en vorstschade bij een N-depositie boven  $1500\text{-}3000 \text{ mol}_e \text{ ha}^{-1} \text{ jr}^{-1}$ .  $\text{NO}_3$ -concentraties in het ondiepe grondwater boven de EU-streefwaarde van  $50 \text{ mg l}^{-1}$  zijn op lange termijn te verwachten bij een atmosferische N toevoer boven  $1500\text{-}3600 \text{ mol}_e \text{ ha}^{-1} \text{ jr}^{-1}$  (paragraaf 4.1).

De kritische depositieniveaus voor het totaal aan zuur zijn hoofdzakelijk berekend met een eenvoudig statisch model. Het criterium hierbij was dat concentraties aan Al in bodemvocht, grondwater en oppervlaktewater beneden een kritisch niveau blijven. De kritische Al-concentraties zijn vastgesteld op grond van toxische effecten op fijne wortels en bodemorganismen (bodemvocht), drinkwaternormen (grondwater) en toxische effecten op vissen (oppervlaktewater). In geval van bodemverzuring is het minimum van (i) een Al-concentratie van  $0,2 \text{ mol}_e \text{ m}^{-3}$ , (ii) een Al-concentratie die bepaald wordt door een kritische molaire Al/Ca-verhouding van 1,0 en (iii) een Al-concentratie die voorkomt dat secundaire Al-verbindingen worden uitgeput, gehanteerd. Modelresultaten toonden aan dat kritische zuurdepositieniveaus lager zijn voor oppervlaktewater en ondiep grondwater ( $300\text{-}500 \text{ mol}_e \text{ ha}^{-1} \text{ jr}^{-1}$ ) dan voor bossen en diep grondwater ( $1100\text{-}1700 \text{ mol}_e \text{ ha}^{-1} \text{ jr}^{-1}$ ). De kritische depositieniveaus voor het totaal aan zuur waren in het algemeen lager dan die voor stikstof (paragraaf 4.2).

#### *Regionale variatie in kritische depositieniveaus*

De regionale variatie in kritische depositieniveaus voor N, S en het totaal aan zuur op bosgronden in Europa en in Nederland is berekend met respectievelijk de modellen START en MACAL (Hoofdstuk 5). Berekeningen met het statische één-laag bodem model START zijn gemaakt voor naald- en loofbossen op 80 bodemtypen, zoals die worden onderscheiden op de FAO-bodemkaart van Europa (paragraaf 5.1). Om overschrijdingen van kritische depositieniveaus te berekenen, is de atmosferische depositie per gridcel van  $1,0$  lengtegraad  $\times$   $0,5$  breedtegraad berekend. Uit de resultaten bleek dat de huidige atmosferische depositie van N- en S-verbindingen op ongeveer de helft van alle Europese bossen hoger is dan het kritische depositieniveau voor deze stoffen. Vooral in Midden- en West-Europa waren de berekende overschrijdingen van kritische depositieniveaus zeer hoog. Dit geldt vooral voor S (een berekende overschrijding tot  $12000 \text{ mol}_e \text{ ha}^{-1} \text{ jr}^{-1}$  in het voormalige Tsjechoslowakije, Polen en Duitsland) en in mindere mate voor N (een berekende overschrijding tot  $3500 \text{ mol}_e \text{ ha}^{-1} \text{ jr}^{-1}$  in Nederland, België en Duitsland). De berekende kritische N-depositieniveaus zijn gerelateerd aan het voorkomen van vegetatieveranderingen in bossen. Berekende kritische N-depositieniveaus werden veel hoger wanneer het risico voor een afname in bosvitaliteit in beschouwing werd genomen. De berekende overschrijding van kritische N-depositieniveaus was in dit geval dus lager, en wel 29% in plaats van 50%. Het bosoppervlak waar kritische N-depositieniveaus worden

overschreden varieerde van 23% tot 62% van het bosoppervlak van Europa, bij een gegeven verwachte onzekerheid in snelheden van kritische N-immobilisatie, N-opname en denitrificatie. Het bosoppervlak waar kritische depositieniveaus voor het totaal aan zuur worden overschreden varieerde van 16% tot 71%, afhankelijk van de gebruikte kritische Al-concentratie en Al/BC-verhouding in de bodemoplossing. Onzekerheden in modelinvoergegevens, zoals verwerkingssnelheden en opnamesnelheden, bleken minder effect te hebben. Ondanks de geschatte onzekerheid is het wel duidelijk dat de huidige atmosferische N en S-belasting op bossen in Midden- en West-Europa (veel) hoger is dan het kritische depositieniveau (paragraaf 5.1).

De berekeningen van kritische depositieniveaus voor Nederlandse bossen werden gemaakt met het statische meer-lagen bodemmodel MACAL voor combinaties van 12 boomsoorten op 23 geaggregeerde bodemtypen, zoals die voorkomen op de 1 : 250 000 bodemkaart van Nederland (paragraaf 5.2). De overschrijdingen van kritische depositieniveaus werden berekend op basis van de atmosferische toevoer per 10 x 10 km gridcel. De kritische depositieniveaus voor N, S en het totaal aan zuur voor bossen bleken sterk te worden overschreden op kalkloze zandgronden in Midden-, Oost- en Zuid-Nederland, vooral in gebieden met intensieve veehouderij. De kritische zuurdepositieniveaus werden hoger in de richting zand- < veen- < löss- < kleigronden. Dit was voornamelijk het gevolg van een toename van de denitrificatie (vooral in veengronden) en van de basenverwerking (vooral in kleigronden) in deze richting. De berekende mediaanwaarden voor het percentage waarmee de huidige belasting moet worden gereduceerd om kritische depositieniveaus op kalkloze gronden te halen, waren 79% voor N, 62% voor S en 76% voor het totaal aan zuur. Bij deze reductieniveaus is er geen sprake van een overschrijding van kritische Al-concentraties ( $0,2 \text{ mol}_c \text{ m}^{-3}$ ) en Al/Ca-verhoudingen ( $1,0 \text{ mol mol}^{-1}$ ) in het gehele bodemprofiel. Wanneer deze kritische waarden alleen in de bovengrond (bijv. de bovenste 30 cm, waar zich de meeste fijne wortels bevinden) niet mogen worden overschreden, wordt het berekende kritische zuurdepositieniveau aanmerkelijk hoger. Wanneer echter als extra criterium wordt gesteld dat de voorraad aan secundaire Al-verbindingen niet op mag raken, dan is het effect van de bodemdiepte gering. Een evaluatie van de verschillende onzekerheden liet zien dat de berekende overschrijding van kritische zuurdepositieniveaus (i) sterk wordt beïnvloed door onzekerheden over kritische Al-concentraties en Al/Ca-verhoudingen, tenzij het voorkómen van Al-uitputting als extra criterium wordt meegenomen, (ii) zeer onzeker is voor klei- en veengronden vanwege de gedane modelveronderstellingen (slechts ca. 7,5% van het Nederlandse bos ligt echter op deze bodems) en (iii) weinig wordt beïnvloed door onzekerheden in modelinvoergegevens. Uit de analyse is geconcludeerd dat ondanks de genoemde onzekerheden, significante emissiereducties nodig zijn om de gewenste kritische zuurdepositieniveaus voor Nederlandse bossen te halen (paragraaf 5.2).

#### *Lange-termijneffecten van zure depositie*

Lange-termijneffecten van huidige depositieniveaus en effecten van depositiescenario's op een aantal karakteristieke bos- en duingronden zijn berekend met de dynamische modellen



SMART en RESAM (Hoofdstuk 6). Het zeer-lange-termijneffect (500 jaar) van een hoog zuurdepositieniveau ( $5000 \text{ mol}_e \text{ ha}^{-1} \text{ jr}^{-1}$ ) op een initieel kalkrijke bodem is vastgesteld op basis van een simulatie met het één-laag bodemmodel SMART (paragraaf 6.1). Hieruit bleek dat de pH boven de 6,5 à 7 blijft totdat de kalkvoorraad is opgelost. SMART berekende een tijdsperiode van ca. 100 jaar voor het volledig oplossen van één procent kalk (calciumcarbonaat) in een bodemlaag van 50 cm. In kalkloze gronden die zich bevinden in een pH-range van ca. 7 tot 4 bepaalde voornamelijk de initiële voorraad uitwisselbare basische kationen de reactie van de bodem op zuurtoevoer. Rond pH 4 veroorzaakte een afname van de basen bezetting aan het adsorptiecomplex een sterke toename van de Al/BC-verhouding in de bodemoplossing. Simulaties van het effect van depositiescenario's toonden aan dat een verandering (bijv. reductie) in zuurdepositie op dergelijke gronden vrijwel direct tot verandering (verlaging) van de Al/BC-verhouding in de bodemoplossing leidt. Bij een constant hoog depositieniveau veroorzaakte het oplossen van secundaire Al-verbindingen een verdere pH-daling beneden 4. Bij een volledige uitputting van deze Al-bron daalde de pH tot ca. 3. De modelanalyse gaf aan dat in zure gronden een pH daling van ca. 4 naar 3 in enkele decennia mogelijk is (paragraaf 6.1).

De reversibiliteit (omkeerbaarheid) van bodemverzuring is nader onderzocht door toepassing van het meer-lagen bodemmodel RESAM (paragraaf 6.2). Hiertoe is het lange-termijneffect (60 jaar) van een reducerend zuurdepositiescenario op de chemische samenstelling van de minerale bodem en van het bodemvocht voorspeld voor een representatieve bosgrond in Nederland (een douglasbos op een holtpodzol). Modelresultaten gaven aan dat er bij een hoge atmosferische toevoer van S en N sprake is van een (i) significante interactie (uitwisseling) tussen  $\text{NH}_4$  en de basische kationen Ca, Mg en K in de boomkroon, (ii) belangrijke rol van N-transformaties (mineralisatie, nitrificatie en wortelopname) en van Al-mobilisatie op de productie en consumptie van zuur (protonen), vooral in de bovenste bodemlagen, (iii) conservatief gedrag van  $\text{SO}_4$  terwijl N nog duidelijk wordt vastgelegd, (iv) sterke relatie tussen de uitspoeling van Al uit de wortelzone enerzijds en de uitspoeling van de som van  $\text{SO}_4$  en  $\text{NO}_3$  anderzijds en (v) dominante rol van secundaire Al-verbindingen in de zuurneutralisatie. Deze resultaten komen alle overeen met de eerder weergegeven resultaten van veld- en laboratoriumstudies. Uit de simulaties bleek tevens dat uitputting van de bovengrond onder bos op relatief korte termijn mogelijk is wanneer de huidige depositieniveaus niet worden gereduceerd. Bij een reductie van het depositieniveau voorspelde RESAM een (i) initiële omkering van netto N-vastlegging naar netto N-mobilisatie, later gevolgd door netto N-vastlegging, (ii) sterke afname in het oplossen van secundaire Al-verbindingen en (iii) relatief snelle ontzuring van de grond, die o.a. tot uiting komt in een toename van de pH en de basenbezetting en een afname van de Al-concentratie in de bodemoplossing (paragraaf 6.2).

Het model RESAM is ook gebruikt om het lange-termijneffect (100 jaar) van het huidige hoge depositieniveau door te rekenen voor een representatieve kalkrijke en kalkloze zandgrond in de Nederlandse kustduinen (paragraaf 6.3). De simulaties gaven aan dat het effect van zure depositie op een kalkrijke duingrond zeer belangrijk wordt, wanneer het

kalkgehalte beneden de 0,3% daalt. Bij dergelijke kalkgehalten bleek de pH in de bovengrond (de bovenste 10 cm) in enkele decennia te dalen van ca. 6,5 tot 3,0. De lage verwerkingssnelheid en de vrijwel verwaarloosbare voorraad aan uitwisselbare kationen en secundaire Al-verbindingen veroorzaken de voorspelde snelle pH-daling in deze gronden. De berekende bijdrage van zure depositie aan de bodemverzuring nam toe van minder dan 15% in een kalkrijke grond tot meer dan 95% in een kalkloze grond. Simulaties voor de kalkloze duingrond gaven aan dat gedurende de simulatieperiode de voorraad aan secundaire Al-bronnen volledig wordt uitgeput tot een diepte van meer dan 50 cm. De hierbij berekende pH-daling van ca. 3,5 à 4,5 tot ca. 3,0 à 3,5 kan gevolgen hebben voor de soortenrijkdom van duinvegetaties (paragraaf 6.3).

#### *Regionale variatie in lange-termijneffecten*

De regionale variatie in de reactie van bosbodems in Europa en Nederland op verschillende depositiescenario's is eveneens met respectievelijk SMART en RESAM onderzocht (Hoofdstuk 7). Het lange-termijneffect van zure depositie op Europese bosgronden is onderzocht voor drie emissie-depositiescenario's, te weten 'Official Energy Pathways' (OEP), Current Reduction Plans (CRP) and Maximum Feasible Reductions (MFR) (paragraaf 7.1). Evenals met START zijn de berekeningen gemaakt voor naald- en loofbossen op 80 bodemtypen in gridcellen van 1,0 lengtegraad x 0,5 breedtegraad. Uit de resultaten bleek dat de mate van verzuring en N-verzadiging in Europese bosgronden niet zal afnemen wanneer de huidige reductieplannen zouden worden uitgevoerd. Het berekende bosoppervlak waar kritische waarden voor de  $\text{NO}_3^-$ - en Al-concentratie en de Al/BC-verhouding in bodemvocht worden overschreden bleef vrijwel constant (Al) of het nam toe ( $\text{NO}_3^-$ , Al/BC). Bodemverzuring nam zeer sterk af in het scenario waarbij wordt uitgegaan van de maximaal mogelijke emissiereductie (het MFR-scenario). Het probleem van N-verzadiging (gedefinieerd als een situatie waarin de beschikbaarheid van anorganisch N groter is dan de vraag naar N door de vegetatie en de microbiële populatie) bleek echter zelfs bij dit scenario nog toe te nemen. N-verzadigde en sterk verzuurde bosgronden waren bij alle scenario's en gedurende de gehele simulatieperiode geconcentreerd in Midden-, West- en Oost-Europa. Zeer hoge Al-concentraties worden vooral voorspeld in het voormalige Tjechoslowakije, Polen en Duitsland, terwijl hoge  $\text{NO}_3^-$ -concentraties zijn berekend voor Nederland, België, Luxemburg en voor grote delen van de voormalige Sovjet-Unie. De onzekerheden in de initiële waarden voor de C/N-verhoudingen en de basenbezetting van de bosbodems hadden wel een groot effect op het voorspelde bosoppervlak waar kritische waarden voor  $\text{NO}_3^-$ - en Al-concentraties en Al/BC-verhoudingen worden overschreden, maar niet zozeer op de voorspelde veranderingen in de tijd (paragraaf 7.1).

Het lange-termijneffect van zure depositie op Nederlandse bosgronden is eveneens onderzocht voor drie emissie-depositiescenario's voor de periode 1965-2050 (paragraaf 7.2). De met RESAM gemaakte berekeningen werden beperkt tot combinaties van zeven belangrijke boomsoorten en veertien kalkloze zandgronden in 20 gebieden met een constant veronderstelde depositie in de ruimte. De beschouwde bos-bodem-combinaties

beslaan ca. 65% van het Nederlandse bosoppervlak. De drie depositiescenario's voor  $\text{SO}_x$ ,  $\text{NO}_x$  en  $\text{NH}_x$  werden gegenereerd met een luchttransportmodel. Daarbij is gebruik gemaakt van (i) historische emissiegegevens (1965-1990), (ii) verwachte emissiereducties gebaseerd op nationale milieubeleidsplannen (1990-2000) en (iii) depositiedoelstellingen voor de jaren 2010 en 2050 (2000-2050). Tot het jaar 2000 waren de drie scenario's gelijk. Een vergelijking van modeluitkomsten voor 1990 en meetresultaten in 150 bosopstanden in hetzelfde jaar toonden een goede overeenkomst voor het N-gehalte in de humuslaag, de basenverzadiging in de minerale bovengrond, de pH en  $\text{SO}_4$ -concentratie in de bodemoplossing. De overeenkomst was redelijk voor de  $\text{NO}_3^-$  en Al-concentratie en de Al/Ca-verhouding in het bodemvocht (met uitzondering van Al in de ondergrond) en vrij slecht voor de  $\text{NH}_4^+/\text{K}$ -verhouding. De voorkomende boomsoort bepaalde sterker de voorspelde bodemvochtsamenstelling dan het depositiegebied waar de opstand zich bevond. De berekende chemische samenstelling van het bodemvocht reageerde zeer snel op de veronderstelde depositiereducties in de drie scenario's. Dit kwam tot uiting in een snelle verhoging van de pH en een snelle verlaging van de Al- en  $\text{SO}_4$ -concentratie en de Al/Ca-verhouding. Er was echter sprake van een duidelijke vertraging in de reactie van  $\text{NH}_4^+$ - en  $\text{NO}_3^-$ -concentraties in bodemvocht op een verlaging van de N-depositie. Dit was hoofdzakelijk het gevolg van de voorspelde N-mobilisatie vanuit de humuslaag. Effecten op de chemische samenstelling van het adsorptiecomplex bleken veel geringer te zijn. Depositiereducties tot een gemiddeld zuurdepositieniveau van  $1400 \text{ mol}_e \text{ ha}^{-1} \text{ jr}^{-1}$  (scenario 2) bleken voldoende te zijn om een substantiële ( $> 10\%$ ) overschrijding van kritische Al-concentraties ( $0,2 \text{ mol}_e \text{ m}^{-3}$ ) en Al/Ca-verhoudingen ( $1,0 \text{ mol}_e \text{ m}^{-3}$ ) in de bovengrond, en van kritische  $\text{NO}_3^-$ -concentraties in de ondergrond ( $0,4 \text{ mol}_e \text{ m}^{-3}$ ) te voorkomen. Dit depositieniveau was ook voldoende om uitputting van secundaire Al-verbindingen te voorkomen (paragraaf 7.2).

### *Conclusies*

De belangrijkste conclusies van dit proefschrift (Hoofdstuk 8) zijn: (i) een verhoogde atmosferische depositie van N en S-verbindingen is de belangrijkste oorzaak ( $\geq 80\%$ ) van de verzuring van kalkloze zandgronden onder bos in Nederland, (ii) de bodemverzuring in kalkloze zandgronden komt vooral tot uiting in een verhoogde mobilisatie en uitspoeling van Al in samenhang met een verhoogde  $\text{SO}_4^-$  en  $\text{NO}_3^-$ -uitspoeling, (iii) de Al-mobilisatie is voornamelijk het gevolg van het oplossen van secundaire anorganische Al-verbindingen, (iv) de huidige depositieniveaus voor N en het totaal aan zuur zijn in Nederland veel hoger dan de kritische depositieniveaus, (v) de onzekerheid in kritische zuurdepositieniveaus, die wordt veroorzaakt door de onzekerheden in kritische Al-concentraties en Al/Ca-verhoudingen is zeer groot, tenzij de kritische Al-concentratie mede wordt gebaseerd op het voorkomen van de uitputting van secundaire Al-verbindingen, (vi) de voorraad aan secundaire Al-verbindingen kan bij het huidige depositieniveau in Nederland in enkele decennia zijn uitgeput, vooral in kalkloze duingronden en (vii) de huidige plannen voor emissiereducties zijn op Europese schaal niet toereikend om de voortschrijdende verzuring te stoppen, terwijl in Nederlandse bosgronden de chemische samenstelling van het bodemvocht (in termen van pH,  $\text{SO}_4^-$ ,  $\text{NO}_3^-$  en Al-concentratie) sterk verbeterd.

## REFERENCES

- Aagaard, P. and H.C. Helgeson, 1982. *Thermodynamic and kinetic constraints on reaction rates among minerals and aqueous solutions. I. Theoretical considerations*. Amer. J. Sci. 282: 237-285.
- Aber, J.D., K.J. Nadelhoffer, P. Steudler and J.M. Melillo, 1989. *Nitrogen saturation in northern forest ecosystems*. Bioscience 39: 378-386.
- Aber, J.D., J.M. Melillo, K.J. Nadelhoffer, J. Pastor and R.D. Boone, 1991. *Factors controlling nitrogen cycling and nitrogen saturation in northern temperate forest ecosystems*. Ecol. Applications 1: 303-315.
- Abrahamson, G. and A.O. Stuanes, 1980. *Effects of simulated acid rain on the effluent from lysimeters with acid, shallow soil rich in organic matter*. In: D. Drablos and A. Tollan (Eds.), Ecological impact of acid precipitation. SNSF Project, Nisk, Norway: 152-153.
- Adams, F. and Z. Rawajfih, 1977. *Basaluminite and alunite a possible cause of sulphate retention by acid soils*. Soil Sci. Soc. Am. J. 41: 686-692.
- Ågren, G.I., 1983. *Model analysis of some consequences of acid precipitation on forest growth*. In: Ecological effects of acid deposition; Report and background papers, 1982. Stockholm conference on the acidification of the environment Expert meeting 1. Solna 1983. (SNV PM; 1636): 233-244.
- Ågren, G.I. and E. Bosatta, 1988. *Nitrogen saturation of terrestrial ecosystems*. Environ. Poll. 54: 185-198.
- Alcamo, J., M. Amann, J.P. Hettelingh, M. Holmberg, L. Hordijk, J. Kämäri, L. Kauppi, P. Kauppi, G. Kornai, and A. Makela, 1987. *Acidification in Europe A simulation model for evaluating control strategies*. Ambio 16: 232-244.
- Alcamo, J., R. Shaw and L. Hordijk, 1990. *The RAINS model of acidification. Science and Strategies in Europe*. Dordrecht, the Netherlands, Kluwer Academic Publishers, 402 pp.
- Appelo, C.A.J., 1982. *Verzuring van het grondwater op de Veluwe*. H<sub>2</sub>O 18: 464-468.
- April, R. and R. Newton, 1985. *Influence of geology on lake acidification in the ILWAS watersheds*. Water Air Soil and Poll. 26: 373-386.
- Aronsson, A., 1980. *Frost hardiness in Scots pine. II Hardiness during winter and spring in young trees of different mineral status*. Studia Forest Suecica 155: 1-27.
- Arp, P.A., 1983. *Modelling the effects of acid precipitation on soil leachates A simple approach*. Ecol. Modelling 19: 105-117.
- Arts, G.H.P., 1988. *Historical development and extent of acidification of shallow soft waters in the Netherlands*. In: P. Matty (Ed.), Air pollution and ecosystems. Proc. Int. Symp. Grenoble, France: 928-933.
- Arts, G.H.P., 1990. *Deterioration of Atlantic soft-water systems and their flora*. Ph.D. Thesis, Catholic University of Nijmegen, the Netherlands, 197 pp.
- Asman, W.A.H., 1987. *Atmospheric behaviour of ammonia and ammonium*. Ph.D. Thesis, Agricultural University Wageningen, the Netherlands.

- Asman, W.A.H., 1990. *Ammonia emission in Europe updated emission and emission variations*. Bilthoven, the Netherlands, National Institute of Public Health and Environmental Protection, Report 2284471008.
- Bache, B., 1974. *Soluble aluminium and calcium aluminium exchange in relation to the pH of dilute calcium chloride suspensions of acid soil*. J. Soil Sci. 25: 331-332.
- Bache, B.W., 1980. *The acidification of soils*. In: T.C. Hutchinson and M. Havas (Eds.), *Effects of acid precipitation on terrestrial ecosystems*. Plenum Press, New York: 183-202.
- Baker, J.P. and C.L. Schofield, 1982. *Aluminium toxicity to fish in acid waters*. Water Air and Soil Poll. 18: 289-309.
- Bakker, T.W.M., 1981. *Nederlandse kustduinen, geohydrologie*. PUDOC, Wageningen, 189 pp.
- Bakker, J.P., 1989. *Nature management by grazing and cutting*. Kluwer Academic Publishers, Dordrecht, the Netherlands, 400 pp.
- Bakker, T.W.M., J.A. Klijn en F.J. Van Zadelhoff 1981. *Nederlandse kustduinen, Landschapsecologie*. PUDOC, Wageningen, the Netherlands, 144 pp.
- Battarbee, R.W., R.J. Flower, A.C. Stevenson, V.J. Jones, R. Harriman and P.G. Appleby, 1988. *Diatom and chemical evidence for reversibility of acidification of Scottish lochs*. Nature 332: 530-532.
- Belmans, C., J.G. Wesseling and R.A. Feddes, 1983. *Simulation model of the water balance of a cropped soil providing different types of boundary conditions SWATRE*. J. Hydrol. 63: 27-286.
- Berdén, M., S.I. Nilsson, K. Rosén and G. Tyler, 1987. *Soil acidification extent, causes and consequences*. National Swedish Environment Protection Board, Report 3292, 164 pp.
- Berdowski, J.J.M., C. Van Heerden, J.J.M. Van Grinsven, J.G. Van Minnen and W. De Vries, 1991. *SOILVEG A model to evaluate effects of acid atmospheric deposition on soil and forest. Volume 1 Model principles and application procedures*. Bilthoven, the Netherlands, Dutch Priority Programme on Acidification, Report 114.1-02, 126 pp.
- Berendse, F. and R. Aerts, 1984. *Competition between Erica tetralix and Molinia caerulea (L.). Moench as affected by availability of nutrients*. Acta Oecol./Oecol. Plant 19(5): 3-14.
- Berendse, F., 1988. *De nutriëntenbalans van droge zandgrondvegetaties in verband met de eutrofiëring via de lucht. Deel 1 Een simulatiemodel als hulpmiddel bij het beheer van vochtige heidevelden*. Wageningen, Centrum voor Agrobiologisch Onderzoek, 51 pp.
- Berg, B. and H. Staaf, 1981. *Leaching, accumulation and release of nitrogen in decomposing forest litter*. In: F.E. Clark and T. Rosswall (Eds.), *Terrestrial Nitrogen Cycles*. Ecol. Bull. 33: 163-178.
- Bergkvist, B. and L. Folkesson, 1992. *Soil acidification and element fluxes of a fagus sylvatica forest as influenced by simulated nitrogen deposition*. Water Air and Soil Poll. 65: 111-133.
- Billet, M.F., E.A. FitzPatrick and M.S. Cresser, 1988. *Long-term changes in the acidity of forest soils in North-East Scotland*. Soil Use and Man. 4: 102-107.

- Billet, M.F., E.A. FitzPatrick and M.S. Cresser, 1990a. *Changes in the carbon and nitrogen status of forest soil organic horizons between 1949/50 and 1987*. Environ. Poll. 66: 67-79.
- Billet, M.F., F. Parker-Jervis, E.A. FitzPatrick and M.S. Cresser, 1990b. *Forest soil chemical changes between 1949/50 and 1987*. J. Soil Sci. 41: 133-145.
- Bisdorf, E. and O.H. Boersma, 1994. *Micromorphological studies*. In: Weathering processes and rates in relation to acidification and vulnerability of forest ecosystems in Northern Europe. Final report in the framework of the STEP programme of the Commission of the European Communities.
- Bloom, P.R. and D.F. Grigal, 1985. *Modelling soil response to acidic deposition in nonsulfate adsorbing soils*. J. Environ. Qual. 14: 489-495.
- Bloom, P.R. and M.S. Erich, 1987. *Effect of solution composition on the rate and mechanism of gibbsite dissolution in acid solutions*. Soil Sci. Soc. Am J. 51: 1131-1136.
- Bloom, P.R., M.B. McBride and R.M. Weaver, 1979a. *Aluminium organic matter in acid soils: salt-extractable aluminium*. Soil Sci. Soc. Am. J. 43: 813-815.
- Bloom, P.R., M.B. McBride and R.M. Weaver, 1979b. *Aluminium organic matter in acid soils: Buffering and solution aluminium activity*. Soil Sci. Soc. Am. J. 43: 488-493.
- Bobbink, R., L. Bik and J.H. Willems, 1988. *Effects of nitrogen fertilization on vegetation structure and dominance of Brachypodium pinnatum (L.) Beauv. in chalk grassland*. Acta Bot. Neerl. 37(2): 231-242.
- Bobbink, R., D. Boxman, E. Fremstad, G. Heil, A. Houdijk and J. Roelofs, 1992. *Critical loads for nitrogen eutrophication of terrestrial and wetland ecosystems based upon changes in vegetation and fauna*. In: P. Grennfelt and E. Thornelof (Eds.): Critical Loads for Nitrogen. Report from a workshop held at Lökeberg, Sweden, 6-10 April 1992. Nordic Council of Ministers, Report 1992, 41: 111-161.
- Boerboom, J.H.A., 1963. *Het verband tussen bodem en vegetatie in de Wassenaarse duinen*. Boor en Spade, 13: 120-155.
- Bormann, F.H., G.E. Likens and J.M. Melillo, 1977. *Nitrogen budget for an aggrading northern hardwood forest ecosystem*. Science 196: 981-983.
- Bouma, J., H.A.J. Van Lanen, A. Breeuwsma, J.M.J. Wüsten and M.J. Kooistra, 1986. *Soil survey data needs when studying modern land use problems*. Soil Use and Man. 2(4): 125-130.
- Boumans, L.J.M. en W. Beltman, 1991. *Kwaliteit van het bovenste freatische grondwater in de zandgebieden van Nederland onder bos- en heidevelden*. Bilthoven, Rijksinstituut voor Volksgezondheid en Milieuhygiëne, Rapport 724901001, 65 pp.
- Boumans, L.J.M. en J.J.M. Van Grinsven, 1991. *Aluminiumconcentraties in het freatische grondwater in de zandgebieden van Nederland onder bos- en heidevelden*. Bilthoven, Rijksinstituut voor Volksgezondheid en Milieuhygiëne, Rapport 724901002, 43 pp.
- Boxman, A.W. en H.F.G. Van Dijk, 1988. *Het effect van landbouw ammonium deposities op bos- en heidevegetaties*. Katholieke Universiteit Nijmegen, 96 pp.

- Boxman, A.W., R.J. Sinke and J.G. Roelofs, 1986. *Effects of ammonium on the growth and kalium (86Rb) uptake of various ectomycorrhizal fungi in pure culture*. Water Air and Soil Poll. 32: 517-522.
- Boxman, A.W., H.F.G. Van Dijk, A.L.F.M. Houdijk and J.G.M. Roelofs, 1988. *Critical loads for nitrogen with special emphasis on ammonium*. In: J. Nilsson and P. Grennfelt (Eds.), *Critical loads for sulphur and nitrogen*. Report from a workshop held at Skokloster, Sweden, 19-24 March, 1988. Miljø rapport 1988 15. Nordic Council of Ministers, København: 295-322.
- Brady, N.C., 1974. *The nature and properties of soils*. (8<sup>th</sup> ed.) Mac.Millan Publ. Co., Inc. New York, 285 pp.
- Bredemeier, M., 1988. *Forest canopy transformation of atmospheric deposition*. Water Air and Soil Poll. 40: 121-138.
- Breeuwsma, A., J.P. Chardon, J.F. Kragt and W. De Vries, 1991. *Pedotransfer functions for denitrification*. In ECE 1991, Soil and Groundwater Research Report II "Nitrate in Soils", Commission of the European Community, Luxembourg: 207-215.
- Breeuwsma, A., J.H.M. Wösten, J.J. Vleeshouwer, A.M. Van Slobbe and J. Bouma, 1986. *Derivation of land qualities to assess environmental problems from soil surveys*. Soil Sci. Soc. Am. J. 50: 186-190.
- Bregt, A.K., J. Denneboom, J. Stolp and J.J. Vleeshouwer, 1986. *BIS, an information system for soil survey and research*. Transactions of the XIII Congress of Int. Soc. Soil Sci., Hamburg, August 1986; Volume III: 1064-1065.
- Brent, R.P., 1973. *Algorithms for Minimization without Derivatives*. Englewood Cliffs, N.J. Prentice-Hall.
- Brinkman, R., 1970. *Ferrollysis, a hydromorphic soil forming process*. Geoderma 3: 199-206.
- Busenberg, E. and C.V. Clemency, 1976. *The dissolution kinetics of feldspars at 25 °C at 1 atm CO<sub>2</sub> partial pressure*. Geochim. Cosmochim. Acta 40: 41-49.
- Butzke, H., 1981. *Versauern unsere Wälder? Erste Ergebnisse der Überprüfung 20 Jahre alter pH-Wert-Messungen in Waldböden Nordrhein-Westfalens*. Forst und Holzwirt 36 (21): 542-548.
- Butzke, H., 1988. *Zur zeitlichen und kleinräumigen Variabilität des pH-Wertes im Waldböden Nordrhein-Westfalens*. Forst und Holzwirt 43 (4): 81-85.
- Calder, I.R. and M.D. Newson, 1979. *Land use and upland water resources in Britain. A strategic look*. Water Resour. Bull. 15: 1628-1639.
- Campbell, N.E.R. and H. Lees, 1967. *The nitrogen cycle*. In: A.D. McLaren and G.H. Peterson (Eds.), *Soil Biochemistry*. Marcel Dekker. Inc., New York: 194-215.
- Cape, J.N. and P.J. Lightowers, 1988. *Review of throughfall and stemflow chemistry data in the United Kingdom*. Institute of Terrestrial Ecology, Edinburgh, Scotland, ITE project T07003 el., 234 pp.
- CBS, 1985. *De Nederlandse Bosstatistiek. Deel 1 De oppervlakte bos van 1980 to 1983*. Den Haag, Centraal Bureau voor de Statistiek, Staatsdrukkerij, 123 pp.

- Chen, C.W., S.A. Gherini, R.J.M. Hudson and J.D. Dean, 1983. *The Integrated Lake-Watershed Acidification Study. Volume 1 Model principles and application procedures.* EPRI EA-3221, Volume 1, Research Project 1109-5, TETRA TECH INC., Lafayette, California, 194 pp.
- Childs, C.W., R.L. Parfitt and R. Lee, 1983. *Movement of aluminium as an inorganic complex in some podzolised soils, New Zealand.* Geoderma 29: 139-155.
- Chou, L. and R. Wollast, 1985. *Steady-state kinetics and dissolution mechanisms of Albite.* Amer. J. Sci. 285: 963-993
- Christensen, B., P.B. Mortensen and T. Petersen, 1985. *Illustration of the present capabilities of the ECCES program system.* Risø National Laboratory, Denmark M-2501, 43 pp.
- Christophersen, N., H.M. Seip and R.F. Wright, 1982. *A model for streamwater chemistry at Birkenes, Norway.* Wat. Resour. Res. 18: 977-996.
- Clark, J.S. and R.G. Hill, 1964. *The pH-percent base relationship of soils.* Soil Sci. Soc. Am. J. 28: 490-492.
- Clays-Josserand, A., R. Lensi and F. Gourbière, 1988. *Vertical distribution of nitrification potential in an acid forest soil.* Soil Biol. Biochem. 20 (3): 405-406.
- Coleman, N.T., S.B. Weed and R.J. McCracken, 1959. *Cation-exchange capacity and exchangeable cations in Pietmont Soils of North Carolina.* Soil Sci. Soc. Am J. 23: 146-149.
- Cosby, B.J., G.M. Hornberger, J.N. Galloway and R.F. Wright, 1985a. *Modeling the effects of acid deposition. Assessment of a lumped parameter model of soil water and streamwater chemistry.* Wat. Resour. Res. 21: 51-63.
- Cosby, B.J., R.F. Wright, G.M. Hornberger and J.N. Galloway, 1985b. *Modeling the effects of acid deposition. Estimation of long-term water quality responses in a small forested catchment.* Wat. Resour. Res. 21: 1591-1601.
- Cosby, B.J., G.M. Hornberger, J.N. Galloway and R.F. Wright, 1985c. *Freshwater acidification from atmospheric deposition of sulfuric acid A quantitative model.* Environ. Sci. Technol. 19: 1144-1149.
- Coulter, R.S. and O. Talibudeen, 1968. *Calcium aluminium exchange equilibria in clay minerals and acid soils.* J. Soil Sci. 19: 237-256.
- Cramer, W. and I.C. Prentice, 1988. *Simulation of regional soil moisture deficits on a European scale.* Norsk geogr. Tidsskr. 42: 149-151.
- Cronan, C.S., W.J. Walker and P.R. Bloom, 1986. *Predicting aqueous aluminium concentrations in natural waters.* Nature 324: 140-143.
- Cronan, C.S., W.A. Reiners, R.C. Reijndols and G.E. Lang, 1978. *Forest floor leaching contributions from mineral, organic, and carbonic acids in New Hampshire subalpine forests.* Science 200: 309-311.
- Cronan, C.S., R. April, R.J. Bartlett, P.R. Bloom, C.T. Driscoll, S.A. Gherini, G.S. Henderson, J.D. Joslin, J.M. Kelly, R.M. Newton, R.A. Parnell, H.H. Patterson, D.J. Raynall, M. Schaedle, C.T. Schofield, E.I. Sucoff, H.B. Tepper and F.C. Thornton, 1989. *Aluminium toxicity in forests exposed to acidic deposition.* Water Air and Soil Poll. 48: 181-192.



- Dahlgren, R.A. and F.C. Ugolini, 1991. *Distribution and characterization of short-range-order minerals in Spodosols from the Washington Cascades*. Geoderma 48: 391-413.
- Dahlgren, R.A. and W.J. Walker, 1993. *Aluminium release rates from selected spodosol Bs horizons: Effects of pH and solid-phase aluminium pools*. Geochim. Cosmochim. Acta 57: 57-66.
- Dancer, W.S., L.A. Peterson and G. Chesters, 1973. *Ammonification and nitrification of N as influenced by soil pH and previous N treatments*. Soil Sci. Soc. Am. J. 37: 67-69.
- David, M.B. and C.T. Driscoll, 1984. *Aluminium speciation and equilibria in soil solution of a Haplorthod in the Adirondack Mountains, New York*. Geoderma 33: 297-318.
- David, M.B., M.J. Mitchell and J.P. Nakas, 1982. *Organic and inorganic sulphur constituents of a forest soil and their relationship to microbial activity*. Soil Sci. Soc. Am. J. 46: 847-852.
- De Boer, W., 1989. *Nitrification in Dutch heathland soils*. Ph.D Thesis, Agricultural University Wageningen, the Netherlands, 96 pp.
- De Boer, W. and A. Tietema, 1990. *Nitrification in Dutch acid forest-and heathland soils mechanisms and effects of biotic and abiotic factors*. Bilthoven, the Netherlands, Dutch Priority Programme on Acidification, Report 106.1, 17 pp.
- Dekker, L.W. 1988. *Verspreiding, oorzaken, gevolgen en verbeteringsmogelijkheden van waterafstotende gronden in Nederland*. Wageningen, Stichting voor Bodemkartering, Rapport 2046, 54 pp.
- Dekker, L.W. and P.D. Jungerius, 1990. *Water repellency in the dunes with special reference to the Netherlands*. Catena Supplement 18, Dunes of the European Coasts: 173-183.
- De Laat, P.J.M., 1985. *Simulatie van verdamping en berekening met MUST*. H<sub>2</sub>O 18: 363-367.
- De Leeuw, F.A.A.M. and J.A. Van Jaarsveld, 1992. *Bepaling van bron-receptor relaties voor verzurende componenten*. Bilthoven, Rijksinstituut voor Volksgezondheid en Milieuhygiëne, Rapport 723001009, 29 pp.
- Depuydt, F., 1972. *De Belgische strand- en duinformaties in het kader van de geomorfologie der zuidoostelijke Noordzeekust*. Kon. Ac. v. Wetensch., Lett. en Schone Kunsten, Brussel, 122 pp.
- De Raeve, F., 1989. Sand dune vegetation and management dynamics. In: F. Van der Meulen, P.D. Jungerius and J. Visser (Eds.), *Perspectives in coastal dune management*. The Hague, The Netherlands, SPB Acad. Publ.: 99-109.
- De Visser, P.H.B. en W. De Vries, 1989. *De gemiddelde waterbalans van bos-, heide- en graslandvegetaties*. Wageningen, Stichting voor Bodemkartering, Rapport nr. 2085, 136 pp.
- De Visser, P.H.B., 1986. *Interactions between soil, vegetations and atmospheric deposition*. Bilthoven, the Netherlands, Dutch Priority Programme on Acidification. Report 02-01, 88 pp.
- De Vries, O. en A.M. Van Vliet, 1945. *Onderzoek naar de bodemgesteldheid van het landgoed de Utrecht nabij Esbeek*. Verslagen van landbouwkundige onderzoekingen, no. 50 (9) A, PUDOC, Wageningen.

- De Vries, W., 1987. *The role of soil data in assessing the large-scale impact of atmospheric pollutants on the quality of soil water*. In: W. van Duijvenbooden and H.G. van Waegeningh (Eds.): Vulnerability of soil and groundwater to pollutants. Proc. Int. Conf. Noordwijk aan Zee, the Netherlands, March 30 - April 3, 1987. Proceedings and Information TNO-CHO/RIVM No. 38: 897-910.
- De Vries, W., 1988. *Critical deposition levels for nitrogen and sulphur on Dutch forest ecosystems*. Water Air and Soil Poll. 42: 221-239.
- De Vries, W., 1990. *Philosophy, structure and application methodology of a soil acidification model for the Netherlands*. In: J. Kamari (Ed.), Environmental Impact Models to Assess Regional Acidification, Kluwer Academic Publishers, Dordrecht: 3-21.
- De Vries, W., 1991. *Methodologies for the assessment and mapping of critical loads and the impact of abatement strategies on forest soils*. Wageningen, the Netherlands, DLO Winand Staring Centre for Integrated Land, Soil and Water Research, Report 46, 109 pp.
- De Vries, W., 1993. *Average critical loads for nitrogen and sulfur and its use in acidification abatement policy in the Netherlands*. Water Air and Soil Poll. 68: 399-434.
- De Vries, W., 1994a. *Rates and mechanisms of cation and silica release in acid sandy soils. 1. Influence of mineral pools and mineral depletion*. Geoderma (submitted).
- De Vries, W., 1994b. *Rates and mechanisms of cation and silica release in acid sandy soils. 2. Effects of pH and aluminium concentration*. Geoderma (submitted).
- De Vries, W. and A. Breeuwsma, 1986. *Relative importance of natural and anthropogenic proton sources in soils in the Netherlands*. Water Air and Soil Poll. 28: 173-184.
- De Vries, W. and A. Breeuwsma, 1987. *The relation between soil acidification and element cycling*. Water Air and Soil Poll. 35: 293-310.
- De Vries, W. and H.D. Gregor, 1991. *Critical loads and critical levels for the environmental effects of air pollutants*. In: M.J. Chadwick and M. Hutton (Eds.), Acid depositions in Europe Environmental effects, control strategies and policy options. York, Stockholm Environmental Institute: 171-216.
- De Vries, W. and G.J. Heij, 1991. *Critical loads and critical levels for the environmental effects of air pollutants*. In G.J. Heij and T. Schneider (Eds.), Acidification Research in the Netherlands Final Report of the Dutch Priority Programme on Acidification. Studies in Environmental Science 46, Elsevier Science Publishers, Amsterdam, the Netherlands: 205-214.
- De Vries, W. and J. Kros, 1989. *The long-term impact of acid deposition on the aluminium chemistry of an acid forest soil*. In: J. Kämäri, D.F. Brakke, A. Jenkins, S.A. Norton and R.F. Wright (Eds.), Regional Acidification Models. Geographic Extent and Time Development: 113-128.
- De Vries, W. and J. Kros, 1991. *Assessment of critical loads and the impact of deposition scenarios by steady state and dynamic soil acidification models*. Wageningen, the Netherlands, DLO Winand Staring Centre for Integrated Land, Soil and Water Research, Report 36, 61 pp.

- De Vries, W. and P.C Jansen, 1994. *Effects of acid deposition on 150 forest stands in the Netherlands. 3. Input output budgets for sulphur, nitrogen, base cations and aluminium.* Wageningen, the Netherlands, DLO Winand Staring Centre for Integrated Land, Soil and Water Research, Report 69.3, 58 pp.
- De Vries, W. and E.E.J.M. Leeters, 1994. *Effects of acid deposition on 150 forest stands in the Netherlands. 1. Chemical composition of the humus layer, mineral soil and soil solution.* Wageningen, the Netherlands, DLO Winand Staring Centre for Integrated Land, Soil and Water Research, Report 69.1.
- De Vries, W., A. Breeuwsma en F. De Vries, 1989a. *Kwetsbaarheid van de Nederlandse bodem voor verzuring.* Wageningen, DLO-Staring Centrum, Rapport nr. 29, 74 pp.
- De Vries, W., J. Klijn and J. Kros, 1994a. *Simulation of the long-term impact of atmospheric deposition on dune ecosystems in the Netherlands.* Journal of Applied Ecology 31: 59-73.
- De Vries, W., J. Kros and C. Van der Salm, 1994b. *Modelling the impact of acid deposition and nutrient cycling in forest soils.* Ecological Modelling (in press).
- De Vries, W., J. Kros and C. Van der Salm, 1994c. *The long-term impact of three emission-deposition scenarios on Dutch forest soils.* Water Air and Soil Poll. 75: 1-35.
- De Vries, W., J. Kros and J.C.H. Voogd, 1994d. *Assessment of critical loads and their exceedance on Dutch forests using a multi-layer steady-state model.* Water Air and Soil Poll. 76 (in press).
- De Vries, W., M. Posch and J. Kämäri, 1989b. *Simulation of the long-term soil response to acid deposition in various buffer ranges.* Water Air and Soil Poll. 48: 349-390.
- De Vries, W., G.J. Reinds and M. Posch, 1994e. *Assessment of critical loads and their exceedance on European forests using a one-layer steady-state model.* Water Air and Soil Poll. 72: 357-394.
- De Vries, W., W. Schöpp and J.P. Hettelingh, 1991. *Comparison of national critical load maps and the CCE critical loads map based on European data only.* In: J.P. Hettelingh, R.J. Downing and P.A.M. De Smet (Eds.), Mapping critical loads for Europe. Bilthoven, the Netherlands, National Institute of Public Health and Environmental Protection. Coordination Centre for Effects, Technical report no. 1: 76-79.
- De Vries, W., J.C.H. Voogd and J. Kros, 1993. *Effects of various deposition scenarios on the aluminium hydroxide content of Dutch forest soils.* Wageningen, the Netherlands, DLO Winand Staring Centre for Integrated Land, Soil and Water Research, Report 68, 32 pp.
- De Vries, W., A. Hol, S. Tjalma en J.C. Voogd, 1990. *Literatuurstudie naar voorraden en verblijftijden van elementen in een bosecosysteem.* Wageningen, DLO-Staring Centrum, Rapport 94, 205 pp.
- De Vries, W., M. Posch, G.J. Reinds and J. Kämäri, 1992a. *Critical loads and their exceedance on forest soils in Europe.* Wageningen, the Netherlands, DLO Winand Staring Centre for Integrated Land, Soil and Water Research, Report 58, 126 pp.
- De Vries, W., M. Posch, G.J. Reinds and J. Kämäri, 1994f. *Simulation of soil response to acidic deposition scenarios in Europe.* Water Air and Soil Poll. 78 (in press.)

- De Vries, W., M.J.P.H. Waltmans, R. Van Versendaal en J.J.M. Van Grinsven, 1988. *Aanpak, structuur en voorlopige procesbeschrijving van een bodemverzuringmodel voor toepassing op regionale schaal*. Wageningen, Stichting voor Bodemkartering, Rapport 2014, 132 pp.
- De Vries, W., J. Kros, R.M. Hootsmans, J.G. Van Uffelen and J.C.H. Voogd, 1992b. *Critical loads on Dutch forest soils*. In: T. Schneider (Ed.), *Acidification on Research Evaluation and Policy Applications*, Studies in Environmental Science 50, Elsevier Science Publishers, Amsterdam, the Netherlands: 307-318.
- De Vries, W., M.M.T. Meulenbrugge, W. Balkema, J.C.H. Voogd and R.C. Sjardijn, 1994g. *Rates, stoichiometry and mechanisms of cation and silica release in acid sandy soils. 3. Differences between soil horizons and soil types*. *Geoderma* (submitted).
- De Vries, W., J.J.M. Van Grinsven, N. Van Breemen, E.E.J.M. Leeters and P.C. Jansen, 1994h. *Impacts of acid atmospheric deposition on concentrations and fluxes of solutes in acid sandy forest soils in the Netherlands*. *Geoderma* (submitted).
- De Vries, W., M. Posch, T. Oja, H. Van Oene, J. Kros, P. Warfvinge and P.A. Arp, 1994i. *Modelling critical loads for the Solling spruce site*. *Modelling of Geo-biosphere Processes*. (Submitted).
- De Wit, J.C.M., W.H. Van Riemsdijk and L.K. Koopal, 1993. *Proton binding to humic substances. 2. Chemical heterogeneity and adsorption models*. *Environm. Sci. Technol.* 2015-2022
- Dickson, W., 1986. *Some data on critical loads for sulphur on surface water*. In: J. Nilsson (Ed.), *Critical loads for nitrogen and sulfur*. Nordic council of Ministers, Report 1986, 11: 143-158.
- Dillon, P.J., R.A. Reid and R. Girard, 1986. *Changes in chemistry of lakes near Sudbury, Ontario following reductions in SO<sub>2</sub> emissions*. *Water Air and Soil poll.* 31: 59-65.
- Dillon, P.J., R.A. Reid and E. de Grosbois, 1987. *The rate of acidification of aquatic ecosystems in Ontario, Canada*. *Nature* 329: 45-48.
- Doing, H., 1966. *Beschrijving van de vegetatie der duinen tussen IJmuiden en Camperduin*. Wageningen, Mededelingen Landbouwhogeschool 66-13, 55 pp.
- Draayers, G.P.J. and J.W. Erisman, 1993. *Atmospheric sulphur deposition to forest stands throughfall estimates compared to estimates from inference*. *Atmospheric Env.* 27A: 43-55.
- Draayers, G.P.J., R. Van Eck and R. Meijers, 1992. *Measuring and modelling dry deposition in complex forest terrain*. In: T. Schneider (Ed.), *Acidification Research Evaluation and Policy Applications*, Studies in Environmental Science 50, Elsevier Science Publishers, Amsterdam, the Netherlands: 285-294.
- Driscoll, C.T. and G.E. Likens, 1982. *Hydrogen ion budget of an aggrading forested ecosystem*. *Tellus* 34: 283-292.
- Driscoll, C.T., J.P. Baker, J.J. Bisopni and C.L. Schofield, 1980. *Effect of aluminium speciation on fish in dilute acidified waters*. *Nature* 284: 161-163.
- Driscoll, C.T., N. Van Breemen and J. Mulder, 1985. *Aluminium chemistry in a forested spodosol*. *Soil Sci. Soc. Am. J.* 49: 437-444.

- Driscoll, C.T., D.A. Schaefer, L.A. Molot and P.J. Dillon, 1989. *Summary of North American data*. In: J.L. Malanchuk and J. Nilsson (Eds.), *The role of nitrogen in the acidification of soils and surface waters*. NORD 1989:92, Nordic Council of Ministers, Copenhagen, Denmark: 6(1)-6(45).
- Duchaufour, P. 1977. *Pedology. Pedogenesis and classification*. George Allen and Unwin, London, U.K., 448 pp.
- Eary, L.E., E.A. Jenne, L.W. Vail and D.C. Girvin, 1989. *Numerical models for predicting watershed acidification*. *Archiv. Environ. Contam. Toxicol.* 18: 29-53.
- Edelman, C.H. en L.A.H. de Smet, 1951. *Over de ontkalking van de Dollardklei*. *Boor en Spade* 4: 104-114.
- Eelerwoude Ingenieursbureau, 1991. *Onderzoek naar de vitaliteit en vitaliteitsbepalende factoren in lijnvormige landschapselementen in Twente*. Rapport project 204HP, 46 pp.
- Eisma, D., 1968. *Composition, origin and distribution of Dutch coastal sands between Hoek van Holland and the island of Vlieland*. *Netherlands J. Sea Res.* 4(2): 123-267.
- Ellenberg, H., 1977. *Stickstoff als Standortfaktor*. *Ecologia Plantarum* 12, 1: 4-21.
- Ellenberg, H., 1985. *Veränderungen der Flora Mitteleuropas unter dem Einfluss von Düngung und Immissionen*. *Schweiz. Z. Forstwes.* 135: 19-39.
- Emmer, I.M. and A. Tietema, 1990. *Temperature dependent nitrogen transformations in acid oak-beech litter in the Netherlands*. *Plant and Soil* 122: 193-196.
- Erisman, J.W., 1990. *Atmospheric deposition of acidifying compounds onto forests in the Netherlands throughfall measurements compared to deposition estimates from inference*. Bilthoven, the Netherlands, National Institute of Public Health and Environmental Protection, Report nr. 723001001, 29 pp.
- Erisman, J.W., 1991. *Acid deposition in the Netherlands*. Bilthoven, the Netherlands, National Institute of Public Health and Environmental Protection, Report nr. 723001002, 72 pp.
- Erisman, J.W., F.A.A.M. De Leeuw en R.M. Van Aalst, 1987. *Depositie van de voor verzuring in Nederland belangrijkste componenten in de jaren 1980 t/m 1986*. Bilthoven, Rijksinstituut voor Volksgezondheid en Milieuhygiëne, Rapport nr. 228473001, 35 pp.
- Faber, P.J. and F. Thiemens, 1975. *Yield levels of Poplar*. Wageningen, the Netherlands, Research Institute for Forestry and Urban Ecology. Extensive report 13(1), 65 pp.
- Falkengren-Grerup, U., 1986. *Soil acidification and vegetation changes in deciduous forest in Southern Sweden*. *Oecologia* 70: 339-347.
- Falkengren-Grerup, U., N. Linnermark and G. Tyler, 1987. *Changes in acidity and cation pools of south Swedish soils between 1949 and 1985*. *Chemosphere* 16: 2239-2248.
- FAO, 1981. *FAO-Unesco soil map of the world, 1 500 000. Volume V Europe*. Unesco Paris 1981, 199 pp.
- FAO, 1988. *Soil map of the World, revised legend*. World soil resources report 60, FAO, Rome, 138 pp.

- Farmer, V.C., J.P. Russell and M.L. Berrow, 1980. *Imogolite and proto-imogolite allophane in spodic horizons. Evidence for a mobile aluminium silicate complex in podzol formation.* J. Soil Sci. 31: 673-684.
- Farrel, E.P., S.I. Nilsson, C.O. Tamm and G. Wiklander, 1984. *Distribution of sulphur fractions in lysimeters previously treated with sulphuric acid, NPK fertilizer and a combination of acid and fertilizer.* For. Ecol. Man. 8: 41-57.
- Fölster, H., 1985. *Proton consumption rates in holocene and present-day weathering of acid forest soils.* In: J.I. Brever (Ed.), *The chemistry of weathering*, Reidel Publ. Co., Dordrecht, the Netherlands: 197-209.
- Foster, N.W., I.K. Morrison and J.A. Nicolson, 1986. *Acid deposition and ion leaching from a podzolic soil under hardwood forest.* Water Air and Soil Poll. 31: 879-889.
- Freyer, J.L., 1990. *SIMPLEX: Non-linear curve fitting algorithm.* University of Amsterdam, Laboratory of Physical Geography and Soil Science, Report 39, 37 pp.
- Fung, P.C., N.S. Bird, G.W. McIntyre and G.G. Sanipelli, 1980. *Aspects of feldspar weathering.* Nuclear Technology 51: 188-196.
- Gaines, G.L. and H.C. Thomas, 1953. *Adsorption studies on clay minerals II. A formulation of the thermodynamics of exchange adsorption.* J. Chem. Phys. 21: 714-718.
- Galloway, J.N., G.E. Likens, W.C. Keene and J.M. Miller, 1982. *The composition of precipitation in remote areas of the world.* J. Geophys. Res. 87: 8771-8776.
- Galloway, J.N., G.E. Likens and M.E. Hawley, 1984. *Acid precipitation Natural versus anthropogenic components.* Science 226: 829-831.
- Gardiner, M.J., 1987. *Representative data for major soil units in the EEC soil map.* An Foras Taluntais, Ireland. Internal Report, 486 pp.
- Gherini, S.A., L. Mok, R.J.M. Hudson, G.F. Davis, C.W. Chen and R.A. Goldstein, 1985. *The ILWAS model formulation and application.* Water Air and Soil Poll. 26: 425-459.
- Gijsman, A., 1990. *Nitrogen nutrition and rhizosphere pH of Douglas fir.* Ph.D Thesis, National University of Groningen, the Netherlands, 132 pp.
- Gimingham, C.H., 1972. *Ecology of heathlands.* John Wiley and Sons, Inc. New York.
- Glatzel, G. and M. Kazda, 1985. *Wachstum und mineralstoffennahrung van buche (Fagus Silvatica) und spitzahorn (Acer platanoides) auf versauertem und schwermetall-belastetem bodenmaterial aus dem einsicherungsberreich.* Z. Pflanzenernähr. Bodenk. 148: 429-438.
- Granhall, U. and T. Lindberg, 1980. *Nitrogen input through biological nitrogen fraction.* In: T. Persson (Ed.), *Structure and function of Northern Coniferous forests. An Ecosystem study.* Ecol. Bull. 32: 333-340.
- Grier, C.C., K.A. Vogt, M.R. Keyes and R.L. Edmonds, 1981. *Biomass production and above - and below - ground production in young and mature Abies amabilis zone ecosystems of the Washington Cascades.* Can. J. For. Res. 11: 155-167.
- Grime, J.P., G.J. Hodgson and R. Hunt, 1988. *Comparative plant ecology; a functional approach to common British species.* Unwin Hyman, London, 742 pp.
- Groenenberg, J.E., J. Kros, C. van der Salm and W. De Vries, 1994. *Application of the model NUCSAM to the Solling spruce site.* Modelling of Geo-biosphere Processes. (submitted).

- Grootjans, A.P., P. Hendriksma, M. Engelmoer and V. Westhoff, 1988. *Vegetation dynamics in a wet dune slack (I) rare species decline on the Wadden island of Schiermonnikoog in the Netherlands*. Acta Bot. Neerl. 37(2): 265-278.
- Gundersen, P., 1991. *Nitrogen deposition and the forest nitrogen cycle role of denitrification*. For. Ecol. Man., 44: 15-28.
- Gundersen, P., 1992. *Mass balance approaches for establishing critical loads for nitrogen in terrestrial ecosystems*. In: P. Grennfeld and E. Thörmelöf (Eds.), *Critical loads for nitrogen*. NORD 1992:41, Nordic Council of Ministers, Copenhagen: 55-109.
- Gundersen, P. and L. Rasmussen, 1990. *Nitrification in forest soils effects from nitrogen deposition on soil acidification and aluminium release*. Rev. Environ. Contam. Toxicol. 113: 1-45.
- Halbäckén, L. and C.O. Tamm, 1986. *Changes in soil acidity from 1927 to 1982-1984 in a forest area of south-west Sweden*. Scand. J. For. Res. 1: 219-232.
- Hall, R.J., C.T. Driscoll, G.E. Likens and J.M. Pratt, 1984. *Physical, chemical and biological consequences of episodic aluminium additions to stream ecosystems*. Limnol. Oceanogr. 30: 212-225.
- Hamilton, G.J. and J.M. Cristie, 1971. *Forest management tables*. Forestry Commission. London, 318 pp.
- Hasselrot, B. and P. Grennfelt, 1987. *Deposition of air pollutants in a wind-exposed forest edge*. Water Air and Soil Poll. 34: 135-140.
- Hauhs, M. and R.F. Wright, 1989. *Acid deposition reversibility of soil and water acidification - A review*. EC Air Pollution Research Report 11, 42 pp.
- Heij, G.J. and T. Schneider, 1991. *Acidification Research in the Netherlands*. Final Report of the Dutch Priority Programme on Acidification. Studies in Environmental Science 46. Elsevier Science Publishers, Amsterdam, the Netherlands, 771 pp.
- Heij, G.J., W. De Vries, A.C. Posthumus and G.M.J. Mohren, 1991. *Effects of air pollution and acid deposition on forests and forest soils*. In: T. Schneider and G.J. Heij (Eds.), *Acidification research in the Netherlands*. Final report of the Dutch Priority Programme on Acidification. Studies in Environmental Science 46, Elsevier Science Publishers, Amsterdam, the Netherlands: 97-137.
- Heil, G.W. and W.M. Diemont, 1983. *Raised nutrient levels change heathland into grassland*. Vegetatio 53: 113-120.
- Heil, G.W., M.J.A. Werger, W. De Mol, D. Van Dam and B. Heijne, 1988. *Capture of atmospheric ammonium by grassland canopies*. Science 239: 764-765.
- Helgeson, H.C., 1971. *Kinetics of mass transfer among silicates and aqueous solution*. Geochim. Cosmochim. Acta 35: 421-469.
- Helgeson, H.C., W.M. Murphy and P. Aagaard, 1984. *Thermodynamic and kinetic constraints on reaction rates among minerals and aqueous solutions. II Rate constants, effective surface area and the hydrolysis of feldspar*. Geochim. Cosmochim. Acta 48: 2405-2432.
- Helling, C.S., G. Chesters and R.B. Corey, 1964. *Contribution of organic matter and clay to soil cation exchange capacity as affected by the pH of the saturating solution*. Soil Sci. Soc. Am. J. 28: 517-520.

- Hendrickx, J.M.H., L.W. Dekker and O.H. Boersma, 1993. *Unstable wetting fronts in water repellent field soils*. J. Environ. Qual. 22: 109-118.
- Hendriks, C.M.A., W. De Vries and J. Van den Burg, 1994. *Effects of acid deposition on 150 forest stands in the Netherlands. 2. Relationship between forest vitality and the chemical composition of the foliage, humus layer and the soil solution*. Wageningen, the Netherlands, DLO Winand Staring Centre for Integrated Land, Soil and Water Research, Report 69.2, 55 pp.
- Henriksen, A., 1988. *Critical loads of nitrogen to surface waters*. In: J. Nilsson and P. Grennfelt (Eds.), *Critical loads for sulphur and nitrogen; report from a workshop held at Skokloster, Sweden, 19-24 March, 1988*. Miljø rapport 1988 15. Nordic Council of Ministers, Copenhagen, Denmark: 385-412.
- Henriksen, A. and D.F. Brakke, 1988. *Estimates of critical loads of sulphur to surface waters*. Environm. Sci. Technol. 22: 8-14.
- Henriksen, A. and T. Hesthagen, 1993. *Critical load exceedance and damage to fish populations*. Oslo, Norwegian Institute for Water Research, Rapport nr. 43, 15 pp.
- Henriksen, A., W. Dickson and D.F. Brakke, 1986. *Estimates for critical loads for sulphur to surface waters*. In: J. Nilsson (Ed.), *Critical loads for nitrogen and sulphur*. Nordic Council of Ministers, Report 1986, 11: 87-120.
- Hettelingh, J.P. and W. De Vries, 1992. *Mapping Vademecum*. Bilthoven, the Netherlands, National Institute of Public Health and Environmental Protection, Report 259101002, 39 pp.
- Hettelingh, J.P., R.J. Downing and P.A.M. De Smedt, 1991. *Mapping critical loads for Europe*. National Institute of Public Health and Environmental Protection. Coordination Centre for Effects, Bilthoven, the Netherlands, Technical report no. 1, 183 pp.
- Hiege, W., 1985. *Wasserhaushalt von Forsten und Wälder und der Einfluss der Wassers auf Wachsthum und Gesundheit von Forsten und Wälder eine Literaturstudie*. Utrecht, the Netherlands, Studiecommissie Waterbeheer, Natuur, bos en Landschap, Rapport 7a, 192 pp.
- Higashi, T., F. De Coninck and F. Gelaude, 1981. *Characterization of some spodic horizons of the Campine (Belgium) with diethionite-citrate, pyrophosphate and sodium hydroxide-tetraborate*. Geoderma 25: 131-142.
- Hoeks, J., 1986. *Acidification of groundwater in the Netherlands*. Nat. Conf. Water Qual. Mod. Int. Natur. Environm., June 10-13th 1986, Bournemouth, England: 493-501.
- Hoekstra, C. and J.N.B. Poelman, 1982. *Dichtheid van gronden gemeten aan de meest voorkomende bodemeenheden in Nederland*. Wageningen, Stichting voor Bodemkartering, Rapport nr. 1582, 47 pp.
- Holdren, G.R. and P.M. Speyer, 1985. *pH dependent changes in rates and stoichiometry of dissolution of an alkali feldspar at room temperature*. Amer. J. Sci. 285: 994-1026.
- Holowaychuk, N. and J.D. Lindsay, 1982. *Distribution and relative sensitivity to acidification of soils Sand River Area*. Alberta, Research Management Division Report 82/13, 93 pp.



- Hommel, P.W.F.M., E.E.J.M. Leeters, P. Mekking and J.G. Vrieling, 1990. *Vegetation changes in the Speulderbos (the Netherlands) during the period 1958-1988*. Wageningen, the Netherlands, DLO Winand Staring Centre for Integrated Land, Soil and Water Research, Report 23, 9 pp.
- Hook, J.E. and L.T. Kardos, 1978. *Nitrate leaching during long-term spray irrigation for treatment of secondary sewage effluent on woodland sites*. J. Environ. Qual. 7: 30-34.
- Hootsmans, R.M. and J.G. van Uffelen, 1991. *Assessment of input data for a simple mass balance model to map critical acid loads for Dutch forest soils*. DLO-Staring Centrum, Interne Mededeling 133, 97 pp.
- Hornberger, G.M., K.J. Beven, B.J. Cosby and D.E. Sappington, 1985. *Shenandoah Watershed Study Calibration of a topography-based variable contributing area model to a small forested catchment*. Wat. Resour. Res. 21: 1841-1850.
- Hornberger, G.M., B.J. Cosby and J.N. Galloway, 1986. *Modeling the effects of acid deposition. Uncertainty and spatial variability in estimation of long-term sulfate dynamics in a region*. Wat. Resour. Res. 22 (8): 1293-1302.
- Houdijk, A.L.M.F., 1990. *Effecten van zwavel en stikstof depositie op bos- en heide vegetaties*. Katholieke Universiteit Nijmegen, Vakgroep Aquatische Ecologie en Biogeologie, 124 pp.
- Houdijk, A.L.F.M., 1993a. *De invloed van verhoogde aluminium-calcium verhoudingen in aanwezigheid van humuszuur en van de uitputting van de aluminiumvoorraad in de bodem op de vitaliteit van de Corsicaanse den*. Katholieke Universiteit Nijmegen, 51 pp.
- Houdijk, A.L.M.F., 1993b. *Atmospheric ammonium deposition and the nutritional balance of terrestrial ecosystems*. Ph.D. Thesis. Catholic University Nijmegen, the Netherlands, 127 pp.
- Hultberg, H., 1988. *Critical loads for sulphur to lakes and streams*. In: J. Nilsson and P. Grennfelt (Eds.), *Critical loads for sulphur and nitrogen; Report from a workshop held at Skokloster, Sweden, 19-24 March, 1988*. Miljø rapport 1988 15. Nordic Council of Ministers, København: 185-200.
- Isermann, K., 1983. *Bewertung natürlicher und anthropogener Stoffeinträge über die Atmosphäre als Standortfaktoren im Hinblick auf die Versauerung Land- und Forstwirtschaftlich genutzter Boden*. VDI-berichte Nr. 500, 307 pp.
- Ivens, W.P.M.F., G.P.J. Draaijers, M.M. Bos and W. Bleuten, 1988. *Dutch forest as air pollutant sinks in agricultural areas. A case study in the central part of the Netherlands on the spatial and temporal variability of atmospheric deposition to forests*. Dutch Priority Programme on Acidification, Report 37-09, 143 pp.
- Ivens, W.P.M.F., A. Klein Tank, P. Kauppi and J. Alcamo, 1989. *Atmospheric deposition of sulphur, nitrogen and basic cations onto European forests observations and model calculations*. In: J. Kämäri, D.F. Brakke, A. Jenkins, S.A. Norton and R.F. Wright (Eds.), *Regional acidification models Geographic extent and time development*, Springer, Berlin: 103-111.

- Iversen, T., J. Saltbones, H. Sandnes, A. Eliassen and H. Øystein, 1989. *Airborne transboundary transport of sulphur and nitrogen over Europe - Model descriptions and calculations*. Oslo, Sweden, Norwegian Meteorological Institute, EMEP/MSC-W Report 2/89.
- James, B.R. and S.J. Riha, 1986. *pH buffering in forest soil organic horizons: relevance to acid precipitation*. J. Environ. Qual. 13: 229-234.
- Janssen, B.H., 1983. *Organische stof en bodemvruchtbaarheid*. Landbouwniversiteit, Wageningen, Intern Rapport, 215 pp.
- Janssen, B.H., 1984. *A simple method for calculating decomposition and accumulation of young organic matter*. Plant and Soil: 76 297-304.
- Janssen, P.H.M., W. Slob en J. Rotmans, 1990. *Gevoeligheidsanalyse en onzekerheids analyse: een inventarisatie van ideeën, methoden en technieken*. Bilthoven, Rijksinstituut voor Volksgezondheid en Milieuhygiëne. Rapport 958805001, 119 pp.
- Jelgersma, S., J. De Jong, W.H. Zagwijn and J.F. Van Regteren Altena, 1970. *The coastal dunes of the western Netherlands; geology, vegetational history and archeology*. Med. Rijks Geol. Dienst, N.S. nr. 21, 166 pp.
- Jenkins, A., J. Kämäri, S.A. Norton, P. Whitehead, B.J. Cosby and D.F. Brakke, 1989. *Models to describe the geographic extent and time evolution of acidification and air pollution damage*. In: J. Kämäri, D.F. Brakke, A. Jenkins, S.A. Norton and J.W. Wright (Eds.) *Regional acidification models Geographic extent and time development*. Springer-Verlag, Berlin Heidelberg: 291-298.
- Johansson, M., I. Savolainen and M. Tähtinen, 1989. *The Finnish integrated acidification model*. In: J. Kämäri, D.F. Brakke, A. Jenkins, S.A. Norton and R.F. Wright (Eds.) *Regional Acidification Models Geographic extent and time development*: 203-211.
- Johnson, D.W., 1980. *Site susceptibility to leaching by H<sub>2</sub>SO<sub>4</sub> in acid rainfall*. In: T.C. Hutchinson and M. Havas (Eds.) *Effects of acid precipitation on terrestrial ecosystems*. Plenum Press, New York: 525-535.
- Johnson, D.W., 1984. *Sulfur cycling in forests*. Biogeochem. 1: 29-43.
- Johnson, D.W. and D.W. Cole, 1977. *Sulphate mobility in an outwash soil in western Washington*. Water Air and Soil Poll. 7: 489-495.
- Johnson, D.W. and D.W. Cole, 1980. *Anion mobility in soils relevance to nutrient transport from forest ecosystems*. Environ. Int. 3: 79-90.
- Johnson, D.W. and D.E. Todd, 1983. *Relationships among iron, aluminium, carbon, and sulfate in a variety of forest soils*. Soil Sci. Soc. of Am. J. 47: 792-800.
- Johnson, D.W., D.W. Cole and S.P. Gessel, 1979. *Acid precipitation and soil sulphate adsorption properties in a tropical and in a temperate forest soil*. Biotropica 11: 38-42.
- Johnson, D.W., D.D. Richter, H. Van Miegroet and D.W. Cole, 1983. *Contributions of acid deposition and natural processes to cation leaching from forest soils A review*. J. Air Poll. Contr. Ass. 33: 1036-1041.
- Johnson, D.W., D.W. Cole, S.P. Gessel, M.J. Singer and R.V. Minden, 1977. *Carbonic acid leaching in a tropical, temperate, sub-alpine and northern forest soil*. Arctic Alpine Res. 9(4): 329-343.

- Johnson, D.W., G.S. Henderson, D.D. Huff, Lindberg, S.E., D.D. Richter, D.S. Shriner, P.E. Todd and J. Turner, 1982. *Cycling of organic and inorganic sulfur in a chestnut oak forest*. *Oecologia* 54: 141-148.
- Johnson, N.M., C.T. Driscoll, J.S. Eaton, G.E. Likens and W.H. McDowell, 1981. *Acid rain, dissolved aluminium and chemical weathering at the Hubbard Brook Experimental Forest, New Hampshire*. *Geochim. Cosmochim. Acta* 45: 1421-1437
- Joslin, J.D. and M.H. Wolfe, 1988. *Responses of red spruce seedlings to changes in soil aluminium in six amended forest soil horizons*. *Can. J. of For. Res.* 18: 1614-1623.
- Joslin, J.D. and M.H. Wolfe, 1989. *Aluminium effects on northern red oak seedling growth in six forest soil horizons*. *Soil Sci. Soc. Am. J.* 53: 274-281.
- Jungerius, P.D. and F. Van der Meulen, 1988. *Erosion processes in a dune landscape along the Dutch coast*. *CATENA* 15(3/4): 217-228.
- Kalisz, P.J. and E.L. Stone, 1980. *Cation exchange capacity of acid forest humus layers*. *Soil Sci. Soc. Am. J.* 44: 407-413.
- Kämäri, J., 1987. *Prediction models for acidification*. *Proc. Int. Symp. on Acidification and Water Pathways, Vol.1, May 4-8, Bolkesjø, Norway*: 405-416.
- Kauppi, P. and M. Posch, 1988. *A case study of the effect of CO<sub>2</sub>-induced climate warming on forest growth and the forest sector A. Productivity reactions of Northern Boreal forests*. In: M.L. Parry, T.R. Carter and N.T. Konijn (Eds.) *The impact of climatic variations on agriculture. Volume 1 Assessments in cool temperate and cool regions*. Kluwer Academic Publishers, Dordrecht, the Netherlands: 183-195.
- Kauppi, P., J. Kämäri, M. Posch, L. Kauppi, and E. Matzner, 1986. *Acidification of forest soils Model development and application for analyzing impacts of acidic deposition in Europe*. *Ecol. Modelling* 33: 231-253.
- Keeney, D.R., 1980. *Prediction of soil nitrogen availability in forest ecosystems a literature review*. *For. Sci.* 26: 159-171.
- Keller, W., J.R. Pitblado and N.I. Conroy, 1986. *Water quality improvements in the Sudbury, Ontario, Canada area related to reduced smelter emissions*. *Water Air and Soil poll.* 31: 765-774.
- Keltjens, W.G. and E. Van Loenen, 1989. *Effects of aluminium and mineral nutrition on growth and chemical composition of hydroponically grown seedlings of five different forest tree species*. *Plant and Soil* 119: 39-50.
- Ketner-Oostra, R. 1993. *Buntgrasduinen na 25 jaar weer onderzocht (Grey hairgrass (Corynephorus canescens) dune re-investigated; Summary in English)*. *De Levende Natuur* 1993, nr. 1: 10-16.
- Khanna, P.K., J. Prenzel, K.J. Meiwes, B. Ulrich and E. Matzner, 1987. *Dynamics of sulfate retention by acid forest soils in an acid deposition environment*. *Soil Sci. Soc. Am. J.* 51: 446-452.
- Kimmins, J.P., D. Binkley, L. Chatarpaul and J. De Catanzaro, 1985. *Biogeochemistry of temperate forest ecosystems Literature on inventories and dynamics of biomass and nutrients*. Petawawa National Forestry Institute, Canada, Information Report PI-X-47E/F, 227 pp.

- Kleijn, C.E. and W. De Vries, 1987. *Characterizing soil moisture composition in forest soils*. In: W. Van Duijvenbooden and H.G. Van Waegening (Eds.), *Vulnerability of soil and groundwater to pollutants*. Proc. Int. Conf. Noordwijk aan Zee, the Netherlands, March 30 - April 3. 1987 Proceedings and Information TNO-CHO/RIVM, No. 38: 591-600.
- Kleijn, C.E., G. Zuidema en W. De Vries, 1989. *De indirecte effecten van atmosferische depositie op de vitaliteit van Nederlandse bossen. 2. Depositie, bodemeigenschappen en bodemvochtsamenstelling van acht Douglas opstanden*. Wageningen, Stichting voor Bodemkartering, Rapport 2050, 96 pp.
- Klein, Th.M., J.P. Kreitinger and M. Alexander, 1983. *Nitrate formation in acid forest soils from the Adirondacks*. Soil Sci. Soc. Am. J. 47: 506-508.
- Klemetsson, L. and B.H. Svensson, 1988. *Effects of acid deposition on denitrification and N<sub>2</sub>O-emission from forest soils*. In: J. Nilsson and P. Grennfelt (Eds.), *Critical loads for sulphur and nitrogen*. NORD 1988:97, Nordic Council of Ministers, Copenhagen, Denmark: 343-362.
- Klijn, J.A., 1981. *Nederlandse kustduinen. Geomorfologie en bodems*. Wageningen, PUDOC, 188 pp.
- Klijn, J.A., 1990. *The younger dunes in the Netherlands; chronology and causation*. In: T.W.M. Bakker, P.D. Jongerius and J.A. Klijn (Eds.) *Dunes of the European coasts; geomorphology-hydrology soils*. CATENA SUPPL. 18: 89-100.
- Klinkhamer, P.G.L. and T.J. De Jong, 1985. *Shoot biomass and species richness in relation to some environmental factors in a coastal dune area in the Netherlands*. Vegetatio 63: 129-132.
- KNMI/RIVM, 1985. *Chemische samenstelling van de neerslag over Nederland*. Bilthoven, Jaarrapport 1985, ISSN 0169-1759, 124 pp.
- Kok, R.M. and G.W. Bultman, 1990. *GENINP Software Requirements Specification*. In: A.H. Bakema et al. (Eds.), *Dutch acidification systems model specifications*. Bilthoven, the Netherlands, Dutch Priority Programme on Acidification, Report nr. 114.1-01: 145-175.
- Kooistra, M.J., 1971. *De chemische samenstelling van de neerslag op Terschelling in het algemeen en de invloed hiervan op de vegetatie*. Utrecht, Rijksuniversiteit, Berichten Fysisch Geografische Afdeling nr. 4, 15 pp.
- Kriebitzsch, W.U., 1978. *Stickstoffnachlieferung in sauren Waldböden Nordwest Deutschlands*. Goltze, Göttingen, Scripta Geobotanica, 14: 1-66.
- Kros, J., W. De Vries, P.H.M. Janssen en C.I. Bak, 1990. *Het gebruik van onzekerheidsanalyse bij modelberekeningen: Een toepassing op het regionale bodemverzuuringsmodel RESAM*. Wageningen, DLO-Staring Centrum, Rapport 65, 127 pp.
- Kros, J., W. De Vries, P. Janssen and C. Bak, 1993. *The uncertainty in forecasting regional trends of forest soil acidification*. Water Air and Soil Poll. 66 29-58.
- Kros, J., P.S.C. Heuberger, P.H.M. Janssen and W. De Vries, 1994. *Regional calibration of a steady-state model to assess critical acid loads*. In *Proceeding of a Symposium on Predictability and nonlinear modeling in natural sciences and economics*. Wageningen Agricultural University, April 5-7, 1993.
- Krug, E.C., 1985. *Acidification of soil and water*. Nature 313: 73.

- Krug, E.C., 1991. *Review of acid-deposition-catchment interaction and comments on further research needs*. Journal of Hydrology 128: 1-27.
- Krug, E.C. and C.R. Frink, 1983. *Acid rain on acid soil a new perspective*. Science 221: 520-525.
- Kundler, P., 1959. *Zur Methodik der Bilanzierung der Ergebnisse von Bodenbildungsprozessen (Profilbilanzierung), dargestellt am Beispiel eines Texturprofils auf Geschiebemergel in Nord-Deutschland*. Z. Pflanzenernähr. Bodenk. 86: 215-222.
- Kuylenstierna, J.C.I. and M.J. Chadwick, 1989. *The relative sensitivity of ecosystems in Europe to the indirect effects of acidic depositions*. In: J. Kämäri, D.F. Brakke, A. Jenkins, S.A. Norton and R.F. Wright (Eds.) *Regional acidification models Geographic extent and time development*, Springer Verlag, Heidelberg, Germany: 3-21.
- Kuylenstierna, J.C.I. and M.J. Chadwick, 1992. *The acidifying input of nitrogen deposition to ecosystems a preliminary method to allow comparison to critical loads for acidity*. In: P. Grennfeld and E. Thörmelöf (Eds.), *Critical loads for nitrogen*. NORD 1992:41, Nordic Council of Ministers, Copenhagen: 359-381.
- La Bastide, J.G.A. and P.J. Faber, 1972. *Revised yield tables for six tree species in the Netherlands*. Wageningen, the Netherlands, Research Institute for Forestry and Urban Ecology, Report 11(1), 64 pp.
- Lammel, R., 1984. *Endgültige Ergebnisse und bundesweite Kartierung der Waldschadens erhebung*. Allg. Forst Z., 39: 340-344.
- Lang, G.E., W.A. Reinvers and G.A. Shellito, 1982. *Tissue chemistry of Abies balsamea and Betula papyrifera var. cordifolia from subalpine forests of northeastern United States*. Can. J. For. Res. 12 311-318.
- Langmyhr, F.J. and P.E. Paus, 1968. *The analysis of inorganic siliceous materials by atomic absorption spectrophotometry and the hydrofluoric acid decomposition technique*. Anal. Chim. Acta 43: 397-408
- Lasaga, A.C., 1983. *Kinetics of silicate dissolution*. Proc. 4<sup>th</sup> Int. Conf. Water Rock Interaction: 269-274
- Leeflang, K.W.H., 1938. *De chemische samenstelling van den neerslag in Nederland*. Chem. Weekblad, 35: 658-664.
- Leemans, R. and W.P. Cramer, 1991. *The IIASA database for mean monthly values of temperature, precipitation, and cloudiness on a global terrestrial grid*. International Institute for Applied Systems Analysis, IIASA, Laxenburg, Austria, Report RR-91-18, 62 pp.
- Leeters, E.E.J.M. en W. De Vries, 1992. *De kwaliteit van de Bodem Verzuring van heide en bosbodems*. In Milieudiagnose 1991. Deel 3 Bodem- en Grondwaterkwaliteit. Bilthoven, Rijksinstituut voor Volksgezondheid en Milieuhygiëne: 49-53.
- Lensi, R., S. Mazurier, F. Gourbière and A. Josserand, 1986. *Rapid determination of the nitrification potential of an acid forest soil and assessment of its variability*. Soil Biol. Biochem. 18 (2): 239-240.
- Lenz, R. and P. Schall, 1991. *Belastungen in fichtendominierten Waldökosysteme. Risikokarten zu Schlüsselprozessen der neuartigen Waldschäden*. AFZ 46: 756-761.

- Leuven, R.S.E.W., H.L.M. Kersten, J.A.A.R. Schuurkes, J.G.M. Roelofs and G.H.P. Arts, 1986. *Evidence for recent acidification of lentic soft waters in the Netherlands*. Water Air and Soil Poll. 10: 387-392.
- Leyton, L., E.R.C. Reijnders and F.B. Thompson, 1967. *Rainfall interception in forest and moorland*. In: W.E. Sopper and H.W. Lull (Eds.), *Int. Symp. on forest hydrology*. Pergamon, Oxford, U.K.: 163-178.
- Likens, G.E. and F.H. Bormann, 1974. *Acid rain a serious regional environmental problem*. Science 184: 1176-1179.
- Likens, G.E., F.H. Bormann and N.M. Johnson, 1969. *Nitrification importance to nutrient losses from a cut-over forested ecosystem*. Science 163: 1205-1206.
- Likens, G.E., F.H. Bormann, R.S. Pierce, J.S. Eaton and N.M. Johnson, 1977. *Biogeochemistry of a forested ecosystem*. Springer Verlag, New York: 1-146
- Liljelund, L.E. and P. Torstensson, 1988. *Critical load of nitrogen with regards to effects on plant composition*. In: J. Nilsson and P. Grennfelt (Eds.), *Critical loads for sulphur and nitrogen; Report from a workshop held at Skokloster, Sweden, 19-24 March, 1988*. Miljø rapport 1988: 15. Nordic Council of Ministers, Copenhagen, Denmark: 363-373.
- Lindsay, W.L., 1979. *Chemical equilibria in soils*. John Wiley and Sons, New York, 449 pp.
- Loman, H. en P. De Willigen, 1972. *Kalkverliezen op zandbouwland*. Haren, Instituut voor Bodemvruchtbaarheid, Rapport nr. 13, 35 pp.
- Lövblad, G., M. Amann, B. Andersen, M. Hormand, S. Joffre and V. Pedersen, 1992. *Deposition of sulphur and nitrogen in the nordic countries: Present and future*. Ambio 21: 339-347.
- Mällkönen, E., J. Derome and M. Kukkola, 1990. *Effects of nitrogen inputs on forest ecosystems. Estimations based on long-term fertilization experiments*. In: P. Kauppi, P. Antilla and K. Kenttämies (Eds.), *Acidification in Finland*. Springer-Verlag, Berlin, Germany: 325-347.
- Matzner, E. and B. Ulrich, 1983. *The turnover of protons by mineralization and ion uptake in a beech (fangus silvatica) and a norway spruce ecosystem*. In: B. Ulrich and J.L. Pankrath (Eds.): *Effects of air pollutants in forest ecosystems*. Reidel Publ. Co., Dordrecht, the Netherlands: 93-103.
- May, H.M., P.A. Helmke and M.L. Jackson, 1979. *Gibbsite solubility and thermodynamic properties of hydroxy-aluminium ions in aqueous solutions at 25°C*. Geochim. Cosmochim. Acta 43: 861-868.
- Mazzarino, M.J., H. Heinrichs and H. Folster, 1983. *Holocene versus accelerated actual proton consumption in German forest soils*. In: B. Ulrich and J.L. Pankrath (Eds.), *Effects of accumulation of air pollutants in forest ecosystems*. Reidel Publ. Co., Dordrecht, the Netherlands: 113-123.
- McCormack, L.H. and K.C. Steiner, 1978. *Variation in aluminium tolerance among six genera of trees*. For. Sci. 24: 565-568.
- McKeague, J.A., 1967. *An evaluation of 0.1M pyrophosphate and pyrophosphate-dithionite in comparison with oxalate as extractants of the accumulation products in podzols and some other soils*. Can. J. Soil Sci. 47: 95-99.

- Mehra, O.P. and M.L. Jackson, 1960. *Iron oxide removal from soils and clays by a dithionite-citrate system buffered with sodium bicarbonate*. Clays and Clay Min. 7: 317-327
- Meiwes, K.J. and P.K. Khanna, 1981. *Distribution and cycling of sulphur in the vegetation of two forest ecosystems in an acid rain environment*. Plant and Soil 60: 369-375.
- Minderman, G. and K.W.F. Leeftang, 1968. *The amounts of drainage water and solutes from lysimeters*. Plant and Soil 28: 61-80.
- Mitscherlich, G. and W. Moll, 1970. *Untersuchungen über die Niederschlags- und Bodenfeuchtigkeitsverhältnisse in einigen Nadel- und Laubholzbeständen in der Nähe von Freiburg*. A.F.J.Z. 141 (3): 49-60
- Mohren, G.M.J., 1991. *Integrated effects (forests)*. In: G.J. Heij and T. Schneider (Eds.), *Acidification research in the Netherlands. Final report of the Dutch Priority Programme on Acidification*. Studies in Environmental Science 46, Elsevier Science Publishers, Amsterdam, the Netherlands: 387-464.
- Mohren, G.M.J., I.I.M. Jorritsma, J.P.G.G.M. Florax, H.H. Bartelink and J.R. Van de Veen, 1991. *FORGRO 3.0: A basic forest growth model: model documentation and listing*. Wageningen, the Netherlands, Research Institute for Forestry and Urban Ecology, Report 524, 137 pp.
- Mokma, D.I. and P. Buurman, 1982. *Podzols and Podzolization*. I.S.M. Monograph 1, Wageningen, the Netherlands, Int. Soil Museum, 126 pp.
- Moore, A.M., 1986. *Temperature and moisture dependence on decomposition rates of hardwood and coniferous leaf litter*. Soil Biol. Biochem. 18: 427-435.
- Mulder, J. and N. Van Breemen, 1987. *Differences in aluminium mobilization in podosols in New Hampshire (USA) and in the Netherlands as a result of acid deposition*. In: T.C. Hutchinson and K.M. Meema (Eds.), *Effects of atmospheric pollutants on forests, wetlands and agricultural ecosystems*, Springer Verlag, Berlin-Heidelberg, Germany: 361-376.
- Mulder, J. and A. Stein, 1994. *The solubility of aluminum in acidic forest soils: Long-term changes due to acid deposition*. Geochim. et Cosmochim. Acta 58: 85-94.
- Mulder, J., C.G.E.M. Van Beek and H.A.L. Dierx, 1990. *Acidification of groundwater in forested sandy deposits in the Netherlands due to acid atmospheric deposition*. Nieuwegein, the Netherlands, KIWA Report SWE 90.015, 36 pp.
- Mulder, J., N. Van Breemen and H.C. Van Eijck, 1989. *Depletion of soil aluminium by acid deposition and implications for acid neutralization*. Nature 337: 247-249.
- Mulder, J., J.J.M. Van Grinsven and N. Van Breemen, 1987. *Impact of acid atmospheric deposition on woodland soils in the Netherlands. III: Aluminium chemistry*. Soil Sci. Soc. Am. J. 51: 1640-1646.
- Mulder, J., N. Van Breemen, L. Rasmussen and C.T. Driscoll, 1988. *Aluminum chemistry of acidic sandy soils with various inputs of acidic deposition in the Netherlands and in Denmark*. In: J. Mulder, *Impact of acid atmospheric deposition on soils: field monitoring and aluminum chemistry*. Ph.D Thesis, Agricultural University, Wageningen, the Netherlands: 77-102.

- Müller, M.J., 1982. *Selected Climatic Data for a Global Set of Standard Stations for Vegetation Science*. Dr. W. Junk Publ., The Hague, the Netherlands.
- Nätscher, L. and U. Schwertmann, 1991. *Proton buffering in organic horizons of acid forest soils*. *Geoderma* 48: 93-106
- Nelleman, C. and T. Frogner, 1994. *Spatial patterns of spruce defoliation seen in relation to acid deposition, critical loads and natural growth conditions in Norway*. *Ambio* (in press).
- Nihlgård, B., 1985. *The ammonium hypothesis; an additional explanation to the forest dieback in Europe*. *Ambio* 14: 2-8.
- Nilsson, S.I., 1985. *Why is Lake Gårdsjön acid? An evaluation of processes contributing to soil and water acidification*. In: F. Andersson and B. Olsson (Eds.), *Lake Gårdsjön. An acid forest lake and its catchment*, *Ecol Bulletins* 37: 311-318.
- Nilsson, J., 1986. *Critical loads for nitrogen and sulphur*. Report 1986: 11, Nordic Council of Ministers, Copenhagen, Denmark: 183 pp.
- Nilsson, S.I. and B. Bergkvist, 1983. *Aluminium chemistry and acidification processes in a shallow podzol on the Swedish west coast*. *Water Air and Soil Poll.* 20: 311-329.
- Nilsson, J. and P. Grennfelt, (Eds.), 1988. *Critical loads for sulphur and nitrogen*. Report from a Workshop held at Skokloster, Sweden, March 19-24, 1988. Miljø rapport 1988: 15. Nordic Council of Ministers, Copenhagen, Denmark, 418 pp.
- Nilsson, S. and O. Sallnäs, in press. *Basic data used by IIASA forest study for European timber assessment analysis*. International Institute of Applied Systems Analysis, Laxenburg, Austria.
- Nilsson, S.I., H.G. Miller and J.D. Miller, 1982. *Forest growth as a possible cause of soil and water acidification: an examination of the concepts*. *Oikos* 39: 40-49.
- Nordstrom, D.K., 1982. *The effect of sulphate on aluminium concentrations in natural waters: some stability relations in the system  $Al_2O_3$ - $SO_3$ - $H_2O$  at 289K*. *Geochim. Cosmochim. Acta* 46: 681-692.
- Olsson, M. and P.A. Melkerud, 1991. *Determination of weathering rates based on geochemical properties of the soil*. In: E. Pulkinen (Ed.): *Environmental geochemistry in Northern Europe*. Proceedings of a Symposium held in Rovaniemi, Finland, 17-19 October, 1989. Geol. Survey of Finland, Special paper 9: 69-78.
- Olsson, M., K. Rosén and P.A. Melkerud, 1991. *Mapping base cation budgets for Swedish forest soils*. In: Proc. second Int. Symp. on Env. Geochem. Uppsala, Sweden, March 1991, 14 pp.
- Olsthoorn, T.N., J.A. Van Jaarsveld, J.M. Knoop, N.D. Van Egmond, J.H.C. Mülschlegel and W. Van Duijvenbooden, 1990. *Integrated modeling in the Netherlands*. In: J. Ferhann, G.A. Mackenzie and B. Rasmussen (Eds.), *Environmental models: Emissions and consequences*: 461-479.
- Oterdoom, J.H., J. Van den Burg en W. De Vries, 1987. *Resultaten van een oriënterend onderzoek naar de minerale voedingstoestand en de bodemchemische eigenschappen van acht Douglasopstanden met vitale en minder vitale bomen in Midden-Nederland*. Wageningen, Instituut voor Bosbouw en Groenbeheer "De Dorschkamp", Rapport nr. 470, 47 pp.



- Pedersen, U., J. Schaug, J.E. Skjelmoen and J.E. Hanssen, 1990. *Data Report 1988. Part 1: Annual Summaries*. Lilleström, Norway, Norwegian Institute for Air Research, EMEP/CCC-Report 4/90.
- Persson, H., 1983. *The distribution and productivity of fine roots in boreal forests*. Plant and Soil 71: 87-101.
- Petersen, T., 1984. *Development of the programm system ECCES for calculating environmental consequences from Energy Systems Status*. Riso National Laboratory Denmark; Report M-2447, 36 pp.
- Pleysier, J.L. and A.S.R. Juo, 1980. *A single-extraction method using silver-thiourea for measuring exchangeable cations and effective CEC in soils with variable charges*. Soil Science 129: 205-211
- Popovic, B., 1984. *Mineralization of carbon and nitrogen in humus from field acidification studies*. Forest. Ecol. Man. 8: 81-93.
- Posch, M., M. Forsius and J. Kämäri, 1993a. *Critical loads of sulphur and nitrogen for lakes 1: Model description and estimation of uncertainty*. Water Air and Soil Poll. 66: 173-192.
- Posch, M., G.J. Reinds and W. De Vries, 1993b. *SMART, Simulation Model for Acidification's Regional Trends*. Model Description and User Manual. Mimeograph Series of the National Board of Waters and the Environment 477, Helsinki, Finland, 43 pp.
- Prenzel, J., 1983. *A mechanism for storage and retrieval of acid in acid soils*. In: B. Ulrich and J.L. Pankrath (Eds.), *Effects of air pollutants in forest ecosystems*. D. Reidel Publ. Co., Dordrecht, the Netherlands, 1983: 157-170.
- Press, W.H., B.P. Flannery, S.A. Teukolsky and W.T. Vetterling, 1986. *Numerical Recipes - The Art of Scientific Computing*. Cambridge University Press, Cambridge, U.K.
- Pruyt, M.J., 1984. *Vegetatie, waterhuishouding en bodem in twee vochtige duinvalleien in het Noordhollands duinreservaat*. Castricum, PWN-Rapport 1.2-38, 97 pp.
- Reddy, K.R., P.S.C. Rao and R.E. Jessup, 1982. *The effect of carbon mineralization on denitrification kinetics in mineral and organic soils*. Soil Sci. Soc. Am. J. 46: 62-68.
- Reurslag, A., G. Zuidema en W. De Vries, 1990. *De indirecte effecten van atmosferische depositie op de vitaliteit van Nederlandse bossen. Deel 3. Simulatie van de waterbalans van acht Douglas-opstanden*. Wageningen, Staring Centrum, Rapport 76. 100 pp.
- Reuss, J.O., 1977. *Chemical and biological relationships relevant to the effect of acid rainfall on the soil-plant system*. Water Air and Soil Poll. 7: 461-478.
- Reuss, J.O., 1980. *Simulations of soil nutrient losses resulting from rainfall acidity*. Ecol. Modelling 11: 15-38.
- Reuss, J.O., 1983. *Implications of the Ca-Al exchange system for the effect of acid precipitation on soils*. J. Environ. Qual. 12: 591-595.
- Reuss, J.O. and D.W. Johnson, 1985. *Effect of soil processes on the acidification of water by acid deposition*. J. Environ. Qual. 14: 26-31.
- Reuss, J.O. and D.W. Johnson, 1986. *Acid deposition and the acidification of soils and waters*. Ecological Studies 59. Springer-Verlag, Berlin, Germany, 119 pp.

- Reuss, J.O., N. Christophersen and H.M. Seip, 1986. *A critique of models for freshwater and soil acidification*. Water Air and Soil Poll. 30: 909-930.
- Reuss, J.O., B.J. Cosby and R.F. Wright, 1987. *Chemical processes governing soil and water acidification*. Nature 329: 27-32.
- Roberts, J., 1983. *Forest transpiration: A conservative hydrological process*. J. Hydrol. 66: 133-141.
- Roberts, T.N., T.A. Clarck, P. Ineson and T.K. Gray, 1980. *Effects of sulphur deposition on litter decomposition and nutrient leaching in coniferous forest soils*. In: T.C. Hutchinson and M. Havas (Eds.), *Effects of acid precipitation on terrestrial ecosystems*. Plenum Press, New York: 381-393.
- Roberts, T.M., R.A. Skeffington and L.W. Blank, 1989. *Causes of type 1 spruce decline*. Forestry 62 (3): 179-222.
- Robie, R.A. and D.R. Waldbaum, 1968. *Thermodynamic properties of minerals and related substances at 298.15 °K (25°C) and one atmosphere (1.013 bars) pressure and at higher temperatures*. Geol. Surv. Bull., 1259 pp.
- Rodin, L.E. and N.I. Bazilevich, 1967. *Production and mineral cycling in terrestrial vegetation*. Oliver and Boyd, Edinburgh and London, 273 pp.
- Roelofs, J.G.M., 1983. *Impact of acidification and eutrophication on macrophyte communities in soft waters in the Netherlands. I Field observations*. Aquatic Botany 17: 138-155.
- Roelofs, J.G.M., 1986. *The effect of air-borne sulphur and nitrogen deposition on aquatic and terrestrial heathland vegetation*. Experientia 42: 372-377.
- Roelofs, J.G.M., L.G.M. Clasquin, I.M.C. Driessen en A.J. Kempers, 1983. *De gevolgen van zwavel en stikstofhoudende neerslag op de vegetatie in heide- en heidevenmilieus*. In: E.H. Adema and J. Van Ham (Eds.), *Proc. Symp. zure regen, oorzaken, effecten en beleid, 's-Hertogenbosch 1983*: 134-140.
- Roelofs, J.G.M., A.J. Kempers, A.L.F.M. Houdijk and J. Jansen, 1985. *The effect of airborne ammonium sulphate on Pinus nigra var. maritima in the Netherlands*. Plant and Soil, 84: 45-56.
- Rosenqvist, I.Th., P. Jorgensen and H. Rueslatten, 1980. *The importance of natural H<sub>2</sub>O<sub>2</sub> production for acidity in soil and water*. In: D. Drablos and A. Tolan (Eds.), *Ecological Impact of Acid Precipitation*. SNSF project Oslo, Norway: 240-241.
- Rosén, K., 1982. *Supply, loss and distribution of nutrients in three coniferous forest watersheds in Central Sweden*. Uppsala, Sweden, Swedish University of Agricultural Sciences, Reports in forest ecology and forest soils 41.
- Rosén, K., 1988. *Effects of biomass accumulation and forestry on nitrogen in forest ecosystems*. In: J. Nilsson and P. Grennfelt (Eds.), *Critical loads for sulphur and nitrogen*, Miljø rapport 1988:15, Nordic Council of Ministers, Copenhagen, Denmark: 269-293.
- Rosén, K., 1990. *The critical load of nitrogen to Swedish forest ecosystems*. Uppsala, Sweden, Swedish University of Agriculture Science, Department of forest soils. Internal Report, 15 pp.

- Rost-Siebert, K., 1983. *Aluminium-Toxizität und -Toleranz an Keimpflanzen von Fichte (Picea abies Karst.) und Buche (Fagus sylvatica L.)*. Allgem. Forstz. 26/27: 686-689.
- Rozema, J., P. Laan, R. Broekman, W.H.O. Ernst and C.A.J. Appelo, 1985. *On the lime transition and decalcification in the coastal dunes of the province of North Holland and the island of Schiermonnikoog*. Acta Bot. Neerl. 34(4): 393-411.
- Runhaar, J., C.L.G. Groen, R. Van der Meijden en R.A.M. Stevers, 1987. *Een nieuwe indeling in ecologische groepen binnen de Nederlandse flora*. Gorteria 13: 276-359.
- Rustad, S., N. Christophersen, H.M. Seip and P.J. Dillon, 1986. *Model for streamwater chemistry of a tributary to Harp Lake*. Ontario, Can. J. Fish. Aquat. Sci. 43: 625-633.
- Ryan, P.J., S.P. Gessel and R.J. Zasoski, 1986a. *Acid tolerance of Pacific Northwest conifers in solution culture. I: Effect of high aluminium concentration and solution acidity*. Plant and Soil 96: 239-257.
- Ryan, P.J., S.P. Gessel and R.J. Zasoski, 1986b. *Acid tolerance of Pacific Northwest conifers in solution culture. II: Effects of varying aluminium concentration of constant pH*. Plant and Soil 96: 259-272.
- Schindler, P.W., 1986. *The significance of in-lake production of alkalinity*. Water Air Soil Poll. 30: 931-944.
- Schneider, T. and A.H.M. Bresser, 1988. *Dutch Priority Programme on Acidification*. Bilthoven, the Netherlands, Report 00-06, 190 pp.
- Schnitzer, M. and S.I.M. Skinner, 1963. *Organo metallic interactions in soils: 1: Reactions between a number of metal ions and the organic matter of a podzol Bh horizon*. Soil Sci. 96: 86-94.
- Schnoor, J. and W. Stumm, 1987. *The role of chemical weathering in the neutralization of acidic deposition*. Schweiz. Z. Hydrol. 48: 171-195.
- Schnoor, J.L., N.P. Nikolaidis and S.E. Glass, 1986. *Lake resources at risk to acidic deposition in the upper midwest*. J. Water Poll. Control Federation 58: 139-148.
- Schoumans, O.F., A. Breeuwsma and W. de Vries, 1987. *Use of soil survey information for assessing the phosphate sorption capacity of heavily manured soils*. In: W. Van Duijvenbooden and H.G. Van Waegeningh (Eds.), *Vulnerability of soil and ground water to pollutants*. Int. Conf. Noordwijk aan Zee, the Netherlands, March 30 - April 3, 1987. TNO-CHO/RIVM Proceedings and Information No. 38: 1079-1088.
- Schulze, E.D., W. De Vries, M. Hauhs, K. Rósen, L. Rasmussen, C.O. Tamm and J. Nilsson, 1989. *Critical loads for nitrogen deposition on forest ecosystems*. Water Air and Soil Poll. 48: 451-456.
- Schütt, P., H. Blaschke, E. Hoque, W. Koch, K.J. Lang and H.J. Schuck, 1983. *Erste Ergebnisse einer botanischen Inventur des 'Fichtensterbens'*. Forstwiss. Zentralbl. 96: 177-186.
- Schutter, M.A.A. en F.A.A.M. De Leeuw, 1991. *Zure depositie in Nederland. Scenarió resultaten voor 1994 en 2000*. Bilthoven, Rijksinstituut voor Volksgezondheid en Milieuhygiëne, Rapport 222101008, 26 pp.
- Schütz, P.R. en G. Van Tol, 1981. *Aanleg en beheer van bos en beplantingen*. PUDOC, Wageningen, 504 pp.

- Schuurkes, J.A.A.R., A.J. Kempers and C.J. Kok, 1988. *Aspects of biochemical sulphur conversions in sediments of a shallow softwater lake*. J. Freshwater Ecol. 4: 369-381.
- Schuurkes, J.A.A.R., M.A. Elbers, J.J.F. Gudden and J.G.M. Roelofs, 1987. *Effects of simulated acid rain on acidification, water quality and flora of small-scale soft watersystems*. Aquatic Bot. 28: 199-226.
- Schwertmann, U., 1964. *Differenzierung der Eisen oxide des Bodems durch Extraction mit Ammoniumoxalat-lösung*. Z. Pflanzenernähr. Bodenk. 105: 194-202.
- Shaffer, P.W., R.P. Hooper, K.N. Eshleman and M. Robbins Church, 1988. *Watershed intake alkalinity generation: A comparison of rates using input-output studies*. Water Air and Soil Poll. 39: 263-273.
- Shriner, D.S. and G.S. Henderson, 1978. *Sulphur distribution and cycling in a deciduous forest watershed*. J. Environ. Qual. 7: 392-397.
- Singh, B.R., 1980. *Distribution of total and extractable S and adsorbed SO<sub>4</sub> in some acid forest soil profiles of southern Norway*. Acta Agric. Scand. 30: 357-363.
- Singh, S. and J.E. Brydon, 1969. *Solubility of basic aluminium sulfates at equilibrium in solution and in the presence of montmorillonite*. Soil Sci. 107: 12-16.
- Singh, B.R. and D.W. Johnson, 1986. *Sulfate content and adsorption in soils of two forested watersheds in southern Norway*. Water Air and Soil Poll. 31: 847-856.
- Singh, B.R., G. Abrahamson and A.O. Stuanes, 1980. *Effect of simulated acid rain on sulphate movement in acid forest soils*. Soil Sci. Soc. Am. J. 44: 75-80.
- Smit, H.P., W.G. Keltjens and N. Van Breemen, 1987. *Effects of soil acidity on Douglas fir seedlings. 2. The role of pH, aluminium concentration and nitrogen nutrition (pot experiment)*. Neth. J. of Agri. Sc. 35: 537-540.
- Smith, R.A. and R.B. Alexander, 1986. *Correlations between stream sulphate and regional SO<sub>2</sub> emission*. Nature 322: 722-724.
- Sollins, P., C.L. Grier, F.M. McGarison, K. Cormack and R. Foyel, 1980. *The internal element cyclus of an old growth Douglas fir ecosystem in Western Oregon*. Ecol. monographs 50: 261-285.
- Steiner, K.C., L.H. McCormack and D.S. Canavera, 1980. *Differential response of paper birch provenances to aluminium in solution culture*. Can. J. For. Res. 10: 25-29.
- Stevens, P., 1987. *Throughfall chemistry beneath Sitka spruce of four ages at Beddgelert Forest, North Wales*. Plant and Soil 101: 291-294.
- Steur, G.G.L., F. De Vries en C. Van Wallenburg, 1985. *Bodemkaart van Nederland 1 : 250 000. Uitgave 1985*. Wageningen, Stichting voor Bodemkartering, 52 pp.
- Steur, G.G.L., F. De Vries and C. Van Wallenburg, 1986. *A new small-scale soil map of the Netherlands*. Proc. 13th Congress Int. Soc. Soil Sci., Hamburg, Aug. 1986: Vol. 3: 1283-1284.
- Strayer, R.F., C.J. Lin and H. Alexander, 1981. *Effect of simulated acid rain on nitrification and nitrogen mineralization in forest soils*. J. Environ. Qual. 10: 547-551.
- Stuyfzand, P.J., 1984. *Effecten van vegetatie en luchtverontreiniging op de grondwater kwaliteit in kalkrijke duinen bij Castricum: lysimeterwaarnemingen*. H<sub>2</sub>O 17: 152-159.

- Sumner, M.E., H. Shahendeh, J. Bouton and J. Hammel, 1986. *Amelioration of an acid soil profile through deep liming and surface application of gypsum*. Soil Sci. Soc. Am. J. 50: 1254-1258.
- Sverdrup, H.U., 1990. *The kinetics of base cation release due to chemical weathering*. Lund University Press, Sweden, 246 pp.
- Sverdrup, H.U. and P.G. Warfvinge, 1988a. *Chemical weathering of minerals in the Gardsjön catchment in relation to a model based on laboratory rate coefficients*. In: J. Nilsson and P. Grennfelt (Eds.), *Critical loads for sulphur and nitrogen; Miljø rapport 1988: 15*, Nordic Council of Ministers, Copenhagen, Denmark: 131-149.
- Sverdrup, H.U. and P.G. Warfvinge, 1988b. *Assessment of critical loads of acid deposition on forest soils*. In: J. Nilsson and P. Grennfelt (Eds.), *Critical loads for sulphur and nitrogen. NORD 1988:97*, Nordic Council of Ministers, Copenhagen, Denmark: 81-129.
- Sverdrup, H., W. De Vries and A. Henriksen, 1990. *Mapping critical loads. A guidance to the criteria, calculations, data collection and mapping of critical loads*. Miljø rapport 1990: 14. Nordic Council of Ministers, Copenhagen, Denmark, 1990, 124 pp.
- Sverdrup, H.U., P. Warfvinge and K. Rosén, 1992. *A model for the impact of soil solution Ca:Al ratio, soil moisture and temperature on tree base cation uptake*. Water Air and Soil Poll. 61: 365-383.
- Tamm, C.O., G. Wiklander and B. Popovic, 1977. *Effects of application of sulphuric acid to poor pine forests*. Water Air and Soil Poll. 8: 75-87.
- Tamminen, P. and M.R. Starr, 1990. *A survey of forest soil properties related to soil acidification in Southern Finland*. In: P. Kauppi, P. Antilla and K. Kenttämies (Eds.), *Acidification in Finland*. Springer Verlag, Berlin, Germany: 235-251.
- Ter Hoeve, J., 1978. *Nadere gegevens over de relatie tussen neerslag en neerslag overschot in bosgebieden*. H<sub>2</sub>O 11: 364-368.
- Teveldal, S., P. Jørgensen and A.O. Stuanes, 1990. *Long-term weathering of silicates in a sandy soil at Vadmoen, Southern Norway*. Clay minerals 25: 447-465.
- Thomas, R., W.G. Van Arkel, H.P. Baars, E.C. Van Ierland, K.F. De Boer, E. Buijsman, T.J.H.M. Hutten and R.J. Swart, 1988. *Emission of SO<sub>2</sub>, NO<sub>x</sub>, VOC and NH<sub>3</sub> in the Netherlands and Europe in the period 1950-2030. The emission module in the Dutch Acidification Systems Model*. Bilthoven, the Netherlands, National Institute of Public Health and Environmental Protection, Report no. 758472002, 118 pp.
- Thompson, M.E., 1987. *Comparison of excess sulfate yields and median values of rivers in Nova Scotia and Newfoundland*. Water Air and Soil Poll. 35: 19-26
- Thornton, F.C., M. Schaedle and D.J. Raynall, 1987. *Effects of aluminium on red spruce seedlings in solution culture*. Environ. Exp. Botany, 27: 489-498.
- Tietema, A., 1992. *Nitrogen cycling and soil acidification in forest ecosystems in the Netherlands*. Ph.D. thesis, University of Amsterdam, the Netherlands, 139 pp.
- Tietema, A. and J.M. Verstraten, 1988. *The nitrogen budget of an oak-beech forest ecosystem in the Netherlands in relation to atmospheric deposition*. Bilthoven, the Netherlands, Dutch Priority Programme on Acidification, Report 04-01, 55 pp.

- Tietema, A. and J.M. Verstraten, 1991. *Nitrogen cycling in an acid forest ecosystem in the Netherlands at increased atmospheric nitrogen input. The nitrogen budget and the effects of nitrogen transformations on the proton budget.* Biogeochemistry 15: 21-46.
- Tietema, A., W. De Boer, L. Riemer and J.M. Verstraten, 1992. *Nitrate production in nitrogen saturated acid forest soils: vertical distributions and characteristics.* Soil Biol. Biochem. 24: 235-240.
- Tietema, A., J.J.H.M. Duysings, J.M. Verstraten and J.W. Westerveld, 1990. *Estimation of actual nitrification rates in an acid forest soil.* In: A.F. Harrison, P. Ineson and O.W. Heal (Eds.), Nutrient cycling in terrestrial ecosystems; Field methods, application and interpretation. Elsevier Applied Science, London and New York: 190-197.
- Tiktak, A. and W. Bouten, 1992. *Modelling soil water dynamics in a forested ecosystem. III: Model description and evaluation of discretization.* Hydrol. processes 6: 455-465.
- Tinhout, A. and M.J.A. Werger, 1988. *Fine roots in a dry Calluna heathland.* Acta. Bot. Neerl. 37(2): 225-230.
- Turner, J.P., 1975. *Nutrient cycling in a douglas-fir ecosystem with respect to age and nutrient status.* Ph. D. Thesis, University of Washington, Seattle, 221 pp.
- Turner, J., D.W. Johnson and M.J. Lambert, 1980. *Sulphur cycling in a Douglas-fir forest and its modification by nitrogen applications.* Oecol. Plant 15: 27-35.
- Tyler, G., 1987. *Probable effects of soil acidification and nitrogen deposition on the floristic composition of oak (Quercus robur L.) forest.* Flora 179: 165-170.
- Ugolini, F.C., R. Minden, H. Dawson and J. Zachara, 1977. *An example of soil processes in the Abies amabilis zone of Central Cascades.* Washington. Soil Sci. 124: 291-302.
- Ulrich, B., 1981a. *Ökologische Gruppierung von Boden nach ihrem chemischen Boden zustand.* Z. Pflanzenernähr. Bodenk. 144: 289-305.
- Ulrich, B., 1981b. *Theoretische betrachtung des ionenkreislaufs in Waldökosystemen.* Z. Pflanzenernähr. Bodenk. 144: 647-659.
- Ulrich, B., 1983a. *A concept of forest ecosystem stability and of acid deposition as driving force for destabilization.* In: B. Ulrich and J.L. Pankrath (Eds.), Effects of air pollutants in forest ecosystems. Reidel Publ. Co., Dordrecht, the Netherlands: 1-29.
- Ulrich, B., 1983b. *Interactions of forest canopies with atmospheric constituents: SO<sub>2</sub>, alkali and earth alkali cations and chloride.* In: B. Ulrich and J. Pankrath (Eds.), Effects of air pollutants in forest ecosystems. Reidel Publ. Co., Dordrecht, the Netherlands: 33-45.
- Ulrich, B., 1983c. *Soil acidity and its relations to acid deposition.* In: B. Ulrich and J. Pankrath (Eds.), Effects of Accumulation of Air Pollutants in Forest Ecosystems, Reidel Publ. Co., Dordrecht, the Netherlands: 127-146.
- Ulrich, B. und E. Matzner, 1983. *Abiotische Folgewirkungen der weitraumigen Ausbreitung von Luftverunreinigung.* Umweltforschungsplan der Bundesminister des Inneren. Forschungsbericht 10402615, BRD, 221 pp.
- Ulrich, B., R. Mayer and P.K. Khanna, 1979. *Die Deposition von Luftverunreinigungen und ihre Auswirkungen in Waldökosystemen im Solling.* Schriften aus der Forstl. Fak. D. Univ. Gottingen und der Nieders. Vers. Anst. Bd. 58, 291 pp.

- Ulrich, B., R. Mayer and P.K. Khanna, 1980. *Chemical changes due to acid precipitation in a loess-derived soil in Central Europe*. Soil sci. 130: 193-199.
- USDA, 1975. *Soil taxonomy, a basic system of soil classification for making and interpreting soil surveys*. Agricultural handbook no. 436, Washington.
- Van Aalst, R.M. en H.S.M.A. Diederer, 1982. *De rol van Stikstof oxiden en Ammoniak bij de depositie vanuit de lucht van bemestende en verzurende stoffen op de Nederlandse bodem*. Delft, TNO rapport R 83/42, 55 pp.
- Van Aalst, R.M. and J.W. Erisman, 1991. *Atmospheric input fluxes*. In: Heij, G.J. and Schneider, T. (Eds.), *Acidification Research in the Netherlands*. Studies in Environmental Science 46; Elsevier Science Publishers, Amsterdam, the Netherlands: 239-288.
- Van Breemen, N., 1973. *Dissolved aluminium in acid sulphate soils and in acid mine waters*. Soil Sci. Soc. Am. J. 37: 694-697.
- Van Breemen, N., 1975. *Acidification and deacidification of coastal plain soils as a result of periodic flooding*. Soil Sci. Soc. Am. J. 39: 1153-1157.
- Van Breemen, N. and R. Brinkman, 1976. *Chemical equilibria and soil formation*. In: G.H. Bolt and M.G.M. Bruggenwert (Eds.), *Soil Chemistry A. Basic elements*. Elsevier Publ. Co., Amsterdam, the Netherlands: 141-170.
- Van Breemen, N., and R. Protz, 1988. *Rates of calcium carbonate removal from soils*. Can. J. of Soil Sci. 68: 449-454.
- Van Breemen, N. and H.F.G. Van Dijk, 1988. *Ecosystem effects of atmospheric deposition of nitrogen in the Netherlands*. Environ. Poll. 54: 249-274.
- Van Breemen, N. and J.M. Verstraten, 1991. *Soil acidification and N cycling*. In: T. Schneider and G.J. Heij (Eds.), *Acidification research in the Netherlands*. Final report of the Dutch Priority Programme on Acidification. Studies in Environmental Science 46, Elsevier Science Publishers, Amsterdam, the Netherlands: 289-352.
- Van Breemen, N., P.A. Burrough, E.J. Velthorst, H.F. Van Dobben, T. De Wit, T.B. De Ridder and H.F.R. Reynders, 1982. *Soil acidification from atmospheric ammonium sulfate in forest canopy throughfall*. Nature 299: 548-550.
- Van Breemen, N., P.H.B. De Visser and J.J.M. Van Grinsven, 1986. *Nutrient and proton budgets in four soil-vegetation systems underlain by Pleistocene alluvial deposits*. J. Geol. Soc. 143: 659-666.
- Van Breemen, N., C.T. Driscoll and J. Mulder, 1984. *Acidic deposition and internal proton sources in acidification of soils and waters*. Nature 307: 599-604.
- Van Breemen, N., C.T. Driscoll and J. Mulder, 1985. *Acidification of soil and water: Reply to E.C. Krug*. Nature 313: 73.
- Van Breemen, N., J. Mulder and C.T. Driscoll, 1983. *Acidification and alkalization of soils*. Plant and Soil 75: 283-308.
- Van Breemen, N., J. Mulder and J.J.M. Van Grinsven, 1987. *Impacts of acid atmospheric deposition on woodland soils in The Netherlands: II Nitrogen transformations*. Soil Sci. Soc. Am. J. 51: 1634-1640.

- Van Breemen, N., W.F.J. Visser and Th. Pape, (Eds.), 1988. *Biogeochemistry of an oak-woodland ecosystem in the Netherlands affected by acid atmospheric deposition*. PUDOC Scientific Publishers, Wageningen, the Netherlands, 197 pp.
- Van Dam, D., H.F. Van Dobben, C.F.J. Ter Braak, and F. De Wit, 1986. *Air pollution as a possible cause for the decline of some phanerogamic species in the Netherlands*. *Vegetatio* 65: 47-52.
- Van Dam, D., G.W. Heil, R. Bobbink and B. Heyne, 1990. *Atmospheric deposition to grassland canopies: Lysimeter budgets discriminating between interception deposition, mineral weathering and mineralization*. *Water Air and Soil Poll.* 53: 83-101.
- Van den Burg, J., 1978. *De groei van Black Alder (Alnus Glutinosa) in Nederland en bodemvruchtbaarheid*. Wageningen, Instituut voor Bosbouw en Groenbeheer, "De Dorschkamp", Rapport nr. 143, 114 pp.
- Van den Burg, J. en H.P. Kiewiet, 1989. *Veebezetting en de naaldsamenstelling van grove den, Douglas en Corsicaanse den in het Peelgebied in de periode 1956 t/m 1988. Een onderzoek naar de betekenis van de veebezetting voor het optreden van bosschade*. Wageningen, Instituut voor Bosbouw en Groenbeheer, "De Dorschkamp", Rapport nr. 559, 76 pp.
- Van den Burg, J. en P.H. Schoenfeld, 1988. *Veranderingen in de groeiplaats van twee generaties naaldboomopstanden op voormalige heidegronden in Drenthe*. Wageningen, Instituut voor Bosbouw en Groenbeheer, "De Dorschkamp", Rapport nr. 491, 124 pp.
- Van den Burg, J., P.W. Evers, G.F.P. Martakis, J.P.M. Relou en D.C. Van der Werf, 1988. *De conditie en de minerale-voedingstoestand van opstanden van grove den (Pinus silvestris) en Corsicaanse den (Pinus nigra var. Maritima) in de Peel en op de zuidoostelijke Veluwe najaar 1986*. Wageningen, Instituut voor Bosbouw en Groenbeheer, "De Dorschkamp", Rapport nr. 519, 66 pp.
- Van der Hagen, H., 1986. *Mogelijkheden voor een verschrallend maaibeheer in twee (ver)natte duinterreinen. Landschapsecologische evaluatie van een natuurbeheersmaatregel*. Nieuwegein, KIWA, Rapport nr. SWE86.007, 75 pp.
- Van der Maarel, E., R. Boot, D. Van Dorp and R. Rijntjes, 1985. *Vegetation succession in the dunes near Oostvoorne, the Netherlands, a comparison of the vegetation in 1959 and 1980*. *Vegetatio* 58: 137-187.
- Van der Maas, M.P. and Th. Pape, 1991. *Hydrochemistry of two Douglas fir ecosystems and a heather ecosystem in the Veluwe, the Netherlands*. Bilthoven, the Netherlands, Dutch Priority Programme on Acidification, Report 102.1-10, 29 pp.
- Van der Meulen, F., H. Van der Hagen and B. Kruijsen, 1987. *Campylopus introflexus. Invasion of a moss in Dutch coastal dunes*. In: W. Joerie, K. Bakker and L. Vlijm (Eds.), *The ecology of biological invasions*. Proc. Kon. Ned. Akad. Wetensch. Series C, Vol. 90, no.1: 73-80.
- Van der Meulen, F. and P.D. Jungerius, 1989. *The decision environment of dynamic dune management*. In: F. Van der Meulen, P.D. Jungerius and J.H. Visser (Eds.), *Perspectives in coastal dune management*: 133-140.



- Van der Meijden, R. en L. Vanhecke, 1986. *Naamlijst van de flora van Nederland en België*. *Gorteria* 13, 5/6: 87-170.
- Van der Salm, C., 1985. *Verzuring van bosbodems in de boswachterij Doorwerth in de periode 1950-1983*. Amsterdam, Fysisch Geografisch en Bodemkundig Laboratorium, Universiteit van Amsterdam, Rapport no. 19, 68 pp.
- Van der Salm, C. and J.M. Verstraten, 1994. *Acid neutralization mechanisms in three acid sandy soils*. *Geoderma* (in press)
- Van der Salm, C., J. Kros, J.E. Groenenberg, W. De Vries and G.J. Reinds, 1994. *Validation of soil acidification models with different degrees of process aggregation on an intensively monitored spruce site*. In: S. Trudgill (Ed.): *Solute modelling in catchment systems*. (submitted).
- Van der Zee, S.E.A.T.M. and W.H. Van Riemsdijk, 1988. *Model for long-term phosphate reaction kinetics in soils*. *J. Environ. Qual.* 17: 35-41.
- Van der Zee, S.E.A.T.M., W.H. Van Riemsdijk and J.J.M. Van Grinsven, 1989. *Extrapolation by time-scaling in systems with diffusion-controlled kinetics and first-order reaction rates*. *Neth. J. Agri. Sci.* 37: 47-60.
- Van Dobben, H.F., 1987. *Effecten van ammoniak op epifytische korstmossen*. In: A.W. Boxman and J.F.M. Geelen (Eds.), *Studiedag effecten van NH<sub>3</sub> op organismen*. Nijmegen, the Netherlands, Katholieke Universiteit Nijmegen: 61-82
- Van Dobben, H., 1991. *Effects on heathlands*. In: G.J. Heij and T. Schneider (Eds.), *Acidification research in the Netherlands: Final Report Second Phase Dutch Priority Programme on Acidification*. *Studies in Environmental Science* 46, Elsevier Science Publishers, Amsterdam, the Netherlands: 139-145.
- Van Dobben, H.T., J. Mulder, H. Van Dam and H. Houweling, 1992. *Impact of atmospheric deposition on the biogeochemistry of Moorland pools and surrounding terrestrial environment*. *Agricultural Research Report* 93, PUDOC Scientific Publishers, Wageningen, the Netherlands, 232 pp.
- Van Dorp, D., R. Boot and E. Van der Maarel, 1985. *Vegetation succession in the dunes near Oostvoorne, the Netherlands, since 1934, interpreted from air photographs and vegetation maps*. *Vegetatio* 58: 123-136.
- Van Grinsven, J.J.M. and W.H. Van Riemsdijk, 1992. *Evaluation of batch and column techniques to measure weathering rates in soils*. *Geoderma* 52: 41-57.
- Van Grinsven, J.J.M., N. Van Breemen and J. Mulder, 1987. *Impacts of acid atmospheric deposition on woodland soils in the Netherlands: I Calculation of hydrological and chemical budgets*. *Soil Sci. Soc. Am. J.* 51: 1629-1634.
- Van Grinsven, J.J.M., G.D.R. Kloeg and W.H. Van Riemsdijk, 1986. *Kinetics and mechanisms of mineral dissolution in a soil at pH values below 4*. *Water Air and Soil Poll.* 31: 981-990.
- Van Grinsven, J.J.M., J. Van Minnen and C. Van Heerden, 1991. *Effects on growth of Douglas fir*. In: T. Schneider and G.J. Heij (Eds.), *Acidification research in the Netherlands. Final report of the Dutch Priority Programme on Acidification*. *Studies in Environmental Science* 46, Elsevier Science Publishers, Amsterdam, the Netherlands: 180-190.

- Van Grinsven, J.J.M., W.H. Van Riemsdijk and N. Van Breemen, 1988. *Weathering and kinetics in acid sandy soils from column experiments: II. base cations*. In: J.J.M. van Grinsven: Impact of acid atmospheric deposition on soils: Quantification of chemical and hydrologic processes. Ph. D. Thesis, Agricultural University Wageningen, the Netherlands: 101-118.
- Van Grinsven, J.J.M., N. Van Breemen, W.H. Van Riemsdijk and J. Mulder, 1987. *The sensitivity of acid forest soils to acid deposition*. Proc. Int. Symp. on Acidification and Water Pathways, Bolkesjø, May 4-8, 1987: 365-374.
- Van Grinsven, J.J.M., W.H. Van Riemsdijk, R. Otjes and N. Van Breemen, 1992. *Rates of aluminium dissolution in acid sandy soils observed in column experiments*. J. Environ. Qual. 21(3): 439-447.
- Van Heesen, H.C., 1970. *Presentation of the seasonal fluctuation of the watertable on soil maps*. Geoderma 4: 257-278.
- Van Jaarsveld, J.A. and D. Onderdelinden, 1993. *TREND; an analytical long-term deposition model for multi-scale purposes*. Bilthoven, the Netherlands, National Institute of Public Health and Environmental Protection, Report no. 228603009, 60 pp.
- Van Miegroet, H. and D.W. Cole, 1984. *The impact of nitrification on soil acidification and cation leaching in a red alder ecosystem*. J. Env. Qual. 13: 586-590.
- Van Oene, H. and W. De Vries, 1994. *Comparison of measured and simulated changes in base cation amounts using a one-layer and a multi-layer soil acidification model*. Water Air and Soil Poll. 72: 41-66.
- Van Oosten, M.F., 1986. *Bodemkaart van Nederland, schaal 1 : 50 000. Toelichting bij de kaarten van de Waddeneilanden Vlieland, Terschelling, Ameland en Schiermonnikoog*. Wageningen, Stichting voor Bodemkartering, 129 pp.
- Van Riemsdijk, W.H. and F.A.M. De Haan, 1981. *Sorption kinetics of phosphate with an acid sandy soil using the phosphatostat method*. Soil Sci. Soc. Am. J. 45: 261-266.
- Van Schuijlenborgh, J. and M.G.M. Bruggenwert, 1965. *On soil genesis in temperate humid climate. V. The formation of the "albic" and "spodic" horizon*. Neth. J. Agric. Sci. 13 (3): 267-279.
- Van Veen, J.A., 1977. *The behaviour of nitrogen in soil: a computer simulation model*. Thesis Free University Amsterdam, 164 pp.
- Van Wallenburg, C., 1988. *De dichtheid van moerige gronden*. Wageningen, the Netherlands, Stichting voor Bodemkartering. Internal Report, 5 pp.
- Van Wesemael, B. and J.M. Verstraten, 1993. *Organic acids in a moder type humus profile under a mediterranean oak forest*. Geoderma 59: 75-88.
- Velbel, M.A., 1986. *Influence of surface area, surface characteristics, and solution composition on feldspar weathering rates*. In: J.A. Davis and K.F. Hayes (Eds.), Geochemical processes at mineral surfaces. ACS Symposium Series No. 323, Amer. Chem. Soc.: 615-634.
- Verhagen, H.L.M. en H.S.M.A. Diederens, 1991. *Vergelijkingsmetingen van de analyse- en monsternemingsmethoden van de vaste en vloeibare fase van bodemmonsters*. TNO-IMW rapport R91/171. Additioneel Programma Verzuringsonderzoek rapport 126-1, 213 pp.

- Vermeulen, A.J., 1977. *Emissieonderzoek m.b.v. regenvangers; opzet, ervaringen en resultaten*. Provinciale Waterstaat N-Holland, Dienst voor Milieuhygiëne, 86 pp.
- Vertegaal, C., J.N.C. Van der Salm, and M.P.J.M. Jansen, 1989. *Omvang en oorzaken van effecten van atmosferische depositie in de duinen*. Resultaten van een enquête onder duinkenners. Leiden, Bureau Duin en Kust, 42 pp.
- Vertegaal, C.T.M., E.G.M. Loumans, T.W.M. Bakker, J.A. Klijn and F. Van der Meulen, 1991. *Monitoring van effectgerichte maatregelen tegen verzuring en eutrofiëring in open droge duinen*. Leiden, Bureau Duin en Kust, 151 pp.
- Verstraten, J.M., J.C.R. Dopheide, J.J.H.M. Duysings, A. Tietema and W. Bouten, 1990. *The proton cycle of a deciduous forest ecosystem in The Netherlands and its implications for soil acidification*. Plant and Soil 127: 61-69.
- Vitousek, P.M. and J.M. Melillo, 1979. *Nitrate losses from disturbed forests: Patterns and mechanisms*. Forest Sci. 25: 605-619.
- Vitousek, P.M., J.R. Gosz, C.C. Grier, J.M. Melillo, W.A. Reiners and R.L. Todd, 1979. *Nitrate losses from disturbed ecosystems*. Science 204: 469-474.
- V&W, 1989. *Derde Nota Waterhuishouding*. Parliamentary Document 21250, 1989, 297 pp.
- Warfinge, P., H. Sverdrup and K. Rósen, 1992a. *Calculating critical loads for N to forest soils*. In: P. Grennfeld and E. Thörmelöf (Eds.): Critical loads for Nitrogen. NORD 1992:41, Nordic Council of Ministers, Copenhagen: 403-418.
- Warfinge, P., M. Holmberg, M. Posch and R.F. Wright, 1992b. *The use of dynamic models to set target loads*. Ambio 21: 369-376.
- Weaver, R.M. and P.R. Bloom, 1977. *Solution activities of aluminium and silicon in highly weathered soils that contain gibbsite and kaolinite*. Soil Sci. Soc. Am. J. 41: 814-817.
- Weaver, G.T., P.K. Khanna and F. Beese, 1985. *Retention and transport of sulphate in a slightly acid forest soil*. Soil Sci. Soc. Am. J. 49: 746-750.
- Westhoff, V., 1989. *Dunes and dune management along the North Sea coast*. In: F. van der Meulen, P.D. Jungerius and J. Visser (Eds.), Perspectives in coastal dune management. SPB Acad. Publ., The Hague, The Netherlands: 44-51.
- Westhoff, V. en A.J. Den Held, 1969. *Plantengemeenschappen van Nederland*. Thieme, Zutphen, 324 pp.
- Weterings, M., 1989. *Verzuring van radebrikgronden onder verschillend historisch gebruik*. Wageningen, Landbouw Universiteit, Internal report, 61 pp.
- Whittaker, H. and G.E. Likens, 1975. *The biosphere and man*. In: H. Lieth and H. Whittaker (Eds.), Primary productivity of the biosphere. Ecol. Studies 14, Springer Verlag, Berlin, Germany: 305-328.
- Wiklander, G., G. Nordlander and R. Anderson, 1991. *Leaching of nitrogen from a forest catchment at Söderåsen in Southern Sweden*. Water Air and Soil Poll. 55: 263-282.
- Witkamp, M. and J. Van der Drift, 1961. *Breakdown of forest litter in relation to environmental factors*. Plant and Soil 15: 295-331.
- Wollast, R., 1967. *Kinetics of the alteration of K-feldspar in buffered solutions at low temperature*. Geochim. Cosmochim. Acta 31: 635-648.
- Wood, J.A., 1989. *Peatland acidity budgets and the effect of acid deposition*. Environment Canada, Discussion Paper no. 5, 34 pp.

- Wright, R.F. and A. Henriksen, 1983. *Restoration of Norwegian lakes by reduction in sulphur deposition*. Nature 305: 422-424.
- Wright, R.F., J. Kämäri and M. Forsius, 1988. *Critical loads for sulfur: modelling time of response of water chemistry to changes in loading*. In: J. Nilsson and P. Grennfelt (Eds.), *Critical loads for sulphur and nitrogen; Report from a workshop held at Skokloster, Sweden, March 19-24, 1988*. Miljø rapport 1988:15. Nordic Council of Ministers, Copenhagen, Denmark: 201-224.
- Wright, R.F., E. Lotse and A. Semp, 1988. *Reversibility of acidification shown by whole-catchment experiments*. Nature 334: 422-424.
- Wright, R.F., M. Holmberg, M. Posch and P. Warfvinge, 1991. *Dynamic models for predicting soil and water acidification: Application to three catchments in Fennoscandia*. Norwegian Institute for Water Research (NIVA), Report 25(1991), 40 pp.
- Wright, R.F., E. Gjessing, N. Christophersen, E. Lotse, H.M. Seip, A. Semp, B. Sletaune, R. Storhaug and K. Wedum, 1986. *Project Rain; Changing acid deposition to whole catchments. The first year of treatment*. Water Air and Soil Poll. 30: 47-63
- Zabowski, D. and F.C. Ugolini, 1990. *Lysimeter and centrifuge soil solutions: seasonal differences between methods*. Soil Sci. Soc. Am. J. 54: 1130-1135.

## ANNEX A: NOTATION OF SYMBOLS IN START, MACAL, SMART AND RESAM

The general notation of symbols in the acidification models is given below.

Entity <sup>1)</sup>	Constituent	Process	Compartment
Am = amount	Al = Aluminium	ad = adsorption	ac = adsorption complex
ct = content	BC = base cations	dd = dry deposition	br = branches
f = factor	C = Carbon	de = denitrification	cb = carbonates
fr = fraction	Ca = calcium	ex = exchange	fl = fresh litter
k = rate constant	Cl = chloride	fe = foliar exudation	hl = humus layer
K = equilibrium constant	CO <sub>2</sub> = carbon dioxide	fu = foliar uptake	lt = litter
R = ratio	H = hydrogen	gu = growth uptake	lv = leaves
T = thickness	HCO <sub>3</sub> = bicarbonate	im = immobilization	mo = micro organisms
	K = potassium	le = leaching	ox = (hydr)oxides
	Mg = magnesium	lf = litterfall	pm = primary minerals
	N = nitrogen	mi = mineralization	rn = root necromass
	Na = sodium	ni = nitrification	rz = rootzone
	NH <sub>3</sub> = ammonia	pr = protonation	ss = subsoil
	NH <sub>4</sub> = ammonium	rd = root decay	st = stems
	NO <sub>3</sub> = nitrate	re = reallocation	
	RCOO = organic anions	ru = root uptake	
	S = sulphur	td = total deposition	
	SO <sub>4</sub> = sulphate	tf = throughfall	
		we = weathering	

<sup>1)</sup> In the computer code the entity *c* is also used for concentration and *F* for flux. In the model description,  $[ ]$  denotes concentration and the prefix *F* is not used since the combination of a constituent and a process (e.g.  $BC_{we}$ ) always refers to a flux.

To avoid redundancy, symbols which only differ in the element involved (e.g.  $frCa_{le}$  and  $frMg_{le}$ ) are denoted once in the list of symbols below, using the code *X* (e.g.  $frX_{le}$ ). Furthermore, symbols which only differ in the subscript min (minimum) or max (maximum) are not denoted separately (e.g.  $k_n$  and not  $k_{n,max}$ ).

Symbol	Explanation	Unit
$\alpha$	a dimensionless exponent	-
<i>A</i>	pre-exponential temperature factor	<i>K</i>
[Ac](crit)	critical acidity concentration	mol <sub>c</sub> m <sup>-3</sup>
Ac <sub>le</sub> (crit)	critical leaching flux of acidity	mol <sub>c</sub> ha <sup>-1</sup> yr <sup>-1</sup>
Ac <sub>ld</sub> (crit)	critical deposition flux of acidity (acid load)	mol <sub>c</sub> ha <sup>-1</sup> yr <sup>-1</sup>
[Al]	actual Al concentration	mol <sub>c</sub> m <sup>-3</sup>
[Al] <sub>e</sub>	Al concentration in equilibrium with Al hydroxide	mol <sub>c</sub> m <sup>-3</sup>
[Al]	inorganic Al concentration	mol <sub>c</sub> m <sup>-3</sup>
[Al](crit)	critical inorganic Al concentration	mol <sub>c</sub> m <sup>-3</sup>

Symbol	Explanation	Unit
$Al_{wo,ox}$	weathering flux of Al due to dissolution of Al hydroxides	$mol_c ha^{-1} yr^{-1}$
$Am_{st}$	amount of stemwood	$kg ha^{-1}$
$Am_m$	amount of root necromass	$kg ha^{-1}$
$Am_{li}$	amount of litter	$kg ha^{-1}$
$AmN_{im}$	amount of nitrogen in the zone where N immobilization occurs	$mol_c ha^{-1}$
[BC <sup>*</sup> ]	Cl-corrected concentration of base cations (Ca+Mg+K+Na-Cl)	$mol_c m^{-3}$
$BC_{dd}^*$	Cl-corrected dry deposition flux of base cations	$mol_c ha^{-1} yr^{-1}$
$BC_{le}^*$	Cl-corrected leaching flux of base cations	$mol_c ha^{-1} yr^{-1}$
$BC_{td}^*$	Cl-corrected total deposition flux of base cations	$mol_c ha^{-1} yr^{-1}$
$BC_{wd}^*$	Cl-corrected wet (bulk) deposition flux of base cations	$mol_c ha^{-1} yr^{-1}$
$BC_{wo}(T)$	weathering rate of base cations at the mean annual temperature T (K)	$mol_c ha^{-1} yr^{-1}$
$BC_{wo}(T_o)$	weathering rate of base cations at a reference temperature $T_o$ (K)	$mol_c ha^{-1} yr^{-1}$
[Ca <sub>a</sub> ]	Ca concentration in equilibrium with Ca carbonate	$mol_c m^{-3}$
CEC	cation exchange capacity of the soil	$mol_c kg^{-1}$
C/N <sub>mo</sub>	C/N ratio of the micro-organisms decomposing the substrate	$g g^{-1}$
C/N <sub>s</sub>	C/N ratio of the substrate (fresh litter, old litter or dead roots)	$g g^{-1}$
ctAl <sub>ox</sub>	Al hydroxide content	$mol_c kg^{-1}$
ctCa <sub>cb</sub>	Ca carbonate content	$mol_c kg^{-1}$
ctC	Carbon content in the soil	$mol_c kg^{-1}$
ctC <sub>im</sub>	Carbon content in the zone where N immobilization occurs	$mol_c kg^{-1}$
ctSO <sub>4,ac</sub>	content of SO <sub>4</sub> at the adsorption complex	$mol_c kg^{-1}$
ctX <sub>br</sub>	content of element X in branches	$mol_c kg^{-1}$
ctX <sub>l</sub>	content of element X in litter	$mol_c kg^{-1}$
ctX <sub>lv</sub>	content of element X in leaves	$mol_c kg^{-1}$
ctX <sub>pm</sub>	content of element X in primary minerals	$mol_c kg^{-1}$
ctX <sub>m</sub>	content of element X in root necromass	$mol_c kg^{-1}$
ctX <sub>st</sub>	content of element X in stems	$mol_c kg^{-1}$
de <sub>exp</sub>	denitrification exponent	-
E	actual evapotranspiration	$m^3 ha^{-1} yr^{-1}$
E <sub>i</sub>	interception evaporation	$m^3 ha^{-1} yr^{-1}$
E <sub>s</sub>	soil evaporation	$m^3 ha^{-1} yr^{-1}$
E <sub>t</sub>	transpiration	$m^3 ha^{-1} yr^{-1}$
ETS	effective temperature sum	°C

Symbol	Explanation	Unit
$f_c$	conversion factor (to convert units from $m^2$ to ha)	$m^2 \text{ ha}^{-1}$
$f_{dd}$	dry deposition factor	-
$ff$	filtering factor	-
$f_p \text{NH}_{4,ru}$	preference factor for the uptake of $\text{NH}_4$ above $\text{NO}_3$	-
$f_{mi}$	reduction factor by which mineralization fractions and mineralization rate constants are multiplied	-
$fr_c$	coverage fraction of a certain land use type in a gridcell	-
$fr_{de}$	denitrification fraction	-
$fr_{de}(z)$	cumulative denitrification fraction in the rootzone at depth $z$	-
$fr_{le}$	leaching fraction	-
$fr_{mi}$	mineralization fraction	-
$fr_{ni}$	nitrification fraction	-
$fr_{ni,hl}$	nitrification fraction in the humus layer	-
$fr_{ni}(z)$	cumulative nitrification fraction in the rootzone at depth $z$	-
$fr_{ru,hl}$	root uptake fraction in the humus layer	-
$fr_{ru}(z)$	cumulative root uptake fraction in the rootzone at depth $z$	-
$frX_{ac}$	fraction of element (cation) X on the adsorption complex	-
$frX_{le}$	foliar exudation fraction of element X	-
$frX_{fu}$	foliar uptake fraction of element X	-
$frX_{re,l}$	reallocation fraction for element X in leaves	-
$frX_{re,r}$	reallocation fraction for element X in (fine) roots	-
$fr_{we}(z)$	cumulative weathering fraction in the rootzone at depth $z$	-
$KAl_{ox}$	equilibrium constant for Al hydroxide dissolution	$\text{mol}^2 \text{ l}^2$
$KAl_{we,ox}$	weathering rate constant of Al from hydroxides	$\text{m}^3 \text{ mol}_c^{-1} \text{ yr}^{-1}$
$KCa_{cb}$	equilibrium constant for Ca carbonate dissolution	$\text{mol}^3 \text{ l}^3 \text{ bar}^{-1}$
$KCa_{we,cb}$	weathering rate constant of Ca from carbonates	$\text{m}^3 \text{ mol}_c^{-1} \text{ yr}^{-1}$
$KCO_2$	product of Henry's law constant for the equilibrium between $\text{CO}_2$ in soil water and soil air, and the first dissociation constant of $\text{H}_2\text{CO}_3$	$\text{mol}^2 \text{ l}^2 \text{ bar}^{-1}$
$k_{de}$	denitrification rate constant	$\text{yr}^{-1}$
$kEI_1$	first Elovich constant	$\text{m}_3 \text{ kg}^{-1} \text{ yr}^{-1}$
$kEI_2$	second Elovich constant	$\text{kg mol}_c^{-1}$
$k_{gc}$	a constant growth rate constant	$\text{kg ha}^{-1} \text{ yr}^{-1}$
$k_{gl}$	a logistic growth rate constant	$\text{kg ha}^{-1} \text{ yr}^{-1}$
$k_{gr}$	annual average growth rate constant	$\text{m}^3 \text{ ha}^{-1} \text{ yr}^{-1}$
$k_{mi,l}$	mineralization rate constant from (old) litter	$\text{yr}^{-1}$
$k_{mi,r}$	mineralization rate constant of root necromass	$\text{yr}^{-1}$

Symbol	Explanation	Unit
$k_{ni}$	nitrification rate constant	$\text{yr}^{-1}$
$k_{pr}$	protonation rate constant	$\text{yr}^{-1}$
$KSO_{4,ad}$	equilibrium constant for $SO_4$ adsorption	$\text{m}^3 \text{mol}_c^{-1}$
$KX_{ex}$	Gaines-Thomas selectivity constant for exchange of element (cation) X against Ca (or BC)	$(\text{mol l}^{-1})^2 X^{-2}$
$kX_{we,pm}$	weathering rate constants of element X (base cations) from primary minerals	$\text{m}^3 \text{mol}_c^{-1} \text{yr}^{-1}$
$MA_{rz}$	moisture amount in the rootzone	$\text{m}^3 \text{ha}^{-1}$
$N_{de}$	denitrification flux	$\text{mol}_c \text{ha}^{-1} \text{yr}^{-1}$
$N_{de}(\text{crit})$	denitrification flux at critical N load	$\text{mol}_c \text{ha}^{-1} \text{yr}^{-1}$
$ni_{exp}$	nitrification exponent	-
$NH_{4,ni}(z)$	cumulative nitrification flux at depth z	$\text{mol}_c \text{ha}^{-1} \text{yr}^{-1}$
$N_{im}(\text{crit})$	critical (long term acceptable) N immobilization flux	$\text{mol}_c \text{ha}^{-1} \text{yr}^{-1}$
$N_{le,min}$	minimum N leaching flux	$\text{mol}_c \text{ha}^{-1} \text{yr}^{-1}$
$NO_{3,de}(z)$	cumulative denitrification flux at depth z	$\text{mol}_c \text{ha}^{-1} \text{yr}^{-1}$
$NO_{3,le}(\text{crit})$	critical leaching flux of $NO_3$	$\text{mol}_c \text{ha}^{-1} \text{yr}^{-1}$
$N_{td}(\text{crit})$	critical N deposition flux (N load)	$\text{mol}_c \text{ha}^{-1} \text{yr}^{-1}$
$\theta$	volumetric moisture content of a soil layer	$\text{m}^3 \text{m}^{-3}$
$\theta_{rz}$	volumetric moisture content of the rootzone	$\text{m}^3 \text{m}^{-3}$
$P$	precipitation	$\text{m}^3 \text{ha}^{-1} \text{yr}^{-1}$
$PE$	precipitation excess	$\text{m}^3 \text{ha}^{-1} \text{yr}^{-1}$
$pCO_2$	partial $CO_2$ pressure in the soil	bar
$\rho$	bulk density of a soil layer	$\text{kg m}^{-3}$
$\rho_{im}$	bulk density of the soil in the zone where N immobilization occurs	$\text{kg m}^{-3}$
$\rho_{rz}$	bulk density of the soil in the rootzone	$\text{kg m}^{-3}$
$\rho_{st}$	density of stemwood	$\text{kg m}^{-3}$
$r$	stoichiometric equivalent ratio of Al to BC in the congruent weathering of silicates	-
$RAICa(\text{crit})$	critical Al/Ca ratio	$\text{mol mol}^{-1}$
$R_{br,st}$	branch to stem ratio	$\text{kg kg}^{-1}$
$R_{COO}_{pr}$	protonation flux of organic anions	$\text{mol}_c \text{ha}^{-1} \text{yr}^{-1}$
$RDA_{mo}$	dissimilation to assimilation ratio of the decomposing microbes	-
$R_{NH_4K}(\text{crit})$	critical $NH_4/K$ ratio	$\text{mol mol}^{-1}$
$R_{NS}_{td}$	ratio of the present N to S deposition	-
$ru_{exp}$	root uptake exponent	-
$SM_{rz}$	soil mass in the rootzone	$\text{kg ha}^{-1}$
$SSC$	sulphate sorption capacity	$\text{mol}_c \text{kg}^{-1}$
$S_{td}(\text{crit})$	critical S deposition flux (S load)	$\text{mol}_c \text{ha}^{-1} \text{yr}^{-1}$
$T$	thickness of a soil layer	m



Symbol	Explanation	Unit
$T_{de}$	thickness of the zone where denitrification occurs	m
$T_{in}$	thickness of the zone where N immobilization occurs	m
$T_{ni}$	thickness of the zone where nitrification occurs	m
$T_{rz}$	thickness of the rootzone	m
$we_{exp}$	weathering exponent	-
[X]	concentration of element X in the soil solution	$\text{mol}_c \text{ m}^{-3}$
(X)	activity of element X in the soil solution	$\text{mol l}^{-1}$
$X_{fe}$	foliar exudation flux of element X	$\text{mol}_c \text{ ha}^{-1} \text{ yr}^{-1}$
$X_{fu}$	foliar uptake flux of element X	$\text{mol}_c \text{ ha}^{-1} \text{ yr}^{-1}$
$X_{gu}$	growth (net) uptake flux of element X	$\text{mol}_c \text{ ha}^{-1} \text{ yr}^{-1}$
$X_{int}$	net interaction flux of element X in the soil	$\text{mol}_c \text{ ha}^{-1} \text{ yr}^{-1}$
$X_{le}$	leaching flux of element X	$\text{mol}_c \text{ ha}^{-1} \text{ yr}^{-1}$
$X_{lf}$	flux of element X by litterfall	$\text{mol}_c \text{ ha}^{-1} \text{ yr}^{-1}$
$X_{mi,fl}$	mineralization flux of element X from fresh litter	$\text{mol}_c \text{ ha}^{-1} \text{ yr}^{-1}$
$X_{mi,lt}$	mineralization flux of element X from 'old' litter	$\text{mol}_c \text{ ha}^{-1} \text{ yr}^{-1}$
$X_{mi,m}$	mineralization flux of element X from root necromass	$\text{mol}_c \text{ ha}^{-1} \text{ yr}^{-1}$
$X_{rd}$	flux of element X by root decay	$\text{mol}_c \text{ ha}^{-1} \text{ yr}^{-1}$
$X_{ru}$	root uptake flux of element X	$\text{mol}_c \text{ ha}^{-1} \text{ yr}^{-1}$
$X_{td}$	total deposition flux of element X to the soil	$\text{mol}_c \text{ ha}^{-1} \text{ yr}^{-1}$
$X_{tot}$	total amount of element X in the soil	$\text{mol}_c \text{ ha}^{-1}$
$Z_X$	charge of element X	-

**ANNEX B: RELATIONSHIPS BETWEEN EMPIRICAL FUNCTIONS DESCRIBING CATION RELEASE**

**Relationships between double logarithmic equations for the release rate against time and against cumulative release**

Describing the release rate of element X,  $RR_{X,t}$ , as (see Eq. 3.5a):

$$RR_{X,t} = \beta_1 \cdot t^{\beta_2} \tag{B1}$$

implies that (see Eq. 3.5b)

$$\log RR_{X,t} = \log \beta_1 + \beta_2 \log t \tag{B2}$$

Rewriting Eq. (B1) gives:

$$t = (RR_{X,t} / \beta_1)^{1/\beta_2} \tag{B3}$$

Integration of Eq. (B1) over  $t$  gives:

$$CR_{X,t} = \frac{\beta_1}{\beta_2 + 1} \cdot t^{\beta_2+1} \tag{B4}$$

where  $CR$  stands for cumulative release. Combining Eq. (B3) and Eq. (B4) yields:

$$CR_{X,t} = \frac{\beta_1^{-1/\beta_2}}{\beta_2 + 1} \cdot RR_{X,t}^{(\beta_2+1)/\beta_2} \tag{B5}$$

Rewriting Eq. (B5) gives:

$$RR_{X,t} = \beta_3 \cdot CR_{X,t}^{\beta_4} \tag{B6}$$

where  $\beta_3 = (\beta_2 + 1) \cdot \beta_1^{1/\beta_2}$  (B7a) and  $\beta_4 = \frac{\beta_2}{\beta_2 + 1}$  (B7b)

Logarithmization of Eq. (B6) gives (see Eq. 3.6):

$$\log RR_{X,t} = \log \beta_3 + \beta_4 \log CR_{X,t} \tag{B8}$$

The relationship between the parameters  $\beta_1$  and  $\beta_2$  in Eq. (B2) and the parameters  $\beta_3$  and  $\beta_4$  in Eq. (B8) is given in the Eqs. (B7a) and B7b).

**The relationship between single logarithmic equations for the cumulative release against time and against release rate**

A single logarithmic relationship is a specific case of the double logarithmic equation. Assuming that the exponent  $\beta_2$  in Eq. (B1) equals -1, i.e.

$$RR_{x,t} = \beta_1 \cdot t^{-1} \tag{B9}$$

and integrating Eq. (B9) gives (see Eq. 3.4):

$$CR_{x,t} = \beta_0 + \beta_1 \ln t \tag{B10}$$

Rewriting Eq. (B10) gives:

$$t = e^{-\beta_0/\beta_1} \cdot e^{CR_{x,t} / \beta_1} \tag{B11}$$

Combination of Eq. (B9) and Eq. (B11) gives:

$$RR_{x,t} = \beta_3 \cdot e^{-\beta_4 \cdot CR_{x,t}} \tag{B12}$$

$$\text{where } \beta_3 = \beta_1 \cdot e^{\beta_0/\beta_1} \tag{B13a} \quad \text{and} \quad \beta_4 = 1 / \beta_1 \tag{B13b}$$

Logarithmization of Eq. (B12) yields (see Eq. 3.7):

$$\ln RR_{x,t} = \ln \beta_3 - \beta_4 CR_{x,t} \tag{B14}$$

The relationship between the parameter  $\beta_0$  in Eq. (B10) and the parameters  $\beta_3$  and  $\beta_4$  in Eq. (B14) can be derived by logarithmization of Eq. (B13a) and substituting  $\beta_1$  by  $\beta_4$  according to Eq. (B13b), which yields (cf Van Riemsdijk and De Haan, 1981):

$$\beta_0 = \frac{1}{\beta_4} \cdot \ln (\beta_3 \cdot \beta_4) \tag{B15}$$

The relationship between the parameter  $\beta_1$  in Eq. (B10) and the parameter  $\beta_4$  in Eq. (B14) is given in Eq. (B13b).

## ANNEX C: SOLUTION METHOD OF THE MODEL SMART

In order to solve the various model equations in SMART, i.e. to compute the concentrations and total amounts of the various ions, the mass balance equation (6.9) is discretized using a time step  $\Delta t$  of one year (since we are interested in the long-term development of forest soils). For the ions with no internal sources ( $\text{SO}_4$ ,  $\text{NO}_3$  and  $\text{NH}_4$ ) Eq. (6.10) applies. Replacing the differential operator  $d[X]/dt$  by its finite difference  $([X]_t - [X]_{t-\Delta t})/\Delta t$  and rearranging Eq. (6.9) yields:

$$[X]_t = \frac{\theta_{rz} \cdot f_c \cdot T_{rz} \cdot [X]_{t-\Delta t} + X_{td,t} \cdot \Delta t}{\theta_{rz} \cdot f_c \cdot T_{rz} + PE \cdot \Delta t} \quad (\text{C1})$$

where  $\Delta t$  is a timestep of one year. Eq. (C1) is solved recursively for  $\text{SO}_4$ ,  $\text{NO}_3$  and  $\text{NH}_4$  after defining an initial concentration,  $[X]_0$ , according to:

$$[X]_0 = (X_{td,0} + X_{int,0}) / PE \quad (\text{C2})$$

$X_{td}$  +  $X_{int}$  are calculated according to Eqs. (6.14), (6.15) and (6.16).

In calcareous soil the Al concentration is set to zero and concentrations of H, BC and  $\text{HCO}_3$  are computed from the charge balance equation (Eq. 6.8) and the two equilibrium equations (Eqs. 6.20 and 6.21):

$$[\text{H}]_t = [\text{NO}_3]_t + [\text{SO}_4]_t + [\text{HCO}_3]_t - [\text{BC}]_t + [\text{NH}_4]_t \quad (\text{C3})$$

$$[\text{HCO}_3]_t = K\text{CO}_2 \cdot p\text{CO}_2 / [\text{H}]_t \quad (\text{C4})$$

$$[\text{BC}]_t = K\text{Ca}_{cb} \cdot [\text{H}]_t^2 / (K\text{CO}_2^2 \cdot p\text{CO}_2) \quad (\text{C5})$$

Combining the Eqs. (C3), (C4) and (C5) yields a non-linear equation for  $[\text{H}]_t$ , which is solved by Brent's method (Brent, 1973) as documented in Press et al. (1986). Once  $[\text{H}]_t$  is computed,  $[\text{HCO}_3]_t$  and  $[\text{BC}]_t$  are calculated from Eqs. (C4) and (C5). To obtain the change in total BC amount the mass balance equation (Eq. 6.9) is rewritten with the aid of Eq. (6.11).

$$\rho_{rz} \cdot f_c \cdot T_{rz} \cdot \frac{d \text{Ca}_{cb}}{dt} + \theta_{rz} \cdot f_c \cdot T_{rz} \cdot \frac{d [\text{BC}]_t}{dt} = \text{BC}_{td,t} + \text{BC}_{int,t} - PE \cdot [\text{BC}]_t \quad (\text{C6})$$

where  $\text{BC}_{int}$  equals growth uptake, since weathering in calcareous soils is ignored in SMART. Defining  $\rho_{rz} \cdot f_c \cdot T_{rz}$  as  $\text{SM}_{rz}$  (soil mass in the rootzone in  $\text{kg ha}^{-1}$ ) and

$\theta_{rz} \cdot f_c \cdot T_{rz}$  as  $MA_{rz}$  (moisture amount in the rootzone in  $m^3 ha^{-1}$ ) and discretizing Eq. (C6), gives:

$$SM_{rz} \cdot Ca_{cb,t} = SM_{rz} \cdot Ca_{cb,t-\Delta t} + MA_{rz} \cdot ([BC]_{t-\Delta t} - [BC]_t) + (BC_{id,t} + BC_{int,t}) \cdot \Delta t - PE [BC]_t \cdot \Delta t \quad (C7)$$

The initial concentration of base cations is taken as:

$$[BC]_0 = (BC_{id,0} - BC_{gu}) / PE \quad (C8)$$

In non-calcareous soils the concentration of H,  $HCO_3$ , Al and BC is calculated by combining the charge balance equation (cf Eq. 6.8):

$$[H]_t = [NO_3]_t + [SO_4]_t + [HCO_3]_t - [Al]_t - [BC]_t - [NH_4]_t \quad (C9)$$

with the equilibria considered (cf Eqs. 6.20 and 6.22), i.e.:

$$[HCO_3]_t = (KCO_2 \cdot pCO_2) / [H]_t \quad (C10)$$

$$[Al]_t = KAl_{ox} \cdot [H]_t^3 \quad (C11)$$

and the change in the total amount of base cations by (cf Eqs. 6.9 and 6.12):

$$MA_{rz} \frac{d [BC]_t}{dt} + SM_{rz} \cdot CEC \frac{d frBC_{ac,t}}{dt} = BC_{id,t} + BC_{int,t} - PE \cdot [BC]_t \quad (C12)$$

which, in its discretized form, reads:

$$[BC]_t = \frac{MA_{rz} \cdot [BC]_{t-1} + (BC_{id,t} + BC_{int,t}) \cdot \Delta t - SM_{rz} \cdot CEC \cdot (frBC_{ac,t} - frBC_{ac,t-\Delta t})}{MA_{rz} + PE \cdot \Delta t} \quad (C13)$$

where BC interaction equals weathering minus growth uptake (cf Eq. 6.13). Furthermore we have the exchange reactions (cf Eqs. 6.23-6.25):

$$\frac{frH_{ac,t}^2}{frBC_{ac,t}} = KH_{ex} \cdot \frac{[H]^2}{[BC]_t} \quad (C14)$$

$$\frac{frAl_{ac,t}^2}{frBC_{ac,t}^3} = KAl_{ox} \cdot \frac{[Al]_t^2}{[BC]_t^3} \quad (C15)$$

$$frH_{ac,t} + frAl_{ac,t} + frBC_{ac,t} = 1 \quad (C16)$$

The solution of this set of equations (C9 to C11 and C13 to C16) can be reduced to the solution of a single non-linear equation in  $frH_{ac,t}$  in the following way: Inserting  $[Al]_t$  from Eq. (C11) into Eq. (C15), taking the third power of Eq. (C14), dividing Eq. (C15) by the resulting expression and taking the square root yields a relation between  $frAl_{ac,t}$  and  $frH_{ac,t}$  according to:

$$frAl_{ac,t} = K \cdot frH_{ac,t}^3 \quad (C17)$$

with the dimensionless constant K given as:

$$K = KAl_{ox} \cdot \left( KAl_{ox} / KH_{ox}^3 \right)^{1/2} \quad (C18)$$

Eq. (C16) immediately yields an expression for  $frBC_{ac,t}$ :

$$frBC_{ac,t} = 1 - frH_{ac,t} - K \cdot frH_{ac,t}^3 \quad (C19)$$

When  $frBC_{ac,t}=0$ , which is generally the case in acid forest soils, there is a simple relationship between  $frH_{ac,t}$  and its complement  $frAl_{ac,t}$  and the K value defined by Eq. (C18), which is displayed in Figure C1.

Since we know  $[BC]_{t-\Delta t}$  and  $frBC_{ac,t-\Delta t}$  from an initialization procedure or from the previous time step,  $[BC]_t$  is expressed in terms of  $frBC_{ac,t}$  (and therefore  $frH_{ac,t}$ ) with the aid of the discretized mass balance equation (Eq. C13). Furthermore, Eq. (C14) is used to express  $[H]_t$  as a function of  $frH_{ac,t}$ :

$$[H]_t = frH_{ac,t} \cdot \left( \frac{[BC]_t}{(KH_{ox} \cdot frBC_{ac,t})} \right)^{1/2} \quad (C20)$$

Finally, inserting all the expressions for  $[HCO_3]_t$  (Eq. C10),  $[Al]_t$  (Eq. C11),  $[BC]_t$  (Eq. C13) and  $[H]_t$  (Eq. C20) into the charge balance equation (Eq. C9) yields a single equation for  $frH_{ac,t}$  which can again be solved by Brent's method.

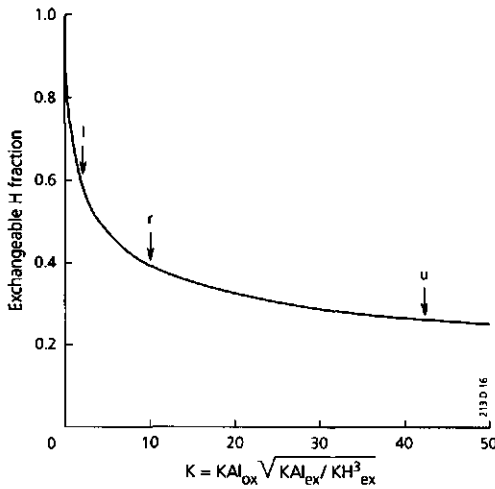


Figure C1 Relationship between the exchangeable H fraction and the dimensionless constant  $K$  for zero base saturation ( $frBC_{ac}=0$ ; cf Eqs. C18 and C19). The arrows refer to the upper ( $u$ ), reference ( $r$ ) and lower ( $l$ ) values of  $KAl_{ox}$ ,  $KAl_{ex}$  and  $KH_{ex}$  (cf Table 6.7)

The initialization of this procedure can be done in two different ways, depending on whether the initial base saturation is known or not. If  $frBC_{ac,t_0}$  is not known, the concentration of base cations is initialized by:

$$[BC]_{t_0} = (BC_{la,t_0} + BC_{we} - BC_{gu}) / PE \quad (C21)$$

Inserting this BC concentration, together with the  $SO_4$ ,  $NO_3$  and  $NH_4$  concentration derived with Eq. (C2), into the charge balance equation (Eq. C9) and using the equilibrium equations for  $HCO_3$  and Al (Eq. C10 and C11) yields the initial values for all solute concentrations. Inserting these values into the exchange equations (Eqs. C14-C16) allows these equations be solved for the exchangeable fractions. If, however,  $frBC_{ac,t}$  is known, we compute  $frH_{ac,t}$  and  $frAl_{ac,t}$  from Eqs. (C19) and (C17), and then use one of the exchange equations (C14 and C15) together with the charge balance equation (C9) and the equilibrium equations (C10 and C11) to compute the initial concentrations.

Finally, the change in the amount of Al hydroxides is computed by combining the mass balance equation (Eq. 6.9) with Eqs. (6.13) and (6.18):

$$MA_{rz} \cdot \frac{d[Al]_l}{dt} + SM_{rz} \cdot \left( CEC \cdot \frac{dfrAl_{ac,t}}{dt} + \frac{dAl_{ox,t}}{dt} \right) = Al_{we} - PE \cdot [Al]_l \quad (C22)$$

Discretizing Eq. (C22) gives:

$$\begin{aligned}
 SM_{rz} \cdot Al_{ox,t} = & SM_{rz} \cdot Al_{ox,t-1} + MA_{rz} \cdot ([Al]_{t-\Delta t} - [Al]_t) + Al_{w0,t} \cdot \Delta t \\
 & - SM_{rz} \cdot CEC \cdot (frAl_{ac,t} - frAl_{ac,t-\Delta t}) - PE \cdot [Al]_t \cdot \Delta t
 \end{aligned}
 \tag{C23}$$

The value of  $Al_{to,t}$  can then be calculated from Eq. (6.13). When the amount of Al hydroxides is depleted, the Al hydroxide equilibrium reaction no longer occurs and Eq. (C17) no longer holds. In this case the system of equations is reduced to a single non-linear equation, this time in  $frBC_{ac,t}$ , in the following way: Putting  $Al_{ox,t} = 0$  in the discretized form of Eq. (C22), we can express  $[Al]_t$  as a linear function in  $frAl_{ac,t}$ :

$$[Al]_t = \frac{MA_{rz} \cdot [Al]_{t-\Delta t} + Al_{in,t-\Delta t} - SM_{rz} \cdot CEC \cdot (frAl_{ac,t-\Delta t})}{MA_{rz} + PE \cdot \Delta t}
 \tag{C24}$$

In the same way as above,  $[BC]_t$  can be expressed as a linear function of  $frBC_{ac,t}$  (cf Eq. C13). Inserting these two linear expressions into the exchange equation (Eq. C15) allows us to express  $frAl_{ac,t}$  as a function of  $frBC_{ac,t}$  alone. From Eq. (C16) we then get  $frH_{ac,t}$  as a function of  $frBC_{ac,t}$ . Furthermore,  $[H]_t$  is given by Eq. (C20). Inserting all these expressions into the charge balance equation (Eq. C20) and using the equilibrium equation for  $HCO_3$  (Eq. C9) yields a single non-linear equation for  $frBC_{ac,t}$ , which is again solved by Brent's method.



## ANNEX D: PUBLICATIONS ON ACID DEPOSITION AND SOIL ACIDIFICATION

### Causes, rates and effects of soil acidification

- Berdowski, J.J.M., D.J. Bakker, J.T. De Smit, G. Van Tol and W. De Vries, 1992. *Technical Evaluation of the TECMENA reports on the forest vitality in the El Maestrazgo and Els Ports area in Spain*, 49 pp.
- Breeuwsma, A. en W. De Vries, 1984a. *Gevolgen van zure regen voor de bodem. 2. Aandeel in de bodemverzuring in Nederland*. Wageningen, Stichting voor Bodemkartering, Rapport nr. 1787, 64 pp.
- Breeuwsma, A. and W. De Vries, 1984b. *The relative importance of natural production of  $H^+$  in soil acidification*. Netherlands Journal of Agricultural Science, 32: 161-163.
- De Visser, P.H.B. en W. De Vries, 1989. *De gemiddeld jaarlijkse waterbalans van bos-, heide en grasland vegetaties*. Wageningen, Stichting voor Bodemkartering, Rapport nr. 2085, 136 pp.
- De Vries, W., 1993a. *De chemische samenstelling van bodem- en bodemvocht van duin gronden in de provincie Zuid-Holland*. Wageningen, DLO-Staring Centrum, Rapport 280, 31 pp.
- De Vries, W., 1994a. *Rates and mechanisms of cation and silica release in acid sandy soils. 1. Influence of mineral pools and mineral depletion*. Geoderma (submitted).
- De Vries, W., 1994b. *Rates and mechanisms of cation and silica release in acid sandy soils. 2. Effects of pH and Al concentration*. Geoderma (submitted).
- De Vries, W. en A. Breeuwsma, 1984a. *Gevolgen van zure regen voor de bodem. 1. Oorzaken van bodemverzuring*. Wageningen, Stichting voor Bodemkartering, Rapport nr. 1786, 60 pp.
- De Vries, W. en A. Breeuwsma, 1984b. *Causes of soil acidification*. Netherlands Journal of Agricultural Science, 32: 159-161
- De Vries, W. en A. Breeuwsma, 1985. *De invloed van natuurlijke zuurbronnen, afvoer van biomassa en zure regen op de verzuring van Nederlandse bosgronden*. Nederlands Bosbouw tijdschrift 57, 4: 111-117
- De Vries, W. and A. Breeuwsma, 1986. *Relative importance of natural and anthropogenic proton sources in soils in the Netherlands*. Water Air and Soil Poll., 28: 173-184
- De Vries, W. and A. Breeuwsma, 1987. *The relation between soil acidification and element cycling*. Water Air and Soil Poll., 35: 293-310
- De Vries, W. and P.C. Jansen, 1994. *Effects of acid deposition on 150 forest stands in the Netherlands. Input output budgets for sulphur, nitrogen, base cations and aluminium*. Wageningen, the Netherlands, DLO Winand Staring Centre for Integrated Land, Soil and Water Research, Report 69.3, 58 pp.
- De Vries, W. and E.E.J.M. Leeters, 1994. *Effects of acid deposition on 150 forest stands in the Netherlands. Chemical composition of the humus layer, mineral soil and soil solution*. Wageningen, the Netherlands, DLO Winand Staring Centre for Integrated Land, Soil and Water Research, Report 69.1.

- De Vries, W., A. Breeuwsma en F. De Vries, 1989a. *Kwetsbaarheid van de Nederlandse bodem voor verzuring. Een voorlopige indicatie in het kader van de Richtlijn "Ammoniak en Veehouderij"*. Wageningen, Staring Centrum, Rapport 29, 74 pp.
- De Vries, W., A. Hol, S. Tjalma en J.C.H. Voogd, 1990. *Voorraden en verblijftijden van elementen in een boscysteem: een literatuurstudie*. Wageningen, Staring Centrum, Rapport 94, 205 pp.
- De Vries, W., M.M.T. Meulenbrugge, W. Balkema, J.C.H. Voogd and R.C. Sjardijn, 1994g. *Rates and mechanisms of cation and silica release in acid sandy soils. 3. Differences between soil horizons and soil types*. Geoderma (submitted).
- De Vries, W., J.J.M. Van Grinsven, N. Van Breemen, E.E.J.M. Leeters and P.C. Jansen, 1994h. *Impacts of acid atmospheric deposition on concentrations and fluxes of solutes in acid sandy forest soils in the Netherlands*. Geoderma (submitted).
- De Vries, W., E.E.J.M. Leeters, C.M. Hendriks, W. Balkema, M.M.T. Meulenbrugge, R. Zwijnen and J.C.H. Voogd, 1992c. *Soil and Soil solution composition of 150 forest stands in the Netherlands in 1990*. In: T. Schneider (Ed.): *Acidification research: Evaluation and policy applications*. Studies in Environmental Science 50, Elsevier Science Publishers, Amsterdam, the Netherlands: 535-536.
- Heij, G.J., J.W. Erisman en W. De Vries, 1992. *De effecten van atmosferische depositie op het Nederlandse bos*. Milieu 7/4: 101-106.
- Heij, G.J., W. De Vries, A.C. Posthumus and G.M.J. Mohren, 1991. *Effects of air pollution and acid deposition on forests and forest soils*. In: G.J. Heij and T. Schneider (Eds.): *Acidification Research in the Netherlands. Final Report of the Dutch Priority Programme on Acidification*. Studies in Environmental Science 46; Elsevier Science Publishers, Amsterdam, the Netherlands: 97-137.
- Hendriks, C.M.A., W. De Vries and J. Van den Burg, 1994. *Effects of acid deposition on 150 forest stands in the Netherlands. Relationships between forest vitality and the chemical composition of foliage, humus layer and soil solution*. Wageningen, the Netherlands, DLO Winand Staring Centre for Integrated Land, Soil and Water Research, Report 69.2, 55 pp.
- Kleijn, C.E. and W. De Vries, 1987. *Characterizing soil moisture composition in forest soil in space and time*. In: W. Van Duyvenbooden and H.G. Van Waegeningh (Eds.), *Vulnerability of Soil and Groundwater to Pollutants*. Proc. Int. Conf. Noordwijk aan Zee, 1987, the Netherlands: 591-600
- Kleijn, C.E., H. Oterdoom, W. De Vries en C. Hendriks, 1987. *De indirecte effecten van atmosferische depositie op de vitaliteit van Nederlandse bossen. Deel 1: Beschrijving van de onderzoeksozpet*. Wageningen, Stichting voor Bodemkartering, Rapport nr. 2010, 74 pp.
- Kleijn, C.E., G. Zuidema en W. De Vries, 1989. *De indirecte effecten van atmosferische depositie op de vitaliteit van Nederlandse bossen. Deel 2. Depositie, bodemeigenschappen en bodemvochtsamenstelling van acht Douglasopstanden*. Wageningen, Stichting voor Bodemkartering, Rapport nr. 2050, 96 pp.

- Leeters, E.E.J.M. en W. De Vries, 1992a. *Verzuring -Belasting en gehalten in de bodem-Gehalten*. In: Milieudiagnose 1991. Deel 1: Integrale rapportage Lucht-, Bodem- en Grondwaterkwaliteit (Pilot study): 23-27
- Leeters, E.E.J.M. en W. De Vries, 1992b. *De kwaliteit van de Bodem - Verzuring - Heide en bosbodems*. In: Milieudiagnose 1991. Deel 3: Bodem- en Grondwaterkwaliteit: 49-53.
- Leeters, E.E.J.M., H. Hartholt, W. De Vries and L.J.M. Boumans, 1994. *Effects of acid deposition on 150 forest stands in the Netherlands. Relationships between deposition level, stand and site characteristics and the chemical composition of needles, soil and soil solution and groundwater*. Wageningen, the Netherlands, DLO Winand Staring Centre for Integrated Land, Soil and Water Research, Report 69.4.
- Loman H., A. Breeuwsma, W. De Vries, J. Hoeks en W. Van Duyvenbooden, 1984. *Verzuring door atmosferische depositie*. Bodem. Publikatiereeks Milieubeheer nr. 84. Ministerie Landbouw en Visserij en Volkshuisvesting, Ruimtelijke Ordening en Milieubeheer, 76 pp.
- Oterdoom, J.H., J. Van den Burg en W. De Vries, 1987. *Resultaten van een oriënterend onderzoek naar de minerale voedingstoestand en bodem-chemische eigenschappen van acht douglasopstanden met vitale en minder vitale bodem in Midden-Nederland, winter 1984/1985*. Wageningen, Rijksinstituut voor Onderzoek in de Bos- en Landschapsbouw "De Dorschkamp", Rapport nr. 470, 47 pp.
- Oterdoom, J.H., R. Postma, A.F.M. Olsthoorn en W. De Vries, 1994. *De indirecte effecten van atmosferische depositie op de vitaliteit van Nederlandse bossen. 5. Vitaliteitskenmerken, naaldsamenstelling, fijne wortels en groei van acht Douglas opstanden*. APV-rapport 18.02, 99 pp.
- Reurslag, A., G. Zuidema en W. De Vries, 1990. *De indirecte effecten van atmosferische depositie op de vitaliteit van Nederlandse bossen. Deel 3. Simulatie van de waterbalans van acht Douglas-opstanden*. Wageningen, Staring Centrum, Rapport 76, 100 pp.
- Rijtema, P.E. and W. De Vries, 1994. *Differences in precipitation excess and nitrogen leaching from agricultural lands and forest plantations*. Biomass & Bioenergy (accepted).
- Van Breemen, N., J.J.M. Van Grinsven and W. De Vries, 1992. *Effects of acid atmospheric deposition on soil and groundwater*. In: Soil pollution and soil protection; international postgraduate course. Wageningen, LUW: 1-22
- Van Grinsven, J.J.M., W. De Vries en N. Van Breemen, 1992. *Effecten van zure depositie op bodem en grondwater*. In: F.A.M. De Haan, C.H. Henkens en D.A. Zeilmaker (Eds.), *Bodembescherming: handboek voor milieubeheer*. Alphen aan den Rijn, Samsom, D2100: 1-45.
- Zevenbergen, Chr. en W. De Vries, 1985. *Evenwichtsreacties (constanten) en bepalingmethoden van aluminium in de bodem (een literatuuroverzicht)*. Wageningen, Stichting voor Bodemkartering, Rapport nr. 1902, 57 pp.

## Critical loads for nitrogen, sulphur and acidity

- Bouma, J., W. De Vries and P.A. Finke, 1994. *Models for predicting environmental impacts*. In: R.C. Wood and J. Dumanski (Eds.), Proc. Int. Workshop on Sustainable Land Management for the 21<sup>st</sup> Century. University of Lethbridge. Lethbridge, Canada, June 20-26, 1993: 239-249.
- De Vries, W., 1988. *Critical deposition levels of nitrogen and sulphur on Dutch forest ecosystems*. Water Air and Soil Poll. 42: 221-239.
- De Vries, W., 1990a. *Kritische depositieniveaus van stikstof en zwavel op Nederlandse bossen*. In: M. Bovenkerk, A.H.M. Bresser en J. Van Ham (Red.), Verzuring. Nationaal symposium over resultaten uit het verzuringsonderzoek en de op grond daarvan voorgestelde maatregelen. Kluwer, Deventer, 1990: 15-22.
- De Vries, W., 1991. *Methodologies for the assessment and mapping of critical loads and the impact of abatement strategies on forest soils*. Wageningen, the Netherlands, DLO Winand Staring Centre for Integrated Land, Soil and Water Research, Report 46, 109 pp.
- De Vries, W., 1992. *Empirical data and model results for critical nitrogen loads in the Netherlands*. In: P. Grennfelt and E. Thörlöf (Eds.), Critical loads for Nitrogen. Report from a workshop held at Lökeberg, Sweden 6-10 April, 1992. Nordic Council of Ministers, Report 1992, 41: 383-402.
- De Vries, W., 1993b. *Average critical loads for nitrogen and sulphur and its use in acidification abatement policy in the Netherlands*. Water Air and Soil Poll. 68: 399-434.
- De Vries, W. and H.D. Gregor, 1991. *Critical loads and critical levels for the environmental effects of air pollutants*. In: M.J. Chadwick and M. Hutton (Eds.): Acid Depositions in Europe: Environmental effects, control strategies and policy options. Stockholm Environment Institute: 171-215.
- De Vries, W. and G.J. Heij, 1991. *Critical loads and critical levels for the environmental effects of air pollutants*. In: G.J. Heij and T. Schneider (Eds.): Acidification Research in the Netherlands. Final Report of the Dutch Priority Programme on Acidification. Studies in Environmental Science 46; Elsevier Science Publishers, Amsterdam, the Netherlands: 205-214.
- De Vries, W. and J. Kros, 1991. *Assessment of critical loads and the impact of deposition scenarios by steady state and dynamic soil acidification models*. Wageningen, the Netherlands, DLO Winand Staring Centre for Integrated Land, Soil and Water Research, Report 36, 61 pp.
- De Vries, W., W. Schöpp and J.P. Hettelingh, 1991a. *Comparison of national critical load maps and the CCE critical loads map based on European data only*. In: J.P. Hettelingh, R.J. Downing and P.A.M. De Smet (Eds.): Mapping critical loads for Europe. Bilthoven, National Institute of Public Health and Environmental Protection, CCE Technical Report 1/RIVM Report 259101001: 76-79.

- De Vries, W., J. Kros and J.C.H. Voogd, 1994d. *Assessment of critical loads and their exceedance on Dutch forests using a multi-layer steady state model*. Water Air and Soil Poll. 76 (in press)
- De Vries, W., G.J. Reinds and M. Posch, 1994e. *Assessment of critical loads and their exceedance on European forests using a one-layer steady-state model*. Water Air and Soil Poll. 72: 357-394.
- De Vries, W., M. Posch, G.J. Reinds and J. Kämäri, 1992a. *Critical loads and their exceedance on forests in Europe*. Wageningen, the Netherlands, DLO Winand Staring Centre for Integrated Land, Soil and Water Research, Report 58, 126 pp.
- De Vries, W., J. Kros, R. Hootsmans, G.J. Van Uffelen and J.C.H. Voogd, 1992b. *Critical loads for Dutch forest soils*. In: T. Schneider (Ed.): *Acidification Research: Evaluation and Policy Applications*. Studies in Environmental Science 50, Elsevier Science Publishers, Amsterdam, the Netherlands: 307-318.
- De Vries, W., M. Posch, T. Oja, H. Van Oene, J. Kros, P. Warfvinge and P.A. Arp, 1994i. *Modelling critical loads for the Solling spruce site*. Modelling of Geo-biosphere Processes (submitted).
- Heij, G.J., J.W. Erisman en W. De Vries, 1992. *De effecten van atmosferische depositie op het Nederlandse bos*. Milieu 1992/4: 101-106.
- Heij, G.J., W. De Vries and G.P.J. Draayers, 1993. *Uncertainties and risks related to exceedances of critical acid loads on forests in the Netherlands*. Proc. Fourth International Symposium on Comparative Risk Analysis and Priority setting for Air Pollution Issues, Keystone, Colorado, USA, June, 7-11, 1993.
- Hettelingh, J.P. and W. De Vries, 1992. *Mapping vademecum*. Bilthoven, National Institute of Public Health and Environmental Protection. Report 259101002, 39 pp.
- Hettelingh, J.P., W. De Vries, W. Schöpp, R.J. Downing and P.A.M. De Smet, 1991. *Methods and data*. In: J.P. Hettelingh, R.J. Downing and P.A.M. De Smet (Eds.): *Mapping critical loads for Europe*. Bilthoven, National Institute of Public Health and Environmental Protection, CCE Technical Report 1 / RIVM Report 259101001: 31-48.
- Hettelingh, J.P., M. Posch, W. De Vries, K. Bull and H.U. Sverdrup, 1992. *Guidelines for the computation and mapping of nitrogen critical loads and exceedances in Europe*. In: P. Grennfelt and E. Thörnelöf (Eds.), *Critical loads for Nitrogen*. Report from a workshop held at Lökeberg, Sweden, April 6-10, 1992. Nordic Council of Ministers, Report 1992, 41: 287-303.
- Posch, M., J.P. Hettelingh, H.U. Sverdrup, K. Bull and W. De Vries, 1993. *Guidelines for the computation and mapping of critical loads and exceedances of sulphur and nitrogen in Europe*. In: R.J. Downing, J.P. Hettelingh and P.A.M. De Smet (Eds.): *Calculation and mapping of critical loads in Europe*. Coordination Centre for effects, Status Report 1993, Bilthoven, the Netherlands: 21-37.
- Schulze, E.D., W. De Vries, M. Hauhs, K. Rosén, L. Rasmussen, C.O. Tamm and J. Nilsson, 1989. *Critical loads for nitrogen deposition on forest ecosystems*. Water Air and Soil Poll., 48: 451-456.
- Sverdrup, H. and W. De Vries, 1994. *Calculating critical loads for acidity with a mass balance model*. Water Air and Soil Poll. 72: 143-162.

- Sverdrup, H., W. De Vries and A. Henriksen, 1990. *Mapping critical loads. A guidance manual to criteria, calculation methods data collection and mapping*. Miljø rapport 1990: 14. Nordic Council of Ministers, Copenhagen, 1990, 124 pp.
- Van der Salm, C., J.C.H. Voogd and W. De Vries, 1993. *SMB - a Simple Mass Balance model to calculate critical loads. Model description and User Manual*. Technical Document 11, Wageningen, the Netherlands, DLO Winand Staring Centre for Integrated Land, Soil and Water Research, 32 pp.

### **Long-term impacts of acid deposition on soils**

- Bakema, A.H., K.F. De Boer, J.W. Erisman, G.J. Heij, J.P. Hettelingh, K.W. Van den Hoek, N.J.P. Hoogervorst, L. Hordijk, R. Thomas and W. De Vries, 1991. *Verzuring*. In: Nationale Milieuverkenning 2, 1990-2010. Bilthoven, RIVM: 184-213.
- Berdowski, J.J.M., C. Van Heerden, J.J.M. Van Grinsven, J.G. Van Minnen and W. De Vries, 1991. *SOILVEG: a model to evaluate effects of acid atmospheric deposition on soil and forest*. Volume 1: Model principles and application procedures. Bilthoven, RIVM, Dutch Priority Programme Acidification, Report 114.1-02, 126 pp.
- De Vries, W., 1987a. *The role of soil data in assessing the large scale input of atmospheric pollutants on groundwater quality*. In: W. Van Duyvenbooden and H.G. Van Waegeningh (Eds.): *Vulnerability of Soil and Groundwater to Pollutants*. Proc. Int. Conf. Noordwijk aan Zee, 1987, The Netherlands: 897-910.
- De Vries, W., 1987b. *A conceptual model for analysing soil and groundwater acidification on a regional scale*. Proc. Int. Symp. on Acidification and Water Pathways. Bolkesjø, 1987, Norway: 185-194
- De Vries, W., 1990b. *Philosophy, structure and application methodology of a soil acidification model for the Netherlands*. In: J. Kämäri (Ed.). *Impact models to assess regional acidification*: 3-21.
- De Vries, W. en J. Kros, 1989a. *De lange termijn effecten van verschillende depositie scenario's op de bodemvochtsamenstelling van representatieve boscystemen*. Wageningen, Staring Centrum, Rapport 30, 89 pp.
- De Vries, W. and J. Kros, 1989b. *The long term impact of acid deposition on the aluminium chemistry of an acid forest soil*. In J. Kämäri, D.F. Brakke, A. Jenkins, S.A. Norton and R.F. Wright (Eds.): *Regional Acidification Models. Geographic Extent and Time Development*: 113-128.
- De Vries, W., M. Posch and J. Kämäri, 1989b. *Simulation of the long-term soil response to acid deposition in various buffer ranges*. *Water Air and Soil Poll.* 48: 349-390.
- De Vries, W., M. Posch and J. Kämäri, 1989c. *Modelling time patterns of forest soil acidification for various deposition scenarios*. In J. Kämäri, D.F. Brakke, A. Jenkins, S.A. Norton and R.F. Wright (Eds.): *Regional Acidification Models. Geographic Extent and Time Development*: 129-150.

- De Vries, W., J.C.H. Voogd and J. Kros, 1993. *Effects of various deposition scenarios on the aluminium hydroxide content of Dutch forest soils*. Wageningen, the Netherlands, DLO Winand Staring Centre for Integrated Land, Soil and Water Research, Report 68, 32 pp.
- De Vries, W., J. Klijn and J. Kros, 1994a. *Simulation of the long-term impact of atmospheric deposition on Dune ecosystems in the Netherlands*. *Journal of Applied Ecology* 31: 59-73.
- De Vries, W. de, J. Kros and C. Van der Salm, 1994b. *Modelling the impact of acid deposition and nutrient cycling in forest soils*. *Ecological Modelling* (in press).
- De Vries, W., J. Kros and C. Van der Salm, 1994c. *The long-term impact of three emission-deposition scenarios on Dutch forest soils*. *Water Air and Soil Poll.* 75: 1-35.
- De Vries, W., J. Kros, C. Van der Salm and J.C.H. Voogd, 1991b. *Effects on forest soils*. In: G.J. Heij and T. Schneider (Eds.): *Acidification Research in the Netherlands*. Final Report of the Dutch Priority Programme on Acidification. *Studies in Environmental Science* 46; Elsevier Science Publishers, Amsterdam, the Netherlands: 169-179
- De Vries, W., M. Posch, G.J. Reinds and J. Kämäri, 1994f. *Simulation of soil response to acidic deposition scenarios in Europe*. *Water Air and Soil Poll.* 78 (in press).
- De Vries, W., O.F. Schoumans, J.F. Kragt and A. Breeuwsma, 1989. *Use of models and soil survey information in assessing regional water quality*. In G. Jousma, J. Bear, Y.Y. Haines and F. Walter (Eds.): *Groundwater contamination: Use of models in decision-making*. Proc. Int. Conf. Amsterdam, 1987, The Netherlands: 419-432.
- De Vries, W., M.J.P.H. Waltmans, R. Van Versendaal en J.J.M. Van Grinsven, 1988. *Aanpak, structuur en voorlopige proces beschrijving van een bodemverzuuringsmodel voor toepassing op regionale schaal*. Wageningen, Stichting voor Bodemkartering, Rapport nr. 2014, 132 pp.
- Groenenberg, J.E., J. Kros, C. Van der Salm and W. De Vries, 1994. *Application of the model NUCSAM to the Solling spruce site*. *Modelling of Geo-biosphere Processes* (submitted).
- Kros, J., P. Janssen, W. De Vries en C. Bak, 1990. *Het gebruik van onzekerheidsanalyse bij modelberekeningen: een toepassing op het regionale bodemverzuuringsmodel RESAM*. Wageningen, Staring Centrum, Rapport 65, 127 pp.
- Kros, J., W. De Vries, P. Janssen and C. Bak, 1993. *The uncertainty in forecasting regional trends of forest soil acidification*. *Water Air and Soil Poll.* 66: 29-58.
- Kros, J., J.E. Groenenberg, W. De Vries and C. Van der Salm, 1994a. *Uncertainties in long-term predictions of forest soil acidification due to neglecting interannual variability*. *Water Air and Soil Poll.* (accepted).
- Kros, J., P.S.C. Heuberger, P.H.M. Janssen and W. De Vries, 1994b. *Regional calibration of a steady-state model to assess critical acid loads*. In: *Proceedings of a Symposium on Predictability and nonlinear modeling in natural sciences and economics*. Wageningen Agricultural University, April 5-7, 1993.

- Posch, M., G.J. Reinds and W. De Vries, 1993. *SMART - A simulation model for Acidification's Regional Trends. Model description and User Manual*. Mimeograph Series of the National Board of Waters and the Environment, Helsinki, Finland, Report 477, 43 pp.
- Tiktak, A., A.H. Bakema, F. Berendse, K.F. De Boer, J.J.M. Van Grinsven, C. Van Heerden, B.J. Heij, G.W. Heil, J. Kros, J.G. Van Minnen, C. Van der Salm, J.C.H. Voogd and W. De Vries, 1992. *Scenario analysis with the Dutch Acidification Systems model (DAS); an example for forests and forest soils*. In: T. Schneider (Ed.): *Acidification Research; Evaluation and Policy Applications*. Studies in Environmental Science 50, Elsevier Science Publishers, Amsterdam, the Netherlands: 319-340.
- Van der Salm, C., W. De Vries and J. Kros, 1994a. *Modelling trends in soil solution concentrations under six forest-soil combinations*. Ecological Modelling (submitted)
- Van der Salm, C., J. Kros, J.E. Groenenberg, W. De Vries and G.J. Reinds, 1994b. *Validation of soil acidification models with different degrees of process aggregation on an intensively monitored spruce site*. In: S. Trudgill (Ed.): *Solute modelling in catchment systems* (submitted).
- Van Oene, H. and W. De Vries, 1994. *Comparison of measured and simulated changes in base cation amounts using a one-layer and a multi-layer soil acidification model*. Water Air and Soil Poll. 72: 41-66.



## CURRICULUM VITAE

Willem (Wim) de Vries werd geboren op 15 april 1959 te Nieuw Lekkerland. In 1977 behaalde hij het Atheneum-B diploma aan de christelijke scholengemeenschap 'De Lage Waard'. In hetzelfde jaar begon hij met de studie Bodemkunde en bemestingsleer aan de Landbouwhogeschool (thans Landbouwuniversiteit) te Wageningen. Het kandidaatsdiploma werd gehaald in 1981 en in 1983 ronde hij de doctoraal studie af. Het vakkenpakket in de doctoraalfase bestond uit een verzwaard hoofdvak bodemscheikunde en bodemnatuurkunde en uit de bijvakken irrigatie en ontwikkelingseconomie.

Van augustus 1982 tot en met mei 1983 bracht hij zijn praktijk door bij het South Australian Department of Agriculture. Daar deed hij onderzoek naar het effect van ontbossing op het chloridegehalte in een drinkwater reservoir. Vanaf september 1983 tot en met 1989 was hij werkzaam bij de voormalige Stichting voor Bodemkartering (STIBOKA). Sinds 1989 is hij werkzaam bij het DLO-Staring Centrum; een fusie van o.a. de voormalige STIBOKA en het Instituut voor Cultuurtechniek en Waterhuishouding (ICW). Zowel bij STIBOKA als bij het DLO-Staring Centrum heeft hij zich hoofdzakelijk bezig gehouden met effecten van zure atmosferische depositie op de bodem. Naast veld- en laboratoriumonderzoek betrof dit vooral het ontwikkelen en toepassen van simulatiemodellen op het gebied van de bodemverzuring. Dit proefschrift vormt de neerslag van een groot deel van het verzuringsonderzoek dat bij STIBOKA en het DLO-Staring Centrum is uitgevoerd.

Wim de Vries is getrouwd en is vader van vier kinderen.